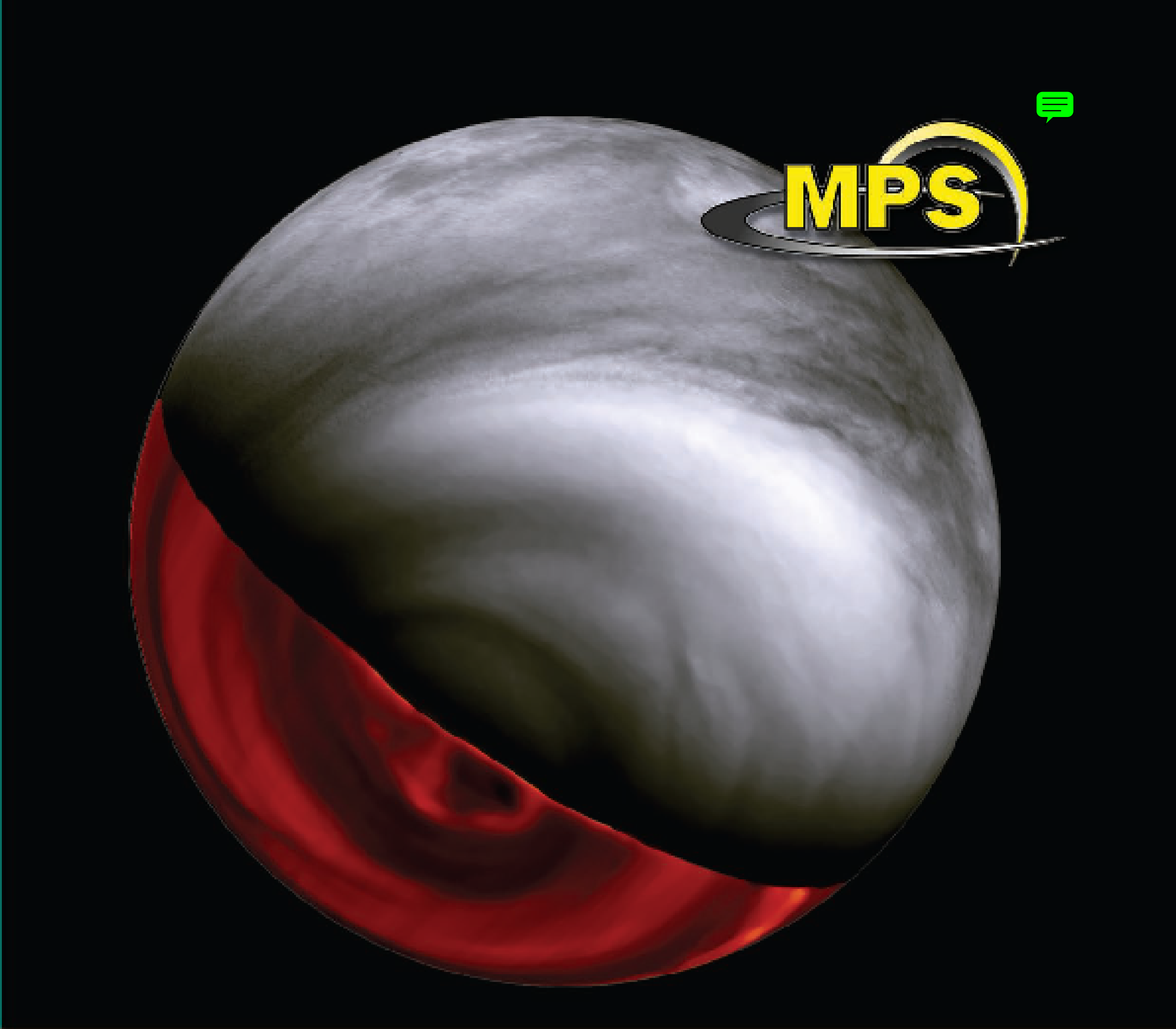

# Max-Planck-Institut
# für Sonnensystemforschung
# Report 2006/2007

MAX-PLANCK-GESELLSCHAFT

# MAX–PLANCK–INSTITUT FÜR SONNENSYSTEMFORSCHUNG

## KATLENBURG–LINDAU

# Report für die Jahre 2006 und 2007

## Update – Oktober 2008


| | |
|---|---|
| *Herausgegeben von der Institutsleitung*: | *Prof. Dr. Sami K. Solanki*<br>*Prof. Dr. Ulrich R. Christensen*<br>*Prof. Dr. Vytenis M. Vasyliūnas* |
| *Redaktion:* | *Dr. Johannes Wicht*<br>*Dr. Patrick W. Daly*<br>*Gerlinde Bierwirth*<br>*Julia Müller* |
| *Koordinatoren des wissenschaftlichen Teils:* | *Dr. Patrick Daly*<br>*Dr. Hermann Böhnhardt*<br>*Prof. Dr. Jörg Büchner*<br>*Dr. Norbert Krupp* |

**Abbildung auf dem Frontumschlag:**

Falschfarbene Abbildungen der Venus Südhemisphäre. Die obere/rechte Seite zeigt eine VMC-Aufnahme der Tagseite im Ultravioletten. Die untere/linke Abbildung ist eine VIRTIS Aufnahme der Nachtseite im nah-infraroten spektralen Fenster bei 1.7 $\mu$m Wellenlänge. Die ultraviolette Aufnahme zeigt die Morphology der oberen Wolkenschicht, während die Infrarotaufnahme tiefere Strukturen zeigt.

**Picture on the Cover:**

False colour image of the Venus southern hemisphere composed of a VMC ultraviolet image on the day side (top/right) and a VIRTIS near-IR image in the 1.7 $\mu$m spectral transparency window on the night side (bottom/left). The images show global morphology at the cloud tops and deep inside the cloud layer.


Erschienen im September 2008.

**Anschrift:**

Max-Planck-Institut für Sonnensystemforschung
Max-Planck-Straße 2
37191 Katlenburg-Lindau
Deutschland
Tel.: +49-(0) 5556-979-0
Fax: +49-(0) 5556-979-240
http://www.mps.mpg.de

# **Inhalt** / Contents

## I **Allgemeines zum Institut** / Institute Overview


Gegenstand und Methoden der Forschung / Subject and Methods of Research . . . . . 1

Struktur und Leitung des Instituts / Structure and Management of the Institute . . . . . 2

Nachruf / Obituary . . . . . 3

Emeritierung Prof. Dr. Vytenis M. Vasyliūnas
Retirement of Prof. Vytenis M. Vasyliūnas . . . . . 4

Personelle Entwicklung / Personnel Development . . . . . 5

Das Kuratorium des Instituts / Board of Trustees of the Institute . . . . . 5

Der Fachbeirat des Instituts / Scientific Advisory Board of the Institute . . . . . 6

Für das Institut aufgewendete Mittel / Institute Resources . . . . . 6


## II **Wissenschaftliche Arbeiten** / Scientific Projects

### *1* ***Sonne und Heliosphäre*** */ Sun and Heliosphere*


Schwerpunktthema: Die Physik solarer Eruptionen . . . . . 9

Highlight: Physics of solar eruptions . . . . . 12

Sonne und Heliosphäre – Übersicht der Projekte / Sun and Heliosphere – overview of projects . . . . . 15

**Solar interior, photosphere and chromosphere**

Solar cycle prediction using precursors and flux transport models . . . . . 16

Modelling the Sun’s open magnetic flux . . . . . 16

A solar surface dynamo . . . . . 17

Current sheets and reconnection in the upper photosphere . . . . . 17

Signature of magnetic reconnection in the solar photosphere . . . . . 18

The origin of the ‘reversed’ granulation . . . . . 19

Flow instabilities of magnetic flux tubes . . . . . 20

Multi-channel high resolution observations of sunspots . . . . . 20

Flux emergence in the solar photosphere – Diagnostics based on 3-D radiation-MHD simulations . . . . . 21

Center-to-limb variations of intensity contrast of simulated faculae and network elements . . . . . 22

High resolution spectroscopy of small-scale solar magnetic elements in the violet CN band-head . . . . . 23

Spectro-polarimetric diagnostics of simulated magneto-convection . . . . . 23

Spectro-polarimetric diagnostics near the solar limb: Simulations versus high-resolution observations . . . . . 23

Classification of line profiles in the network and internetwork based on Hinode data and comparison with
MHD simulations . . . . . 24

Low-lying loops in the quiet Sun internetwork region . . . . . 25

Oscillations in penumbral filaments . . . . . 25

The nature of running penumbral waves . . . 26
Moving magnetic features . . . 26
Tracking of moving magnetic flux concentrations around sunspots in the photosphere . . . 27
The vertical extension of penumbral filaments . . . 27
Magnetohydrostatic model of sunspot filamentary structure . . . 28
Automated detection of bright points and faculae at various disk positions . . . 28
Fine structure and dynamics of sunspot umbral dots: Evidence for their convective nature . . . 28
Validation of three methods proposed to derive the photospheric plasma motion . . . 29
Photospheric plasma flows preceding the 'Bastille Day' flare period . . . 30
Derivation of the photospheric plasma motion in AR 8210 in preparation of Hinode observations . . . 30
On the relations between chromospheric emissions and magnetic field in the quiet Sun . . . 31
Measurement of the magnetic canopy . . . 32
Velocity distribution of chromospheric downflows . . . 33
Spectropolarimetric observations of the He I 10830 Å multiplet in an active region filament . . . 33
Chromospheric fibrils observed in Ca II *K* . . . 34
The intensity contrast of solar granulation: comparing Hinode results with MHD simulations . . . 35
Strong horizontal magnetic field in a surface dynamo simulation . . . 36
Comparison of magnetoconvection simulations with the approximation of thin flux tubes . . . 36
Evidence of magnetic field wrapping around penumbral filaments . . . 37
Discovery of inward moving magnetic enhancements in sunspot penumbrae . . . 38
Evidence of convective rolls in a sunspot penumbra . . . 38
Magnetic structures of an emerging flux region in the photosphere and chromosphere . . . 39

**Solar transition region and corona**

Magnetic structure of the solar transition region as observed in various ultraviolet lines . . . 39
Current-free electric double layer in coronal funnel . . . 40
Plasma outflows and open magnetic fields in a quiet-sun region . . . 40
The inverse Evershed effect in transition region emission as observed by SUMER . . . 41
Nonlinear force-free magnetic field extrapolation . . . 42
Segmentation of loops from coronal EUV images . . . 42
Fundamental principles of stereoscopy and their application to the STEREO mission . . . 43
Inversion of coronal Zeeman and Hanle observations . . . 43
Properties of solar polar coronal plumes constrained by UVCS data . . . 44
Preprocessing of vector magnetograph data for a nonlinear force-free magnetic field reconstruction . . . 44
Testing nonlinear force-free extrapolations . . . 44
Magnetic stereoscopy: I. Theory . . . 45
Magnetic stereoscopy: II. Application . . . 45
An optimization principle for the computation of MHD equilibria in the solar corona . . . 46

Computing nonlinear force-free fields in spherical coordinates . . . 46
Nonlinear force-free modelling of coronal magnetic fields, Part I: a quantitative comparison of methods 47
Evolution of a coronal loop system . . . 47
Search for photospheric footpoints of transition region loops . . . 48
Loop segmentation . . . 49
Magnetic field extrapolation with MHS model . . . 49
Solar coronal-hole plasma densities and temperatures . . . 50
Jets or high-velocity flows in the solar corona . . . 50
Fe XIX plasma jets in the solar corona . . . 50
A nanoflare model of emission line radiance distributions in active region coronae . . . 51
A hot coronal downflow . . . 51
Transverse loop oscillations . . . 52
Statistical study of Doppler shift oscillations seen in hot coronal loops . . . 52
Hanle effect in H I Ly-$\alpha$ and $\beta$: Diagnostic of coronal magnetic fields . . . 53
Force-free magnetic field extrapolation in simulations of the solar atmosphere . . . 54
Simulation of three-dimensional magnetic reconnection sites at the Sun . . . 54
The topological skeleton as a predictor of 3-D magnetic reconnection sites in the solar atmosphere . . . 55
Investigation of reconnection in the solar corona by Hinode observations . . . 55
Linearly unstable low-frequency current driven plasma waves in the solar corona . . . 56
High frequency electron/electron modes in solar coronal plasma . . . 57
Vlasov code simulation of collisionless solar plasma instabilities . . . 57
Anomalous collisions in the solar atmosphere are stronger than predicted by the quasi-linear theory . . . 58
Anomalous resistivity of solar coronal plasmas due to electrostatic double layers . . . 59
Log-normal intensity distribution of the quiet-Sun FUV continuum . . . 59
Multi-spacecraft observations of polar coronal plumes . . . 60
The redshifted footpoints of coronal loops . . . 61
3-D plume . . . 61
3-D loop . . . 62
SOHO/SUMER observations of prominence oscillation before eruption . . . 62
SUMER observations of molecular hydrogen in active region plage . . . 63
Small-scale flows in simultaneous SUMER and TRACE high-cadence observations . . . 63
Emission heights of coronal bright points on Fe XIII radiance map . . . 64
MHS model . . . 64
Attenuation of Alfvén waves in straight and curved coronal slabs . . . 64
Loop morphology and flows above a sunspot . . . 65
Evolution of a flaring active region as a sequence of nonlinear force-free field extrapolations . . . 65
Coronal equilibria . . . 66

Magnetic structure of Flares . . . 67

Preprocessing of vector magnetograms . . . 67

Magnetic modelling for Solar Orbiter . . . 68

**Solar wind and heliosphere**

Kinetic properties of the solar corona and solar wind . . . 68

Reviews on the origin and evolution of the solar wind and its response to the solar activity cycle . . . 68

Limits on the core temperature anisotropy of solar wind protons . . . 69

Ion-cyclotron beam instabilities in a coronal funnel . . . 69

Ion-cyclotron drift instabilities in the nonuniform corona . . . 70

Collisionless damping of parametrically unstable Alfvén waves . . . 71

Diffusion plateaus in the velocity distributions of protons in fast solar wind . . . 71

On the evolution of the solar wind proton temperature anisotropy from 0.3 to 2.5 AU . . . 72

**Past solar activity and Sun-Earth relations**

Variations of total solar irradiance (TSI) . . . 72

A cross-calibrated sunspot area time series since 1874 . . . 72

Reconstruction of solar UV irradiance in cycles 21 – 23 . . . 73

Spectral irradiance variations: Comparison between observations and the SATIRE model on solar rotation time scales . . . 74

Modelling solar cycle variation of spectral line properties . . . 74

Dependence of sunspot brightness on sunspot size and cycle phase . . . 74

Historical Ca spectroheliograms: making an old resource available for new studies . . . 75

Stellar variability: using the solar paradigm to model variability of active stars . . . 76

Grand minima and maxima of solar activity . . . 76

The latitudinal dependence of the sunspot cycle: a new diagnostic of dynamo models . . . 76

**Ongoing and future solar missions and instruments**

Lessons from the SUMER/SOHO ultraviolet spectrograph . . . 77

SOHO/SUMER: Status and perspectives . . . 77

STEREO Update . . . 78

TIP-2 . . . 78

SWAP and LYRA instruments on PROBA-2 . . . 79

SUNRISE: A balloon-borne telescope for high resolution observations of the Sun . . . 80

Thermal design for EUS (EUV Spectrograph) onboard Solar Orbiter . . . 81

SOLAR ORBITER: Programmatic issues . . . 81

The EUS instrument . . . 82

The Solar Orbiter EUI instrument . . . 83

The Solar Orbiter PHI instrument . . . 83

The SPICE instrument proposed for the HELEX / Solar Orbiter mission . . . 84

Analysis of PHI instrument performance . . . 84

Thermal design of a VUV telescope mirror for Solar Orbiter instruments . . . 86

Magnetic modelling for SO/VIM . . . 86

Solar microscopy: Unveiling the Sun's basic physical processes at their instrinsic scales . . . 87

Proposal to ESA to fly a coronal magnetic field mapper, COMPASS . . . 87

**Solar-stellar connections, interstellar dust and Cosmic Rays**

Theoretical mass loss rates of cool stars . . . 87

The fraction of DA white dwarfs with kilo-gauss magnetic fields . . . 88

The Ca II infrared triplet as a stellar activity diagnostic: Test and calibration . . . 88

Doppler imaging of the RS CVn Star Sigma Geminorum . . . 89

Triggered Star formation by outflow-driven shells . . . 90

Properties of young protostellar objects: a peculiar source . . . 90

A magnetic communication scenario for hot Jupiters . . . 91

Formation of coherent structures and particle acceleration at the front of dense relativistic $e^+ - e^-$ jets expanding into the interstellar medium . . . 91

Understanding WMAP results: The low-$l$ anomalies and dust in the vicinity of the solar system . . . 91

Monitoring the interstellar dust flow through the solar system . . . 92

Anomalous cosmic ray from ENA measurements with SOHO/CELIAS/HSTOF . . . 92

Estimating the thickness of the heliosheath from CELIAS/HSTOF and Voyager 1 data . . . 93

Interstellar dust in the solar system . . . 93

Combined models of magnetic flux generation and transport in cool stars . . . 94

The FeH $F^4\Delta$-$X^4\Delta$ system and its diagnostic capability for investigating solar and stellar magnetic fields 94

**Fundamental science**

Eigenfunctions of the radial operator and the spin-orbit-coupling operator for a relativistic binary . . . 95

Solar Axions . . . 95

## 2 ***Planeten, ihre natürlichen Satelliten und Kometen*** / *Planets, their moons and comets*

Schwerpunktthema: Höhepunkte der Venus-Express-Mission . . . 97

Highlight: Venus Express Highlights . . . 102

Planeten, ihre natürlichen Satelliten und Kometen – Übersicht der Projekte / Planets, their moons and comets – overview of projects . . . 109

**Planetary interiors**

Dipole moment scaling for planetary dynamos . . . 110

Magnetic structures in Earth-like dynamo simulations . . . 110

Magnetic field reversal statistics . . . 111

Magnetic core-mantle coupling . . . 112

Torsional oscillation in dynamo simulations . . . 112

Statistical properties of the multipole coefficients of the geomagnetic field . . . 112
Double diffusive convection in planetary ion cores . . . 113

**Terrestrial planets research – Mercury**

A dynamo model for Mercury . . . 114
Driving Mercury's Dynamo . . . 114
Mercury's tidal Love number from laser altimetry . . . 115

**Terrestrial planets research – Venus**

Venus Express – the first European mission to planet Venus . . . 116
Venus Express scientific support . . . 116
Morphology of Venus in the polar region . . . 116
VMC monitors global weather on Venus . . . 116
Venus Cloud Altimetry . . . 117
Venus cloud tops winds . . . 117
Global cloud morphology of Venus from the Venus Monitoring Camera . . . 119
Convection in the upper clouds of Venus . . . 120
Venus Monitoring Camera sees the surface through the thick cloud veil . . . 120
Vertical thermal structure and winds on the Venusian's Mesosphere derived from HHSMT CO spectral-line observations . . . 121
Venus Express ASPERA-4 Experiment Observes Ion Outflow from Venus Atmosphere . . . 121
Plasma environment on Venus . . . 122
Magnetic pile-up boundary and magnetic barrier on Venus . . . 122
Bow shock and ion composition boundaries at Venus – Venus Express ASPERA-4 . . . 123
The plasma environment of Venus: comparison of Venus Express ASPERA-4 measurements with 3D hybrid simulations . . . 123

**Terrestrial planets research – Mars**

Study of the Martian water cycle by the PFS and OMEGA experiments onboard the Mars Express . . . 125
Martian aerosols and HRSC stereo images . . . 125
New images of Mars from the OSIRIS camera system on Rosetta . . . 126
Presence of a strongly ferrimagnetic phase in bedrock at Meridiani Planum, Mars? . . . 128
The ring of Mars: Close to discovery? . . . 129
Remnant of a geyser like eruption in a Martian crater . . . 129
Magnetic properties of Martian atmospheric dust . . . 130
Indication of long-lasting dry periods on Mars from the chemistry and mineralogy of atmospheric dust . 130
Simulation of the water cycle on Mars . . . 132
Semi-annual oscillations in the atmosphere of Mars . . . 132
Seasonal changes of the baroclinic wave activity of Mars simulated with a Global Circulation Model . . 133
Comparison of microwave observations of Martian temperature and winds with model simulations . . . 133

Study on winter polar warmings and the meridional transport on Mars with model simulations . . . . . 135

Temperature inversion during the 2001 global dust storm on Mars — SWAS with MAOAM . . . . . . . 135

Middle atmosphere polar warmings on Mars: Simulations and validation study . . . . . . . . . . . . . . 136

New dynamical core for MAOAM . . . . . . . . . . . . . . . . . . . . . . . . . . . . . . . . . . . . . . 136

MARSIS on Mars Express . . . . . . . . . . . . . . . . . . . . . . . . . . . . . . . . . . . . . . . . . . 137

Solar wind/ionosphere interface on Mars from comparative analysis of MEX-ASPERA-3 and MEX-MARSIS observations . . . . . . . . . . . . . . . . . . . . . . . . . . . . . . . . . . 140

Pickup protons at Mars and their acceleration at the bow shock . . . . . . . . . . . . . . . . . . . . . . 142

Suprathermal Electrons as a Source of Aurora on Mars . . . . . . . . . . . . . . . . . . . . . . . . . . 142

Inflations of the magnetospheric cavity on Mars due to crustal magnetization . . . . . . . . . . . . . . 143

Influence of crustal magnetization on solar wind induced escape . . . . . . . . . . . . . . . . . . . . . 143

Field-aligned currents and parallel electric field potential drops on Mars . . . . . . . . . . . . . . . . . 144

Peaked Electron distributions on Mars . . . . . . . . . . . . . . . . . . . . . . . . . . . . . . . . . . . 145

Plasma moments in the environment of Mars . . . . . . . . . . . . . . . . . . . . . . . . . . . . . . . . 146

Energetic electron asymmetries in the Martian magnetosphere . . . . . . . . . . . . . . . . . . . . . . 146

Project MOMA . . . . . . . . . . . . . . . . . . . . . . . . . . . . . . . . . . . . . . . . . . . . . . . . 147

**Outer planets research – Jupiter and Saturn**

Comparison of periodic substorms at Jupiter and Earth . . . . . . . . . . . . . . . . . . . . . . . . . . 148

Observations of Saturnian magnetosphere and interaction of magnetospheric particles with moons . . . 149

**Outer planets research – Ice Giants**

A Deep Convection Model for the Zonal Flows on the Ice Giants . . . . . . . . . . . . . . . . . . . . . 154

**Cometary research**

The recent mega-outburst of comet 17P/Holmes at millimeter wavelengths . . . . . . . . . . . . . . . . 155

Millimeter-wavelength spectroscopy as a tool for studying the rotation of active comets: the case study of comet 8P/Tuttle . . . . . . . . . . . . . . . . . . . . . . . . . . . . . . . . . . . . . . 156

Submillimeter monitoring of HCN in fragment C of comet 73P/Schwassmann-Wachmann 3 . . . . . . . 156

Deep Impact at comet 9P/Tempel 1: Exploring the Dust Component . . . . . . . . . . . . . . . . . . . 157

Physical and composition properties of short-periodic and Oort Cloud comets . . . . . . . . . . . . . . 159

**Cometary research – ROSETTA**

CONSERT on board ROSETTA . . . . . . . . . . . . . . . . . . . . . . . . . . . . . . . . . . . . . . . 160

Detailed report on COSAC (2006/07) . . . . . . . . . . . . . . . . . . . . . . . . . . . . . . . . . . . 160

The ROSETTA Lander PHILAE . . . . . . . . . . . . . . . . . . . . . . . . . . . . . . . . . . . . . . 161

Retrieval Simulation for the MIRO Instrument on the Rosetta Orbiter . . . . . . . . . . . . . . . . . . . 161

Scientific observations with OSIRIS onboard Rosetta . . . . . . . . . . . . . . . . . . . . . . . . . . . 163

OSIRIS images from Rosetta Earth swing-by . . . . . . . . . . . . . . . . . . . . . . . . . . . . . . . 164

**Other small bodies**

Pluto-Charon and Triton: . . . . . 165

Surface exploration of Kuiper Belt Objects and Cometary Nuclei . . . . . 165

**General studies**

Linearity Improvement of sub-millimeter heterodyne spectrometers . . . . . 166

Improvement of instrument performance in ground-based (sub)millimeter observations . . . . . 166

Herschel Solar System Observations (HSSO) . . . . . 167

HIFI absolute flux calibration using opaque molecular spectra in the Martian atmosphere . . . . . 168

Development of Wide Bandwidth SAW Chirp Filters with Improved Magnitude Response . . . . . 169

A tool to study rings around satellites . . . . . 170

Photoelectron modelling . . . . . 170

Multi-fluid modelling of solar wind interaction with planetary bodies . . . . . 171

DAWN Framing Camera . . . . . 172

### *3 Atmosphäre, Ionosphäre und Magnetosphäre der Erde/* *Terrestrial Atmosphere, Ionosphere, Magnetosphere*

Overview of Magnetospheric research . . . . . 173

Future Exploration of Planetary Magnetospheres . . . . . 174

The Earth's magnetosphere and the Cluster Mission . . . . . 174

The Galileo Mission, new insights about planetary magnetospheres . . . . . 175

The 5-day signal in the mesospheric water vapour concentration in high latitudes in 2003 . . . . . 177

Long-term trends of the concentration of the minor constituents in the mesosphere – a model study . . . 177

A new 22 GHz water vapour heterodyne spectrometer . . . . . 178

Forces in the magnetosphere-ionosphere-Earth system . . . . . 178

Rotationally driven interchange instability . . . . . 179

The Cluster Mission . . . . . 179

Multipoint observations of ions in the energy range 30–235 keV upstream of Earth's bow shock . . . . 180

Cluster encounter with an electron beam during a substorm . . . . . 180

Motion of flux transfer events . . . . . 180

Substorm observations in the magnetotail with Cluster during high-speed plasma streaming from the Sun 181

The non-cusp Earth's magnetopause observed by Cluster . . . . . 181

RAPID contribution to the Cluster Active Archive . . . . . 182

The German Cluster Data Centre . . . . . 183

## III Selbständige Nachwuchsgruppe Helio- und Asteroseismologie / Independent Junior Research Group of the Max Planck Society "Helio- and Asteroseismology"

Measurement of the meridional flow with Fourier-Hankel decomposition . . . . . 185

Solar-cycle variation of rotation and meridional circulation . . . . . 185

Accurate travel-time measurements . . . 186
High resolution time-distance helioseismology . . . 186
Travel-time sensitivity kernels for vector flows . . . 188
Three-dimensional sensitivity kernels for ring-diagram analysis . . . 188
Solar supergranular structure from local helioseismology . . . 188
Surface magnetic field effects in local helioseismology . . . 189
Penumbral acoustic anomaly . . . 189
Imaging the interaction of solar waves with a sunspot . . . 190
Simulations of wave propagation: The Semi-spectral Linear MHD (SLiM) code . . . 190
Testing the SLiM code . . . 191
Three-dimensional numerical simulation of wave propagation through model sunspots . . . 191
Asteroseismology of K Giants . . . 192
Beyond mean-field theories of atomic Fermi gases . . . 192
Initial-value formalism for spherically symmetric matter distributions in General Relativity . . . 193
HELAS local helioseismology database . . . 193
German Data Center for the Solar Dynamics Observatory . . . 194
Helioseismology with Solar Orbiter . . . 194

## IV International Max Planck Research School

Übersicht / Overview . . . 195
Vorstand / *Chair* . . . 196
Lehrveranstaltungen / *Lectures* . . . 196
Abgeschlossene Dissertationen / *Finished PhDs* . . . 196
Laufende Dissertationen / *Ongoing PhDs* . . . 198
Preise / *Awards* 2006 – 2007 . . . 199

## V Rechenzentrum, Elektroniklabor, Mechanik, Haustechnik und Ausbildung / Computer Centre, Electronic Laboratory, Mechanics, Physical Plant and Education

Rechenzentrum . . . 201
Elektroniklabor . . . 203
Abteilung Mechanik . . . 203
Verwaltung – Teilbereich Haustechnik . . . 205
Ausbildung . . . 205

## VI Personelle Gliederung / Personnel

Kollegium, wissenschaftliche Mitglieder / Board of directors, scientific members . . . 207

Wissenschaftliche und wissenschaftlich-technische Mitarbeiter / Scientific staff . . . . . . . . . . . . . 207

## VII **Wissenschaftliche Zusammenarbeit** / Scientific Collaboration

Wissenschaftler, die als Gäste längere Zeit am MPS tätig waren / Long-term scientific visitors at MPS . . . . . 213

Wissenschaftler, die als Gäste nur kurzzeitig am MPS tätig waren / Short-term scientific visitors to MPS . . . . . 214

Längere Aufenthalte von Wissenschaftlern des MPS an anderen Instituten / Long-term visits of MPS scientists to other institutes . . . . . 216

Projekte in Zusammenarbeit mit anderen Institutionen / Projects in collaboration with other institutions . . . . . 216

Projektförderungen durch das Bundesministerium für Bildung und Forschung (BMBF) und andere Institutionen / Project grants by BMBF and other institutions . . . . . 226

Lehrtätigkeiten / Teaching . . . . . 227

IMPRS Vorlesungen / IMPRS lectures . . . . . 227

Weitere Lehrtätigkeiten oder Kurse / Other lectures or courses . . . . . 228

Mitgliedschaften in wissenschaftlichen Gremien / Membership in scientific councils . . . . . 228

Gutachtertätigkeiten / Review reports . . . . . 228

Tätigkeiten als Convener/ Convenerships during scientific meetings . . . . . 230

Organisation von Workshops/Workshop organisation . . . . . 230

Öffentlichkeitsarbeit / Public relations . . . . . 231

TV- und Hörfunkauftritte / Media coverage . . . . . 231

Pressenotizen / Press releases . . . . . 231

Erich-Regener-Vortragsreihe / Erich-Regener lecture series . . . . . 232

Institutsführungen, Ausstellungen und spezielle Events / Guided tours, exhibitions, and special events . 233

Vorträge außerhalb des MPS / External presentations . . . . . 233

Auszeichnungen / Awards . . . . . 235

Herausgebertätigkeiten / Editorships . . . . . 236

Direktionsberaterkreis des MPS / „Direktionsberaterkreis“ at MPS . . . . . 236

40 Jahre in der MPG / 40 years at MPG . . . . . 236

25 Jahre in der MPG / 25 years at MPG . . . . . 237

## VIII **Berichte, Vorträge und Veröffentlichungen** / Reports, Talks and Publications

Interne MPS-Berichte / Internal MPS reports . . . . . 239

Experimentvorschläge / Proposals . . . . . 239

Tee-Seminare / Tea Seminars . . . . . 240

IMPRS Solar System Seminars / IMPRS Solar System Seminars . . . . . 243

Instituts-Seminare / Institute seminars . . . . . 245

MPS-Kolloquien / MPS Colloquia . . . . . 245
Vorträge 2006 / Talks 2006 . . . . . 248
Vorträge 2007 / Talks 2007 . . . . . 271
Veröffentlichungen 2006 / Publications 2006 . . . . . 285
Veröffentlichungen 2007 / Publications 2007 . . . . . 303

# I. Allgemeines zum Institut / Institute Overview

## Gegenstand und Methoden der Forschung / Subject and Methods of Research

Die verschiedenen Objekte des Sonnensystems bilden den Gegenstand der Forschung am MPS. Ein großes Forschungsgebiet betrifft die Sonne, ihre Atmosphäre, das vom Sonnenwind beeinflusste interplanetare Medium, sowie den Einfluss der schwankenden solaren Partikel- und Wellenstrahlung auf die Erde und auf andere Planeten. Das zweite große Forschungsthema befasst sich mit dem Inneren, den Oberflächen, Atmosphären, Ionosphären und Magnetosphären der Planeten, ihrer Monde, sowie von Kometen und Asteroiden.

Eine wichtige Rolle spielt die Auswertung von Bildern und Spektren, die mit Instrumenten auf Raumsonden oder von erdgebundenen Teleskopen gewonnen werden. Damit werden die Sonne, Planeten (insbesondere Mars und Venus), Monde (Titan), Kometen und andere Kleinkörper erforscht. Die Korona der Sonne wird mit optischen Instrumenten im gesamten Spektralbereich vom Sichtbaren bis zum weichen Röntgenlicht vom Weltraum aus beobachtet, und ihre Plasmaeigenschaften werden mit spektroskopischen Methoden diagnostiziert. Die untere Atmosphäre der Sonne (die Photosphäre und Chromosphäre) wird anhand von spektropolarimetrischen Messungen sowohl vom Boden als auch vom Weltraum aus untersucht. Dabei geht es vor allem um die Bestimmung des solaren Magnetfeldes, welches eine grundlegende Rolle für eine Vielzahl solarer Phänomene spielt. Ein neues Arbeitsgebiet ist die Untersuchung des Sonneninneren durch Analyse von beobachteten Schwingungen an ihrer Oberfläche (Helioseismologie). Geologische Vorgänge und die mineralogische Zusammensetzung an den Oberflächen planetarer Körper, sowie die Eigenschaften von Planetenatmosphären werden durch abbildende und spektrometrische Verfahren im sichtbaren Spektrum und nahen Infrarotbereich untersucht. In-situ-Methoden zur chemischen Untersuchung von Kometen- und Planetenoberflächen, sowie geophysikalische Untersuchungen des Planeteninneren werden in Zukunft eine Rolle spielen.

In den Magnetosphären der Erde und anderer Planeten, im Sonnenwind und in der Umgebung von Kometen werden Teilchen und Wellen von Instrumenten auf Raumsonden in-situ gemessen. Die chemische Zusammensetzung, die räumliche Verteilung der Teilchen sowie das Studium von Transportvorgängen und Beschleunigungsprozessen stehen dabei im Vordergrund. Bei der überwiegend experimentell ausgerichteten Arbeitsweise des Instituts spielt die Entwicklung und der Bau von Instrumenten und die Gewinnung und Auswertung von Messdaten eine Hauptrolle. Diese Aktivitäten werden jedoch intensiv von theoretischen Arbeiten und der Bildung von physikalischen Modellen begleitet. Das Schwergewicht liegt hierbei auf der numerischen Simulation in den Bereichen planetare und solare Dynamos, atmosphärische Zirkulationsmodelle, MHD-Prozesse in der Konvektionszone und Atmosphäre der Sonne, Physik ionosphärischer und magnetosphärischer Plasmen, sowie Konvektionsströmungen im Gesteinsmantel terrestrischer Planeten und in den Gashüllen der Riesenplaneten.

---

*The objects of the solar system are at the focus of research at MPS. One important area of research includes the Sun, its atmosphere, the interplanetary medium filled with and influenced by the solar wind, as well as the influence of the variable radiation of solar particles and waves on the Earth and other planets. The second major research field involves the interiors, surfaces, atmospheres, ionospheres, and magnetospheres of the planets and their moons, as well as those of comets and asteroids.*

*The analysis of images and spectra obtained from instruments on spacecrafts or from ground-based telescopes play an important role for the exploration of the Sun, the planets (especially Mars and Venus), moons (Titan), comets, and other small bodies. The solar corona is observed with optical instruments in space covering the entire spectral range from visible to soft x-rays, and its plasma properties are analysed by spectroscopic methods. The Sun's lower atmosphere (the photosphere and chromosphere) is investigated by means of spectral polarisation measurements, both from the ground and from space. In this case, it is the solar magnetic field that is of key interest. It plays a fundamental role in a multitude of solar phenomena. A new field of endeavour is the study of the solar interior by analysing the observed oscillations on the surface (helioseismology). Geological processes and mineralogical composition on the surfaces of plane-*

*tary bodies, as well as the properties of the atmospheres of planets are investigated with imaging and spectrometric techniques in the visible and near infrared spectral regions. In-situ methods for chemical analysis of cometary and planetary surfaces, as well as geophysical investigations of the interiors of planets will play an important role in the future.*

*In the magnetospheres of the Earth and other planets, in the solar wind and in the neighbourhood of comets, particles and waves are measured in-situ from space-borne instruments. The chemical composition, the spatial distribution of particles, and the study of transport mechanisms and energisation processes are at the forefront of the research into these topics. As the institute is primarily involved in experimental investigations, the development and construction of instruments together with the analysis of acquired data play a major role. These activities are accompanied by intensive theoretical efforts and the creation of physical models. The emphasis here lies on numerical simulations of planetary and solar dynamos, atmospheric circulation models, MHD processes in the convection zone and solar atmosphere, the physics of ionospheric and magnetospheric plasmas, as well as on convection currents in the solid mantle of terrestrial planets and in the gas envelopes of the giant planets.*

## **Struktur und Leitung des Instituts /** Structure and Management of the Institute

Mit der Emeritierung von Dr.-Ing. H. Rosenbauer am 30. Juni 2004 wurde das Institut in drei Abteilungen gegliedert: der Abteilung Sonne und Heliosphäre unter den Leitung von Prof. Dr. S. K. Solanki, der Abteilung Planeten und Kometen unter der Leitung von Prof. Dr. U. R. Christensen, sowie der Abteilung Magnetosphäre unter der Leitung von Prof. Dr. V. M. Vasyliūnas. Nach der Emeritierung von Prof. Vasyliūnas am 1. Oktober 2007 bleiben nunmehr zwei Abteilungen bestehen. Am 1. September 2005 wurde das Institut um die Selbständige Nachwuchsgruppe Helio- und Asteroseismologie der MPG erweitert. Eine technische Abteilung und die Verwaltung sind zentral organisiert und stehen allen wissenschaftlichen Abteilungen zur Verfügung. Die zentralen technischen Einrichtungen umfassen eine Mechanische Abteilung, bestehend aus Konstruktion und Werkstätten, ein Entwicklungslabor für Elektronik, ein Rechenzentrum und eine Fachbibliothek.

Das Institut wurde durch das Gesamtkollegium der Direktoren Prof. Dr. U. R. Christensen, Prof. Dr. S. K. Solanki und Prof. Dr. V. M. Vasyliūnas (bis 30. September 2007) gemeinschaftlich geleitet.

Geschäftsführender Direktor war bis zum 31. Dezember 2007 Prof. Dr. U. R. Christensen. Er wurde in dieser Funktion von Prof. Dr. S. K. Solanki abgelöst.

Das Kollegium wird in seiner Arbeit durch einen technischen Geschäftsführer (Dr. I. Pardowitz), einen Verwaltungsleiter (A. Poprawa), und einen Direktionsberaterkreis unterstützt. Letzterer besteht aus drei Mitarbeitern des wissenschaftlich-technischen Bereiches, die von allen Mitarbeitern des Instituts für eine einjährige Amtsperiode gewählt werden.

Für die einzelnen Forschungsvorhaben werden innerhalb der Abteilungen jeweils Projektgruppen gebildet, die nach Abschluss des Projektes wieder aufgelöst werden.

---

*Following the retirement of Dr.-Ing. H. Rosenbauer at June 30, 2004 the institute was reorganized into three departments: the department Sun and Heliosphere headed by Prof. Dr. S. K. Solanki, the department Planets and Comets headed by Prof. Dr. U. R. Christensen, and the department Magnetosphere headed by Prof. Dr. V. M. Vasyliūnas. After the retirement of Prof. Vasyliūnas on October 1, 2007 two departments now remain. In addition, the Independent Junior Research Group of the Max Planck Society "Helio- and Asteroseismology" was created on September 1, 2005. A technical department and the administration are centrally organized and serve all research departments. The technical department comprises a mechanical department, including design office and workshop, an electronics laboratory, a computing center, and a library.*

*The institute was jointly managed by the directors Prof. Dr. U. R. Christensen, Prof. Dr. S. K. Solanki, and Prof. Dr. V. M. Vasyliūnas (until September 30, 2007), who constitute the board of directors).*

*Prof. Dr. U. R. Christensen served as managing director until December 31, 2007 and was superseded by Prof. Dr. S. K. Solanki.*

*The board of directors is assisted by a technical manager (Dr. I. Pardowitz), the head of administration (A. Proprawa), and a director's advisory committee. The latter consists of three members of the scientific-technical staff who are elected for a one-year period by the complete staff.*

*A dedicated project group is formed for the duration of each research project. Every institute member can take the initiative to start a new project and to form the corresponding group.*

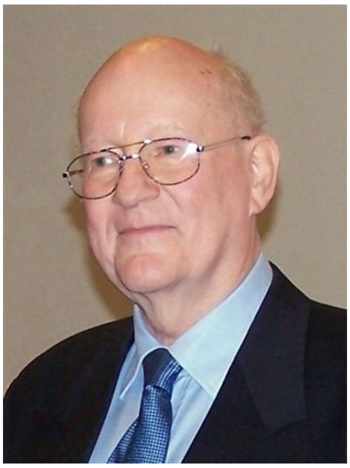

Professor Dr. Tor Hagfors
18.12.1930 – 17.01.2007

## **Nachruf** / Obituary

Professor Tor Hagfors wurde am 18. Dezember 1930 in Oslo, Norwegen, geboren und verstarb am 17. Januar 2007 im Alter von 76 Jahren. Im Jahr 1992 wurde er als Direktor an das Max-Planck-Institut für Aeronomie berufen und verblieb in dieser Position bis zu seiner Emeritierung im Jahr 1998.

Ein Wissenschaftlerleben lang interessierte sich Tor Hagfors dafür, Radiowellen von der Erde aus als Mittel für die Fernerkundung einzusetzen. Als die Autorität in der Radarerforschung der Ionosphäre und der Planeten leitete er für viele Jahre international führende Radioobservatorien. Während seiner Zeit am MPAe war er maßgeblich an der Einrichtung und Weiterentwicklung vieler Radiowellenexperimente beteiligt: EISCAT und seiner Ausweitung nach Svalbard, HEATING, SOUSY, der Modernisierung von STARE, und der Entwicklung eines neuen hochauflösenden abbildenden Radiometers.

In einem Alter, in dem viele sich auf ihren Lorbeeren ausruhen würden, nahm Prof. Hagfors nochmal richtig Fahrt auf. Er begann an der Entwicklung eines neuen Radiometers mitzuwirken, das tiefe Frequenzen nutzt, um das Innere von Himmelskörpern zu erforschen. Von einem Satelliten aus sollte dieses Gerät zunächst die Marskruste bis in eine Tiefe von einigen hundert Metern erkunden. Dies war das erste Experiment seiner Art, und viele Kritiker warnten, dass es niemals in der Lage sein würde, auch nur irgendetwas unter der Planetenoberfläche auszumachen. Tor Hagfors jedoch plante und arbeitet unermütlich weiter, bis MARSIS schließlich Realität wurde. Heute ist das Experiment erfolgreich am Mars im Einsatz.

Die oberflächen-durchdringende Radartechnik wurde auch vorgeschlagen, um zum ersten Mal die interne Struktur eines Kometen zu erforschen. Trotz Zweifeln an der Durchführbarkeit dieses Vorhabens erreichte Tor Hagfors schließlich, dass die Radartechnik auch auf Rosetta eingesetzt wird. Das Experiment ist unterwegs und wird im Jahr 2014 ein Rendezvous mit einem Kometen haben. Bis zu seinem Ende blickte Tor Hagfors in die Zukunft und schlug vor, ein Radarexperiment einzusetzen, um die Frage nach einem Ozean im Untergrund des Jupitermondes Europa zu klären. Das Experiment ist Teil der vorgeschlagenen LAPLACE Mission.

In seinen letzten Jahren als Direktor des MPAe war Tor Hagfors massgeblich an den ambitionierten Plänen für die Umgestaltung des Instituts beteiligt. Befreit von der administrativen Last eines Direktors führte er seine erfolgreiche wissenschaftliche Arbeit nach der Emeritierung bis zu seinem Tode fort. Wir vermissen ihn.

---

*Professor Dr. Tor Hagfors was born in Oslo, Norway, on December 18, 1930, and died at an age of 76 years on January 17, 2007. Tor Hagfors was invited as director to the Max-Planck-Institute for Aeronomie (MPAe) in 1992, a position he retained until he became emeritus in 1998.*

*Tor Hagfors' science interests were governed by lifelong activity in ground based research applying radio waves as remote sensing diagnostic tools. As "The Authority" in the field of ionospheric radar research and planetary radar astronomy Tor Hagfors for many years headed internationally leading radio-observatories. While at MPAe Tor Hagfors supported and advanced ground-based radio wave experiments: EISCAT and its expansion to Svalbard, HEATING, SOUSY, modernization of STARE and development of a new high resolution imaging radiometer.*

*At an age when most decide to rest on their laurels Tor Hagfors pushed ahead. He joined the efforts to use low frequency radars to probe the interior of solar system bodies. In particular to mount a radar on a spacecraft to sound the outer layers of Mars to depths of several hundred meters. It was the first experiment of its kind, and there were warnings that it would never reveal anything below the surface. But Tor Hagfors worked and planned in favor of the experiment, and eventually it was realized with MARSIS, which is now in successful operation at Mars. The subsurface radar technique was also chosen to explore the inner structure of a comet – something never attempted before. Doubts about the feasibility of such measurements abounded, but Tor Hagfors contributed significantly to its acceptance in the ROSETTA mission. The experiment is* *now on the way to rendezvous with a comet in 2014. Towards the end Tor still kept an eye on the horizon arguing for radar soundings of Jupiter's icy moon Europa to probe it for an underground ocean. A radar experiment is included in the proposal for the upcoming LAPLACE mission.*

*During his last years as director Tor Hagfors played an important role in realizing the ambitious plans for reorientation of the institute. After retirement Tor Hagfors, now relieved from administrative burdens, continued his fruitful scientific work until his untimely death. We miss him. , Erling Nielsen*

## Emeritierung Prof. Dr. Vytenis M. Vasyliūnas

Retirement of Prof. Vytenis M. Vasyliūnas

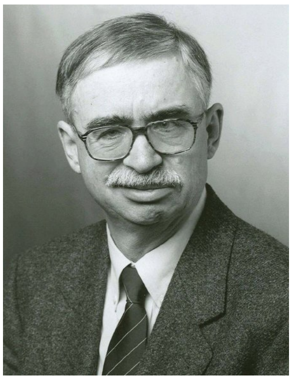

Am 30.09.2007 ist Prof. Dr. Vytenis M. Vasyliūnas nach 32-jähriger Tätigkeit am Institut in den Ruhestand getreten.

Prof. Dr. Vytenis M. Vasyliūnas hat sich wissenschaftlich vor allem mit theoretischer Weltraumplasmaphysik beschäftigt. In diesem Feld ist er nach wie vor ein sehr gefragter Spezialist. Besonders bei der Beschreibung der Wechselwirkungsprozesse zwischen der Magnetosphäre und der Ionosphäre der Erde und anderer Planeten konnte sich Prof. Vasyliūnas einen hochangesehenen Ruf erarbeiten. Bahnbrechende Veröffentlichungen aus den siebziger und achtziger Jahren sind weiterhin Standardwerke auf diesem Gebiet der Physik und liefern auch heute noch die Grundlagen für Studenten, die gerade erst ihre Karriere beginnen.

Geboren am 25. September 1939 in Kaunas (Litauen) studierte Prof. Vasyliūnas Physik an der Harvard University und erlangte seinen Doktortitel 1966 am renommierten Massachusetts Institute of Technology (M.I.T.), wo er bis 1970 als Assistant Professor of Physics und bis 1975 als Professor of Physics arbeitete.

Seine Karriere in der Max-Planck-Gesellschaft begann er am 1. August 1975 als Wissenschaftliches Mitglied am damaligen Max-Planck-Institut für Aeronomie (heute Max-Planck-Institut für Sonnensystemforschung). Seit seinem Amtsantritt als Direktor im Jahr 1978 führte Prof. Vasyliūnas das Institut in teilweise kritischen Phasen als Geschäftsführender Direktor im Wechsel mit seinen Direktorenkollegen insgesamt drei Mal (1984 – 1986, 1991 – 1993 und 1998 – 2000).

Neben mehr als 100 wissenschaftlichen Publikationen in hochangesehenen Fachjournalen erhielt Prof. Vasyliūnas 1975 den James B. Macelwane-Preis der American Geophysical Union. Er wurde 2003 Associate der Royal Astronomical Society London, war Forschungstipendiat der Alfred P. Sloan Foundation (1971 – 1973) und ist Mitglied der American Geophysical Union.

Neben der Wissenschaft beschäftigt sich Prof. Vasyliūnas auch sehr intensiv mit der Musik. Als begnadeter Organist hat er in vielen Kathedralen und Kirchen dieser Welt gespielt. So ist ein Orgelkonzert von Prof. Vasyliūnas jedes Mal ein besonderes Highlight auf der jährlichen Fachtagung der American Geophysical Union in San Francisco.

Auch nach seiner Emeritierung wird Prof. Vasyliūnas weiterhin wissenschaftlich arbeiten. Ergebnisse der Missionen CLUSTER, GALILEO oder CASSINI interessieren ihn sehr. Man darf also weiterhin auf bahnbrechende Veröffentlichungen eines einzigartigen Wissenschaftlers hoffen.

---

*On September 30, 2007, Prof. Vytenis M. Vasyliūnas began his retirement after 32 years of involvement at this Institute. His major scientific achievements were primarily in the field of theoretical space plasma physics, in which he is still a leading expert. In particular, his descriptions of the interaction processes between the magnetosphere and ionosphere of the Earth and other planets has earned Vasyliūnas a very respected reputation. His innovative publications in the seventies and eighties are still considered standard references in this area of physics and provide the groundwork for students just starting their careers.*

*Born on September 25, 1939 in Kaunas, Lithuania, Vasyliūnas studied physics at Harvard University, receiving his doctorate in 1966 from the Massachusetts Institute of Technology (M.I.T.), where he then worked as Assistent Professor of Phyics until 1970 and as Professor of Physics until 1975.*

*His career with the Max Planck Society began on August 1, 1975 as a Scientific Member of the then Max*

*Planck Institute for Aeronomy (the previous name for the MPI for Solar System Research). Since becoming a director in 1978, Vasyliūnas has headed the Institute, sometimes through critical phases, as Managing Director in rotation with the other directors for a total of three times (1984 – 1986, 1991 – 1993, and 1998 – 2000).*

*With more than 100 publications in respected scientific journals, Vasyliūnas received the James B. Macelwane Prize from the American Geophysical Union in 1975. He has been elected Associate of the Royal Astronomical Society of London in 2003, was a Research Fellow of the Alfred P. Sloan Foundation (1971 – 1973), and is a member of the American Geophysical Union.*

*Apart from science, Vasyliūnas is also very deeply involved with music. As a gifted organist, he has played in many cathedrals and churches around the world. An organ concert by Vasyliūnas is a standard program highlight at the annual fall meetings of the American Geophysical Union in San Francisco.*

*Even after his retirement, Vasyliūnas will still be scientifically active. He is very much interested in the results of the ongoing Cluster, Galileo, and Cassini Missions. We can still hope to experience exciting new publications from the exceptional scientist.*

Norbert Krupp, Axel Korth

## **Personelle Entwicklung /** Personnel Development

In den Jahren 2006 und 2007 hat sich die Zahl der Mitarbeiterinnen und Mitarbeiter des Instituts entsprechend dem Sozialplan verändert.

Die Zahl der Planstellen verringerte sich bis Ende Dezember 2007 auf 96. Davon waren 26 mit Wissenschaftlern besetzt. Damit ist der Stellenabbau gemäß des Teilschließungsbeschlusses abgeschlossen. Die Zahl der am Institut wissenschaftlich Tätigen war jedoch mit Einbeziehung der aus Mitteln des BMBF finanzierten Wissenschaftler und der Doktoranden beträchtlich größer und betrug am 31. Dezember 2007 etwa 138.

Mitarbeiter, die nach dem Sozialplan ausgeschieden sind:

2006: Elke Hartmann, Roswitha Komossa, Peter Mutio, Claudius Römer, Hartmut Sommer, Robert Uhde

2007: Manfred Güll, Hermann Hartwig, Christiane Heise, Dietmar Hennecke, Klaus-Dieter Preschel,Inge Reuter, Helmut Schüddekopf, Ilse Schwarz

In den Ruhestand traten:

2006: Werner Hundertmark, Dr. Jörg-Rainer Kramm, Egon Pinnecke, Dr. Arne K. Richter, Dorothee Schreiber, Prof. Rainer Schwenn

2007: Anita Brandt, Dr. Axel Korth

---

*During the years 2006 and 2007 the number of institute staff was reduced according to the social plan.*

*The number of permanent positions decreased to 96 by the end of December 2007. Of these 26 were filled by scientists. The number of people working scientifically, through BMBF-financed scientists and through Ph.D. students, was nevertheless substantially greater, consisting of 138 on 31st December 2007.*

*Staff members who have left according to the social plan are:*

*2006: Elke Hartmann, Roswitha Komossa, Peter Mutio, Claudius Römer, Hartmut Sommer, Robert Uhde*

*2007: Manfred Güll, Hermann Hartwig, Christiane Heise, Dietmar Hennecke, Klaus-Dieter Preschel, Inge Reuter, Helmut Schüddekopf, Ilse Schwarz,*

*The following have retired:*

*2006: Werner Hundertmark, Dr. Jörg-Rainer Kramm, Egon Pinnecke, Dr. Arne K. Richter, Dorothee Schreiber, Prof. Rainer Schwenn*

*2007: Anita Brandt, Dr. Axel Korth*

## **Das Kuratorium des Instituts /** Board of Trustees of the Institute

Dem Kuratorium des Instituts gehörten in den Jahren 2006 und 2007 die folgenden Mitglieder an:

Dr. Josef Lange, Staatssekretär im Niedersächsischen Ministerium für Wissenschaft und Kultur, Hannover;

Prof. Dr. Oskar von der Lühe, Kiepenheuer-Institut für Sonnenphysik, Freiburg;

Frau Erika Mann, Mitglied des Europäischen Parlaments, Hannover;

Dr. Fritz Merkle, OHB-System GmbH, Bremen;

Prof. Dr. Hermann J. Opgenoorth, Head, Solar System Mission Division, ESA-ESTEC, Noordwijk, Niederlande;

Thomas Oppermann, Mitglied des Bundestags, Göttingen.

Das Kuratorium tagte am 26. September 2007 in Lindau.

---

*The following were members of the board of trustees of the institute in the years 2006 and 2007:*

*Prof. Dr. Stefan Dreizler, Institute for Astrophysics, University Göttingen;*

*Helge Engelhardt, Ministerialdirigent, BMBF (German Federal Ministry for Education and Research), Bonn;*

*Dr. Thomas Galinski, DLR (German space agency), Bonn;*

*Prof. Dr. Jürgen Hesselbach, President, Technical University Braunschweig;*

*Dr. Hanna von Hoerner, von Hoerner und Sulger GmbH, Schwetzingen;*

*Markus Hoppe, Vice president, University Göttingen;*

*Dr. Josef Lange, permanent secretary in the Lower Saxony Ministry for Science and Culture, Hannover;*

*Prof. Dr. Oskar von der Lühe, Kiepenheuer Institute for Solar Physics, Freiburg;*

*Ms. Erika Mann, member of the European Parliament, Hannover;*

*Dr. Fritz Merkle, OHB-System GmbH, Bremen;*

*Prof. Dr. Hermann J. Opgenoorth, Head, Solar System Mission Division, ESA-ESTEC, Noordwijk, The Netherlands;*

*Thomas Oppermann, member of the Bundestag, Göttingen.*

*The board of trustees met on 26 September 2007 in Lindau.*

## **Der Fachbeirat des Instituts /** Scientific Advisory Board of the Institute

Im Jahr 2001 wurde vom Präsidenten der Max-Planck-Gesellschaft ein neuer Fachbeirat für das Institut berufen. In den Jahren 2001 -- 2007 gehören dem Fachbeirat die folgenden Mitglieder an:

Prof. Dr. D. Crisp, Pasadena, CA, USA;
Prof. Dr. G. Hensler, Wien, Österreich;
Dr. L. J. Lanzerotti, Murray Hill, NJ, USA;
Prof. Dr. John W. Leibacher, Tucson, AZ, USA;
Prof. Dr. P. Lognonné, Saint Maur, Frankreich;
Prof. Dr. E. R. Priest, St. Andrews, Großbritannien;
Prof. Dr. R. Rosner, Chicago, IL, USA;
Prof. Dr. D. J. Southwood, Paris, Frankreich;
Prof. Dr. D. J. Stevenson, Pasadena, CA, USA.

Im Berichtszeitraum fand die Zusammenkunft des Fachbeirats vom 24. — 26. September 2007 im MPS in Lindau statt.

---

*In 2001 a new advisory board for the institute was appointed by the President of the Max Planck Society. During the years 2001 -- 2007 the following were members of the scientific advisory board:*

*Prof. Dr. D. Crisp, Pasadena, CA, USA;*
*Prof. Dr. G. Hensler, Vienna, Austria;*
*Dr. L. J. Lanzerotti, Murray Hill, NJ, USA;*
*Prof. Dr. John W. Leibacher, Tucson, AZ, USA;*
*Prof. Dr. P. Lognonné, Saint Maur, France;*
*Prof. Dr. E. R. Priest, St. Andrews, UK;*
*Prof. Dr. R. Rosner, Chicago, IL, USA;*
*Prof. Dr. D. J. Southwood, Paris, France;*
*Prof. Dr. D. J. Stevenson, Pasadena, CA, USA.*

*During the period of this report the advisory board met in Lindau from 24 -- 26 September 2007.*

## **Für das Institut aufgewendete Mittel /** Institute Resources

Die vom Bund und den Ländern getragene und durch die Generalverwaltung der Max-Planck-Gesellschaft zugeteilte Grundausstattung des Instituts an Personal- und Sachmitteln betrug im Jahre 2006 7,7 Millionen Euro für Personal und 2,6 Millionen Euro für Sachausgaben. An Investitionsmitteln (Geräte mit Preisen über 5.000 Euro) wurden 0,5 Millionen Euro bewilligt. Für das Jahr 2007 lauten diese Zahlen: 6,7 Millionen Euro für Personal, 2,4 Millionen Euro für Sachausgaben und 0,5 Millionen Euro für Investitionen.

Besondere Forschungsvorhaben sind durch das BMBF (Bundesministerium für Bildung und Forschung) und die ESA (European Space Agency) gefördert worden. Vom BMBF (DLR) erhielt das Institut 2006 insgesamt 5,3 Millionen Euro und 2007 7,8 Millionen Euro. Die entsprechenden Beträge der ESA waren 0,4 Millionen Euro und 0,3 Millionen Euro.

Für diese Förderungen, ohne die viele experimentelle Forschungsvorhaben nicht durchführbar gewesen wären, möchten wir auch an dieser Stelle ausdrücklich danken.

---

*The basic funding of the institute, from the federal and state governments and allocated through the administrative headquarters of the Max Planck Society, amounted to 7.7 million euros for personnel and 2.6 million euros for materials in 2006. Capital investment funds (equipment over 5000 euros) of 0.5 million euros were approved. For 2007 the figures are: 6.7 million euros for personnel, 2.4 million euros for materials, and 0.5 million euros for capital investment.*

*Special research needs were funded by BMBF (German Federal Ministry for Education and Research) and ESA (European Space Agency). From BMBF (DLR) the institute received 5,3 million euros in 2006 and 7.8 million euros in 2007. The corresponding sums from ESA were 0.4 million euros and 0.3 million euros.*

*For this financial assistance, without which many experimental research programmes would not be possible, we wish to express our gratitude.*

# II. Wissenschaftliche Arbeiten / Scientific Projects

## 1. *Sonne und Heliosphäre / Sun and Heliosphere*

### *Schwerpunktthema:*

### Die Physik solarer Eruptionen

(English version see page 12)

Seit dem Januar 2007 befinden sich die Sonden der STEREO-Mission der NASA auf ihren Umlaufbahnen um die Sonne und liefern zum ersten Mal simultane Aufnahmen unseres Zentralgestirns und ihrer Umgebung von zwei verschiedenen Standpunkten aus. Wissenschaftler des MPS entwickeln Auswerteverfahren, um aus diesen Aufnahmen dreidimensionale Modelle der Plasmastrukturen in der Sonnenatmosphäre zu erzeugen und die Ergebnisse mit Magnetfeldmodellen der Sonnenkorona zu vergleichen. Ziel der Untersuchungen ist das Verständnis von energiereichen Eruptionen und Massenauswürfen der Sonnenkorona.

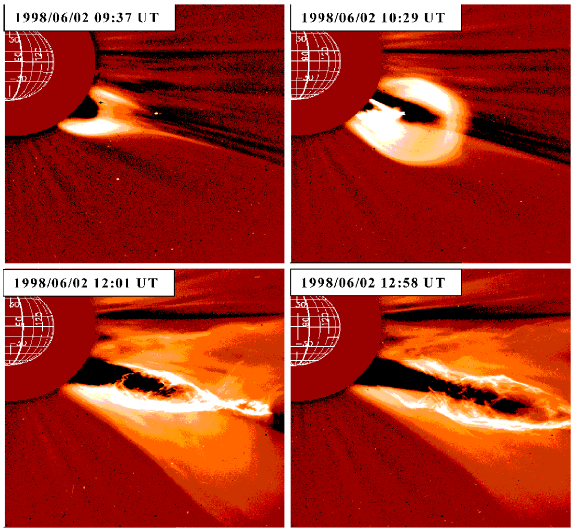


Abb. 1: Beobachtung eines koronalen Massenauswurfs durch den LASCO-Koronagraph auf der ESA-Raumsonde SOHO. Die Sonne ist ausgeblendet hinter der Scheibe in der linken oberen Ecke. Der Kreis deutet ihre Größe und Position an. [Urheber: LASCO-Konsortium]

#### Solare Eruptionen – wenn die Korona aus dem Gleichgewicht gerät

Mit der Eroberung und der Nutzung des erdnahen Weltraumes ist die Menschheit in eine gänzlich neue Umwelt vorgestoßen, die der Aktivität der Sonne in weit größeren Maße ausgesetzt ist als ihr angestammter Lebensraum. Neben der intensiven Ultraviolett (UV) und Röntgen-Strahlung der Sonne wird diese neue Umgebung stark von der Wechselwirkung der Erdmagnetosphäre mit dem Sonnenwind geprägt. Dieser Fluß aus Ionen von Wasserstoff, Helium und wenigen schwereren Elementen entweicht kontinuierlich aus der Sonnenatmosphäre und strömt mit mehr als einer Millionen km/h in den interplanetaren Raum hinaus.

In den 70 Jahren des vorherigen Jahrhunderts wurde entdeckt, dass im Sonnenwind abrupte Störungen eingebettet sind, die von plötzlichen Eruptionen auf der Sonnenoberfläche ausgehen (Abb. 1). Enorme Gasmassen von bis zu $10^{10}$ Tonnen (etwa die Masse eines Kometen) werden dabei in den Weltraum geschleudert und rasen als Plasmawolke von Magnetfeldern zusammengehalten in den interplanetaren Raum hinaus.

Bewegen sich diese Gaswolken zufällig auf die Erde zu, haben sie starke Auswirkungen auf die Magnetosphäre der Erde. Während der normale Sonnenwind vom Magnetfeld der Erde an der Magnetopause in einem Abstand von etwa 10 – 15 Erdradien um die Erde herumgelenkt wird, staucht der enorme Druck der Gaswolken den Abstand dieser äußeren Grenze des Erdmagnetfeldes auf bis zu der Hälfte zusammen. Eine sichtbare Begleiterscheinung dieser Wechselwirkung ist eine erhöhte Polarlichtaktivität bis nach Mitteleuropa hinein.

Als weitere Folgeerscheinung eines CMEs (coronal mass ejections) werden Protonen der Korona und des Sonnenwindes während einer Eruption auf Energien von einer Millionen Elektronenvolt und mehr beschleunigt. Diese Teilchen können tief in die Erdatmosphäre eindringen. Astronauten im All sind dann für mehrere Stunden einer verstärkten Strahlendosis ausgesetzt und die Elektronik von Telekommunikations- und Fernsehsatelliten kann durch das Teilchenbombardement zerstört werden.

### Das Magnetfeld – das Energiereservoir der Korona

Der genaue Mechanismus dieser Eruptionen ist noch weitgehend unverstanden. Jedoch weist die enorme Energie von $10^{14}$ TWh (zum Vergleich: der weltweite Primärenergieverbrauch lag 2001 bei etwa $10^5$ TWh), die bei einer typischen Eruption in einigen 10 Minuten freigesetzt wird, darauf hin, dass das Magnetfeld der Sonnenatmosphäre eine entscheidende Rolle spielt. Die Energiedichte des Magnetfeldes übersteigt die thermische und die Strömungsenergie in der Sonnenkorona um mehrere Zehnerpotenzen, daher stellt das Magnetfeld dort für dynamische Prozesse ein fast unbegrenztes Energiereservoir dar.

Da das Magnetfeld elektrisch geladenes Gas einschließt, behindert es Plasmabewegungen in der Korona, solange sich das Feld in einem Gleichgewichtszustand befindet. Zu bestimmten Zeitpunkten scheint die magnetische Konfiguration jedoch das Gleichgewicht zu verlieren, und sie ändert sich abrupt durch Feldlinenverschmelzung. Die dabei freigesetzte Energie kann das Plasma sowohl aufheizen als auch in Form einer Eruption beschleunigen. Die Aufheizung ist als Röntgen-Flare beobachtbar, während die Eruption bei hinreichender Energie einen koronalen Massenauswurf zur Folge hat.

Eine genaue Kenntnis des Magnetfeldes ist daher ein Schlüssel zum Verständnis der Eruptionen und Massenauswürfe. Weltweit werden große Anstrengungen unternommen, die Struktur des koronale Magnetfeldes zu ermitteln. Bislang ist jedoch nur das Feld der untersten Atmosphärenschichten über den Zeeman- und Hanle-Effekt einer Messung zugänglich. Das Feld in den höheren Schichten muß daraus über Extrapolationsrechnungen bestimmt werden (Abb. 2). Das MPS ist führend in der Entwicklung von numerischen Codes für die Lösung dieses nichtlinearen Randwertproblems. Gegenwärtig beschränken sich diese Rechnungen noch auf begrenzte Gebiete der Sonnenoberfläche, meist auf isolierte aktive Regionen, in denen sich ein großer Teil des magnetischen Flusses aus dem Sonneninneren konzentriert. Die Rechnungen gestatten es, die Veränderungen der magnetischen Konfiguration einer aktive Region, insbesondere das Anwachsen der Energie und Helizität zu verfolgen. Auf diese Weise hoffen die Wissenschaftler, kritische Werte dieser Größen zu bestimmen, mit deren Hilfe sich die koronalen Eruptionen vorhersagen lassen.

### STEREO – die Mission der dritten Dimension

Bislang sind die Sonneneruptionen und die daraus resultierenden Massenauswürfe nur aus Erdnähe beobachtet worden. Wir wissen aus diesen Beobachtungen, dass sie unterschiedlich häufig vorkommen: Zu Zeiten des alle 11 Jahre wiederkehrenden Aktivitätsminimums der Sonne sind sie eher selten und treten im Mittel alle zwei Wochen auf, während der dazwischen liegenden Aktivitätsmaxima können allerdings mehrere Eruptionen an einem Tag ausgelöst werden. Ein Manko der bisherigen Beobachtungen war, dass sie vor allem die Eruptionen auf der Sonnenperipherie erfassten, die dann mehr oder weniger im rechten Winkel zur Erde beschleunigt wurden. Massenauswürfe, die auf die Erde zurasten, ließen sich nur schlecht gegen den alles überstrahlenden Sonnenhintergrund beobachten.

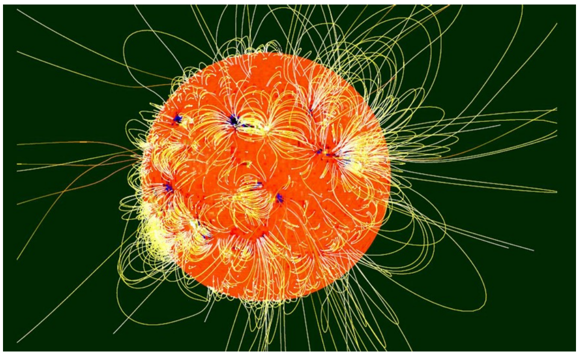

Abb. 2: Magnetfeld der Sonne während des Aktivitätsmaximums. Das photosphärische Magnetfeld (gelb: positive, blau: negative Polarität) wurde mit dem Michelson Doppler Imager auf der Raumsonde SOHO gemessen und in die Sonnenkorona hinein extrapoliert. Die Feldlinien zeigen die Topologie des koronalen Magnetfeldes. [Urheber: Max-Planck-Institut für Sonnensystemforschung]

Hier bringt die STEREO-Mission eine entscheidende Verbesserung. Die Mission besteht aus zwei Sonden, die die Sonne in der Ebene der Ekliptik auf leicht unterschiedlichen Umlaufbahnen umkreisen, eine etwas schneller, die andere etwas langsamer als es der Bahngeschwindigkeit der Erde entspricht. Von der Sonne aus gesehen entfernen sich die Sonden so im Mittel von der Erde um etwa 22 Grad pro Jahr. Mit zunehmendem Abstand bieten sie somit einen Blick auf die Sonne und den umgebenden Weltraum aus zwei unabhängigen Betrachtungswinkeln. Beide Sonden sind mit EUV-Teleskopen und Weißlichtkoronagraphen ausgestattet, welche die Sonne und ihre Umgebung bis zur Erdbahn beobachten. Diese Aufnahmen aus den verschiedenen Blickwinkeln ermöglichen zum ersten Mal eine dreidimensionale Rekonstruktion der beobachteten Strukturen auf der Sonnenoberfläche, in der Sonnenkorona und in der umgebenden Heliosphäre. Insbesondere können so Massenauswürfe und ihre Ausbreitungsrichtung zum ersten Mal dreidimensional erfasst und zuverlässige Prognosen gemacht werden, ob sie sich auf die Erde zubewegen. Eine typische Zeitspanne von zwei Tagen, die die Gaswolke benötigt, um die Erde zu erreichen, gibt den Betreibergesellschaften von Satelliten genügend Zeit, Vorkehrungen zum Schutz der empfindlichen Elektronik ihrer Satelliten zu treffen.

**Erste Ergebnisse der STEREO-Mission.**

Für die Rekonstruktion werden Verfahren ähnlich der Luftbildstereoskopie oder der Computertomographie in modifizierter Form auf die Bilddaten der STEREO-Mission angewendet. Im ersten Jahr nach dem Start der Mission betrug der Abstand der Sonden noch weniger als etwa 40 Grad, so dass die Rekonstruktionsverfahren auf einen kleinen Basiswinkel abgestimmt waren.

In den EUV-Aufnahmen der Sonne sind aktive Regionen die auffälligsten Phänomene. Das bis zu 1 Millionen Grad heisse, in einzelnen magnetischen Flussröhren eingefangene Plasma strahlt intensiv in den EUV-Wellenlängen während die mit 6000 Grad kühle Sonnenoberfläche dunkel erscheint. Die stereoskopische Rekonstruktion der sichtbaren Plasmabögen sollte somit dem Verlauf magnetischer Feldlinien entsprechen. In Abb. 3 sind die kontrastverstärkte EUV-Beobachung einer aktiven Region und ihre dreidimensionale Rekonstruktion gegenübergestellt. Die rekonstruierten Plasmabögen sind dabei in gelb dargestellt, aus Extrapolationen des Oberflächenmagnetfeldes errechnete Feldlinien in rot.

Ein wichtiges Ziel der STEREO Mission ist die Vorhersage der Ausbreitung von Massenauswürfen, insbesondere wenn sie sich in Richtung auf die Erde zubewegen. Im Koronagraphen sind Plasmawolken eines Massenauswurfs durch eine erhöhte Streulichtintensität, hervorgerufen durch die Streuung des Sonnenlichts an der Plasmawolke, sichtbar. Die Grenzfläche der Plasmawolke kann daher mit einem beobachteten starken Gradienten des Streulichts identifiziert werden. Jedoch zeigt sich auf diese Weise im Koronagraphen nur die Projektion dieser Grenzfläche in der jeweiligen Blickrichtung des Instruments. Mit den Koronagraphen der STEREO-Sonden stehen zum ersten Mal simultane Beobachtungen aus zwei Blickrichtungen zur Verfügung, so dass sich Teile dieser Grenzfläche rekonstruieren lassen.

Leider ist die Aktivität der Sonne im Moment sehr gering, so dass bislang die Stereorekonstruktion an nur wenigen Exemplaren eines Massenauswurfs ausprobiert werden konnte. Sie wird aber in den kommenden Jahren anwachsen und die Häufigkeit von koronalen Eruptionen wird deutlich zunehmen.

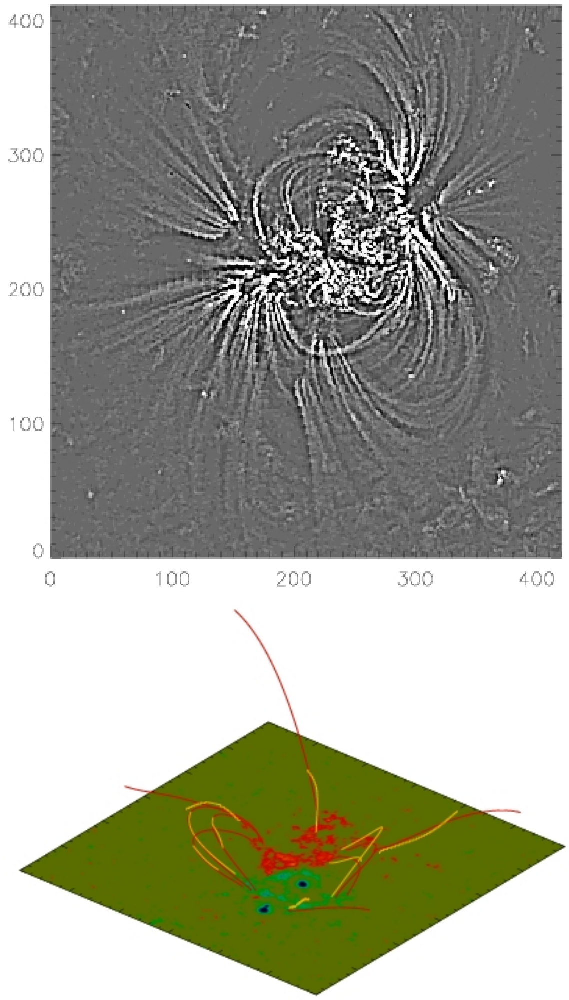


Abb. 3: EUV Beobachtung von Plasmabögen einer aktiven Region in der Spektrallinie $\lambda = 17.7$ nm durch eine der STEREO-Sonden (oben) und ihre stereoskopische Rekonstruktion (unten). Die rekonstruierten Plasmabögen sind gelb, die Feldlinien des Magnetfeldes der aktiven Region aus Extrapolationsrechnungen sind rote gezeichnet. Die Farbkodierung auf dem unteren Rand zeigt das gemessene Magnetfeld in der Sonnenphotosphäre (blau: negative, rot: positive Polarität, grün: verschwindende Feldstärke). [Urheber: Max-Planck-Institut für Sonnensystemforschung]

Der Abstand der STEREO-Sonden zur Erde und von einander nimmt ebenfalls kontinuierlich zu, so dass auch die Beobachtungsbedingungen für Massenauswürfe günstiger werden. Der größere Basiswinkel lässt in Zukunft einerseits genauere Rekonstruktionen zu, andererseits werden die Massenauswürfe, die sich auf die Erde zubewegen, sich dann von den STEREO-Sonden aus gesehen seitlich ausbreiten und weitere Teile der Grenzfläche der Plasmawolke werden sichtbar. Insbesondere die interessante Frontfläche der Wolke wird sich dann rekonstruieren lassen und genaue Rückschlüsse über die Ausbreitungsgeschwindigkeit und -richtung zulassen.

## *Highlight:*

## Physics of solar eruptions

### Physics of solar eruptions

Since January 2007 the two spacecraft of NASA's STEREO mission orbit the Sun and provide us for the first time with simultaneously observed images of the Sun from two different viewpoints. The scientists at the MPS have developed analysis tools to generate three-dimensional models of plasma structures in the solar corona and compare them with models of the coronal magnetic field. These investigations aim at a better understanding of energetic eruptions and mass ejections of the solar corona.

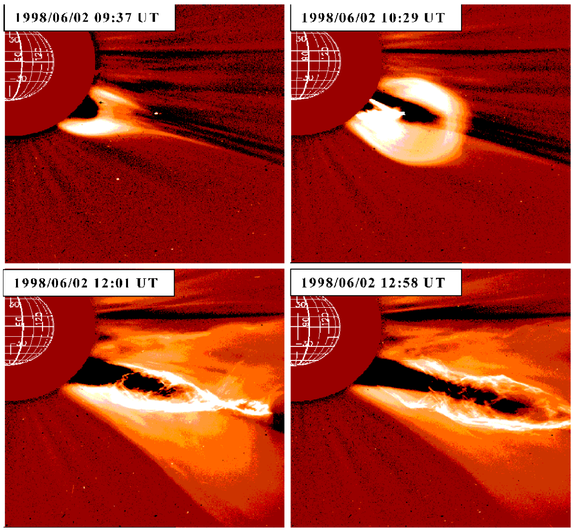


Fig. 1: Observation of a coronal mass ejection by the LASCO coronagraph on board the ESA spacecraft SOHO. The Sun is occulted in this observation behind the disk in the upper left, the circle indicates its size. [©LASCO-Konsortium]

### Solar eruptions – when the corona loses its equilibrium

With the conquest and the exploitation of near-earth space, man advanced into a totally new environment, which is exposed to solar activity to a much larger degree than his natural habitat. Besides the intensive UV and X-ray radiation, conditions of this new environment are strongly controlled by the interaction of the Earth's magnetosphere with the solar wind. This continuous flow of protons, helium ions and few heavier ions escapes from the solar atmosphere and blows out into interplanetary space with a speed of more than a million km/h.

In the seventies of the last century space missions discovered that strong occasional disturbances were embedded in the solar wind which were caused by eruptions on the solar surface (Fig. 1). During these events, huge masses of up to $10^{10}$ tons (about the mass of a comet) of gas confined by magnetic fields are ejected into space and rush into interplanetary space. They were named coronal mass ejecta (CME), accordingly.

Under normal conditions, the background solar wind is deflected by the Earth's magnetosphere in a standoff distance of about 15 Earth radii. When Earth is hit by a CME gas cloud, its magnetosphere is strongly deformed. Due to its intense pressure, the CME may compress the front side magnetosphere so that magnetosphere boundary distance is reduced to only have the normal value. As a consequence of this interaction, aurorae may be observed at unusually low latitudes in middle Europe.

As a further consequence of a CME, protons and heavier particles of the solar wind are accelerated to millions of electron volt. These particles then can penetrate deeply into the Earth's atmosphere. Astronauts in space are then exposed to enhanced radiation for several hours and the electronics of satellites for communication, navigation and other purposes could be destroyed.

### The magnetic field – the energy reservoir of the solar corona

The precise mechanism of a CME eruption is still unknown. The enormous energy of $10^{14}$ TWh released in such an event within some tens of minutes (for a comparison, the world's energy consumption in 2001 was about $10^5$ TWh), is evidence of the magnetic field playing an important role. The energy density of the magnetic field exceeds the thermal, bulk kinetic and gravitational energy by several orders of magnitudes. It therefore provides an almost unlimited energy reservoir for dynamical processes in the solar corona.

The magnetic field confines electrically charged particles on thin flux tubes and plasma motion is limited to drifts along the field direction. In case the magnetic configuration loses its equilibrium, its topology then may abruptly change by field line reconnection. This process usually converts magnetic field energy into plasma kinetic energy which appears as both heat and bulk flow. The sudden release of heat is observed as flares in EUV and X-rays in the solar corona and accelerated plasma bulk flows may initiate a coronal mass ejection if directed away from the solar surface.

The precise knowledge of the field is therefore a key to the understanding of flares, eruptions and coronal mass ejections. Large efforts are therefore made world wide to determine the coronal magnetic field. So far, only the field close to the solar surface, in the photo- and chromosphere, can be observed making use of the Zeeman and the Hanle effects. At larger heights in the corona, the field can only indirectly be determined by extrapolating the field from the surface (see Fig. 2). The MPS is a leading developer in algorithms which solve this nonlinear boundary value problem. At present, these calculations are limited to regions above the solar surface with a size of typically 0.1 solar radii, usually above largely isolated active regions, in which most of the magnetic flux emanating from the Sun is concentrated. Our calculations allow to follow the changes in the magnetic configuration, the gradual increase in magnetic energy and helicity supplied by dynamo precesses in the solar interior and their abrupt decrease after an eruption. Monitoring these parameters, we hope to be able to derive critical parameters, which will help us to predict coronal mass ejections.

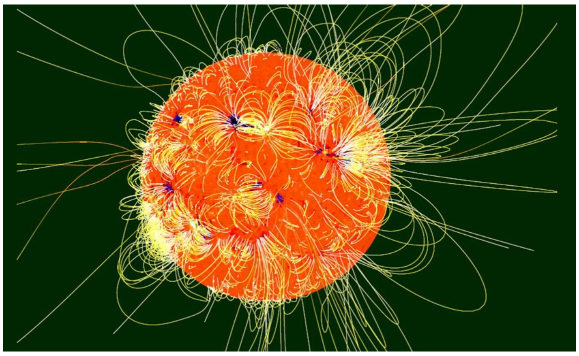

Fig. 2: The magnetic field of the Sun during the activity minimum. The photospheric line of sight field was measured by the MDI instrument on SOHO (positive polarity in yellow, negative polarity in blue. The coronal field is represented by field lines and was derived by extrapolation of the measured surface field. [©Max-Planck-Institut für Sonnensystemforschung]

## STEREO – the mission to the third dimension

So far, eruptions and coronal mass ejections have only been observed from Earth or earth bound satellites. From these observations, we know that the occurrence of coronal mass ejections is strongly correlated with the solar activity cycle with an 11 years period. During low activity, mass ejections occur rarely at a rate of about one every few weeks, at maximum activity, there may be several a day. A severe drawback of past observations was that from the Earth preferentially CMEs released on the solar periphery and moving roughly at 90 degrees to the Earth-Sun line could be perceived. Those CMEs which were accelerated towards Earth and which affected us most could only badly be discerned against the bright solar background.

At this point, the new STEREO mission brings about an essential improvement. The mission provides twin spacecraft which orbit the Sun in the ecliptic plane at a distance of about 1 AU, on slightly faster, the other slightly slower than Earth. The separation of the two spacecraft in heliospheric longitude thus increases by about 22 degrees per year. With increasing distance they provide a view onto the Sun from two independent vantage points. Both spacecraft are equipped with EUV telescopes and white-light coronagraphs. The latter have a field of view which extends to almost 1 AU and allow to survey the whole space from the Sun to the Earth's orbit. The two view directions allow for the first time to reconstruct observed plasma structures in three dimensions. In particular we can now determine the generation and the propagation direction of coronal mass ejections in three dimensions. Reliable predictions can be made whether the mass ejections move towards Earth and if so, when then will arrive there. The typical propagation time of about two days gives satellite companies a chance to switch off and protect satellite electronics.

## First results from the STEREO mission

The three-dimensional reconstruction from the STEREO images is achieved with analysis tools similarly applied to areal photography or computer tomography. During the first year of operation, the angular distance between the spacecraft was less than 40 degrees and the reconstruction tools were tuned to a small stereo base.

Active regions are the most prominent features in most EUV images of the Sun. Plasma at temperatures beyond about a few 100 000 degrees radiates intensively at various EUV wavelengths while the cool solar surface at about 6000 degrees remains dark. As the hot plasma is confined in thin magnetic flux tubes the reconstruction of these visible plasma arcades should outline the magnetic field lines. In Fig. 3 we display one of the pair of contrast enhanced EUV images and a three-dimensional reconstruction which results from it. The reconstructed plasma arcades are drawn in yellow, field lines resulting from an extrapolation of the surface field in red.

An important goal of the STEREO mission is the prediction of coronal mass ejections, in particular if they propagate in direction towards Earth. In coronagraphs, the plasma clouds become visible by the enhancement of scattered sun light from the increased plasma density of the cloud. The surface of the cloud then co-

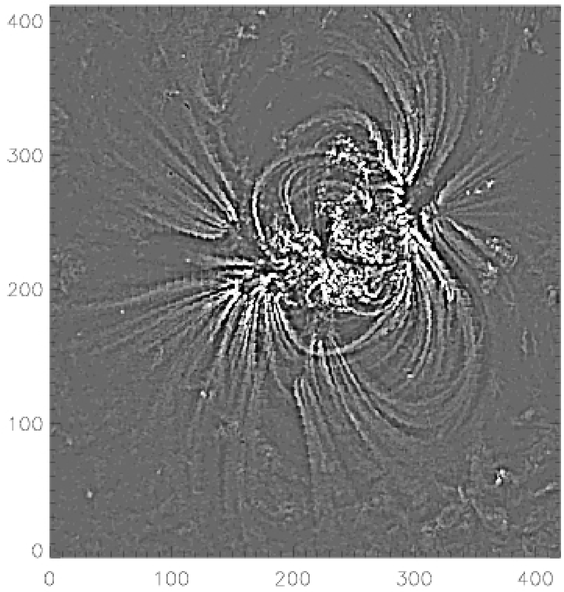


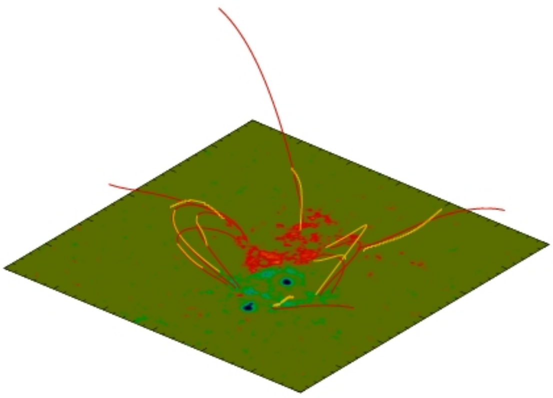

Fig. 3: EUV observations of arcades of hot plasma associated with an active region (top) and their stereoscopic reconstruction (bottom). The observations were made by the STEREO spacecraft at a wavelength of $\lambda$=17.7 nm. On the right, the reconstructed loops are drawn in yellow, close magnetic field lines from an extrapolation of surface field measurements are drawn in red. The surface field is represented on the bottom plane by a colour code (blue: negative, red: positive polarity, green: vanishing field strength) [©Max-Planck-Institut für Sonnensystemforschung]

incides with the boundary of the region of enhanced stray light in the image. However, from each vantage point of the STEREO spacecraft a different part of the cloud surface projects onto the respective coronagraph image so that conventional stereoscopic reconstruction algorithms have to be modified.

Unfortunately, the Sun's activity has been at its minimum during the first year of operation so that the reconstruction for CMEs could be applied to only a few faint examples. For the coming years, the solar activity will increase and more and stronger mass ejections will be observed.

In addition, the distance between the STEREO spacecraft will increase continuously which also will improve the conditions of observation for mass ejections, especially for those which propagate towards Earth. These will be seen as near limb events from the STEREO spacecraft. With these observations we will then be able to reconstruct the front part of the CME cloud surface and measure very precisely the speed and direction of the cloud's motion.

(B. Inhester und T. Wiegelmann)

## **Sonne und Heliosphäre – Übersicht der Projekte /**
## Sun and Heliosphere – overview of projects

Dargestellt ist die Dauer der verschiedenen Projektphasen (farbcodiert) einzelner Instrumente. Kurze Beschreibungen findet man in den einzelnen Jahres- bzw. Tätigkeitsberichten des MPS.

The different project phases of each instrument are shown colour-coded. Short descriptions of these instruments can be found in the annual reports of the MPS.

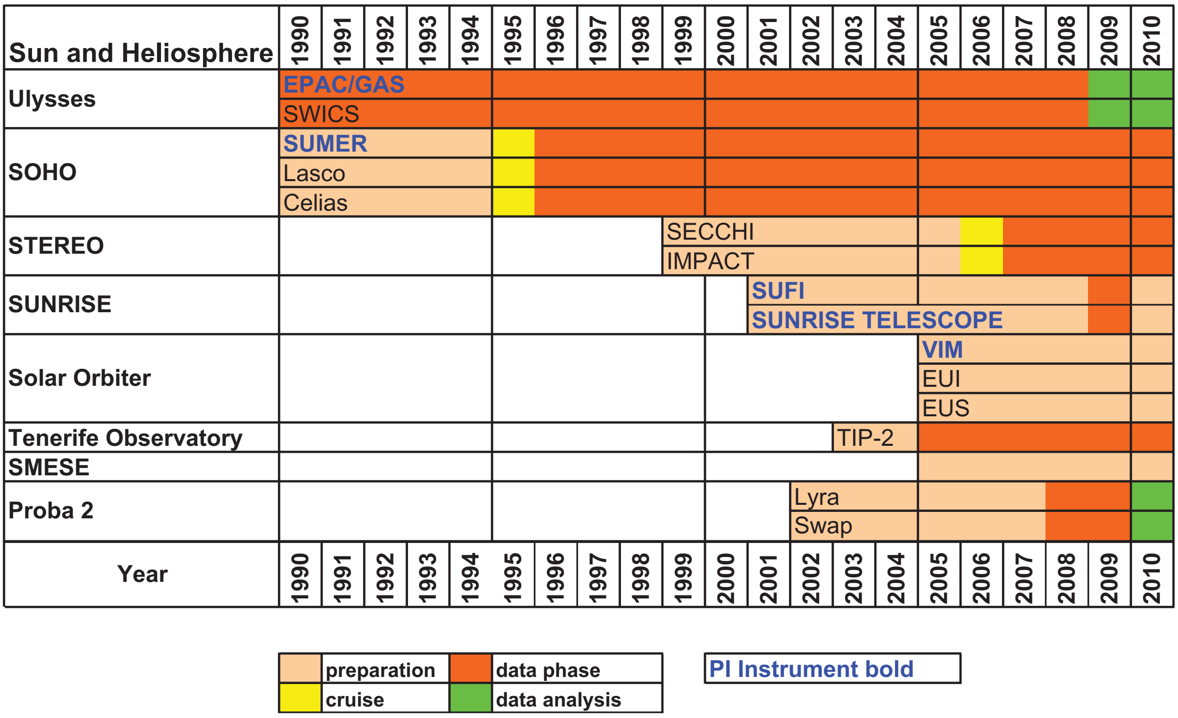

# Wissenschaftliche Einzelberichte/
*Individual scientific reports*

(nur in Englisch)

## Solar interior, photosphere and chromosphere

### Solar cycle prediction using precursors and flux transport models

It has been suggested in recent publications that a method based on a flux-transport Babcock-Leighton-type dynamo model may permit a reliable prediction of solar-cycle amplitudes. Predictions on the basis of 'precursors' (such as polar field strength, activity a few years before solar minimum, level of geomagnetic disturbances, etc.) around the preceding activity minimum have been used, with variable success, already for some time.

We have studied the origin of the predictive skill of such methods. To assess the dynamo-based approach, we have used a simple flux transport model for the azimuthally averaged radial magnetic field at the solar surface. A source term describes the emergence of new flux based on observational sunspot data. We consider the magnetic flux diffusing over the solar equator as a predictor, since this quantity is directly related to the global dipole field from which a Babcock-Leighton dynamo generates the toroidal field for the next activity cycle. If the source is represented schematically by a narrow activity belt drifting with constant speed over a fixed range of latitudes between activity minima, our predictor shows considerable predictive skill with correlation coefficients up to 0.95 for past cycles (see Fig. 4). However, the predictive skill is completely lost when the actually observed emergence latitudes are used.

This result and the partial success of some of the precursor methods originates from the fact that the precursor amplitude is largely determined by the sunspot activity a few years before solar minimum. Since stronger cycles tend to rise faster to their maximum activity (known as the Waldmeier effect), the temporal overlapping of cycles leads to a shift of the minimum epochs that depends on the strength of the following cycle. This information is picked up by precursor methods and also by our flux transport model with a schematic source. Therefore, their predictive skill does not require a memory, i.e., a physical connection between the surface manifestations of subsequent activity cycles. In fact, we have shown that such methods can be applied with success to random sequences of synthetic activity cycles with fully independent amplitudes, as long as the cycles overlap and exhibit the Waldmeier effect.

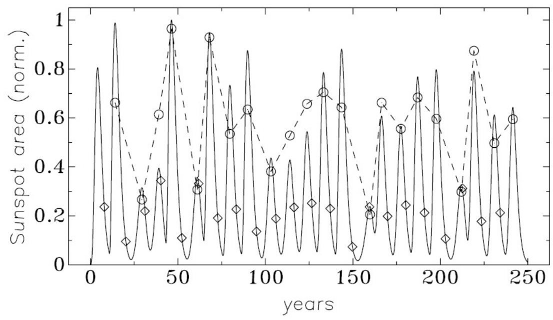


Fig. 4: Predicted cycle amplitudes (open circles, connected by the dashed line) based upon the activity level three years before the preceding minimum (diamonds) for a series of 23 synthetic solar cycles (full line) with a random distribution of maxima. The quality of the 'prediction' of the random amplitudes (correlation coefficient $r = 0.84$) is comparable to that based on real sunspot data ($r = 0.89$).

(R. Cameron and M. Schüssler)

### Modelling the Sun's open magnetic flux

The fraction of the Sun's magnetic surface flux which is not contained in closed loops but reaches out far into the heliosphere is denoted as the Sun's open magnetic flux. Measurements outside the ecliptic plane with *Ulysses* have shown that the strength of the radial component of the heliospheric field is largely independent of latitude (except for a sudden polarity change at the heliospheric current sheet), so that the solar open flux is almost uniformly distributed on spherical surfaces. This result gives the opportunity to infer the total open flux and its time variation on the basis of the interplanetary magnetic field measured near Earth. The results can then be used to test and calibrate models that extrapolate the heliospheric field from its photospheric sources. Such calibration is particularly important for reconstructing the solar open flux in the past (before the epoch of in-situ measurements) with solar surface flux transport simulations based upon sunspot group areas, sunspot numbers, or other proxies.

Our work consists of two steps. Firstly, we have evaluated the consistency of field extrapolation models based on the observed photospheric flux distribution with direct measurements of the heliospheric magnetic field. Since the widely used potential field source surface (PFSS) model does not give a good representation of the latitude-independent heliospheric field, we have used the more realistic current sheet source surface (CSSS) model with a source surface located outward of 10 $R_\odot$ to extrapolate the field on the basis of the Wilcox Solar Observatory (WSO) synoptic maps of the solar surface field from 1976 – 2005. We find that this approach yields good agreement with the direct measurements of the near-Earth field and, at the same time, a latitude-independent heliospheric field.

In a second step, we have used a surface flux transport code to simulate the evolution of the surface field and the corresponding open flux determined with the CSSS model on the basis of emerging bipolar magnetic flux derived from the USAF/NOAA SOON sunspot group record (see Fig. 5). It turns out, that the results fairly well reproduce the measured near-Earth field, provided that the average tilt angle of emerging bipolar magnetic regions is somewhat smaller than commonly assumed, but consistent with sunspot group observations. Our model is the first that consistently reproduces the open flux and the total unsigned surface flux together with the azimuthally averaged flux.

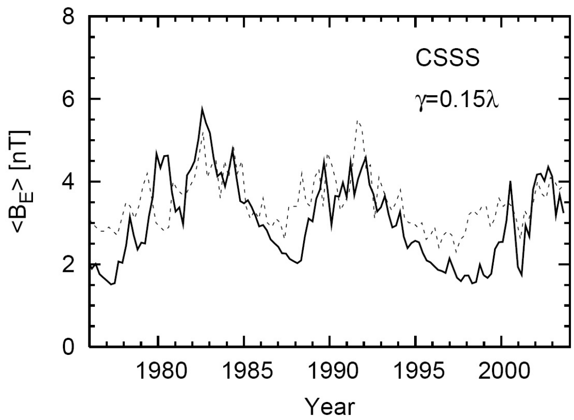


Fig. 5: Temporal evolution of the mean unsigned radial field at 1 AU: comparison between measurements (dashed line, OMNI data) and our combinded surface flux transport and CSSS field extrapolation model with input from the SOON sunspot group areas (full line).

These results provide a firm basis for the reconstruction of the open flux in the past, using existing records of sunspot groups and sunspot numbers.

(I. Baumann and M. Schüssler)

### A solar surface dynamo

Magnetic fields in the quiet solar photosphere (often referred to as 'intranetwork fields') are of considerable interest in connection with the heating of the upper solar atmosphere. Observations indicate that small-scale, mixed-polarity magnetic fields are ubiquitous in the quiet Sun and contribute significantly to the total magnetic energy and unsigned flux in the photosphere outside active regions.

It has been suggested that the intranetwork fields result from local fast dynamo action on the basis of granular convection. In fact, such (non-helical) turbulent dynamo action was found in MHD simulations of incompressible thermal convection at high Rayleigh number in a closed box. However, it was unclear whether these results carry over to the case of realistic solar granulation without artificial boundary effects and including all relevant physics (compressibility, partial ionization, radiative transfer).

We have carried out a simulation with the MURaM radiative MHD code in a computational box with a horizontal extension of 4.9 Mm × 4.9 Mm and a height of 1.4 Mm, ranging between the top of the photosphere down to about 800 km below the visible solar surface. With a grid resolution of 7.5 km in the horizontal directions and 10 km in the vertical, we reached a magnetic Reynolds number of ∼2600, which was sufficient for self-excited dynamo action: a very weak random seed field grew with an *e*-folding time of about 10 min (granular time scale) until it reached saturation after about 3 hours, reaching a mean (unsigned) flux density of about 25 G near the visible surface.

The dynamo-generated field is strongly intermittent (exponential probability density functions) and of mixed polarity on small scales near the solar surface (see Fig. 6). Downward convective pumping of magnetic energy through the (open) lower boundary of the computational box is significant (up to 80 % of the work against the Lorentz force is lost in that way), but not sufficient to shut down dynamo action.

(A. Vögler and M. Schüssler)

### Current sheets and reconnection in the upper photosphere

We have studied the decay of a mixed-polarity field in the solar photosphere based on a high-resolution simulation with the MURaM radiative MHD code. The computational box with a horizontal extension of 6 Mm × 6 Mm and a height of 1.4 Mm has been resolved by 1152 × 1152 × 200 grid cells, corresponding to a cell size of 5.2 km horizontally and 7 km vertically.

We find that the reconnection associated with the decay of the field takes place preferentially in the upper photosphere, where narrow currents form between the expanding patches of opposite-polarity magnetic flux (see Fig. 7 for an example). The thickness of the current sheets is at the resolution limit of the simulation (10 – 15 km), strong Joule heating leads to temperatures of about 9000 K, and reconnection drives flows with velocities of the order of 10 km $s^{-1}$ in the upper photosphere. The strong heating leads to a brightening of the current sheet even in the visible continuum.

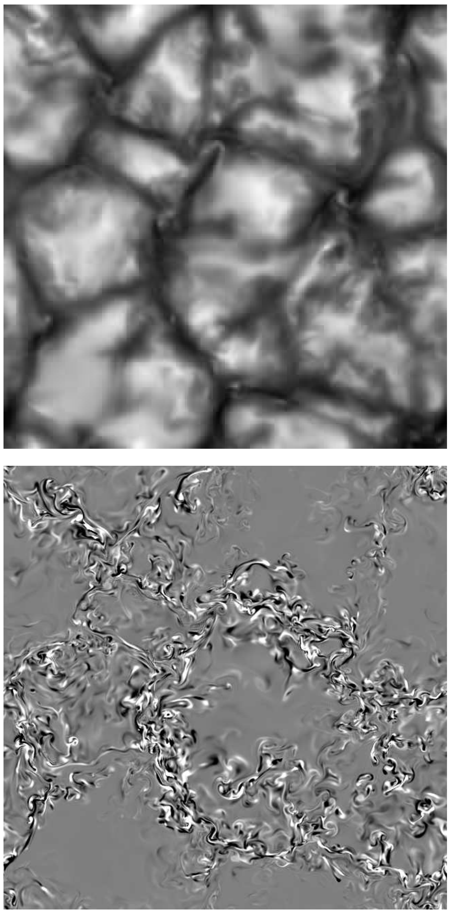

Fig. 6: Snapshot from a surface dynamo simulation. Upper panel: (bolometric) brightness map, showing the granulation pattern. Lower panel: grey-scale map (saturated at ±250 G) of the vertical magnetic field component at the solar surface (Rosseland optical depth equal to unity). The field shows an intricate small-scale pattern with rapid polarity changes and an unsigned flux density of about 25 G. Local flux concentrations can reach kilogauss values. The size of the maps is 4.9 Mm × 4.9 Mm on the Sun.

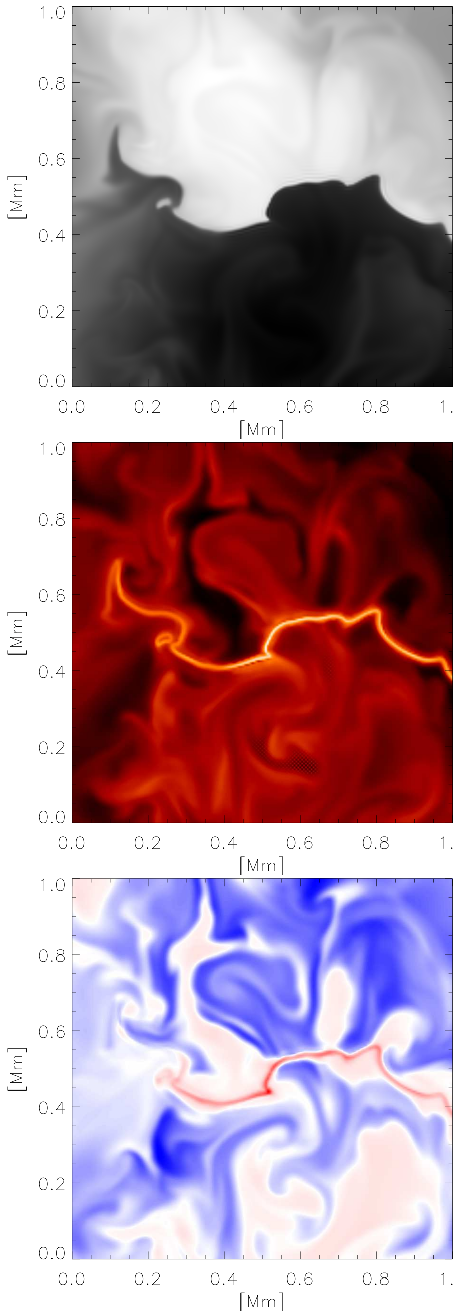


Fig. 7: A simulated current sheet ∼450 km above the visible surface. *Top:* Map of the vertical magnetic field component (black: upward, white: downward, extrema ∼ ±400G); *middle:* temperature, maximum ∼9000 K; *bottom:* vertical velocity (blue: upflow, red: downflow). The reconnection-driven downflow velocity exceeds 10 km s$^{-1}$.

The structure of the current sheets represents 'textbook cases': local peaks of gas pressure and temperature at the current sheet, vertical reconnection flows along the sheet and horizontal flows transporting magnetic flux towards the sheet and reconnection region.

(M. Schüssler, R. Cameron, and A. Vögler)

**Signature of magnetic reconnection in the solar photosphere**

Realistic 3-D radiation magneto-convection simulations, which take into account the presence of mixed polarities on the solar surface (as are ubiquitous in the quiet Sun and also common along neutral lines of active regions) reveal magnetic reconnection in photoshperic layers (specially in the upper photosphere) at sites where opposite polarity magnetic fields are pushed together by photospheric convective motions. The sites of magnetic reconnection are prominent in the simulations as locations of very close opposite polarity fields, strong localized heating and localized downflows. We have searched for observational signatures of such reconnection sites and have picked a typ-

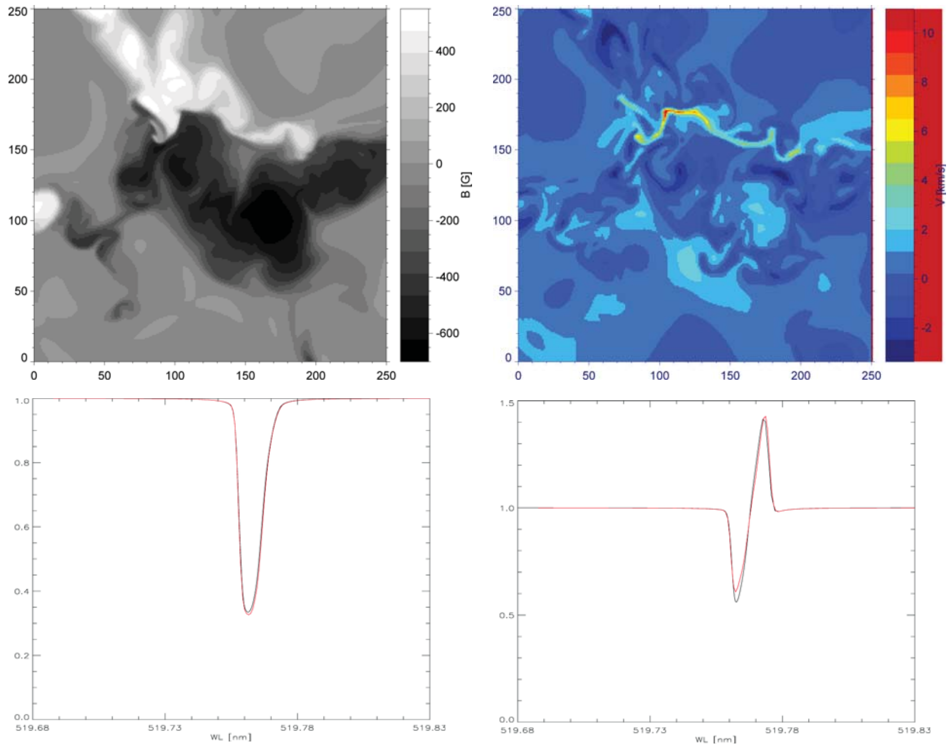


Fig. 8: Upper left: vertical magnetic field at approximately 300 km above $\tau = 1$ at the location of the reconnection (strong fields of either polarity are white and black, respectively). Upper right: map of vertical velocity (blue: upflow, red: downflow) of the same region. Lower left: normal profile of Fe II 519.7 nm line (black and red solid lines represent LTE and NLTE cases respectively). Lower right: the line profile at the location of the reconnection in the original spatial resolution of MHD simulations.

ical reconnection event for close examination in order to find the best diagnostics in spectral and polarimetric signals.

For this purpose several lines with different formation heights have been considered. We discovered that a number of the considered spectral lines exhibits an intensity reversal redwards of their cores right at the location of the reconnection, and the most promising ones even display prominant emission in the red wing at the current sheet. The redshift of the reversal is a product of the strong downflow velocity at the current sheet (Fig. 8). According to the simulations, the feature stays visible even after reducing the spatial resolution to mimic observations with the SST (Swedish Solar Telescope) on La Palma under very good seeing conditions. It is planned to use our next observing run at the SST to search for the signature of magnetic reconnection in the photosphere.

(S. Danilovic, S. K. Solanki, and M. Schüssler in collaboration with J. Bruls (Kiepenheuer Institut für Sonnenphysik))

**The origin of the ‘reversed’ granulation**

While white-light or continuum images show granulation as a pattern of isolated bright patches within a network of dark intergranular lanes, observations in the wings of strong spectral lines (representing higher layers in the solar photosphere) exhibit a reversed pattern of contrasts: bright intergranular lanes and darker granules.

We have studied the origin and physical nature of the reversed granulation pattern by means of radiative hydrodynamics simulations with the MURaM code, providing a realistic model of the near-surface layers of the convection zone and the photosphere. While the pattern of horizontal temperature fluctuations at the base of the photosphere consists of relatively hot granular cells bounded by the cooler intergranular downflow network, we find that the amplitude of the temperature fluctuations diminishes with increasing height in the photosphere. At a height of z = 130 – 140 km in the photosphere, the pattern of horizontal temperature fluctuations reverses so that granular regions become relatively cool compared to the intergranular network.

Detailed analysis of the trajectories of fluid elements through the photosphere (Fig. 9) reveals that the motion of the fluid is non-adiabatic, owing to strong radiative cooling when approaching the surface of optical depth unity followed by reheating by the radiation field from below. The temperature structure of the photosphere results from the competition between expansion of rising fluid elements and radiative heating. The former acts to lower the temperature of the fluid whereas the latter acts to increase it towards the radiative equilibrium temperature with a net entropy gain. After the fluid overturns and descends towards the convection zone, radiative energy loss again decreases the entropy of the fluid. Radiative heating and cooling of fluid elements that penetrate into the photosphere and overturn do not occur in equal amounts. The imbalance in the cumulative heating and cooling of these fluid elements is responsible for the reversal of temperature fluctuations with respect to height in the photosphere.

(M. C. M. Cheung and M. Schüssler in collaboration with F. Moreno Insertis (Instituto de Astrofísica de Canarias, Spain))

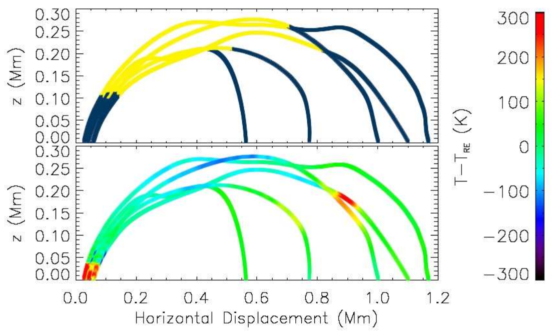


Fig. 9: Trajectories of fluid elements projected on a common vertical plane. The elements rise in a granular upflow (to the left), ascend and travel horizontally, overturn, and finally re-enter the convection zone. On the upper panel, the colour coding represents the sign of the radiative energy exchange: dark blue indicates radiative cooling while yellow denotes heating of the fluid element. On the lower panel, the trajectories are colour-coded according to the deviation of their gas temperature from the corresponding value of the radiative equilibrium temperature. The fluid elements are radiatively heated when their temperature falls below the radiative equilibrium value.

## Flow instabilities of magnetic flux tubes

Astrophysical magnetic fields become highly structured and intermittent when they are embedded in an electrically conducting plasma in turbulent motion with high magnetic Reynolds number. The stability properties of magnetic flux filaments in the presence of flows are relevant in various astrophysical situations, for instance in connection with magnetoconvection and the storage of magnetic flux in stellar interiors and accretion disks, for the maintainance of magnetic structures in stellar atmospheres, or for collimated outflows and jets.

Physical processes involving magnetic flux filaments are often studied in the context of the approximation of thin magnetic flux tubes, whereby the filaments are treated as bundles of magnetic field lines whose diameter is small compared to all other relevant length scales. We have used this approximation to investigate, in ideal MHD, the linear stability of magnetic flux tubes under the influence of perpendicular external flows as well as with (internal or external) longitudinal flows along the field lines.

We find that external perpendicular flows can drive monotonic as well as oscillatory instability (overstability). In a gravitationally stratified medium, the stability condition depends on direction and magnitude of the external velocity as well as on its first and second derivatives with respect to depth. The range of the flow-driven instabilities typically extends to modes with much shorter wavelengths along the flux tube than for the buoyancy-driven undulatory Parker instability.

In the case of longitudinal flows along the field lines, we find Kelvin-Helmholtz instability for flow velocities exceeding a critical speed that depends on the Alfvén speed and on the ratio of the internal and external densities (see Fig. 10). Inclusion of a friction term proportional to the relative transversal velocity leads to a friction-driven instability connected with backward (or negative energy) waves. If stratification effects are included, the Kelvin-Helmholtz instability and the friction-driven instability can set in for flow speeds significantly smaller than the Alfvén speed.

Ongoing work addresses the consequences of these instabilities for magnetic flux storage in stellar convection zones.

(V. Holzwarth, D. Schmitt, and M. Schüssler in collaboration with A. Ferriz Mas (University of Vigo, Orense, Spain))

## Multi-channel high resolution observations of sunspots

In August 2006 a multi-channel polarimetry and imaging campaign was carried out at the Swedish Solar Telescope (SST) in La Palma, Canary Islands. Photometric observations in Ca II $K$, G-band and two continuum wavelengths were combined with 2-D-spectro-polarimetric scans through the Zeeman-active

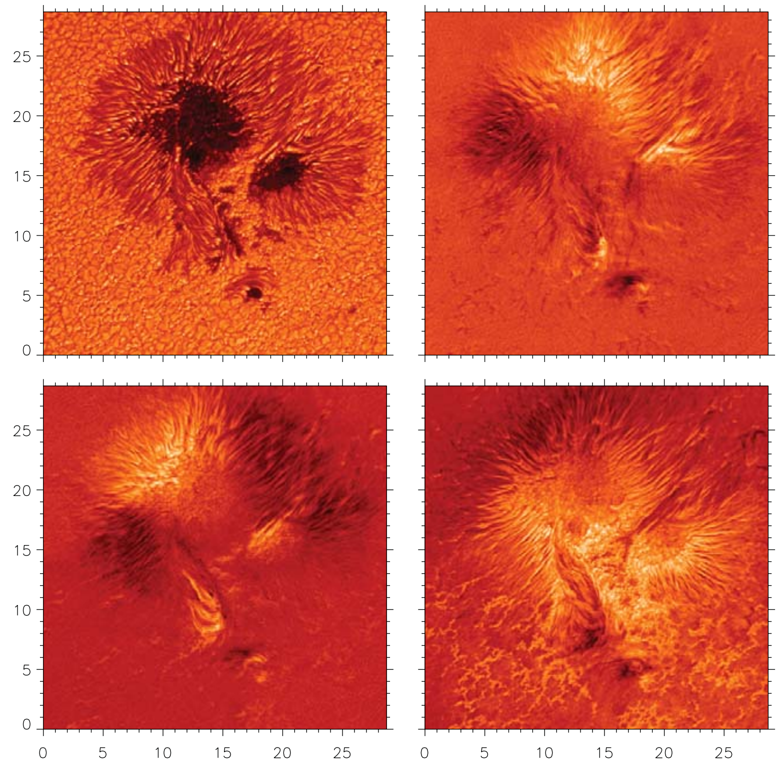


Fig. 11: Broad band continuum image (upper left) and Stokes $Q$, $U$ and $V$ images (at Fe I 6303 Å−75 mÅ) of a mature sunspot in NOAA 10904. Axis labels are given in Mm.

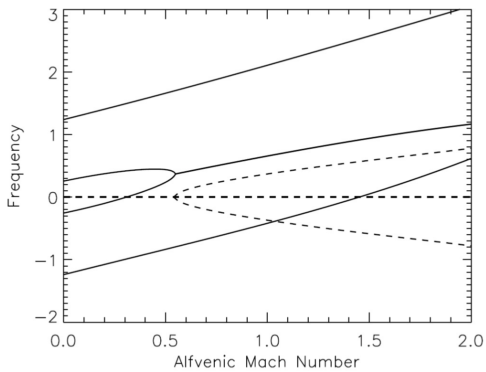


Fig. 10: Linear modes of a horizontal flux tube in the case of longitudinal flow, external stratification, and no friction. Shown are the real parts (oscillation frequencies) and imaginary parts (growth rates) of the complex (normalized) frequencies as functions of the Alfvénic Mach number of the longitudinal flow. Kelvin-Helmholtz instability sets in when the real parts of the two (mainly) transversal modes merge. The two modes whose real parts cross the zero line represent backward modes, i.e. reverse their direction of propagation for sufficiently large flow velocity. They become unstable 'negative energy waves' when dissipation by friction is included.

Fe I 6303 Å line. The sunspot group NOAA 10904 was traced during its transit across the solar disk.

By using the STT adaptive optics system and state-of-the-art post-facto image reconstruction techniques angular resolutions close to the diffraction limit of the 1-m telescope aperture were achieved. Polarimetric data were corrected for instrumental polarization effects (deconvolution with telescope matrices) in order to obtain the full Stokes vectors (magnetic field vectors) at each pixel of the field of view and at 6 spectral positions along the profile of the scanned iron line (see Fig. 11). This is probably the most complete polarimetric data set ever obtained at such a high spatial resolution.

These photospheric and chromospheric data give insights into the complex magnetic field and flow topologies in and around the observed sunspots. In addition, the reorganization of magnetic field lines during a weak flare erupting above the sunspot penumbra has been identified.

(J. Hirzberger, T. Riethmüller, P. Kobel, and S. K. Solanki)

### Flux emergence in the solar photosphere – Diagnostics based on 3-D radiation-MHD simulations

We investigate the observational signature of flux tube emergence in the solar photosphere in Stokes profiles calculated in 3-D radiation-MHD simulations. The

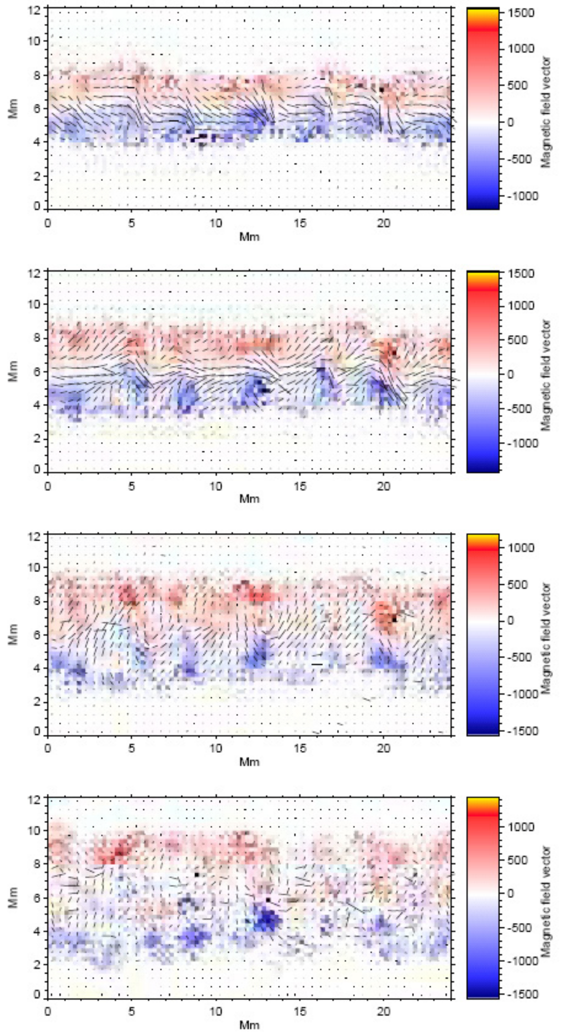


Fig. 12: Maps of retrieved magnetic field vector for a time sequence of emergence (time increases from top to bottom pannels). Note the twisted structure of the emerging field shown by the arrows representing the projection of the horizontal component of the field. The colours represent the vertical (line-of-sight) component of the magnetic field [in Gauss].

simulations consider the emergence of a twisted magnetic flux tube through the solar surface. We study different stages in the emergence process, starting from the early appearance of the flux tube at the solar surface (see Fig. 12). At every stage we numerically compute line profiles, degraded to the typical spatial resolution of the observations. Then, following observational practice, we apply Milne-Eddington-type inversions to the synthetic spectra in order to retrieve different atmospheric parameters. We find that both observations and simulations agree on the general picture of an upwardly emerging horizontal flux tube with sub-kilogauss field strength. The simulations show that after interaction with granulations, the field distribution gets more vertical and concentrated in intergranular lanes. During this process the initially upwardly emerging flux tube, slows down and the magnetized plasma concentrates in intergranular lanes with downflowing motion. The analysis of the magnetic field vector indicates that the magnetic flux tube was less twisted in published observational studies comparing to simulations. However, the complexity of magnetic flux emergence revealed by recent Hinode simulations is well mimicked by the synthetic data.

(L. Yelles Chaouche, S. K. Solanki, M. Schüssler, and A. Lagg in collaboration with M. Cheung (Lockheed Martin))

### Center-to-limb variations of intensity contrast of simulated faculae and network elements

Observations of the total solar irradiance from space revealed changes on all time scales. Such irradiance variations are closely related to manifestations of magnetic activity at the Sun's surface. Sunspots and active region faculae are considered to be the dominant contributors. So far all successful reconstructions of solar irradiance have made use of empirical brightness contrast of magnetic features, which are central for the success of any model. We aim to use fully self-consistently computed contrasts. In a first step the contrast obtained from MHD simulations are compared with observed values. Observations demonstrate that the contrast of photospheric magnetic features depends on the amount of magnetic flux and disc position. Consequently we performed quantitative analysis of the computed continuum contrast of small-scale magnetic features in a series of realistic radiative 3-D MHD simulations reproducing quiet Sun, network and active regions depending on the amount of magnetic flux and heliocentric angle. We found that the hydrodynamic models, i.e. without magnetic field, appear brighter at disc center and darker near the limb than the MHD models with a non-zero magnetic field. The output of the simulations was compared with results obtained by the MDI on SOHO after taking into account the instrumental parameters of MDI (spatial resolution, filter profiles, scattered light). The computed center-to-limb variation (CLV) of the continuum intensity in different models exhibits a good correlation with observations by MDI. The CLV of the continuum contrast of magnetic features depends on the magnetic flux per pixel or magnetogram signal. Stronger magnetogram signals correspond to a high density of wider flux tubes, which appear dark at the disc center, but bright near the limb. Weak magnetogram signals usually correspond to narrow flux tubes and appear bright at the disc center and also near the limb. The reason for this is the *hot wall* effect which we see in detail in the models near the limb. A typical CLV of the continuum contrast of faculae increases towards the limb, reaches a maximum and then decreases again. The results of this investigation will form an input for the modelling of the variations of the total solar irradiance.

(V. Zakharov, M. Schüssler, S. Shelyag, S. K. Solanki, A. Vögler, and T. Wenzler)

### High resolution spectroscopy of small-scale solar magnetic elements in the violet CN band-head

When observing the Sun through a 1 nm wide interference filter centered near 430 nm (the G band ) or near 388 nm (violet CN band) at sub-arcsec spatial resolution small-scale photospheric magnetic features often appear brighter than the non-magnetic surroundings, in contrast to observations in the continuum at nearby wavelengths. These G-band bright points (BP) are used to monitor the small-scale photospheric magnetic fields without the need of magnetograms.
The lateral inflow of radiation into evacuated flux-tubes or flux-sheets, which describe the photospheric small-scale magnetic features, leads to an enhanced inside temperature which dissociates molecules whose number is thereby decreased as compared to the surroundings. This effect produces a weakening of CH and CN absorption lines, providing a brightness excess, i.e. a BP. Our recent high-resolution spectroscopic observations of individual CH and CN spectral lines in BPs clearly confirm this effect.
A comparison between CN and CH bands in BPs gives different results in observations and radiative 3-D MHD simulations. Observations show that the BPs have on average a 1.4 times higher contrast in the violet CN band than in the G band, while simulations predict the same contrast. It is not clear if this disparity is due to shortcomings of the simulations, or due to different levels of scattered light (in the instrumentation or in the terrestrial atmosphere) at these wavelengths.
To resolve this uncertainty, we carried out the first radiative computations in realistic 3-D MHD models of the violet CN band. This spectral domain contains not only CN lines but also some CH line. We clearly identify the strong decrease in absorption of the individual molecular lines within bright magnetic elements. We compare the change in line-core depths of CN and CH lines in computed spectra with that obtained in our spectroscopic observations of BPs.
Preliminary results show that in BPs the ratio of contrasts in CN line-cores to those in CH line-cores lies in a range between 0.9 and 2.0 with a mean value around 1.2. The ratio of these contrasts decreases with increasing continuum intensity of BPs. This agrees qualitatively with the results of our observations. However, the values are smaller in the simulations. This suggests that even state-of-the-art 3-D radiative MHD simulations, that otherwise are highly successful in reproducing observations, have missing ingredients.

(V. Zakharov, A. Gandorfer, and S. K. Solanki)

### Spectro-polarimetric diagnostics of simulated magneto-convection

The Stokes diagnostics of radiative magneto-convection simulations provides a tool to study the correspondence of physical processes in the solar (sub)photosphere, which are described by the simulations, to spectro-polarimetric observations. Stokes profiles of Zeeman-sensitive lines of neutral iron in the visible and infrared spectral ranges emerging from the simulated atmosphere have been calculated in order to study their relation to the relevant physical quantities and compare with observational results (Fig. 13). We have analyzed the dependence of the Stokes-$I$ line strength and width as well as of the Stokes-$V$ signal and asymmetries on the magnetic field strength. Furthermore, we have evaluated the correspondence between the actual velocities in the simulation with values determined from the Stokes-$I$ (Doppler shift of the center of gravity) and Stokes-$V$ profiles (zero-crossing shift). We confirm that the line weakening in strong magnetic fields results from a higher temperature (at equal optical depth) in the magnetic flux concentrations. We also confirm that considerable Stokes-$V$ asymmetries originate in the peripheral parts of strong magnetic flux concentrations, where the line of sight cuts through the magnetopause of the expanding flux concentration into the surrounding convective downflow.

(S. Shelyag, M. Schüssler, S. K. Solanki, and A. Vögler)

### Spectro-polarimetric diagnostics near the solar limb: Simulations versus high-resolution observations

The aim of this investigation is to understand the detailed formation of Stokes profiles and thus to lay the foundation of the physical interpretation of spectro-polarimetric diagnostics in an active region plage near the limb. We use 3-D radiation-MHD simulations with unipolar fields of an average strength of 200 G and 400 G, which is distributed between weak fields and flux tubes in which the field typically reaches kilogauss values. We generate synthetic Stokes spectra by radiative transfer calculations, then we smear the simulated Stokes signal to reproduce observational condi-

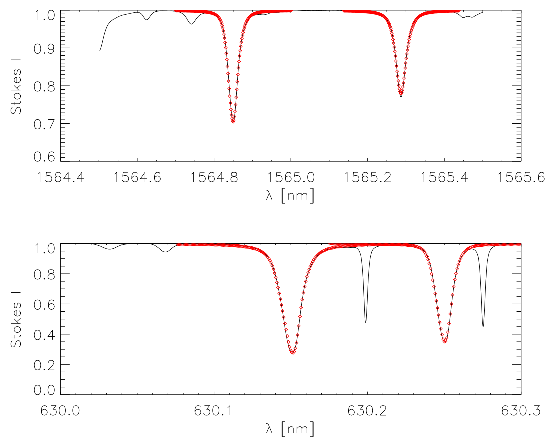


Fig. 13: Comparison between synthetic Fe I line profiles (red symbols) for two pairs of infrared (top) and visible (bottom) lines, respectively, with the observed quiet-Sun profiles (solid curves) from the Liège spectral atlas. The synthetic profiles have been spatially averaged over the 6 Mm × 6 Mm computational domain for one simulation snapshot with a mean vertical field of 10 G. They agree with the observed profiles to within a few percent.

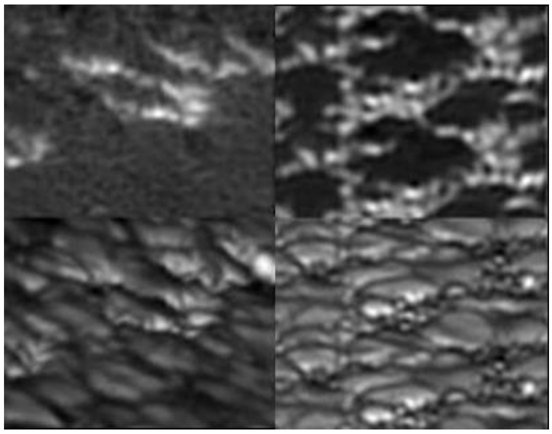

Fig. 14: Observed continuum (lower left panel), and Stokes $V$ signal at -50 mÅfrom Fe I 6302 line center (upper left). Right panels: corresponding simulated images.

tions (Fig. 14). The synthetic data treated in this manner statistically reproduce spectro-polarimetric high resolution observations at $\mu = 0.39$ (Fig. 14) obtained by the SOUP instrument with the Swedish Solar Telescope in 2006 by L. Rouppe van der Voort and M. van Noort. After establishing the similarity between observations and simulations, we investigate in more detail individual features in the simulations corresponding to magnetic flux concentrations, and identify the properties and origin of their Stokes signatures. It is found that along any given ray passing through the magnetic element the polarized Stokes parameters are formed over a very narrow region. Also, Stokes $Q$ and $U$ are preferentially formed at a different height (along different rays) than Stokes $V$. The formation of Stokes $V$ asymmetry along these inclined rays largely follows the classical picture of velocity and magnetic field gradients at the flux-tube boundary, but also displays some unexpected new twists.

(L. Yelles Chaouche and S. K. Solanki in collaboration with Luc Rouppe van der Voort and M. van Noort (Royal Swedish Academy Science, Stockholm))

**Classification of line profiles in the network and internetwork based on Hinode data and comparison with MHD simulations**

A quiet Sun region covering 31″ × 88″ at $\mu = 0.6$ scanned by the Spectro-polarimeter (SP) on Hinode was used for the analysis of Stokes $V$ profiles in 630.25 nm line. The noise level of Stokes signals vary across the scan around values of $10^{-3}$ (in units of the continuum intensity, $I_c$) (see Fig. 15). We carried out a Principle Component Analysis (PCA) to classify the observed Stokes $V$ and separately the $Q$ and $U$ profiles. PCA allows functions of diverse shapes to be grouped into classes that are not predefined, so that preconceptions of what the profiles should look like do not enter into the analysis. The shapes of the profiles are diagnostically important, since they give information on unresolved structure and vertical gradients of physical quantities in the solar atmosphere. The percentage distribution of the different classes of profiles was studied as well as their spatial distribution.

The analysis shows that the fraction of irregular profiles is largest in the weak-field internetwork regions. The positions of irregular profiles are in the edges of the patches of a given magnetic polarity, or in the regions of mixed polarities. Because of the position on the solar disk, many profiles are found to show negative asymmetry. Area asymmetry histograms show a slight offset to negative values. Area asymmetry of the spatially averaged Stokes $V$ profile decreases with the Stokes $V$ amplitude, and actually reverses in the network. The amplitude asymmetry of the averaged $V$ profile does not change significantly with Stokes $V$ amplitude.

The observed PCA classes of Stokes profiles agree rather well with similarly determined classes from radiation MHD simulations due to Vögler *et al.* (2005).

(S. Danilovic, A. Lagg, S. K. Solanki, M. Schüssler, and A. Vögler in collaboration with L. Khomenko (Instituto de Astrofisica de Canarias, Tenerife, Spain))

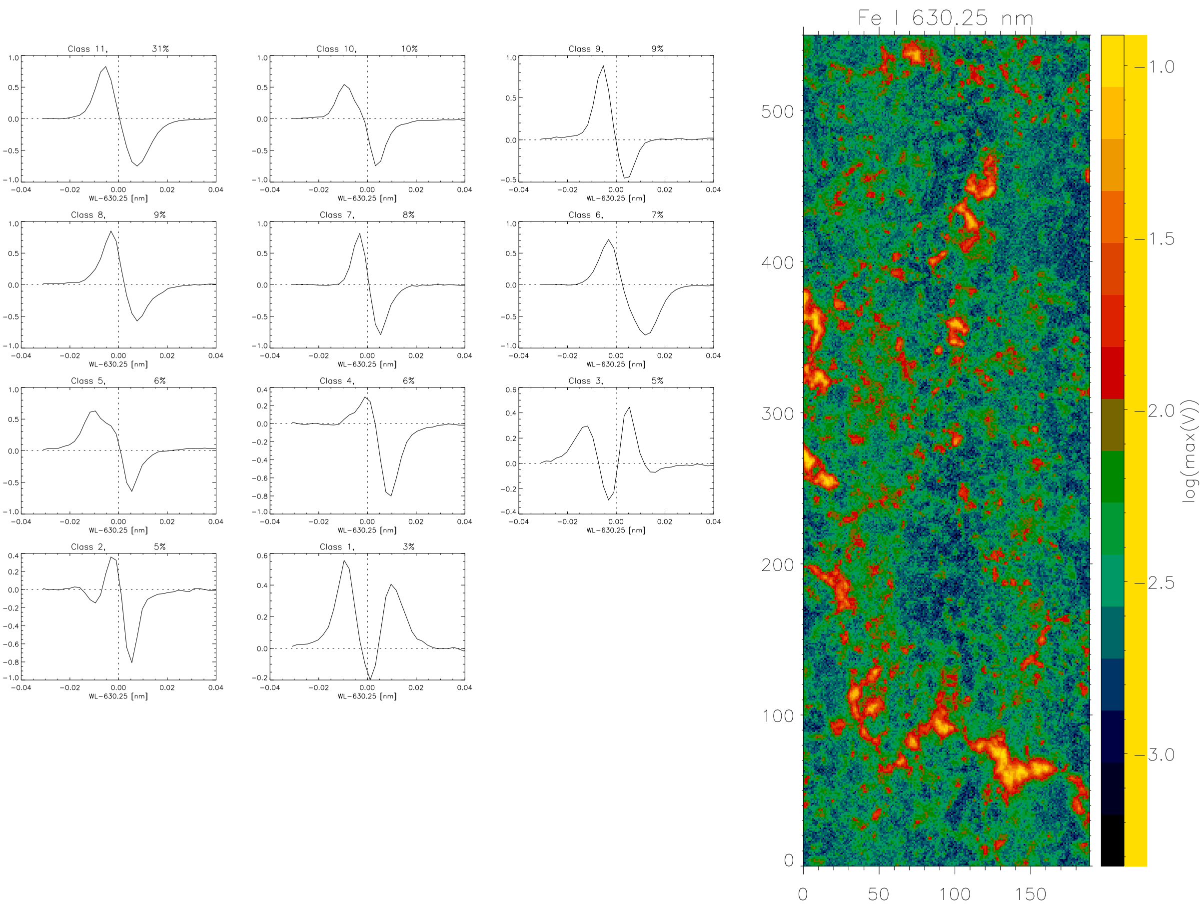


Fig. 15: Right: V amplitude map of the region we investigated. Left: Class profiles for the threshold value of $4 * 10^{-3}\ I_c$ (36 % of all the pixels lie above the noise threshold and are analysed in the illustrated case).

### Low-lying loops in the quiet Sun internetwork region

A number of studies support the presence of horizontal magnetic fields in quiet Sun internetwork regions. However, the origin and connectivity of these fields is still unknown. In order to obtain a better idea of this structure we have obtained long exposures of spectropolarimetric data in the very magnetically sensitive 1.56 micron lines recorded in the internetwork near the center of the solar disk. The data were inverted to obtain the magnetic field vector, the line-of-sight velocity and the thermal structure of the field. It was noticeable that patches of linear polarization often lay between patches of opposite circular polarization. After the inversion these locations could be identified as opposite polarity internetwork features connected by short (2 – 6 arcsec long) low-lying magnetic loops, whose tops lie in the photosphere. About 10 – 20 % of the total magnetic flux in the internetwork was found to be in the form of such loops.

(S. K. Solanki in collaboration with M. Martínez González, M. Collados, and B. Ruiz Cobo (Instituto de Astrofisica de Canarias, Tenerife, Spain))

### Oscillations in penumbral filaments

The objective of this study was to identify wave modes in a sunspot penumbra. Spectropolarimetric time series data of the photospheric Fe I 15662 Å and Fe I 15665 Å lines were simultaneously inverted using a model comprising two atmospheric components in each spatial pixel – one permeated by a nearly horizontal magnetic field (flux tube, FT), the other with a less-inclined magnetic field (magnetic background, MB) – and a non-magnetic straylight component.

Fourier phase difference analysis was performed on the line-of-sight velocities retrieved from both components to determine time delays between the velocity signals, while vertical separations between the signals in the two components were calculated from the Stokes velocity response functions. Time delays between the oscillations in the two components in the frequency range 2.5 – 4.5 mHz were combined with speeds of atmospheric wave modes to determine wave travel distances. These were compared to expected path lengths obtained from response functions of the observed spectral lines in the two different atmospheric components. High-$\beta$ fast-mode (i.e., modified $p$-mode) waves exhibit the best agreement with the observations. This is the first time that such waves have been identified in a sunspot penumbra.

(D. S. Bloomfield, S. K. Solanki, and A. Lagg in collaboration with J. M. Borrero (High Altitude Observatory, USA) and P. S. Cally (Monash University, Australia))

### The nature of running penumbral waves

Running penumbral waves (RPWs) are observed as intensity and/or velocity fronts in the chromosphere above sunspot penumbrae moving outwards from the umbra. We sought to confirm whether this phenomenon is due to either i) trans-sunspot waves in the chromosphere or ii) a visual pattern of upward-propagating waves. Full Stokes spectropolarimetric time series data of the photospheric Si I 10827 Å line and the chromospheric He I 10830 Å multiplet were inverted using a Milne-Eddington inversion code.

Spatial pixels were paired together between the outer umbral (as well as inner penumbral) photosphere and the penumbral chromosphere using solar inclinations retrieved by the inversion. These dual-height pairings of line-of-sight velocity time series were studied for signatures of wave propagation using a Fourier phase difference analysis. The dispersion relation for acoustic waves including radiative cooling, modified to incorporate inclined directions of wave propagation (i.e., reduced gravity and increased path length), fits well the observed pattern of Fourier phase differences between the pairs of photospheric and chromospheric pixels (Fig. 16).

The observed signature of RPWs comes from low-$\beta$ slow magneto-acoustic waves that are initially excited by a common photospheric source which then experience increasing propagation distances to the chromospheric sampling height from travelling along increasingly inclined field lines. As such, delays of increasing magnitude are observed in same-wavefront arrival times at increasing radial distance through sunspot penumbrae. The pattern of these delayed wavefronts gives rise to the apparent outward motion of RPWs. We have thus demonstrated that the observed RPWs are in effect low-$\beta$ slow-mode waves propagating along the magnetic field lines.

(D. S. Bloomfield, A. Lagg, and S. K. Solanki)

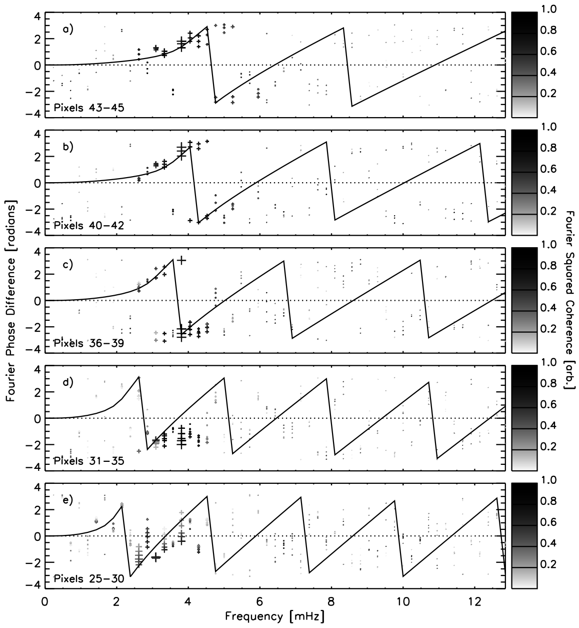


Fig. 16: Fourier phase differences between line-of-sight velocities from spatially offset pairs of photospheric and chromospheric pixels. Panels present groups of pixel pairs moving from those with chromospheric pixels closest to the umbra/penumbra boundary ($a$) toward those in the outer penumbra ($e$). Solid curves show dispersion relations calculated using group averages of field inclinations retrieved by the inversion (40°, 45°, 53°, 63°, and 65° for $a$ to $e$, respectively).

### Moving magnetic features

Moving magnetic features (MMFs) are small magnetic concentrations, often composed of pairs of opposite polarity, that are found in the moat around a sunspot and are seen to move away from the spot. Earlier we had shown that the MMF pairs are ordered such that the polarity opposite to the sunspot is present closer to it, while the feature with the same polarity is located further away from the spot. In addition, their exact orientation and the direction of their motion follows the superpenumbral fibrils seen in H$\alpha$ (i.e. they probably follow the magnetic field direction of the magnetic canopy surrounding the sunspot). Based on these observations a new model of MMF pairs was proposed. It was suggested that MMF pairs are the footpoints of small U-loops emanating from the canopy.

We have now extended this work to include more sunspots observed by the Michelson Doppler Imager (MDI) in its high resolution mode, taking care to choose mature and very regular sunspots with a very clean moat in order to rule out disturbances to the MMF statistics by other nearby magnetic fields. In addition to the properties of the MMFs determined in the earlier work (orientation, direction and speed of motion, lifetime, position of initial appearance, etc.), we also studied two additional parameters of interest for testing our model: the presence of up and downflows in the MMFs and the evolution of the horizontal speed of an MMF as a function of time. We find that the trailing MMF shows a downflow, while the leading MMF does not. Also, we find that the proper motion of the MMFs slows down with distance from birthplace, but is not a significant function of distance from the sunspot.

Both the improved statistics of the known parameters and the new parameters are in good agreement with the proposed model. The downflow in the trailing MMF of a pair is expected due to the downflow of Evershed-flow material into the solar interior through the U-loop. Since the Evershed flow comes from the sunspot, we do not expect any significant flow in the leading MMF of the pair, exactly as observed. Similarly, the speed of the MMF is expected to decrease with time after birth, due to drag from the surroundings on the U-loop, which is pushed out by the inertia of the Evershed-flowing material (the initial speed of MMF pairs is generally higher than the normal moat flow speed).

(J. Zhang, S. K. Solanki, and J. Woch in collaboration with J. Wang (National Astronomical Observatories Beijing, China))

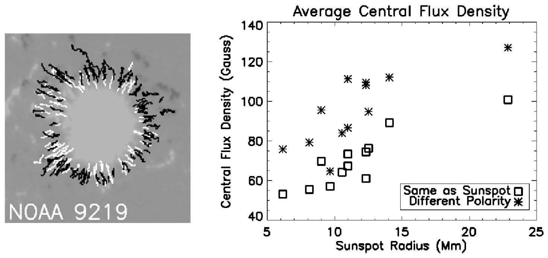


Fig. 17: *Left:* This positive sunspot, NOAA 9219, released 93 positive and 118 negative moving flux concentrations within 7.5 hours. On a lightened magnetogram, we drew the traces of those positive moving flux concentrations in white colour, and the traces of negative ones in black. On average, those having a different polarity than the sunspot (in this case negative, or black) appear and disappear 2Mms closer to the penumbra than those having the polarity of the sunspot (in this case, positive, white), but these two kinds have similar lifetimes (1hr 40min) and displacements (3.4 Mm). *Right:* For each moving flux concentration, we calculated the average flux density of it's central pixel over it's lifetime. Having put the data from 12 sunspot altogether, we find that the average magnetic flux density (and flux) of the moving flux concentrations released by a sunspot is generally proportional to the diameter of the mother sunspot. Moreover, those moving flux concentrations with different polarity as the sunspot are usually stronger; statistics also show that they reach their magnetic maximum (flux and flux density) much earlier than the other type.

**Tracking of moving magnetic flux concentrations around sunspots in the photosphere**

During the decay process of sunspots, their magnetic fluxes decrease with time. Small magnetic flux concentrations of both the same as and opposite to the sunspots' magnetic field were observed to be moving away from sunspots, which might have contributed to the decay of sunspots (see Fig. 17). Using time series of MDI/SOHO high-resolution line-of-sight magnetograms, we developed an automatic computerized tracking method and traced the flow of flux concentrations around several mature sunspots. We statistically analyzed the kinematic and magnetic characteristics of these flows, and studied these statistical values' dependency upon the size, flux, and phase of the sunspots. The possible physics nature of these flows and the relationship between them and the decrease of the sunspots' total flux are discussed.

(Xiaobo Li, J. Büchner, and H. Zhang)

**The vertical extension of penumbral filaments**

Studies of the fine structure of the penumbra as inferred from the uncombed field model, consisting of a nearly horizontal flux tube embedded in a surrounding magnetic field, were continued. The inversions previously restricted to the 1.56 $\mu$m data, were now applied to penumbral spectropolarimetric data from the neutral iron lines at 6300 Å. These lines differ from the 1.56 $\mu$m lines employed earlier in that they are formed somewhat higher in the photosphere and, importantly, display a large Stokes $V$ asymmetry due to the large sensitivity of these lines. The inversion infers very similar radial dependences in the physical quantities (LOS velocity, magnetic field strength etc.) as those previously obtained from the inversion of the Fe I 1.56 $\mu$m lines. In addition, the large Stokes $V$ asymmetry exhibited by the 6300 Å lines helps to constrain the vertical size of the penumbral flux tubes. The uncombed field model, which is composed of horizontal flux tubes embedded in an inclined field, is able to reproduce the observed area asymmetry with striking accuracy. The data suggest that the horizontal flux tubes have a thickness of 100 – 300 km in the vertical direction.

(J. M. Borrero, S. K. Solanki, and A. Lagg in collaboration with H. Socas-Navarro and B. Lites (High Altitude Observatory, Boulder, USA))

**Magnetohydrostatic model of sunspot filamentary structure**

The filamentary structure of sunspot penumbrae is often described in terms of flux tubes. The equilibrium configuration for such penumbral flux tubes has so far been studied under the thin-flux-tube approximation, which greatly simplifies their treatment. However, the thin-flux tube approximation has limited applicability in the solar photosphere, since the radius of the penumbral flux tubes is typically comparable to the pressure scale height.

A first step towards a more realistic modelling of penumbral flux tubes beyond the thin-flux-tube approximation has been taken and analytical solutions for the static momentum equation obtained that describe horizontal flux tubes with a circular cross section, embedded in a surrounding atmosphere that harbours a potential magnetic field. The basic idea is to set up a generic magnetic and velocity field that satisfies certain conditions: Maxwell's equations, boundary conditions, observations etc. These magnetic field and velocity vectors are brought into the momentum equation. By requiring force balance, the density and pressure (and therefore temperature) distribution inside the flux tube are determined.

Interestingly, the inferred pressure, density and temperature stratification reproduce intensity features similar to dark core penumbral filaments and penumbral grains revealed by observations.

(J. M. Borrero)

**Automated detection of bright points and faculae at various disk positions**

It has long been known that small-scale magnetic flux concentrations (the so-called magnetic elements) appear mainly as Bright Points (BPs) near solar disk center, while faculae correspond to their signature near the limb. However, the exact relationship between these two radiative features is not clear, e.g., are BPs and faculae associated with similar magnetic flux concentrations (size, field strength)? A center-to-limb study of this relationship is of importance for comparison with the geometry and temperature stratification of flux-tube models, and to provide a new observational constraint for MHD simulations.

We have obtained the center-to-limb variations of brightness contrast and relative number density for both BPs and faculae, and studied how their morphology changes as a function of the viewing angle. To achieve this with statistical significance, faculae and BPs have to be detected separately in an automated way. We have identified the most useful criteria for separating BPs, faculae and granules from each other in images of solar active region and network, and developed a selection technique.

We applied our detection algorithm to simultaneous G-band (430 ± 0.5 nm) and G-continuum (436 ± 0.5 nm) images recorded at the 1-m Swedish Solar Telescope (SST). These data cover active regions at various heliocentric angles from disk center to the limb. Due to excellent seeing conditions, a phase-diversity reconstruction allowed almost diffraction-limited resolution to be achieved (angular resolution $\sim 0.1$ arcsec). We find that the number of BPs gradually drops towards the limb, while the number of faculae gradually rises, so that at many disk locations both types of brightness features are present. Even at disk center our algorithm detects facular structures, suggesting the presence of strong but highly inclined fields (see Fig. 18).

(P. Kobel, V. Zakharov, J. Hirzberger, A. Gandorfer, and S. K. Solanki)

**Fine structure and dynamics of sunspot umbral dots: Evidence for their convective nature**

Umbral dots (UDs) are small bright features found in sunspot umbrae. Although various statistical analyses of their properties have been carried out, their evolution is not well studied. Such a study is particularly pressing in view of successful recent numerical simulations by Schüssler and Vögler (2006). We have taken two approaches to studying their nature.

In the first approach we have inverted Hinode spectropolarimetric data of UDs and found that they differ from the diffuse umbral background almost exclusively in the low photosphere. There they display higher temperatures, a significantly lower field strength and (at least for brighter ones near the umbral boundary) strong blueshifts (see Fig. 19). The obtained structure is in good agreement with the predictions of the simulations of Schüssler and Vögler (2006), suggesting that UDs are small-scale convective features.

The second approach we have taken is more statistical. We have analyzed a 110-minute time series of high resolution images of the umbra of a mature sunspot acquired with the 1-m Swedish Solar Telescope (SST) on La Palma. After image reconstruction via the multi frame blind deconvolution technique and following destretching and sub-sonic filtering a resolution near the telescope's diffraction limit of $0.18''$ (130 km) at the observed wavelength was reached.

Nearly 13000 UDs were found in the analyzed time

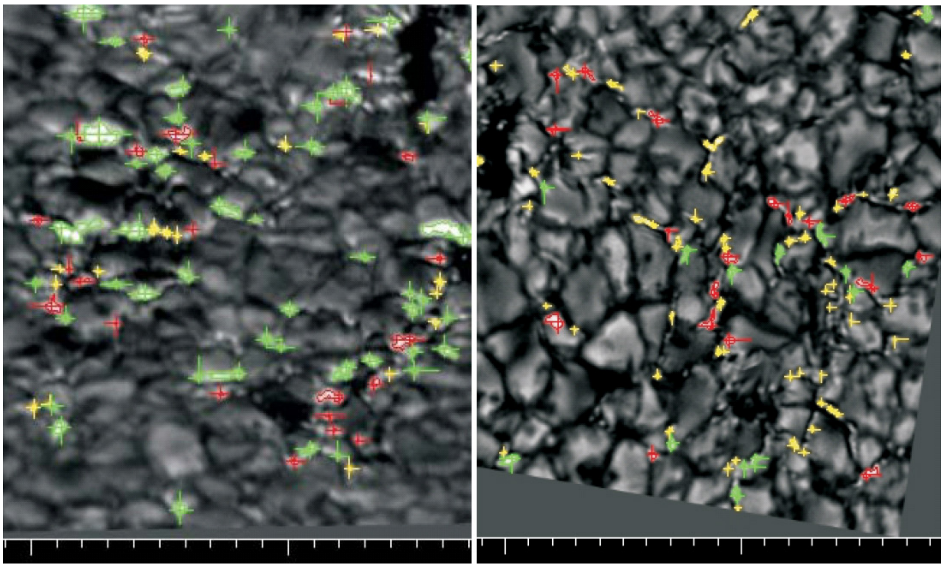

Fig. 18: Left: Near limb image (heliocentric angle = 60 degs) with mostly detected faculae (green contours). The image is oriented such that the solar radius vector points upwards in the direction of the limb. Right: Disk center image with mostly detected bright points (yellow contours). The red contours correspond to bright features classified in none of the two categories by our algorithm. Both images were recorded in the G-band. Tickmarks are at distances of seconds of arc.

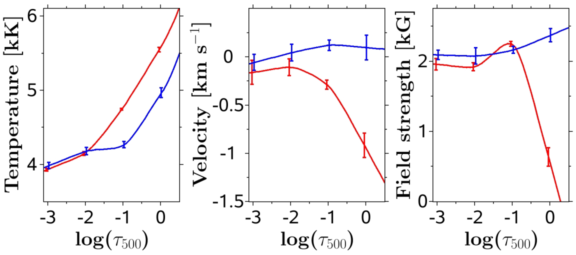


Fig. 19: Atmospheric stratification of a typical peripheral umbral dot (UD) obtained from the Stokes profiles at the location of the UD's center (red lines) and the diffuse background near the UD (blue lines). The formal errors of the inversion at the used optical depth nodes are indicated by bars. Negative LOS velocity values indicate upflows.

series of 310 images. The histogram of the effective UD diameters shows a peak at 0.31″ (225 km), which is significantly above the resolution limit. The mean filling factor is 12 % and the mean nearest neighbour distance is 0.63″ (460 km). The mean peak intensity of the UDs is 52 % of the intensity of the undisturbed photospere, and just 0.12 % of all UDs are found to be brighter than the quiet Sun, in contrast to earlier claims.

The UDs showed striking horizontal motions, moving on average at a rate of 380 ms$^{-1}$, which corresponds also to typical speeds of internetwork elements. Many UDs are seen to enter the umbra after breaking away from the penumbra and from a light bridge, while others are born inside the umbra. Brighter UDs are often found to be strung along (curved) lines and to move along these. We were able to determine the average brightness and size evolution of an umbral dot over its lifetime.

(T. Riethmüller, A. Gandorfer, A. Lagg, S. K. Solanki, and V. Zakharov)

### Validation of three methods proposed to derive the photospheric plasma motion from observed magnetic fields

The photospheric plasma and its magnetic field evolution are closely related due the high values of the magnetic Reynolds number in this region. In this sense, the photospheric plasma velocity field can be estimated from the evolution of magnetic features. Several methods have been suggested that calculate the photospheric plasma velocity field from a sequence of photospheric magnetograms: Local Correlation Tracking – LCT (November 1988), a combination of induction equation and LCT – reveals the ILCT method (Welsch *et al.*, 2004) and the Minimum Energy Fit – MEF – method (Longcope, 2004). In order to test the validity of these methods we applied them to the same model data, a spheromak magnetic field. For this sake we modeled a photospheric motion by moving the spheromak-field at the boundary by 4 pixels upward and 4 pixels horizontally at an angle of 35 degrees. The pixel size corresponds to 2 arcsec at the solar surface and the time interval between the initial and final magnetic field configurations corresponds to 1.5 hours. The velocity fields obtained by all methods differ in the horizontal direction mostly

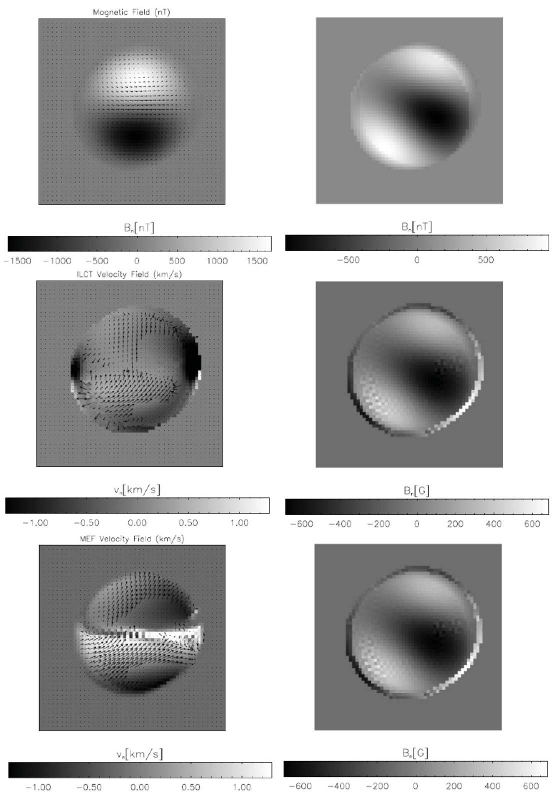


Fig. 20: Top left – three components of the magnetic field at the base of the spheromak; Top right – variation of the normal component of the magnetic field; Center left – velocity field obtained by using the ILCT method; Center right – variation of the magnetic field normal component obtained using ILCT velocity field; Botton left – velocity field obtained using MEF method; Botton right – variation of the magnetic field normal component obtained using MEF velocity field.

above the polarity inversion line and near the edge of the spheromak (boundary effect) while the vertical velocities were correctly obtained near the field reversals. Fig. 20 shows the velocity field obtained using ILCT method (Center left), the variation of the magnetic field normal component obtained using the ILCT velocity field (Center right) and the velocity field obtained using MEF method (Botton left) and the variation of the magnetic field normal component obtained using the velocity field obtained by the MEF method (Botton right).

(J. C. Santos and J. Büchner in collaboration with M. V. Alves (Sao Jose dos Campos, Brazil))

### Photospheric plasma flows preceding the 'Bastille Day' flare period

The 'Bastille Day' flare on July $13^{th}$ and $14^{th}$, 2000 was one of the strongest flare events ever observed. The multi-wavelengths observations available for this event provide rich information to study the causes of flare eruptions. One of the open questions is the possible role of the emergence and submergence of photospheric magnetized plasma flows for the eruption of flares which, in addition to the horizontal photospheric plasma motion, can influence the dynamics of the solar atmosphere located above such events. Near the polarity inversion line (PIL) the rate of flux emergence and submergence can be obtained from the observed magnetic field evolution, not, however, away from PIL. The horizontal motion in the solar photosphere cannot be directly measured as well. The observed evolution of the photospheric magnetic field can, however, provide valuable information that can be used to estimate photospheric plasma flows since the latter are closely related to the evolution of the magnetic flux.

We used three methods to estimate the photospheric plasma motion from vector magnetic field observations of the active region NOAA 9077, observed by the Huairou Solar Observing Station (HSOS) of the National Astronomical Observatories of China before and after the 'Bastille Day' flare on July $13^{th}$ and $14^{th}$, 2000 (Fig. 21).

Our analysis shows that the velocity fields obtained by LCT, ILCT and MEF reveal results of different reliability in dependence on the strength of the vertical magnetic field. Generally the more accurate ILCT and MEF methods provide larger values of the horizontal plasma velocities than those obtained by LCT. The vertical plasma flow velocity components, which can be obtained only by ILCT and MEF, reveal both emerging and submerging flows, the highest flow velocities were obtained in regions of weak vertical magnetic fields, in particular near field reversal lines. Outside these regions ILCT and MEF provide quite different results for emergence and submergence, there their reliability with respect to the determination of up- and downflows is very limited.

(J. C. Santos and J. Büchner in collaboration with H. Zhang (National Astronomical Observatory, Bejing, China))

### Derivation of the photospheric plasma motion in AR 8210 in preparation of Hinode observations

After its successful launch the Hinode spacecraft is providing excitingly high resolution optical observations of the solar corona and simultaneously determines photospheric vector magnetic fields. In order to investigate the relation between the observable highly structured coronal dynamics or, e.g., the eruption of solar flares, with the observed photospheric magnetic

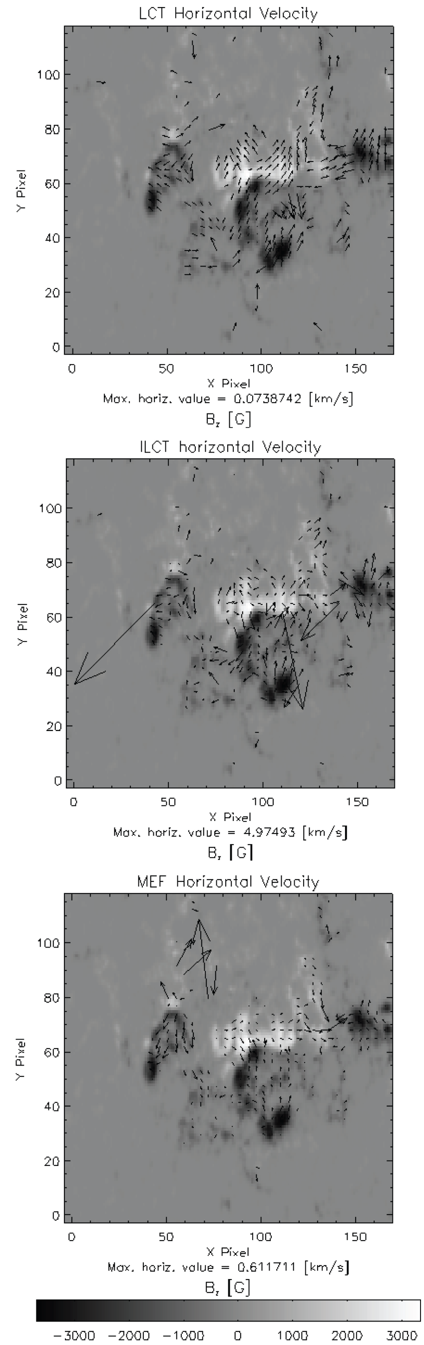


Fig. 21: Horizontal velocity obtained from the evolution of the photospheric magnetic field measured for AR9077 between July $13^{th}$, at 02:50 UT, and July $14^{th}$, at 10:25 UT. The arrows show the velocity direction and the gray scale depicts the vertical component of the magnetic field.

fields it is necessary to combine the two ends of the cause-consequence chain. This is possible, practically, only by means of numerical simulations (see the contribution "Investigation of reconnection in the solar corona by Hinode observations"). For forward numerical simulations starting from photospheric observations it is, however, necessary to know not only the photospheric vector magnetic fields, but also the photospheric plasma motion. The photospheric plasma velocities might be estimated by using the observed evolution of the magnetic field. Several methods have been suggested that calculate the photospheric plasma velocity field from a sequence of photospheric vector magnetograms: Starting with a local correlation tracking – LCT – and combining it with the induction equation for the vertical magnetic field component Welsch *et al.* (2004) developed the ILCT method and Longcope (2004) the Minimum Energy Fit (MEF) method. In order to verify the applicability of these methods for their future use in interpreting Hinode observations we tested them using vector magnetograms of AR8210 obtained on 1 May 1998, between 17:13 UT and 21:29 UT.

The results obtained for the horizontal and vertical components of the velocity are shown in Fig. 22. The upper plot corresponds to the ILCT method, the lower to MEF. As a result ILCT revealed a pattern which agrees well with earlier, independent investigation of the photospheric flows in AR 8210, while the results of MEF are less plausible. The reason might be that they seem to depend critically on the choice of the area covered, while ILCT depends more on the local magnetic field properties.

(J. C. Santos and J. Büchner)

**On the relations between chromospheric emissions and magnetic field in the quiet Sun**

Chromospheric brightness recorded in the UV and in the cores of strong spectral lines is known to depend on the underlying photospheric magnetic field. Similar relations are also expected at millimeter wavelengths, but have never been determined. We analyzed observational data from 4 instruments, including UV images at 1600 Å from TRACE, Ca II K-line filtergrams from BBSO, radio images at 3.5 mm from the Berkeley–Illinois–Maryland Array (BIMA) and MDI/SOHO longitudinal photospheric magnetograms (Fig. 23). For the first time interferometric millimeter data with the highest currently available resolution were included in such an analysis.

We found a power law to be a good representation for the relationship between photospheric magnetic field and emissions from chromospheric heights at all wavelengths. Power laws also describe the various flux-flux relationships, irrespective of the considered resolution.

Our analysis also shows that the dependence of chromospheric brightness on magnetic field is quite dif-

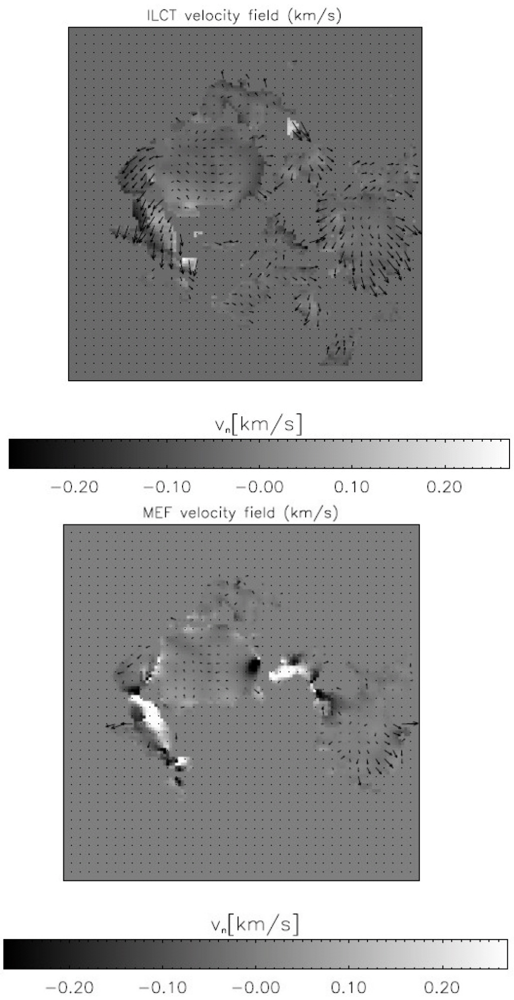


Fig. 22: Horizontal velocity obtained from the evolution of the photospheric magnetic field of the active region AR 8210 on 1 May 1998 between 17:13 UT and 21:29 UT. The arrows indicate the horizontal velocity direction and the gray scale depicts the vertical component. The upper plot depicts the results obtained by using the ILCT method, the lower those obtained by a MEF.

ferent for the network and internetwork regions. The power-law exponents in the relation between Ca II K-line intensity (or TRACE 1600 Å intensity) and network magnetic flux are found to be similar to those obtained by Schrijver *et al.* (1989) for active regions (power law exponent of $\simeq$ 0.6). In contrast almost no dependence of Ca II K-line, 1600 Å and 3.5 mm intensity on magnetogram signal was found in the internetwork. This result supports the idea that different heating mechanisms are acting in the internetwork (acoustic) and network (magnetic).

(M. Loukitcheva and S. K. Solanki in collaboration with S. White (University of Maryland, USA))

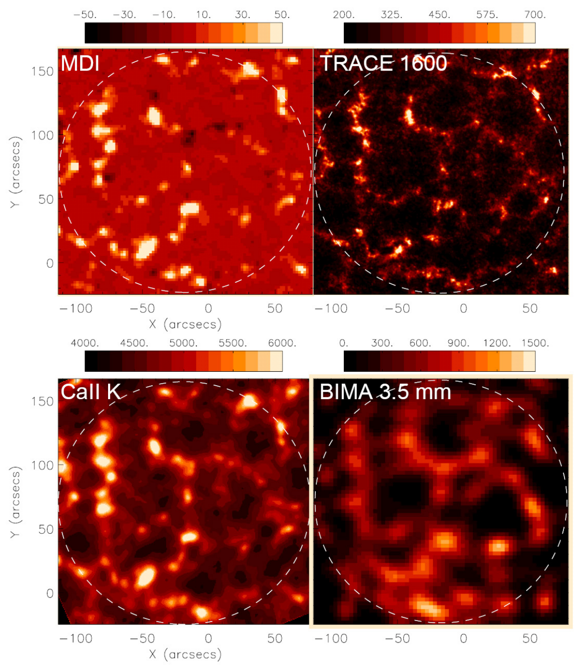


Fig. 23: Portrait of the quiet solar chromosphere at the center of the Sun's disk at 4 wavelengths. From top left to bottom right: MDI longitudinal photospheric magnetogram, UV 1600 Å image from TRACE, Ca II K-line center image from BBSO and BIMA image at 3.5 mm.

### Measurement of the magnetic canopy

Measurements have been carried out with the goal to answer the question whether the concept of a magnetic canopy – horizontal magnetic field lines spanning over the supergranular cells at a heigh of 800 to 1500 km – is correct. The canopy concept was introduced by Gabriel (1976) and Giovanelli (1980). In the following years research activities concentrated on the determination of the parameters of the canopy magnetic field, like height above the photosphere and magnetic field strength. Also, the first models explaining how low-lying canopies can be produced were constructed (Solanki and Steiner, 1990). Schrijver and Title (2003) fundamentally questioned the canopy concept: the presence of unresolved, relatively strong inter-network field concentrations of the order of a few Mx cm$^{-2}$ destroy the classical, wineglass shaped canopy.

First attempts to measure the weak fields of the magnetic canopy using the He I 10830 Å line are presented in Fig. 24: the Stokes vector represents a $2'' \times 2''$ average over the central part of a supergranular cell. The observation was obtained with the new TIP-2 instrument at the German Vacuum Tower Telescope, the heliospheric angle was 60° ($\mu = \cos\Theta = 0.5$). Clearly, a Stokes $V$ signal is present. An inversion involving Zeeman and a simplified version of Hanle diagnostics

(Lagg *et al.*, 2004) reveals magnetic field strengths of $< 100$ G and an inclination angle with respect to the solar surface of 60° to 120°.

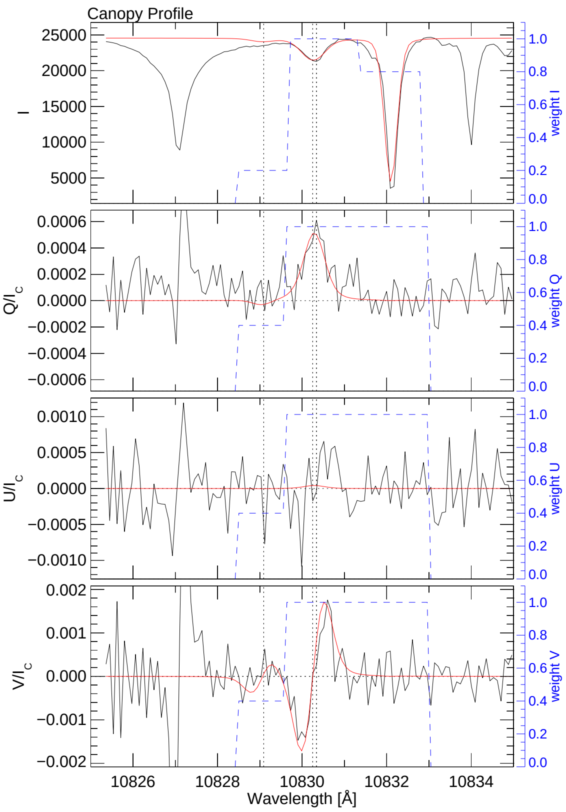


Fig. 24: Observation of a quiet region: the measured Stokes vector (black) was analyzed using a Milne-Eddington type inversion (Lagg *et al.*, 2004). The best-fit profile is shown in red. The values obtained for the magnetic field vector are $|B| < 100$ G, inclination to the solar surface $\gamma = 60 - 120°$. The dashed blue line shows the weighting scheme used for the inversion.

The presence of a significant Stokes $V$ signal and the absence of measurable linear polarization resulting from the Zeeman effect above a supergranular cell (see Fig. 24) point to the fact that a significant portion of the magnetic field lines is rooted in the network, in contradiction to the Schrijver and Title (2003) model. Further analysis of this data set, especially the proper treatment of the Hanle effect, responsible for the linear polarization signal, is required to confirm the presence of the canopy. Additionally, the measurement must be repeated over multiple supergranular cells at different $\mu$ values.

(A. Lagg, S. K. Solanki, J. Woch, and A. Gandorfer)

### Velocity distribution of chromospheric downflows

An unexpected result found by Lagg *et al.* (2007) was the presence of a strongly supersonic downflow in the chromospheric layers of an emerging flux region. However, it was not clear how common such downflows are nor what their properties can be. We have analysed the velocity distributions of a large dataset composed of 35 maps of the Stokes $I$, $Q$, $U$, and $V$ profiles of nine active regions and four rasters of quiet Sun areas obtained in the chromospheric He I 1083.0 nm triplet. The data were recorded at the Tenerife Infrared Polarimeter (TIP) at the German Vacuum Tower Telescope (VTT) of the Spanish observatory of Izaña, Tenerife. The line-of-sight velocities were determined by applying a multi-Gaussian fit to the intensity profiles. Single and double component fits were carried out for all datasets. In order to characterise all scanned regions, every observed dataset was divided in regions showing a magnetic signal (*magnetic regions*) and no magnetic signal (*'field free' regions*). We find that 18.7% of all observed pixels show strong downflows as evidenced by a second line profile component, generally shifted by more than 8 $\mathrm{km\,s^{-1}}$ relative to the rest wavelegth, while 12.1 % of all observed pixels show supersonic downflows above 10 $\mathrm{km\,s^{-1}}$. The distribution of these strong downflows displays two distinct populations. The slower one (near sonic and weakly supersonic flows) has line-of-sight velocities up to 17 $\mathrm{km\,s^{-1}}$ and is associated with moderate to strong magnetic signal (see Fig. 25). Strongly supersonic downflows (reaching up to 60 $\mathrm{km\,s^{-1}}$) are found at places with weak to moderate magnetic signal. We find that rapid downflows are in most cases associated with pores and sunspots, although they often do not exactly overlie them. However, strong downflows are also seen in the quiet Sun, far away from any magnetic activity.

(R. Aznar Cuadrado, S. K. Solanki, and A. Lagg)

### Spectropolarimetric observations of the He I 10830 Å multiplet in an active region filament

Atlthough the magnetic structure of quiet prominences and filaments has been revealed through Hanle-effect measurements, very little is known about the magnetic field in active prominences or filaments. We analysed full Stokes vector measurements of the chromospheric He I 10830 Å multiplet in an active region filament during a flare, i.e. when the filament was in its phase of activity. The data were recorded with the new Tenerife Infrared Polarimeter (TIP 2) at the German Vacuum Tower Telescope (VTT). During observations on 2005 May 18, a flare of GOES class C2.0 erupted in the west part of the active region NOAA 10763 causing, most probably, the activation of the filament. In the scanned region, the filament and the flare ribbons were visible in the H$\alpha$ slit jaw camera images.

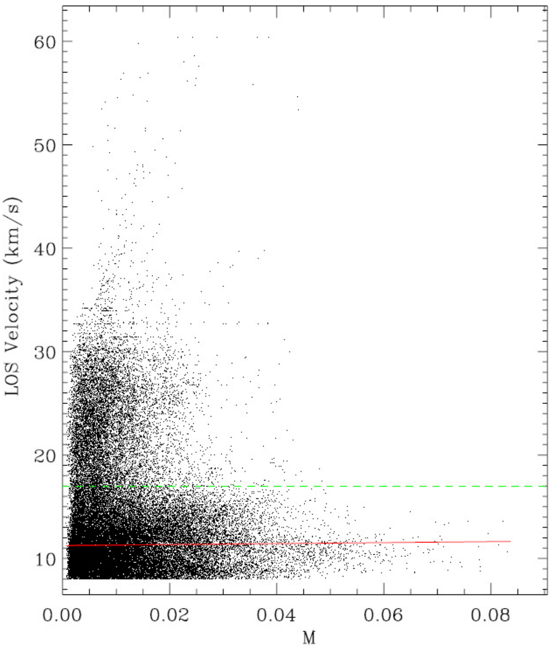


Fig. 25: Scatter plot of the LOS velocities measured in the second component of the chromospheric He I 1083.0 nm line versus the magnetic field signal $M$ defined as $M = \sqrt{Q^2 + U^2 + V^2}/I_c$, where $I_c$ is the continuum intensity. The green dashed line represents an imaginary boundary of the two distinct populations of the chromospheric downflows distribution. The red solid line shows a linear fit to the slower population.

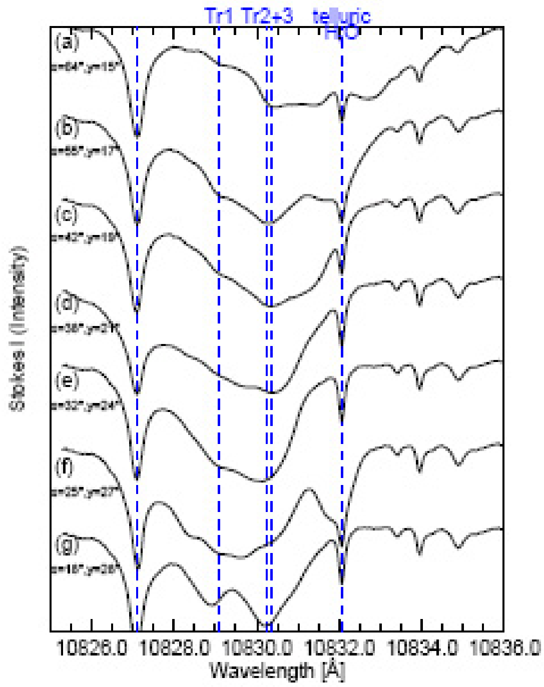


Fig. 26: Examples of the observed Stokes $I$ profiles, with their pixel positions marked on their left side.

The analysis of the He Stokes profiles observed during the scan reveals huge differences in the profile shapes. In Fig. 26 we present some examples of observed Stokes $I$ profiles at different pixel positions. At the top we see a profile displaying a very strong redshift, while the lower profiles exhibit an increasing amount of blueshift.

In some profiles of Fig. 26, e.g., (b) and (c), blueshifted and redshifted components of the He multiplet coexist.

Line-of-sight velocities and the magnetic field vector values in the chromosphere are deduced from the observed Stokes profile by applying an inversion code to the He I lines. In particular, we measure supersonic upflows with velocities up to 60 km/s and supersonic downflows with velocities up to 100 km/s in the filament.

The inversion of the whole map shows that the He blueshifted components belong to mostly transversal field lines in the body of the filament. These field lines are found to be curving upwards on both sides of the filament. This picture suggests the presence of dipped field lines that are moving upward, carrying with them the filament material. During this movement, we also observe filament material flowing down along field lines having the same polarity as the photospheric field (i.e. they have the opposite inclination with respect to the dipped field lines). These downflows are faster at the filament end points. The field lines are found to be almost parallel to the filament axis in the plane perpendicular to the line of sight. The two main theoretical models of prominence support (dip or flux rope models) have been used to interpret the results obtained. Even if the observed dipped field lines are predicted by both models, globally our observations can be explained better in terms of the flux rope model than the dip model.

(C. Sasso, A. Lagg, S. K. Solanki, and R. Aznar Cuadrado in collaboration with M. Collados (IAC))

### Chromospheric fibrils observed in Ca II *K*

In August 2007 a multi-channel polarimetry and imaging campaign was carried out at the Swedish Solar Telescope (SST) in La Palma, Canary Islands. Photometric observations in the Ca II *K* 3934 Å line and two continuum wavelengths were combined with imaging spectro-polarimetric scans through the Zeeman-sensitive Fe I 6302 Å line.

The Ca II *K* line is used to probe the structure of the solar chromosphere. Former observations of that line typically show a structure of diffuse brigthenings in magnetic regions and an even more diffuse pattern produced by various wave motions. This appearance is different from chromospheric observations using other spectral lines, e.g. H$\alpha$ which typically show a filamentary structure of so-called mottles or spicules.

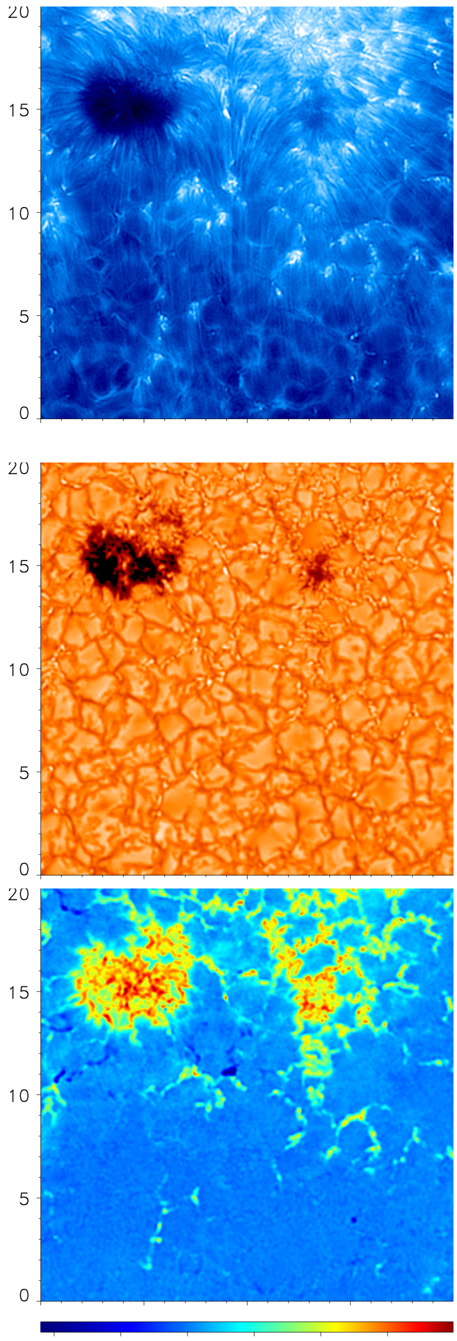

Fig. 27: Ca II $K$ 3934 Å line center image, red continuum image and line-of-sight magnetic field map of active region NOAA 10966. The region is located at a heliographic position of $\mu = 0.99$. Axis labels are given in Mm.

The present observations were obtained with a rather narrow filter of only 1.1 Å width which keeps the chromospheric contributions in the filtergrams in active and network regions high. In addition, the data were obtained by using the SST adaptive optics system and were reconstructed from seeing effects using speckle interferometric techniques. Thus the spatial resolution of resulting data is close to the diffraction limit of the SST which is about 0.1 arcsec at the wavelength of Ca II $K$ (72 km). These high resolution observations (see Fig. 27) show for the first time a clear filamentary structure of the chromosphere as seen in Ca II $K$. The width of the observed filaments is on average around 0.13 arcsec which is significantly smaller than the well-known H$\alpha$ fibrils. The fibril length is small in regions of strong magnetic activity and spreads out to lengths up to more than 10 arcsec above quiet regions. The bright endpoints of the fibrils are clearly co-spatial with photospheric magnetic field concentrations (pores, bright points). The natural interpretation of these fibrils is that they follow the magnetic canopy, a horizontal magnetic field overlying comparatively field-free gas in the lower chromosphere internetwork regions.

Using time series of Ca II $K$ filtergrams the dynamics of these fibrils can be characterized. Several kinds of dynamic phenomena are clearly discernible. Power maps calculated in various frequency bands indicate that fibrils in plage regions channel waves with frequencies below the acoustic cutoff frequency into the chromosphere and fibrils extending over quiet Sun form a canopy structure that suppresses oscillations from below.

(A. Pietarila, J. Hirzberger, V. Zakharov, and S. K. Solanki)

### The intensity contrast of solar granulation: comparing Hinode results with MHD simulations

The root-mean-square of the normalized continuum intensity fluctuations within an area on the solar disk is mainly determined by the intensity variation between the bright granules and the darker intergranular lanes and thus usually referred to as the *granulation contrast.* It is a key property of solar surface convection since it is connected with the temperature difference between rising (granules) and descending gas masses (intergranules) and thus related to the efficacy of the convective energy transport. Reliable measurements of the granulation contrast are notoriously difficult since the observed contrast suffers significantly from image degradation by the optical system and, most importantly in the case of ground-based telescopes, by seeing and straylight effects due to the terrestrial atmosphere.

A new era has begun with the launch of the 50-cm Solar Optical Telescope (SOT) on the *Hinode* satellite. The good performance and low straylight level of the spectro-polarimeter, together with the complete absence of atmospheric effects, open the possibility to obtain a much more reliable determination of the granulation contrast at 630 nm. In Fig. 28 we have compared the intensity contrast of a *Hinode* Spectro-Polarimeter continuum map of the quiet Sun with the prediction from an MHD simulation with the MURaM code.

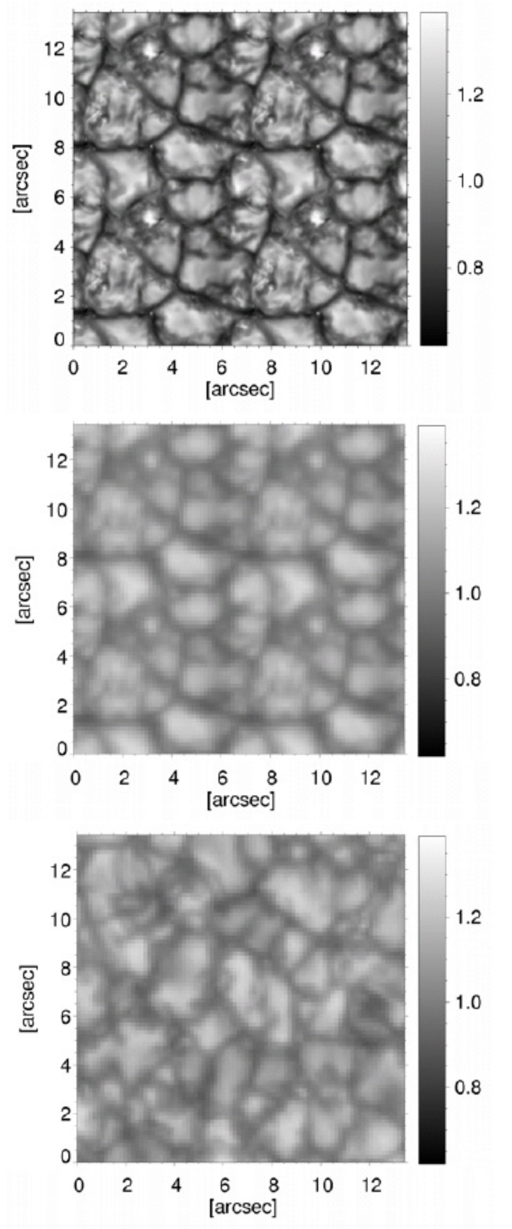


Fig. 28: Continuum images at 630 nm from the simulation snapshot with original resolution *(top panel)* and after degrading *(middle panel)*, in comparison with a detail of the observed Hinode/SP map of the same size *(bottom panel)*. The periodic simulation box is shown fourfold for better visibility.

While the discrepancy between the original contrast on the basis of the simulation (14.4 %) and the observed contrast (7 %) is large, consideration of the basic optical properties of the *Hinode* system and a slight defocus are sufficient to bring the degraded contrast of the 3-D radiative MHD simulation and the observed rms continuum contrast at nearly into agreement. The remaining discrepancy (of about 0.4 % in contrast) can be ascribed to the combined effects of straylight, other low-order optical abberations, and instrument electronics.

(S. Danilovic, A. Gandorfer, A. Lagg, M. Schüssler, and S. K. Solanki in collaboration with A. Vögler (University of Utrecht), Y. Katsukawa and S. Tsuneta (National Astronomical Observatory of Japan))

### Strong horizontal magnetic field in a surface dynamo simulation

Observations with the spectro-polarimeter aboard the *Hinode* satellite have revealed strong (and actually dominant) horizontal magnetic fields in the 'quiet' solar photosphere, i.e., outside active regions and network. We have examined the results of numerical 3-D radiative MHD simulations with the MURaM code in order to understand the origin of such strong horizontal fields. As shown in Fig. 29, we find dominating horizontal fields in the middle photosphere consistent with the *Hinode* observations in the case of surface dynamo runs, where turbulent shear flows in the intergranular lanes generate a strongly intermittent magnetic field from a small seed field. This dynamo-generated field is of mixed polarity on small horizontal length scales, so that the unsigned vertical flux decreases strongly with height: patches of opposite-polarity flux are connected by low-lying loops, whose height scale is roughly comparable to the horizontal distance of their footpoints. As a consequence, the horizontal field component dominates over the vertical optical depth unity. In addition, the overturning granular upflows lead to an expulsion of horizontal flux, so that horizontal magnetic field loops form above granules.

(M. Schüssler in collaboration with A. Vögler (University of Utrecht))

### Comparison of magnetoconvection simulations with the approximation of thin flux tubes

The structure and dynamics of small vertical photospheric magnetic flux concentrations has been often treated in the framework of an approximation based upon a low-order truncation of the Taylor expansions of all quantities in the horizontal direction, together

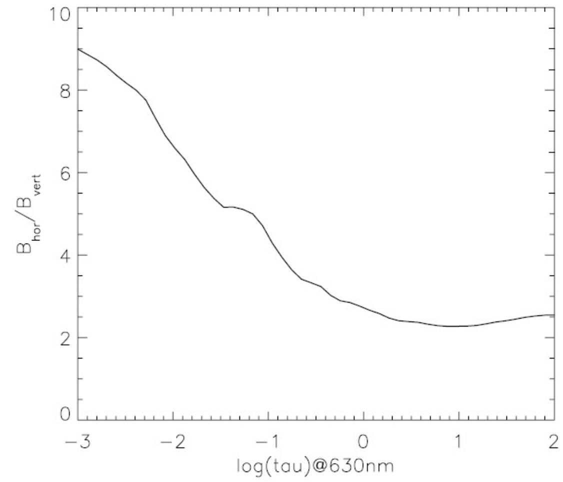


Fig. 29: Ratio of the root-mean-square of the horizontal field component to the horizontally averaged unsigned vertical field as a function of continuum optical depth at 630 nm wavelength, $\log(\tau_{630})$. In the optical depth interval $-2 < \log(\tau_{630}) < -1$ (relevant for the formation of the FeI lines used in the *Hinode* spectro-polarimeter), the ratio is roughly in the range 4–6. This is consistent with the estimates derived on basis of the observational results (cf. Lites et al., 2008).

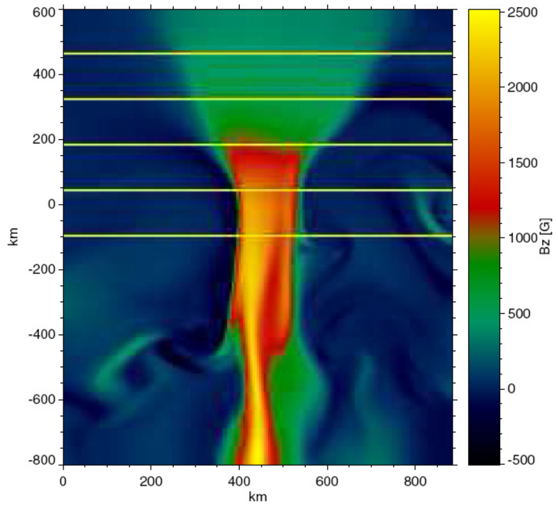


Fig. 30: Vertical cut through a simulated magnetic flux sheet. Colours indicate the vertical magnetic field strength. Zero on the vertical scale corresponds to the average height of optical depth unity. The horizontal lines indicate the height levels along which the magnetic field profiles are drawn in the subsequent figure.

with the assumption of instantaneous total pressure balance at the boundary to the non-magnetic external medium. Formally, such an approximation is justified if the diameter of the structure (a flux tube or a flux sheet) is small compared to all other relevant length scales (scale height, radius of curvature, wavelength, etc.). The advent of realistic 3-D radiative MHD simulations opens the possibility to check the consistency of the approximation with the properties of the flux concentrations that form in the course of the simulation. An example of such comparison is described here. Fig. 30 (from a simulation with MURaM code) shows the magnetic field strength in a vertical cut through a magnetic flux sheet that has formed in an intergranular lane. Fig. 31 shows horizontal profiles of the vertical magnetic field component at various heights in comparison with the profiles derived on the basis of the static thin flux tube approximation (up to second order). The curvature of the profiles in the upper layers reflects the growing importance of the magnetic curvature force. Altogether, the comparison indicates that the approximation is not inconsistent with the results of full 3-D simulations. The differences between approximation and simulation are due to the asymmetry and the dynamics of the simulated structure.

(L. Yelles, M. Schüssler, and S. K. Solanki)

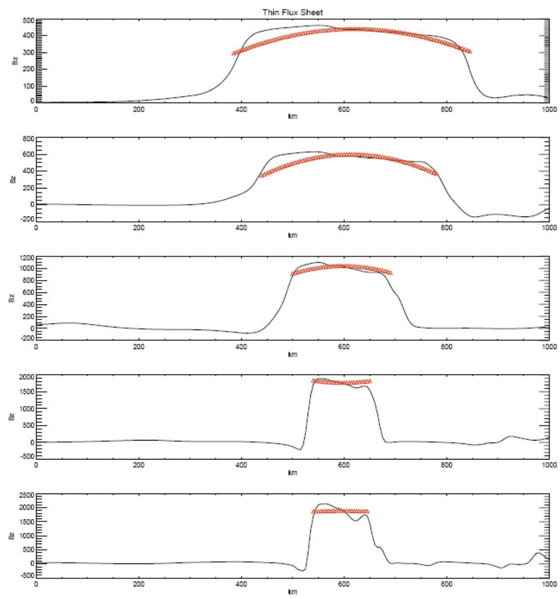


Fig. 31: Profiles of the vertical magnetic field component along the horizontal lines in the previous figure. The black lines show the results from the simulation, the red symbols indicate the corresponding profiles according to the second-order approximation of thin flux tubes (modified for the case of flux sheets).

## Evidence of magnetic field wrapping around penumbral filaments

The constant high-spatial resolution of spectropolarimetric observations from the Solar Optical Telescope on-board the Hinode spacecraft allow the fine structure of the penumbral magnetic fields to be investigated at a new level of detail and precision. The Stokes vector of two neutral iron lines at 630 nm is inverted at every spatial pixel to retrieve the depth-dependence of the magnetic field vector, line-of-sight velocity and thermodynamic parameters. We show that the measured Stokes spectra are consistent with the wrapping of an inclined field around the horizontal filaments. The wrapping effect is stronger for wider filaments. In addition, we find that the external magnetic field can penetrate into the intraspines, leading to non-radial magnetic fields inside them. Such a structure of the penumbral magnetic field has been predicted by different models of penumbral fine structure, but never been resolved observationally.

(S. K. Solanki in collaboration with J. M. Borrero and B. W. Lites (High Altitude Observatory, Boulder, USA))

## Discovery of inward moving magnetic enhancements in sunspot penumbrae

Sunspot penumbrae show a fine structure in continuum intensity which displays considerable dynamics. In particular, bright penumbral gains are found, which constantly move in the direction of the umbra. The magnetic field, in contrast, although also highly structured, has so far appeared to be relatively static.

Using continuum images, longitudinal magnetograms and Dopplergrams, recorded in high resolution mode by the Michelson Doppler Imager (MDI) instrument on the Solar and Heliospheric Observatory (SOHO), we probed the evolution of magnetic features in the inner penumbrae of two regular sunspots, and characterized their fundamental properties. The relationship between magnetic features, corresponding brightness in continuum images and Dopplergrams was also considered.

We noted local enhancements of the line-of-sight (LOS) component of the magnetic field in the inner part of the penumbral region that move inward towards the umbra-penumbra boundary with a radial speed of about 0.3 km $s^{-1}$. These local inward-moving enhancements of the LOS component of the magnetic fields appear to be relatively common. They are associated with dark structures and tend to display downflows relative to the penumbral background. We also confirmed the presence of outward moving magnetic enhancments in the outer half of the penumbra, which turn into moving magnetic features upon leaving the sunspot. The behaviour of both the inward moving and the outward moving magnetic enhancements is consistent with the rising flux-tube model of Schlichenmaier (2002).

(S. K. Solanki and J. Woch in collaboration with J. Zhang (National Astronomical Observatories, Beijing, China))

## Evidence of convective rolls in a sunspot penumbra

The structure of sunspot penumbrae has been enriched by the recent discovery of twisting motion of penumbral fibrils by Ichimoto et al. (2007). In order to constrain the geometry and the associated magnetic field of such penumbral filaments we observed a mature sunspot, located at heliocentric angle $\theta = 40.5^o$, using the 1-m Swedish Solar Telescope (SST). We obtained high-quality full Stokes vector scans over the Fe I ($\lambda = 630.2$ nm) line simultaneously with high-resolution images in the blue continuum and in the G-band. The near-diffraction limited spatial resolution ($\approx 0.11$ arcsec in the blue channel and $\approx 0.25$ arcsec in the spectro-polarimetric data) was achieved by applying speckle image reconstruction techniques.

We confirmed the presence of continuous lateral motions, directed towards disc-center, of dark and bright features across bright filaments, leading to a visual impression of rotations around their axes. The limb-side of the filaments clearly shows blue shifts whereas its center-side is red shifted. The LOS velocity changes by $\Delta v \approx 0.9\,\mathrm{km\,s^{-1}}$ which is in good agreement with the horizontal motions obtained in the blue continuum. The profile looks very asymmetric, so that the blue shift is much stronger than the red shift. The center-ward side of the filament has enhanced magnetic field strength and greatly reduced inclination, whereas at the limbward side the magnetic field is weaker and almost horizontal.

To explain the observed signature we proposed a qualitative model shown in Fig. 32. In this model, bright filaments with reduced and strongly inclined magnetic field are embedded in the more vertical and stronger magnetic fields, which are highly evacuated. These filaments have internal convective flows, e.g. in form of rolls, moving upwards at the center of the filaments and downwards at their sides. This can explain apparent lateral motions seen in the center-ward sides of the filaments oriented perpendicularly to the line-of-symmetry of the sunspot when they are viewed away from the solar disc center. Such convective rolls have reduced magnetic field which is oriented horizontaly along the filament.

(V. Zakharov, J. Hirzberger, and S. K. Solanki)

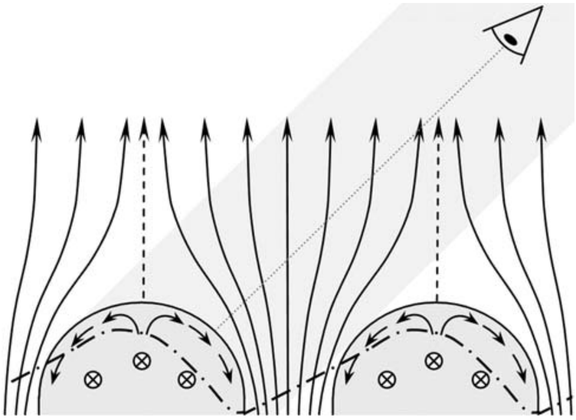

Fig. 32: Schematic illustration of the field and flow structure in penumbral filaments. The dashed-dotted line delineates the unit optical level ($\tau_c = 1$). Vertical arrows denote magnetic field lines and thick arrows inside the filaments outline convective flows. Circled crosses inside the filaments indicate magnetic fields inside the filaments oriented along their axes.

### Magnetic structures of an emerging flux region in the photosphere and chromosphere

We present maps of the full magnetic field vector of an emerging flux region in both the photosphere and chromosphere, which was based on spectropolarimetric observations by the Tenerife Infrared Polarimeter II (TIP II) mounted on the Vacuum Tower Telescope (VTT). This study goes beyond that published by Solanki *et al.* (2003) in: (1) TIP II was used to get a bigger field of view with higher spatial and spectral resolution than TIP; (2) We scanned this region with the slit parallel to the dark loop-like structures monitored by the H$\alpha$ slit-jaw images, enabling us to observe an entire loop at the same time.

A reliable inversion based on the Milne-Eddington approximation was performed to the full Stokes vectors of the chromospheric He I 10830 Å line and the photospheric Si I 10827.1 Å line. The magnetic and velocity structure of freshly emerged loops are determined in both atmospheric layers. We find that: (1) the magnetic vector in the upper chromosphere is more regular than in the photosphere. In both layers the field is close to horizontal in the emergence zone and relatively vertical in the footpoints. In the photosphere, small patches of dipolar features are observed within the emergence zone, known as Moving Dipolar Features (MDFs). In the upper chromosphere, however, there is no counterpart for those features; (2) the magnetic field strength decreases with height as the magnetic flux is expanding. The field strength within the emergence zone varies from 300 to 600 G in the photosphere and drops to below 300 G in upper chromosphere. The gradient of the longitudinal magnetic component is 0.3 G/km inside the footpoints; (3) Following the technique of Solanki (2003), a series of shallow horizontal young loops are reconstructed in 3 dimensions based on the magnetic field vector in the upper chromosphere.

(Z. Xu, A. Lagg, and S. K. Solanki)

## Solar transition region and corona

### Magnetic structure of the solar transition region as observed in various ultraviolet lines emitted at different temperatures

The solar atmosphere is known to be structured on all scales by the Sun's magnetic field, which controls the mass supply to the solar corona and the energy and momentum transport of the coronal plasma. Our knowledge of the magnetic field in the transition region (TR) and corona mainly stems from the extrapolation of the field as measured in the photosphere and chromosphere. The new aspect of our analysis is the correlative use of plasma and field measurements, e.g. stemming from SUMER and MDI on SOHO, together with the coronal magnetic field as obtained by force-free-field extrapolation. Similar analyses have already been carried out to study the plasma flows in actice regions, to link flows and fields in an equatorial coronal hole, and to study the solar wind origin in a coronal funnel (see the previous Annual Report 2004/2005).

Here the structure of the solar transition region in a polar coronal hole of the Sun is studied. In particular, the detailed association of the coronal magnetic field with the radiance patterns as seen in various far ultraviolet (FUV) emission lines is investigated. A comparison on small scale is made of the coronal magnetic field, as obtained by extrapolation of the photospheric field to heights of several tens of megameters, with the radiance maps of several FUV lines, which are emitted by ions of various elements at different ionization stages and correspond to different local coronal temperatures. By a correlation analysis of the emission pattern with the magnetic field (network and carpet of loops), the so-called correlation height of the emission can be determined.

In particular, at mesoscopic scales of several megameters the regions with strong emission (originating from multiple small closed loops) are found to be located at low heights, whereas weak emissions (coming from locally open, i.e. farther reaching fields) appear to originate at greater heights. These findings are consistent with similar results obtained at large scales for large loops and big coronal holes. Our correlation-

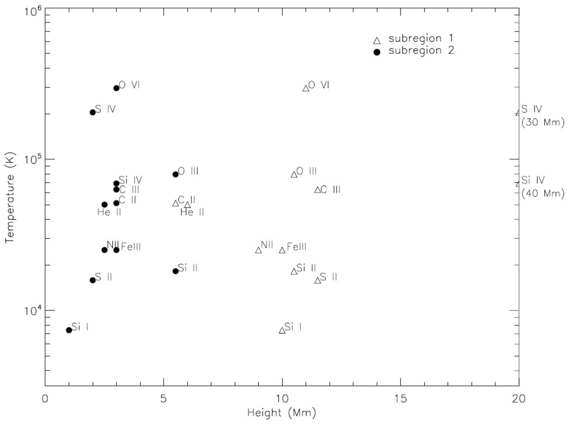


Fig. 33: Ionization temperatures and the correlation heights of 12 selected emission lines in two different sub-regions of a polar coronal hole. The triangle symbol indicates the data from sub-region 1 (open funnel), while the filled-circle symbol shows the data from sub-region 2 (closed loop).

height analysis of the FUV emission lines confirms the notion that plasma at different temperature can coexist at the same height. This fact is illustrated in Fig. 33 which shows the results for two regions (funnel and loop) in a coronal hole. In conclusion, the TR there is not thermally stratified but strongly nonuniform and magnetically structured.

(E. Marsch in collaboration with G.-Q. Zhuo, J.-S. He, and C.-Y. Tu (Department of Geophysics, Peking University, Beijing, China))

## Current-free electric double layer in coronal funnel

Current-free double layers (CFDLs) have been recently discovered in a number of laboratory devices, when a low collisional plasma is forced to expand from a high magnetic field source region to a low magnetic field diffusion region. This experimental setup bears a striking resemblance to the natural conditions prevailing in the magnetic funnels of the solar corona. It was commonly thought that magnetic-field-aligned potential disruptions were driven by electron currents, although the theoretical possibility of a CDFL has been known of for some time. Given its recent experimental verification, we make a contribution to solar plasma physics by investigating the possibility of CFDLs in coronal funnels, which have much in common with the laboratory experiments.

This work does not call on the traditional explanations of solar wind plasma supply and initial acceleration; rather, we suggest that the basic mechanism lying at the origin of the solar wind is ion acceleration through an electrostatic double layer created by chromospheric plasma expanding upward in a coronal funnel. For both coronal funnels and the plasma vessel, the plasma density decreases proportionally to the magnetic field, the magnetic fields are of the same order of magnitude, and the plasma acceleration is almost the same, leading to a typical speed of 10 km $s^{-1}$. In the laboratory experiments, the electrons heated by the applied radio frequency in the source supply the power for the double layer, whereas in case of the solar atmosphere an electron energization mechanism still has to be identified at the bottom of a funnel. Nevertheless, we believe that a CFDL is a way to accelerate the plasma up into the corona.

(E. Marsch in collaboration with R. W. Boswell and C. Charles (Research School of Physical Sciences and Engineering, Australian National University, Canberra, Australia))

## Plasma outflows and open magnetic fields in a quiet-sun region

It is well known that the fast solar wind mainly originates in coronal holes. Whether quiet-Sun regions are also sources of the solar wind is an open question, which we study here by using the ultraviolet spectra and magnetic-field data obtained from SOHO. The previous finding of relatively large blue shifts at the intersections of magnetic network boundaries at middle solar latitudes is confirmed. However, we believe that these intersection sites are not the sources of the solar wind. To show this, we make a potential-field extrapolation of the magnetic field from the photosphere into the corona up to 80 Mm height, which is together with an EIT image presented in Fig. 34. It indicates that many of those network intersections that are associated with blueshifts are not related to open field lines. Only the regions appearing dark in the Fe XII 19.5 nm image, may be considered as genuine sources of solar wind, because their pattern seems to be consistent with the distribution of open field lines.

The outflows from the strong blue-shift locations may just feed plasma to the magnetic carpet, i.e. to the closed-field loops in the solar transition region and lower corona. The dark regions in the Fe XII image of EIT could correspond to real sources of solar wind, but since a weak outflow cannot feed much plasma into a magnetic tube from its bottom, the original material for the solar wind still must be provided by side flows, and is perhaps released by reconnection. It is also possible that the open field lines are just small threads of a large coronal loop. The low density and low field strength inside the loop will then result in weak ultraviolet emission. If we reduce the top height from 80 to 40 Mm, the pattern of the cross points at 20 Mm of

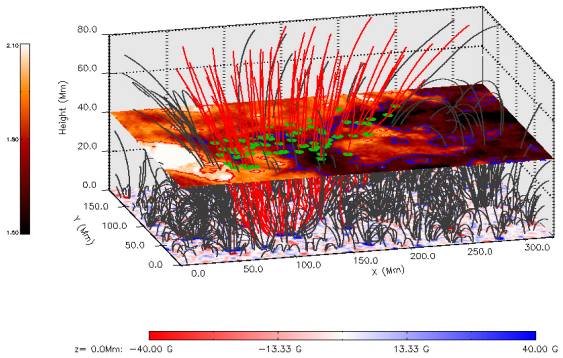


Fig. 34: Illustration of the 3-D coronal magnetic field lines. The foot points of the field lines at $z = 0$ Mm have a $|B_z|$ that is larger than 7.5 gauss. The red colour denotes open field lines and black closed ones. The Fe XII radiance (colour coded by the left vertical bar) image is placed at the inferred emission height of 40 Mm. The intersection points (green dots) of the open field lines with the plane at 40 Mm do not everywhere, yet mostly coincide with regions of low radiance.

the open field lines may compare better with the dark regions in the 19.5 nm EIT image. Thus there remains an uncertainty in fixing the true height of the source region of the low emission.

(E. Marsch in collaboration with C.-Y. Tu and J.-S. He (Department of Geophysics, Peking University, Beijing, China))

### The inverse Evershed effect in transition region emission as observed by SUMER

One of the most peculiar spectroscopic signatures of sunspots is the observed opposite shift of spectral lines observed in (disk) center-ward and limb-ward penumbral areas. The effect was discovered one century ago in photospheric lines by Evershed at Kodaikanal and named after him. In the photosphere, blueshifts are always observed in the center-ward side of the penumbra and are, since then, generally interpreted as nearly horizontal flows directed outward from the sunspot umbra.

Such flows reach speeds of few km/s and appear to be mainly associated to dark penumbral channels when observed at $< 1''$ resolution. In contrast, an opposite flow at higher atmospheric layers (chromosphere and transition region) into the sunspot is also observed (see Fig. 35 top). This inverse Evershed flow – not to confuse with downflows in sunspot plumes (distinct velocity channels seen in emission lines formed at higher temperatures, such as Ne VIII) – has been much less studied, particularly in the transition region.

Spectroscopic observations of a big sunspot at different aspect angles clearly show the inverse Evershed effect at transition region temperatures up to 0.18 MK. The motions seem to occur in a collar of radially directed filamentary structures, with widths comparable to the 1 Mm SUMER spatial resolution and characterised by different plasma velocities. The inverse Evershed flow appears to be confined to a region within roughly twice the penumbral radius and terminates abruptly near a patch of opposite magnetic polarity located on the limb-ward side of the sunspot.

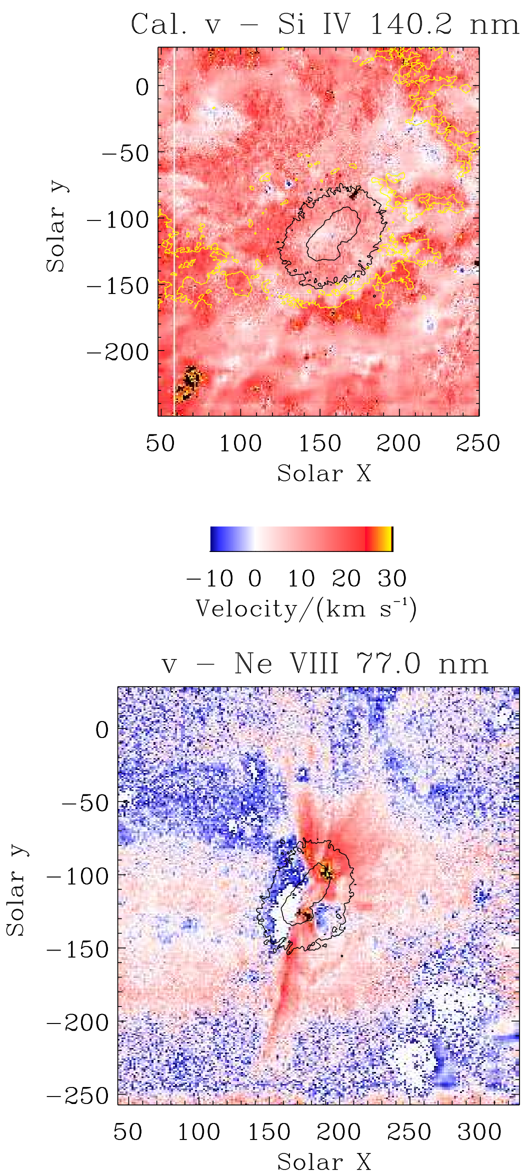


Fig. 35: Si IV (top) and Ne VIII (bottom) Doppler maps (umbral/penumbral boundaries as black contours). The inverse Evershed flow is observed in the Si IV map in sectors not covered by the prominent northern and southern plumes seen in the hotter lines.

(L. Teriaca, W. Curdt, and S. K. Solanki)

### Comparison of the Grad-Rubin and Wheatland-Sturrock-Roumeliotis algorithms for nonlinear force-free magnetic field extrapolation

We compare the performance of two alternative algorithms which aim to construct a force-free magnetic field given suitable boundary conditions. For this comparison, we have implemented both algorithms on the same finite element grid which uses Whitney forms to describe the fields within the grid cells. The additional use of conjugate gradient and multigrid iterations result in very effective codes. The conjugate gradient iteration steps are especially adaped to the algebraic structure of our nonlinear problem so that an exact line-search is performed at every iteration step. The Grad-Rubin and Wheatland-Sturrock-Roumeliotis algorithms both perform well for the reconstruction of a known analytic force-free field. For more arbitrary boundary conditions the Wheatland-Sturrock-Roumeliotis approach has some difficulties because it requires overdetermined boundary information which may include inconsistencies (a semi-analytic test-field as shown in Fig. 36). This is assumed to be even more severe if applied to real data. The Grad-Rubin code on the other hand loses convergence for strong current densities. There are signs that this occurs when stationary solutions to the boundary value problem cease to exist. At least for the example we have investigated, the maximum possible boundary current density we were able to reconstruct seems to be not far from the limit beyond which a force-free field cannot exist anymore for a given normal magnetic field intensity on the boundary.

(B. Inhester and T. Wiegelmann)

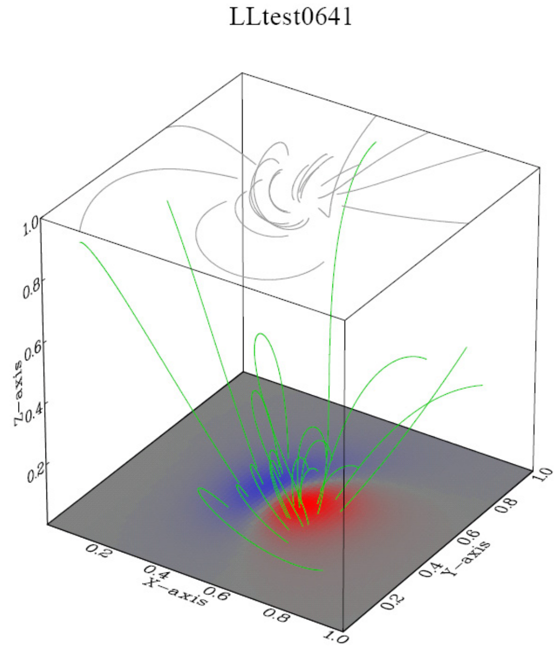


Fig. 36: Representative field lines of the reconstructed Low and Lou (1990) nonlinear force-free model. The colour code at the bottom represents $B_z$, the top plane shows the vertical projection of the field lines.

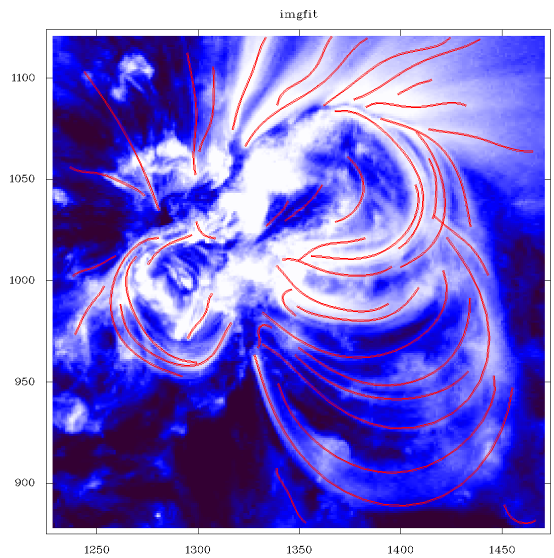


Fig. 37: Example of loop structures extracted from an active region on one of the first STEREO/SECCHI images.

### Segmentation of loops from coronal EUV images

Solar EUV images offer a wealth of information about the structure of the solar chromosphere, transition region and corona. Moreover, these structures are in continuous motion so that the information collected by these images will be enormous and must often be reduced for further analysis. One standard task often encountered is to extract the shape of bright loops from these images to be used for stereoscopic loop reconstruction or for comparison with projections of magnetic field lines derived from models of the solar magnetic field (Fig. 37).

In terms of image intensities, these features are elongated ridge-like intensity maxima. To discriminate the maxima, we need information of the spatial derivatives of the image intensity. Commonly, the derivative estimates are strongly affected by image noise and need to be regularized. The result is expressed in a discrete vector field of ridge points (ridgels) which are positioned on the ridge center and have the intrinsic orientation of the local ridge direction. Schemes are proposed to connect ridgels to smooth, spline-represented curves which fit the observed loops. Finally, a half-automatted user interface allows to merge or split, eliminate or select loop fits obtained from the above procedure.

(B. Inhester, Li Feng, and T. Wiegelmann)

**Fundamental principles of stereoscopy and their application to the STEREO mission**

We discuss the basic principles of stereoscopy and their relevance to the reconstruction of coronal loops and other plasma striations to be observed with the STEREO/EUVI imager (Fig. 38). The aim of the paper is to make the STEREO community familiar with these principles and to give hints how they may apply to the analysis of data from the recently launched STEREO mission.

We disucss the geometry of the solar coronal stereo problem, explain the fundaments of epipolar geometry and how the images from the STEREO telescopes should be rectified for further stereoscopy analysis. Next, we give an introduction to our tie-point reconstruction algorithm and consider ambiguities in the reconstruction results and resolution errors. Ghost features which unavoidably result from a straight-forward stereo reconstruction are analysed, and rules and constraints are listed which help to distinguish the true reconstructions from these ghosts.

Finally, we mention extensions to plain stereoscopy such as a third view, a tomography-based approach and also, how magnetic field information can be used to improve the reconstruction.

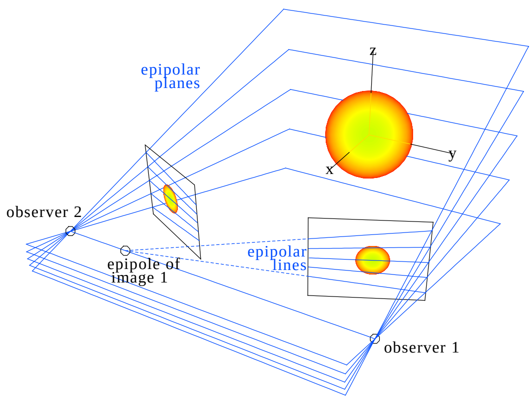


Fig. 38: Orientation of epipolar planes in space and the respective epipolar lines in the images for two observers (e.g., spacecraft) looking at the Sun. The observers telescope screens are derived from a projective geometry camera model.

(B. Inhester)

**Inversion of coronal Zeeman and Hanle observations to reconstruct the coronal magnetic field**

Hanle-effect observations of forbidden coronal line transitions and recently also longitudinal Zeeman-effect measurements of coronal lines show quantitative signatures of the weak coronal magnetic field. The interpretation of these observations is, however, complicated by the fact that they are the result of line-of-sight integrations through the optically thin corona. We study by means of simulated observations the possibility of applying tomographic techniques in order to reconstruct the 3-D magnetic field configuration in the solar corona from these observations (Fig. 39). The reconstruction problem relates to a family of similar problems termed vector tomography. It is shown that Zeeman data and Hanle data alone obtained from vantage points in the ecliptic plane are sensitive only to certain magnetic field structures: The Zeeman observations cannot respond to the divergence of the emissivity weighted magnetic field, the Hanle observations do not see its curl. For a full reconstruction it is therefore necessary to combine the longitudinal Zeeman and Hanle effect data and also include observations of the solar surface magnetic field. The inversion algorithm we have developed is capable to yield a reconstruction of the entire coronal magnetic field without the assumption of the field to be force-free.

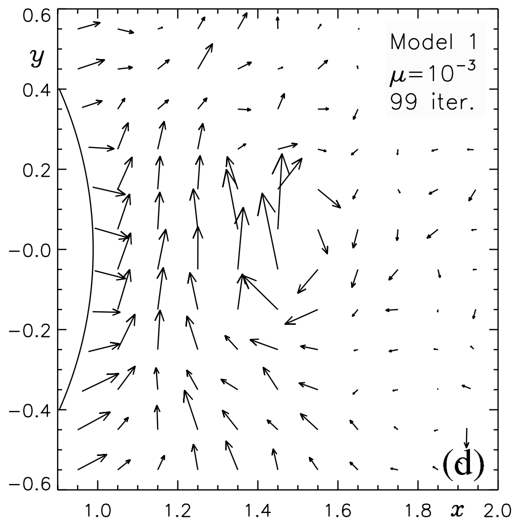


Fig. 39: Example of a reconstructed current loop. The figure show the original and the reconstructed magnetic field distribution in a plane perpendicular to the loop. The curl marks the loop center which carries a loop-aligned current.

(B. Inhester and M. Kramar)

### Properties of solar polar coronal plumes constrained by UVCS data

Polar plumes are nearly radially directed brightenings seen above the solar limb at the locations of the polar coronal holes. In recent years there have been conflicting claims regarding their physical properties, in particular the outflow speed of the solar wind within them. We investigate the plasma dynamics (outflow speed and turbulence) inside polar plumes using a new approach. We compare line profiles observed by the Ultraviolet Coronagraph Spectrometer (UVCS) instrument on SOHO at the minimum between solar cycles 22 and 23 with model calculations. We compute line profiles and total intensities of the H I Ly$\alpha$ line and the O VI doublets. The presence of polar plumes has a marked effect on the profile shapes of the O VI lines. The observed profile shapes and intensities are reproduced best by a small solar wind speed at low altitudes in plumes that increases with height to reach ambient interplume values above roughly 3 – 4 $R_\odot$. We also find that plumes very close to the pole give narrow profiles at heights above 2.5 $R_\odot$, which are in conflict with the observations. This suggests a tendency for plumes to be located away from the pole. The inclusion of plumes in the model computations provides an improved correspondence with the observations and confirms previous results showing that published UVCS observations in polar coronal holes can be roughly reproduced without the need for a large temperature anisotropy.

(S. K. Solanki in collaboration with N.-E. Raouafi and J. W. Harvey (National Solar Observatory, Tucson, USA))

### Preprocessing of vector magnetograph data for a nonlinear force-free magnetic field reconstruction

Knowledge regarding the coronal magnetic field is important for the understanding of many phenomena, like flares and coronal mass ejections. Because of the low plasma beta in the solar corona the coronal magnetic field is often assumed to be force-free, and we use photospheric vector magnetograph data to extrapolate the magnetic field into the corona with the help of a nonlinear force-free optimization code. Unfortunately the measurements of the photospheric magnetic field contain inconsistencies and noise. In particular the transversal components (say Bx and By) of current vector magnetographs have their uncertainties, see Fig. 40. Furthermore the magnetic field in the photosphere is not necessarily force-free and often not consistent with the assumption of a force-free field above. We develop a preprocessing procedure to drive the observed non force-free data towards suitable boundary conditions for a force-free extrapolation. As a result we get a data set which is as close as possible to the measured data and consistent with the force-free assumption.

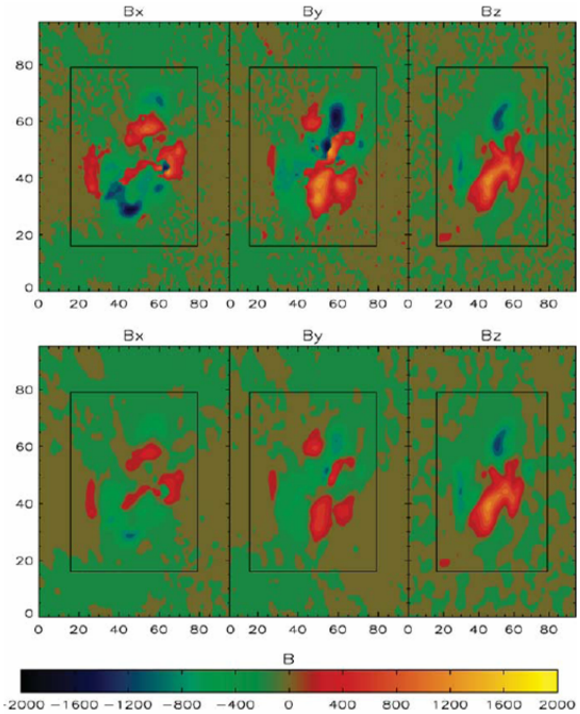


Fig. 40: Top panel: vector magnetogram of AR 7321 taken with SFT at October 26, 1992. Bottom panel: After applying our preprocessing procedure.

(T. Wiegelmann and B. Inhester in collaboration with T. Sakurai (National Astronomical Observatory of Japan, Tokyo))

### Testing nonlinear force-free coronal magnetic field extrapolations with the Titov-Démoulin equilibrium

As the coronal magnetic field can usually not be measured directly, it has to be extrapolated from photospheric measurements into the corona. We test the quality of a nonlinear force-free coronal magnetic field extrapolation code with the help of a known analytical solution. The nonlinear force-free equations are numerically solved with the help of an optimization principle. The method minimizes an integral over the force-free and solenoidal condition. As boundary condition we use either the magnetic field components on all six sides of the computational box in Case I or only on the bottom boundary in Case II. We check the quality of the reconstruction by computing how well force-freeness and divergence-freeness are fulfilled and by comparing the numerical solution with the analytical solution which is shown in Fig. 41. The comparison is done with magnetic field line plots and several quantitative measures, like the vector correlation, Cauchy Schwarz, normalized vector error, mean vector error and magnetic energy. For Case I the reconstructed magnetic field shows good agreement with the original magnetic field topology, whereas in Case II there are considerable deviations from the exact solution. This is corroborated by the quantitative measures, which are significantly better for Case I. Despite the strong nonlinearity of the considered force-free equilibrium, the optimization method of extrapolation is able to reconstruct it; however, the quality of reconstruction depends significantly on the consistency of the input data, which is given only if the known solution is provided also at the lateral and top boundaries, and on the presence or absence of flux concentrations near the boundaries of the magnetogram.

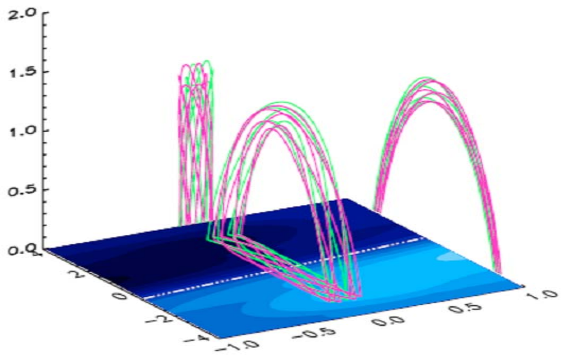


Fig. 41: Magnetic field topology for the Titov-Demoulin equilibrium.

(T. Wiegelmann, B. Inhester, B. Kliem, G. Valori, and T. Neukirch)

**Magnetic stereoscopy: I. Theory**

The space mission STEREO will provide images from two viewpoints. An important aim of the STEREO mission is to get a 3-D view of the solar corona. We developed a programme for the stereoscopic reconstruction of 3-D coronal loops from images taken with the two STEREO spacecraft. A pure geometric triangulation of coronal features leads to ambiguities because the dilute plasma emissions complicate the association of features in image 1 with features in image 2. As a consequence of these problems the stereoscopic reconstruction is not unique and multiple solutions occur. We demonstrate how these ambiguities can be resolved with the help of different coronal magnetic field models (potential, linear and nonlinear force-free fields). The idea is that, due to the high conductivity in the coronal plasma, the emitting plasma outlines the magnetic field lines. Consequently the 3-D coronal magnetic field provides a proxy for the stereoscopy which allows to eliminate inconsistent configurations. Fig. 42 shows schematically how our newly developed stereoscopy-programme works. The combination of stereoscopy and magnetic modelling is more powerful than one of these tools alone. We test our method with the help of a model active region and plan to apply it to the solar case as soon as STEREO data become available.

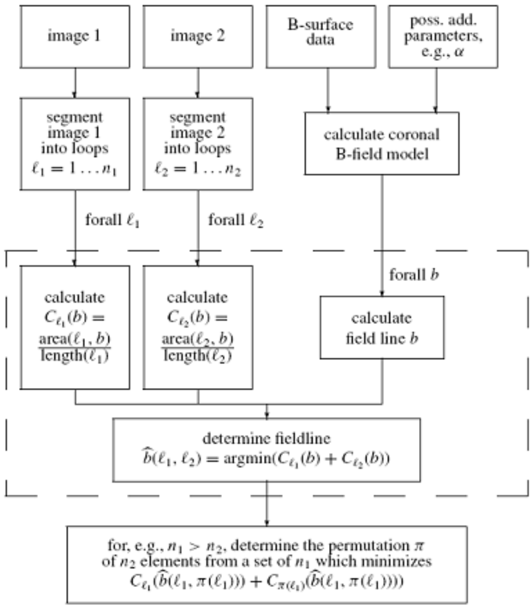


Fig. 42: This figure shows schematically how our newly developed stereoscopy-programme works.

(T. Wiegelmann and B. Inhester)

**Magnetic stereoscopy: II. Application**

Based on the stereoscopy theory described in Part I, we present here an application of the magnetic stereoscopy tool to the coronal loops observed by TRACE in the active region NOAA 8891. Designed for the newly launched STEREO mission, we aim to reconstruct the 3-D geometry of coronal loops. Taking advantage of the solar rotation, two TRACE image pairs observed on 1 March and 2 March 2000, are used as the STEREO-A and B EUVI images. The stereoscopic reconstruction is composed of three steps. First we identify loop structures in two TRACE images observed from two viewpoints approximately 17 degrees apart. In a second step, we extrapolate the magnetic field in the corona with the linear force-free field model from the photospheric SOHO/MDI data. Finally combining the extrapolated field lines and 1D loop curves from two different viewpoints, we obtain the 3-D loop structures with the magnetic stereoscopy tool (Fig. 43). We demonstrate that by including the magnetic modelling this tool is more powerful than pure geometrical stereoscopy, especially in resolving the ambiguities generated by classical stereoscopy. By assuming that the loop structures are quasi stationary in this active region, we obtain the 3-D geometry for the most possible loop pair. We will apply this tool to the simultaneous SECCHI/EUVI data in the near future.

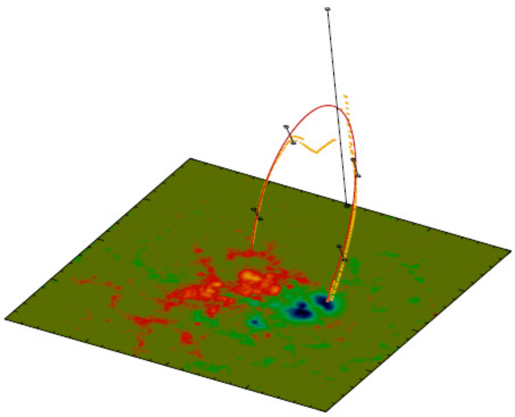

Fig. 43: Magnetic stereoscopy of a loop pair. Yellow points give the solution of the 3-D reconstruction, the red line is the best fitting 3-D magnetic field line. The reconstruction error bars at five points along the 3-D magnetic field line are also shown.

(L. Feng, T. Wiegelmann, B. Inhester, S. K. Solanki, and P. Ruan in collaboration with W. Q. Gan (Purple Mountain Observatory, Nanjing, China))

### An optimization principle for the computation of MHD equilibria in the solar corona

We develop an optimization principle for computing stationary MHD equilibria. Our code for the self-consistent computation of the coronal magnetic fields and the coronal plasma uses non-force-free MHD equilibria. Previous versions of the code have been used to compute nonlinear force-free coronal magnetic fields from photospheric measurements. The programme uses photospheric vector magnetograms and coronal EUV images as input. We tested our reconstruction code with the help of a semi-analytic MHD-equilibrium. The quality of the reconstruction was judged by comparing the exact and reconstructed solution qualitatively by magnetic field-line plots and EUV-images and quantitatively by several different numerical criteria. Our code is able to reconstruct the semi-analytic test equilibrium with high accuracy see Fig. 44. The stationary MHD optimization code developed here has about the same accuracy as its predecessor, a nonlinear force-free optimization code. The computing time for MHD-equilibria is, however, longer than for force-free magnetic fields. We also extended a well-known class of nonlinear force-free equilibria to the non-force-free regime for purposes of testing the code. We demonstrate that the code works in principle using tests with analytical equilibria, but it still needs to be applied to real data.

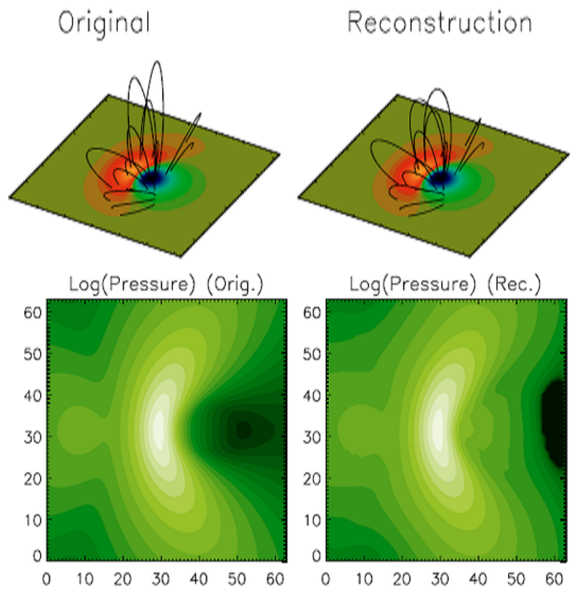


Fig. 44: Top: Coronal magnetic field model. Bottom: artificial EUV-images (LOS integrated plasma pressure). Left: Original, Right: Reconstruction.

(T. Wiegelmann in collaboration with T. Neukirch (University of St. Andrews, School of Mathematics and Statistics, Scotland))

### Computing nonlinear force-free fields in spherical coordinates

We developed the world wide first code for the extrapolation of global nonlinear force-free coronal magnetic fields in spherical coordinates, see Fig. 45. The programme uses measured vector magnetograms on the solar photosphere as input and solves the force-free equations in the solar corona. The method is based on an optimization principle and the heritage of the newly developed code is a corresponding method in Cartesian geometry. We tested the newly developed code with the help of a semi-analytic solution and rate the quality of our reconstruction qualitatively by magnetic field line plots and quantitatively with a number of comparison metrics. We find that we can reconstruct the original test field with high accuracy. We are planning to apply our code to full disk vectormagnetograms from SOLIS and SDO as soon as these data become available.

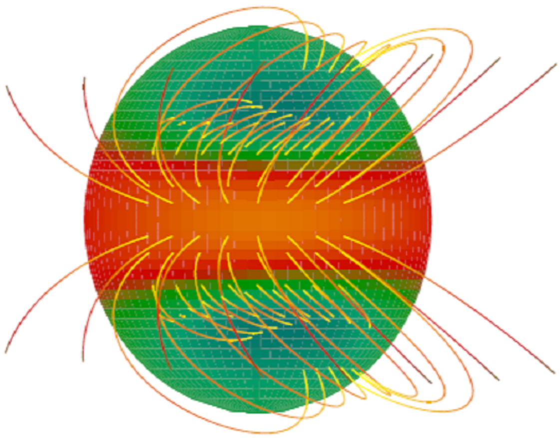

Fig. 45: Some example field lines for a nonlinear force-free coronal magnetic field model.

(T. Wiegelmann)

### Nonlinear force-free modelling of coronal magnetic fields, Part I: a quantitative comparison of methods

We compare six algorithms for the computation of nonlinear force-free (NLFF) magnetic fields (including optimization, magnetofrictional, Grad Rubin based, and Green's function-based methods) by evaluating their performance in blind tests on analytical force-free-field models for which boundary conditions are specified either for the entire surface area of a cubic volume or for an extended lower boundary only. Figures of merit are used to compare the input vector field to the resulting model fields. Based on these merit functions, we argue that all algorithms yield NLFF fields that agree best with the input field in the lower central region of the volume, where the field and electrical currents are strongest and the effects of boundary conditions weakest. The NLFF vector fields in the outer domains of the volume depend sensitively on the details of the specified boundary conditions; best agreement is found if the field outside of the model volume is incorporated as part of the model boundary, either as potential field boundaries on the side and top surfaces, or as a potential field in a skirt around the main volume of interest. For input field (B) and modeled field (b), the best method included in our study yields an average relative vector error $E_n = < |B - b| > / < |B| >$ of only 0.02 when all sides are specified and 0.14 for the case where only the lower boundary is specified, while the total energy in the magnetic field is approximated to within 2 %. The models converge towards the central, strong input field at speeds that differ by a factor of one million per iteration step. The fastest-converging, best-performing model for these analytical test cases is the Wheatland, Sturrock, and Roumeliotis (2000) optimization algorithm as implemented by Wiegelmann (2004). In parallel we have implemented the Grad-Rubin and the Wheatland-Sturrock-Romumeliotis-optimization algorithm using improved numerical convergence schemes (Fig. 46). We also carried out further tests with more complicated test configurations.

(T. Wiegelmann and B. Inhester in collaboration with C. J. Schrijver (Lockheed Martin Advanced Technology Center, Palo Alto, USA) and the NLFF-consortium)

### Evolution of a coronal loop system

The temporal variation of a loop system that appears to be changing rapidly is examined. The analyzed data were obtained on 15 May 1999, with the Transition Region and Coronal Explorer (TRACE) during an observing campaign and consist of observations in the Fe IX/Fe X 171 Å and Fe XII 195 Å passbands taken at a cadence of $\sim 10$ min as shown in Fig. 47. The special interest in this loop system is that it looks like one expanding loop; however, careful examination reveals that the loop consists of several strands and that new loop strands become visible successively at higher altitudes and lower loop strands fade out during the one hour of our observations. These strands have different widths, densities, and temperatures and are most probably consisting of, at least, a few unresolved thinner threads. Several geometric and physical parameters are derived for two of the strands, and an effort is made to determine their 3-D structure based on the extrapolation of the magnetic field lines. Electron density estimates allow us to derive radiative and conductive cooling times and to conclude that these loop strands are cooling by radiation.

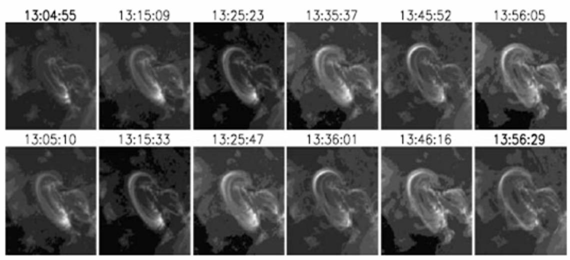


Fig. 47: Time sequence images of the loop system observed with TRACE at 171 Å (first row) and 195 Å (second row) with a time cadence of $\sim 10$ min.

(T. Wiegelmann in collaboration with G. Tsiropoula, K. Tziotziou (National Observatory of Athens, Institute for Space Applications and Remote Sensing) and T. Zachariadis, C. Gontikakis, H. Dara (Academy of

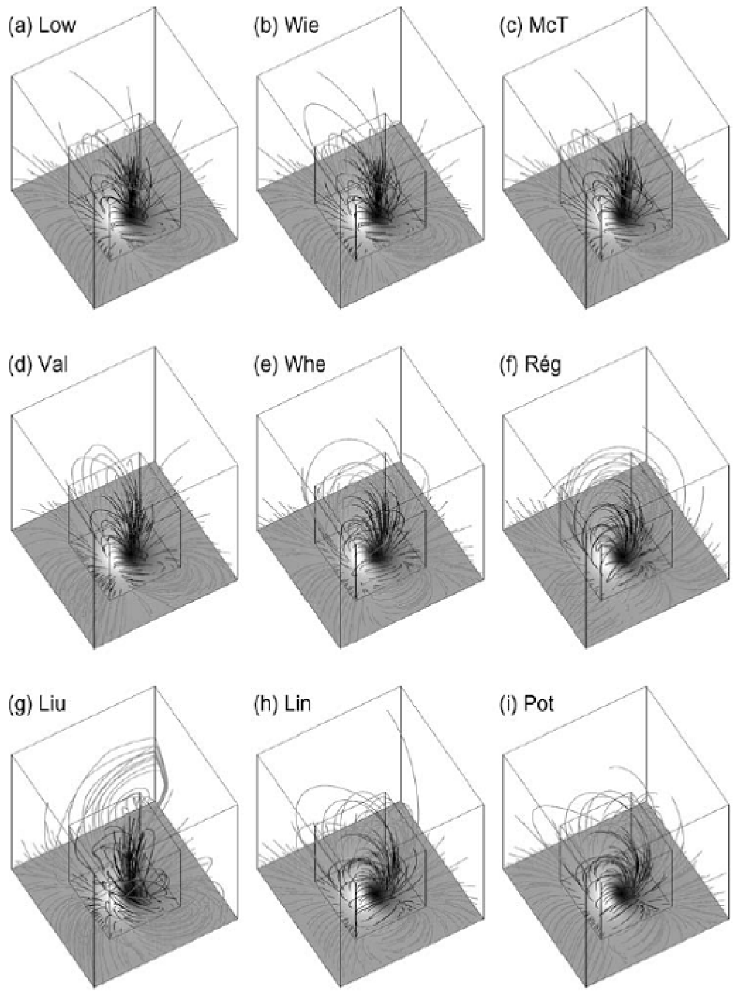


Fig. 46: Magnetic field lines for Case I in which all six sides boundaries were provided to the modelers. (a) Low and Lou input model; (b) Wiegelmann; (c) McTiernan; (d) Valori; (e) Wheatland; (f) Régnier; (g) Liu; (h) Linear force-free field; (i) potential field.

Athens, Research Center for Astronomy and Applied Mathematics))

### Search for photospheric footpoints of transition region loops

Sensitive VUV observations show the upper solar atmosphere to consist of a hierarchy of loop structures with different temperatures and extents. These loops fill most of the quiet Sun transition region (TR), and their footpoints do not seem to be associated with known traditional magnetic structures. They lie across the network boundaries with the footpoints in the interior of supergranulation cells without obvious magnetic counterparts. The magnetic measurements employed so far do not have enough spatial resolution and sensitivity to reveal magnetic structures in cell interiors, however, it has been known for long that such structures exist. A complex magnetic field pervades the seemingly non-magnetic quiet photosphere. Theoretical arguments suggest that a significant part of such photospheric magnetic field actually reaches TR and coronal heights, providing natural candidates for the so-far unidentified TR loop footpoints.

We carried out an observational study during March 2006 and aimed at identifying such photospheric footpoints. The study requires simultaneous observations of the quiet Sun TR loops and the magnetic fields in cell interiors. We observed the C III 977 Å line with SOHO/SUMER to trace TR loops, whereas the photospheric magnetic fields are identified employing high spatial resolution G-band images obtained with the Dutch Open Telescope (DOT). G-band bright points (BPs) are proxies for intense kG magnetic concentrations. Our simultaneous SOHO/SUMER DOT observations show interesting preliminary results. Among others, (1) the BPs are associated with TR bright features, but they tend to avoid the brightest parts, (2) the BPs are associated with TR downflows as expected from TR loop models, and (3) the BPs avoid locations of large TR line widths, locations often characterized by the presence of explosive events.

(L. Teriaca and U. Schühle in collaboration with J. Sanchez Almeida (Instituto Astrofisico de Canarias, Spain), P. Sütterlin, R. J. Rutten (Sterrekundig Instituut, Utrecht University, The Netherland), and D. Spadaro (INAF-Osservatorio Astronomico di Catania, Italy))

### Loop segmentation tool for EUVI images

The SECCHI/EUVI on the newly launched STEREO mission provides us with a great number of high spatial resolution images of the coronal loops in the solar corona. In order to test model assumptions, e.g., of the magnetic field and obtain accurate loop properties, one standard task encountered is to extract the shape of the bright loops from the images. In terms of the EUV image intensities, these loop features are elongated ridge-like intensity maxima. Our loop segmentation tool advances in three major steps. According to the spatial derivatives of the image intensity, we at first identified the ridge points which may located in the coronal loops and interpolate the precise position of the ridge point in the direction across the loop where the intensity obtains its maximum. The second step is to connect the identified ridge points to curves based on the algorithm of co-circularity condition. Finally we smooth the connected curves by a polynomial fit, possibly connect curves which appear to be aligned and eliminate those whose length is very small. An application of this loop segmentation tool to the SECCHI/EUVI data is shown in Fig. 48.

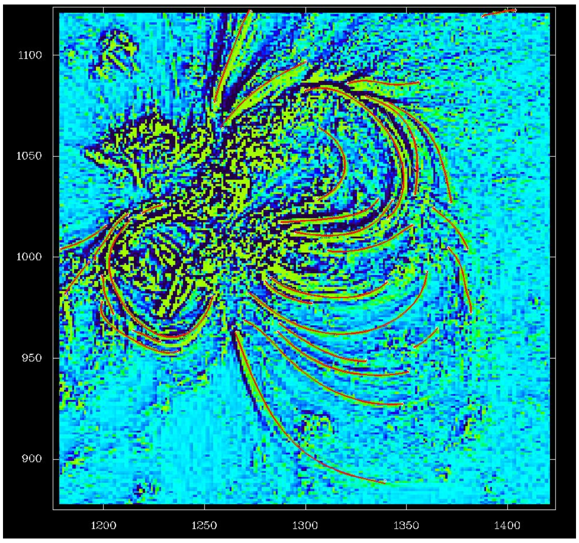


Fig. 48: Loop segments identified in the SECCHI/EUVI image observed on 12 December 2006 are shown with the red lines.

(B. Inhester, L. Feng, and T. Wiegelmann)

### Magnetic field extrapolation with MHS model

Current measurements provide the photospheric magnetic field (e.g, from MDI on SOHO) and line-of-sight integrated 2-D coronal images (e.g. EIT). Our aim is to use these observations to reconstruct the 3-D-structure of the solar corona. Here we do the reconstruction in two steps. We compute a global coronal magnetic field model with the help of a potential or linear force-free model. In a subsequent step we model the coronal plasma radiation with the help of scaling laws. Scaling laws which relate loop emissivities with plasma parameters will be tested with these models.

We extrapolate the magnetic field in the solar corona with potential field model and linear force-free model, and fill in the loops with the plasma according to the scaling laws. We cannot compare our temperature distribution with observations directly. In order to enable direct comparisons of our model with observations, we intend to calculate the plasma emissivities in the corona and integrate the emissivities in line of sight to produce artificial images. After that, we can compare our simulations and observations directly. STEREO provides the opportunity to observe the sun from two view directions. We will apply an advanced model, such as MHS model (e.g. Neukirch, 1995), to compute the coronal magnetic field and the plasma self-consistently (Fig. 49).

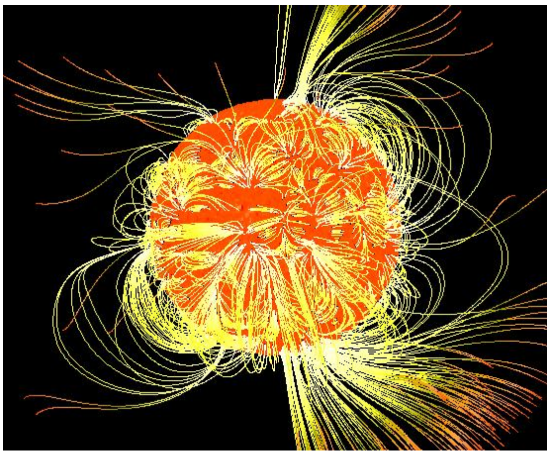

Fig. 49: Field lines constructed with MHS model. MDI(1913) magnetogram is the boundary condition.

(P. Ruan, T. Wiegelmann, B. Inhester, S. K. Solanki, and L. Feng)

**Solar coronal-hole plasma densities and temperatures**

Polar plumes extending from the Sun into the solar corona have long been seen during eclipses, and can now be studied without this restriction with telescopes and spectrometers on board of spacecraft. Despite the large amount of observational data available on this prominent phenomenon, it is not clear whether plumes contribute substantially to the fast solar-wind streams emanating from coronal holes. An understanding of the processes leading to the formation of bright plumes and the surrounding darker inter-plume regions in coronal holes requires a good knowledge of the physical conditions in plumes and their environment. This investigation aims at measuring the electron densities and temperatures in these regions with the help of radiance ratios of ultraviolet emission lines obtained by SUMER on SOHO. It finds densities of about $7 \times 10^7$ cm$^{-3}$ in bright plumes and $1.3 \times 10^7$ cm$^{-3}$ in inter-plume lanes at $\approx 45$ Mm above the limb. At this height, the total plume cross-section relative to the size of the coronal hole was found to be less than 8 %. The densities drop by a factor of roughly two over the next 80 Mm in height, in lanes a little less than seen in plumes. In this height range, the electron temperatures in plumes are $\approx 7.5 \times 10^5$ K and $\approx 1.13 \times 10^6$ K in inter-plume regions. The effective ion temperatures, deduced from the line widths, are higher and nearly independent of the altitude in plumes, whereas they increase in inter-plume regions, starting from an even higher level. No systematic dependence of the line-of-sight bulk velocities on the brightness could be found in the coronal-hole plasma.

(K. Wilhelm)

**Jets or high-velocity flows in the solar corona**

A large variety of jet-like phenomena are often observed in the solar atmosphere such as surges, spicules, sprays, EUV and X-ray jets. We analysed active region EUV dynamic events (Fig. 50) observed simultaneously at high cadence with SUMER/SOHO and TRACE. Although the features appear in the TRACE Fe IX/X 171 Å images as jets seen in projection on the solar disk, the SUMER spectral line profiles suggest that the plasma has been driven along a curved large scale magnetic structure, a pre-existing loop. The SUMER observations were carried out in spectral lines covering a large temperature range from $10^4$ K to $10^6$ K. We found that sudden heating from an energy deposition, most likely resulting from magnetic reconnection is followed by high velocity plasma flow. The Doppler velocities were found to be in the range from 90 to 160 km s$^{-1}$. The heating process has a duration which is below the exposure time of 25 s while the lifetime of the events is from 5 to 15 min. The additional check of soft X-ray Yohkoh images shows that the features most probably reach 3 MK (X-ray) temperatures. The spectroscopic analysis showed no existence of cold material during the events.

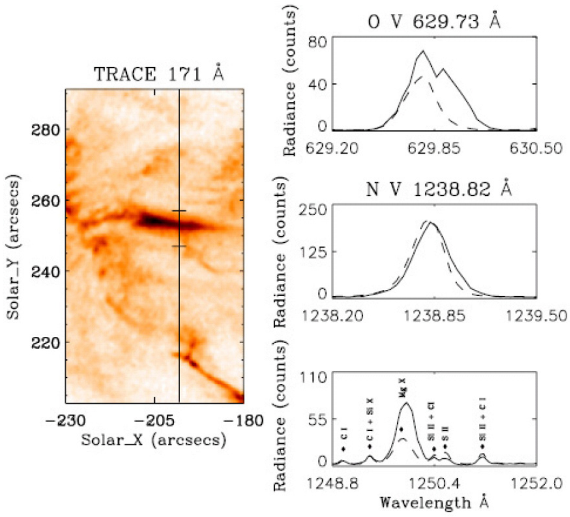


Fig. 50: Left: TRACE 171 Å colour reversed intensity image showing one of the analysed jets. The vertical line corresponds to the position of the SUMER slit, while the two horizontal lines outline the slit partition which is shown on the right in the SUMER data. Right: The analysed spectral line profiles of the jet (solid line) and a reference spectrum (dashed line).

(M. S. Madjarska, D. E. Innes, and W. Curdt in collaboration with J. G. Doyle (Armagh Observatory, Northern Ireland))

**Fe XIX plasma jets in the solar corona**

High velocity X-ray jets at the time of flares are not understood but are expected. Jets of the type reported here were a surprise. They were seen off limb, in the corona above an evolving, but not flaring, active region. They may be linked to an erupting prominence just infront of the active region. The jets were seen in the Fe XIX line, so have a temperature around $10^7$ K. They have Doppler velocities of 200 – 400 km/s, widths of a few arcsecs and lifetimes of 5 – 20 min.

Fig. 51 shows the SUMER spectrum of one of the jet events. In this example there are two narrow jets, separated by 5 arcsec, with line shifts of 400 km/s. These jets appeared to start together and faded after 10 min. A third jet is visible in the image about 100 arcsec further south. These very hot jets are sometimes simultaneous or precede colder, $10^5$ K, jets and brightenings.

(D. E. Innes and P.-F. Chen)

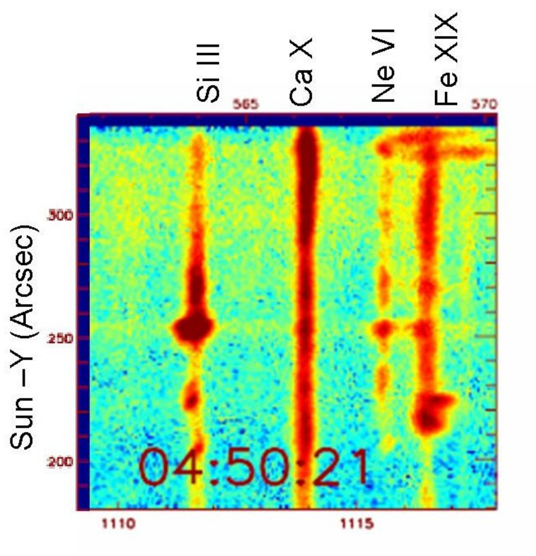


Fig. 51: SUMER spectrum of Fe XIX jets, seen off limb above an active region on 27 September 2000.

### A nanoflare model of emission line radiance distributions in active region coronae

Nanoflares are small impulsive bursts of energy that blend with and possibly make up much of the solar background emission and could be the heat source for the solar corona. The majority would be small fluctuations on the overall background and impossible to detect, so their energy contribution to coronal heating is estimated by extrapolating the energy frequency distribution of larger flares. If the power-law index of the energy frequency distribution is greater than 2, the energy of nanoflares is greater than the contribution from large flares.

Here we use a simple nanoflare model based on three key parameters: the flare rate, the flare damping time, and the power-law slope of the flare energy frequency distribution to simulate emission line radiances observed by SUMER in the corona above an active region. The three lines analysed, Fe XIX, Ca XIII, and Si III have very different formation temperatures, damping times and flare rates but all suggest a power-law slope greater than 2. Thus nanoflares may provide a significant fraction of the flare energy to active region coronae.

Fig. 52 compares model light curves with Fe XIX light curves obtained by SUMER observing in the corona of an active region. The simulated light curves on the left are for three different values of the power-law index. As the index increases the background becomes smoother and single flares more prominent. The values greater than 2 match the observed light curves, on the right, better. Previously an event counting analysis

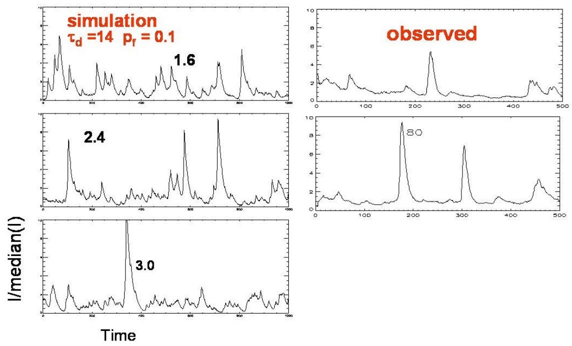


Fig. 52: Fe XIX light curves. Left: simulated nanoflares with flare frequency 0.1 per time step, decay time 14 time steps and power-law index 1.6, 2.4 and 3.0 (as labelled). Right: observed Fe XIX light curves.

of the same Fe XIX dataset gave a slope of 1.8.

(D. E. Innes and S. K. Solanki in collaboration with H. Safari (Institute for Advanced Studies in Basic Sciences, Zanjan, Iran) and A. Pauluhn (Paul Scherrer Institut, Villigen, Switzerland))

### A hot coronal downflow

Inflowing structures following flares and coronal mass ejections have been reported repeatedly in the literature. However, in coronal data these were dark and were interpreted as plasma voids moving down. In contrast to this we have discovered a bright coronal downflow in the course of a prominence eruption-associated coronal mass ejection (CME) imaged by EIT (Extreme ultraviolet Imaging Telescope) and LASCO (Large Angle Spectrometric Coronagraph) on board SOHO (Solar and Heliospheric Observatory) as well as SXT on Yohkoh and the coronagraphs on Mauna Loa (see Fig. 53). Evolution of the prominences seen by EIT was tracked into the LASCO/C2 and C3 fields-of-view where the prominences developed into the core of a typical three-part CME. The downflow showed a very rapid acceleration, with initial velocities projected on the plane of the sky far in excess of the free-fall speed, followed by a strong deceleration. The downflow followed a curved path which may be explained by material following the apex of a contracting magnetic loop sliding down along other field lines. This observation provides strong support for the pinching off of the field lines drawn out by the erupting prominences and the contraction of the arcade formed by the reconnection.

(D. Tripathi, S. K. Solanki, R. Schwenn, V. Bothmer, and M. Mierla in collaboration with G. Stenborg (Catholic University of America, Washington, USA), D. F. Webb (Boston College, USA), and H. E. Mason (University of Cambridge, Great Britain))

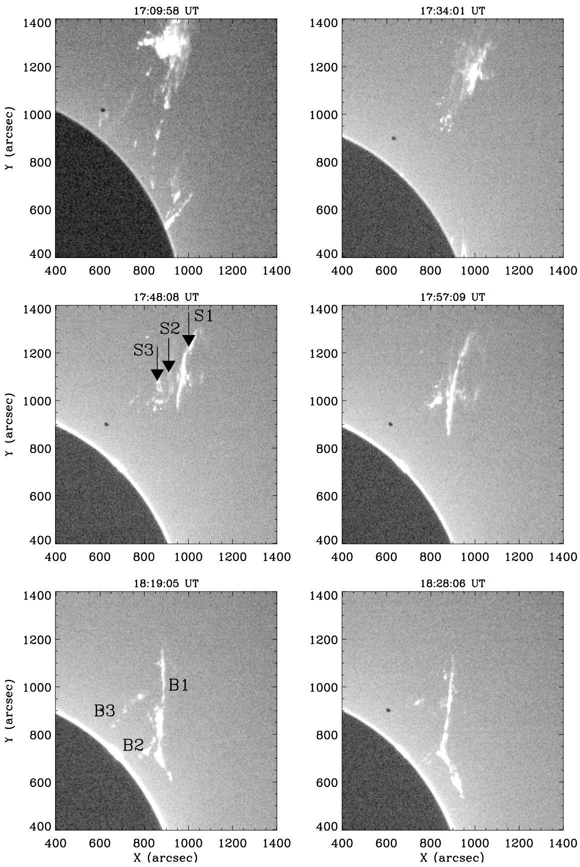


Fig. 53: Sequence of images taken by the Hα coronagraph of the Advanced Corona Observing System at Mauna Loa Solar Observatory showing the morphology of downflowing gas associated with a prominence erruption and a CME (and with hot gas visible in SXT).

**Transverse loop oscillations**

The observation of oscillations of a coronal loop allows important parameters of the loop to be determined. In particular, it provides an estimate of the magnetic field strength of the oscillating loop. Transverse loop oscillations belong to the most widely studied oscillation modes. In a curved loop transverse oscillations have two polarizations whose properties differ. E.g., the vertical oscillation (which is like a breathing mode) is partly compressible, while the horizontal oscillation is not. Both polarizations have been observed. In the period covered by this report two types of studies of these oscillations have been undertaken.

The first is to test how unique the identification of the two polarizations is under different viewing directions of the oscillating loop. We find that for many geometries it is not readily possible to distinguish between the two polarizations and show that a number of oscillations assigned to the horizontal polarization may well be misidentified vertical oscillations.

The other type of study is numerical simulations of vertical loop oscillations. In earlier 2-D simulation work we reproduced the observed signatures of vertical oscillations relatively well, with the exception of the damping: the synthetic oscillations showed a much too rapid damping compared with the observations.

In the period of time covered by this report we have concentrated on extending the simulations in two directions:

a) Introduction of gravity: we computed the equilibrium and the oscillations in the presence of a gravity-induced stratification in the studied curved loop. We find that the main results obtained without gravity are in general also valid including gravity. However, we observe that the mechanism for damping the oscillations appears to change when gravity is included. The details are still being studied.

b) In an attempt to increase the damping time we also excited waves using a damped periodic signal (instead of a single pulse as we had modelled in our earlier work; the single pulse produced too rapid damping). In this case the damping time becomes distinctly longer: the less damped the driver, the less damped the loop oscillation. In this way the damping time to oscillation period ratio can be made consistent with the observations. Further work needs to be done in order to test if this really implies that the observed vertical oscillations are excited by a periodic driver.

(S. K. Solanki in collaboration with M. Selwa, T. J. Wang, L. Ofman (NASA Goddard Space Flight Center, Greenbelt, USA), and K. Murawski (UMCS Lublin, Poland))

**Statistical study of Doppler shift oscillations seen in hot coronal loops**

Among the recent discoveries of SUMER/SOHO are Doppler shift oscillations in hot coronal loops, triggered by microflares at their footpoints. They are seen in time series of hot flare lines such as Fe XIX 1118 Å and Fe XXI 1354 Å, obtained in the corona above active regions on the limb. They have been interpreted as signatures of magnetoacoustic standing waves. Studies of their properties can provide us with a variety of information, including the excitation site, the excitation mechanism, the energy dissipation and the coronal magnetic field.

In order to understand the properties of these oscillations a statistical study is required. A wavelet-based method for the automatic identification of the oscillations has been developed and tested on SUMER data.

We would like to determine the percentage of active region microflares that trigger oscillations, find which modes are excited, their periods, damping times as well as the temperature range of the lines in which they are observed. An example of the intensity and Doppler shift time series of the emission line Fe XIX 1118 Å is shown in the Fig. 54. The contours are calculated using the wavelet-based analysis of Doppler shifts. One can see that the oscillations occur during small flare-like events and their amplitude does not depend on the amplitude of the brightenings. They occur at the positions of the intersection of the SUMER slit with the hot coronal loops but not all the loops are seen to oscillate. So far, only the first harmonic mode of the oscillations has been observed, corresponding to an excitation site at one of the footpoints.

The Hinode mission launched in August 2006 will give us an opportunity to make high-cadence imaging and spectral observations of active region loops at any position on the Sun, and thus will provide us with the loop geometry and oscillations characteristics at different heights.

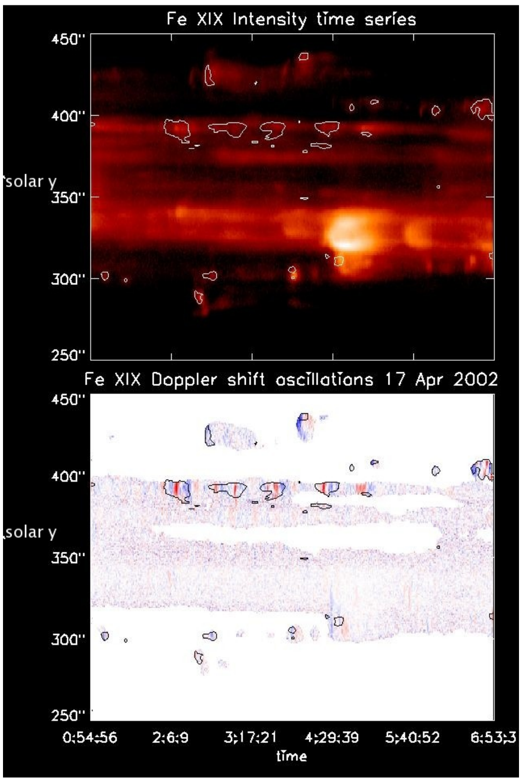


Fig. 54: Wavelet detection of Doppler shift coronal oscillations. Six hour time series of the Fe XIX 1118 Å line observed with SUMER/SOHO above the active region 9901 on the west limb on the 17th of April 2002. The contours outlining the oscillations have been obtained by applying the wavelet-based method.

(D. Tothova, D. E. Innes, and S. K. Solanki)

**Hanle effect in H I Ly-$\alpha$ and $\beta$: Diagnostic of coronal magnetic fields**

The coronal magnetic field is poorly known, mainly due to the weakness of the field and of the coronal radiation. The most widely used technique of solar magnetic field measurements, the Zeeman effect, is mainly restricted to the polarization signal of forbidden spectral lines (e.g., Fe XIV 530.3 nm green line) in the corona and provides only partial information on the vector (strength or direction projected on the plane of the sky; but not both).

The Hanle effect, i.e., the modification of the linear polarization parameters of resonant scattered radiation by a local magnetic field, presents an alternative for inferring the coronal field. The Hanle effect works best in the UV wavelength range for typical fields less than 100 Gauss. It needs very high polarimetric sensitivity. Advantages with respect to the Zeeman effect are that the Hanle effect is not sensitive to the cancellation of unresolved magnetic fields of opposite polarities and it is less sensitive to the exact spectral resolution of the measurements.

Unfortunately, there are still many unknowns regarding the selection of the most suitable spectral lines for the Hanle effect. We have therefore started a programme to compute a set of strong FUV coronal spectral lines in the presence of a realistic distribution of the coronal magnetic field. The aim of this work is the selection of spectral lines that might be of use for future space instruments to measure the coronal magnetic field. The lines being considered are: Ly $\alpha$ 1216 Å, Ly-$\beta$ 1026 Å, Ly-$\gamma$ 973 Å, Ly-$\delta$ 950 Å, and O VI 1031.91 Å.

The employed magnetic field model is obtained from the global potential field extrapolation from measured photospheric magnetograms (synoptic charts of the magnetic field). The coronal field structure is considered both at solar activity minimum and maximum.

Fig. 55 gives the obtained direction of the plane of polarization with respect to the tangent to the solar limb for a synthetic coronagraphic observation in H Ly-$\beta$. It is clear from this preliminary study that a significant and practically measurable Hanle signal can be obtained, sufficient to allow the determination of the coronal field. We also find, for example, that under typical coronal conditions Ly-$\beta$ is superior to Ly $\alpha$ for the measurement of the magnetic vector.

(S. K. Solanki and T. Wiegelmann in collaboration with N.-E. Raouafi (National Solar Observatory, Tucson, USA))

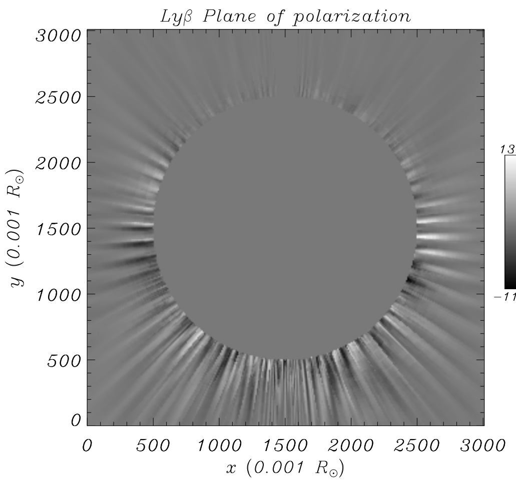


Fig. 55: Rotation angle of the polarization plane with respect to the tangent to the solar limb obtained through the Hanle effect in H I Ly-$\beta$. The magnetic field utilized in the calculation is a potential field extrapolation from photospheric magnetograms.

**Force-free magnetic field extrapolation for MHD boundary conditions in simulations of the solar atmosphere**

Modern investigations of the solar atmosphere provide a wealth of new information on the magnetic and plasma structure. A valuable tool to interpret these data is numerical simulation of the magnetic coupling between the different regions of the solar atmosphere starting from the photosphere, where the magnetic field can be determined with the highest spatial resolution, through the chromosphere and the corona. Existing solar simulation models usually use model magnetic fields on meso-scales or address global solar phenomena to investigate the influence of the photospheric boundary conditions such as magnetic shear, plasma motion, emerging flux, etc. A first mesoscale simulation model based on a statistical model of line of possible photospheric sight magnetic fields and plasma motions has been used by Gudiksen and Nordlund (2002) to study coronal heating. As a next step in this development it is desirable, however, to incorporate the observed photospheric magnetic fields in magnetohydrodynamic simulations in concrete case-specific studies, in order to allow a comparison of the results with corona observations. In order to start the simulations with magnetic fields extrapolated from the photospherically observed ones we developed the Seehafer 1978 approach toward an appropriate boundary symmetry model of force-free magnetic field extrapolations consistent with MHD equations-compatible boundary conditions. The symmetry properties we chose for our approach are depicted in Fig. 56. A comparison with other extrapolation models shows good compatibility, although different results are obtained near the boundaries, which anyway have to be removed from the region of interest as far as possible.

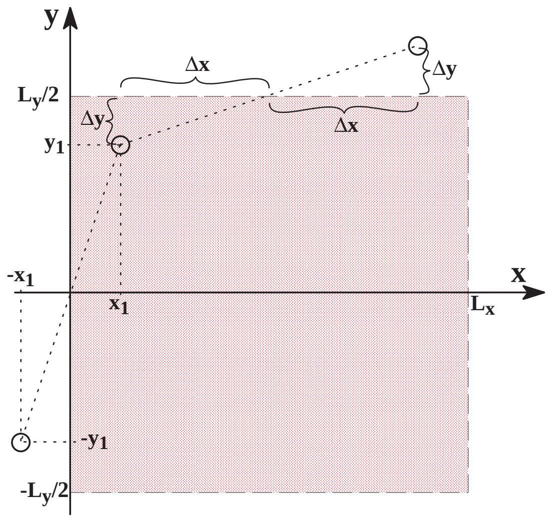


Fig. 56: Illustration of the line symmetry model which enables a force-free magnetic field extrapolation consistent with the MHD equations at the boundaries of solar atmospheric simulation boxes.

(J. Büchner in collaboration with A. Otto (University of Fairbanks, USA))

**Simulation of three-dimensional magnetic reconnection sites at the Sun**

Reconnection was conjectured by Giovanelli in 1946 to explain particle acceleration in solar flares. Since then there is no generic theory of reconnection in three dimensions. Petschek's 1964 theory, used as a standard, was derived for a two-dimensional magnetized plasma flow in regions containing an X-type singularity of the magnetic field. It was questioned in endless disputes and arguments, especially, what its three-dimensional real world analogue would be. This is especially important since remote sensing of the solar atmosphere has shown that the coronal magnetic field configurations are essentially three-dimensional. It is appropriate to search for the natural magnetic configuration and pre-conditions of reconnection of the corona by means of numerical simulations based on the observed photospheric magnetic field and motion. We recently have developed an appropriate simulation approach. Applying our approach to observed photospheric configurations we diagnosed three-dimensional magnetic reconnection by looking for regions of enhanced parallel electric fields. This provides an appropriate diagnostics tool for three-dimensional solar reconnection as the geometry and topology of the acting fields and flows is very complex. Fig. 57 depicts the resulting potential drop due to electric fields parallel to the coronal magnetic field by mapping it down to the corresponding photospheric magnetic footpoints. This way we are able to compare the actual sites of three-dimensional reconnection directly with the observed signatures of reconnection like precipitating accelerated electrons and local heating areas (Bright Points).

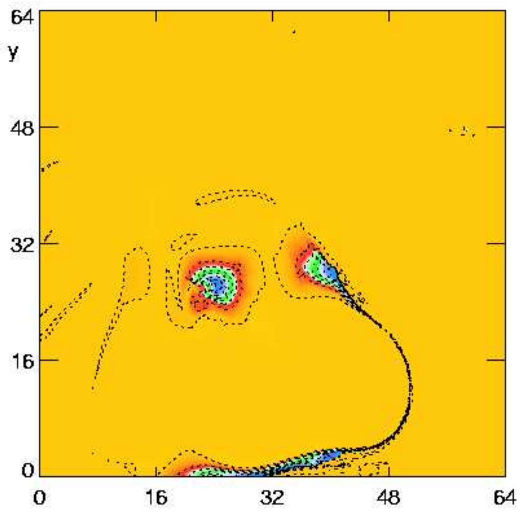


Fig. 57: Electric potential drop along the magnetic field, mapped down to the photosphere. This potential drop is due to parallel electric fields caused by three-dimensional magnetic reconnection. They were obtained by a simulation of the response of the solar atmosphere to an observed evolution of the photospheric magnetic field.

(J. Büchner)

### The topological skeleton as a predictor of 3-D magnetic reconnection sites in the solar atmosphere

The local heating of coronal plasma is thought to be due to three-dimensional magnetic reconnection. In order to verify this hypothesis we looked for a link between observations of heating in the solar atmosphere and the 3-D structure of the magnetic field in which reconnection might occur. For this sake our previous results of three-dimensional numerical MHD simulations of an observed EUV bright point in the solar atmosphere, based on MDI line-of-sight magnetogram data of June 13, 1998, were analyzed by a topological method which is based on the consideration of single magnetic charges (monopoles) instead of the distributed photospheric magnetic field topology. Three different methods were applied to reduce the magnetograms to a set of point magnetic sources.

We found that the calculated topological structure (see Fig. 58) corresponds well to the locations where increased parallel reconnection electric fields have built up in the simulation model. In fact, the simulation of the observed rotation of one magnetic source region within the bright point area has produced the parallel electric fields along the topological separatrix surface(s) bounding the magnetic flux of that source region. All three magnetogram reduction methods produce similar results for the large-scale magnetic field structure. We conclude that the magnetic-topology method is useful for predicting the location of coronal bright points, which will be found especially in modern high-resolution EUV data, like of Hinode. The choice of the magnetogram reduction algorithm does not seem to greatly affect the large-scale topological features of the resultant reconstructed magnetic field.

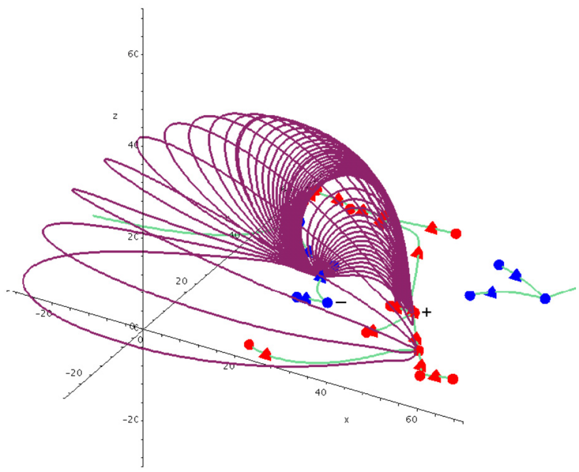


Fig. 58: Perspective view of the separatrix dome covering the rotating magnetic flux tube region, with monopolar magnetic charges calculated using the smoothed magnetic field technique.

(J. Büchner and B. Nikutowski in collaboration with Rh. Mc Lean (Armagh Observatory, Northern Ireland) and E. R. Priest (Scotland, U.K.))

### Investigation of reconnection in the solar corona by Hinode observations

Hinode observations are going to provide rich information which will enable a better understanding of magnetic reconnection in the solar atmosphere. So far different models exist of reconnection in three dimensions with different consequences for flare and CME triggering as well as for solar particle acceleration. Most of these models are qualitative, cartoon-like, i.e. they can neither be verified nor falsified quantitatively by observations. Numerical simulation approaches are necessary to describe the nonlinear, non-local (and ranging over extremely different scales) physical processes, which are not directly observable. We discuss key aspects which have to be taken into account in order to develop appropriate forward simulation models which are able to specify the nature of solar reconnection by a direct comparison with Hinode observations. As a starting point we discuss how to use the vector magnetic field information provided by SOT as an initial condition for the simulations. We further consider the use of the time series of SOT vector magnetic field observations to derive appropriate boundary conditions simulation models able to describe the energy input into the chromosphere and corona. Further, an appropriate coupled plasma – neutral gas model is suggested, able to describe the consequences of the sub-photospheric energy input for reconnection causing electron acceleration, indirectly observable by XRT, and plasma heating, observable by EIS. Since location, triggering conditions and strength of reconnection depend on microscopic dissipation processes, we shortly review the appropriate transport coefficients for solar coronal conditions. We show by an example that different resistivity models might reveal completely different locations and sizes of three-dimensional reconnection and of the corresponding electric fields in the solar corona. The differences can be verified by Hinode observations as one can see by comparing Fig. 59 and Fig. 60.

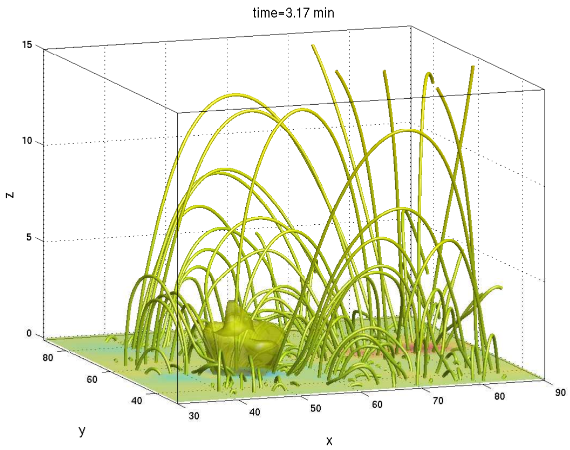


Fig. 59: Isosurface of enhanced parallel current densities ($j_{par} = 7.5 j_{norm}$) obtained by a simulation of a driven solar corona.

(J. Büchner)

**Linearly unstable low-frequency current driven plasma waves in the solar corona**

We have studied the linear stability of parallel (force-free) currents in the solar corona for all wave propagation directions with respect to the magnetic field. For this sake we have considered a configuration that can be inferred for solar coronal current concentrations: an

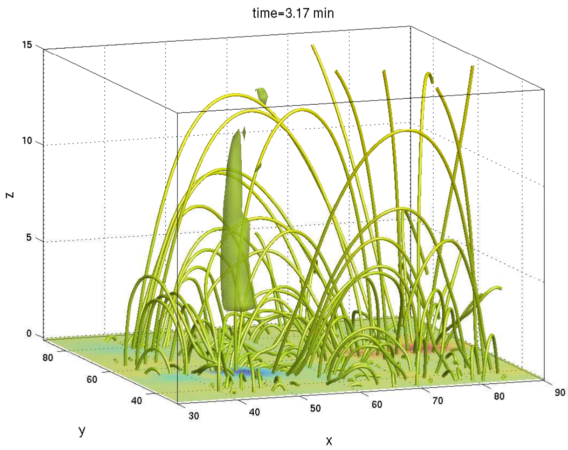


Fig. 60: Isosurface ($u_{ccv||} = 0.2 v_A$) of the parallel current carrier velocity obtained by the same simulation of a driven solar corona.

electron drift parallel to the magnetic field at the background of a stationary ion gas. It is thought that such currents lead to the development of electrostatic instabilities which can strongly enhance the transport in the collisionless coronal plasma, causing, e.g., anomalous resistivity, heat conduction etc. Due to their relative importance for collisionless transport we have focused first on low-frequency wave instabilities including ion-acoustic, Buneman and lower-hybrid modes, which for perpendicular propagation directions usually is called the modified two-stream instability. We did not limit ourselves, to either the parallel or the perpendicular direction. Instead we studied all linearly unstable wave modes in the framework of a multi-fluid description. For this sake we developed a special dispersion solver. A particular result is depicted in Fig. 61. Shown are the (colour coded) growth rates, normalized to the ion plasma frequency for Buneman-like, quasi-perpendicular propagation (upper panel) and for Lower Hybrid (LH)-like, quasi-parallel wave modes (lower panel). Both are shown as a function of the electron drift velocity and the plasma $\beta$. As one can see the LH modes become especially important for stronger magnetization (small plasma $\beta$) and higher drift speeds. Estimating the saturation level of the growing waves by particle trapping in the generated potential wells (strong turbulence case) we found that both, oblique and parallel waves, contribute wave power to the turbulence by the same order of magnitude.

(K. W. Lee, J. Büchner and N. Elkina)

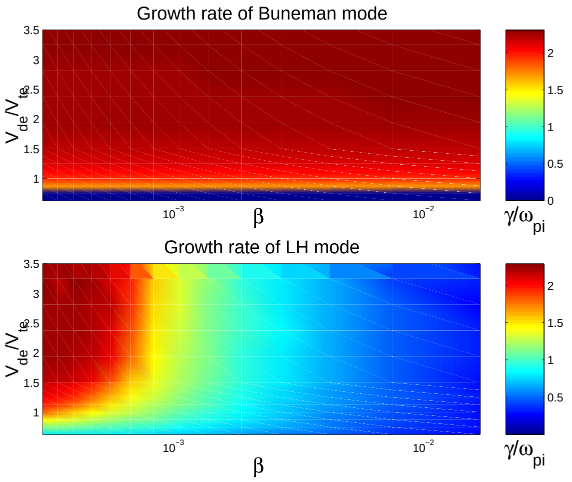


Fig. 61: Growth rates, normalized to the ion plasma frequency (colour code see to the right), for Buneman-like, quasi-perpendicular propagation (upper panel) and for Lower-Hybrid-like, quasi-parallel wave modes (lower panel), both shown as a function of the electron drift velocity and the plasma $\beta$.

## High frequency electron/electron modes in solar coronal plasma

Especially during solar flares RHESSI and other spacecraft have observed intense nonthermal electromagnetic radiation, ranging up to the $\gamma$-ray frequencies. The observations imply that strong energetic electron beams are precipitating which eventually radiate X-rays through the Bremsstrahlung mechanism in the collisional plasma of the lower corona. However, on their way from the initial acceleration site the high energy electron flows form return beams, often called "return currents" which cancel the net current flow. As a result two-electron-stream instabilities may be excited by the current-neutralized beams which can cause energy loss of the electron beams toward plasma heating. To understand the evolution of such current-neutralized beam-plasma instabilities, we have performed parametric studies of the linear stability of such beams in the parameter range of densities, temperatures and velocity ratios typical for the solar atmosphere. We found that a two-fluid approach is appropriate for typical solar plasma parameters. Also, while earlier studies of this problem were limited to one dimension and to very diluted electron beams, we have extended the analysis to higher dimensional beam-plasma situations with beams of arbitrary density and also to electromagnetic waves. We have analyzed arbitrary propagation angles of the waves with respect to magnetic field and beam direction. We have found that in addition to the well-studied Buneman instability, new high-frequency wave instabilities occur. Fig. 62 depicts in its left panel the growth rates and in the right panel the real frequencies in dependence on the wave-vector directions for the high-frequency waves caused in the return-beam plasma situation of the solar corona. As one can see for dilute beams the forward propagating high-frequency electron plasma waves grow faster than the backward directed well known low-frequency ion-acoustic-type waves. Hence, the high-frequency waves are expected to dissipate the beams toward heating the background coronal plasma. To which extent has still to be investigated.

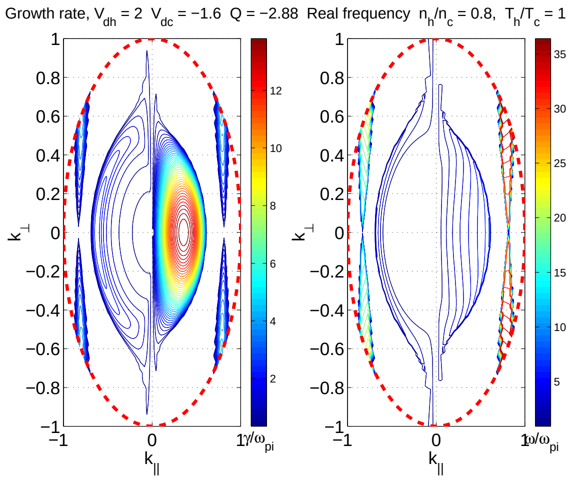


Fig. 62: Growth rates (left panel) and real frequencies (right panel) shown in dependence on the wave-vector directions for the high frequency waves caused by return-beam flows in the solar corona.

(K. W. Lee, J. Büchner and N. Elkina)

## Vlasov code simulation of collisionless solar plasma instabilities

In order to understand the strongly nonlinear evolution and consequences of collisionless solar plasma instabilities it is necessary to carry out kinetic plasma simulations. Currently appropriate numerical schemes run on modern fast CPU, large memory parallelized computer systems. This allows the development of kinetic codes which directly solve the Vlasov equation describing collective collisionless plasmas. For many years due to restricted computer resources, collisionless plasmas have been simulated mainly by introducing macro-particles in a particle-in-cell (PIC) approach. The mathematical advantage in using Lagrange-Euler PIC codes is their replacement of the treatment of the advection-type partial differential Vlasov equation by the solution of ordinary differential equations of macro-particle motion. Physically PIC-codes re-coarse-grain the continuous collisionless plasma distribution function flows introducing, this

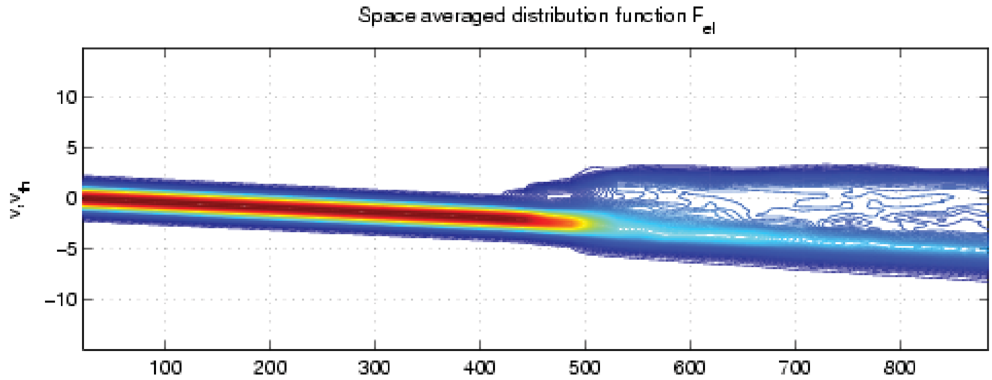


Fig. 63: Vlasov-code simulation of currents in the solar corona: Shown is the space-averaged electron distribution function $F_{el}$. After the switch-on of an external electric potential due to the interaction of strongly magnetized coronal plasmas first the parallel electric current increases. However, after the corresponding electron drift reaches the threshold of an ion-acoustic instability (at about $t\omega_{pe} \approx 450$) the distribution function flattens and the current is strongly reduced due to the wave-particle interaction of electrons with the growing electric potential of the plasma waves. A Vlasov-code simulation allows to determine the resulting so called anomalous collisionless transport properties.

way un-physically large shot-noise of the finite number macro-particles. In other words, PIC codes replace the usually huge plasma parameter $n\lambda_D^3 \approx 10^{10}$ of space plasmas by the much smaller number of particles per cell of the order of $n_m\lambda_D^3 \approx 100$, where $n_m$ is the number density of macro-particles and the Debye length $\lambda_D$ the typical size of a simulation cell. The arising noise problem limits the applicability of PIC codes to the investigation of insensitive to fine nonlinear resonances and collective field-particle interaction phenomena. The small number of macro-particles does not allow to describe the acceleration of a few particles to high energies. Modern Vlasov codes provide a powerful tool for low-noise studies of collisionless plasmas with a fine resolution of the phase space including those regions where trapping occurs or where particles move at speeds close to wave velocities. The obvious price for the noise reduction is the numerical effort. Due to the lack of a right-hand side, the Vlasov-equation causes a filamentation of the distribution function into small-scale structures, which have to be treated numerically correctly. We discuss this and other important aspects of direct Vlasov code simulations and demonstrate their abilities by a number of space physics applications. We argue that the total numerical effort of Vlasov codes which solve the same sensitive to noise and fine phase space structures problem does not exceed the effort necessary for a similarly accurate PIC code.

An example of such investigations is shown in Fig. 63. Shown is the space-averaged electron distribution function $F_{el}$. After the switch-on of an external electric potential due to the interaction of strongly magnetized coronal plasmas a mainly parallel to the magnetic field directed (“froce-free”) electric current arises. After the corresponding electron drift reaches the threshold of a plasma instability (in the Figure at about $t\omega_{pe} \approx 450$) the drift-distribution function starts to flatten and the current becomes limited due to the wave-particle interaction of electrons with the growing electric potential of the plasma waves. Our Vlasov-code simulation allows to determine the resulting so called “anomalous”, i.e. the typical for the solar coronal plasma transport properties.

(N. Elkina and J. Büchner)

**Anomalous collisions in the solar atmosphere are stronger than predicted by the quasi-linear theory**

An outstanding open question in solar physics is that of the transport properties of the collisionless coronal plasma, where binary collisions are inefficient and, instead, collective wave-particle interactions determine transport and dissipation. In order to obtain macroscopic transport coefficients one has to solve kinetic equations together with the Maxwell equations for the interacting electromagnetic fields, an essentially nonlinear problem. For weak turbulence the quasi-linear and other weakly nonlinear theories provide predictions for the saturated field fluctuations and the so called anomalous resistivity, the normal mode of current dissipation in collisionless space plasmas. Unfortunately, there has been no generic expression for “anomalous” quasi-collisions found, yet, which could be used for a macroscopic description like the Spitzer-Braginski expressions for binary collisional transport, not applicable in the solar corona. In collisionless plasmas it is often replaced by the so called “Sagdeev-formula”, obtained from quasi-linear theory arguments. By means of numerical simulations we have tested the "Sagdeev-formula" for ion-acoustic plasma waves. Fig. 64 compares the evolution of the simulated effective collision frequency $\nu$ with the value predicted by quasi-linear theory, calculated for the simulated wave energy. Our simulations have shown that the effective collision rate can exceed the quasi-linear prediction by two orders of magnitude.

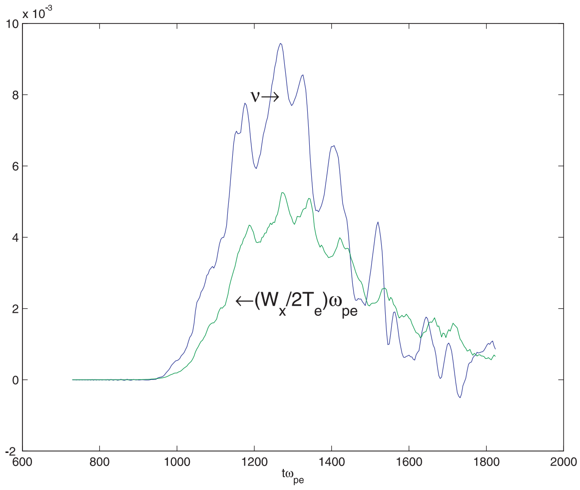


Fig. 64: Evolution of the simulated effective collision frequency $\nu$ compared to the (enhanced by a factor of 100 for better comparison) quasi-linear Sagdeev-formula prediction, calculated for the simulated wave energy.

(J. Büchner and N. Elkina)

### Anomalous resistivity of solar coronal plasmas due to electrostatic double layers

The anomalous electric resistivity of solar plasmas is an important issue of coronal DC heating and reconnection. The linear stability theory of isothermal current driven plasmas predicts an ion-acoustic instability if the relative drift velocity of the current carrying particles exceeds a certain threshold. The spectrum of waves, excited by a marginal instability, is very narrow. Hence, the wave power at saturation and the corresponding electric resistivity due to wave-particle interaction cannot be obtained by means of a quasilinear, weak-turbulence approach and the nonlinear single-mode theory provides too small saturation amplitudes. To solve the nonlinear problem a newly developed unsplit conservative Eulerian-Vlasov code is applied to simulate a strongly magnetized current-driven plasma, which can be considered in 1D1V (one spatial, one velocity space direction). Instead of periodic boundary conditions, usually used as they are simpler to treat, open boundaries are implemented which allow to maintain a constant current flow. Simulated is a typical coronal plasma for the real mass ratio $m_i/m_e = 1836$. The initial spontaneous instability is followed by a three-stage nonlinear evolution: First electron trapping leads to the formation of electron phase space holes. Due to a steepening of the leading edges of the potential wells the electron phase space holes gradually become asymmetric, they grow in size and deepen. The phase space holes accelerate until they move much faster than the initial ion-acoustic waves. The interaction of the current carriers with the asymmetric potential wells causes a non-vanishing net momentum transfer between the particles and the self-generated electric field. After a few ion plasma periods ion trapping starts until, finally, an electrostatic double layer arises. We found that the nonlinear saturated state of the system is dominated by the particle interaction with coherent phase space structures. The corresponding anomalous resistivity is slightly modulated with an oscillation period. For a macroscopic description its major part can be parameterized by means of an effective collision rate of the order of half the ion plasma frequencies (see Fig. 65).

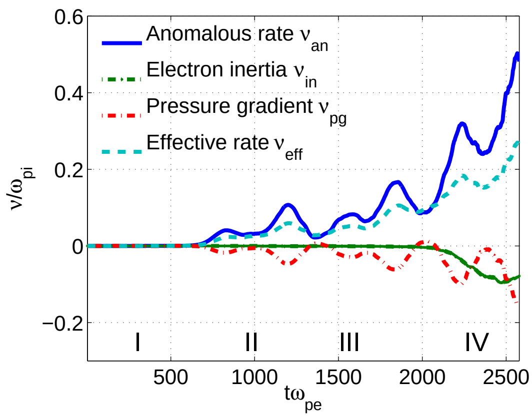


Fig. 65: Evolution of the momentum exchange rate of the interaction with the electrostatic structures ($\nu_{an}$, blue solid line), its reduction by the electron inertia- ($\nu_{in}$, green dashed-dotted line) and by pressure-gradient-contributions ($\nu_{pg}$, oscillating with $\omega_{pi}$ red dashed-dotted line) as well as the resulting box-averaged effective collision rate ($\nu_{eff}$, blue dashed line).

(J. Büchner and N. Elkina)

### Log-normal intensity distribution of the quiet-Sun FUV continuum

We have analysed the distribution of the radiances in a large raster image obtained by SOHO/SUMER in chromospheric FUV continuum emission of the quiet Sun. These results have been used to constrain atmospheric models.

According to semi-empirical atmospheric models the continuum emission around 140 nm originates from chromospheric layers where the temperature rises from low values at near-radiative equilibrium to a plateau of ≈6 000 K. We study raster images and intensity distribution histograms and find that a single log-normal distribution matches these observations very well, and that the spatial structure observed corresponds to a mixture of features at supergranular and smaller scales (see Fig. 66. The data suggest that chromospheric heating originates through dissipation of magnetic free-energy fields of small size and magnitude in underlying photospheric intergranular lanes. It has been suggested that such fields can be produced by photospheric dynamos at the intergranular scale and/or by complex fields emerging in a "magnetic carpet". Such fields are expected to have sufficient free-energy to power the chromospheric heating. Plasma instabilities, such as the Farley-Buneman instability, would allow this free-energy to be dissipated in the chromosphere.

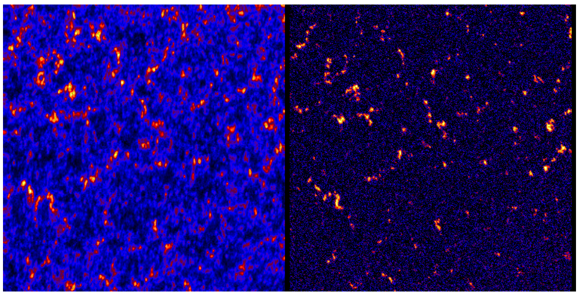

Fig. 66: The supergranular pattern in a quiet-Sun region. Left: 300" × 300" raster in the continuum emission near 140 nm. Right: hires MDI-magnetogram (abs. values). The dominating magnetic field is believed to be the source of chromospheric heating.

(W. Curdt in collaboration with J. M. Fontenla, J. Harder (LASP Boulder), and E. H. Avrett (CfA Cambridge))

**Multi-spacecraft observations of polar coronal plumes**

The mysterious polar coronal plumes, first observed during solar eclipses, have been the target of instruments on four spacecraft and ground-based observatories in April 2007. Early in April, the southern polar coronal hole was well developed, the South pole being tipped towards the Earth with a pole angle of 6.2°. The X-Ray Telescope (XRT) and the EUV Imaging Spectroscope (EIS) on *Hinode* observed the coronal hole (CH) on the disk, while SUMER on *SOHO* obtained a large raster of 300″ × 600″ above the limb. Images taken by the Extreme UltraViolet Imager (EUVI) instruments on *STEREO A* and *B* have been analysed to provide 3-D information about the plumes. The reconstruction is based on displacements of identifiable structures seen in stereoscopic view (see Fig. 67).

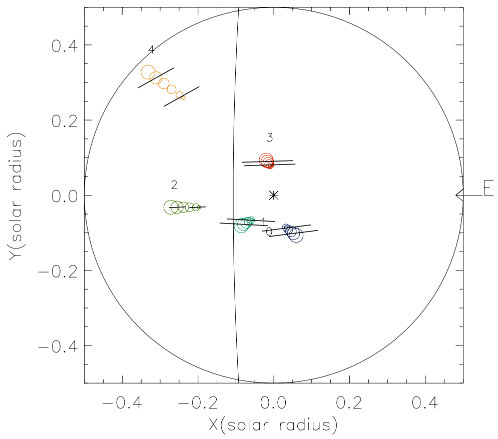


Fig. 67: Results of the 3-D reconstruction in epipolar projection (view onto the southern polar region). The scales are in solar radii and the out-of-plane distances of the fitted positions are coded by the symbol size. The smallest circles denote the footpoints on the disk. The viewing direction from the Earth and the visible limb are indicated.

Several coronal bright points (BP) are seen in soft X rays by XRT and in Fe XII 19.5 nm emission by EIS. Two of the plume footpoints determined from EUVI are close to locations of bright points (not shown here), which are thought to be the footpoints of plumes.

We established the 3-D plume geometry from EUVI images, although still with significant uncertainties, and to link them to other observations. Extrapolating the plume structures to the base of the corona, we could associate some plume footpoints with BPs. The temporal radiance variations in BPs are not reflected in any corresponding changes in the plumes.

The spatial radiance variations of the high-FIP element neon as compared to low-FIP magnesium, which outline the plume pattern, indicate abundance anomalies.

We applied plasma diagnostics based on emission line ratios to derive the electron density, confirming that plumes have higher densities than their environment (see Fig. 68). These observations thereby favour the view that the cross-sections of plumes are restricted along the LOS direction, and thus the total area occupied by all plumes is small compared to the size of the CH. This suggests that the plume contribution to the fast solar wind is relatively small.

(W. Curdt, K. Wilhelm, and L. Feng in collaboration with S. Kamio (National Astronomical Observatory of Japan)

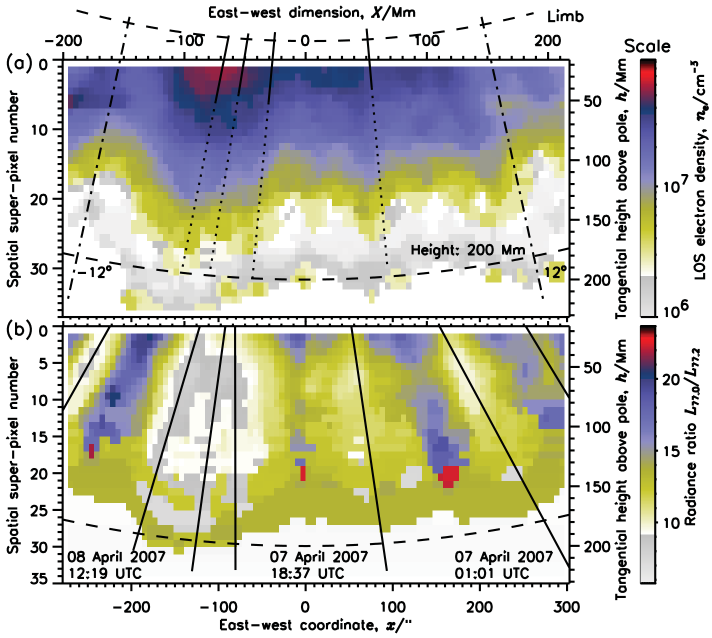

Fig. 68: SUMER raster above the southern coronal hole. The solar limb is indicated in the upper margin by a dashed line, and the radial directions from the center of the disk at ±12° with respect to the negative $y$ axis are shown as dashed-dotted lines.

**a)** The density-sensitive ratio of the Si VIII emission lines near 144 nm yields an estimate of the electron density, $n_e$. Superimposed on the density plot are, in solid lines, the projections of the 3-D plume reconstructions from the EUVI observations. Plume number 4 is not within the SUMER scan range. The projections are extrapolated by dotted lines.

**b)** Variations in the radiance ratio $R = L_{77.0}/L_{77.2}$ are indicative of an elemental abundance anomaly caused by the difference in first ionization potential of high-FIP element neon and low-FIP element magnesium. The ratio $R$ exhibits very clear signatures of plume and interplume regions. The combined SUMER results on plume projections are shown as solid lines for a comparison with the EUVI results.

### The redshifted footpoints of coronal loops

The average redshift in transition region emission has puzzled solar scientists since decades, since the continously downflowing material must empty the solar corona within minutes, if not balanced by a replenishing process. We report observations of the SUMER spectrograph (shown in Fig. 69), which clearly indicate a steady downflow in both footpoints of coronal loops observed at transition region (TR) and lower corona temperatures. We also show and quantify a correlation existing between this Doppler shift and the spectral radiance. Our results indicate a strong correlation which holds from the chromosphere to the lower corona. We suggest that the downflow in the footpoints of closed loops may be a common phenomenon on all scales, which could explain, why on a statistical basis bright pixels tend to be more redshifted, thus solving the net redshift problem. The observation of steady downflow in redshifted footpoints is indicative of a quiescent transport mechanism and seems to be in conflict with impulsive heating.

(W. Curdt, I. E. Dammasch, B. N. Dwivedi, and S. Parenti)

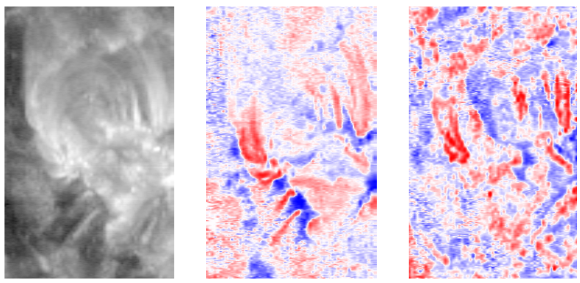

Fig. 69: Example of redshifted loop legs from 21 May 2004 showing Ne VIII emission both as radiance (left) and as Doppler map (center). It is also seen in the emission of O IV (right). The Doppler map reveals strong redshift of 20–30 km/s at both loop legs. These observations suggest a quasi-continuous downflow at all TR temperatures.

### 3-D reconstruction of polar plumes from EUVI/SECCHI images

We present the first stereoscopic reconstruction of the three-dimensional structures of polar plumes based on the two simultaneously recorded images taken by the EUVI telescopes in the SECCHI instrument package onboard the recently launched STEREO mission. The reconstructed polar plumes were observed on April

7th, 2007 when the two spacecraft were well below the solar equatorial plane, an appropriate time for the observation of the plumes in the south polar coronal hole. The heliocentric separation of the two spacecraft was 3.6 degrees at that time. We determine locations of the footpoints of five EUV polar plumes on the solar surface as well as their inclinations relative to the line-of-sight and to their local radial directions. The five plumes are all within 21° of the south pole and their inclinations to the line-of-sight of STEREO A(head) and to the radial directions are on average 107° and 28°, respectively. Of the three plumes in front of the limb only one is associated with an EUV bright point. Fig. 70 shows the projections of the 3-D plumes onto the solar equatorial plane. For each plume the size of the circle is proportional to the distance of the 3-D point to the solar surface.

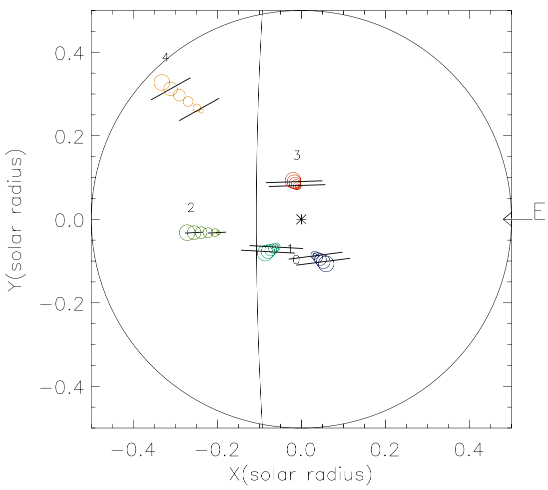


Fig. 70: The projections onto the equatorial plane of the 3-D plumes with the associated error bars (black solid lines). The solar limb as seen by the Earth is indicated by the curve near the south pole which is marked by a star symbol. The view direction from the earth is indicated by the arrow marked E at the right edge.

(L. Feng, B. Inhester, S. K. Solanki, T. Wiegelmann, and B. Podlipnik in collaboration with the STEREO/SECCHI team R. A. Howard, S. Plunkett, and J.-P. Wuelser)

### 3-D reconstruction of coronal loops from EUVI/SECCHI images

We present the first reconstruction of the three-dimensional shape of magnetic loops in an active region based on images recorded simultaneously from two different vantage points on 8 June 2007. The images were taken by the two EUVI telescopes of the SECCHI instrument onboard the recently launched STEREO spacecraft when the heliocentric separation of the two space probes was 12 degrees. We demostrate that these data allow a reliable three-dimensional reconstruction of sufficiently bright loops to be obtained. The result is compared with field lines derived from a coronal magnetic field model extrapolated from a photospheric magnetogram recorded nearly simultaneously by SOHO/MDI. We attribute discrepancies between reconstructed loops and extrapolated field lines to the inadequacy of the linear force-free field model used for the extrapolation. Fig. 71 shows the reconstructed loops and best fit magnetic field lines from a viewpoint which is different from STEREO A and B.

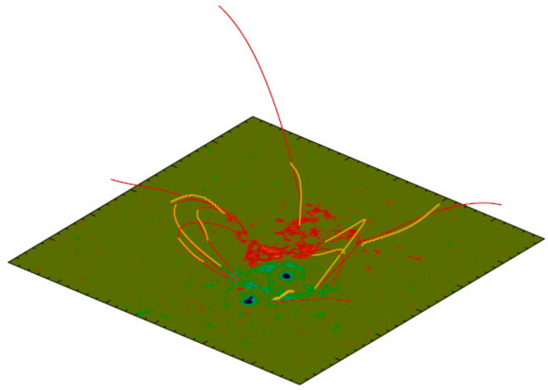

Fig. 71: The reconstructed 3-D loops (yellow lines) and extrapolated field lines (red lines) seen from a view point NE of the active region. The coloured background represents a photospheric magnetogram, with the opposite magnetic polarities being coloured green and red.

(L. Feng, B. Inhester, S. K. Solanki, T. Wiegelmann, and B. Podlipnik in collaboration with the STEREO/SECCHI team: R. A. Howard and J.-P. Wuelser)

### SOHO/SUMER observations of prominence oscillation before eruption

As a large-scale eruptive phenomenon, coronal mass ejections (CMEs) often reveal some precursors in the initiation phase, e.g., X-ray brightening, filament darkening, etc, which are useful for CME modelling and space weather forecast. With the SOHO/SUMER spectroscopic observations of the 26 September 2000 event, we propose another precursor for CME eruptions, i.e., long-time prominence oscillations.

A prominence oscillation-and-eruption event was observed by ground-based H$\alpha$ telescopes and space-borne EUV imaging and spectroscopic instruments. In particular, the SUMER slit was observing the prominence in sit-and-stare mode. The observations show that a siphon flow was moving from the proximity of the prominence to a far site, which was followed by repetitive H$\alpha$ surges and continual prominence oscillations (see Fig. 72). The oscillation lasted 4 hours before the prominence erupted as a blob-like CME. The analysis of the multiwavelength data indicates that the whole process fits well into the emerging flux trigger mechanism for CMEs. The emerging flux drives a siphon flow due to increased gas pressure where the background polarity emerges and H$\alpha$ surges due to magnetic reconnection where the opposite polarity emerges. The magnetic reconnection triggers the prominence oscillations, as well as its loss of equilibrium, which finally leads to the eruption of the prominence.

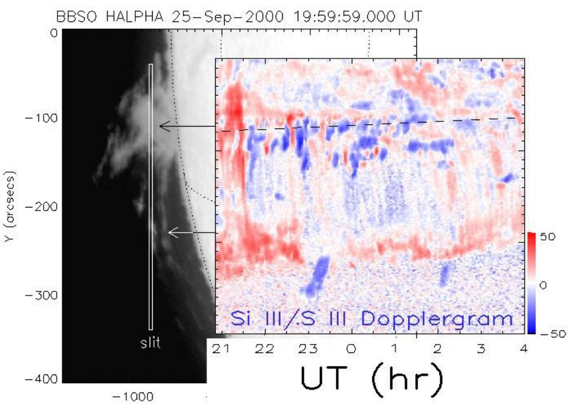


Fig. 72: Left: H$\alpha$ image showing the prominence and the position of the SUMER slit. Right: the time evolution of the Si III/S III 1113 Å Doppler shift. Oscillations with a period of about 20 min were seen along the dashed line at the height of the top arrow.

(P. F. Chen (Nanjing University, China), D. E. Innes, and S. K. Solanki)

### SUMER observations of molecular hydrogen in active region plage

SUMER-Hinode co-observations detected small concentrations of $H_2$ in active region plage at the footpoints of X-ray microflares. In six hours of observation, six of the seven $H_2$ sites in the SUMER rasters were near a footpoint of a brightening X-ray loop, seen with Hinode/XRT (Fig. 73). The seventh is associated with an unusually strong transition region plasma outflow.

The observed $H_2$ 1119.10 Å line is excited by O VI line emission at 1031.94 Å which is formed in the transition region. The $H_2$ intensity depends on both the strength of the O VI and the atmospheric opacity of the chromosphere between the O VI and $H_2$ layers.

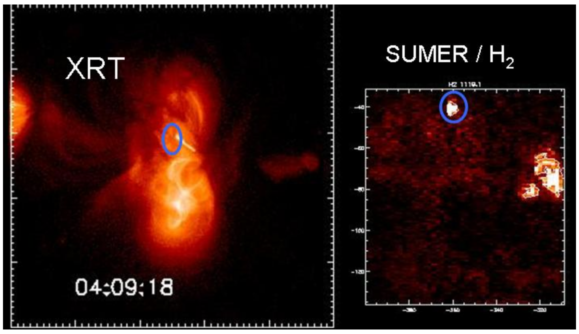


Fig. 73: Hinode/XRT image showing the active region with the microflare footpoint circled where strong molecular hydrogen was observed with SUMER. The molecular hydrogen footpoint emission, observed at 04:09 UT, is circled in the SUMER raster alongside. The other bright region of molecular hydrogen, at the right edge of the raster, is the sunspot.

Unfortunately, the observing sequence did not include the O VI line. As a proxy, we investigated the correlation between the intensities of $H_2$ and the Si III line at 1113.24 Å which, like O VI, is also formed in the transition region. There was no simple relationship between the two and several events that appeared bright in Si III showed no signature in $H_2$.

We conclude that an increase in O VI transition region emission cannot be the only reason for enhanced $H_2$ excitation and suggest that a chromospheric opacity decrease is also required. Microflare energy dissipation may heat the chromosphere, reducing its opacity, so that O VI microflare emission is able to reach the lower layers of the chromosphere and excite the $H_2$. Future observations with SUMER will measure the O VI 1031.94 Å and $H_2$ intensities almost simultaneously, in order to test this hypothesis.

(D. E. Innes)

### Small-scale flows in simultaneous SUMER and TRACE high-cadence observations

The physical properties of small-scale transient flows observed simultaneously at high cadence with the SUMER spectrometer and the TRACE imager in the plage area of an active region were studied. The major objective of this work was to provide a better understanding of the nature of transient phenomena in the solar atmosphere by using high-cadence imager and spectrometer co-observations at similar spatial and temporal resolution. A sequence of TRACE Fe IX/X $\lambda$171 Å and high-resolution MDI images were analysed together with simultaneously obtained SUMER observations in spectral lines covering a temperature range from 10 000 K to 1 MK. Numerous transient flows in small-scale loops (up to 30 Mm) were observed in the plage area of an active region. These flows have temperatures from 10 000 K (the low temperature limit of our observations) to 250 000 K. The coronal response of these features is uncertain due to a blending of the observed coronal line Mg X λ624.85 Å. The duration of the events ranges from 60 s to 19 min depending on the loop size. Some of the flows reach supersonic velocities. We found that Doppler shifts often associated with explosive events or bi-directional jets can actually be identified with flows (some of them reaching supersonic velocities) in small-scale loops. Additionally, we demonstrate how a line-of-sight effect can give misleading information on the nature of the observed phenomena if only either an imager or a spectrometer is used.

(M. S. Madjarska in collaboration with J. G. Doyle (Armagh Observatory, Northern Ireland))

### Emission heights of coronal bright points on Fe XIII radiance map

The study of coronal bright points (BPs) is important for understanding coronal heating and the origin of the solar wind. Previous studies indicated that coronal BPs have a highly significant tendency to coincide with magnetic neutral lines in the photosphere. We studied for the first time the emission heights of the BPs above the photosphere in the bipolar magnetic loops that are apparently associated with them. As BPs are seen in projection against the disk their true emission heights are unknown. The correlation of the BP locations on the Fe XII radiance map from EIT with the magnetic field features (in particular neutral lines) was investigated in detail. The coronal magnetic field was determined by an extrapolation of the photospheric field to different altitudes above the disk. It was found that most BPs sit on or near a photospheric neutral line, but that the emission occurs at a height of about 5 Mm. Some BPs, while being seen in projection, still seem to coincide with neutral lines, although their emission takes place at heights of more than 10 Mm. Such coincidences almost disappear for emissions above 20 Mm.

We also projected the upper segments of the 3-D magnetic field lines above different heights, respectively, on to the tangent x–y plane, where x is in the east-west and y in the south-north direction. The shape of each BP was compared with the respective field-line segment nearby. This comparison suggests that most coronal BPs are actually located on the top of their associated magnetic loops. Finally, we calculated for each selected BP region the correlation coefficient between the Fe XII intensity enhancement and the horizontal component of the extrapolated magnetic field vector at the same x–y position in planes of different heights, respectively. We found that for almost all the BP regions we studied, the correlation coefficient increases with increasing height to a maximal value and then decreases again. The height corresponding to this maximum was defined as the correlation height, which for most BPs was found to be smaller than 20 Mm.

(E. Marsch in collaboration with H. Tian, C.-Y. Tu, and J.-S. He (Department of Geophysics, Peking University, Beijing, China))

### Reconstructing the solar corona self-consistently with a magnetohydrostatic model during solar activity minimum

In the absence of regular large-scale coronal magnetic field measurements there is a need to determine the magnetic field at high accuracy from photospheric measurements. If we aim to determine also the plasma distribution, then there is a need to go beyond force-free models and complete a full magnetohydrostatic (MHS) field. We take an analytic MHS model to extrapolate the magnetic field in the corona from photospheric magnetic field measurement. The boundary conditions are given by a synoptic magnetogram at the photospheric level and by a source-surface model at the outer boundary. In the model, the electric current density can be decomposed into two components: one component is aligned with the magnetic field lines, whereas the other component flows in spherical shells. The second component of the current produces finite Lorentz forces that are balanced by the pressure gradient and the gravity force. We derive the 3-D distribution of the magnetic field and plasma self-consistently in one model. The density in the model is higher in the equatorial plane than in the polar region. We compare the magnetic field distribution of our model with potential and force-free field models for the same boundary conditions and find that our model differs from both. Magnetic field lines from these three different models are shown in Fig. 74.

(P. Ruan, T. Wiegelmann, B. Inhester, T. Neukirch, S. K. Solanki, and L. Feng)

### Attenuation of Alfvén waves in straight and curved coronal slabs

The attenuation and dissipation of Alfvén waves under coronal conditions has been the topic of considerable theoretical study over the years and has gained in interest ever since the discovery of coronal loop oscillations. We have considered impulsively generated Alfvén waves in coronal loops to investigate the role of energy leakage on wave attenuation, which includes

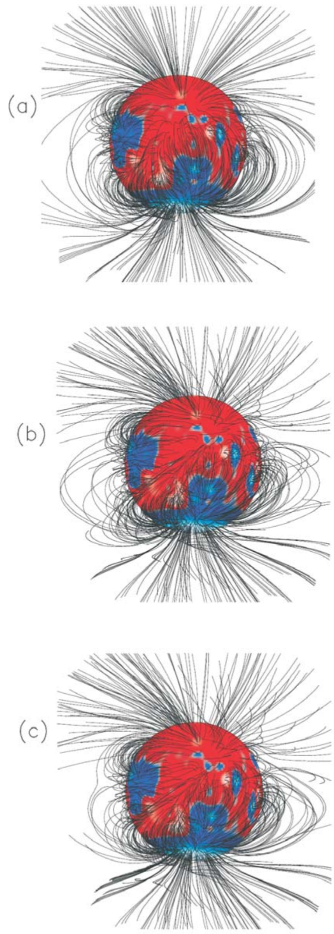


Fig. 74: Magnetic field lines in the corona for Carrington rotation 1919 from different models: (a): potential field model, (b): LFFF model with $\alpha = 0.4$, (c): MHS model with $\alpha = 0.4$ and $a = 0.2$.

lateral leakage, leakage into dense photospheric regions and nonlinear driving of magnetosonic waves.

A coronal loop was modelled as a straight magnetic slab, but also as a curved slab of smooth mass density profiles. We performed numerical simulations that solve the 2,5 D ideal magnetohydrodynamic equations to determine the signatures of Alfvén waves.

The numerical results show that lateral leakage of Alfvén waves is significant in comparison to leakage into the photospheric regions for realistic corona to photospheric density ratios. Energy leakage is enhanced by curvature of magnetic field lines and for large amplitude Alfvén waves for which nonlinear driving of magnetosonic waves is more significant than in the linear regime.

(S. K. Solanki in collaboration with M. Gruszecki, K. Murawski (Institute of Physics, UMCS, Lublin, Poland), and L. Ofman (The Catholic University of America, NASA Goddard Space Flight Center))

**Loop morphology and flows above a sunspot**

A striking feature of sunspots is the presence of photospheric nearly-horizontal flows directed outward from the sunspot umbra (Evershed effect), while the opposite is observed in the chromosphere (inverse Evershed effect). The inverse Evershed effect is also detected from space VUV spectra at temperatures up to the transition region where supersonic flows in sub-resolution structures are observed.

We have used SUMER to make maps of the line-of-sight velocity (Doppler shifts) showing that the inverse Evershed effect, observed at transition region temperatures up to 0.18 MK, displays unresolved features. To obtain more insight into the nature of the unresolved flow structures, maps of magnetic field strength and direction were obtained by applying a Milne-Eddington type inversion using one magnetic atmospheric component and a stray-light component to Hinode/SOT data.

Fig. 75 shows some of the field lines (obtained via nonlinear force-free extrapolation) overplotted to SUMER radiance and velocity maps. The comparison reveals information on the morphology and dynamics of the corona above the sunspot and, in particular, on the inverse Evershed effect that results from a combination of long reaching loops and a corolla of radially directed short loops surrounding the penumbra. These loops, with average width somewhat smaller than the 1 Mm SUMER spatial resolution and characterised by different plasma velocities, end in the ring of opposite polarity flux at the edge of the moat around the sunspot.

(L. Teriaca, T. Wiegelmann, A. Lagg, S. K. Solanki, and W. Curdt in collaboration with T. Sekii (National Astronomical Observatory of Japan, Tokyo 181-8588, Japan) and the Hinode/SOT Team)

**Evolution of a flaring active region as a sequence of nonlinear force-free field extrapolations**

The solar corona is structured by magnetic fields. As direct measurements of the coronal magnetic field are not routinely available, it is extrapolated from photospheric vector magnetograms. When magnetic flux emerges from below the solar surface and expands into the corona, the coronal mangetic field is destabilized leading to explosive events like flares or coronal mass ejections.
We study the temporal evolution of flaring active region (AR) NOAA 10540 from 18 to 21 January 2004 and are in particular interested in the free magnetic energy available to power the flares associated with it. We use photospheric vector magnetograms measured

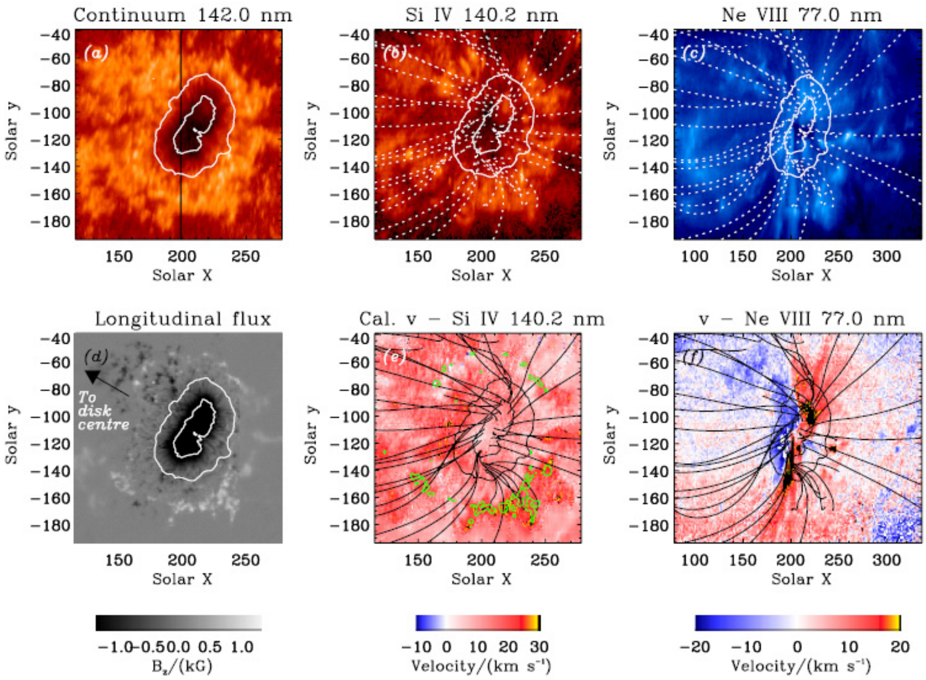


Fig. 75: SUMER radiance *(a - c)* and velocity *(e - f)* maps. Panel *(d)* shows the $B_Z$ field. On panel *(e)* the positive $B_Z$ level of 300 G is shown in green. Note that the velocity map in panel *(e)* has an absolute calibration while that in *(f)* is computed against the average over the FOV. Umbra and penumbra contours are from the SOT-SP continuum. On panels (*b*, *c*, *e*, and *f*) the dotted lines trace some of the extrapolated field lines.

with the Solar Flare Telescope (SFT) of the National Astronomical Observatory of Japan (NAOJ), located in Tokyo. We extrapolate these measurements into the corona with the help of a nonlinear force-free field model. This coronal magnetic field model is based on a well tested multigrid-like optimization code with which we are able to estimate the energy content of the 3-D coronal field, as well as an upper limit for its free magnetic energy. Furthermore, the evolution of the energy density with height and time is studied.

The coronal magnetic field energy in AR 10540 increases slowly during the days before a M6.1 flare and drops significantly after it. We estimated the energy which has been set free during this event as $\propto 10^{25}$ *J* which is sufficient to power a large flare (see Fig. 76).

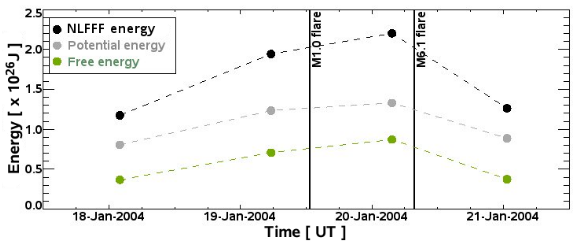


Fig. 76: Total magnetic energy of the nonlinear force-free field (black), potential field (gray), and free magnetic energy (green) before/after two M-class flares.

We also estimated the energy density in the flaring region, i.e., the amount of stored energy per unit volume, which is highest before the occurrence of the M6.1 flare and is mainly concentrated in low heights ($\approx$ 20 Mm) above the photosphere.

(J. K. Thalmann and T. Wiegelmann)

### Optimization approach for the computation of magnetohydrostatic coronal equilibria in spherical geometry

We developed an optimization method for computing nonlinear magnetohydrostatic equilibria in spherical geometry with the aim to obtain self-consistent solutions for the coronal magnetic field, the coronal plasma density and plasma pressure using observational data as input. Previous versions of the code have been used to compute nonlinear force-free coronal magnetic fields from photospheric measurements in Cartesian and spherical geometry, and magnetostatic-equilibria in Cartesian geometry. We test our code with the help of a known analytic 3-D equilibrium solution of the magnetohydrostatic equations. We find that the method reconstructs the equilibrium accurately, with residual forces of the order of the discretisation error of the analytic solution. The correlation with the reference solution is better than 99.9 %

and the magnetic energy is computed accurately with an error of $< 0.1\%$. In Fig. 77 we outline how our newly developed code can be used to reconstruct the coronal magnetic field and plasma from observational data. The basic idea is to compute first a nonlinear force-free field from observed vector magnetograms and then model the plasma along the loops. Artificial images from the model plasma are compared with observed coronal EUV images, which allows us to improve the plasma model. Optional the plasma density can be reconstructed with tomographic methods. Our newly developed magnetohydrostatic code uses the resulting magnetic field and plasma configuration as input for the computation of a self-consistent equilibrium.

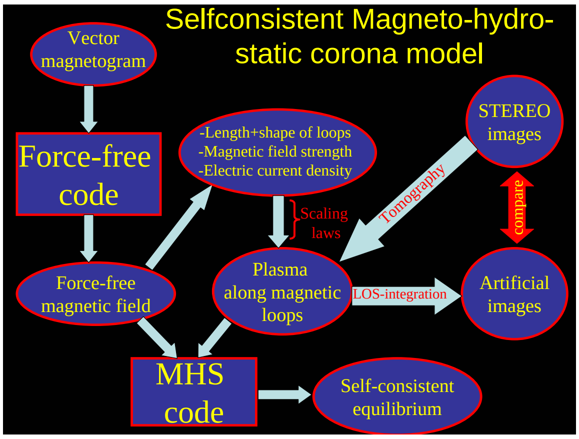


Fig. 77: How can we model the solar corona from observed quantities like the magnetic field vector in the photosphere and coronal EUV images?

(T. Wiegelmann, P. Ruan, and B. Inhester in collaboration with T. Neukirch (University of St. Andrews))

### Changes of Magnetic Structure in 3-D Associated with the $X3.4$ Flare of 13 December 2006

Recent observations demonstrated that sunspot structure can change rapidly and irreversibly after flares. One of the most puzzling results is the increase in magnetic shear around flaring magnetic polarity inversion line after flares. However, all these observations were made at the photosphere level. We study the altitude variation of the non-potentiality of the magnetic fields associated with the $4B/X3.4$ flare of 13 December 2006. The vector magnetograms with unprecedented quality from Hinode before and after the flare are used as the boundary conditions to extrapolate the 3-dimensional nonlinear force-free magnetic fields and the potential fields. The former are computed with the optimization algorithm and the later with Greens function method. At the photosphere boundary, magnetic shear increases after the flare in a local area close to the flaring magnetic polarity inversion line. Two measures of the magnetic non-potentiality, the weighted mean shear (top panel in Fig. 78) and the total magnetic shear (bottom panel in Fig. 78), are calculated in this area at progressively higher altitude. By comparing their altitude variation profiles before and after the flare, we find that the non-potentiality of the local area increases after the flare below about 8 Mm and decreases from that height to about 70 Mm. Beyond 70 Mm, the magnetic fields approach potential for both times.

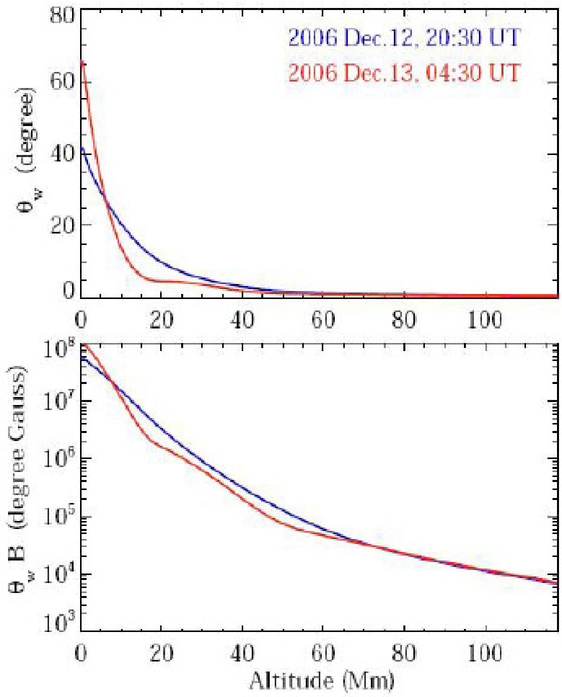


Fig. 78: Weigted mean shear (top panel) and total magnetic shear (bottom panel) in the flaring region as a function of altitude. Blue: before the flare, red: after the flare.

(T. Wiegelmann in collaboration with Ju Jing, Haimin Wang (New Jersey Institute of Technology and Big Bear Solar Observatory), Yoshinori Suematsu (NAOJ), and Masahito Kubo (High Altitute Observatory))

### Can we improve the preprocessing of photospheric vector magnetograms by the inclusion of chromospheric observations?

The solar magnetic field is key to understanding the physical processes in the solar atmosphere. Unfortunately, we can measure the magnetic field vector routinely with high accuracy only in the photosphere. These measurements are extrapolated into the corona under the assumption that the field is force-free. That condition is not fulfilled in the photosphere, but is in the chromosphere and corona. In order to make the observed boundary data consistent with the force-free assumption, we therefore have to apply some transformations before nonlinear force-free extrapolation codes can be legitimately applied. We developed a minimization procedure that uses the measured photospheric field vectors as input to approximate a more chromospheric-like field. The procedure includes force-free consistency integrals, spatial smoothing, and - newly included in the version presented here - an improved match to the field direction as inferred from fibrils as can be observed in, e.g., chromospheric $H\alpha$ images. We test the procedure using a model active-region field that included buoyancy forces at the photospheric level. The proposed preprocessing method allows us to approximate the chromospheric vector field to within a few degrees and the free energy in the coronal field to within one percent, which represent very significant improvements over the earlier method.

(T. Wiegelmann and J. K. Thalmann in collaboration with C. J. Schrijver, M. L. DeRosa (Lockheed Martin Advanced Technology Center, Palo Alto, USA) and T. R. Metcalf, deceased)

### Nonlinear force-free magnetic fields: The influence of uncertainties in photospheric field measurements

It is expected that inaccuracies in the magnetic vector obtained in the photosphere influence the field extrapolated into the corona, but this has never been studied in a systematic manner. The aim of this study is to investigate how inaccuracies introduced into the photospheric magnetic field vector map from the inversion of asymmetric and noisy Stokes parameters influence the extrapolation of nonlinear force-free magnetic fields. We compute nonlinear force-free magnetic fields based on simulated vector magnetograms, which have been produced by the inversion of Stokes profiles, computed from a 3-D radiation MHD simulation snapshot. These extrapolations are compared with extrapolations starting directly from the field in the MHD simulations, which is our reference. We investigate how line formation and instrumental effects such as noise, limited spatial and spectral resolution and limited spectral sampling influence the resulting magnetic field structure. The reconstructed field is most accurate if ideal Stokes data are inverted and becomes less accurate as an increasing number of instrumental effects and noise are included. In all cases we find, however, that a force-free reconstruction agrees with the reference field significantly better than a potential field extrapolation starting directly from the magnetic field at a given geometric level in the MHD data cube.

(T. Wiegelmann, L. Yelles Chaouche, S. K. Solanki, and A. Lagg)

## Solar wind and heliosphere

### Kinetic properties of the solar corona and solar wind

The kinetic plasma physics of the solar corona and solar wind are reviewed with emphasis on the theoretical understanding of the in-situ measurements of solar wind particles and waves, as well as on the remote-sensing observations of the solar corona made by means of ultraviolet spectroscopy and imaging. In order to explain coronal and interplanetary heating, the microphysics of the dissipation of various forms of mechanical, electric and magnetic energy at small scales (e.g., contained in plasma waves, turbulences or non-uniform flows) must be addressed. We therefore scrutinise the basic assumptions underlying the classical transport theory and the related collisional heating rates, and also describe alternatives associated with wave-particle interactions. We elucidate the kinetic aspects of heating the solar corona and interplanetary plasma through Landau- and cyclotron-resonant damping of plasma waves, and analyse in detail wave absorption and micro instabilities. Important aspects (virtues and limitations) of fluid models, either single- and multi-species or magnetohydrodynamic and multi-moment models, for coronal heating and solar wind acceleration are critically discussed. Also, kinetic model results which were recently obtained by numerically solving the Vlasov–Boltzmann equation in a coronal funnel and hole are presented. Promising areas and perspectives for future research are outlined finally.

(E. Marsch)

### Reviews on the origin and evolution of the solar wind and its response to the solar activity cycle

The coronal origins of the solar wind and the sources of the steady streams and transient flows caused by solar magnetic eruptions were discussed in two tutorial review papers, given at a workshop held within the International Living With a Star (ILWS) programme in Goa, India, and at the symposium of the International Astronomical Union (IAU) in Cairo, Egypt. The solar wind response to the solar activity cycle was discussed in a review article resulting from the Paris COSPAR meeting. The magnetic field of the Sun and the plasma properties of its atmosphere, such as temperature distribution, density stratification, photospheric convection and waves in the corona, determine the origin, energetics and evolution of the solar wind. The solar wind comes in three main kinds, as steady fast streams, variable slow flows and transient slow and fast coronal mass ejections. The three types of solar wind are closely associated with and largely determined by the structure and activity of the coronal magnetic field. The plasma characteristics and magnetic features of the solar wind source regions are reviewed. The boundary conditions in the mostly closed corona (streamers and loops), in the transiently opening corona (eruptive prominences and loops) and in the lastingly open corona (funnels and holes) are analyzed. The resulting three-dimensional structure of the solar wind and the evolution of the inner heliosphere over the solar cycle are discussed. The variations of the solar wind ram pressure and consequent variations of the global heliosphere are briefly addressed.

(E. Marsch)

**Limits on the core temperature anisotropy of solar wind protons**

We analyse the temperature anisotropy of the protons in the solar wind and thereby concentrate on plasma data obtained in the year 1976 of the Helios 1 and Helios 2 missions. We derive the core proton temperatures $T_\perp$ and $T_\parallel$, in the directions perpendicular and parallel to the magnetic field, as well as the core parallel plasma beta, $\beta_\parallel$. The data are separately analysed for two distance ranges, $R \leq 0.4$ AU and $R > 0.4$ AU, and divided into 24 bins for the plasma beta, in the range from 0.1 to 10, and into 72 bins for the total temperature anisotropy, $A = 1 - T_\perp/T_\parallel$, which is here considered in the range from $-0.9$ to 0.9. The number of spectra in each bin is determined to obtain occurrence distributions. The statistical results are presented in two-dimensional histograms. For each column we define a critical upper and lower limit of the anisotropy (indicated by red lines in Fig. 79). Empirical limits for $A$ are determined as a function of $\beta_\parallel$ and compared with the theoretical thresholds (yellow lines) for the mirror and firehose instability, as obtained from published linear stability analyses and numerical simulations. Nearer to the Sun the solar wind core protons are found to be largely stable against growth of the firehose mode. But they stay close to the fluid nonresonant as well as the kinetic resonant instability thresholds at larger solar distances (see Fig. 79).

(E. Marsch in collaboration with L. Zhao (Department of Atmospheric, Oceanic, and Space Sciences, University of Michigan, Ann Arbor, USA) and C.-Y. Tu (Department of Geophysics, Peking University, Beijing, China))

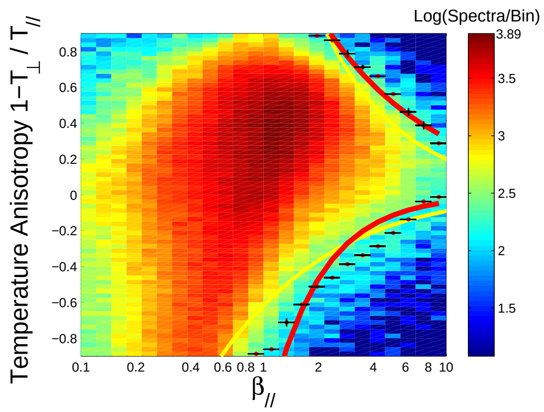


Fig. 79: Two-dimensional histogram of the solar wind proton anisotropy measured within the radial distance range with $R > 0.4$ AU. The core temperature anisotropy $A$ is shown as a function of the parallel plasma beta of the core protons. The colour coding logarithmically indicates the number of spectra per bin. The colour scale itself is linear. Black horizontal bars in each $\beta_\parallel$-column indicate where the logarithm of the number of spectra equals 2.2, which is used as a limiting value. The red lines are theoretical fits to these marginal data points. The theoretical thresholds are shown by yellow lines for the mirror (upper curve) and firehose (lower curve) instability. The total number of proton spectra analysed is 193 902.

**Ion-cyclotron beam instabilities in a coronal funnel**

Spectroscopic solar observations suggest the resonant ion-cyclotron wave-particle interactions as a principal mechanism for heating and accelerating ions in the magnetically open coronal holes. However, the mechanism responsible for the generation of the ion-cyclotron waves remains unclear. One possible scenario is that ion beams emanating from small-scale reconnection events can drive micro-instabilities which might in turn excite ion-cyclotron waves. In the framework of the collisionless multi-fluid model, a Fourier plane-waves linear perturbation analysis is performed in order to study ion beam-driven electromagnetic instabilities. While neglecting the electron inertia this model allows one to take into account ion-cyclotron wave effects that are absent from the one-fluid MHD model. Realistic models of the density and temperature, as well as a 2-D analytical model describing a funnel open-field region, are used to define the background plasma. Assuming realistic beam velocities taken from observations of small-scale reconnection events, it is demonstrated (Fig. 80 and Fig. 81) that the free energy provided by the ion beam propagating parallel the ambient field can drive micro-instabilities through ion-cyclotron resonant excitation.

(R. Mecheri and E. Marsch)

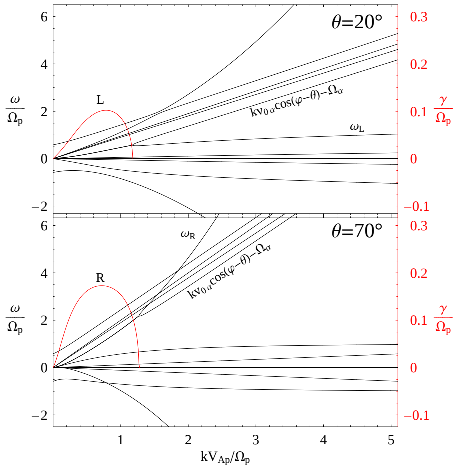


Fig. 80: Dispersion curves in a beam plasma with electrons ($n_{0e}$), protons ($n_{0p}$) and alpha particles ($He^{2+}$, $n_{0\alpha}/n_{0p} = 0.1$ and $v_{0\alpha} = 350$ km/s) at a funnel location, with a magnetic field inclination angle of 82° with respect to the normal on the solar surface and a proton Alfvén speed $V_{Ap} \approx 175$ km/s. Wave frequency (black) and growth rate (red), both normalized to the proton cyclotron frequency $\Omega_p$, are shown versus the normalized wave number $kV_{Ap}/\Omega_p$. Note, for an angle of propagation $\theta = 20°$ (i.e., quasi-perpendicular propagation), the left-hand resonant excitation (L) of the ion-cyclotron mode ($\omega_L$) and for $\theta = 70°$ (i.e., quasi-parallel propagation) the right-hand resonant excitation (R) of the fast mode ($\omega_R$). The plasma beta values are $\beta_e = 0.4\,\beta_b = 4\,\beta_\alpha = 0.004$.

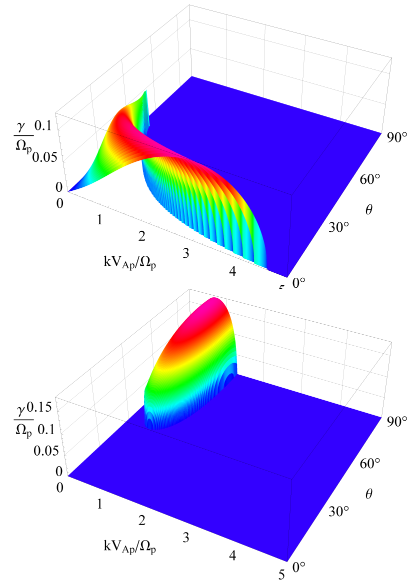


Fig. 81: Growth rate as a function of the angle of propagation $\theta$ and the normalized wave number $kV_{Ap}/\Omega_p$ of the left-hand (top) and the right-hand (bottom) resonant ion-cyclotron instabilities in the case of an alpha particle ($He^{2+}$) beam plasma. For the relevant parameters see Fig. 80.

## Ion-cyclotron drift instabilities in the nonuniform corona

Recent observations revealed that the solar atmosphere is highly structured in density, temperature and magnetic field. The presence of these gradients in the plasma leads to the appearance of electric currents which in the weakly collisional corona can provide free energy for driving microinstabilities. These instabilities are very relevant since they may constitute an important source of ion-cyclotron waves, which have been concluded to play a key role in coronal heating but whose coronal origin remains unclear. Considering a density stratification transverse to the magnetic field, we studied the possible occurrence of gradient-induced microinstabilities under typical funnel conditions. A Fourier plane-waves perturbation analysis is performed in the framework of the multi-fluid model. While neglecting the electron inertia this model allows one to take into account ion-cyclotron wave effects that are absent from the one-fluid MHD model. Realistic models of density and temperature as well as a 2-D analytical magnetic field model are used to define the background plasma in the open-field region of a polar coronal hole. We demonstrate that, assuming typical transverse density length scales taken from radio observations, the current generated by a relative gradient-drift between electrons and ions can provide enough free energy for driving waves unstable. This instability results from the coupling of two slow-mode waves into one single unstable mode (Fig. 82 and Fig. 83).

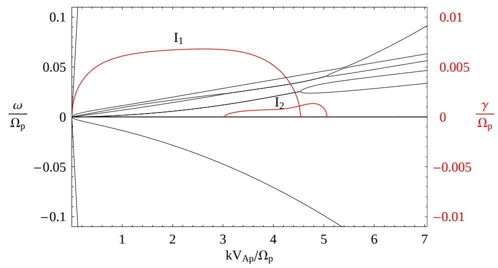


Fig. 82: Three-fluid drift plasma dispersion curves at a funnel location with a magnetic field inclination angle of 85.3° and for an angle of propagation $\theta = 85°$, both with respect to the normal on the solar surface. The plasma consists of electrons ($n_{0e}$), protons ($n_{0p}$) and alpha ($He^{2+}$) particles (with $n_{0\alpha} = 0.1\, n_{0p}$) in relative drift. The drift currents are due to a density stratification perpendicular to the magnetic field with a length scale L = 1 km. Note the appearance of two instabilities ($I_1$ and $I_2$) resulting from the coupling of slow modes. The frequency (in black) and growth rate (in red) are normalized to the proton cyclotron frequency $\Omega_p$, and the wavenumber k to $\Omega_p/V_{Ap}$ where $V_{Ap}$ is the proton Alfvén speed. The corresponding plasma beta values are $\beta_e = 1.2\,\beta_p = 4\,\beta_\alpha \approx 0.09$. Here $T_{0\alpha} = 3\,T_{0p} = 3\,T_{0e}$.

(R. Mecheri and E. Marsch)

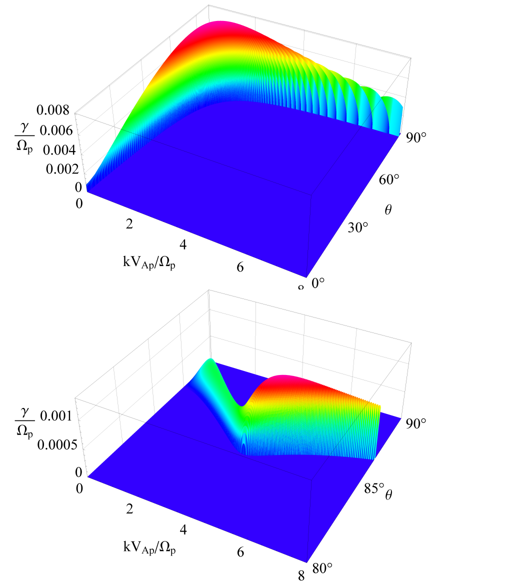


Fig. 83: Growth rate of the $I_1$ (top) and $I_2$ (bottom) slow modes instabilities (shown in Fig. 82) as a function of the propagation angle $\theta$ and the normalized wave number $kV_{Ap}/\Omega_p$. The density length scale perpendicular to the magnetic field is L = 1 km. For the relevant parameters see caption of Fig. 82.

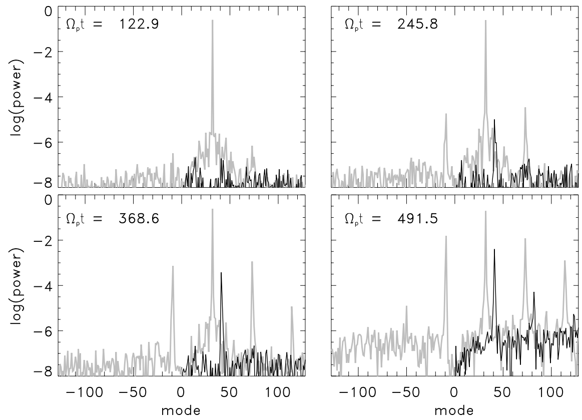


Fig. 84: Evolution (shown at four instances of time in units of the proton gyroperiod) of the wave power spectrum for the magnetic field fluctuations (gray line) and density fluctuations (dark line) as function of the wave mode number for a left-hand polarized pump wave. Its relative amplitude $B$ is 0.5, the mode number is $m = +32$, $\beta_e = 1.4$, and $\beta_p = 0.01$.

### Collisionless damping of parametrically unstable Alfvén waves

Linear Vlasov theory and one-dimensional hybrid simulations were used to study the parametric instabilities of a circularly polarized parallel-propagating Alfvén wave in a homogeneous, magnetized, and collisionless plasma. The linear and the weakly nonlinear development of the instabilities of the Alfvén waves were analysed and discussed, including kinetic effects. The structure, growth, and damping of the driven ion-acoustic-like waves (see Fig. 84) were investigated. The dispersion relation reproduces the fluid characteristics of the instabilities in the case that protons are cold, but it contains an infinite number of roots in the general case. It was shown that at low proton plasma beta ($\beta \approx 0.1$), kinetic effects break the degeneracy of the mode-coupling solutions of the fluid theory, and thus one can unambiguously identify the growing and the damped modes. It was further found that, contrary to traditional thought, kinetic effects remain important even for very low $\beta$ in the late stages of the linear evolution, leading to a de-phasing effect between the plasma pressure and the density fluctuation. The relevance of the results to the experimental identification of the instabilities, to the generation of local turbulence, and to the reduction of cross helicity in the solar wind were pointed out.

(E. Marsch in collaboration with J. Araneda (Departamento de Fisica, Universidad de Concepción, Chile) and A. Viñas (NASA Goddard Space Flight Center, Greenbelt, Maryland, USA))

### Diffusion plateaus in the velocity distributions of protons in fast solar wind

In a collisionless plasma, such as the fast solar wind, wave-particle interactions play the decisive role in determining the shape of particle velocity distribution functions (VDFs). In our analysis we provide observational evidence for the resonant interaction of the protons with ion-cyclotron/Alfvén waves which propagate outward from the Sun along the interplanetary magnetic field. According to quasi-linear theory, the protons thereby diffuse in velocity space, a process that can lead to the formation of plateaus in their VDF. This diffusion plateau formation naturally explains the observed thermal anisotropies in the core of the proton VDFs. (For an example see Fig. 60 on page 57 of the previous annual report.)

With respect to whether the diffusion plateau was actually reached (which is assessed and quantified by the parameter $\epsilon$ that measures in percentage the relative deviation from a plateau), we investigated a large number (about 10000) of individual VDFs from several distinct fast solar wind streams observed between 0.3 and 1 AU. All these measurements were made by Helios 2 during the solar minimum in 1976 and 1977. The proton VDFs were provided by the plasma instrument and modelled by a superposition of multiple Gaussians, such that the plasma dispersion relation for parallel-propagating Alfvén/cyclotron waves could readily be solved numerically. Thus the details of the proton VDFs could be well represented in the dispersion relation, which made our theoretical analysis as self-consistent as possible, and proton thermal effects on the wave dispersion relation were naturally taken into account. The results are presented in Fig. 85, which shows $\epsilon$ as evaluated on the sunward and earthward parts of each VDF versus heliocentric distance for fast solar wind. Apparently, towards the sun the proton core VDF reveals a stable plateau which hardly changes with radial distance.

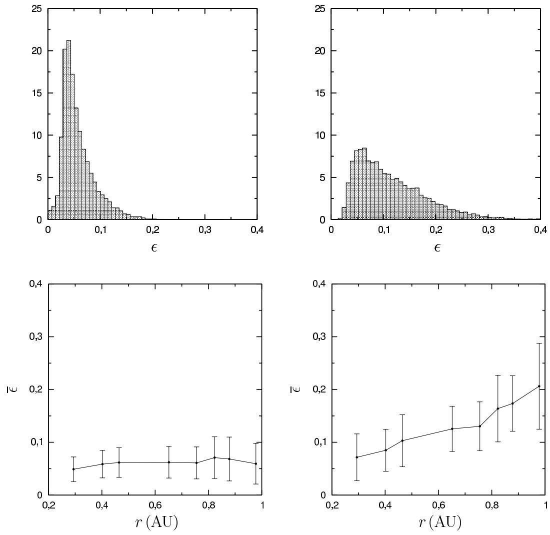


Fig. 85: (top) Histograms of $\epsilon$, which both are normalized to unity and comprise the values of this parameter describing the deviation of a proton VDF from its self-consistent diffusion plateau on the antibeamward (left) and beamward (right) side of the proton core, respectively. (bottom) Mean values and variances of $\epsilon$ plotted against heliocentric distance for fast solar wind. An $\epsilon$ of zero indicates a complete plateau.

(M. Heuer and E. Marsch)

### On the evolution of the solar wind proton temperature anisotropy from 0.3 to 2.5 AU

In a research letter we reported a detailed analysis of the proton temperature anisotropy evolution in the solar wind from 0.3 to 2.5 AU, on the basis of Helios and Ulysses observations. We found an important dependence of the anisotropy regulation mechanisms on heliocentric distance. The fast wind data show a distinct path in the relevant parameter space, whereby the first part of the trajectory is well described by an anticorrelation between the proton temperature anisotropy $T_{\perp p}/T_{\parallel p}$ and the parallel plasma beta, $\beta_{\parallel p}$, while beyond 1 AU the evolution in parameter space changes, and the data result in agreement with the constraints placed by the fire-hose instability. The slow wind data show a more irregular behaviour, and in general it is not possible to recover a single evolution path. However, on small temporal scale we found that different slow streams populate different regions of the parameter space. This suggests that when considering single streams the anisotropy in slow wind possibly follows an evolution path as well.

(E. Marsch in collaboration with a team of people from different institutes, lead by L. Matteini (Universita degli Studi di Firenze, Italy))

## Past solar activity and Sun-Earth relations

### Variations of total solar irradiance (TSI)

Variations of total solar irradiance (TSI) have been measured since 1978. For earlier times, TSI has been reconstructed using models that make use of available data (e.g., sunspot areas since 1874 or sunspot numbers since 1611). For a comparison with climate records extending across the Holocene a much longer reconstruction of TSI is needed. In earlier work we provided the main missing ingredient of such a reconstruction, a long-term record of sunspots, based on cosmogenic $^{14}C$ records. Its use, however, requires a change in the modelling approach, since only 10-year averages of sunspot numbers can be reconstructed from $^{14}C$. After the adaptation of the models, a preliminary reconstruction of TSI throughout the Holocene has been carried out. It is shown in Fig. 86, where the blue line represents the best estimate of TSI and the red curves indicate the estimated cycle amplitude. On average, the Sun has been 0.6 W/m$^2$ brighter during the last 60 years than averaged over the whole Holocene, and it spent less than 10% of the time at such high activity levels. Further work on this topic is underway.

(L. Vieira, S. K. Solanki, N. A. Krivova, and L. Balmaceda)

### A cross-calibrated sunspot area time series since 1874

A complete and homogeneous historical record of sunspot areas is a valuable proxy of solar variability and has been widely used, e.g., to study the characteristics of the solar cycle or to reconstruct total and spectral irradiance at earlier times. The Royal Greenwich Observatory regularly measured this and other related parameters between 1874 and 1976. After that time records from a row of different observatories are available. These, however, show systematic differences and often have significant gaps. We compared

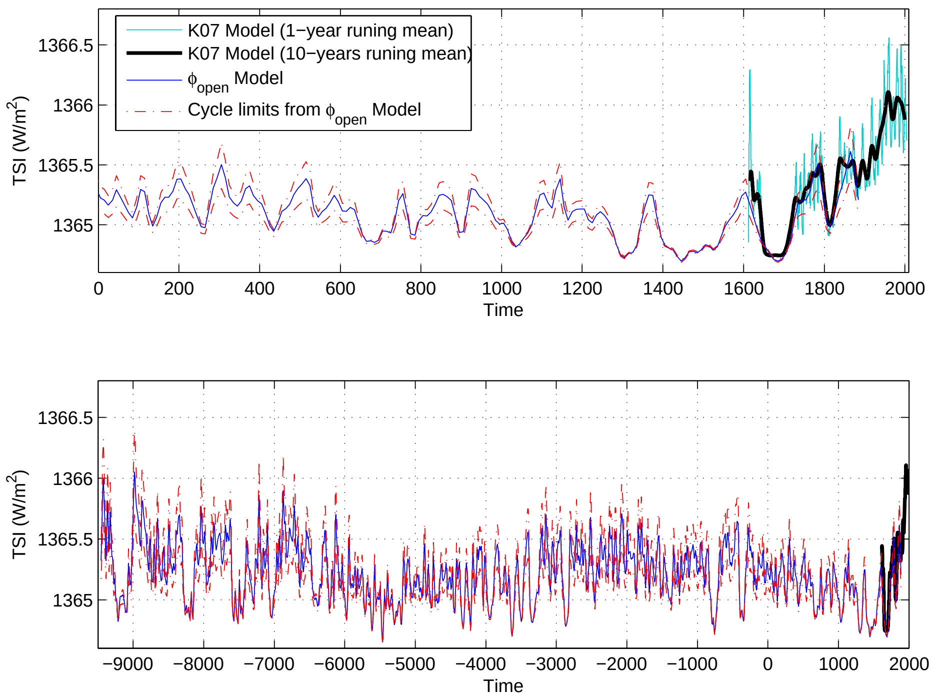


Fig. 86: Reconstructed TSI over the last 11 400 years (blue line). The red curves mark the estimated cycle amplitude, the light blue and black lines show the 1-yr and 10-yr running means, respectively, for the reconstruction by Krivova et al. (2007) based on the modelled evolution of the solar photospheric magnetic flux.

the data from different observatories when they overlap and determined the corresponding calibration factors. Using these data we compiled a complete and cross-calibrated time series.

The new composite sunspot area record was used to reconstruct solar total and UV irradiance variations. Variations in solar irradiance on time scales longer than approximately a day are caused by dark sunspots and bright faculae. Due to different wavelength dependences of their contrast, the contribution of faculae is higher in the UV than in the visible or IR, whereas the contribution of sunspots is almost negligible in the UV. Therefore employment of faulty sunspot data to reconstruct solar total and UV urradiance can lead to systematic differences between them. Thus, Foukal (2002) claimed on the basis of reconstructions using uncalibrated and thus biased data that UV irradiance does not follow total irradiance and is irrelevant for the Earth's climate. However, we show that when appropriately calibrated sunspot areas are employed, both total and UV solar irradiance behave similarly.

(L. Balmaceda, S. K. Solanki, and N. A. Krivova)

**Reconstruction of solar UV irradiance in cycles 21 – 23**

Solar irradiance variations show a strong wavelength dependence. Whereas the total solar irradiance varies by about 0.1% over the solar cycle, variations at wavelengths around the Ly-$\alpha$ emission line near 121.6 nm reach up to 100%. These variations may have a significant impact on the Earth's climate system. Being almost completely absorbed in the upper atmosphere, solar UV radiation below 300 nm affects stratospheric chemistry and controls production and destruction of ozone.

Initial work aimed at extending our SATIRE model (Spectral and Total Irradiance REconstructions) to reproduce the SUSIM measurements of the spectral irradiance in the UV right down to Ly-$\alpha$ wavelengths. In the next step we employed the SOHO MDI and NSO Kitt Peak magnetograms and continuum images, to reconstruct solar UV irradiance back to 1974. Gaps in the daily record are filled in using such proxies of solar UV irradiance as Mg II index and radio flux at 10.7 cm. The reconstructed Ly-$\alpha$ irradiance agrees well with an independent composite of UARS SOLSTICE mesurements and proxy models (Fig. 87).

(N. A. Krivova, S. K. Solanki, T. Wenzler, and B. Podlipnik in collaboration with L. Floyd (Interferometrics Inc., USA))

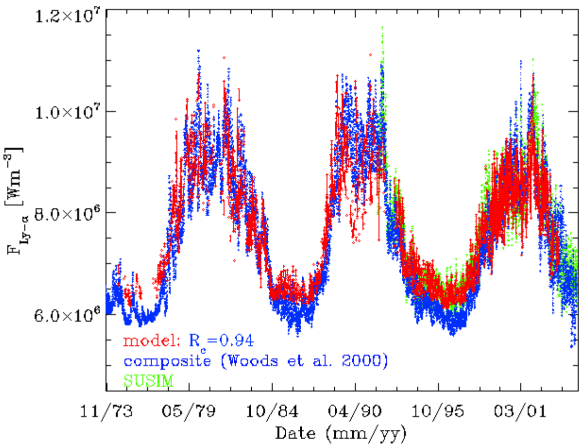


Fig. 87: Solar Ly-$\alpha$ irradiance since 1974: reconstructed (red), measured by the SUSIM instrument (green) and compiled by Woods et al. (blue). This latter record includes measurements by the space instruments AE-E, SME, UARS SOLSTICE and TIMED SEE, as well as proxy models based on Mg C/W and F10.7 indices, all adjusted to the absolute level of SOLSTICE.

### Spectral irradiance variations: Comparison between observations and the SATIRE model on solar rotation time scales

Until very recently, the spectral dependence of the solar variability had mainly been determined in the UV, in particular by the measurements taken by the SUSIM and SOLSTICE instruments onboard UARS. Information in the visible was restricted to the three colour channels of the SPM instrument of SOHO/VIRGO, though degradation hampered the use of these data beyond time scales of the order of a couple of months. The irradiance variability at most other wavelengths had to be inferred using indirect methods, including models of solar spectral irradiance. Thanks to missions such as SORCE and SCIAMACHY, the observational outlook has now become much better and we have, for the first time, variability observations that span from the UV to the near IR. This allows us to test the reliability of spectral irradiance calculations between 200 and 1600 nm based on the SATIRE model over three solar rotations in 2004.

We compare our model calculations with spectral irradiance observations taken with SORCE, SOHO/VIRGO and UARS/SUSIM. The variability as a function of wavelength as well as time series in a number of selected wavelength regions covering the UV to the near IR were analysed. We also show the facular and spot contributions to the total calculated irradiance. In most wavelength regions, the variability agrees well between all sets of observations and the model calculations. The model does particularly well between 400 and 1300 nm, but fails below 220 nm as well as for some of the strong NUV lines. Our calculations clearly show the shift from faculae-dominated variability in the NUV to spot-dominated variability above approximately 400 nm. At wavelengths between approximately 310 and 350 nm the model calculations currently provide the best estimates of solar variability due to the low sensitivity of SUSIM and SORCE in this range.

(N. A. Krivova and S. K. Solanki in collaboration with Y. C. Unruh (Blackett Laboratory, Imperial College London, UK) and J. Harder, G. Kopp (LASP, Boulder, USA))

### Modelling solar cycle variation of spectral line properties

In addition to measurements of the irradiance of the Sun, there are also observations of the variations of the depths and equivalent widths of individual spectral lines over the solar cycle, such as Mn I 539.4 nm. Such observations have been regularly carried out by W. Livingston for two solar cycles at the Kitt Peak National Solar Observatory. The Mn line is particularly interesting since its parameters show an unusually large amplitude change over the solar cycle, compared with other spectral lines (e.g. of iron or carbon). One explanation proposed for this phenomenon is the optical pumping by the Mg II k line.

We have taken another approach and started from the assumption that it is simply the change in the coverage of the solar surface by magnetic features which is responsible. We couple the radiative transfer of this and other lines, but excluding optical pumping, with the SATIRE model (Spectral and Total Irradiance Reconstructions) used to reconstruct, e.g., total irradiance during the satellite era. With this approach we could well reproduce the behaviour of the Mn line as well as simultaneously observed Fe I lines with exactly the same value of the single free parameter in SATIRE as used for the reconstruction of total solar irradiance. This suggests that there is no need to invoke optical pumping effects to explain the behaviour of the Mn line.

(S. Danilovic, S. K. Solanki, and N. A. Krivova in collaboration with W. Livingston (National Solar Observatory, USA) and I. Vince (Astronomical Observatory, Serbia))

### Dependence of sunspot brightness on sunspot size and cycle phase

Albregtsen and Maltby, (1978) reported an increase in umbral core brightness from the early to the late phase of the solar cycle from the analysis of 13 sunspots which cover solar cycles 20 and 21. At the same time, they did not find any dependence of umbral brightness on the size or the type of the sunspot. We have revisited this topic by analysing continuum images of more than 160 sunspots observed by the MDI instrument onboard the SOHO spacecraft between March 1998 and March 2004, i.e. a sizable part of solar cycle 23. The advantage of this data set is its homogeneity, with no seeing fluctuations. A careful stray light correction, which is validated using the Mercury transit of 7 May 2003, was carried out before the umbral and penumbral intensities are determined. The influence of the Zeeman splitting of the nearby Ni I spectral line on the measured 'continuum' intensity was also taken into account.

No significant variation in umbral core, mean umbral and mean penumbral intensities with solar cycle was found, in contrast to the earlier findings. We found, however, a strong and clear dependence of the umbral brightness on sunspot size. The penumbral brightness also displays a weak dependence. The deduced brightness-radius relationship has numerous implications, such as those for the energy transport in umbrae or irradiance reconstructions.

(S. K. Solanki and N. A. Krivova in collaboration with S. K. Mathew (Udaipur Solar Observatory, India) and V. Martínez Pillet (Instituto de Astrofísica de Canarias, Spain))

**Historical Ca spectroheliograms: making an old resource available for new studies**

Various observatories around the globe started regular full-disc imaging of the solar atmosphere in the Ca II K line since the early decades of the 20th century. The archives made by these observations have the potential of providing far more detailed information on solar magnetism than just the sunspot number and area records to which most studies of solar activity and irradiance changes are restricted.

We have analysed the image content of three Ca II K spectroheliogram time series, specifically those obtained by the digitization of the Arcetri, Kodaikanal and Mt Wilson photographic archives, in order to estimate their potential value for studies focussing on time scales longer than the solar cycle. We have also compared the results to those for similar present-day observations taken with the Meudon spectroheliograph and with the Rome-PSPT. We show that historic data suffer from stronger geometrical distortions and photometric uncertainties than the present-day observations. The photometric uncertainties mostly originate from the photographic calibration of the original data and from stray-light effects. We also show that the image contents of the three analysed series vary in time. These variations are due to instrumentation changes and aging, as well as changes of the observing programmes. Our results imply that the main challenge for the analysis of historic data is their accurate photometric calibration. This problem must be solved before thay can provide reliable information about solar magnetism and activity over the last century. Moreover, inter-calibration of results obtained from independent time series is required to reliably trace changes of solar properties with time from the analysis of such data. Different approaches to calibrating the data while simultaneously removing stray light have also been tested (Fig. 88). Final results have not yet been obtained.

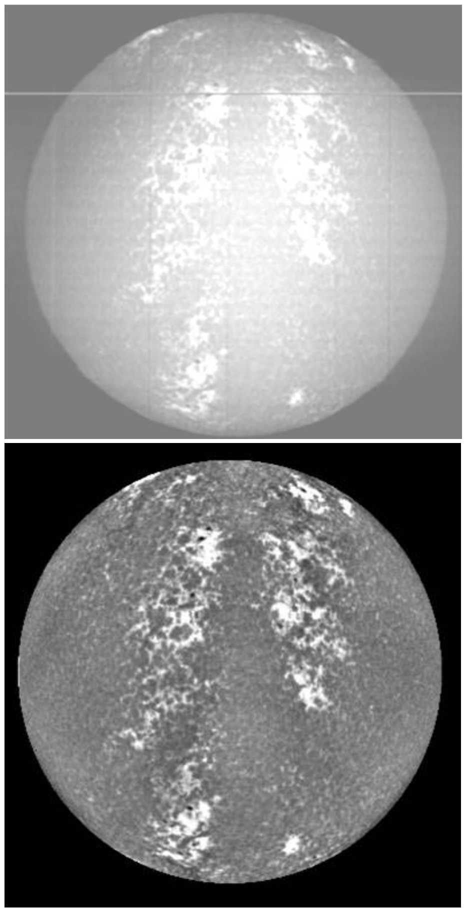

Fig. 88: Examples of Ca II images before our corrections (top) and after (bottom).

(S. K. Solanki and N. A. Krivova in collaboration with I. Ermolli (Rome Observatory, Italy) and A. Tlatov (Pulkovo Observatory, Russia))

### Stellar variability: using the solar paradigm to model variability of active stars

Relatively inactive stars like the Sun are brighter around the maxima of their activity cycles. Stars that are significantly more active display the opposite behaviour: they are darker at times of higher activity. This suggests that for the more active stars it is not the faculae that dominate the brightness changes over the time scale of the activity cycle, but rather the starspots. It has been suggested that the variability of these stars has an origin different from the Sun and there had been no quantitative modelling to test whether the variability of stars with high activity could be treated by extrapolating from the Sun or not.

We started from the models that we developed to compute the irradiance variations of the Sun and determined the amounts by which the surface coverage by faculae and sunspots changes over the solar cycle. We find that although the absolute value of the area coverage due to faculae increases much more than of sunspots from activity minimum to maximum, the ratio of the area covered by spots to that covered by facule increases quite strongly, since facular area increases nearly linearly with Ca II H and K flux, while the sunspot area increases almost quadratically. If we take the solar relations and extrapolate them to the activity levels of the stars we reproduce the average behaviour of the stars reasonably well (with no free parameter at our disposal). The scatter shown by the stellar data points can be largely explained by taking into account that we are observing the stars at random angles, and not just along the equator as is the case for the Sun. At other angles the ratio of facular brightening to spot darkening is different due to the different center-to-limb behaviour of their brightness.

(S. K. Solanki in collaboration with R. Knaack (ETH Zürich) and Y. Unruh (Imperial College London))

### Grand minima and maxima of solar activity

A record of sunspot number spanning the whole Holocene clearly shows the presence of numerous periods of particularly low sunspot number lasting multiple decades (so called grand minima) as well as similar periods of particularly high sunspot number (grand maxima) (see Fig. 89). The statistics of such grand minima and maxima are expected to provide new observational constraints on dynamo models. We have identified between 20 and 30 grand minima and maxima during the Holocene and have studied the distribution of their duration and of the waiting time between two events. We find that the occurrence of grand minima and maxima does not exhibit a cyclic variability, but rather seems to be driven by a stochastic or chaotic process. The waiting time distribution of both grand minima and grand maxima differs significantly from an exponential distribution, implying that these events tend to cluster together, with long event-free periods between the clusters. Grand minima can be distinguished according to their lengths, and fall into two classes: short Maunder type (30 – 90 years long) and the longer Spörer type (more than 110 years long). The grand maxima do not show such a distinction.

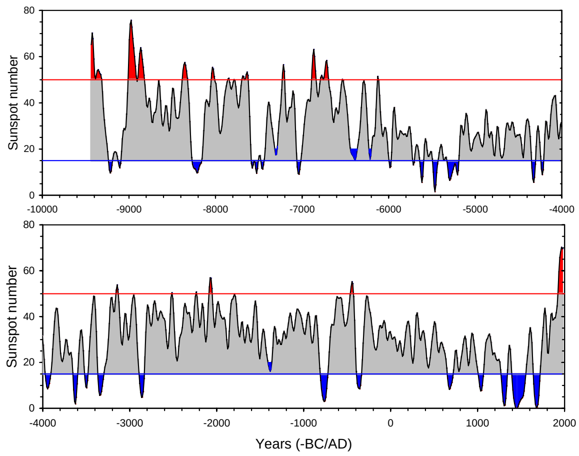


Fig. 89: Sunspot number throughout the Holocene reconstructed from $^{14}C$ in tree trunks. The data set has been smoothed to remove the very short-term variations and has been spread over two panels to improve visibility. Blue and red areas denote grand minima and maxima, respectively.

(S. K. Solanki in collaboration with I. G. Usoskin (University of Oulu, Finland) and G. A. Kovaltsov (Ioffe Physical Institute, Russia))

### The latitudinal dependence of the sunspot cycle: a new diagnostic of dynamo models

The sunspot cycle is one of the main diagnostics of the solar dynamo. Its temporal variation has consequently been studied in great detail. The latitude-distribution of solar activity as represented by sunspots has been far less studied. To develop it as a novel diagnostic of the solar dynamo is the aim of this work.

We first determined the latitudinal distribution of a sunspot cycle by integrating the butterfly diagram at each latitude over the length of each cycle. We then formed the five lowest moments of the latitudinal distribution of all complete sunspot cycles since 1874 and compared these moments with each other.

The three lowest moments correlate remarkably well with each other. For example, the mean latitude of the sunspots during a cycle and the latitude range are correlated at the 0.96 level. A clear asymmetry is seen between the two hemispheres, with the southern solar hemisphere showing consistently larger, and more positive correlations than the northern hemisphere. The same analysis when applied to different simple dynamo models reveals significant differences between the models and demonstrates that such moments are a useful diagnostic of the exact dynamo mechanism acting in the Sun.

Remarkably, dynamos without a meridional flow provide results closer to those of the Sun's northern hemisphere, while a dynamo with a meridional flow produces fields more similar to those in the Sun's southern hemisphere. This may provide a clue to the cause of the persistent north-south asymmetry of solar activity

(S. K. Solanki and D. Schmitt in collaboration with T. Wenzler (ETH Zürich))

## Ongoing and future solar missions and instruments

### Lessons from the SUMER/SOHO ultraviolet spectrograph

Our understanding of the high-temperature solar atmosphere is to a large extent based on spectroscopic observations of emission lines and continuum radiation in the vacuum-ultraviolet (VUV) wavelength range of the electromagnetic spectrum. The VUV radiation is produced by transitions of atoms and ions, or to some extent, of molecules. The atomic and ionic emission lines have formation temperatures between 10 000 K and several million kelvin, representative of the chromosphere, the transition region and the corona. The molecular lines and the continua originate in cooler regions of the Sun. Radiation at VUV wavelengths is strongly absorbed by the Earth's atmosphere and can only be detected with instruments on sounding rockets and spacecraft above the atmosphere. Detailed studies of the spectral radiances together with atomic physics data furnish information on the electron density and temperature of the solar atmosphere, as well as on elemental abundances, whereas Doppler line-shift measurements show bulk plasma motions, turbulence, and ion temperatures. Research in this field was presented in a review paper using measurements of the Solar Ultraviolet Measurements of Emitted Radiation (SUMER) instrument on the ESA/NASA Solar and Heliospheric Observatory (SOHO). In addition, the instrumental techniques were described as well as the scientific use of the data obtained over a period of ten years.

Most of the data acquired by SOHO are in the public domain and can be obtained from http://sohowww.nascom.nasa.gov/data/archive.html or http://idc-medoc.ias.u-psud.fr/jsp/AvailableData.jsp.

In addition, the SUMER data are available in IDL-restore-file format from http://www.mps.mpg.de/projects/soho/sumer/FILE/SumerEntryPage.html.

(K. Wilhelm)

### SOHO/SUMER: Status and perspectives

During the last years, the Solar Ultraviolet Measurements of Emitted Radiation (SUMER) spectrograph has been operated only in campaign mode with 4 to 6 observational blocks per year, and pointing was selected preferably to off-limb targets. This policy was a reaction to extrapolations showing that otherwise the instrument would reach the overall limit of accumulated photons seen by the detectors much too early. This measure was very successfull in extending the expected life time. Moreover, what at first glance could be interpreted as a restriction has proven to be an opportunity for a change of scientific objectives that allowed the exploration of a new field of investigation (cf., the highlight 'Coronal Seismology' on page 12 of the 2002/2003 annual report or Wang *et al.* (2003)).

In June 2004, however, an unexpected problem with detector 'A' started: multiple rows of the active detector array were accumulated into single rows just like an artificial binning (recently, a similar effect was reported by the UVCS team; the UVCS instrument on SOHO is equipped with identical, SUMER-type detectors). Since this degradation was progressing also during no-activity periods, the data-taking policy was changed again, and now observations with high photon loads were allowed for detector 'A'. This opened new opportunities for joint observations with ground-based observatories focussing on chromospheric science. Even raster scans in the very bright H I Lyman-$\alpha$ emission line at 1215 Å were performed for the very first time (cf., article 'The structure and dynamics ...' by Teriaca et al. on page 34 of the 2004/2005 annual report).

Detector 'B', which was only used occasionally, is fully operational. It was kept as a resource to be used for joint observations with the Japanese-US-UK mission Hinode, operational since September 2006. After first collaborative observations already in November, two major multi-spacecraft campaign were successfully performed during the periods 2 – 29 April and 2 – 16 November 2007 supported by SOHO (SUMER, CDS, MDI, EIT, UVCS), TRACE, STEREO, Hinode (SOT, EIS, XRT), and various ground-based observatories. In total, 31 studies were run at least twice, and it can be expected that the annual rate of publications using SUMER data, which was still on a high level of 40 peer-reviewed papers will be boosted by the outcome of this campaign.

The intensive use of the remaining detector lead to some degradation. It is however clear, that enough resources are left to repeat such campaigns, and there are definite plans to overlap with the operational phase of the NASA mission *Solar Dynamics Observatory (SDO)* scheduled for launch in December 2008.

(W. Curdt, U. Schühle, K. Wilhelm, and L. Teriaca)

### STEREO Update

The lift off of the two STEREO spacecraft (sc) Ahead (A) and Behind (B) happened from Cape Canaveral Air Force Station with a Boeing Delta II rocket on 25 October 2006. Switch on of the SEP (Solar Energetic Particles) packages on the Behind and the Ahead SC occurred on 13 November and on 14 November 2006 respectively. The SEP package consists of SEPT (Solar Electron Proton Telescope), LET (Low Energy Telescope), HET (High Energy Telescope), and SIT (Suprathermal Ion Telescope) instruments. The SIT and SEPT instruments had at switch on their doors still closed on both spacecraft. They were opened in December 2006 and January 2007. Since then the SEP package is working nominally, except for some optimisations which have to be done in the next months.
During the commissioning phase the instrument on both STEREO SC were calibrated, and cross calibrations with the Wind and ACE SC were undertaken. In the attached Fig. 90 from the Ahead and the Behind SC good agreement between the ion spectrum from SEPT and the proton spectrum from SIT on STEREO is found. The same good agreement holds for the various ion spectra from SIT and ULEIS on ACE.
Meanwhile two instrument papers have been finished and accepted and are ready for publication in Space Science Reviews. Further papers will be prepared on the 1) Study of the quiet corona (Solar Minimum), 2) the first ICME and ground event observed with STEREO during solar minimum, and the particle population during Corotating Interaction Regions (CIRs).

(A. Korth and U. Mall)

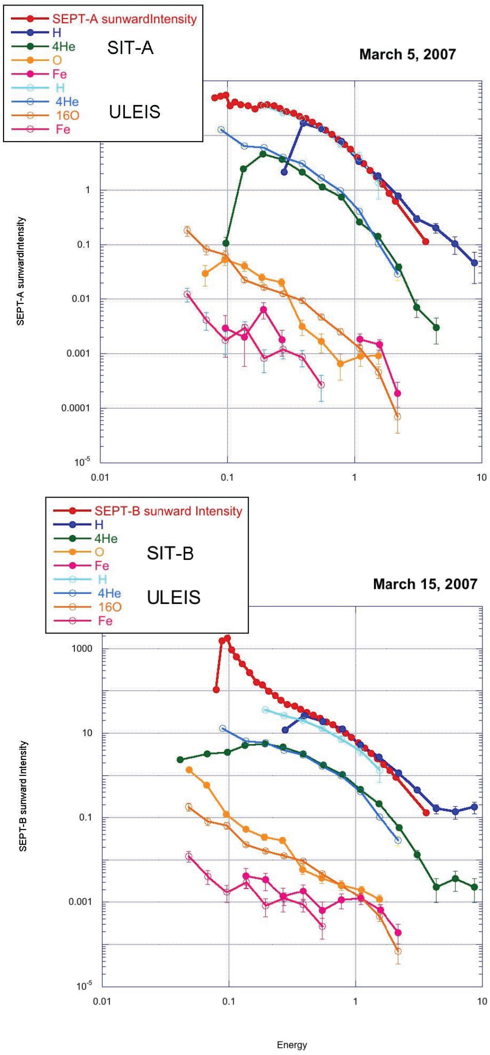


Fig. 90: Spectra taken by instruments on STEREO-A and STEREO-B compared with spectra taken onboard the ACE spacecraft.

### TIP-2

Since May 2005 the new Tenerife Infrared Polarimeter 2 (TIP-2) is operational at the German Vacuum Tower Telescope (VTT) on Tenerife. Compared to the TIP instrument, the new spectro-polarimeter enhanced the field of view to 77″ along the slit, allowing most active regions to be covered with one single scan. Full Stokes vector measurements in the wavelength range from 10800 to 16000 Å can be obtained with a polarimetric accuracy of $10^{-4}$. Combined with the powerful Kiepenheuer Adaptive Optic System (KAOS) a spatial resolution of 0.7″ is achievable. With the installation of the Gregor telescope (planned for 2008) TIP-2 will be capable of observing at a resolution of 0.35″.

To demonstrate the capabilities of TIP-2 we show a scan of an active region recorded during the first observing campaign when the full field of view of 77″ was available. Fig. 91 shows Stokes $I$, $Q$, $U$ and $V$ maps of an active region in the photospheric Si I 10827 Å line and the chromospheric He I 10830 Å line

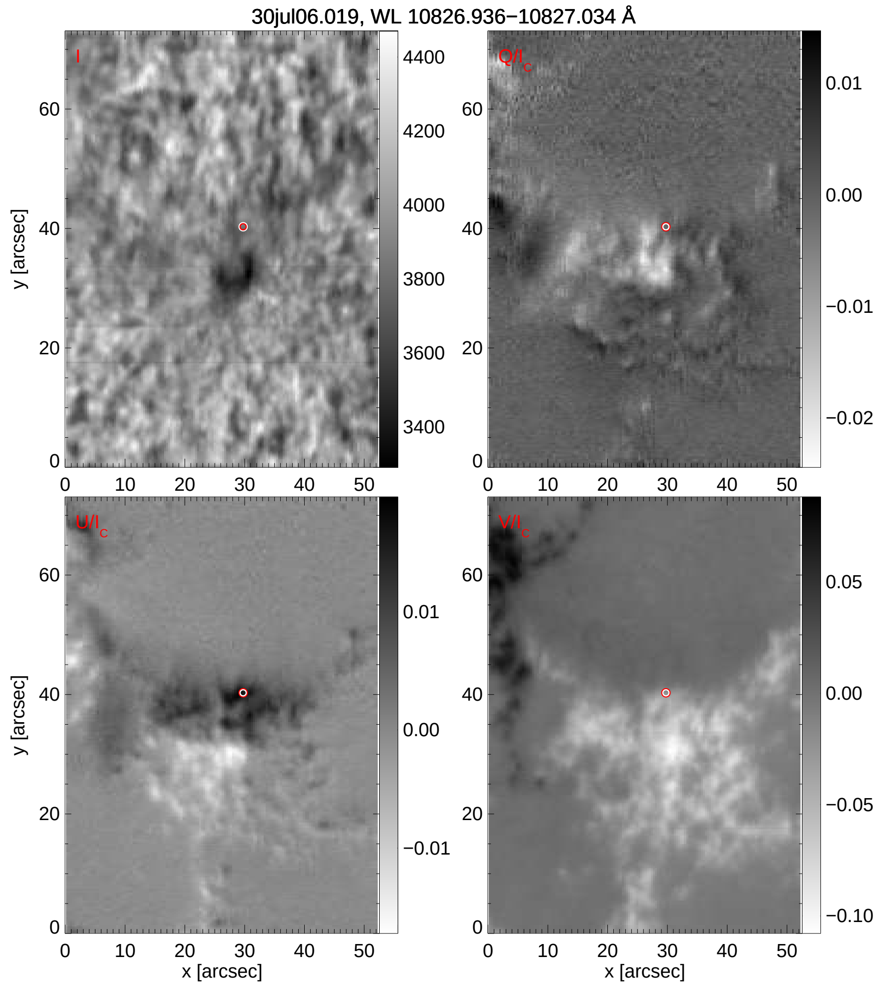


Fig. 91: Stokes $I$, $Q$, $U$ and $V$ map of an active region containing a small pore close to the the core of the Si I 10827 Å line. The images are composite maps of the individual slit spectra for the wavelength range given in the image title.

at the solar position 35°W, 9°N. The angle of the solar vertical to the line of sight was 35°. The region of $52'' \times 77''$ was scanned in 150 scanning steps from UT 18:33 until 19:05 on 30 July 2006. The exposure time per slit position was 10 s, resulting in a signal to noise ratio of $\approx 1000$ (RMS-noise). The image was stabilized using KAOS, the estimated spatial resolution of the image was limited by the seeing to $\approx 1.5''$. Standard data reduction routines as provided by the IAC have been used to calibrate the images and to remove instrumental crosstalk.

(A. Lagg and S. K. Solanki in collaboration with M. Collados Vera (IAC Tenerife))

### SWAP and LYRA instruments on PROBA-2

PROBA-2 is a technology oriented ESA micro-satellite mission to be launched in 2007. The solar instrumentation on this platform has been built by a Belgian-Swiss-German consortium (ROB, CSL, PMOD/WRC, IMOMEC, MPS, BISA). It consists of the ultraviolet radiometer LYRA and the extreme ultraviolet imaging telescope SWAP. LYRA (Fig. 92) will measure continuously during the mission the ultraviolet solar irradiance in four broad wavelength bands between 1 nm and 240 nm, while SWAP is a filtergraph telescope that will provide solar coronal images at 1-minute cadence in a passband at 17.4 nm, the Fe IX/Fe X spectral lines, corresponding to the one million degrees temperature plasma. Both instruments carry technologically new instrumentation: LYRA will use newly developed UV detectors, SWAP makes use of a new off-axis optical design and fly for the first time a CMOS active pixel camera.

The German (MPS) contribution was to carry out the calibration of the two instruments in collaboration with the Physikalisch-Technische Bundesanstalt (PTB) at the Berlin Electron Storage ring for Synchrotron radiation (BESSY II).

The calibration of the SWAP instrument has been per-

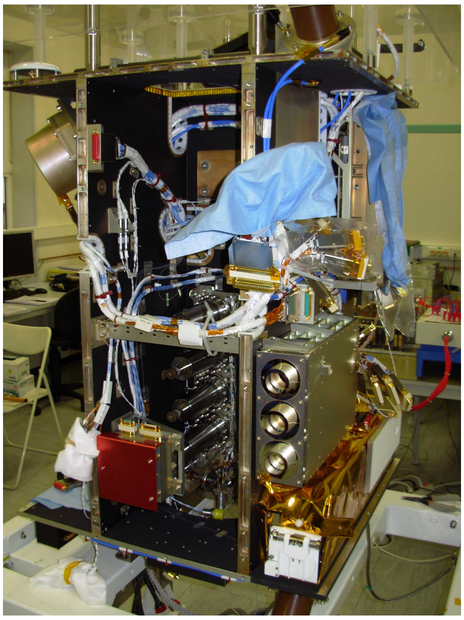

Fig. 92: The radiometer LYRA and the filtergraph telescope SWAP mounted on the PROBA-2 platform in early March 2007. The solar instruments are mounted on the vertical panel in the lower right corner of the image.

formed at the grazing incidence (GI) beamline using the large goniometer inside the 2-meter diameter vacuum chamber of PTB. The response inside the spectral passband has been characterized as well as the absolute radiometric sensitivity of the instrument by mapping the aperture with the monochromatic, collimated beam from the synchrotron that was calibrated by PTB with a reference detector.

The LYRA instrument consists of three units of four channels each, with different passbands in the spectral range from 1 nm to 240 nm. Each channel consists of a spectral filter selecting the passband and a single photodetector. For the different LYRA channels, newly developed detectors have been fabricated and calibrated that will be flown for the first time on a space mission. The detectors are based on diamond as a wide-band-gap material, which is blind to visible light (therefore called “Blind to Optical Light Diamond -– BOLD” detectors). The visible blindness bears major advantages for solar UV observations from space, as they require less spectral filters and no low-temperature operation. To cover the large spectral range, the grazing incidence and the normal incidence beamlines of the PTB/BESSY facilities had to be used. The detectors developed under this project and, finally, all twelve channels of the LYRA instrument have been calibrated at these beamlines.

(U. Schühle)

**SUNRISE: A balloon-borne telescope for high resolution observations of the Sun**

SUNRISE is a balloon-borne solar telescope with an aperture of 1 m, working in the UV and visible optical domain. The main scientific goal of SUNRISE is to study the structure and dynamics of the magnetic field in the atmosphere of the Sun at high spatial resolution. SUNRISE will provide diffraction-limited images of the photosphere and chromosphere with an unprecedented resolution down to 35 km at wavelengths around 220 nm. Focal-plane instruments are a UV filter imager (SUFI), a Fabry-Perot imaging magnetograph (IMaX), and a spectrograph/polarimeter (SUPOS). Stratospheric long-duration balloon flights of SUNRISE over the North Atlantic and/or Antarctica are planned, starting in summer 2009. SUNRISE is a joint project of the Max-Planck-Institut für Sonnensystemforschung (MPS), Katlenburg-Lindau, with the Kiepenheuer-Institut für Sonnenphysik (KIS), Freiburg, the High-Altitude Observatory (HAO), Boulder, the Lockheed-Martin Solar and Astrophysics Lab. (LMSAL), Palo Alto, and the Spanish IMaX consortium.

Project status:
The SUNRISE gondola system (Fig. 93) has been launched for a successful test flight on 3 October 2007 from Fort Sumner, New Mexico, USA. The test flight instrumentation consisted of a 30-cm telescope with a UV sensitive CCD camera and SUFI flight filters, main parts of the instrument control system, including the main on-board computer, power distribution units and the data storage system. As the main aim of the test flight the gondola pointing performance could be verified, and measurements of the atmospheric transmission at dedicated UV wavelengths could be done. Control hardware/software as well as commanding and telemetry could be successfully tested in flight.

The lightweighted Zerodur primary mirror has been manufacted by SAGEM in France. The CDR for the Zerodur mirror was successfully held in September 2006, shaping and lightweighting of the blank was finished mid 2007, and it was polished after that. After integration into the SUNRISE telescope mirror cell the final surface treatment using ion beam figuring was done. Now the aluminmum coating can be deposited.

The assembly and integration of the SUNRISE telescope now takes place at the Kayser-Threde company in Munich. All CFRP components as well as the steel central frame have been assembled and after the integration of the main mirror cell the telescope will be aligned and interferometrically tested. Expected delivery date for the telescope is June 2008.

The optical concept of the postfocus instrumentation

Fig. 93: The SUNRISE gondola during the launch preparations for the successful test flight on 3 October 2007 in Fort Sumner, USA.

has been optimized with a clear separation of spectral intervals. The polarimetric spectrograph SUPOS now works at 854.2 nm (Ca II line), all UV wavelenghts will be analyzed by the imaging filtergraph SUFI. The optical design was analyzed regarding alignment and manufacturing tolerances. All optical components have been manufactured and are within specifications. These components have been mounted on an aluminum breadboard optical bench unit which serves optical verification and calibration purposes in the laboratory. After successful calibration the optical components will be mounted on the flight unit optical bench, which has been manufactured from CFRP.

The flight hardware of the instrument control system, main-on-board computer, power distribution unit and data storage systems have been assembled and environmentally tested. Qualification models have successfully been used during the test flight. Further development of the on-board and ground segment software is ongoing.

(A. Gandorfer, P. Barthol, M. Schüssler, S. K. Solanki and the MPS engineering team in collaboration with teams led by M. Knölker (High Altitude Observatory, Boulder, USA), V. Martínez Pillet (Instituto de Astrofisica de Canarias, La Laguna, Tenerife/Spain), A. Title (Lockheed Palo Alto Research Laboratory, USA), and W. Schmidt (KIS, Freiburg))

### Thermal design for EUS (EUV Spectrograph) onboard Solar Orbiter

Measurements for reflection, transmission and absorption properties of a primary mirror (quarz) with SiC coatings were analyzed. Aim is to determine the heat absorbed in the mirror and reflected into the instrument, and to find a configuration which minimizes both. Also analysed are other materials (B4C, Zerodur) for which material properties are available from the literature. It was found that at a distance of 0.22 AU from the Sun, a configuration with a 10-nm thick SiC coating on a circular quarz substrate of 6-cm diameter reflects 12.6 Watts of heat into the instrument, while 7 Watts are absorbed in the mirror and 58 Watts are transmitted, i.e. most heat is simply passing through the configuration and won't negatively influence the spectrograph. This provides an elegant solution of the thermal problems produced by going so close to the Sun.

(A. Theissen, U. Schühle, and W. Curdt)

### SOLAR ORBITER: Programmatic issues

The Solar Orbiter mission was proposed in early 2000 by a European team led by MPS scientists. After a successful first assessment study, Solar Orbiter was selected in September 2000 by the ESA executive as the next solar physics mission. Ever since MPS has remained a major player in the design of Solar Orbiter and the defintion of its scientific objectives, and has continued this role in various teams and working groups (see the previous annual report). However, the mission was delayed several times by various reasons, and in the recent past it went through serious political ups and downs, concerning its budget, payload funding and status within ESA. Although the mission was reconfirmed in 2006 as an essential part of the present science programme, the Science Programme Committee (SPC) of ESA has not finally approved but only confirmed it with a possible launch in 2015 (before the new Cosmic Vision science programme starts), given that the mission stays within the fixed cost cap of 300 M Euro foreseen for it in the ESA science budget.

Facing the much higher (by about 120 M Euro) cost estimate for the Solar Orbiter mission including launch and operation, international collaboration had to be sought for in order to save the mission. To review the scientific and technical status of Solar Orbiter, a well attended (about 250 participants) and highly successful second workshop was organized by E. Marsch (MPS), K. Tsinganos (University of Athens) and R. Marsden (ESA) and held in Athens in October 2006, with strong international attendance including many American colleagues. At that occasion the idea was promoted to join ESA's Solar Orbiter with NASA's Sentinels to save money and exploit the obvious science synergies. A Joint Science and Technology Definition Team (JSTDT) was therefore appointed by ESA and NASA (with Co-Chairs: E. Marsch and R. Lin) to define the new scientific goals, orbital characteristics, and technical constraints, and to look also into the payload optimization of the combined missions.

Future milestones of this common activity were: In May 2007 the JSTDT met again and finally in September, to produce and deliver a concise report on the joint missions and prepare its presentation to the advisory structure of the agencies, and then in November to ESA's decision making council, the Science Programme Committee (SPC). In their three meetings, the JSTDT of ESA and NASA succeeded in solving the key problems of a joint mission scenario and defined the common highly synergetic science programme now named HELEX, which encompasses the four Sentinels and the Solar Orbiter as so-called Heliophysical Explorers with planned launches in 2017, respectively 2015. Joint announcements of opportunity were released by both agencies on 18 October 2007, inviting the community to propose instruments for the payload of the Solar Orbiter mission, which is going to be implemented first and launched by an American Atlas V rocket.

MPS intends to participate in this mission with key instrumentation for imaging and spectroscopy in the visible and extreme ultraviolet light. Over the past years, the instruments of main interest to MPS were the VIM, EUI, EUS, and COR (usual names used in the strawman payload), which by now are well defined technically and scientifically. The first three of these are subsequently described in separate sections below. During the last three months of 2007 the involved instrument teams were occupied with science meetings, completing their writing assignements, carrying out technical studies, and defining the final instrument designs. The due date for proposal delivery was 15 January 2008. The actually proposed instruments and funded participations will be described in detail in the next annual report.

(E. Marsch)

### The EUS instrument

Among the four top mission goals of the Solar Orbiter

- Determine the properties, dynamics and interactions of plasma, fields and particles in the near-Sun heliosphere
- Investigate the links between the solar surface, corona and inner heliosphere
- Explore, at all latitudes, the energetics, dynamics and fine-scale structure of the Sun's magnetized atmosphere
- Probe the solar dynamo by observing the Sun's high-latitude field, flows and seismic waves

the first three require EUV spectroscopy. The Extreme Ultraviolet imaging Spectrograph (EUS) is a high-resolution telescope/spectroscope designed to reach ambitious performance parameters such as a spatial resolution of 150 km and a spectral resolution good enough to resolve Dopplershifts of 1 km/s over a wide temperature range. Three spectral bands are foreseen to cover the entire range of temperatures of the solar atmosphere: the 116-126-nm band with the bright H I Ly-$\alpha$ line, the 95-105-nm band with the O VI doublet, and the 70-80-nm band with the Ne VIII doublet. The latter will be particularly suited to observe the emanating solar wind at higher latitudes, a capability unique to Solar Orbiter.

The limited spacecraft resources such as mass and power require a simple and efficient design. The instrument will be built with a two-mirror optical system (cf., Fig. 94), where the collimator also acts as the dispersion element and carries a toroidal variable line space grating (TVLS) and a highly efficient imaging detector.

We have made an optical study to show the feasibility of the three wavelength bands, with a specially proposed design for the long-wavelength channel (the 116-126-nm band), which also includes in second order the important spectral range between 58 nm and 63 nm. Further studies have been carried out for the thermal design. A particularly useful solution has been found for the reduction of the thermal heat load on the primary mirror: A thin mirror coating of silicon carbide will reflect radiation within the useful wavelength range in the VUV, while it transmits most of the visible and infrared part of the solar spectrum. We have carried out experimental studies to produce such mirror coatings to determine the optimum coating thickness that minimizes the absorption of solar energy. For the three wavelength channels, we have cameras under development which make use of the CMOS-APS readout chips that are also foreseen for other Solar Orbiter remote-sensing instruments. They will be coupled with micro-channel plate intensifiers with a distribution of photocathode materials, optimized for each spectral range. The system throughput and expected count rate based on SUMER spectral data have been calculated and found to be compatible, given the small aperture size dictated by the Solar Orbiter model payload.

The consortium forming now around the CDS and SUMER teams involved in the SOHO (Solar and Heliospheric Observatory) mission is led by the Rutherford-Appleton-Laboratory (UK). A strong Co-

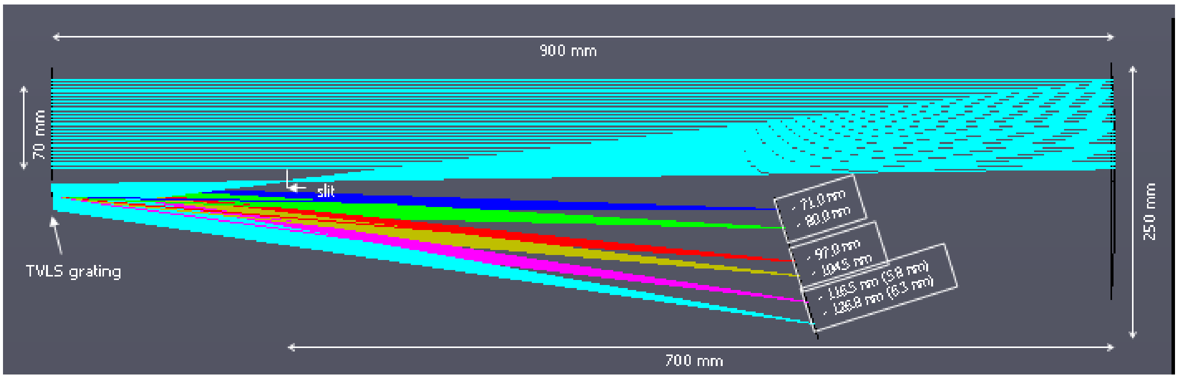


Fig. 94: The proposed EUS optical design.

investigator participation is given by the large involvement in the instrument design and development.

(W. Curdt, U. Schühle, L. Teriaca, and A. Theissen)

### The Solar Orbiter EUI instrument

The Extreme-Ultraviolet Imager (EUI) is a suite of remote-sensing telescopes designed for imaging at high resolution the structures in the solar atmosphere, from the chromosphere to the corona. The instrument package contains three high-resolution imagers (HRI) and a full-Sun imager (FSI). EUI will observe and analyse the morphology and dynamics of the solar atmosphere at the base of the corona. A full-Sun imager will show the structure of the whole Sun at coronal temperatures, while three high-resolution telescopes will show, in selected wavelength bands, the details of the structures that are in the close-up field-of-view of the Solar Orbiter.

In response to the call for Letters of Intent by ESA on 11 July 2006 a consortium was formed by agreement between involved parties to propose the EUI instrument.

The contribution to the EUI suite under responsibility of MPS will be the HRI telescope for the hydrogen Lyman-$\alpha$ line (121.6 nm). The most important – while most intense – line of the solar atmosphere is of great value for the diagnostics of the chromosphere and transition region.

An optical design study was made to evaluate the performance characteristics of the telescope. Being an order of magnitude larger than the wavelength of current EUV imagers, the Lyman-$\alpha$ imager must fit within the given envelopes for the Solar Orbiter payload instruments and fulfil the optical requirements. A Ritchey-Chrétien telescope was designed in conjunction with the other EUI channels and was studied and verified to fulfil all requirements.

To provide an efficient camera for the Lyman-$\alpha$ wavelength, an intensifier system is necessary, which can be coupled with a CMOS-APS (Active Pixel Sensor) image readout system that will be identical to all EUI focal plane units. We have designed and built a breadboard unit of such a camera, also in regard to a possible contribution to the EUS instrument of Solar Orbiter. Several technological production steps have been established and implemented, that can be carried out at MPS, to build such a camera system in house.

The Announcement of Opportunity (AO) by ESA for the Solar Orbiter Payload was issued on 18 October 2007. A proposal was written to be submitted by J. F. Hochedez (Royal Observatory of Belgium) as Principal Investigator with the Centre Spacial de Liège (CSL) hosting the project office and three Lead-Co-Investigators of MPS, Institut d'Astrophysique Spatiale (IAS), and Mullard Space Science Laboratory (MSSL) of the University College London, representing the contributions from Germany, France and the United Kingdom, respectively (Hochedez *et al.*, 2007).

(U. Schühle, W. Curdt, E. Marsch, S. K. Solanki, L. Teriaca, and A. Theissen in collaboration with T. Appourchaux (IAS, F), J. M. Defise (CSL, B), L. Harra (MSSL, GB), J. F. Hochedez (ROB, B), and others)

### The Solar Orbiter PHI instrument

A Visible Light Imager and Magnetograph (VIM) is a primary instrument of the remote sensing package of ESA's Solar Orbiter mission. A consortium for implementation of such an instrument, led by the MPS, has been established. This consortium has responded to ESA's call for submission of Letters of Intent (July 2006). It has also submitted an Instrumental Interface Document (January 2007) including a detailed opto-mechanical design and a management plan. On 18 October 2007 ESA has released an Announcement of Opportunity (AO) for the Solar Orbiter payload. The consortium has responded to this AO (January 2008) with a proposal for a Polarimetric and Helioseismic Imager (PHI, see Fig. 95) as an implementation of the VIM instrument.

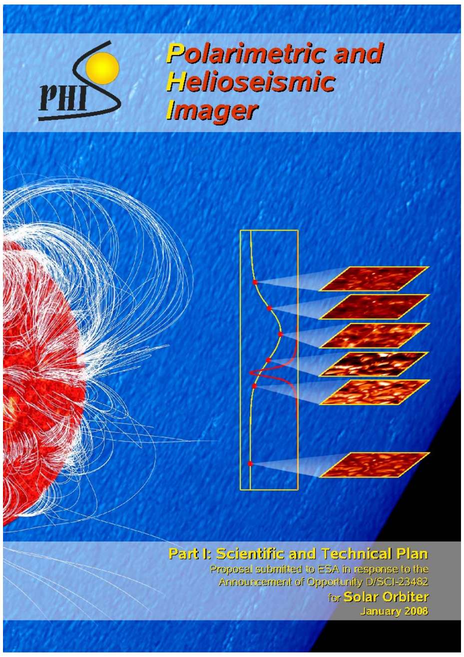


Fig. 95: Cover Page of the proposal for a Polarimetric and Helioseismic Imager (PHI) for Solar Orbiter.

The proposed design (see Fig. 96) is based on two optical telescopes – a High Resolution Telescope (HRT) and a Full Disk Telescope (FDT) – as well as a Filtergraph coupled alternately to either telescopes. This concept allows measuring the full magnetic field vectors and the velocity fields at the photospheric level by scanning across a magnetically sensitive spectral line. The heart of the filtergraph will be a tunable solid state double-etalon made out of thin lithiumniobate ($LiNbO_3$) wafers. In order to verify the feasibility of such a filter, an etalon has been built and characterized. First tests for space qualification have successfully been carried out (Schühle *et al.*, 2006) and further tests are underway to fully verify that the filter can operate under the Solar Orbiter environmental conditions.

(A. Gandorfer, H. Hartwig, J. Hirzberger, A. Lagg, U. Schühle, S.K. Solanki, J. Woch, and L. Yelles Chaouche in collaboration with T. Appourchaux (IAS, Paris), M. Sigwarth (KIS, Freiburg), V. Martínez Pillet (IAC, Tenerife) and others)

### The SPICE instrument proposed for the HELEX / Solar Orbiter mission

Most of the top mission goals of Solar Orbiter and the Heliophysical Explorers (HELEX) science programme require ultraviolet spectroscopy. The 'Spectral Imaging of the Coronal Environment' (SPICE) is an instrument proposal in response to the announcement of opportunity issued by ESA and NASA for the strawman Extreme Ultraviolet Spectrometer (EUS) on Solar Orbiter. SPICE is a high-resolution telescope/spectroscope designed to achieve ambitious performance parameters, such as a spatial resolution of 150 km and a spectral resolution good enough to resolve Dopplershifts of 3 km/s over a wide temperature range. Two spectral bands are foreseen to cover the entire range of temperatures in the solar atmosphere: the 97 – 105 nm band with the O VI doublet, and the 70 – 79 nm band with the Ne VIII doublet. The latter will be particularly suited to observe the emanating solar wind at higher solar latitudes, a capability unique to Solar Orbiter. SPICE is designed for observations of the solar disk as well as for coronal observations off the limb out to three solar radii.

The limited spacecraft resources such as mass and power require a simple and efficient design. Therefore, the instrument will be built as a two-mirror optical system, where the collimator also acts as the dispersive element consisting of a grating with toroidal variable line space (TVLS), and with a highly efficient imaging detector.

We have made an optical study to show the feasibility of both wavelength bands, with a special design proposed for the long-wavelength channel, which in second order also includes the important spectral range between 48.5 nm and 52.5 nm. Further studies have been carried out for the thermal design. A particularly useful solution has been found for the reduction of the thermal heat load on the primary mirror: A thin mirror coating of silicon carbide will reflect the radiation within the useful wavelength range in the vacuum ultraviolet, while it will transmit most of the visible and infrared part of the solar spectrum (c.f. Schühle *et al.*, 2007).

The system throughput and the expected count rate based on SUMER spectral data have been calculated and found to be compatible, given that a small aperture size is dictated by the thermal requirements on the Solar Orbiter model payload.

The international consortium, which formed around the CDS and SUMER teams involved in the SOHO (Solar and Heliospheric Observatory) mission, is led by the Southwest Research Institute (USA).

(W. Curdt, U. Schühle, E. Marsch, and A. Theissen)

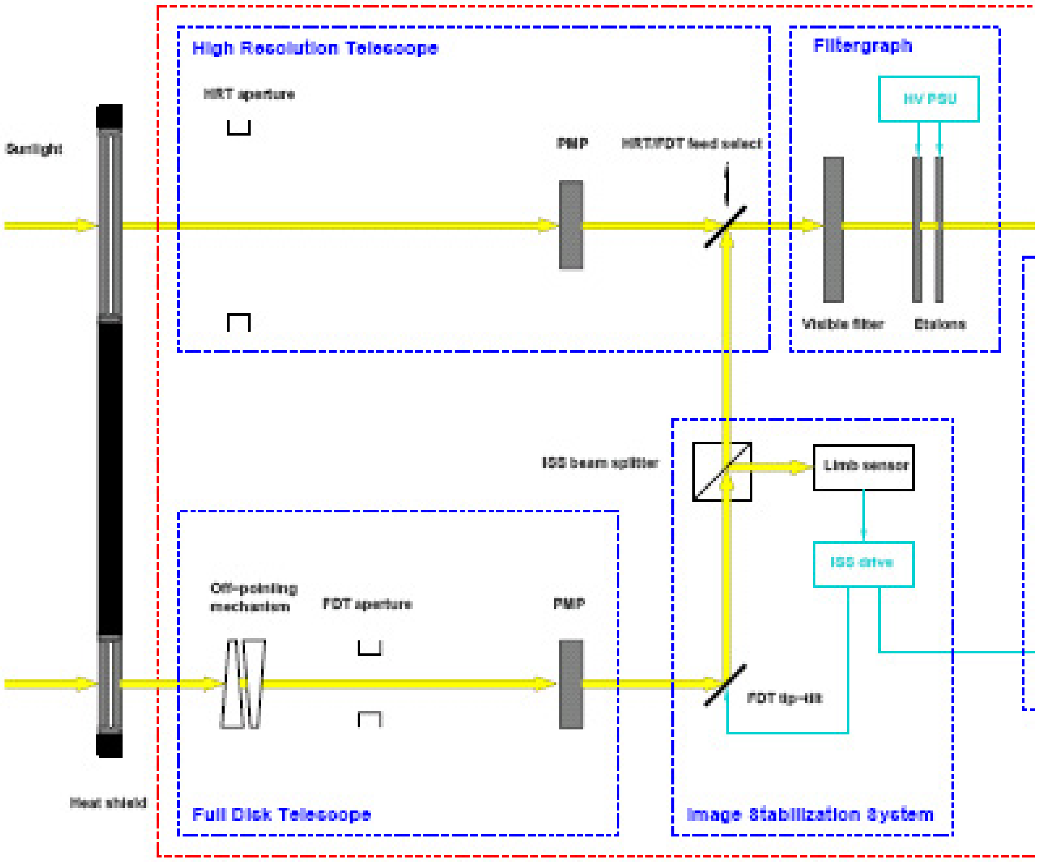


Fig. 96: Functional diagram of the PHI instrument.

**Analysis of PHI instrument performance**

We performed simulations of the instrument performance (see Fig. 96) of the Polarimetric and Helioseismic Imager (PHI) on board the Solar Orbiter (SO) spacecraft. The peculiar orbit of SO allowing for an unprecedented view onto the solar poles and a two-week period of quasi-heliostationary observations per orbit, has one major disadvantage: the rate for the transmission of PHI science data is limited to an average value of 20 kbit/s. This restriction requires a sophisticated on-board data compression, since conventional, JPEG-type algorithms do not suffice to transfer the desired scientific information to Earth. Milne-Eddington (ME) type inversions of the radiative transfer equation offer a robust determination of science parameters derived from the measurement of the raw Stokes vector. The results of such inversions directly reveal the relevant physical parameters of the solar atmosphere: Magnetic field strength and direction, and line of sight velocity. With only a minimum loss in science information the data volume compared to the raw data can be reduced by a factor of 10 to 20.

In order to achieve the optimum performance of PHI a thorough study of the instrument performance was carried out. This study involved a full-fledged simulation of the PHI instrument, taking into account all relevant instrument parameters. We simulated PHI measurements by pointing the hypothetical telescope towards an artificial Sun, represented by the most realistic magnetohydrodynamic (MHD) simulations currently available for the uppermost layer of the solar surface (Vögler *et al.*, 2005). The Stokes vector maps resulting from artificial measurements with the PHI telescope were inverted using a ME-based inversion (Lagg *et al.*, 2004). Comparisons between the atmospheric parameters resulting from these inversions (see Fig. 97) and the MHD simulations deliver a realistic estimate for the performance of the instrument. Fig. 98 shows the width of the narrow band filter, used for recording a Stokes map at a certain wavelength within the spectral line of interest. The filter width was varied from 25 to 300 mÅ. The four panels of the plot show the variation of the standard deviation of differences between the MHD data and the measured values of the parameters magnetic field strength, inclination, azimuth, and the line-of-sight direction. The analysis clearly demonstrates that the optimum choice for the filter width is in the range between 70 and 120 mÅ, where the difference between simulated observations and MHD data is smallest. Thus, the baseline design filter width for PHI was set to 100 mÅ.

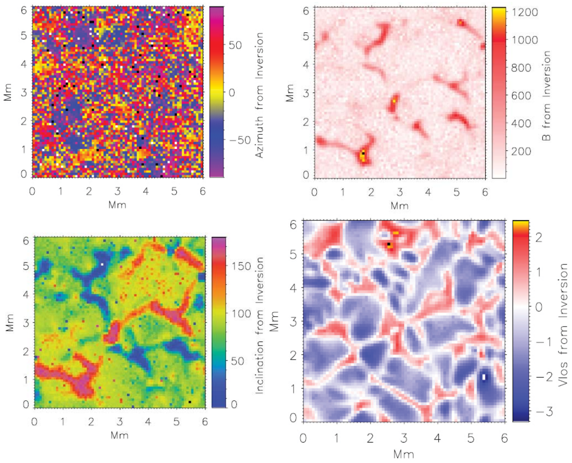


Fig. 97: Simulated data of the PHI instrument; upper left: magnetic field strength [G], upper right: magnetic field inclination [degrees], lower right: magnetic field azimuth [degrees] and lower left: line-of-sight flow velocity [km s$^{-1}$].

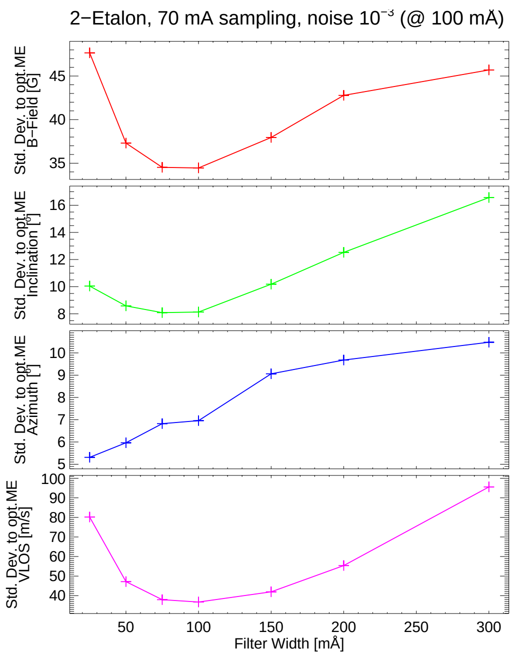


Fig. 98: Performance of the PHI instrument depending on the width of the narrow band filter: The simulated PHI measurements clearly show an optimum instrument performance near 100 mÅ.

(A. Lagg, J. Woch, J. Hirzberger, A. Gandorfer, A. Feller, and S. K. Solanki)

**Thermal design of a VUV telescope mirror for Solar Orbiter instruments**

We have made experimental studies with thin silicon carbide (SiC) coatings on transparent substrates (quartz sample plates) to evaluate their reflective properties in the vacuum ultraviolet (VUV) spectral range between 58 nm and 123 nm. Additional measurements of reflection, transmission and absorption properties in the visible have been made and analyzed. The aim is to determine the heat absorbed in the mirror and reflected into the instrument, and to find a configuration which minimizes both, while keeping a good reflectance in the VUV.

A thin SiC coating of 10 nm thickness is found to be a very promising compromise between high VUV reflectivity and low vis/IR absorption. The overall absorption of the solar spectrum by such a mirror is less than 8 % (Schühle *et al.*, 2007). This provides an elegant solution of the thermal problems produced by going so close to the Sun.

The investigations have been extended to boron carbide thin coatings, which is an alternative to silcon carbide as a VUV reflective material.

(U. Schühle, W. Curdt, and A. Theissen)

**Nonlinear force-free magnetic field modelling for VIM on Solar Orbiter**

The aim of this work is to investigate how photon noise and errors in the retrieval of solar magnetic parameters from measured Stokes profiles influences the extrapolation of nonlinear force-free coronal magnetic fields from photospheric vector magnetograms. To do so we use a nonlinear force-free extrapolation code based on an optimization principle. The extrapolation method has been extensively tested and applied to data from various telescopes. Here we apply the code to artificial vector magnetograms obtained from 3-D radiation-MHD simulations. As a reference case we compute the coronal magnetic field from an ideal magnetogram and compare the result with more realistic magnetograms based on simulated Solar Orbiter/VIM-measurements, see Fig. 99. We investigate the effects of noise, ambiguities, spatial resolution, inversion mechanism of Stokes profiles etc. We rate the quality of the reconstructed coronal magnetic field qualitatively by magnetic field line plots and quantitatively by a number of comparision metrices, e.g., the vector correlation with the exact solution and how accurately the free magnetic energy is computed. Not surprisingly, instrument effects and noise influence the quality of the nonlinear force-free coronal magnetic field model. The extrapolations from realistic vector magnetograms show a reasonable agreement with the ideal reconstruction, however, and are in particular significantly better than extrapolations based on line-of-sight magnetograms only. High-quality VIM data will thus allow reasonably accurate extrapolations that can serve as the basis for magnetic-coupling science through a comparison with observations from EUS and EUI.

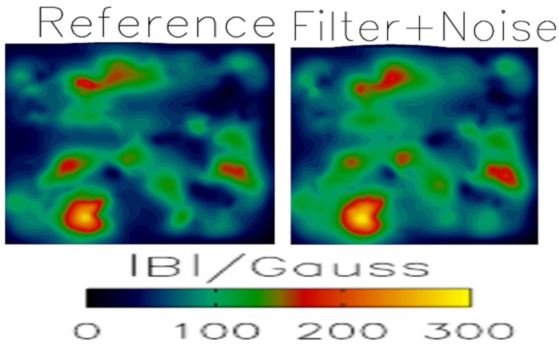


Fig. 99: Strength of the coronal magnetic field in the height 400 km. The field has been etrapolated from an ideal artifical vector magnetograms (left) and a magnetogram obtained from the inversion of Stokes profiles, including instrument effects and noise (right).

(T. Wiegelmann, S. K. Solanki, L. Yelles, and A. Lagg)

**Solar microscopy: Unveiling the Sun's basic physical processes at their instrinsic scales**

Many of the basic physical processes on the Sun responsible for solar activity and the Sun's influence on the Earth take place at intrinsic scales that have yet to be observationally resolved. These or similar processes also take place in a variety of other astrophysical systems, but are even further from being resolved. The Sun provides the most promising physical system on which such processes will finally be resolved. We identified some of the important physical scales and estimated the sizes of solar instruments needed to resolve them. Given the very large size of the ideal instrument, we also considered instrumentation that would have a resolution intermediate between the one currently achievable and that needed to resolve fully the basic processes. This instrumentation could form the core payload of a next-generation solar mission. It would include a large EUV/FUV telescope of 1 – 2 m in diameter, and thus require resources that would put it in the ESA cornerstone class.

(S. K. Solanki and E. Marsch)

**Proposal to ESA to fly a coronal magnetic field mapper, COMPASS**

The existence of the million-degree solar corona overlying the solar surface, which is at a comparatively cool 5800 K, is one of the major and most enduring enigmas in astrophysics. In spite of considerable progress in our knowledge of the solar corona's physical structure, dynamics and heating based on data from SOHO and other spacecraft, we are still far from a final solution of this problem. One of the major factors limiting progress towards finding the mechanism causing coronal heating and activity is that the Sun's magnetic field determines the structure, dynamics and the energetics of the corona, but our knowledge of this field is very limited and incomplete. The magnetic field is measured dominantly at the solar surface, many thousands of km away from the corona. The techniques available for measuring the coronal field from the ground all have serious shortcomings and only provide very limited and incomplete information on this key quantity.

The concept of a mission, COMPASS (COronal Magnetism, Plasma and Activity Studies from Space), has been worked out that aims at closing this serious gap in our knowledge by mapping the magnetic field in the solar transition region and corona, both on the solar disk and outside the solar limb.

Since the coronal magnetic field is weak (on the order of 1 – 100 G) compared to the well-measured surface field, we need to use novel techniques to probe it. COMPASS will take a multipronged approach. It will record the Hanle effect, a quantum mechanical interference effect that influences the polarisation in spectral lines, as well as the Zeeman effect in different wavelength bands. Lines in the EUV and FUV part of the spectrum are the most promising for observing the magnetic field in the solar transition region and corona. Therefore this is the spectral region on which the proposed mission will concentrate. In addition, it will also observe highly ionized spectral lines in the infrared (IR) solar spectrum in order to get a complementary picture of the field.

(S. K. Solanki, J. Büchner, W. Curdt, A. Gandorfer, B. Inhester, A. Lagg, D. Markiewicz-Innes, E. Marsch, U. Schühle, M. Schüssler, and J. Woch in collaboration with S. Fineschi (University of Turin, Italy) and the COMPASS Team)

## Solar-stellar connections, interstellar dust and Cosmic Rays

### Theoretical mass loss rates of cool stars

The stellar mass loss rate is important for the rotational evolution of a star and for its interaction with the circumstellar environment. The analysis of astrospheric absorption features enables an empirical determination of mass loss rates of cool stars other than the Sun. In collaboration with M. Jardine (University of St. Andrews, UK), I have developed a model for the wind properties of cool main-sequence stars, which comprises their wind ram pressures, mass fluxes, and terminal wind velocities. The wind properties are determined through a polytropic magnetised wind model, assuming power laws for the dependence of the thermal and magnetic wind parameters on the stellar rotation rate. We use empirical data to constrain theoretical wind scenarios, which are characterised by different rates of increase of the wind temperature, wind density, and magnetic field strength. Scenarios based on moderate rates of increase yield wind ram pressures in agreement with most empirical constraints, but cannot account for some moderately rotating targets, whose high apparent mass loss rates are inconsistent with observed coronal X-ray and magnetic properties. For fast magnetic rotators, the magneto-centrifugal driving of the outflow can produce terminal wind velocities far in excess of the surface escape velocity. Disregarding this aspect in the analyses of wind ram pressures leads to overestimations of stellar mass loss rates. The predicted mass loss rates of cool main-sequence stars do not exceed about ten times the solar value (Fig. 100). We expect the impact of stellar winds on planetary atmospheres to be less severe and the detectability of magnetospheric radio emission to be lower than suggested in previous investigations.

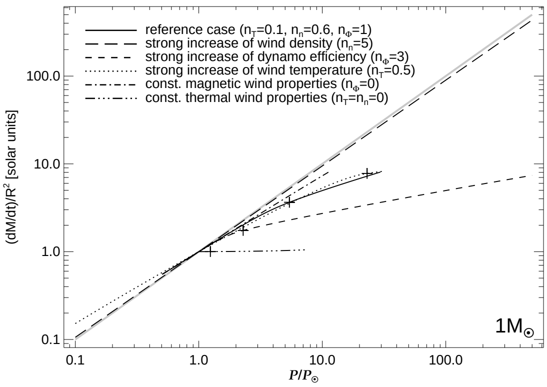


Fig. 100: Self-consistent mass loss rates per surface area, $\dot{M}/R^2$, as a function of the wind ram pressure, $\mathcal{P}/\mathcal{P}_\odot$.

(V. Holzwarth)

### The fraction of DA white dwarfs with kilo-gauss magnetic fields

The distribution of the strength of the magnetic field on white dwarfs has strong implications for the origins of these fields and the progenitors of these stars. According to current estimates about 10 % of all white dwarfs have fields in excess of 1 MG. This result is well established. Of greater interest, but less certain is the fraction of white dwarfs with weaker fields, since it requires particularly sensitive observations to detect fields in the kG regime. So far only a handful of white dwarfs had been observed with the required sensitivity (mainly in an earlier study we had carried out; Aznar Cuadrado *et al.* 2006). According to this and other previous studies the fraction of white dwarfs with kG fields is roughly 25 %.

Our aim was to improve the statistics by a new sample of ten white dwarfs in order to determine the ratio of magnetic to field-free white dwarfs. Mean longitudinal magnetic field strengths were determined by means of high-precision circular polarimetry of H$\beta$ and H$\gamma$ with the FORS1 spectrograph of the VLT "Kueyen" 8-m telescope. In one of our objects (LTT 7987) we detected a statistically significant (97 % confidence level) longitudinal magnetic field varying between $(-1 \pm 0.5)$ kG and $(+1 \pm 0.5)$ kG. This would be the weakest magnetic field ever found in a white dwarf, but at this level of accuracy, systematic errors cannot be completely ruled out. We also observed the sdO star EC 11481-2303 but could not detect a magnetic field. The sum of all VLT observations carried out so far with uncertainties of typically 1000 G or less suggest that 15 – 20 % of white dwarfs have kG fields. Together with previous investigations, the fraction of kG magnetic fields in white dwarfs amounts to about 11 – 15 %, which is close to the current estimations for highly magnetic white dwarfs (>1 MG).

(R. Aznar Cuadrado and S. K. Solanki in collaboration with S. Jordan (Universität Heidelberg), R. Napiwotzki (University of Hertfordshire), and H. M. Schmid (ETH Zürich))

### The Ca II infrared triplet as a stellar activity diagnostic: Test and calibration with high resolution observations

The aim of this work is to determine and test the best way of deriving activity-level information and errors from the Ca II IRT lines, in preparation of the GAIA Cornerstone mission by ESA, by which the Ca II IRT spectral range will be spectroscopically observed for millions of stars.

We have analysed high resolution spectra (R≈ 86 000) of a sample of 42 late-type active stars (with measured $\log R'_{\rm HK}$ spanning from $\approx -3$ to $\approx -5$) acquired with the Italian 3.6-m Telescopio Nazionale Galileo (TNG) using the SARG spectrometer in the 4960 – 10110 Å range. The high quality of the spectra and the good activity-level coverage allow us to measure two different chromospheric indicators that can be derived from the Ca II infrared triplet (Ca II IRT) lines: the residual equivalent width (EQW), $W_{\rm IRT}$, and the chromospheric indicator $R_{\rm IRT}$.

The diagnostic power of the Ca II IRT lines as magnetic activity indicators has been investigated by many authors in the past. However, there are some problems in the use of these lines as chromospheric diagnostics, such as the dependence of their central depressions on $v \sin i$ and the photospheric contribution. Andretta *et al.* (2005) suggested the $R_{\rm IRT}$ index as a good estimator of the chromospheric contribution to the Ca II IRT lines which takes into account the proper subtraction of the photospheric quiescent contribution. The $R_{\rm IRT}$ index is calculated for each observed star as the difference between the computed NLTE-$v \sin i$-convolved photospheric central intensity and the observed one. A new candidate for chromospheric indicator is the core-residual EQW, $W_{\rm IRT}$, given by the area of the positive profile obtained as the difference between the calculated NLTE-$v \sin i$-convolved photospheric and the observed profiles.

We correlate the Mount-Wilson purely chromospheric emission indicator $\log R'_{\rm HK}$ with $R_{\rm IRT}$ and the $W_{\rm IRT}$ indexes. This analysis indicates that the Ca II IRT lines are good chromospheric diagnostics. We find that both $W_{\rm IRT}$ and the $R_{\rm IRT}$ quantities can be used as chromospheric indicators, although the former exhibits a tighter correlation with the $\log R'_{\rm HK}$ index. Furthermore, we find that the total chromospheric excess EQW in the Ca II IRT is almost linearly correlated with the excess in the Ca II H & K doublet, as estimated through the $\log R'_{\rm HK}$ index.

(R. Aznar Cuadrado in collaboration with I. Busà (INAF/Osservatorio Astrofisico di Catania), L. Terranegra, V. Andretta, and M. T. Gomez (INAF/Osservatorio Astronomico di Capodimonte))

### Doppler imaging of the RS CVn Star Sigma Geminorum

In contrast to the Sun, other stars remain point sources even in observations with the best telescopes. Doppler imaging is a valuable tool for indirectly making rough images of stellar surfaces. Using this technique, we can reconstruct stellar surface maps from a time-series of high-resolution spectral line profiles.

We made a Doppler Imaging analysis of Sigma Geminorum based on 70 spectra observed with the Nordic Optical Telescope (NOT) on La Palma and with the Telescope Bernard Lyot (TBL) at the Observatory at Pic du Midi in the period of February 1998 – December 2001. The inversion technique based on the Occamian approach was applied to the observations in order to reconstruct 4 surface images for different epochs. To test the reliability of the results we made reconstructions with different sets of atomic lines (Fe I 6173 Å, Ni I 6175 Å, Ni I 6177 Å, Fe I 6180 Å, Fe I 6430 Å and Ca I 6439 Å) as well as with Mean Line Profiles calculated from 808 Fe I lines for observations taken in December 2001.

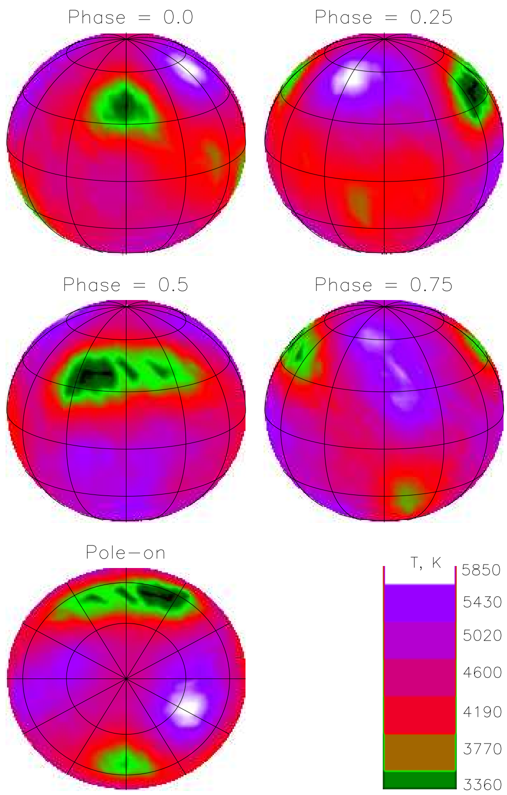


Fig. 101: Reconstructed surface map of $\sigma$ Gem for December 2001 for 6 atomic lines (Fe I 6173 Å, Ni I 6175 Å, Ni I 6177 Å, Fe I 6180 Å, Fe I 6430 Å and Ca I 6439 Å) is shown at four orbital phases with the coordinate grid of 30° in both latitude and longitude. Plotted is the effective temperature distribution given by the colour scale, which is clarified by the bottom right panel.

Tests with different spectral lines and different techniques show that $\sigma$ Gem has multiple low-latitude spots. On the visible hemisphere there are 2 – 3 spot groups located in general below a latitude of 45° (green to black in Fig. 101). There is no sign of a polar or high-latitude spot, as present on more rapidly rotating stars. This may have to do with the relatively slow rotation of $\sigma$-Gem ($P_{rot} \approx$ 19.6 days), which would mean that the Coriolis force is not as strong as on more rapid rotators. These results are robust and are found using different groups of spectral lines.

(A. A. Semenova and S. K. Solanki in collaboration with S. Berdyugina (ETH, Zürich) and P. Petit (Observatoire Midi-Pyrénées, Toulouse))

**Triggered Star formation by outflow-driven shells**

When an area of active or recent star formation (SF) is found, a question can be raised: is the SF there happening spontaneously or is it being triggered? Places where there is no apparent trigger would be a possible evidence of its spontaneous nature, but in areas where there are indications of triggered SF the determination of the possible causes is difficult. Star forming areas contain population of young stellar objects (YSOs), then the mentioned question can be addressed studying the interactions between components of the YSOs and their surrounding interstellar medium.

According to a triggered star formation scenario (e.g. Martin-Pintado and Cernicharo, 1987) outflows powered by YSOs shape the molecular clouds, can dig cavities, and trigger new SF. NGC 1333 is an active site of low and intermediate star formation in Perseus and is a suggested site of self-regulated star formation (Norman and Silk, 1980). Therefore it is a suitable target for a study of triggered star formation (e.g. Sandell and Knee, 2001). On the another hand, continuum sub-mm observations of star forming regions can detect dust thermal emission of embedded sources (which drive outflows), and further detailed structures.

Within the framework of our wide-field mapping of star formation regions in the Perseus and Orion molecular clouds using SCUBA at 850 and 450 $\mu$m, we map NGC 1333 with an area of around $14' \times 21'$. The maps show more structure than the previous maps of the region observed in sub-mm. We have unveiled the known embedded SK 1 source (in the dust shell of the SSV 13 ridge) and detailed structure of the region, among some other young protostars.

In agreement with the SK 1 observations, our map of the region shows lumpy filaments and shells/cavities that seem to be created by outflows. The measured mass of SK 1 ($\sim 0.07$ M$_\odot$) is much less than its virial mass ($\sim 0.2 - 1$ M$_\odot$). Our observations support the idea of SK 1 as an event triggered by outflow-driven shells in NGC 1333 (induced by an increase in gas pressure and density due to radiation pressure from the stellar winds, that have presumably created the dust shell). This kind of evidences provides a more thorough understanding of the star formation regulation processes.

(M. Rengel in collaboration with K. Hodapp (Institute for Astronomy, Hilo) and J. Eislöffel (Thüringer Landessternwarte Tautenburg)).

**Properties of young protostellar objects: a peculiar source**

The earliest stage of star formation, in which a deeply embedded protostar is known to exist, is the so-called Class 0 phase. The physical properties of class 0 sources have not been well studied due to the difficulties of being deeply embedded in dense molecular cloud cores and being heavily obscured by the envelope material, and are rare due to their short dynamical lifetime. Recent developments of mm and sub-mm observational techniques have revealed such deeply embedded very young protostars as sub-mm point sources, and our understanding about the initial condition of star formation has significantly progressed.

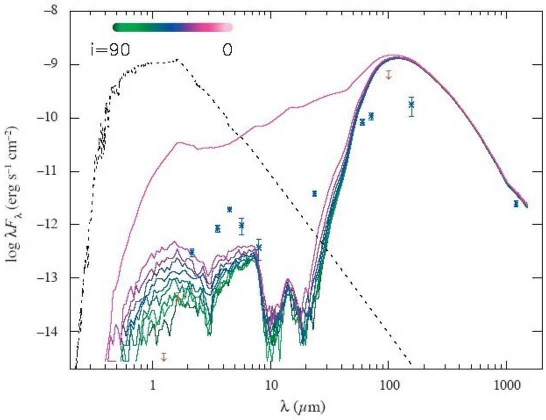


Fig. 102: Photometric data of Lupus 3 MMS plotted on the calculated Class 0 SED by Whitney et al. (2003). The solid lines represent the SEDs seen from the different viewing angles. The broken line represents the spectrum of the central object (T$_{eff}$ = 4000 K)

A nearby (d $\sim$ 150 pc) star-forming region, the Lupus 3 molecular cloud, has been surveyed for dense gas and dust cores and embedded objects in radio ($H^{13}CO^+$ J = 1-0 line and 1.2 mm continuum) and infrared (JHK$_s$L'MN bands and $H_2$ v = 1-0 s(1) line) wavelengths. These observations unveil a filamentary cloud, three dense cores, an embedded mm source (MMS), and an associated elongated object in the K band. The spectral energy distribution (SED) analysis of the MMS shows that it is a remarkably cold class 0 object with molecular outflow detected in the CO (J = 3-2 line), and peculiarly with near-IR detections (Fig. 102). From the estimated low bolometric temperature (39.5 K), faint bolometric luminosity (0.16 L$_\odot$), and sufficiently large envelope mass (0.52 $M_\odot$), the MMS is expected to be in a very early phase ($10^4$ yr) of mass accretion. The K-band elongated feature appears to be scattered light originated from the embedded central object of the MMS seen through the outflow cavity opening toward HH 78 on the near side as shown by the blue-shifted CO wings. The MMS has been also detected by the Spitzer Space Telescope (SST), and its near-IR images exhibit butter y-shaped nebulosity emission as scattered light through the bipolar cavities in contrast to that in the K band. Together with the SST and NTT JHK photometric data, the observed SED has a short-wavelength cut-off suggesting a low effective temperature (<1400 K) of the central object.

This study represents a report of a class 0 object which also exhibits near-IR emission. This is interpreted as a young protostar embedded in a thick dust envelope with outflow cavities.

(M. Rengel in collaboration mainly with K. Tachihara (Kobe University))

### A magnetic communication scenario for hot Jupiters

The observations of enhanced chromospheric activity on HD 179949 as well as on $\nu$ And with the same periods as their close-in planets seem to indicate some kind of magnetic interaction between star and planet. A constraint to any possible model are the large phase angles of 60° and 169°, respectively. We developed a simple model, which considers the propagation of Alfven waves within the stellar wind flow relative to the planet. The model is similar to the one used to explain the current system between Io and Jupiter. We found that our model can explain the observed large phase angles (see Fig. 103).

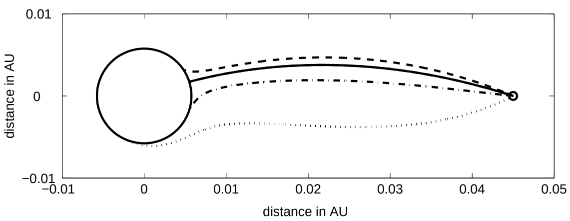


Fig. 103: Alfvén characteristics c-A in the equatorial plane for a star with a rotation period of 9 d and four different orbital periods Porb of the planet in the same stellar wind, i.e. the fact that this corresponds to different star masses is ignored here in order to better illustrate the effect of the relative velocity. The solid line is a magnetic field line in the stellar wind. It is equivalent to c-A with Porb = 9 d. The dashed line corresponds to Porb = 12 d, the dash-dotted to Porb = 6 d and the dotted to Porb = 3 d.

(J. Büchner in collaboration with S. Preusse, A. Kopp, and U. Motschmann)

### Formation of coherent structures and particle acceleration at the front of dense relativistic $e^+ - e^-$ jets expanding into the interstellar medium

We investigated the formation of large amplitude coherent structures due to the injection of dense relativistic jets into the dilute ambient interstellar medium. We found that a two-stream instability between jet and ambient plasma particles takes place. By means of open-boundary conditions relativistic Vlasov-code simulations we studied the nonlinear evolution of these waves. We found that a major wave package is excited locally at the jet front. Later quasi-stationary wave patterns are formed behind the jet front (Fig. 104). They trap the majority of the plasma particles causing significant heating of the core plasma and particle acceleration.

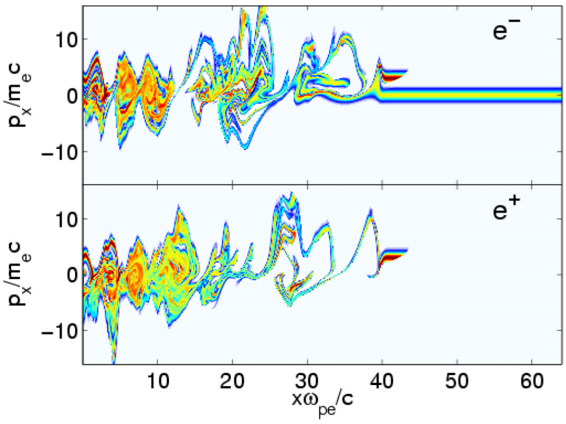


Fig. 104: Electron and positron distribution functions in $(x, p_x)$ at $t\omega_{pe} = 86$. The shock front forms at the interface between jet and surrounding media as one can see in the electron phase space (upper panel).

(N. Elkina and J. Büchner)

### Understanding WMAP results: The low-$l$ anomalies and dust in the vicinity of the solar system

Analyses of the cosmic microwave background (CMB) radiation maps produced by the Wilkinson Microwave Anisotropy Probe (WMAP) have revealed anomalies not predicted by the standard cosmological theories. It has been suggested that a dust cloud in the vicinity of the solar system may be the cause for these anomalies. We have been investigating the thermal microwave emission by dust particles at wavelengths of several millimetres in order to provide quantitative estimates of the contribution of the solar system-bound dust to the CMB (see Fig. 105).

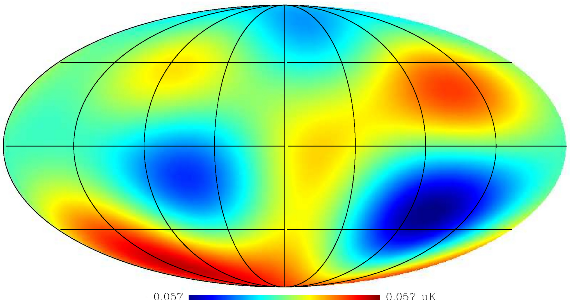


Fig. 105: Superposition of the quadrupole and octopole of the multipole expansion of the cosmic microwave background (CMB) temperature fluctuations in the ecliptic coordinates. The alignment of the two multipoles with the solar system geometry is surprising.

Our thermal emission models are based on the Mie scattering theory for perfect homogeneous spheres, assuming the particles are composed either of a silicate or carbonaceous material, or ice. The spatial distributions of dust under our consideration include the smooth background zodiacal cloud, asteroid dust bands, meteor streams along the orbits of selected comets, as well as the prominent Taurid meteor complex. Hypothetical clouds of interstellar dust are also taken into consideration, e.g. the monodirectional flow of particles focussed by solar gravity. The local interstellar clouds are on our to-do list. While the known dust clouds are ruled out based on the photometric, spectral and spatial configuration arguments, properties of a hypothetical dust cloud that can be held responsible for the anomalous observations are being inferred.

(V. Dikarev, O. Preuß, S. K. Solanki, and H. Krüger in collaboration with A. Krivov (FSU Jena))

### Monitoring the interstellar dust flow through the solar system

The Ulysses spacecraft has been orbiting the Sun on a highly inclined ellipse almost perpendicular to the ecliptic plane (inclination 79°, perihelion distance 1.3 AU, aphelion distance 5.4 AU) since it encountered Jupiter in 1992. The in-situ dust detector on board continuously measured interstellar dust grains with masses up to $10^{-13}$ kg, penetrating deep into the solar system. The flow direction is close to the mean apex of the Sun's motion through the local interstellar medium (parallel to the flow of neutral interstellar hydrogen and helium gas), and, on average, the grain impact velocities exceed the local solar system escape velocity, even if radiation pressure effects are neglected. The grains act as tracers of the physical conditions in the local interstellar cloud (LIC), showing that the intrinsic size distribution of interstellar grains in the LIC extends to grain sizes larger than those detectable by astronomical observations. The existence of such 'big' interstellar grains is also indicated by observations of radar meteors entering the Earth's atmosphere. The Ulysses measurements showed that the dust-to-gas mass ratio in the local interstellar cloud is at least a factor of two higher than the standard interstellar value derived from cosmic abundances, implying the existence of inhomogeneities in the diffuse interstellar medium on relatively small length scales. The interstellar dust stream in the inner solar system is altered by the solar radiation pressure force, gravitational focussing and interaction of charged grains with the time varying interplanetary magnetic field.

The dust measurements from Ulysses' third passage through the outer solar system obtained in 2004 to 2006 imply an at least 30° shift in the approach direction of interstellar grains. The reason for this shift remains mysterious. Whether it is connected to a secondary stream of interstellar neutral atoms shifted from the main neutral gas flow is presently unclear. However, given that the neutral gas stream is shifted along the ecliptic plane while the shift in the dust flow is offset from the ecliptic, a connection between both phenomena seems unlikely.

(H. Krüger and the Ulysses dust team)

### Properties of anomalous cosmic ray (ACR) as deduced from ENA measurements with SOHO/CELIAS/HSTOF

Remote observation of the low energy end (up to few 100 keV) of the energetic ion spectrum in the heliosheath is possible by using the energetic neutral atoms (ENAs) coming from neutralization of those ions. The ENAs of possibly heliosheath origin were first detected by CELIAS/HSTOF onboard SOHO. Until recently, the interpretation of these data was difficult, because of large uncertainties concerning the ion spectrum in the heliosheath and in the heliosphere. In particular, this applied to the low energy anomalous cosmic ray ions, which cannot penetrate into the inner heliosphere. After the Voyager 1 crossing of the termination shock it has become possible to compare the results deduced from the ENA observations to the ion spectra measured in situ.

The low-energy ion flux measurements by LECP instrument on Voyager 1 downstream from the shock can be combined with the HSTOF ENA measurements to estimate the hydrogen column density in the heliosheath. With the ion spectrum given by the proton and helium in-situ post-shock data and the ENA spectrum by the CELIAS/HSTOF ENA data, the hydrogen column density can be determined. This approach presumes that the LECP ion fluxes can be used in place of the averages over the sector of the heliosheath covered by the HSTOF observations. The resulting hydrogen column density must be understood as an average over the same sector (within the apex or nose sector of the heliosphere, that is including both the forward part of the heliosheath and the flanks). The result of the simultaneous fit to the hydrogen and helium spectra corresponds to an average thickness within the selected sector of the heliosheath of about 75 AU (or about 30 AU in the apex direction). Based on this estimate from the CELIAS/HSTOF ENA and the LECP energetic ion data onboard Voyager 1, the latter should leave the heliosheath region beyond the year 2014.

(M. Hilchenbach in collaboration with K. C. Hsieh (University of Arizona, Tucson, USA) and A. Czechowski (Polish Academy of Sciences, Warsaw, Poland))

### Estimating the thickness of the heliosheath from CELIAS/HSTOF and Voyager 1 data

The heliosheath (the transition region between the solar wind termination shock and the heliopause, also called the inner heliosheath), into which Voyager 1 recently moved, has been for some time considered a probable source of the energetic neutral atoms (ENAs), both H and He, observed since the year 1996 by the HSTOF/CELIAS instrument on board the Solar and Heliospheric Observatory. These ENAs are thought to originate as heliosheath energetic ions that become neutralized by charge exchange with the low-energy neutral atoms that enter the heliosheath from interstellar space (Fig. 106) We show that the fluxes of protons and He ions in the heliosheath reported by the Voyager 1 Low Energy Charged Particle (LECP) experiment are consistent with this hypothesis. We used recent Voyager 1 measurements of the ion fluxes beyond the termination shock and the SOHO HSTOF/ CELIAS measured fluxes of the energetic neutral hydrogen and helium at 1 AU to estimate the neutral hydrogen column density in the heliosheath. Our best estimate is $1.13 \times 10^{14}$ cm$^{-2}$. The result corresponds to an average thickness of the heliosheath, in the forward part of the heliosphere (within 155° from the nose direction and 17° from the ecliptic), of L $\sim$ 75 AU for an average hydrogen density of 0.1 cm$^3$ in the heliosheath.

(M. Hilchenbach and R. Kallenbach in collaboration with A. Czechwoski, K. C. Hsieh, and J. Kota)

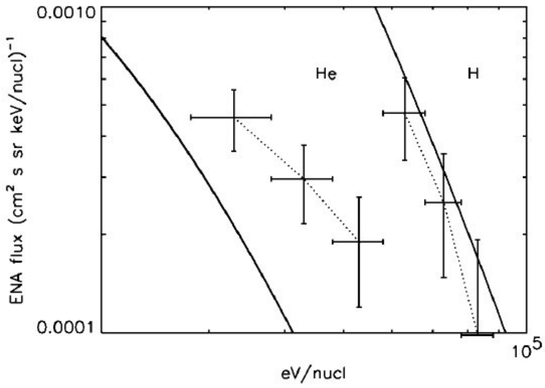


Fig. 106: Best-fit hydrogen and helium ENA spectra compared with the CELIAS/HSTOF ENA data. The data presented in the Figure cover the forward part and flanks of the heliosheath. The heliotail sector is excluded. Vertical error bars show 1-$\sigma$ statistical errors. Horizontal bars denote energy bins.

### Interstellar dust in the solar system

The Ulysses spacecraft has been has been measuring interstellar dust in the solar system since it encountered Jupiter in 1992. The in-situ dust detector on board continuously measured interstellar dust grains with masses up to $10^{-13}$ kg, penetrating deep into the solar system (Grün et al., 1993; Krüger *et al.*, 2007). On average, the grain impact velocities exceed the local solar system escape velocity, even if radiation pressure effects are neglected, and the grains act as tracers of the physical conditions in the local interstellar cloud (LIC). The Ulysses measurements showed that the intrinsic size distribution of interstellar grains in the LIC extends to grain sizes larger than those detectable by astronomical observations. Furthermore, the dust-to-gas mass ratio in the LIC is at least a factor of two higher than the standard interstellar value derived from cosmic abundances, implying the existence of inhomogeneities in the diffuse interstellar medium on relatively small length scales.

The interstellar dust stream in the inner solar system is altered by the solar radiation pressure force, gravitational focussing and interaction of charged grains with the time varying interplanetary magnetic field (IMF). Until 2004, the interstellar dust flow direction was close to the mean apex of the Sun's motion through the LIC (i.e. parallel to the flow of neutral interstellar hydrogen and helium gas). Since 2005, the Ulysses measurements imply an at least 30° shift in the approach direction of interstellar grains (Krüger *et al.*, 2007) (Fig. 107). The reason for this shift remains mysterious. Whether it is connected to a secondary stream of interstellar neutral atoms shifted from the main neutral gas flow is presently unclear. Given, however, that the neutral gas stream is shifted along the ecliptic plane while the shift in the dust flow is offset from the ecliptic, a connection between both phenomena seems unlikely.

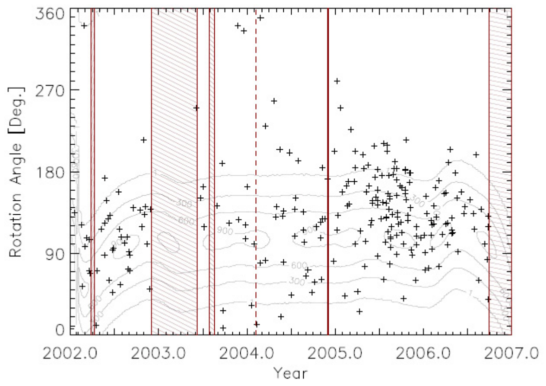


Fig. 107: Impact direction (i.e. spacecraft rotation angle at dust particle impact) of interstellar grains measured with Ulysses from 1 January 2002 to 31 December 2006. Ecliptic north is close to 0°. Each cross indicates an individual impact. Contour lines show the effective sensor area for particles approaching from the upstream direction of interstellar helium. A vertical dashed line shows Jupiter closest approach on 5 February 2004, five shaded areas indicate periods when the dust instrument was switched off.

(H. Krüger and the Ulysses dust team)

## Combined models of magnetic flux generation and transport in cool stars

We have developed a model which connects the deep-seated dynamos to the surface magnetic flux in stars with outer convection zones, such as the Sun. The link is the buoyant rise of magnetic flux tubes from the field generation layer through the convection zone. During their ascent, rotationally induced forces lead to a poleward deflection of the rising tubes and to a deformation, which manifests itself as a tilt angle of emerged bipolar magnetic regions at the surface. Both effects can be crucial for the further evolution of the surface flux. As a first example, we have used a thin-layer $\alpha\Omega$ dynamo model with Sun-like radial shear in the convective overshoot region. We have carried out numerical simulations of the rise of Parker-unstable thin flux tubes from the dynamo layer up to the surface, which in turn determine the latitudes and the tilt angles of the emerging flux loops. This information has been put into a surface flux transport model with Sun-like differential rotation, meridional flow, and turbulent magnetic diffusion, which simulates the evolution of bipolar magnetic regions. Fig. 108a shows the surface evolution of the magnetic flux density averaged over stellar longitude (azimuth), for a star with solar internal structure, rotating 2.6 times faster than the Sun (a 'younger Sun'). The periodic variation of the generated magnetic flux (the interior dynamo) is no longer visible in the variation of magnetic flux integrated over the entire surface (Fig. 108b). For a more active Sun-like star rotating about 13 times faster than the Sun, the surface emergence pattern of magnetic fields is very different from that of the dynamo-generated magnetic field in the deep convection zone. This result underlines the importance of taking the flux rise process into account, when confronting models of deep-seated stellar dynamos with observations of active cool stars.

(E. Işık, D. Schmitt, and M. Schüssler)

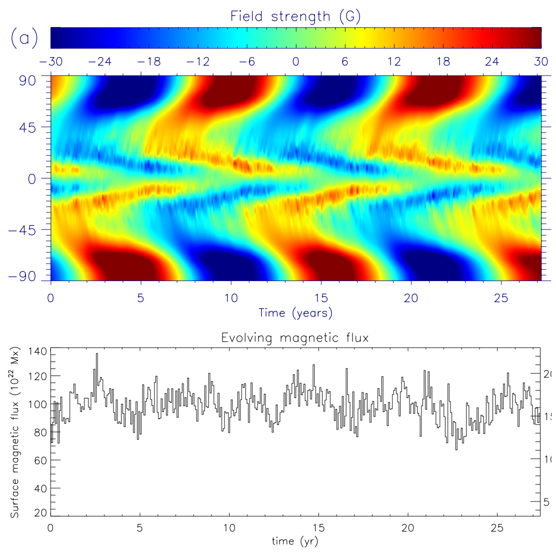


Fig. 108: (a) Time-latitude diagram of the azimuthally averaged magnetic flux density for a Sun-like star rotating 2.6 times faster than the Sun. (b) Time variation of the total unsigned surface magnetic flux. The values are averaged over 1-month time intervals.

## The FeH $F^4\Delta$-$X^4\Delta$ system and its diagnostic capability for investigating solar and stellar magnetic fields

For the study of cool stellar atmospheres and the internal structure of sunspots and starspots, lines of diatomic molecules are ideal tools, given their temperature and pressure sensitivities which are typically higher than of atomic lines. The Wing-Ford FeH $F^4\Delta$-$X^4\Delta$ system represents such a diatomic molecule that is, in addition, highly sensitive to magnetic fields. The FeH $F^4\Delta$-$X^4\Delta$ system is produced by transitions between two electronic states with a coupling of the angular momenta that is intermediate between limiting Hund's cases (a) and (b). The current theoretical description of these transitions, including the involved molecular constants, are only based on intensity measurements because until now polarimetric observations have not been available. This significantly limits their diagnostic value. Furthermore, so far the theory was optimized to reproduce energy levels and line strengths without taking magnetic sensitivities into account.

Our goal was to investigate the diagnostic capabilities of the current theoretical description of the molecule FeH. Using the best available Hamiltonian, we carried out the perturbation calculation of the molecular Zeeman effect for this transition and computed the Landé factors of the energy levels and of transitions. We extracted Landé factors from a comparison of observed and calculated Stokes $I$ and $V$ profiles. Certain spectral lines, more frequently with high magnetic sensitivity, exhibited discrepancies between the theory and observations. We extended the theoretical model with a semi-empirical approach to obtain a diagnostic tool that is able to reproduce many of the interesting spectral lines.

We found that the current theory successfully reproduces the magnetic properties of a large number of lines in the $F^4\Delta$-$X^4\Delta$ system and that the modified Hamiltonian allows us to synthesize and successfully reproduce the most sensitive lines. Thus our observations have provided valuable constraints on empirical molecular constants and Landé factors. In conclusion, the FeH $F^4\Delta$-$X^4\Delta$ system is found to be a very sensitive magnetic diagnostic tool. Polarimetric data of these lines, in contrast to intensity measurements, provide us with more direct and detailed information to study the coolest parts of sunspot and starspot umbrae, and cool active dwarfs.

(A. Lagg and S. K. Solanki in collaboration with N. Afram, S. V. Berdyugina, and D. M. Fluri (ETH Zürich))

## Fundamental science

### Eigenfunctions of the radial operator and the spin-orbit-coupling operator for a relativistic binary

The exact eigenfunctions of a relativistic binary (like, e.g., positronium) of two fermions bound by the Coulomb force are calculated. We consider the Dirac equation for two distinguishable fermions (as in a hydrogen-like atom, where we have a proton and an electron) including the electrostatic potential but without radiative corrections. As shown in a previous paper, this quantum-mechanical problem can be treated exactly. To solve the eigenvalue problem in particle-antiparticle space, we make an ansatz that involves four independent spatial functions for each particle species. We provide the exact solution for the radial eigenfunction (four-component spinor) of the hamiltonian in terms of generalized hypergeometric functions, which are determined through a complex matrix recursion relation. In addition, an equivalent set of coupled first-order, or uncoupled second-order, differential equations which may be solved numerically is provided. The exact eigenfunctions of the two spin-orbit-coupling operators for the binary system are also calculated. To evaluate them we use the spherical harmonics for the relative angular momentum, and describe the combined spin states by help of the natural basis constructed from tensor products of the single-spin eigenvectors and by exploiting the algebraic properties of the spin-helicity operators.

(E. Marsch)

### Solar Axions

According to the QCD standard model the strong interaction should violate CP (simultaneous charge conjugation and parity) symmetry. However, the experimental evidence suggests that CP symmetry is conserved to a very high degree. To resolve this "CP problem" the axion, a chargeless, weakly interacting, low-mass elementary particle, was introduced. It is postulated that due to the Primakov effect axions are produced from two photons each in the core of the Sun and radiated out. They can convert back into photons in the presence of a magnetic field.

The CERN Axion Solar Telescope (CAST) experiment makes use of this property to search for these axions by applying a strong magnetic field and then searching for the X-ray signature of the decaying axions. So far, tight upper limits have been set on the relevant coupling constant within a given range of energies. Currently, this range is being extended with the help of changes to the instrumentations.

In parallel, the possibility of employing solar X-ray and EUV data to determine or at least set upper limits on the solar axion flux is being explored.

(S. K. Solanki and L. Teriaca in collaboration with K. Zioutas (CERN and University of Patras) and the CAST collaboration)

# 2. *Planeten, ihre natürlichen Satelliten und Kometen / Planets, their moons and comets*

## *Schwerpunktthema:*

## Höhepunkte der Venus-Express-Mission

(English version see page 102)

Venus Express ist die erste ESA-Mission zum Planeten Venus. Ihre wichtigsten wissenschaftlichen Ziele sind globale Untersuchungen der Atmosphäre, der Plasma-Umgebung und der Planetenoberfläche aus dem Orbit. Venus Express basiert auf dem Mars-Express-System, das an die spezifischen Bedingungen der Mission angepasst wurde. Es bietet eine vielseitige Plattform sowohl für Nadir- und Limb-Messungen als auch für Sonnen-, Stern-, und Radiookkultation. Der Satellit trat im April 2006 in ein hoch elliptisches polares Orbit um seinen Zielplaneten ein. Periapsis und Apoapsis sind 250 km bzw. 66 000 km vom Planetenzentrum entfernt, die Periode des Orbits beträgt 24 Stunden. Die Kernmission war nominal für den Zeitraum vom 4. Juni 2006 bis zum 2. Oktober 2007 angesetzt, was in etwa zwei siderischen Venustagen entspricht.

Die Payload besteht aus sieben Experimenten und beinhaltet ein leistungsfähiges Ensemble aus einer abbildenden Kamera, einem Fernerkundungsspektrometer, Instrumenten für die Untersuchung des den Planeten umgebenden Plasmas und des magnetischen Feldes sowie ein Radioexperiment. Das MPS ist vielfältig am Venus Express Programm beteiligt: Die Venus Monitoring Camera (VMC), für die die PI-Verantwortung am MPS liegt, studiert die Wolkenstrukturen und die Dynamik der Atmosphäre und ermöglicht eine Kartierung der Oberflächentemperatur des Planeten. Dieses Engagement wird durch wissenschaftliche Beteiligungen am abbildenden Spektrometer VIRTIS und am Analyser of Space Plasmas and Energetic Atoms (ASPERA-4) vervollständigt. Für ASPERA-4 hat das MPS zudem Hardware entwickelt. Ferner unterstützt das MPS die ESA bei der Planung und Koordination der wissenschaftlichen Messungen.

### Wolkenstruktur und Dynamik

Das abbildende Spektrometer auf Venus Express nutzt die große Exzentrizität des polaren Orbits, um die Wolkenschichten in einem spektralen Bereich von Ultraviolett bis zum thermischen Infrarot mit bisher unerreichtem Detailreichtum aufzuzeichnen. Dabei wurden alle Breiten und Sonnenstände mit Auflösungen von etwa 50 km in der Apoapsis bis zu einigen hundert Metern in der Periapsis abgedeckt. Die multispektralen Abbildungen ermöglichen es zum ersten Mal, die Wolkenstrukturen in drei Dimensionen zu rekonstruieren. Darüber hinaus erlauben es die Limb-Messungen sowie die Stern- und Sonnenokkultationstechniken, die vertikale Struktur des Nebels über der Wolkendecke (upper haze) zu untersuchen.

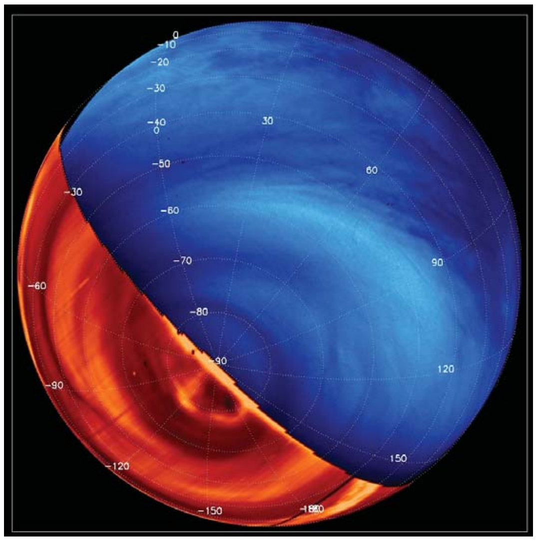

Abb. 109: Falschfarbene Abbildungen der Venus Südhemisphäre. Die blaue Abbildung zeigt eine VMC-Aufnahme der Tagseite im UV. Die rote Abbildung ist eine VIRTIS Aufnahme der Nachtseite im nah-infraroten spektralen Fenster bei 1.7 $\mu$m Wellenlänge.

Abb. 109 zeigt die Kombination eines VMC-Bildes im Ultravioletten (UV) auf der Tagseite, mit einem VIRTIS-Bild auf der Nachtseite, das im transparenten Nah-Infrarot-Fenster bei 1.7 $\mu$m Wellenlänge aufgenommen wurde. Die Strukturen im UV-Bild geben die unregelmäßige Verteilung eines unbekannten Absorbers in der oberen Wolkenschicht zwischen etwa 55 bis 70 km Höhe wieder, die wiederum auf unterschiedliche dynamische Zustände in der Atmosphäre zurückgeht. Die scheckige, fleckige Wolkenstruktur in niedrigen Breiten unter 40°S spricht dafür, dass hier turbulente Konvektion eine größere Rolle spielt, angetrieben durch die in niedrigen Breiten stärkere Sonneneinstrahlung, die zum großen Teil von der oberen Wolkenschicht in etwa 55 bis 65 km Höhe absorbiert wird. Zu den Polen hin werden die scheckigen Wolken durch streifige Gebilde abgelöst, was für eine geordnete, mehr laminare Bewegung in mittleren Breiten spricht. Die Region zwischen 50° und 70°S wird von einem hellen, fast strukturlosem Band dominiert. Dies lässt vermuten, dass hier Aerosole einen Großteil der Sonneneinstrahlung reflektieren, bevor sie den UV-Absorber erreicht. In den Polregionen hingegen findet man kreis- und spiralförmige Strukturen mit einem Durchmesser von einigen hundert Metern (siehe Abb. 109).

In niedrigen und mittleren Breiten kann die Helligkeit der Wolkenschicht von einem Tag zum nächsten deutlich variieren. Starke Winde und mikrophysikalische Wolkenbildungsprozesse wie Nukleation und Koagulation scheinen hier die Durchsichtigkeit der oberen Wolkenschicht relativ schnell zu verändern.

Der im nahen Infrarot aufgenommene Teil der Abb. 109 zeigt die Strahlung, die auf der Nachtseite von der unteren Atmosphäre durch das spektrale Fenster bei 1.7 $\mu$m Wellenlänge dringt. Hier gehen die Strukturen auf die unterschiedliche Durchsichtigkeit der Hauptwolkenschicht in 50 bis 55 km Höhe zurück. Die Helligkeit variiert etwa um eine Größenordnung, was einer Änderung in der Opazität um einen Faktor zwischen 20 und 40 entspricht. Bei dem spektralen Fenster mit einer Wellenlänge von 1.7 $\mu$m ist der Kontrast noch stärker.

Die von Venus Express aufgedeckten Wolkenstrukturen sind im Wesentlichen in Form eines globalen Wirbels organisiert (Abb. 109). Sowohl die UV-Bilder von der Tagseite als auch die Infrarot-Aufnahmen von der Nachtseite zeigen, dass dieser Wirbel die gesamte Südhemisphäre bedeckt und mindestens bis zur Untergrenze der Wolkendecke bei 50 km hinunter reicht. Frühere Beobachtungen der Nordhemisphäre zeigen ein sehr ähnliches Bild, die Wolkenstruktur scheint also symmetrisch zum Äquator zu sein. Diese Wirbel haben eine verblüffende Ähnlichkeit mit Hurrikanen auf der Erde, ihre Größen und die jeweiligen Antriebskräfte dürften sich aber deutlich unterscheiden.

Der sehr elliptische Orbit von Venus Express ermöglicht es, bestimmte Regionen und Phänomene sowohl sehr detailliert als auch in ihrem globalen Kontext abzubilden. Abb. 110 vergleicht Beispiele von Wolkenstrukturen auf mittleren und kleinen Skalen in UV VMC-Aufnahmen und nah-infraroten VIRTIS-Bildern. Abb. 110A und 110B zeigen Details des Überganges von den fleckigen Wolken zu den streifigen Strukturen bei etwa 40° bis 50° südlicher Breite. Abb. 110C zeigt die durch Konvektion ziselierten feinen Wolkenstrukturen nahe am subsolaren Punkt. Die abbildenden Instrumente haben auch verschiedene Wellenphänomene beobachtet: Nahe der Pole entdeckte die VMC lange grade Strukturen, die kürzere Wellen in ihrer Umgebung auszulösen scheinen (Abb. 110D). Und VIRTIS zeichnete Wellen auf, die mit den Spiralarmen des globalen Wirbels zusammenhängen (Abb. 110E).

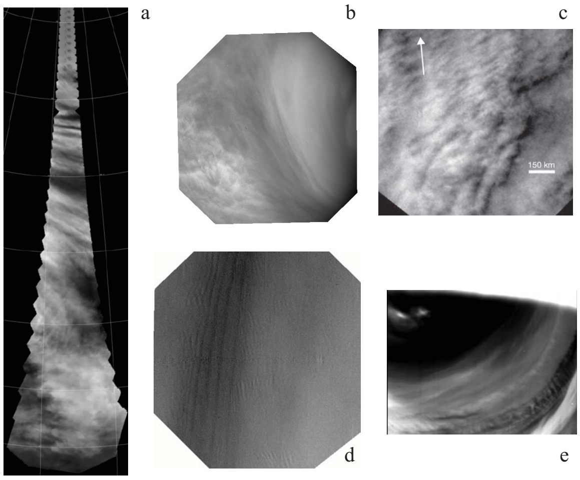


Abb. 110: Wolkenstrukturen auf mittleren und kleinen Längenskalen. A: Mosaik aus UV VMC-Aufnahmen während der Periapsis von Orbit Nr: 261; B: UV VMC-Abbildung der Übergangsregion in mittleren Breiten; C: hochaufgelöste UV VMC-Abbildung der fleckigen, konvektiven Wolken in niedrigen Breiten; D: Wellen in der Polarregion (etwa 70°N) aufgenommen im VMC UV-Kanal. E: Wellen in der tieferen Wolkenschicht bei mittleren Breiten, aufgenommen von VIRTIS im Nah-Infrarot.

VIRTIS-Aufnahmen im nah-infraroten $CO_2$-Absorptionsband erlauben es, global die Höhe der Wolkenoberdecke zu kartieren, da die Intensität der Absorption von der Dicke der Wolkenschicht abhängt. Abb. 111 zeigt ein UV VMC-Bild, überlagert mit farbkodierten Höhenangaben, die auf gleichzeitigen VIRTIS Aufnahmen im 1.6 $\mu$m $CO_2$ Band basieren. In niederen und mittleren Breiten liegt die Höhe der Wolkenoberdecke bei etwa 70 km und nimmt ab einer Breite von etwa 55° zu den Polen hin ab, wo sie bis auf 65 km im Auge des Wirbels sinkt. Die Höhe variiert also um mehr als eine Skalenhöhe. (Höhe in der der Druck um den Faktor e abnimmt.) Überraschenderweise macht sich die scharfe Grenze des hellen Bandes im UV-Bereich nicht als Höhenänderung bemerkbar (Abb. 111). Daraus schließt man, dass sich die dunklen Strukturen bei niedrigen Breiten und das helle Band bei mittleren Breiten auf vergleichbarer Höhe befinden.

Frühere Beobachtungen und Modelle der Venusatmosphäre haben gezeigt, dass es mindestens zwei unterschiedliche dynamische Zustände gibt: Die Troposphäre (0 bis 60 km Höhe) und die untere Mesosphäre (bis etwa 80 km Höhe) zeigen fast ausschließlich zonale Winde, die in Richtung der Planetenrotation wehen. Die Geschwindigkeit erreicht an der Wolkenoberseite ein Maximum und nimmt dann zur Planetenoberfläche hin und über den Wolken ab. Die Thermosphäre (100 bis 200 km Höhe) nimmt an einer globalen Zirkulation zwischen Tag- und Nacht-

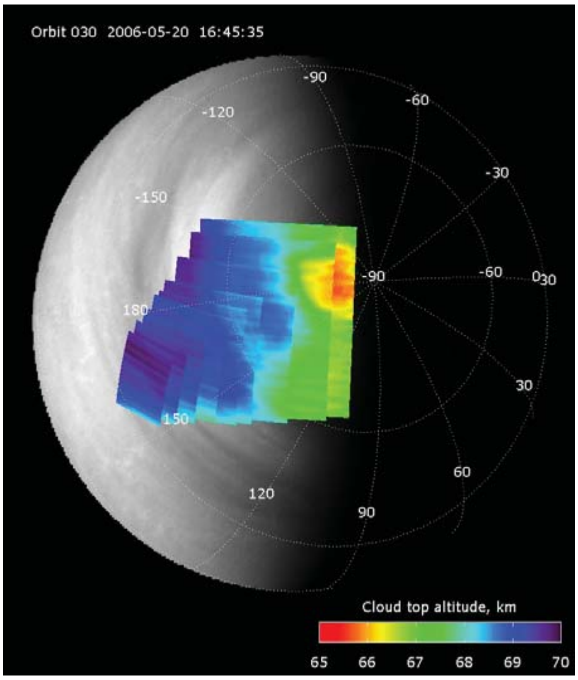


Abb. 111: Höhe der Wolkenoberseite. Das Farbmosaik der Höhe basiert auf VIRTIS-Daten im nah-infrarotem $CO_2$-Band. Es wurde einer VMC-Aufnahme im Ultravioletten überlagert, die gleichzeitig aufgenommen wurde.

seite teil, die von Temperaturdifferenzen zwischen dem subsolaren und dem antisolaren Punkten getrieben wird.

Die abbildenden Spektrometer auf Venus Express haben die Atmosphärenbewegung in verschiedenen Höhen beobachtet, angefangen an der unteren Wolkengrenze (etwa 50 km) bis hinauf zur unteren Mesosphäre (etwa 140 km). Die Windgeschwindigkeiten werden dadurch ermittelt, dass man die Bewegung von Wolkenstrukturen verfolgt. Abb. 112 zeigt über die Breite gemittelte Geschwindigkeitsprofile der zonalen Winde in unterschiedlichen Höhen, basierend auf VIRTIS- und auf VMC-Daten. In allen Höhen bleibt die Windgeschwindigkeit in der Wolkenzone bis zu einer Breite von 50° nahezu konstant, dann jedoch nimmt sie zum Pol hin schnell ab. Interessanterweise fällt dieser Übergang mit der Grenze zwischen fleckigen und streifigen Wolken zusammen. Ein Vergleich mit den zyklostrophischen Winden, die aus VIRTIS Temperaturmessungen abgeleitet wurden, zeigt eine recht gute Übereinstimmung für mittlere und hohe Breiten. Dies bestätigt die Annahme, dass es sich bei den zonalen Winden um zyklostrophische Winde handelt. Vorläufige Studien zur Zeitabhängigkeit dieser Winde deuten darauf hin, dass sie am späten Morgen am schwächsten sind und zum Nachmittag hin zunehmen. Die meridionalen Nord-Süd-Winde sind wesentlich schwächer (0 – 20 m/s) und darum wesentlich schwerer zu messen. Sie werden vom Äquator bis zu mittleren Breiten hin stärker, werden dann zum Pol hin wieder schwächer und kehren nahe am Pol sogar ihre Richtung um.

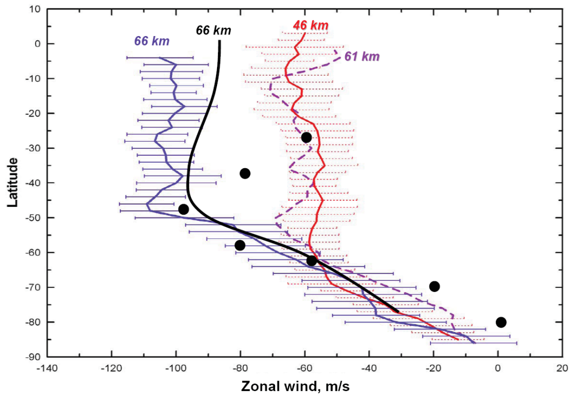


Abb. 112: Breitenabhängigkeit der gemittelten zonalen Ost-West-Windgeschwindigkeiten in der Südhemisphäre. Blau: UV, 380 nm, Tagseite; violett: Nah-infrarot, 980 nm, Tagseite; rot: Nah-infrarot, 1.74 $\mu$m, Nachtseite); schwarz: VMC-Aufnahme bei 365 nm, Nachtseite. Die Fehlerbalken der violetten und schwarzen Profile sind jenen der blauen Kurve vergleichbar. Die Höhenangaben an den Profilen sind etwa auf 2 bis 3 km genau. Die schwarzen Punkte zeigen ein zyklostrophisches Windprofil in 66 km Höhe. Mit Ausnahme des schwarzen Profils beruhen alle Kurven auf VIRTIS-Daten.

### Plasma-Umgebung

Venus hat kein inneres Magnetfeld, es bildet sich aber durch die Ionosphäre an der Tagseite des Planeten eine vom Sonnenwind induzierte Magnetosphäre. Dadurch kann die Energie des Sonnenwindes teilweise auf die Ionen der oberen Atmosphäre übertragen werden. Diese werden so beschleunigt und können vom Planeten entweichen. Daher ist die Untersuchung der Wechselwirkung mit dem Sonnenwind ganz wesentlich für das Verständnis der Entwicklung der Venusatmosphäre. Die Plasma-Umgebung des Planeten wird durch das ASPERA-4 Experiment (Analyzer of Space Plasmas and Energetic Atoms) mit drei verschiedenen Sensoren untersucht: einem für Neutralteilchen, einem für Ionen und einem für Elektronen. Die Messungen von Venus Express fallen in eine Periode geringer solarer Aktivität und ergänzen so die Messungen des Pioneer Venus Orbiter, die 1985 – 1992 im Maximum der solaren Aktivität vorgenommen wurden.

Venus Express durchquert auf seinem Orbit um Venus verschiedene Plasmaregionen und -grenzen, nämlich die Bugstoßwelle, den Magnetosheath, die induzierte Magnetosphärengrenze, den Plasmamantel, die Ionopause und die Ionosphäre (siehe Abb. 113). Die Grenzschichten lassen sich deutlich in den

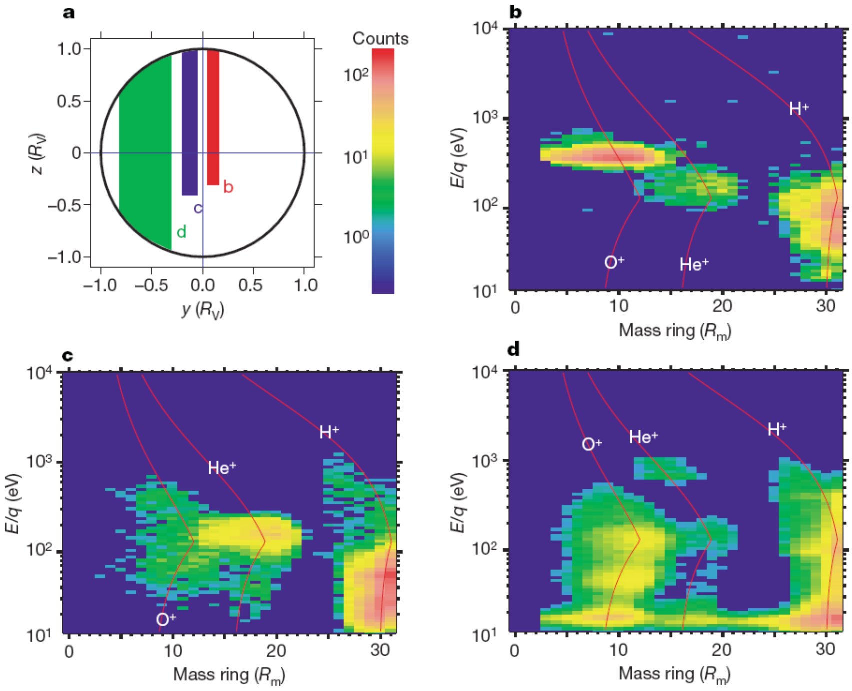


Abb. 114: Zusammensetzung und Energieverteilung des entweichenden Ionenplasmas. a: Geometrie der drei räumlichen Bereiche, in denen Energie/Massen-Spektrogramme bestimmt wurden, im Venus-Solar-Elektrischen Koordinatensystem (VSE). b-d: Energie/Massen-Spektrogramme summiert über 33 Orbits während des Zeitraums 18. Mai bis 30. Dezember 2006 in der elektrisch positiven Hemisphäre (b), in der elektrisch negativen Hemisphäre (c) und im Plasmamantel (d). Vertikale Achsen zeigen Energie pro Ladung, horizontale Achsen Massenkanäle des Sensors. Die Farben skalieren die durchschnittlichen Zählraten im Messzeitraum. Rote Linien deuten Ionen gleicher Masse an.

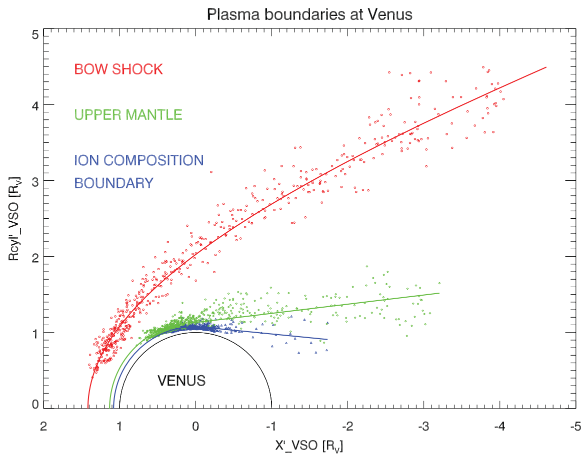


Abb. 113: Beobachtungen der Plasmagrenzen durch das Ionen- und Elektronenspektrometer an Bord von Venus Express während des ersten Jahres der Mission. Durchquerungen der Bugstoßwelle (rot), der induzierten Magnetosphärengrenze (‘Oberer Plasma Mantel’, grün) und Ionopause (‘Grenze der Ionenzusammensetzung’, blau) und entsprechende Fits an den Datenpunkten. Die horizontale Achse definiert die Venus-Sonnen-Linie, die vertikale Achse den Abstand von dieser Linie.

Magnetfeld- und Plasmamessungen identifizieren. Das ASPERA-4 Experiment hat erstmals die Komposition des vom Planeten entweichenden Plasmas bestimmt. Die Beschleunigung des planetaren Ionenplasmas wird durch drei Prozesse verursacht: durch das konvektive elektrische Feld (‘Pick-Up’), durch Instabilitäten an der Magnetosphärengrenze, die Plasmawolken ablösen, und durch Polarisationsfelder auf der Nachtseite des Planeten, wo das induzierte Magnetfeld nahezu radial ist. ASPERA-4 hat zwei verschiedene Kanäle für den Ionenabfluss entdeckt: entlang einer Plasmaschicht im Zentrum des Magnetosphärenschweifs und entlang der Magnetosphärengrenze. Die Energieverteilung der Ionen in beiden Kanälen ist sehr unterschiedlich: Ionen in der Plasmaschicht haben Energien im Verhältnis 4/2/1 für $O^+/He^+/H^+$ (siehe Abb. 114), während Ionen an der Magnetosphärengrenze nahezu Sonnenwindgeschwindigkeit aufweisen. Für einen gewöhnlichen Pick-Up-Prozess würde man allerdings nach der Ionenmasse ein Energieverhältnis von 16/4/1 erwarten. Vermutlich ist die Differenz durch eine nach Ionenmasse unterschiedliche Absorption in dem Plasmafluss verursacht.

Wie zu erwarten, wird der Ionenabfluss durch das induzierte elektrische Feld bestimmt. Alle drei Ionenarten zeigen ähnliche räumliche Verteilungen, was nahelegt, dass zum Beispiel $H^+$ und $He^+$ Ionen beide planetaren Ursprungs sind. Der gesamte Ionenabfluss vom Planeten lässt sich aus dem Integral des gemessenen Flusses bestimmen, aber die räumliche Abdeckung im ersten Jahr der Mission ist nicht ausreichend, um einen durchschnittlichen Fluss zu bestimmen. Es lassen sich aber bereits die Verhältnisse der abfliessenden Ionensorten mit $Q(\mathrm{H}^+)/Q(\mathrm{O}^+) = 1.9$ und $Q(\mathrm{He}^+)/Q(\mathrm{O}^+) = 0.07$ angeben, $\mathrm{He}^+$ tritt allerdings nur in sehr geringer Intensität auf. Diese Zusammensetzung weicht erheblich von der Zusammensetzung der äußeren Ionosphäre bei 300 km Höhe ab, die vom Pioneer Venus Orbiter mit $n(\mathrm{H}^+)/n(\mathrm{O}^+) = 0.1$ and $n(\mathrm{He}^+)/n(\mathrm{O}^+) = 4 \times 10^{-3}$ bestimmt wurde. Diese Anreicherung von leichteren Ionen im entweichenden Plasma kann zwei Ursachen haben: der Pick-Up-Prozess ist entweder erst bei größeren Höhen wirksam oder die Beschleunigung erfolgt durch Polarisationsfelder, in denen leichtere Ionen höhere Geschwindigkeiten erreichen.

Das Verhältnis von Wasserstoff zu Sauerstoff im entweichenden Plasma ist ein kritischer Parameter für das Verständnis von Wassermangel und Oxidationszustand der Venusatmosphäre. Das hier gemessene Verhältnis von $Q(\mathrm{H}^+)/Q(\mathrm{O}^+) = 1.9$ gilt allerdings nur für Ionen und lässt sich mit Neutraldichtemodellen auf ein Abflussverhältnis von 2.2 für neutrale Atome und Ionen skalieren. Dies kommt dem stöchiometrischen Verhältnis von 2 für das Wassermolekül sehr nahe. Ein leichter Überschuss an $\mathrm{H}^+$-Ionen lässt sich durch Protonen des Sonnenwindes erklären, die in geringer Zahl die Magnetosphärengrenze durchdringen können. Dass der gegenwärtig gemessene Abfluss von Wasserstoff und Sauerstoff im stöchiometrischen Verhältnis von Wasser erfolgt, bedeutet, dass sich der Oxidationsgrad der Venusatmosphäre nach der Ausbildung eines Gleichgewichtszustandes nicht mehr geändert hat – im Gegensatz zu Mars, bei dem ein höherer Wasserstoff-Abfluss eine fortschreitende Oxidation nahelegt. Diese Beobachtungen sind im Einklang mit Messungen des Pioneer Venus Orbiters. Die absolute Abflussrate und ihre Bedeutung für die Entwicklung der Atmosphäre wird im weiteren Verlauf der Venus Express Mission bestimmt. Das erste Messjahr erlaubt jedoch bereits die Angabe einer unteren Grenze von $10^{25}$ Ionen/s für den Ionenabfluss vom gesamten Planeten, der Großteil dieses Abflusses erfolgt durch die Plasmaschicht im Schweif des Planeten.

Die beobachtete relative Häufigkeit von $\mathrm{He}^+$ im entweichenden Plasma von Venus ist überraschend hoch. Dies könnte wiederum durch die gegenüber Sauerstoff höhere Beschleunigungseffizienz in den Polarisationsfeldern verursacht sein. Im Vergleich zu Mars erzeugt die höhere Schwerkraft der Venus größere Druckgradienten in der Nachtatmosphäre. Dies kann zu entsprechend stärkeren Polarisationsfeldern führen. Während also die höhere Schwerkraft einen thermischen Abfluss aller Atome und Ionen erschwert, scheint sie über die Polarisationsfelder einen Abfluss der leichteren Ionen zu fördern. Das wichtigste Ergebnis dieser Beobachtungen ist allerdings der Nachweis eines noch heute wesentlichen Ionenabflusses durch den Plasmaschweif von Venus. Weitere Beobachtungen im Verlaufe der Mission werden es erlauben, die Abhängigkeit des Abflusses von der solaren Aktivität und damit seine Bedeutung für die Geschichte des Wassers auf Venus zu bestimmen.

**Planetenoberfläche**

Venus Express konnte zum ersten Mal unter Ausnutzung des spektralen Fensters bei einem $\mu$m Wellenlänge die Temperatur der Planetennachtseite kartieren. Speziell nimmt VIRTIS ein Mosaik der Südhemisphäre auf und zwar während des von der Apoapsis wegführenden Teils des Orbits. VMC hingegen schießt Nahaufnahmen der Äquatorregion, wenn sich die Raumsonde in der Ekliptikebene befindet. So wird eine Verunreinigung durch Streulicht verhindert. Abb. 115 zeigt ein thermisches Mosaik der Äquatorregion, das VMC während der nominalen Mission erstellt hat. Die Helligkeitskontraste in diesen Aufnahmen der Nachtseite haben verschiedene Ursachen. Neben der Oberflächentemperatur tragen zu einem geringeren Grade auch das Emissionsvermögen der Oberfläche sowie die Durchlässigkeit der Wolkendecke bei. Diese beiden zusätzlichen Effekte müssen erst herausgerechnet werden. Man nimmt im Allgemeinen an, dass sich die Oberfläche im thermischen Gleichgewicht mit der Atmosphäre befindet. Dann folgt die Temperatur der Topographie und nimmt mit der Höhe gemäß dem atmosphärischen Temperaturgradienten ab. Abb. 115 zeigt eine Temperaturkarte, in der die wesentlichen Elemente der Oberflächenreliefs klar zu erkennen sind, obwohl die Auflösung aufgrund von Mehrfachreflektionen in der dichten Atmosphäre wohl nicht mehr als 50 km beträgt. Die Beobachtungen decken die Hinemoa Planitia sowie die Beta- und die Phöberegion ab. An den Ostflanken der Phöberegion sind bereits einige Venera und Pioneer Forschungssatelliten im Zeitraum von 1970 bis 1980 gelandet.

Das Hauptziel der thermischen Karten ist es, aktive Vulkane aufzuspüren und nach Korrelationen zwischen dem Emissionsvermögen der Oberfläche und der vom Magellan Radar erfassten Geologie zu suchen. Die Interpretation dieser Karten stellt eine echte Herausforderung dar, da die Oberfläche ja von einer dicken Wolkendecke mit einer Opazität von 20 bis 40 verschleiert wird.

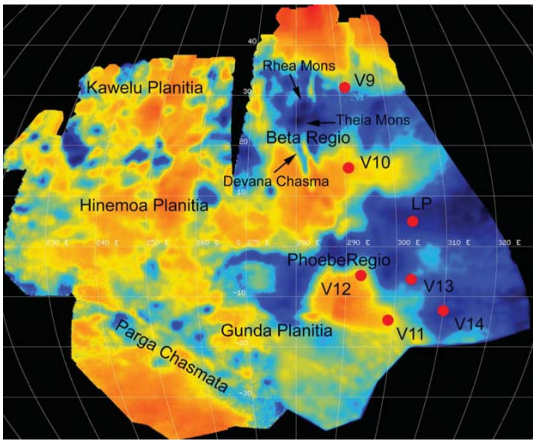


Abb. 115: Temperaturkarte um die Beta- und Phöbe-Gebiete sowie der Hinemoa Planitia. Die Temperaturen basieren auf VMC-Daten. Rote Punkte zeigen die Landestellen der Venera-Missionen (V-9,V-14) und der Pioneer-Venus-Large-Probe. Die Farbkodierung gibt die gemessene Helligkeit wieder.

Die nominale Kernmission hat gezeigt, dass es sich bei Venus Express um eine gelungene Kombination aus einer flexiblen Raumsonde mit einer leistungsfähigen Payload und einer effektiven Bodenkontrolle und Auswertung handelt. Die erste Missionsverlängerung wurde bis zum Mai 2009 genehmigt. Diese zusätzliche Zeit wird es erlauben, die räumliche und zeitliche Abdeckung des Planeten zu verbessern und die bisher entdeckten Phänomene detaillierter zu untersuchen. Neue Arten des Raumsondenbetriebs werden ebenfalls zur Anwendung kommen. So wird man etwa die Instrumente im "Spot-pointing"-Betrieb möglichst lange auf einen ausgewählten Punkt ausrichten, um diesen über einen längeren Zeitraum und unter verschiedenen Winkeln zu beobachten. Der Nadir-Pendel-Betrieb erlaubt es, die Dauer der Beobachtungen auf der Tagseite auszudehnen und dabei gleichzeitig die thermischen Toleranzen einzuhalten. Im July und August 2008 wird die Periapsis von 250 bis 350 km auf 180 bis 280 km reduziert, so dass ASPERA und MAG Plasma und Magnetfeld in einer geringeren Höhe untersuchen können.

## *Highlight:*

## Venus Express Highlights

Venus Express is the first European (ESA) mission to the planet Venus. Its main science goal is to carry out a global survey of the atmosphere, the plasma environment, and the surface of Venus from orbit. The spacecraft, based on the Mars Express bus modified for the conditions at Venus, provides a versatile platform for nadir and limb observations as well as solar, stellar, and radio occultation. In April 2006 Venus Express was inserted in an elliptical polar orbit around Venus with a pericentre height of about 250 km and an apocentre distance of roughly 66,000 km and an orbital period of 24 hours. The nominal mission lasted from 4 June 2006 until 2 October 2007, which corresponds to about two Venus sidereal days.

The payload consists of seven experiments. It includes a powerful suite of remote sensing imagers and spectrometers, instruments for in-situ investigation of the circumplanetary plasma and magnetic field, and a radio science experiment. MPS is deeply involved in the Venus Express programme. Venus Monitoring Camera (VMC) – the PI instrument – studies the cloud morphology and dynamics of the Venus atmosphere and contributes to the thermal mapping of the surface. These investigations are complemented by a scientific participation in the imaging spectrometer VIRTIS experiment. MPS was involved in the hardware manufacturing and takes part in the science investigations with the Analyzer of Space Plasmas and Energetic Atoms (ASPERA-4) experiment. In addition, MPS provides scientific support to ESA coordinating scientific observations and planning.

### Cloud Morphology and Dynamics

The spectro-imaging instruments in the Venus Express payload use the highly eccentric polar orbit of the satellite to investigate the Venus cloud layer in the spectral range from UV to thermal IR in unprecedented detail at all latitudes and local solar times with spatial resolution ranging from about 50 km at the apocentre to a few hundred meters at pericentre. Multispectral imaging provides for the first time an opportunity to reconstruct the global cloud morphology in 3-D. Also limb observations and stellar/solar occultation techniques allow the instruments to reveal the vertical structure of the upper haze. Fig. 109 shows a synthetic view of the planet produced by combining the VMC UV image on the day side with the VIRTIS image taken in the 1.7 $\mu$m spectral transparency window on the night side. The UV markings are produced by inhomogenities in the horizontal and vertical distribution of an unknown absorber in the upper cloud layer, their morphology indicating variations in the dynamic state at about 70 km altitude. At low latitudes ($< 40°$S) the mottled and patchy cloud pattern suggests the significant role of convection in the vicinity of the sub-solar point, where a large fraction of the solar energy is deposited in the upper cloud layer (55 – 65 km). Further towards the pole, mottled clouds give way to streaky features, indicating a transition to a more regular quasi-laminar flow in the mid-latitudes. The mid-latitudes (50 – 70° S) are dominated by a bright, almost featureless band, implying the presence of a large amount of purely scattering aerosol that masks the UV absorber. Circular and spiral dark features a few hundred kilometers across appear in the polar regions (see Fig. 109).

The brightness in the middle and high latitudes shows remarkable variability on a daily time scale. This indicates vigorous dynamical and microphysical processes like nucleation and coagulation that change the upper cloud opacity.

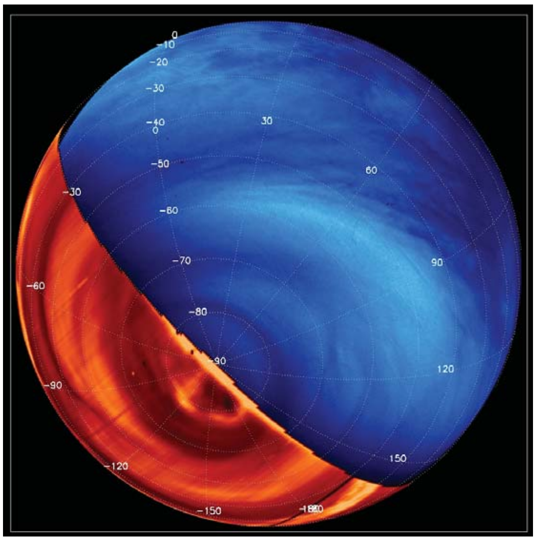

Fig. 109: False colour image of the Venus southern hemisphere composed of a VMC UV image on the day side (blue) and a VIRTIS near-IR image in the 1.7 $\mu m$ spectral transparency window on the night side (red).

The near-IR part of the image in Fig. 109 shows emission leaking from the hot lower atmosphere (about 35 km) through the spectral transparency window at 1.7 $\mu$m on the night side. Here the contrasts mark spatial variations of the opacity of the main cloud deck at roughly 50 – 55 km altitude. Brightness variations by about a factor of 10 roughly correspond to opacity variations between 20 and 40. The opacity contrast is even higher in the 1.7 $\mu$m spectral window. The cloud morphology revealed by Venus Express imaging apparently has a global vortex-like organization. Day-side UV and night-side near-IR observations imply that this pattern covers the whole southern hemisphere and persists at least down to the cloud bottom (about 50 km). The comparison with earlier observations in the northern hemisphere suggests that the global cloud patterns are remarkable symmetric with respect to the equator. Moreover, the planetary vortex on Venus has some striking morphological similarities to the hurricanes on Earth, although the scales and driving forces are quite different in these two cases. The highly eccentric orbit of Venus Express allows the imaging instruments to zoom in certain regions and phenomena and to put high resolution images in a global context. Fig. 110 shows examples of meso- and small-scale cloud morphology seen in the VMC UV and VIRTIS near-IR images.

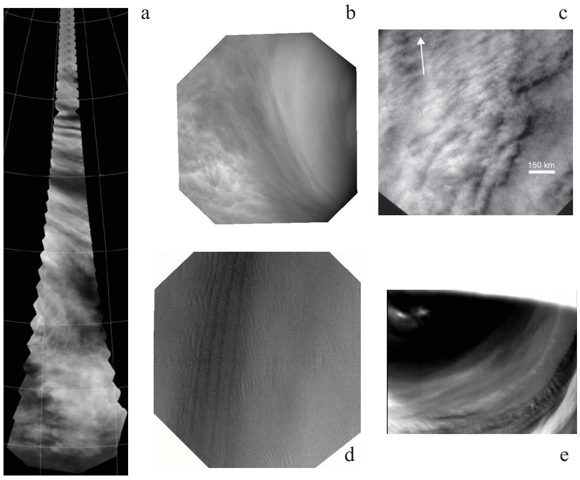

Fig. 110: Meso- and small-scale cloud morphology. A: A mosaic composed of VMC UV images taken during pericentre pass in orbit no. 261. B: VMC UV image of the mid-latitude transition region. C: VMC high resolution UV image of the convective clouds at low latitudes. D: Waves in the polar region ($\sim$ 70°N) captured by the VMC UV channel. E: Mid-latitude waves in the deep cloud seen by VIRTIS in the near-IR.

Fig. 110A and Fig. 110B show the details of the transition from patchy clouds at low latitudes to streaky features in middle latitudes which occurs between 40° and 50° south. The fine structure of the convective clouds at low latitudes close to the sub-solar point is shown in Fig. 110C. The imaging instruments observed a variety of waves. In the polar regions, VMC detected long straight regular features that seemed to induce short waves nearby as shown in Fig. 110D. The waves associated with the spiral arms of the global vortex were seen by VIRTIS in the deep cloud (see Fig. 110E). VIRTIS imaging in the near-IR $CO_2$ absorption bands, whose relative depth is proportional to the cloud top pressure, provides an opportunity to map the cloud top altitude directly all over the globe. Fig. 111 shows a VMC UV image with an overlaid colour mosaic of the cloud top altitude derived from simultaneous VIRTIS measurements in the 1.6 $\mu$m $CO_2$ band. The cloud top in the low- and mid-latitudes is located at roughly 70 km. It begins descending at about 55° south and sinks as deep as 65 km in the vortex eye. Thus the cloud top altitude varies by more than a scale height over the planet. Surprisingly, the sharp outer boundary of the UV bright band is not evident in the cloud top maps, implying that both UV dark low latitude and bright mid-latitude clouds are located at about the same altitude level.

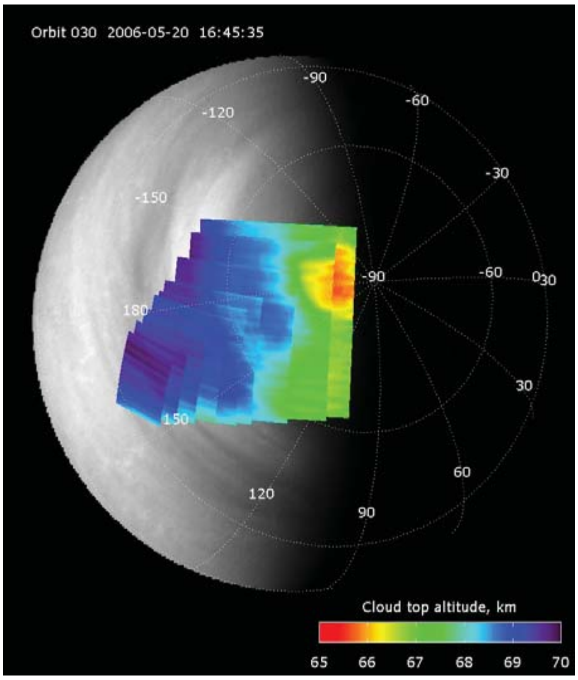


Fig. 111: Altimetry of the cloud tops. The colour mosaic of the cloud top altitude derived from VIRTIS spectral imaging in the near-IR $CO_2$ bands is overplotted on a simultaneously captured VMC UV image.

Early observations and models established that the Venus atmosphere has at least two dynamical regimes. The troposphere (0 – 60 km) and lower mesosphere up to about 80 km are in the state of super-rotation: retrograde almost purely zonal motion with a wind speed that peaks at the cloud top and decreases towards the surface and above the clouds. The thermosphere (100 – 200 km) is involved in a global day-to-night circulation driven by temperature differences between the sub-solar and anti-solar points. Spectro-imaging instruments onboard Venus Express observed atmospheric motions at altitudes from the cloud base ($\approx$ 50 km) up to the lower mesosphere (about 140 km). The wind speeds are derived from tracking the motions of cloud features. Fig. 112 shows the latitude profile of zonal wind at several altitudes derived from VIRTIS and VMC imaging. At all heights the wind speeds within the cloud deck remain almost constant with latitude below 50° south, but quickly fade out poleward of this latitude. Interestingly, this boundary coincides with the transition in cloud morphology (see Fig. 109). The comparison to the thermal wind derived from the VIRTIS temperature sounding indicates that the cyclostrophic approximation works quite well, at least in the upper cloud region in middle and high latitudes (see Fig. 112). Preliminary studies suggest that zonal winds have a minimum in the late morning, increasing in the afternoon. The meridional winds are much weaker (0 – 20 m/s) and more difficult to measure. They tend to increase from the equator to mid-latitudes where the meridional wind speed reaches a maximum and then decreases and even inverts its direction near the pole.

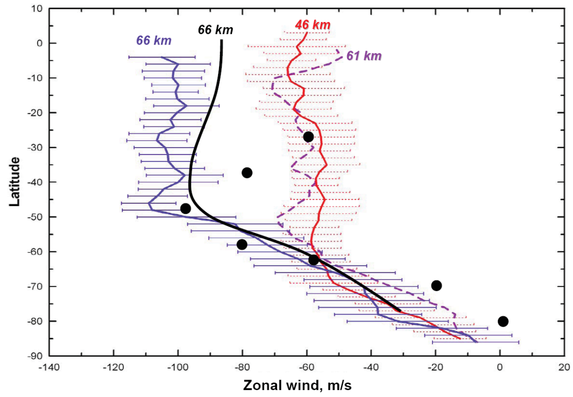


Fig. 112: Mean latitude profiles of the zonal wind speed in the southern hemisphere derived from VIRTIS images (blue: UV, 380 nm, day side; purple: near-IR, 980 nm, day side; red: near-IR, 1.74 $\mu$m, night side) and VMC UV images (365 nm, black curve). Error bars for the purple and black profiles are similar to those of the blue one. Figures on the curves give the altitude with 2 – 3 km accuracy. Black dots show cyclostrophic wind calculations for roughly 66 km altitude based on the VIRTIS temperature sounding.

## Plasma Environment

Venus has no internal magnetic field. The interaction of the solar wind with the planet therefore results in the formation of an induced magnetosphere. In the induced magnetosphere the solar wind energy may be transfered to the planetary ions of the upper atmosphere resulting in acceleration, escape and loss. Therefore the investigation of the interaction processes is crucially important for understanding the evolution of the atmosphere. Venus Express investigates the circumplanetary plasma environment by means of three techniques. The ASPERA-4 experiment (Analyzer of Space Plasmas and Energetic Atoms) measures in-situ fluxes of energetic neutral atoms, ions and electrons. Venus Express measurements are taken at solar minimum, thus complement-ing the Pioneer Venus plasma studies that were acquired during solar maximum.

Venus Express passes through different regions and boundaries, namely bow shock, magnetosheath, and induced magnetosphere boundary, formed by interaction of the solar wind with the planet (see Fig. 113), their boundaries clearly identified in the magnetic field and plasma measurements. The ASPERA-4 experiment has established for the first time the composition of escaping planetary ions. At Venus, ion acceleration is produced by three mechanisms: by ion pick-up (that is, by acceleration in the convection electric field), by instabilities at the induced magnetosphere boundary resulting in detached plasma clouds, and by polarization electric fields at low altitudes in the night-side ionosphere where the field is nearly radial. ASPERA-4 observed two different populations of the accelerated planetary ions, namely ions escaping through the plasma sheet and ions escaping through the induced magnetosphere boundary layer. The energy distributions of these two populations are different. The ratio of the $O^+$/$He^+$/$H^+$ energies in the plasma sheet is about 4/2/1 (see Fig. 114c). The ion energy is therefore a function of mass, suggesting that ion pick-up is an acceleration mechanism in the plasma sheet, in general agreement with the previous simulations for $O^+$. However, ordinary pick-up would result in a 16/4/1 ratio. The difference may be due to species-dependent assimilation into the plasma flow.

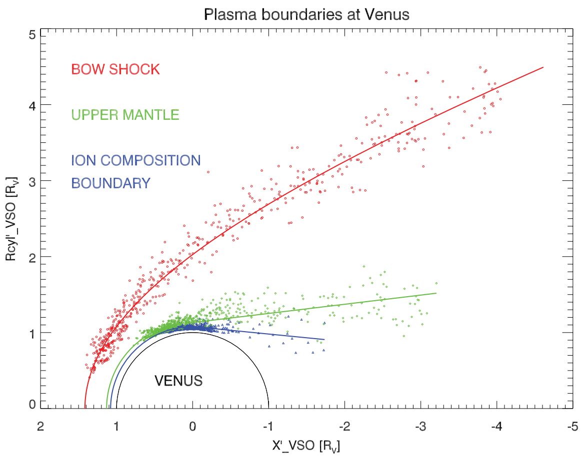


Fig. 113: Plasma boundary crossings observed by the ion and electron spectrometers on board Venus Express during the first year of the mission. Crossings of the bow shock (red), induced magnetospheric boundary (upper mantle, green) and ionopause (ion composition boundary, blue) and respective fits to the data. The horizontal axis is defined by the Venus-Sun line, the vertical axis by the distance from that line.

The ion escape considered here occurs through two main regions: the plasma sheet and a boundary layer at the induced magnetosphere boundary (see Fig. 113). As expected, the alignment of the plasma sheet plane and the ion energy are controlled by the electric field. All three species show similar spatial distributions, confirming that both $H^+$ and $He^+$ are indeed of planetary rather than solar-wind origin. The escape rates are obtained by integrating the measured flux. Although the spatial coverage is still not sufficient to obtain the total average escape rate, one can obtain reliable flux ratios. These are $Q(H^+)/Q(O^+) = 1.9$ and $Q(He^+)/Q(O^+) = 0.07$. The escaping plasma consists primarily of $H^+$ and $O^+$ ions with some admixture of $He^+$. The measured composition differs significantly from the plasma composition at the ionopause altitude (300 km) for solar minimum conditions, where the respective number-density ratios are $n(H^+)/n(O^+) = 0.1$ and $n(He^+)/n(O^+) = 4 \times 10^{-3}$. The observed enrichment of escaping plasma in light species may result from two causes. First, the ion pick-up process operating primarily at higher altitudes, 600 – 700 km, in which the densities of light species are increased with respect to heavier ions. Second, acceleration by the polarization electric field increasing the flux of lighter ions with respect to heavier, because lighter ions gain higher velocities for the same energy.

The ratio of the escape rates of hydrogen and oxygen is a critical parameter in understanding both the dryness and the oxidation state of the Venusian atmosphere. The measured ratios concern only ions and do not include the escape of the respective atoms. Scaling the measured ratio $Q(H^+)/Q(O^+) = 1.9$ to account for the neutral losses, we arrive at a ratio for the total (neutral atoms plus ions) loss of 2.2, very close to the stoichiometric value of 2 for the water molecule. Some excess of $H^+$ could be due to solar wind protons, which may penetrate through the induced magnetosphere boundary in small amounts and contribute to the measured H1 flux in the boundary layer. That the present escape of hydrogen and oxygen through the wake takes place in the stoichiometric ratio of water implies that the atmosphere of Venus did not change its oxidation state after steady state conditions had been reached, in contrast with that of Mars. This result is thus consistent with the suggestion from atmospheric and ionospheric observations by the Pioneer Venus orbiter that Venus loses the constituents of water in a ratio that maintains the system's oxidation state. The absolute escape rates, including the implications for long-term water evolution, will be determined later. However, the initial analysis gives a reliable lower limit of 1025 $s^{-1}$ for the escape of $H^+$, most of which occurs through the plasma wake.

The observed relative abundance of $He^+$ in the escaping plasma from Venus is surprisingly high. This may

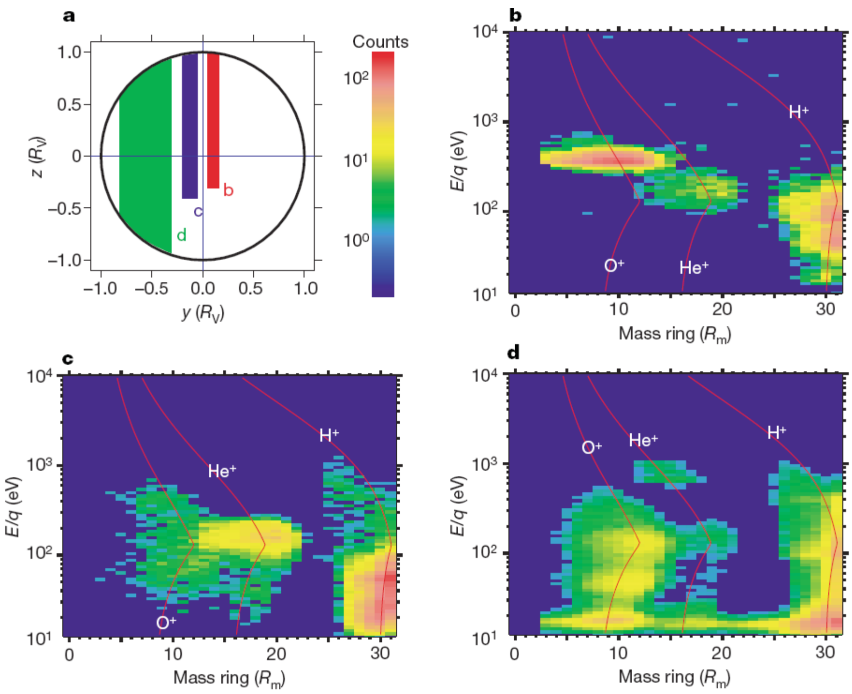


Fig. 114: Composition and energy distribution of the escaping plasma. a: Geometry of the three spatial regions where the energy-mass matrixes were collected in the Vse (Venus-solar-electrical) coordinate system. b-d: The energy-mass matrixes accumulated over 33 orbits during the period from May 18 through 30 December 2006 for the +Y lobe (b),-Y lobe(c) and IMB layer (d). Vertical axes are energy/charge (E/q) ratio, the horizontal axes are the position of the ion impact on the detector (a sensor mass ring, $R_m$), and the colour codes the counts that were accumulated over all directions and averaged over occurrences. The red lines represent constant mass.

be due to the more effective acceleration caused by the polarization field. The higher pressure gradients associated with the stronger gravitational field on Venus results in a higher polarization field that operates over larger distances at Venus than at Mars. Thus, whereas the stronger gravitational field of Venus reduces the Jeans escape of the heavier main constituents of the atmosphere, almost paradoxically it facilitates the loss of the lighter species. The main result of these observations, however, is the establishment of potentially important ion escape from present-day Venus through the plasma wake region. Further observations in this region as the solar cycle progresses will establish the variability of these escape rates and will improve our ability to infer the history of Venus's water.

## Surface Investigations

For the first time Venus Express has carried out systematic thermal mapping of the surface in the 1 $\mu$m transparency window on the night side. VIRTIS acquires mosaics of the Southern hemisphere from apocentre and the ascending branch of the orbit. VMC takes close-up images of the equatorial region when the spacecraft is in eclipse, so the observations are not polluted by stray light. Fig. 115 shows a thermal mosaic of the equatorial regions obtained by VMC during the nominal mission. The brightness contrasts are caused by variations in surface temperature and to lesser extent its emissivity, as well as a large contribution from the overlying cloud opacity, which must be removed to reveal the surface temperature. The surface is assumed to be in thermal equilibrium with the atmosphere so its temperature follows the topography, with higher regions progressively colder according to the atmospheric lapse rate. Thus major relief features are clearly recognized in the map in Fig. 115, although the spatial resolution is severely degraded by multiple scattering in the thick atmosphere to about 50 km at best. The observations covered Hinemoa Planitia and Beta and Phoebe Regio, the eastern flanks of which were visited by several Venera and Pioneer Venus descent probes between 1970 and 1980.

The main goals of surface thermal mapping are to search for active volcanism and to identify correlations between emissivity anomalies and the geological units seen in the Magellan radar data. Interpretation of the thermal maps like those shown in Fig. 115 is a challenging task since the surface is observed through the cloud deck with an opacity of about 20 – 40.

The nominal mission demonstrated that Venus Ex-

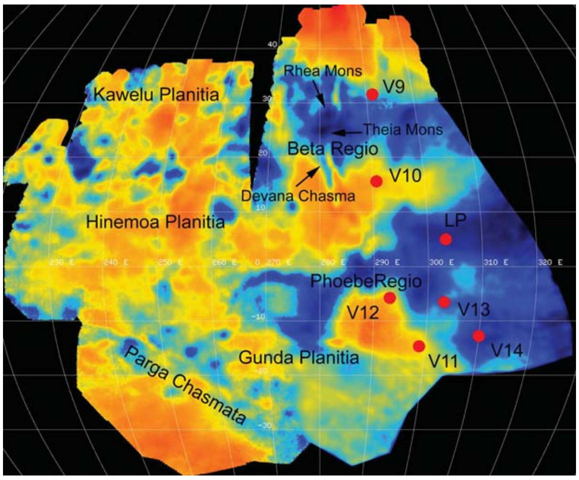


Fig. 115: VMC thermal map of Beta and Phoebe regions and Hinemoa Planitia. Red dots show Venera (V-9,-14) and Pioneer Venus Large Probe (LP) landing sites. Colour codes correspond to the measured brightness.

press is an excellent combination of a flexible spacecraft, capable payload, and efficient ground segment. The first mission extension has been approved until May 2009, allowing Venus Express to extend the spatial and temporal coverage of the planet to carry out detailed observations of the phenomena discovered during the nominal mission. New modes of the spacecraft science operations can also be implemented, such as spot pointing to keep a selected target in the field of view of the instruments for longer time and to observe it at a varying angle. When applied to limb tracking this provides longer observations of the limb. Finally, a nadir "pendulum" mode allows the instruments to extend the duration of dayside observations while staying within allowed thermal conditions. In July – August 2008 the pericentre altitude will be reduced from 250 – 350 km to 180 – 280 km. This will allow ASPERA-4 and MAG to continue plasma and magnetic field investigations at lower altitude.

(D. V. Titov, W. J. Markiewicz, M. Fraenz, J. Woch, N. Krupp, E. Dubinin, R. Moissl, C. Martinecz, A. Piccialli, H. U. Keller, and U. Christensen)

## **Planeten, ihre natürlichen Satelliten und Kometen – Übersicht der Projekte /**
## Planets, their moons and comets – overview of projects

Dargestellt ist die Dauer der verschiedenen Projektphasen (farbcodiert) einzelner Instrumente. Kurze Beschreibungen findet man in den einzelnen Jahres- bzw. Tätigkeitsberichten des MPS.

The different project phases of each instruments are shown colour-coded. Short descriptions of these instruments can be found in the annual reports of the MPS.

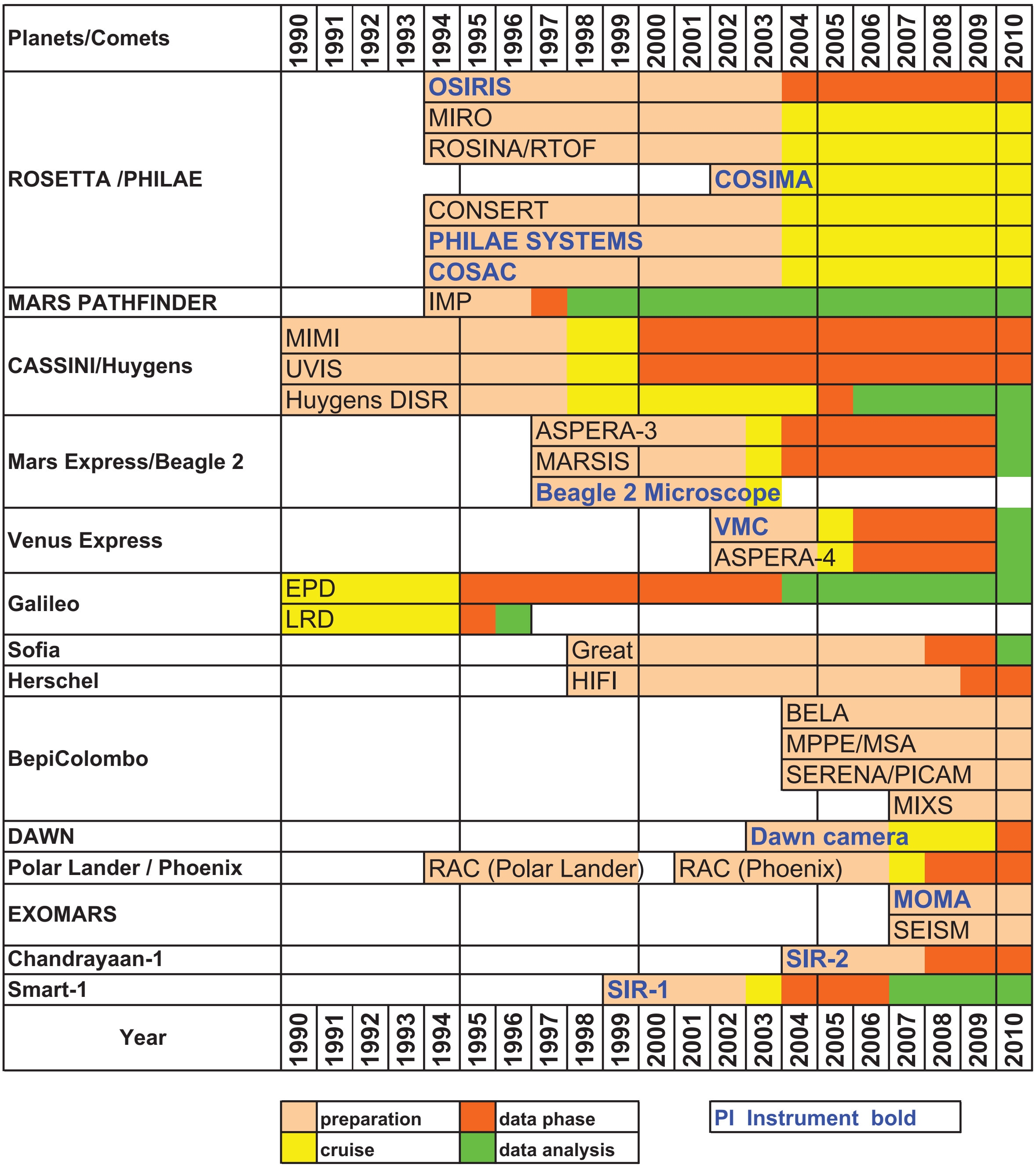

## Wissenschaftliche Einzelberichte/
*Individual scientific reports*

(nur in Englisch)

## Planetary interiors

### Dipole moment scaling for planetary dynamos

The magnetic dipole moment is the most fundamental observable property of planetary magnetic fields. We have extended our previous scaling analysis (Christensen and Aubert, 2006), which dealt with internal dynamo properties, and derived scaling laws for the dipole moment in rotating convection-driven numerical dynamo models. We have used results from 145 dynamo models, mostly our own with some additions from the literature, that cover a variety of boundary conditions, heating modes, and a wide section of parameter space. We show that the time-averaged dipole moment depends on the convective buoyancy flux $F$. Two distinct regimes are found above the critical magnetic Reynolds number for onset of dynamo action. In the first regime the external magnetic field is dipole-dominant, whereas at larger buoyancy flux or slower rotation the external field is dominated by higher multipoles, and the dipole moment is reduced by a factor of 10 or more relative to the dipolar regime. For dynamos driven by inner core buoyancy sources, the dipole moment $M$ increases like $M \sim F^{1/3}$ in the dipolar regime. Reversing dipolar dynamos tend to cluster near the multipolar transition, which is shown to depend on a local Rossby number parameter (Fig. 116). The geodynamo lies close to this transition, suggesting an explanation for polarity reversals and the possibility of a weak dipole early in Earth history. Internally-heated dynamos generate smaller dipole moments overall and show a gradual transition from dipolar to multipolar states. Our scaling yields order-of-magnitude agreement with the dipole moments of Earth, Jupiter, Saturn, Uranus, Neptune, and Ganymede. For Mercury it predicts a multipolar-type dynamo; see page 114 for a specific model explaining the observed properties of Mercury's field (Olson and Christensen, 2006).

(U. Christensen in collaboration with P. Olson (Baltimore))

### Magnetic structures in Earth-like dynamo simulations

Visualizing the complex action in simulations of planetary dynamo regions is notoriously difficult. Fieldlines are a well established concept for visualizing the magnetic field morphology. However, choosing the key fieldlines that highlight the most important features proves difficult. Also, using fieldlines to show dynamical changes is not straightforward since there is no clear concept for the evolution of a particular fieldline.

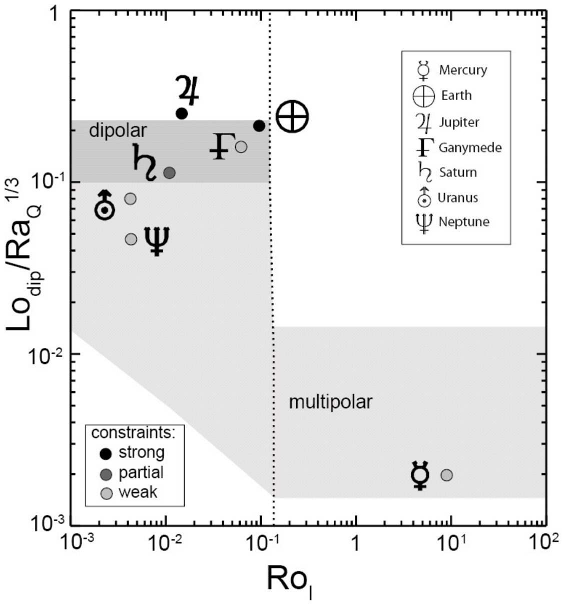


Fig. 116: Dimensionless planetary dipole moment, normalized by Rayleigh number, versus the local Rossby number. The shading (dipolar dark and multipolar light grey) indicates the predicted dipole moment in the different regimes. Symbols for planets are shaded according to the strength of the constraints on the control parameters $Ra_Q$ and $Ro_l$.

Julien Aubert has developed a Matlab tool that tries to overcome these deficiencies, the Dynamical Magnetic Fieldline Imager (DMFI). We have used this tool to analyze three different numerical dynamo simulations that were geared to simulate Earth's dynamo and included magnetic field reversals and excursions. DMFI preforms three main steps: 1) In a first step DMFI draws fieldlines through, for example, 10 predefined anchor points until they hit the outer boundary of the dynamo region. 2) DMFI then determines the points of maximum magnetic energy along each of these lines. 3) These points are used as the new fieldline anchor points to illustrate the next evolution step of the numerical simulation. Steps 2) and 3) are repeated over and over to visualize the selected dynamo sequence. After some cycles the fieldlines have converged to depict the most active dynamo regions.

DMFI helped us to identify three main magnetic field features that were present in all three different models analyzed. Magnetic cyclones and anticyclones are correlated with convective flow vortices rotating in prograde and retrograde direction, respectively. Magnetic anticyclones are the main players in establishing the mean dipole field while magnetic cyclones are mostly diffusive features. The third important structure type are magnetic upwellings that seem to be connected to convective plumes. Magnetic upwellings are attached to the inner core and preferably rise inside the tangent cylinder, an imaginary cylinder touching the inner core equator, or at the equatorial region. They can create a significant amount of inverse magnetic field that annihilates the normal direction dipole field. This paves the road for field reversals and excursions. A significant braking of the equatorial flow symmetry with strong upwellings rising either in the northern or in the southern hemisphere seems to be a necessary prerequisite. The upwellings have to be strong enough and persistent enough to kill off the normal polarity dipole. Alternatively, two or more upwellings can team up to do the job. Both scenarios are unlikely which may explain the rareness of reversals.

Fig. 117 shows two magnetic upwellings somewhat north of the equator. They have already lead to a large dipole tilt, a reversal will follow. The north-south stretching fieldlines seen to the left of the inner core in the side view form a magnetic anticyclone.

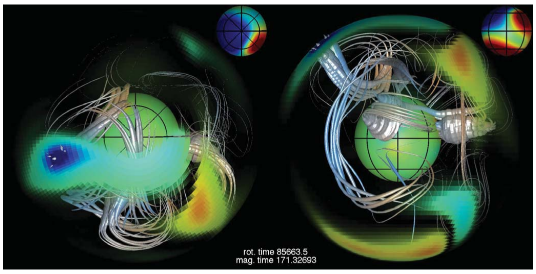


Fig. 117: Magnetic fieldlines visualizing the dominant magnetic structures during a field reversal. North-polar and side view are shown at left and right, respectively. The inner core is represented by the central sphere. Colour coded radial magnetic field is shown on the inner core, the outer boundary (depicting only the dominant field patches), and a level representing Earth's surface in the upper right corner of both panels.

(J. Wicht in collaboration with J. Aubert (IPG Paris) and J. Aurnou (UCLA))

### Magnetic field reversal statistics

Magnetic field reversals are particularly spectacular geomagnetic processes. The broader interest in reversals is based on the fact that the magnetic field strength is significantly reduced during these events. This bears potential health risks as well as an increased liability of electronical devises. Accessing the statistical properties of magnetic field reversals is therefore of prime interest.

More than 100 consecutive reversals are documented for Earth. We have chosen a simple but nevertheless fully self consistent convection driven dynamo model to simulate 140 numerical reversals. The Hurst measure $H$ indicates whether a statistical sequence contains a long-term memory ($0.6 \leq H \leq 1.0$), is Poissonian without any memory ($0.4 \leq H \leq 0.6$), or is chaotic ($0.0 \leq H \leq 0.4$).

Analysis of the paleomagnetic polarity interval record suggests that this sequence contains a long-term memory since $H$ typically exceeds 0.9. This result does not change significantly when shorter polarity intervals are neglected that may rather be excursions. The numerical model, on the other hand, is clearly Poissonian with Hurst measures around 0.5.

Dynamo simulations suggest that excursions and reversals go back to the same internal process, both being characterized by a particular low relative dipole strength. We have therefore included excursions in our analysis, not only assessing intervals between two consecutive reversals but also between two consecutive excursions or an excursion and a reversal. The mean duration of this new type of interval, that we call inter-event interval, is significantly decreased since longer stable polarity intervals are now interrupted by excursions. However, both interval types clearly follow a Poissonian distribution (see Fig. 118) and the Hurst measure is also very similar.

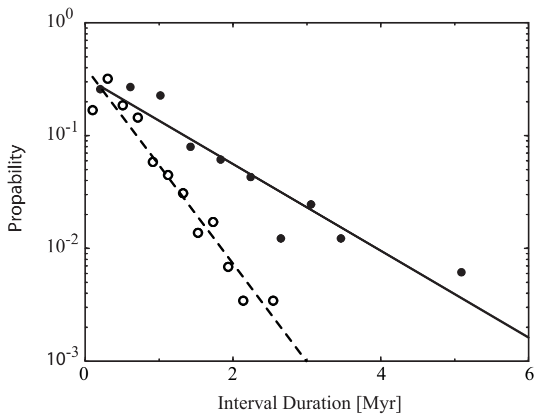


Fig. 118: Histogram of stable polarity interval and inter-event interval durations shown as solid and open symbols, respectively. Inter-event intervals are intervals between consecutive reversals and/or excursions. A Poisson distribution has been fitted in both cases and is shown as a solid and a dashed line, respectively. The goodness of fit is 20% for both with a mean reversal of roughly one per Myr. for polarity intervals and two per Myr. for inter-event intervals.

(J. Wicht in collaboration with A. Jonkers (University of Liverpool))

**Magnetic core-mantle coupling**

From geomagnetic field observations at or above the Earth's surface, the *rms* strength of the radial magnetic field component at the core-mantle boundary (CMB) is 0.31 mT at spherical harmonic degrees less than 13. The spatial spectrum of the CMB field is nearly white, excluding the dipole. An open question is at what spatial scale the magnetic power spectrum starts to drop off and what the total field strength including the small scales is. Observations of the Earth's nutation require dissipative core-mantle coupling, although the nature of this coupling is unknown. Magnetic coupling can occur when a thin layer of high electrical conductivity exists in the lowermost mantle, or at the top of the core when mechanically coupled to the mantle. In that case the nutation observations constrain the mean radial CMB field strength to 0.69 mT (Buffett, B.A., Mathews, P.M., Herring, T.A., J. Geophys. Res., 107, doi: 10.1029/2000JB000056, 2002), implying substantial magnetic energy at spherical harmonic degrees exceeding one hundred. Ohmic dissipation increases with the inverse square length scale of the magnetic field and an open question is, if such a field spectrum would imply an unreasonable amount of dissipation. We have addressed this question by analysing a numerical dynamo model whose spectrum is Earth-like at low harmonic degrees and whose magnetic Reynolds number matches the probable core value. When the model field is scaled to the present-day geomagnetic dipole, it predicts 0.7 – 1 TW of ohmic dissipation in the core, which is well within the plausible range. We conclude that electromagnetic core-mantle coupling by a field that contains substantial energy at short wavelength is a viable hypothesis.

(U. Christensen in collaboration with B. A. Buffett (Chicago))

**Torsional oscillation in dynamo simulations**

Earth's fast rotation and the low viscosity of liquid iron promote a particular dynamical state in Earth's liquid iron core that is called geostrophy. Geostrophy implies that flow variations in the direction of the planets rotation axis are minimized. The only motions where these variations truly vanish are the motions of concentric geostrophic cylinders that share the planets rotation axis as their common symmetry axis. These cylinders are coupled by inertial, viscous, and Lorentz forces, and the latter contribution is thought to dominate in Earth's core. The magnetic field line component perpendicular to the rotation axis couples the cylinders like torsional strings. Disturbances in the motion of one cylinder travel as one dimensional Alfvén waves towards the inner core and the core-mantle boundary along these strings. This effect may excite torsional eigen-oscillations that are thought to account for a good deal of the decadal magnetic field variations and have reportedly been identified in the geomagnetic field.

We have performed several dynamo simulations to explore whether similar features can be found in the numerical models (see Fig. 119). The Alfvén waves are indeed present when inertial and viscous forces are small. However, these waves where always quickly modified and strongly damped so that significant eigen-oscillations could never develop. Moreover, scaling analysis predict that the inertial forces may amount to 10% of the Lorentz forces in Earth's core (Christensen and Aubert, 2006). Our simulations show that the Alfvén waves then loose their significance and should not be identifiable in Earth's core. The interpretation of secular variation features in terms of core dynamics is indeed difficult and non-unique, and we suggest to explore alternative interpretations that take inertial effects into account.

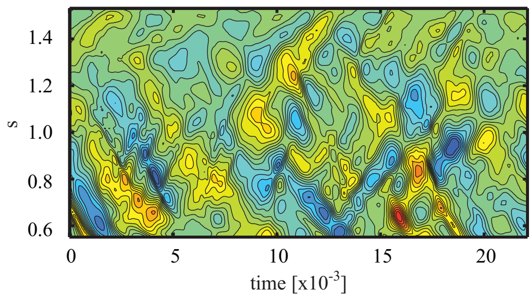


Fig. 119: Traveling Alfvén waves can clearly be identified in the variation of the motion of geostrophic cylinders. We show this flow variation between the inner core boundary (cylindrical radius s = 0.56) and close to the core-mantle boundary (s = 1.56) for a numerical model where viscous and inertial effects are small.

(J. Wicht and U. R. Christensen)

**Statistical properties of the multipole coefficients of the geomagnetic field**

The Earth has had a magnetic field for several billion years. The main component is the dipole, which is variable on all time scales from a few 100 yr and longer. A spectacular aspect of this variability are the sudden dipole polarity reversals, which occur on average every few $10^5$ yr.

The magnetic field is generated by induction processes in the fluid outer core of the Earth. Because of the non-linear interaction of the flow and the magnetic field, this dynamo action is a complex MHD problem. A self-consistent approach requires numerical solution of the MHD equations in a rotating and convecting spherical shell. The numerical dynamo models developed at the MPS exhibit many of the characteristics of the geomagnetic field.

The objective of the project is a systematic quantitative analysis of the output of these geodynamo models. To this end we extract the (first) multipole components of the magnetic field from the magnetohydrodynamical simulations of the geodynamo and subsequently compare them with analytical theory.

The stochastic differential equations for the mode coefficients lead to a Fokker-Planck equation for the probability distribution of the multipole coefficients, from which the statistical properties such as the mean square amplitudes, the autocorrelation functions, cross correlations, the mean reversal rates of the axial dipole etc. can be derived.

By comparing theory and numerical simulations we hope to gain insight into the inner working of the geodynamo, especially in the likelihood of polarity reservals.

(C. St-Jean-Leblanc, D. Schmitt, J. Wicht, and U. Christensen in collaboration with P. Hoyng (Utrecht))

**Double diffusive convection in planetary ion cores**

Thermal convection is considered as the main heat transport mechanism in planetary interiors. In the case of planetary cores, the heat required for driving convection in the liquid part of the core comes mainly from the secular cooling, latent heat release due to the solidification of the iron alloy, and possibly from radiogenic heat sources. The release of the compositionally light constituents at the inner core-outer core boundary due to solidification suggests that compositional heterogeneities may significantly contribute to the driving force for convection. Thus, both the thermal and the compositional components are important in powering the convection in planetary interiors. The different diffusivities of these two components, however, may lead to more complex and interesting convection patterns, especially when these components act in opposite direction. Such double diffusive convection (DDC) phenomena have been extensively analyzed in oceanography, magma chamber dynamics, and metallurgy.

In the case of planetary cores, thermo-chemical convection has been studied by using the concept of codensity, by combining thermal and compositional density variations into a single co-density variable, under the assumption of the same diffusivity for both the components. In order to give up this simplification we have modified our code to now solve for thermal and chemical variations with two separate equations. The code was first tested for the case of convection of an infinite Prandtl number incompressible fluid under the Boussinesq approximation for a range of buoyancy ratios and Lewis numbers ($Le$, ratio of thermal to compositional diffusivity). In these models, convection started as simple oscillations but more complex oscillation patterns were observed as $Le$ was increased. These complex oscillations yielded a steady state convection pattern with the further increase in $Le$.

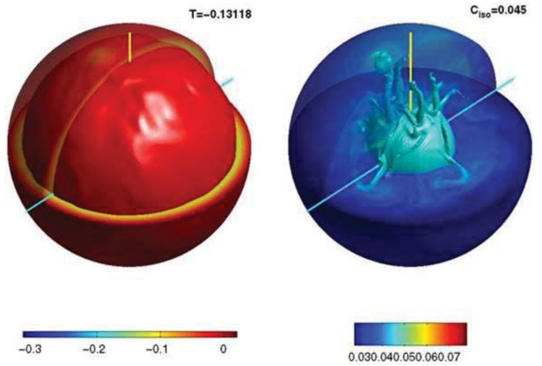


Fig. 120: Isosurfaces of thermal buoyancy (left) and chemical buoyancy (right) for numerical simulations of a planetary core dynamo. Thermal effects stabilize the outer part of the core, chemical effects drive convection in the deeper part. The chemical plumes are much narrower than comparable thermal features since the chemical diffusivity is an order of magnitude smaller here. The narrower plumes can more easily penetrate the outer part of the core where they may drive significant flows. This leads to a stronger magnetic field generation than in the simplifying co-density case where chemical and thermal components are assumed to have the same larger diffusivity.

Furthermore, we tested the code by reproducing the results of convection and magnetic field generation for the case of Mercury-like parameters, earlier studied by using co-density formulation. In this model, a sub-adiabatic CMB heat flow was assumed leading to the stable stratification in the upper part of the core and vigorous convection in the deeper part of the outer core. Next, we analyzed the effect of double-diffusive convection on the magnetic field generation for the same set of parameters but by taking compositional diffusivity an order of magnitude smaller than the thermal diffusivity and redistributing the net buoyancy flux into equivalent thermal and compositional buoyancy fluxes. The results are drastically different from those obtained for the equivalent co-density case. In the DDC model we observe generation of thin narrow plumes of light constituents penetrating into thermally stratified layer of the outer core (see Fig. 120). Long-term time averaged velocity and magnetic fields show that both quantities are significantly larger in the double-diffusive case. More examinations are needed to access whether the smallness of Mercury's magnetic field can still be explained by a stably stratified outer layer in this more realistic DDC scenario.

(J. Wicht and U. R. Christensen in collaboration with Ajay Manlik (National Geophysical Research Institute, Hyderabat, India))

## Terrestrial planets research – Mercury

### A dynamo model for Mercury

The magnitude of Mercury's global magnetic field at the planet's surface is only 1 % of the geomagnetic field strength. The field is large-scaled and probably dominated by the axial dipole, although the limited data obtained during the Mariner 10 flybys and the contribution of magnetospheric currents do not allow for a unique characterization of the internal field. An origin by an Earth-like dynamo appears doubtful, because the implied balance of Lorentz and Coriolis force inside Mercury's core should result in a field with 30 % of the geomagnetic field strength. We suggest a special type of dynamo that works deep in Mercury's fluid core below a stagnant layer. According to thermal evolution models the heat flux in Mercury's core is less than what can be conducted along an adiabatic temperature gradient. The models also predict the existence of a solid inner core. The rejection of sulphur associated with its growth would drive compositional convection. The combination of two sources of buoyancy leads to a deep unstable layer, while in the upper part of the fluid core the stabilizing thermal gradient dominates. For plausible values of the heat flow at the core-mantle boundary, the size of the inner core, and the sulphur concentration, we estimate that the unstable layer has 20 – 60 % of the outer core's thickness. Numerical models show that a dynamo operating in such a system generates a strong internal magnetic field that is dominated by small spatial scales (Fig. 121, top). The contribution of the dipole and the quadrupole are weak in the dynamo region, but in contrast to the small-scale components they vary less rapidly with time. The dynamo field diffuses through the stagnant layer, where its rapidly changing parts are strongly damped by the skin effect. The axisymmetric dipole and quadrupole components pass with some attenuation and dominate the field structure outside the core (Fig. 121, bottom). Non-axisymmetric modes are more strongly attenuated, even at low harmonic degree. In some models the dipole dominates the surface field, whereas in others the axial quadrupole may be stronger at some times. The field strength at the surface is 20 – 200 % of the observed strength for different models. Because of the suppression of high frequencies by the filtering effect, the surface field varies only on time scales of more than 1000 years. Future observations by space missions will allow to test the model predictions, such as the strong dominance of axisymmetric low-order field components and the lack of detectable secular variation on a decadal time scale (Christensen, 2006).

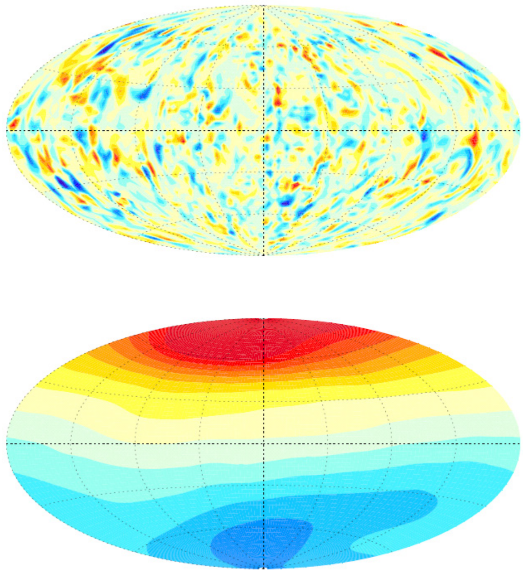

Fig. 121: Snapshot of the radial magnetic field at the upper end of the dynamo region (top) and at Mercury's surface (bottom). The contour steps are 50,000 nT for the interior field and 100 nT for the surface field.

(U. R. Christensen and J. Wicht)

### Driving Mercury's Dynamo

The knowledge about Mercury's core is scarce. The inner core size, the core temperature, the core sulfur content, all these key properties are largely unknown. Thermal evolution models suggest that the heat flux through the core-mantle boundary is likely sub-adiabatic since the planet has formed a thick lithosphere early in its history. This rules out thermal convection as the main driving force for Mercury's dynamo. Light elements released from a freezing inner core are an alternative source for powering convection and thereby the dynamo. We have calculated the power available to fuel the dynamo for different reasonable sulfur contents and core-mantle boundary (CMB) heat fluxes scanning all possible inner core sizes.

The prescribed CMB heat flux controls the inner core growth by limiting the associated latent heat release and therefore determines not only the available thermal but also the chemical power. The thermally stabilizing effect of the sub-adiabatic CMB heat flux causes the outer part of the core to be quasi stagnant, thereby limiting the available power. A scaling based on numerical dynamo simulations (Christensen *et al.*, 2006) allows to derive the Elsasser number and magnetic Reynolds number for the different models explored. These two quantities are measures for the magnetic field strength and the flow vigoure respectively (see Fig. 122). Planetary dynamo theory and numerical simulations suggest that the Elsasser number should be at least of order one and that the magnetic Reynolds number cannot be below 50. These conditions restrict the possible parameters for Mercury's interior. If, for example, Mercury's inner core radius amounts to more than 45% of the total core radius, the heat flux through the core-mantle boundary has to exceed $1\mathrm{mW/m^2}$ (see Fig. 122). Numerical simulations have shown (Christensen, 2006) that an Elsasser number of order one can be reconciled with the planets weak measured field strength.

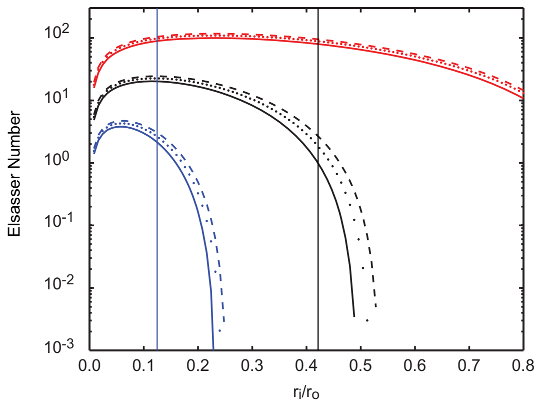


Fig. 122: Estimated Elsasser number for Mercury's convective core dynamo. Three different values for the core-mantle boundary heat flux ($0.1\mathrm{mW/m^2}$ in blue, $1\mathrm{mW/m^2}$ in black, and $10\mathrm{mW/m^2}$ in red) and three different sulfur weight fractions (1% as solid line, 2% as dotted line, and 3% as dashed line) are explored. The vertical lines mark relative inner core sizes that correspond to a magnetic Reynolds number of 50 beyond which dynamo action is deemed impossible.

(J. Wicht, U. R. Christensen, and M. Buske)

### Mercury's tidal Love number from laser altimetry

The BELA laser altimeter on board the BepiColombo MPO spacecraft will map the entire surface of Mercury and should in principle allow for the retrieval of the tidal elevation of order one meter and of the forced libration amplitude of order 40 arcseconds caused by solar gravitation. In the frame of our BELA MPS laser project funded by the German Aerospace Agency DLR, we created synthetic altimetry data and inverted them simultaneously for the long-wavelength topography, the amplitude of the forced libration $\phi_{\mathrm{lib}}$, and the tidal Love number $h_2$. The precise values of $\phi_{\mathrm{lib}}$ and $h_2$ reveal information on the interior structure of Mercury such as the thickness of the liquid outer core. In previous simulations, we assumed an idealized scenario with MPO's orbit in resonance with Mercury's rotation and with uniform data acquisition from all parts of the orbit. We found that the Love number can be recovered within a few percent error. Recently, we have studied the more realistic case of a non-resonant and elliptical MPO orbit with the restriction that no measurements are possible at altitudes above 1000 km due to an insufficient number of photons returned from Mercury's surface to the receiver of BELA. With proper weighting of the data set, such that a uniform spatial coverage of Mercury's surface and a uniform temporal coverage of the tidal period is simulated, the Love number can still be extracted with high accuracy. In particular, we have characterized how much the uncertainties $\Delta h_2$ and $\Delta\phi_{\mathrm{lib}}$ are decreasing with the maximum degree of inversion in the spherical harmonic expansion of the static topography which we apply in our simulations (c.f. Fig. 123). We find that under realistic conditions and assuming realistic instrumental uncertainties and realistic computer resources, it should be feasible to test the most recent models on the interior structure of Mercury from an analysis of BepiColombo laser altimeter data records (Koch, Christensen and Kallenbach, 2008). In turn, the simulations have helped us to define requirements for the BELA instrument design which is now approaching maturity for implementation in the hardware phases C and D.

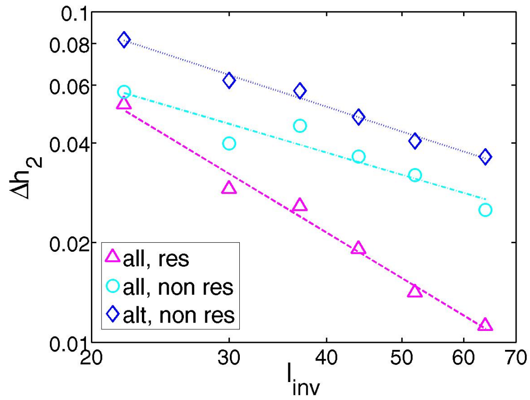


Fig. 123: Errors of the Love number vs. maximum harmonic degree of inversion for a resonant spacecraft orbit (triangles), a non-resonant orbit (squares), and a non-resonant orbit with data limited to spacecraft altitudes up to 1000 km (0diamonds). The lines represent the results of linear regressions.

(C. Koch, U. R. Christensen, and R. Kallenbach)

## Terrestrial planets research – Venus

### Venus Express – the first European mission to planet Venus

Venus Express is the first ESA mission devoted to global investigation of the atmosphere, the plasma environment, and the surface of Venus (Fig. 124). The spacecraft that carries seven instruments onboard was launched from the Baikonur Cosmodrome in Kazakhstan by the Russian Sojuz-Fregat launcher on 9 November 2005. On 11 April 2006 Venus Express was successfully inserted into orbit and started observations. The nominal mission ended in October 2007. Now Venus Express is in extended mission that will last till May 2009. MPS is deeply involved in many aspects of the mission: scientific support of the mission planning and operations, procurement of the Venus Monitoring Camera (VMC) instrument and its operations (PI experiment), hardware participation in the ASPERA-4 experiment, scientific analysis of the data from VMC, ASPERA, and VIRTIS experiments. Also, MPS participates in the development of the future strategy for Venus exploration. D. Titov was the member of the Steering Committee of the European Venus Explorer proposal for the ESA Cosmic Vision Programme and is the member of the Science and Technology Definition Team of the future NASA Flagship mission to Venus.

(D. Titov)

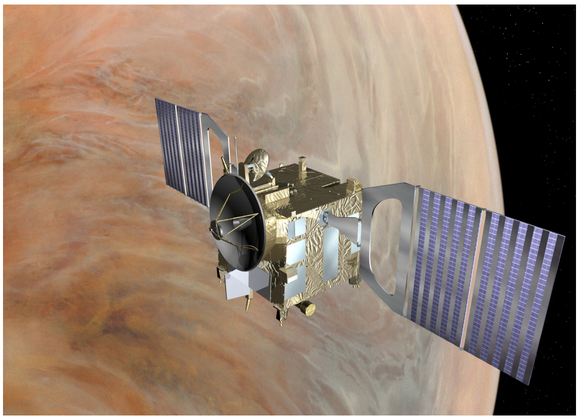

Fig. 124: An artist's view of Venus Express in orbit (credit ESA).

### Venus Express scientific support

Venus Express science planning is based on synergy between experiments to provide complete coverage of science themes and fulfill the mission goals. Planning of the orbital operations is a complex process that takes into account requests from all experiments, operational constraints and mission resources. A concept of "science cases" – typical observations in orbit – was developed and used to build the Science Activity Plan (SAP) for both nominal and extended mission (June 2006 – May 2009), which is currently being successfully implemented. The versatile spacecraft allows us to combine pericentre nadir observations, off-pericentre and apocentre mosaics, limb observations, solar, stellar and Earth occultation. The observation timelines are developed in a coordinated way to optimize the payload activity, maximize the overall mission science return, and to fit into the available mission budgets.

(D. Titov)

### Morphology of Venus in the polar region

VMC and VIRTIS experiments onboard Venus Express deliver highly complementary imaging and spectro-imaging observations of Venus in the spectral range from UV to thermal IR. The polar orbit of Venus Express is very well suited for investigation of the southern hemisphere. Fig. 125 shows global views of the southern hemisphere taken by the UV channel of VMC from a distance of about 60,000 km. A bright mid-latitude band separates darker low latitudes from the polar regions in which global streaks indicate atmospheric parcels spiraling towards the pole. The polar vortex originally discovered at thermal infrared wavelengths (Fig. 126), is now observed by VMC as the dark oval UV feature (Figs. 125a, 126). Correlation of the VMC UV markings with VIRTIS thermal IR patterns in the polar region could imply a common nature of both phenomena that is probably connected to global circulation at high latitudes. The global cloud pattern at high latitudes resembles very much the structure of Earth hurricanes, but the Venus polar vortex is 3 – 4 times larger. We observe strong variations of the global cloud top patterns with time scale of about a day indicating quick dynamical and microphysical processes at the cloud tops.

(D. Titov, W. J. Markiewicz, H. U. Keller, R. Moissl, and P. Russo)

### VMC monitors global weather on Venus

Venus is completely shrouded by thick clouds that consist mainly of concentrated (∼75%) sulfuric acid ($H_2SO_4$) forming in photochemical reactions between sulfur dioxide ($SO_2$) and water molecules exposed to direct solar light at the top of the clouds. The nature of the second chemical specie that forms cloud particles and strongly absorbs ultraviolet light is not known. The VMC UV filter picks up the spectral feature of

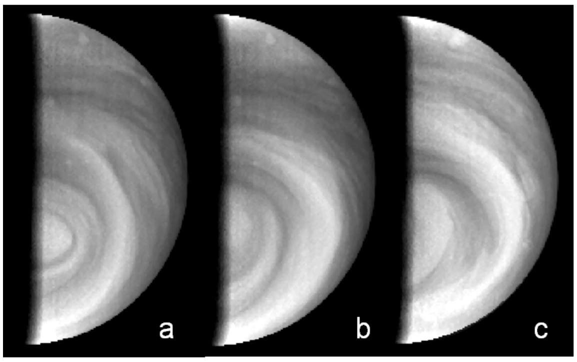


Fig. 125: Polar views of Venus taken by VMC in the UV filter.

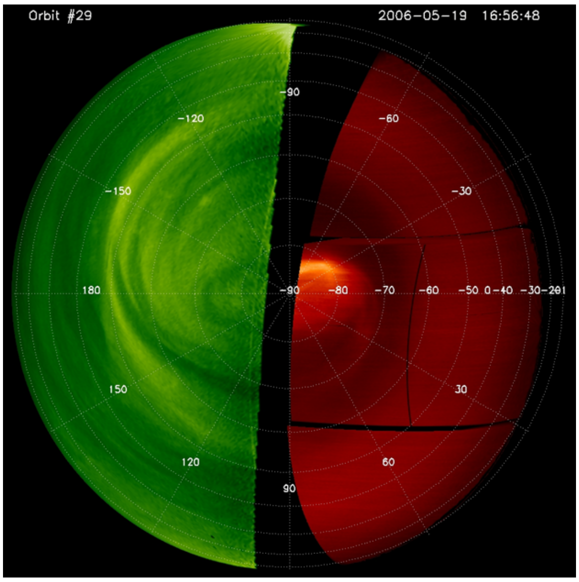


Fig. 126: VMC UV image (left, false colour) taken simultaneously with the VIRTIS thermal-IR mosaic (right). Bright vortex in thermal IR has its counterpart in the UV image. Dark region around ("cold collar") corresponds to the bright mid-latitude belt in VMC images.

the unknown UV absorber. The images in Fig. 127 were acquired by VMC in July 2007. Dark markings that usually dominate in low latitudes indicate higher abundance of the unknown UV absorber at the cloud tops. Bright features are produced by sulfuric acid aerosol, the high latitude "cap" being the most prominent of them.

This portrait gallery, each of them taken only a few days apart, demonstrates how remarkably variable appearance of the Venus face is. The dark clouds can be obscured by a bright sulfuric acid veil during 1 – 2 days and then disappear in equally short time. During such events brightness of the southern high latitudes can increase by about 30% while the "cap" extends beyond its usual boundary at ~50° S (orbit 470) almost to the equator (orbits 459, 463).

The VMC observations are consistent with the previous conclusions that the brightening is caused by increase of the amount of the polar haze that masked the top of the main cloud. The time scale of the changes that encompass the whole planet is strikingly short. This "global weather" suggests fast dynamical, chemical, and microphysical processes that form and remove upper haze on the time scale of days. The processes of diffusive growth of sulfuric acid particles, eddy mixing, and sedimentation are too slow at these altitudes. Homogeneous nucleation can lead to formation of a large amount of new particles of submicron size ($r \sim 0.1\ \mu m$). This process can be rather quick providing the system reaches high values of supersaturation ($\sim 10 - 100$) that in case of the Venus upper atmosphere implies either abrupt cooling or injection of large amount of $SO_2$ molecules in this region. Both mechanisms imply some changes in the dynamical regime all over the planet. In the systems with large number density ($n \sim 10^4\ cm^{-3}$) that usually form in homogeneous nucleation, the coagulation is an effective process to decrease the number of particles and opacity within few days. It is also possible that changes in haze density are caused by solar wind interacting with Venus upper atmosphere. If this is so then VMC is monitoring space weather effects on our sister planet.

(D. Titov, W. J. Markiewicz, L. Veiera, and H. U. Keller)

### Venus Cloud Altimetry

Joint observations by VIRTIS and VMC allow us to study the altitude of the cloud top in different regions seen in VMC images. VIRTIS spectra in the $CO_2$ near-IR bands are used for this task. Fig. 128 shows the preliminary result of cloud top altimetry indicating that the altitude of the cloud tops varies from ~72 km in the bright mid-latitude band to ~65 km in the polar vortex. This corresponds to about 1.5 scale height of the atmosphere.

(N. Ignatiev, D. Titov, W. Markiewicz, and N. Manoel)

### Venus cloud tops winds

The Venus Monitoring Camera imaging sequences with about 8 hours duration and good temporal resolution allows one to determine the winds at the cloud tops (~70 km) by tracking UV markings on the Venus disc. Fig. 129 shows the preliminary results on zonal winds. The latitude wind profiles show almost constant velocity of 90 – 100 m/s at low latitudes (<40 deg) in agreement with the earlier measurements. However, above 40 deg latitude the wind

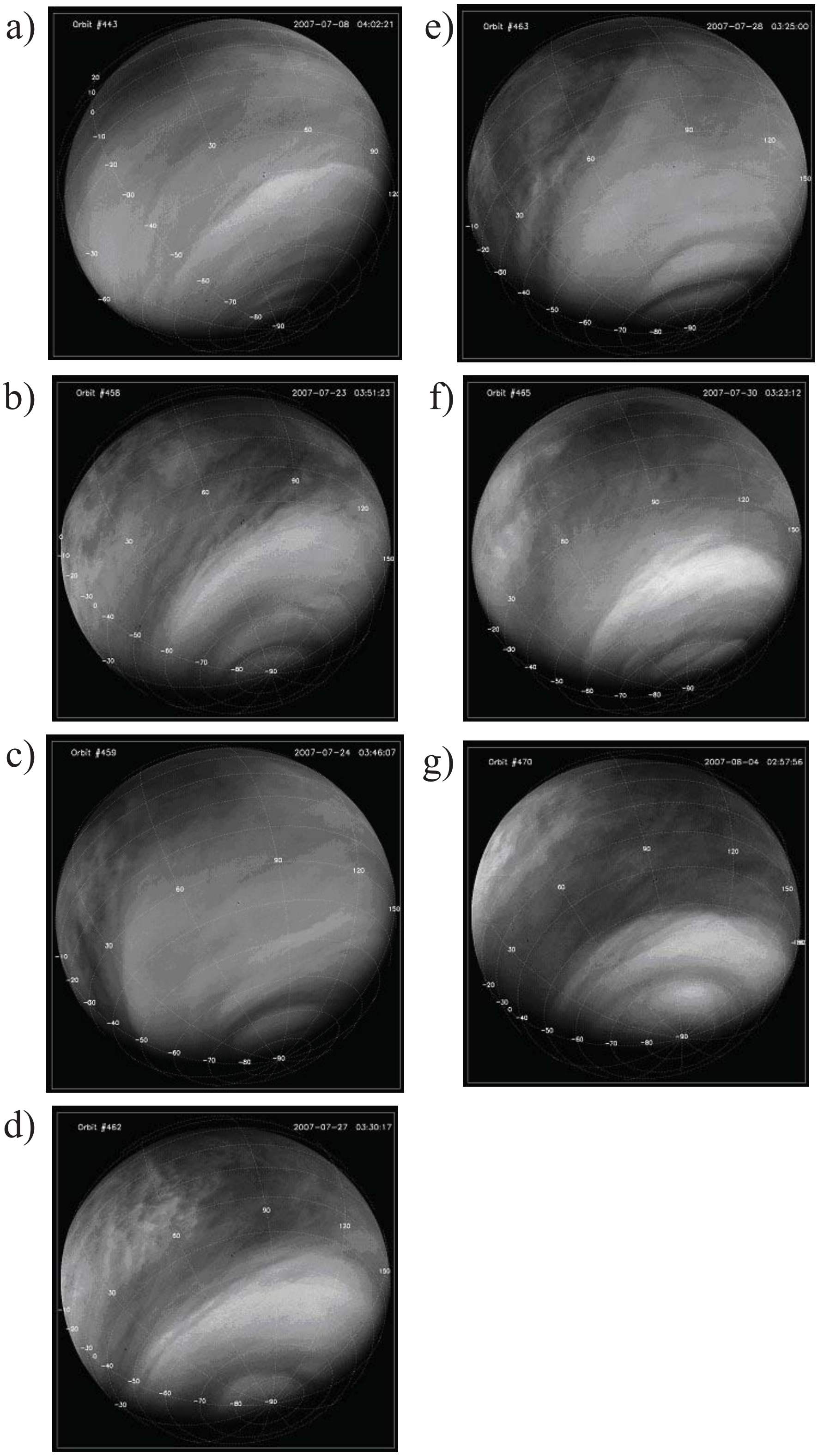


Fig. 127: These images were captured by VMC in the UV filter in July 2007. In this particular season the Venus Express spacecraft approached the planet from the day side that created ideal illumination conditions. All images were acquired from the distance of ~35,000 km with spacecraft pointing in nadir. VMC spatial resolution was ~25 km/px. Atmosphere rotates counterclockwise.

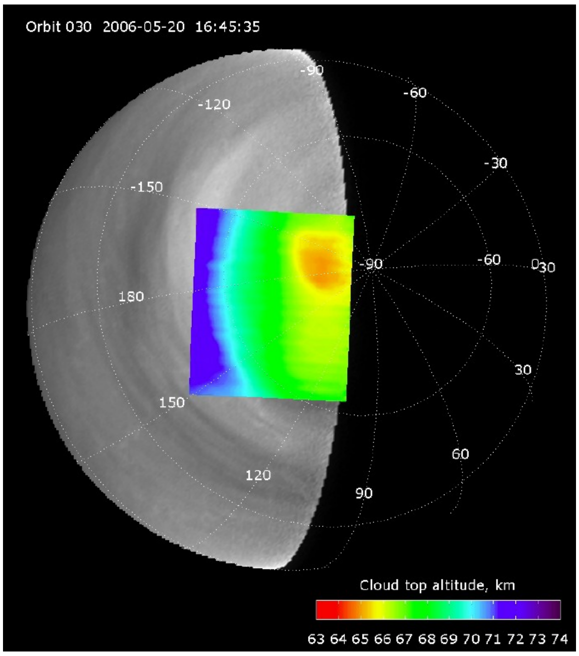


Fig. 128: Altimetry of the cloud tops from the VIRTIS and VMC data analysis.

velocity quickly decreases towards the pole. Red circles show the latitude profile of the thermal wind derived from the VIRTIS temperature sounding under the assumption of cyclostrophic balance. The thermal wind profile fits the observations well in the middle latitude, while showing serious discrepancies in low and high latitudes that can indicate breaking of the cyclostrophic assumption.

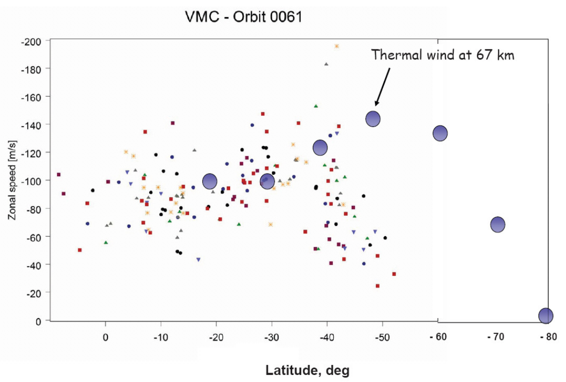


Fig. 129: Latitudinal profile of the zonal wind derived from the cloud tracking in VMC images (lines with error bars) compared to the cyclostrophic wind calculated from the VIRTIS temperature sounding (red circles).

(R. Moissl, I. Khatuntsev, S. Limaye, A. Piccialli, W. J. Markiewicz, D. Titov, N. Ignatiev, and H. U. Keller)

**Global cloud morphology of Venus from the Venus Monitoring Camera**

Venus is completely covered by a thick cloud layer. Its upper part is composed of sulfuric acid and other aerosols of unknown origin. The cloud tops are involved in fast retrograde zonal motion (super-rotation) with the wind speed exceeding 100 $ms^{-1}$. The mechanism maintaining super-rotation is still not understood. Here we report observations of Venus with the Venus Monitoring Camera (VMC) on board the Venus Express spacecraft. Taking advantage of the VMC high resolution imaging and the polar orbit, we investigate both global and small scale properties of these clouds, their temporal and latitudinal variations, and derive wind velocities. Fig. 130 shows an UV image of the southern hemisphere taken by VMC from a distance of $\sim$40,000 km. It shows a global cloud structure from the southern pole to the equator. A bright polar band, a dark mid-latitude band, and bright streamers on the boundary between them, observed by earlier missions, are well visible in this VMC image. One or several global dark streaks are always present within the polar cap region indicating atmospheric parcels spiraling towards the pole. The dark oval feature close to the terminator at the pole is the polar dipole seen in UV, originally discovered at the thermal infrared wavelength.

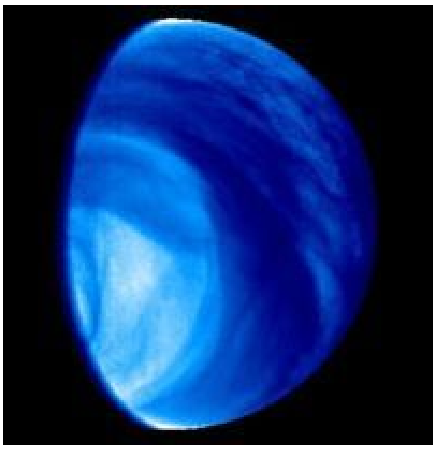

Fig. 130: Global view of Venus in UV from the Venus Monitoring Camera (false colour). The South pole is in the lower left corner. Direction of super-rotation is anti-clockwise.

The eccentric orbit of Venus Express allows one to zoom in the cloud features while the spacecraft approaches the planet. The mosaic in Fig. 131 shows that a mottled and chaotic cloud pattern at low latitudes gives way to approximately zonally oriented streaks at about 20° latitude and indicates the transition from the dynamical regime that is dominated by local convection at the sub-solar point to the one with quasi-laminar flow.

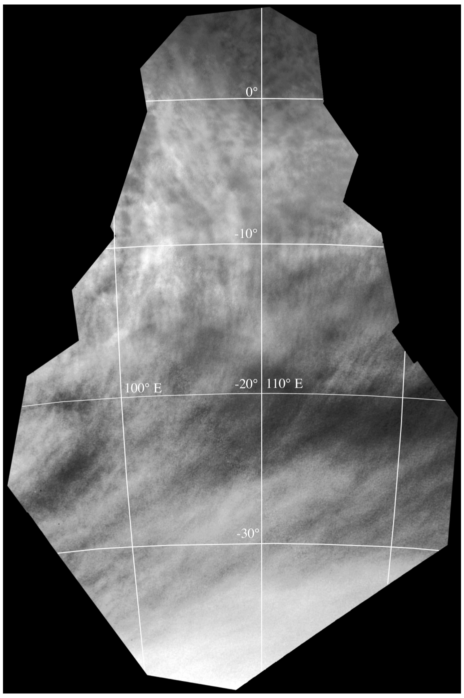


Fig. 131: Mosaic composed of the VMC UV images taken at close approach.

(W. J. Markiewicz, D. Titov, H. U. Keller, R. Moissl, P. Russo, and G. Portyankina)

**Convection in the upper clouds of Venus**

Fig. 132 shows details of the Venus equatorial region near sub-solar point (local noon). These cellular patterns are believed to be convection cells. They are most prominent in the early afternoon but can be found also near the sub-solar point on the morning side. Further from the sub-solar point the patterns return to wavy and streaky morphology even in the equatorial region. The morphology of the clouds is dominated here by very small scale cells. Nevertheless, many interesting linear features can also be seen. The horizontal scale of the convection cells is about 20 km. Because the convection is most likely in the upper cloud deck which is 10 km thick the aspect ratio (diameter/depth) of the cells is about 2. This is five times smaller than the lower aspect ratio limits estimated based on previous poorer resolution data. We believe that these convection cells were actually clusters of cells now individually resolved as seen in Fig. 132. The presently derived small aspect ratio means that the convection is most likely confined to the upper cloud. The large aspect ratio was believed to imply that the convection cells reach all the way down to the surface. The sub-solar region is where the Venus atmosphere absorbs most of the solar radiation. This energy has to be somehow distributed throughout the planet to drive super-rotation. With deep convection the transport of energy could be efficiently accomplished dynamically. The present conclusion about the convection being shallow implies that the energy transport near the sub-solar point is most likely radiative. If this is indeed the case, our picture of the Venus atmosphere, at least with respect to the vertical transport of mass, momentum, and energy, has to be reassessed.

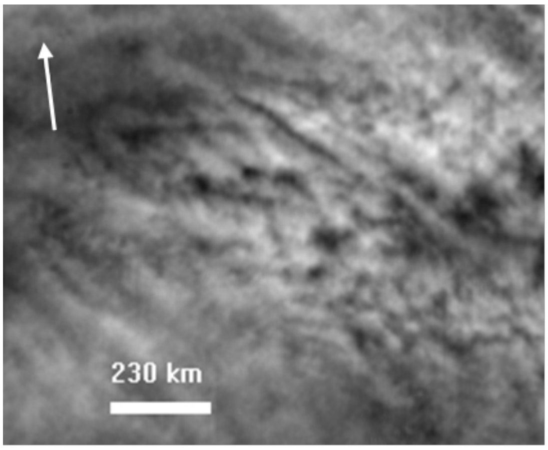


Fig. 132: High resolution image of Venus cloud structure taken by the VMC.

(W. J. Markiewicz, D. Titov, R. Moissl, and H. U. Keller)

**Venus Monitoring Camera sees the surface through the thick cloud veil**

Infrared radiation emitted by the hot (735 K) surface of Venus escapes to space after multiple scatterings in the 25 km thick cloud layer. VMC uses this weak glow to map the planet on the night side.

Fig. 133 shows the infrared mosaic of the Venus surface composed of about 1000 individual VMC images. Orange colour corresponds to lowlands with higher surface temperature and hence stronger thermal emission. Highlands and mountains with elevations of up to 5 km above the “sea” level are about 40 K colder and appear blue in the mosaic. The atmospheric blurring limits spatial resolution of the Venus surface imaging by about 50 km.

The mapped area includes the most typical geological units on Venus. Beta and Phoebe Regions represent *tesserae* – the oldest terrains on the planet. The Magellan radar sounding detected anomalously high reflectivity of the tops of Rhea and Theia mountains indicating the presence of conductive, semiconductive, ferroelectric or ferromagnetic materials. Vast orange-yellow region in Fig. 133 is Hinemoa Planitia – relatively young lowlands that cover about 70% of the

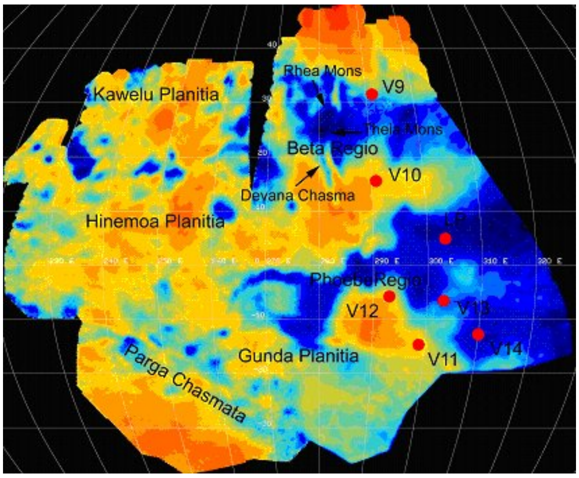


Fig. 133: False colour mosaic of the Venus surface composed of VMC images taken in April and August 2007 in 1 $\mu$m filter. Red circles mark the landing sites of the Soviet Veneras (V) and Pioneer Venus Large Probe (LP).

Venus surface. They formed about 700 Million years ago due to volcanic eruptions that covered almost the entire planet. The elongated feature connecting Beta and Phoebe Regios – Devana Chasma – is a rift zone, resembling the East-African rift on Earth. Rifts are expected to be the centers of current volcanic activity on Venus.

The surface mosaics are currently used to study variation of mineralogical composition and correlate them with topography and radar reflectivity. They are also used to search for ongoing volcanic activity: few square kilometers flows of hot lava can be detected in such images as bright spots.

(A. Basilevsky, E. Shalygin, F. Scholten, D. Titov, and W. J. Markiewicz)

### Vertical thermal structure and winds on the Venusian's Mesosphere derived from HHSMT CO spectral-line observations

Submillimetre observations of the $^{12}$CO J = 2–1 line carried out with the Heinrich Hertz Submillimeter Telescope (HHSMT) were used to determine vertical thermal profiles and winds in Venus' mesosphere. The data was taken 2 days after the second MESSENGER flyby of Venus (on 5 June 2007 at 23:10 UTC) during 5 days. This data was part of a coordinated observational campaign in support of the ESA Venus Express mission. Fig. 134 shows an example of an observed and a best-fit spectra (the later obtained from the radiative transfer model) – black and red lines, respectively –, retrieved vertical temperature profile, retrieved mesospheric CO volume mixing ratio, and wind velocity for the spectral line observation.

Day-to-day and day-to-night temperature variations and short-term fluctuations of the mesospheric zonal flow were evident in our data. Furthermore, retrieved winds showed variations of around 100 m s$^{-1}$ between June 14 and June 15. We found a temperature peak at 90-100 km that seems to support the new finding of the extensive layer of warm air detected by SPICAV onboard Venus Express (Bertaux et al. 2007, Nature 450, 646).

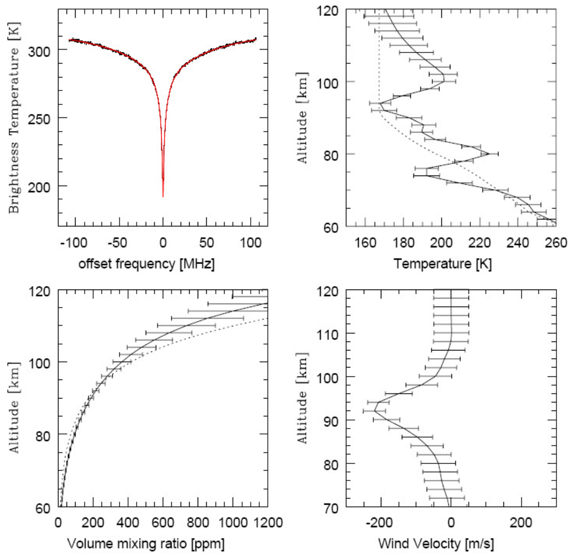


Fig. 134: Top-left panel: example of a spectrum (Obs. No. 34) observed on 15 June 2007. A best-fit synthetic line (red line) is displayed. Top-right panel: retrieved vertical temperature profile (solid line). Bottom-left panel: retrieved mesospheric CO volume mixing ratio (solid line). Bottom-right panel: wind velocity.

(M. Rengel, P. Hartogh, and C. Jarchow)

### Venus Express ASPERA-4 Experiment Observes Ion Outflow from Venus Atmosphere

For a long time it has been one of the great puzzles of planetary science why the atmospheres of Earth, Mars and Venus are so different. Specifically it was not clear how a planet with a gravity similar to Earth can loose all the water from its atmosphere. Now observations made by the ASPERA-4 experiment onboard the Venus Express spacecraft for the first time indicate an explanation of this puzzle (Barabash *et al.*, 2007). All planets with an atmosphere are surrounded by a layer of ions, the ionosphere, because the solar ultra-violett radiation ionizes the outer regions of the atmospheres. The laws of photochemistry dictate that mainly hydrogen and oxygen can gain enough energy to dominate the outer atmospheres. The Sun emitts a continuous stream of hot protons and Helium nuclei into interplanetary space – the solar wind. In contrast to Earth

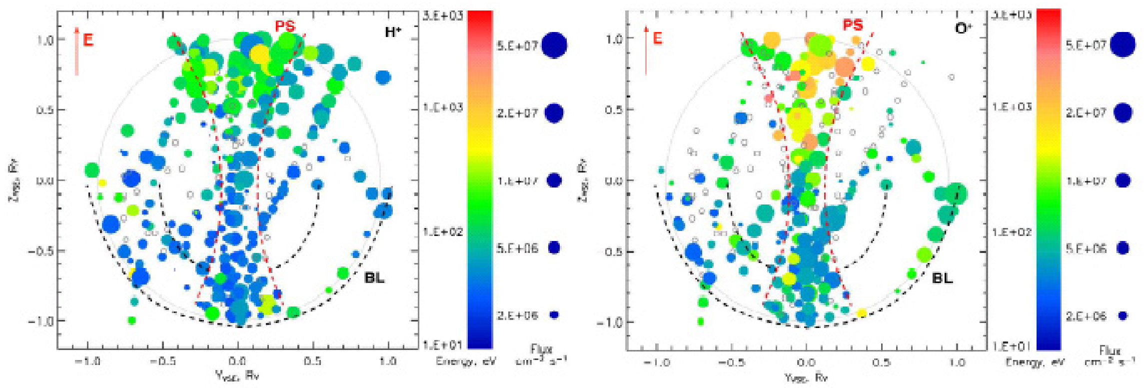


Fig. 135: Flux of ions/cm$^2$s in the plasma tail of Venus as observed by the ASPERA-4 experiment onboard Venus Express. The left panel shows the flux of hydrogen, the right panel the flux of $O^+$ ions. The coordinate plane is oriented such that the electric field induced by the solar wind points upward. The axes are in units of Venus radii (RV = 6051 km). The flux intensity is indicated by the colour scale and by the size of dots. The plasma sheet (PS) formed by the electric field (E) is indicated by red lines.

the upper atmosphere of Venus is not protected against this hot ion flow by a magnetic field. Nevertheless the solar wind itself carries a magnetic field from the surface of the Sun which is deflected by the ionosphere. This deflection causes a barrier against the solar wind flow which inhibits a direct impact of the solar wind into the atmosphere and also limits the outflow of ions from the planetary ionosphere. Thus it was so far not clear how the planet can loose a significant amount of ions from its ionosphere.

The ASPERA-4 experiment on the Venus Express spacecraft was designed to measure the outflow of ions from the planet along the orbit of the spacecraft which slowly precedes around the planet at an orbital period of 24 hours. During the first year of operation of Venus Express the outflow of ions from the planet could be measured in large areas of the Venus space environment. These measurements show that there is indeed a very significant outflow of oxygen, hydrogen and also Helium ± ions in the plasma tail which forms behind the planet through the deflection of the solar wind flow. We have mentioned before that the solar wind carries an embedded magnetic field which is deflected by the planetary ionosphere. Since the solar wind ions flow with a very high speed (around 500 km/s) around the planet, the embedded magnetic field induces a strong electric field in the ionosphere. In Fig. 135 the observations of the ASPERA-4 experiment are displayed in a coordinate system which is oriented along this induced electric field. We can observe that the planetary ion outflow collimates in a narrow region dominated by a positive electric field – the plasma sheet. This indicates that the electric field induced by the solar wind is able to pull out ions from the planetary ionosphere. The ratio of oxygen to hydrogen ions is about 1:2 which means that water molecules are probably the source of these ions. The flux intensities shown in Fig. 135 are not corrected for the sensitivity of the ion sensor such that the hydrogen flux numbers appear lower.

(M. Fränz, C. Martinecz, E. Dubinin, and J. Woch)

### Plasma environment on Venus

The ASPERA-4 instrument on Venus Express has provided us with the first preliminary maps of the distribution of the solar wind and planetary plasma around Venus (Fig. 136). The main regions can be clearly identified: solar wind streaming supersonically relative to Venus forms a bow shock which deflects the wind around the planet in the magnetosheath region, transition region or mantle where the proton fluxes are strongly reduced and the magnetosphere dominated by oxygen ions. The mantle is mainly occupied by protons of solar origin and by planetary protons that underwent a charge-exchange process. It is observed that most of escaping planetary ions form a 'planetary wind' within a cylindrical volume behind the planet. This flow is driven by the momentum transfer from solar wind.

(E. Dubinin, M. Fränz, J. Woch, and C. Martinecz)

### Magnetic pile-up boundary and magnetic barrier on Venus

The ASPERA-4 instrument on Venus Express has performed the first ion composition measurements within the magnetic barrier separating the solar wind and

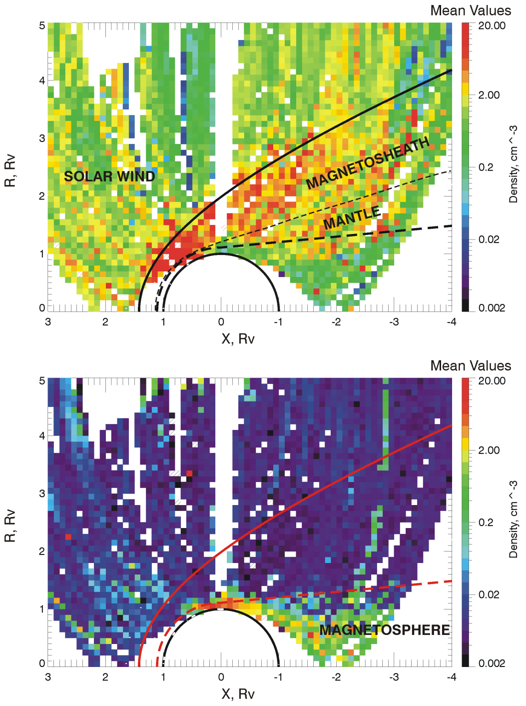


Fig. 136: Maps of the mean values of proton and oxygen number densities in cylindrical coordinates based on the ASPERA-4 measurements onboard Venus Express.

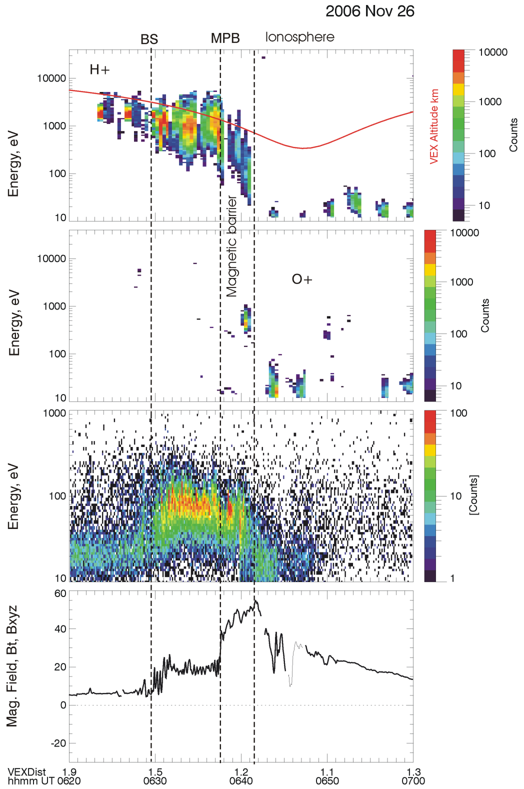


Fig. 137: From top to bottom are the energy-time spectrograms of protons, oxygen ions, electrons, and the magnetic field value measured by the ASPERA-4 and MAG instruments onboard Venus Express. The spacecraft subsequently crossed the bow shock (BS), magnetosheath, the magnetic pile-up boundary (MPB), the magnetic barrier and entered the ionosphere. The red curve shows the altitude (km) of the spacecraft above Venus.

ionospheric plasmas on Venus (Fig. 137). It is observed that a strong pile-up of the interplanetary magnetic field and the formation of the magnetic barrier occurs due to an efficient mass-loading of solar wind by planetary ions. A sharp and shock-like magnetic pile-up boundary (MPB) is detected by the magnetometer (MAG). This implies an abrupt momentum transfer from the magnetosheath plasma to the magnetic field stresses and planetary (mostly oxygen) ions. Origin and mechanism responsible for such a transition layer is a subject of detailed study since it is a permanent feature of the induced magnetospheres which has no adequate explanation yet.

(E. Dubinin, M. Fränz, J. Woch, U. Motschmann, K.-H. Glassmeier, and C. Martinecz)

### Location of the bow shock and ion composition boundaries at Venus – initial determinations from Venus Express ASPERA-4

For the first time since 1992 when the Pioneer Venus Orbiter (PVO) ceased to operate, there is again a plasma instrument in orbit around Venus, namely the ASPERA-4 (Analyzer of Space Plasmas and Energetic Atoms) flown on Venus Express (which was inserted into an elliptical polar orbit about the planet on 11 April 2006).

Based on measurements made by the constituent ion and electron sensors of ASPERA-4 during their first five months of operation, we determine the locations of both the Venus bow shock and the ion composition boundary under solar minimum conditions (Fig. 138). In contrast to previous studies based on PVO data, we employ a 3-parameter fit to achieve a realistic shape for the bow shock. We use a different fit technique for the ion composition boundary because this latter boundary cannot be represented by a conic section. Additionally we investigate the dependence of the location of the bow shock on solar wind ram pressure (based on ASPERA-4 solar wind data).

(C. Martinecz)

### The plasma environment of Venus: comparison of Venus Express ASPERA-4 measurements with 3D hybrid simulations

We use data of the ASPERA-4 ion and electron spectrometers on board Venus Express (VEX) to deter-

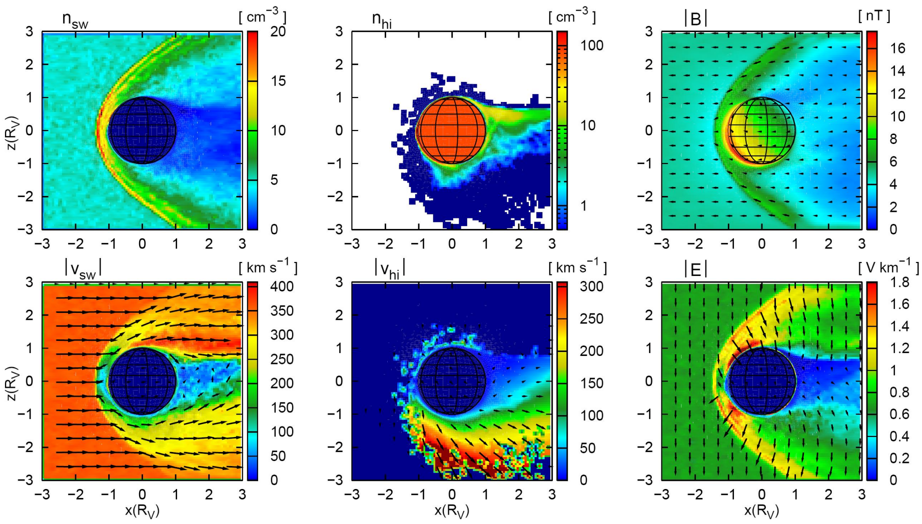


Fig. 139: Cut through the simulation box along the polar plane, i. e. one looks from the western (dusk) side (in the sense of orbital motion) on Venus. The plasma flow comes in from the left (+x-axis), the interplanetary magnetic field is orientated into the plane (+y-axis) and thus, the solar wind electric field points away from the planet (-z-axis). The figures illustrate from left to right in the first row the solar wind density ($n_{sw}$), the heavy ion density ($n_{hi}$) and the background magnetic field; and in the second row the solar wind bulk velocity ($|v_{sw}|$), heavy ion bulk velocity ($|v_{hi}|$) and the convective electric field. In the density plots a clear separation between the solar wind and ionospheric plasma takes place forming the so-called ion composition boundary (ICB) in the northern hemisphere. In the south hemisphere there is no clear ICB due to the mass loading effect, i. e. the planetary ions are accelerated in the direction of the convective electric field and are picked-up by the solar wind flow. The solar wind electric field $\vec{E} = -\vec{v} \times \vec{B}$ vanishes where the heavy ion plasma dominates.

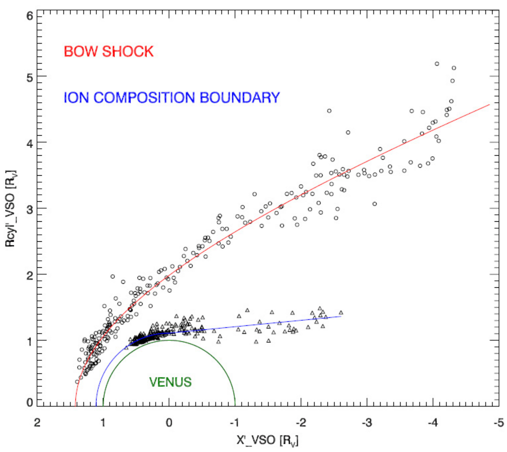


Fig. 138: Venusian bow shock (red line) and ion composition boundary (blue line) fits to Venus Express observations in an aberrated Venus-centered Solar Orbital (VSO) coordinate system under the assumption of cylindrical symmetry in Venusian radii. The circles represent the in- and outbound bow shock crossings and the triangles the in- and outbound ion composition boundary crossings based on the first 5 months of ELS (Electron Spectrometer) and IMA (Ion Mass Analyzer) observations.

mine the locations and shapes of the plasma boundaries (bow shock, ion composition boundary and mantle) at Venus. We also investigate the variation of the terminator bow shock position as a function of the solar wind dynamic pressure and solar EUV flux. We find that the bow shock is independent of the ram pressure, at least during solar minimum, and do not observe yet an effect on the terminator bow shock location because the EUV flux is small over the period of observation. However, the large variations visible in the bow shock positions can be attributed to variations in the magnetic field strength since the bow shock position should depend on the upstream Mach number.

We compare the results with a 3D hybrid simulation, originally developed for the interaction of the solar wind with weak comets. In the hybrid model, ions are treated as individual particles moving in self-consistently generated electromagnetic fields and electrons are modeled as a massless charge neutralizing fluid. The planetary heavy ion plasma is generated by an oxygen ionosphere and exosphere adapted to a profile, which depends on the solar zenith angle (Chapman layer).

A first comparison between observations and simulations indicates that the hybrid model is able to produce an adequate picture of the global plasma environment at Venus (Fig. 139). The positions of the simulated plasma boundaries are in good agreement with the observations, but we found a significant discrepancy in the absolute values of the considered parameters. The comparison of the model data with the boundary positions and plasma moments obtained by the ASPERA-4 experiment allows us to evaluate the accuracy of the model which then can be used to estimate boundary positions and escape fluxes from the planet under conditions different from today.

(C. Martinecz)

## Terrestrial planets research – Mars

### Study of the Martian water cycle by the PFS and OMEGA experiments onboard the Mars Express

Water vapour is the most variable trace gas in the atmosphere of Mars. This implies that the gas is strongly involved in exchange with non-atmospheric reservoirs on the planet like polar caps, regolith, and possibly permafrost. One of the main goals of the Mars Express mission is to understand the Martian water cycle. Two experiments onboard the spacecraft – the Planetary Fourier Spectrometer (PFS) and the infrared mapping spectrometer OMEGA – are very well suited to study the composition of the atmosphere and the surface of Mars. Data analysis carried out at MPS is focused on the study of Martian atmospheric water, in particular, its seasonal behaviour and peculiarities related to outstanding relief features like Tharsis volcanoes.

*Seasonal water cycle*

Retrievals of the atmospheric water amount were based on the fitting of the PFS spectrum in the region of the 2.56 $\mu$m $H_2O$ band. The processing of the entire available dataset yielded intriguing results about the water vapour content and its variations between January 2004 and April 2005. This time covers the season between $L_S$ = 331° of Mars Year 26 to $L_S$ = 196° of the consecutive year. Fig. 140 shows the seasonal behaviour of the atmospheric water content. The mean column density of the equinox season before northern summer is 8.2 pr.$\mu$m. The maximum reached values during northern summer ($L_S \sim 110°$) are 65 pr.$\mu$m, centered around 75°N latitude. After $L_S$ = 130° the maximum vanishes quickly within half a Martian month. Manifestation of the equatorward water transport is seen as a "tongue" of 15 – 20 pr. $\mu$m that progressed southward and reached the equator at about $L_S$ = 190°. The observations strongly suggested that atmospheric water is not uniformly mixed vertically but is rather confined to the lower few kilometers above the surface. The geographical distribution shows two maxima over Arabia Terra and the Tharsis highlands which are most probably caused by atmosphere-ground interaction and by atmospheric circulation.

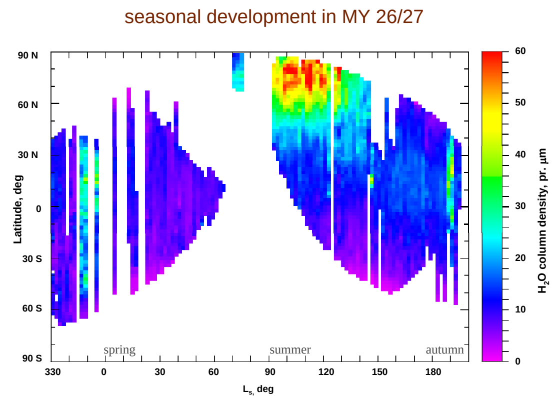


Fig. 140: The seasonal map of water vapour between $L_S$ = 330° of MY 26 and $L_S$ = 200° of MY 27.

*Water vapour anomaly above Tharsis volcanoes*

The behaviour of atmospheric water in the vicinity of the Tharsis volcanoes was studied with the OMEGA infrared mapping spectrometer data (Fig. 141). OMEGA observations over the volcanoes cover quite uniformly a whole Martian year, at different times of the day, allowing a complete seasonal and diurnal survey. The mixing ratio of water vapour shows a peculiar strong enrichment on the top of the volcanoes compared to the surrounding valley, which persists for most of the year and which shows a clear seasonal trend.

The reasons of such an enrichment of water vapour in the rarefied atmosphere of the volcanoes' summit is most likely due to local circulation effects. The extreme topography of the Tharsis region triggers an upslope wind which transports water vapour from the valley to the top of the mountains. This water pump is probably more hindered during the summer due to the low altitude of the saturation layer. The study of the local behaviour of the atmospheric water continues, focusing on comparisons with observations from the Mars rovers Spirit and Opportunity and regions of pronounced topography features like Hellas Basin and Valles Marineris.

(D. V. Titov, M. Tschimmel, and L. Maltagliati)

### Martian aerosols and HRSC stereo images

HRSC is the stereo camera of Mars Express, Europe's mission to Mars. From 2004 the camera has mapped a large fraction of the red planet in stereo and in colour at resolutions of 15 - 50 meters. Digital terrain models, routinely derived from the stereo information, have a similar resolution, both in the horizontal and in the vertical direction. The mission still continues.

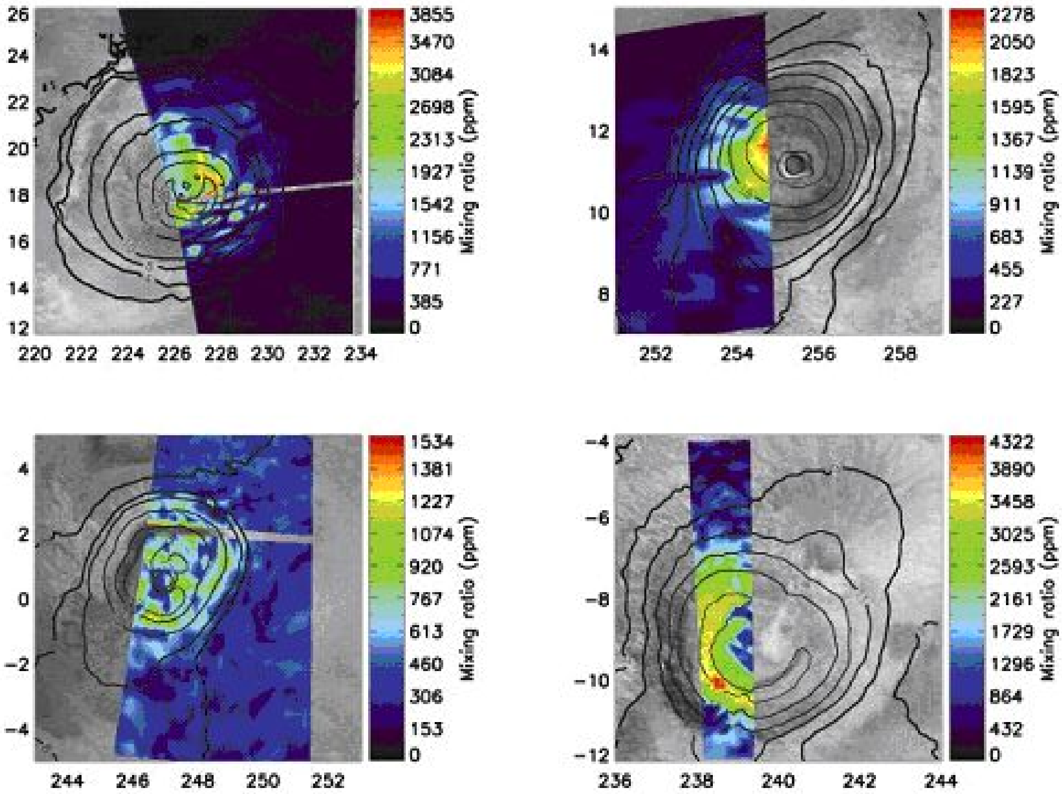


Fig. 141: Atmospheric water vapour above four Tharsis volcanoes retrieved from the OMEGA observations.

The Martian atmosphere contains large amounts of dust and other aerosols that reduce the contrast and spatial resolution of orbiter images. These also invoke a strong diffuse reddish illumination onto the surface, which differs strongly from that of the direct solar illumination, thus changing the observed colours. Interpreting images of the Martian surface requires careful analysis of these atmospheric effects. HRSC stereo imagery offers a unique and powerful tool to study the effects of the Martian atmosphere on orbiter images.

The magnitude of atmospheric effects in the first place depends on the optical depth of the atmosphere. We developed and extensively tested software to estimate this optical depth from shadows or from HRSC's stereo information. Our analyses of HRSC images show that the optical depth strongly depends on altitude (Fig. 142). On average the airborne dust appears to have the same scale-height as the atmosphere itself, meaning that the dust usually is well mixed. However, locally we found strong deviations.

By now, our analysis of HRSC images has made it clear that aerosol properties show important differences from place to place and from time to time. For example, during the autumn of 2006 we analyzed various limb scans taken with the HRSC camera that all show thin whitish or bluish hazes above altitudes of about 50 kilometers. Such hazes are highly variable and localized, but typically may have optical depths of order 0.01, as compared to 0.5 for the airborne dust. Somewhat surprisingly, it appears that these high altitude hazes significantly increase the albedo of the planet. The likely reason is that high altitude hazes contain small and probably icy particles that show strong backscattering. As an effect, the high hazes directly reflect a lot of sunlight back into space. In contrast, the airborne dust sends most of the scattered solar radiation towards the surface.

(N. M. Hoekzema, O. J. Stenzel, W. J. Markiewicz, E. Petrova, and H. U. Keller)

### New images of Mars from the OSIRIS camera system on Rosetta

A series of images of Mars were taken by Rosetta's Optical, Spectroscopic, and Infrared Remote Imaging System (OSIRIS) in February 2007 during the swing-by maneuver.

In the lead image (Fig. 143), an orange (red), green and near-UV colour filter composite image of Mars is shown; the UV channel (the blue colour) has been enhanced. The enhanced UV signal clearly shows the

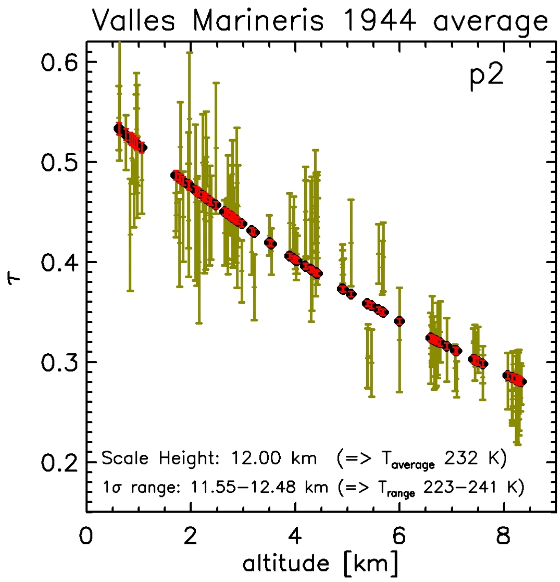


Fig. 142: The scale height of optical depth in the atmosphere of Mars is usually, but certainly not always, very similar to the scale-height of the local atmosphere itself. Here is an example of optical depth as a function of altitude in one of the canyons of Valles Marineris. It was measured with the shadow method from an image taken with Mars Express' stereo camera HRSC during orbit 1944 of the orbiter.

presence of the cloud systems covering most of the Martian disk.

At this time of the Martian year (southern spring), a large fraction of Mars' atmosphere is evaporating from the southern polar cap and will migrate to the northern polar cap during nothern winter.

The first colour image (Fig. 144) was generated using the OSIRIS orange (red), green and blue colour filters.

The ultraviolet image (Fig. 145) was taken on 24 February 2007 with the OSIRIS wide-angle camera through the 'OH' colour filter, intended for the indirect detection of water when observing comet 67/P Churyumov-Gerasimenko.

Clouds are visible at the North polar cap of Mars and at the morning 'limb' (border or outermost edge of a celestial body). A high-altitude cloud is also visible and shown in the inset.

Atmospheric structures can be seen in the next pair of images taken by the OSIRIS narrow-angle camera (Figs. 146 and 147). The images have been produced through a special combination of the green and red colour filters, emphasising the brightness difference. This image processing step enhances the structures in the atmosphere, either dust or clouds.

The images were acquired on 24 February at 19:28 CET from a distance of about 240,000 km; image resolution is about 5 km/pixel.

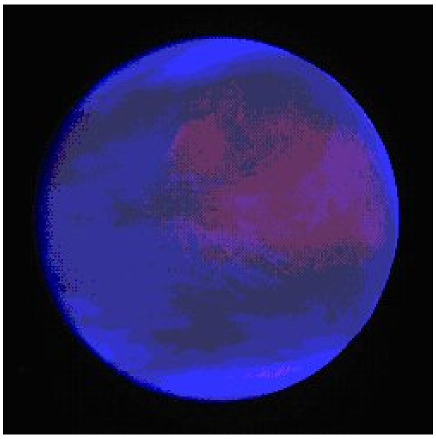

Fig. 143: Image of Mars seen by OSIRIS: A cloudy day on Mars.

Fig. 144: True-colour image of Mars seen by OSIRIS.

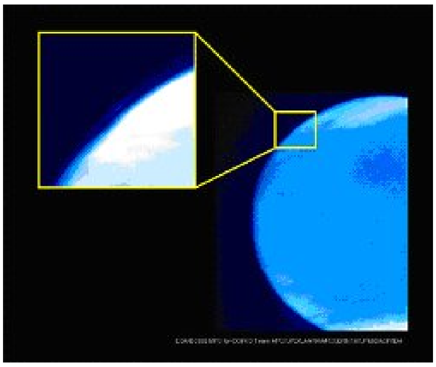

Fig. 145: OSIRIS ultraviolet image of Mars.

Phobos is the inner moon of Mars. Fig. 148 shows Phobos in front of the Mars disk. A sequence of images was acquired through different colour filters following the moon on its orbit around Mars.

The Phobos images were acquired on 24 February, 21:08 UTC.

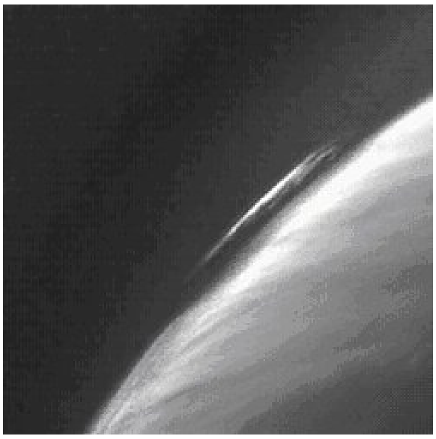

Fig. 146: Evening clouds at Mars as seen from 240,000 km distance.

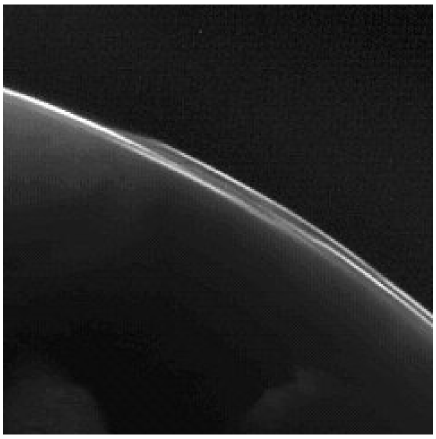

Fig. 147: OSIRIS image of atmospheric structures of Mars (morning clouds).

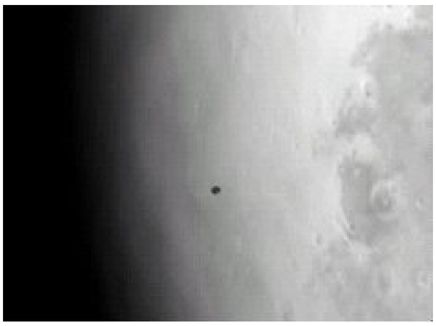

Fig. 148: Phobos transit in front of the Mars disk.

(H. Sierks)

**Presence of a strongly ferrimagnetic phase in bedrock at Meridiani Planum, Mars?**

The Rock Abrasion Tool (RAT) onboard the Mars Exploration Rovers (MER) is a grinding tool designed to remove dust coatings and/or weathering rinds from rocks and expose fresh rock material. Four magnets of different strengths that are built into the structure of the RAT (Fig. 149) have been attracting substantial amounts of magnetic material during RAT activities on both rovers.

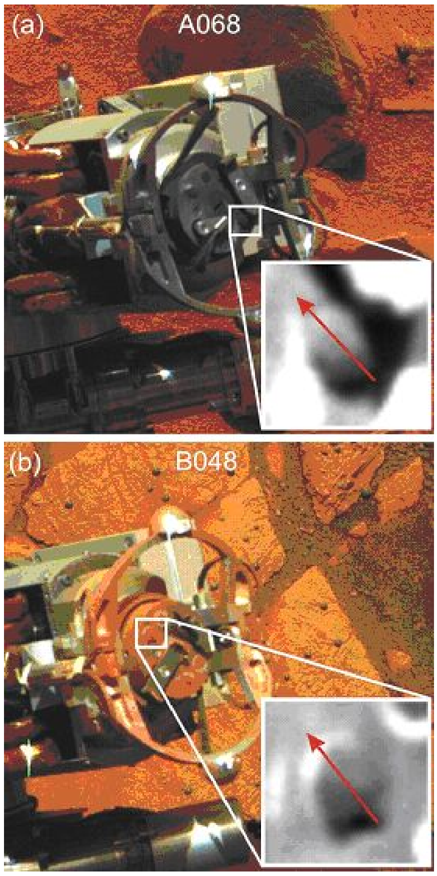


Fig. 149: False-colour images of the RAT acquired with the Panoramic Camera. (a) MER-A, sol 068. The inset shows one of the magnetic particle accumulations (partially shadowed by the grinding bit) as seen through the blue filter (480 nm). The red arrow indicates the luminosity gradient analyzed. (b) Same as (a), but for MER-B, sol 048. The colour images have been generated in a controlled way (with the RGB components stretched from 0 to 0.05 $W/m^2/sr/nm$ in both cases). The scene is brighter on B048 as compared to A068. Note the difference in colour between abraded rock particles on A068 and B048. Scale: The circular plane at the bottom of the RAT is 33.4 mm in diameter.

The RAT magnet experiment as performed on Spirit (MER-A) demonstrates the presence of a strongly ferrimagnetic phase in Gusev crater rocks, which, based on Mössbauer and visible/near-infrared reflectance spectra, is interpreted as magnetite. The amount of abraded rock material adhering to the magnets varied strongly during the mission and is correlated in a consistent way to the amount of magnetite inferred from Mössbauer spectra for the corresponding rock.
The RAT magnet experiment as performed on Opportunity (MER-B) also indicates the presence of a

strongly ferrimagnetic phase in outcrops, although the evidence is weaker than in the case of Spirit. According to data from the $\alpha$-particle-x-ray spectrometer (APXS) and the Mössbauer spectrometer (MB), the Eagle crater outcrops (studied during the primary mission of Opportunity) should not contain magnetite, and their magnetization should not exceed 0.03 $Am^2/kg$. However, the topographic profiles of the magnetic particle accumulations (as inferred from a radiometric analysis, cf. insets in Fig. 149) extend to a maximum height of about 1.0 and 0.6 mm for A068 and B048, respectively. Assuming rotational symmetry for these particle accumulations the following volumes are calculated: 11.3 $mm^3$ for A068 versus 4.7 $mm^3$ for B048. Weighting these volumes by the cumulated grind depths that were achieved prior to acquisition of the images we find that the saturation magnetization should be $0.30 \pm 0.05$ $Am^2/kg$ (Goetz *et al.*, JGR 113, 2008), thus an order of magnitude larger than the above value that was inferred from APXS/MB data. We conclude that Eagle crater outcrops might contain a small amount of a strongly ferrimagnetic phase such as magnetite ($Fe_3O_4$) or maghemite ($\gamma$-$Fe_2O_3$). None of these phases was identified by MB spectroscopy, either because its abundance is below the MB detection limit, or because the ferrimagnetic phase has MB parameters very similar to those of hematite ($\alpha$-$Fe_2O_3$), which is the mineral believed to cause the sextet in the observed spectra.

(W. Goetz and S. F. Hviid in collaboration with M. B. Madsen (University of Copenhagen))

**The ring of Mars: Close to discovery?**

The rings of Mars have long been predicted to originate from the Martian moons Phobos and Deimos. Bombarded by interplanetary meteoroids, the moons generate surface ejecta several orders of magnitude more massive than the projectiles. However, these ejecta are only fast enough to escape from the satellites, but too slow to leave the planet. Thus, they stay in orbits close to that of the parent satellite. Perturbed by the solar radiation pressure and planetary oblateness, they form a thin equatorial ring due to Phobos and a thick tilted torus due to Deimos.

These dust clouds are very faint, however, and one needs extremely sensitive imaging systems in order to detect their elusive radiation close to the bright extended source of light, Mars. Feasibility studies have been performed for the detection of the rings with the OSIRIS camera on board the Rosetta spacecraft that has had an opportunity in February 2007 to capture the rings at the time of its close encounter with Mars, i.e. when the ring was at a long angular distance from the planet. The OSIRIS observations are under scrutiny at the MPS. Predictions for other telescopes have also been computed, e.g. for the Spitzer telescope in the infrared light (see Fig. 150) and with the ESO VLT in a Mars-occulting mode, late in December 2007 near the opposition of Mars at the time when the rings are seen fairly edge-on.

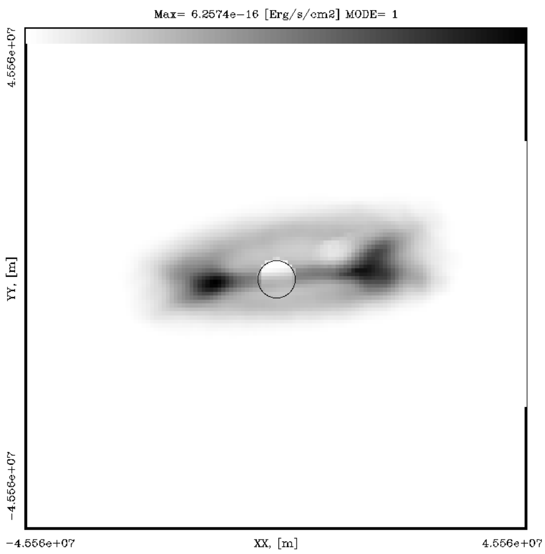


Fig. 150: Radiance map for the Deimos torus around Mars predicted for January 1, 2008, for the 3.6 $\mu$m filter of the IRAC camera on board the Spitzer telescope.

(V. Dikarev, H. Krüger, and M. Küppers in collaboration with A. V. Krivov (FSU Jena, Germany))

**Remnant of a geyser like eruption in a Martian crater**

Images of a Martian crater show an intriguing distribution of water ice. The crater is at 71°N, 103°E. At the floor of this crater an almost circular region of water ice is observed while the rest of the crater floor appears defrosted. This effect was first found in the MOC image M23-01916 (Wide Angel Camera) taken during late Martian Spring, at solar longitude $L_S = 110°$. A year later an image taken by the HRSC camera at $L_S = 154°$ shows the same effect (Fig. 151). Both images indicate that the material underneath the ice is darker than the rest of the crater floor. Our models of the seasonal cycle of condensation of water ice agree well with the observations (Fig. 152). Our simulations show, that the formation of a long lasting or permanent ice layer in the center of the crater is possible only when below it the regolith has thermal inertia higher than the rest of the crater. We also show that in the present climate it is not possible to accumulate any significant amount of water ice over the years. This is possible, if the atmosphere contained only several times more water vapour than today. Another explanation however is much more likely. The dark material on the edge of the ice is most likely basaltic lava. We believe that some time in the past there was a volcanic heating below the surface which resulted in rapid flow of water from below the surface. This liquid water, while entering the atmosphere rapidly, froze once the heat source was exhausted. What we are looking at is the top surface of a cylinder of water ice wedged in the ground. The main implication of this is that the cryosphere, at least in the past and very likely still today, is water ice rich and deep. To date it has only been possible to argue for the existence of water ice in the near surface layer from gamma ray data and other studies.

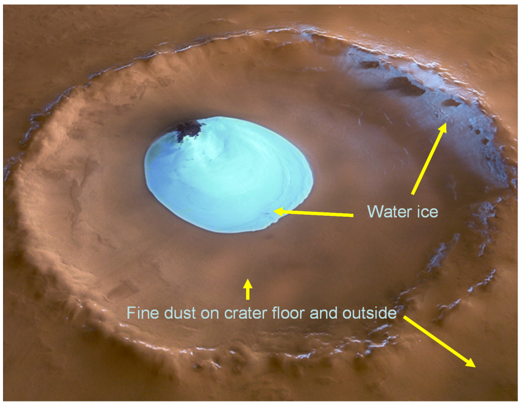


Fig. 151: HRSC image of a Martian crater.

(W. J. Markiewicz, K. J. Kossacki, and H. U. Keller)

### Magnetic properties of Martian atmospheric dust

The Martian atmospheric dust is of interest since it represents the end product of the weathering processes active on Mars. A characterization of the chemical and morphological properties of the dust can lead to a better understanding of the processes that formed the dust.

The surface and aeolian dust on Mars is rich in iron compounds, and significant quantities of dust have been observed to stick to permanent magnets that are either exposed to the dusty atmosphere or inserted into the soil. All successful lander missions to Mars (Viking (1976), Mars Pathfinder (1997) and the Mars Exploration Rovers (2004)) have carried permanent magnets of various designs for the purpose of studying dust magnetic properties (Fig. 153). The magnetism of the aeolian dust stems from its content of magnetite, which derives from mechanical weathering of magnetite-rich surface rocks. A strong correlation between the elements titanium and iron is observed

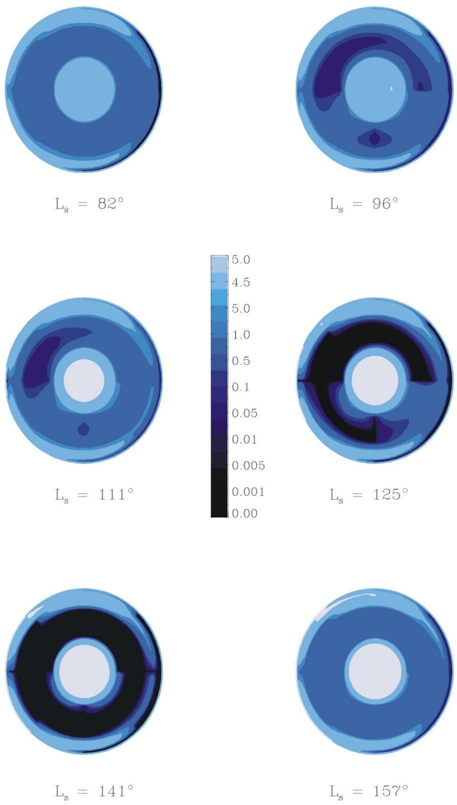


Fig. 152: Skewing water ice remnants of a geyser eruption.

in dust attracted to permanent-magnet surfaces, suggesting that the magnetite responsible for the magnetization of the soil is actually titanomagnetite. Overall the dust can be shown to have a saturation magnetization of less than 2 $Am^2\ kg^{-1}$. However, some grains are significantly more magnetic, and by interaction with a permanent magnet it is possible to separate the airborne dust into populations of more and less magnetic grains. Sub-populations attracted to a magnet have been seen to have magnetizations above 7.2 $Am^2\ kg^{-1}$. The wide-spread presence of magnetite and other easily-oxidized minerals like olivine in rocks and in the global Martian dust implies that the Martian surface has been largely devoid of liquid water for a long time.

(S. F. Hviid and W. Goetz)

### Indication of long-lasting dry periods on Mars from the chemistry and mineralogy of atmospheric dust

The ubiquitous atmospheric dust on Mars is well mixed by periodic global dust storms, and such dust carries information about the environment in which it once formed and hence about the history of water on

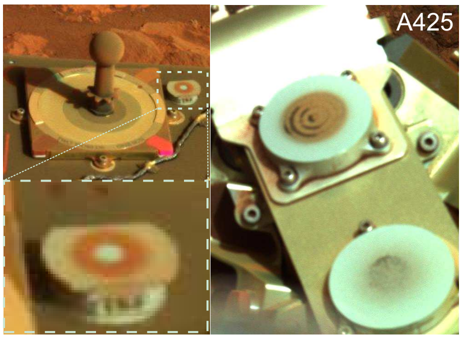


Fig. 153: Magnetic targets on the Mars exploration rovers, left: sweep magnet, right: filter and capture magnets.

Mars. The Mars Exploration Rovers (MER) have permanent magnets to collect atmospheric dust for investigation by instruments on the rovers. In particular, dust attracted to the strong Capture magnet and the somewhat weaker Filter magnet (both located on the front part of the rover deck, Fig. 154) can be studied by instruments mounted to the end of the robotic arm: Microscopic Imager (MI), Alpha-particle-x-ray spectrometer (APXS) and Mössbauer spectrometer (MB).

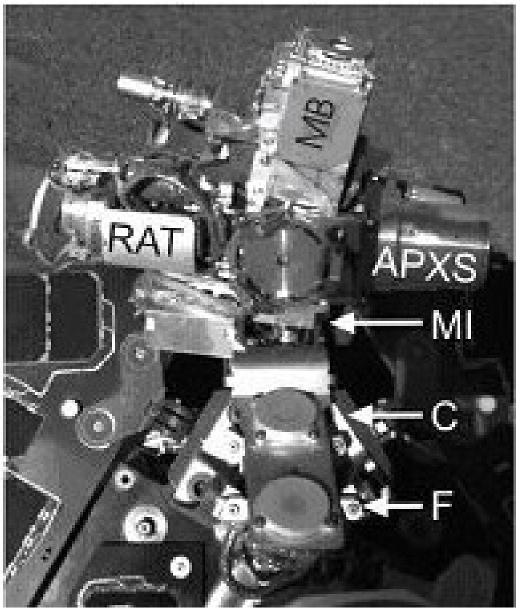


Fig. 154: Context image (Navcam, MER-B, sol 328) showing the instruments mounted to the end of the robotic arm (APXS: Alpha-particle-x-ray spectrometer, MB: Mössbauer spectrometer, RAT: Rock Abrasion Tool, MI: Microscopic Imager) and the magnets (C: capture magnet, F: filter magnet).

An MB spectrum of dust attracted to the capture magnet is shown in Fig. 155 together with spectra of bright Martian soil and of magnetite ($Fe_3O_4$): About half of the iron atoms turn out to belong to a magnetite phase, while the majority of the remaining iron atoms are interpreted to belong to olivine and pyroxene (Goetz *et al.*, 2007, 2008). This result is interesting in two respects: 1) The magnetism of the aeolian dust apparently stems from its content of magnetite. This suggests that the dust is derived from mechanical weathering of magnetite-rich surface rocks. Moreover a strong correlation between the elements titanium and iron is observed (Fig. 156), suggesting that the magnetite responsible for the magnetization of the dust is actually titanomagnetite (Goetz *et al.*, 2007, 2008). 2) Olivine is known to be easily re-worked by the action of liquid water. The presence of olivine in aeolian dust taken together with the one in all soils (MER-A and MER-B) as well as in the large majority of rocks encountered by MER-A implies that the Martian surface has been largely devoid of liquid water for a long time.

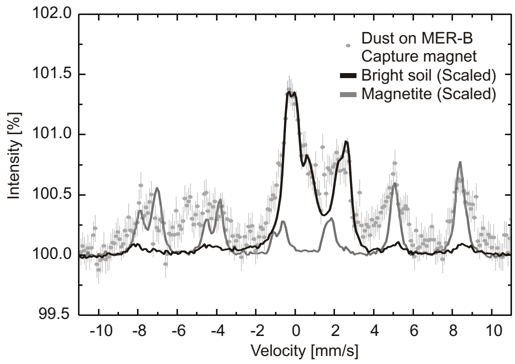


Fig. 155: Mössbauer spectrum of Martian airborne dust (data points with error bars) as attracted to the capture magnet (MER-B, sol 328-330). Also shown: Spectrum of bright Martian soil (black solid line) and magnetite on the calibration target onboard the rover (grey solid line).

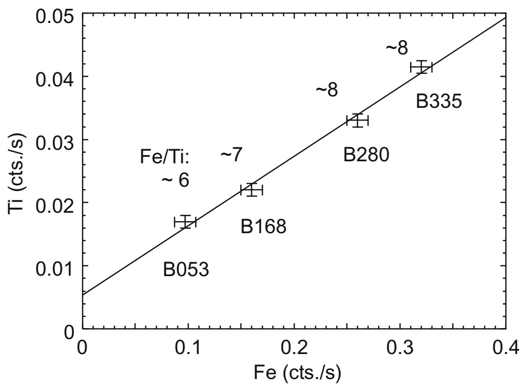


Fig. 156: Elemental composition (Fe, Ti) of dust on the MER-B capture magnet (APXS raw data). The amount of Fe and Ti increases over time (sol numbers ranging from 53 through 335), while the ratio Fe/Ti remains essentially constant.

(W. Goetz and S. F. Hviid in collaboration with M. B. Madsen (University of Copenhagen))

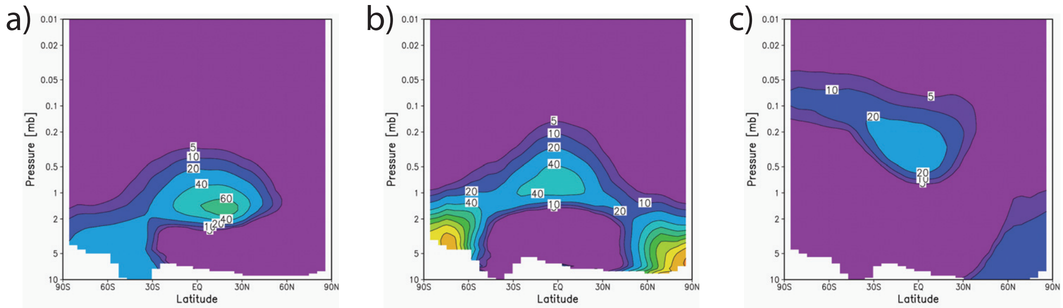


Fig. 157: Zonal-mean mass mixing ratio of water ice [ppm] in (a) Ls = 90°, (b) Ls = 180° and (c) Ls = 270° simulated in the MGCM.

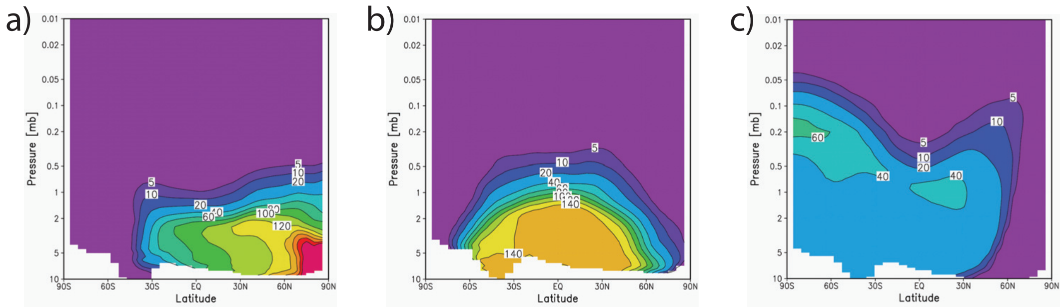


Fig. 158: Same as Fig. 157, except for water vapour [ppm].

### Simulation of the water cycle on Mars

There is already a lot of data about the column density distributions of water vapour and water ice derived from orbiters around Mars. In addition, ground-based millimeter- and submillimeter telescopes have detected the hygropause (cut-off height of water vapour) on Martian low- and mid-latitude. The 3-dimensional simulation of the atmospheric water cycle is an important step in understanding the Martian atmosphere, for the theoretical interpretation of the observational data. We are starting to introduce a water cycle in our Martian general circulation model (MGCM). Figs. 157 and 158 show the vertical-height cross-sections of simulated water ice and water vapour distributions. Water vapour can exist only below the water ice clouds. If we define the hygropause as the highest point with the water vapour of ~5 ppm, it is 0.5 – 1.0 mb (15 – 20 km height) for a solar longitude Ls = 90° and 180°. During Ls = 270°, the hygropause reaches above ~0.2 mb (~30 km height). These results are consistent with the past millimeter wave observations. The seasonal changes of the hygropause are being observed by also the upcoming Herschel space telescope. Combined with it, this model will help to investigate the meridional transport of water on Mars.

(T. Kuroda and P. Hartogh in collaboration with D. Sakai and M. Takahashi (Center for Climate System Research, University of Tokyo, Japan))

### Semi-annual oscillations in the atmosphere of Mars

The semi-annual oscillation (SAO), mean zonal winds alternating with a 6-month period, is a well-known phenomenon in tropics on Earth. In this study we report on the first detection of the SAO in the Martian atmosphere. The semi-annual periodicity is found in the difference between day- and night-time atmospheric temperatures, a good proxy for solar tides, measured from Mars Global Surveyor (Fig. 159). Simulations with our Martian general circulation model (MGCM) proved that this modulation of tidal amplitudes is a manifestation of the SAO of zonal winds in Martian tropics (Fig. 160). Our numerical experiments revealed significant differences in driving mechanisms of the SAO between Mars and Earth. On Mars, unlike on Earth, equatorial Kelvin waves supply only small retrograde torque to the mean circulation. Instead, thermal tides and quasi-stationary planetary waves induced by Martian topography contribute strongly to the prograde (super-rotation) acceleration. The existence of the SAO on Mars suggests that this phenomenon is not a result of the unique terrestrial environment, but a more general consequence of wave-mean flow interactions in atmospheres of fast-rotating planets.

(T. Kuroda, A. S. Medvedev, and P. Hartogh in collaboration with M. Takahashi (Center for Climate System Research, University of Tokyo, Japan))

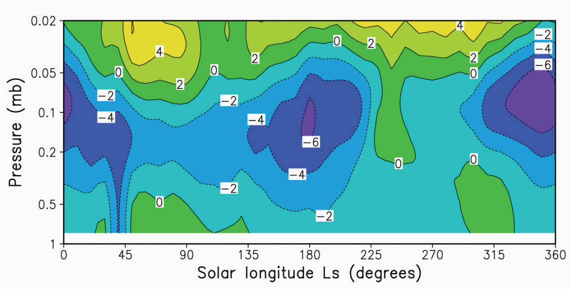


Fig. 159: Seasonal change of the temperature difference between local day and night divided by 2, $(T_{2PM} - T_{2AM})/2$, averaged between 10°S and 10°N from the MGS-TES limb observations. The data in this plot are for the period from $L_s$=125° in Mars Year 24 (April 1999) to $L_s$=125° in Mars Year 25 (March 2001). The contour interval is 2 K.

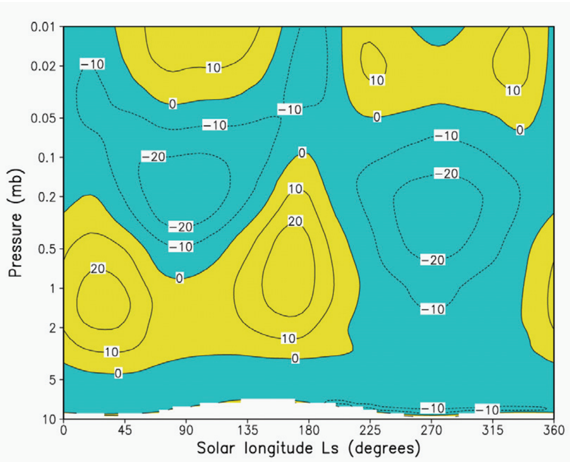


Fig. 160: The composite annual cycle of the simulated mean zonal wind averaged between 10°S and 10°N simulated in the MGCM. The contour interval is 10 m s$^{-1}$, westerly wind is shaded with yellow.

## Seasonal changes of the baroclinic wave activity in the northern hemisphere of Mars simulated with a Global Circulation Model

Simulations of baroclinic waves in the northern hemispheric Martian atmosphere have been performed for different seasons and different dust opacities using a general circulation model of the Martian atmosphere.

In the simulations for the weak dust load, the wave with zonal wave number 2 and 3.1 Sols period is dominant near the surface, while the wave with zonal wavenumber 1 and 5.5 Sols period is dominant at higher altitudes, in "autumn" ($L_S$ = 195 – 225°). In "winter" ($L_S$ = 280 – 300°), the wave with zonal wavenumber 1 and 6.6 Sols period is dominant in all altitudes. These wave structures and seasonal changes are consistent with observations from the Mars Global Surveyor, and they can be explained by seasonal changes of the atmospheric fields (vertical shear of zonal wind, distributions of the potential vorticity gradient and energetic particle fluxes, see Fig. 161). It is also simulated that strong dust storms in solstitial season contribute to the significant reduction of the baroclinic wave activity, as observed by the Viking Landers, due to the stabilization of the jet stream with respect to baroclinic disturbances and the associated weakening of the wave excitation.

(T. Kuroda, A. S. Medvedev, and P. Hartogh)

## Comparison of microwave observations of Martian temperature and winds with general circulation model simulations

Microwave observations of the temperature and wind in the middle atmosphere of Mars are compared with the results of simulations with our Martian general circulation mode (MAOAM). The simulated global-mean mesospheric temperature during a northern summer solstice is ∼ 10 K lower than at spring and autumn equinoxes, which is consistent with JCMT observations in 1996-97, although the absolute values are 30 – 40 K higher than in observations. The wind velocity in the middle atmosphere in the model is comparable to the observations, except that the eastern wind in the afternoon is ∼ 100 m s$^{-1}$ weaker. The wind velocity was directly measured from Doppler shifts of CO lines. We emphasize that these wind data obtained from the microwave measurements are unique for the Martian atmosphere. The descending landers (Viking and Mars Pathfinder) performed the only other available wind measurements. The simulated temperature in the Martian mesosphere is considerably higher than the JCMT microwave data show. However, the model temperature at 60 – 70 km is ∼ 10 K lower in summer solstice than in spring and autumn equinoxes, which is consistent with the measurements. One possible reason for this discrepancy is the strong winter polar warming that is simulated in the model (Medvedev and Hartogh, 2007). Moreover, it is still difficult to determine the characteristics of the mesospheric temperature, because the available observational data is very sparse, and there are differences of 20 – 30 K between the observational data. R. T. Clancy and B. J. Sandor (1989) describe that the higher (compared to other measurements) temperature derived from the Viking descent is due to either the effect of dust raised to higher altitudes or strong near-infrared heating by $CO_2$ in the northern summer. Because the Viking descent occurred during daytime in summer at the latitude of ∼ 22° N, the observed temperature represents a local snapshot, whereas the JCMT observations cover the global-mean temperature. More observational data are needed for constraining and validating model results. As for the wind velocity, the large difference

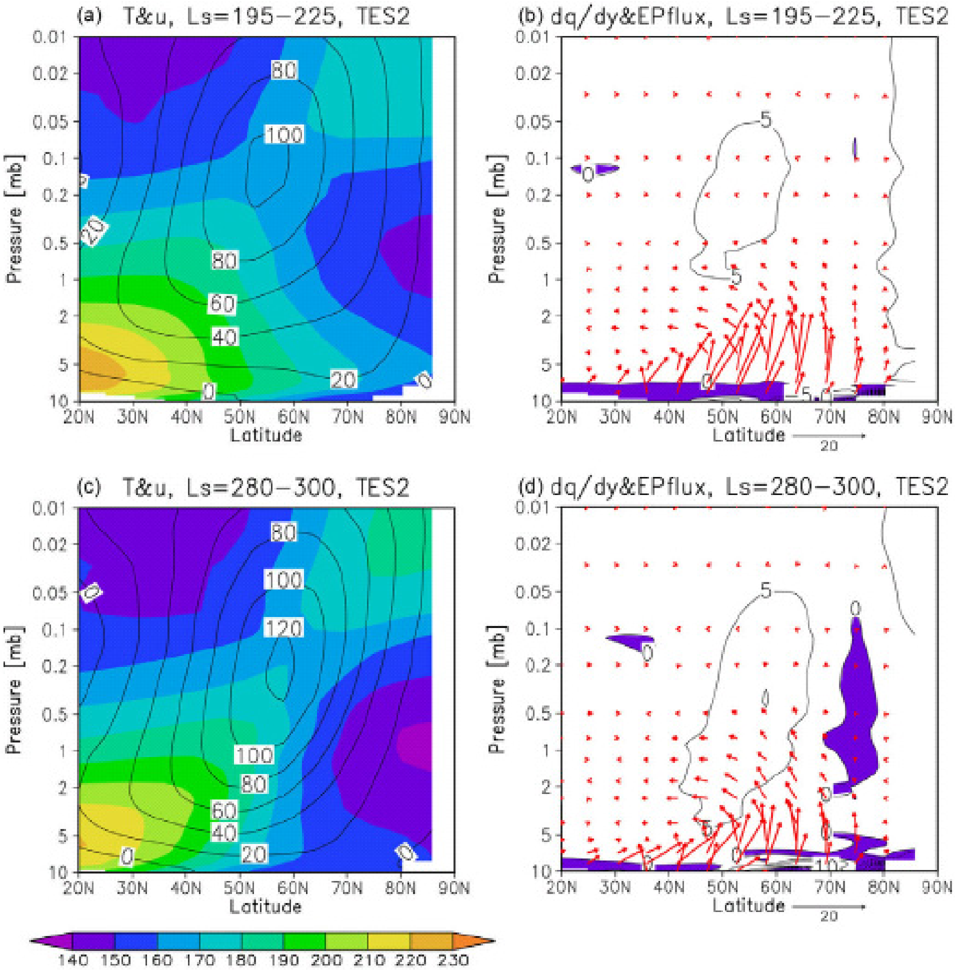


Fig. 161: Zonal-mean atmospheric fields simulated for the weak dust load: (a) Temperature [K] (shades) and zonal wind [m $s^{-1}$] (contours); (b) The Eliassen-Palm fluxes due to transient eddies (red arrows) and the meridional gradient of the potential vorticity multiplied by the radius of Mars [in units $10^{-4}$ $s^{-1}$] averaged for the "autumn" ($L_S$ = 195 – 225°). Shaded are the negative values; (c) and (d) are the same as (a) and (b), respectively, except for the "winter" ($L_S$ = 280 – 300°).

between the measurements and simulations is seen only for the eastern wind in afternoons. Other Martian GCMs (Forget *et al.*, 1999) did not reproduce the strong eastern wind observed by JCMT either, as described in Clancy *et al.*, (2006). To a large degree, the simulated wind velocity is related to the temperature distribution through the so-called thermal wind relation:

$$\left(f + \frac{2u\,\tan\phi}{a}\right)\frac{\partial u}{\partial z} = -\frac{g}{aT}\frac{\partial T}{\partial \phi}$$

where $f$ is the Coriolis parameter, $u$ is the zonal wind velocity, $\phi$ is the latitude, $a$ is the radius of planet, $z$ is the height, $g$ is the acceleration of gravity and $T$ is the temperature. To maintain the eastern wind velocity of $\sim 180$ m $s^{-1}$ at 60 km from above equation, as observed by JCMT, the value of $\partial T/\partial\phi \sim$ -16 K is required. For example, the temperature at the latitude of 57° S must be $\sim 16$ K higher than that at the equator, from the surface and up to 60 km. In the model, $\partial T/\partial\phi$ is almost zero from the surface up to $\sim 40$ km at the local times 2 – 3 pm, which explains a weaker eastern wind. The atmospheric heating in mid latitude and polar region in the southern hemisphere below $\sim 60$ km should be mainly due to the heating by $CO_2$ infrared band or dust. Our GCM uses a simplified parameterization of Forget *et al.* (1999) for heating effects by $CO_2$ infrared band, therefore the improvement of it or of the dust distribution might contribute to the production of stronger easterlies. In addition, ion drag may affect the wind velocities. Because of the thin air and weaker magnetic field, the effects of ions can influence the middle atmosphere of Mars.

(T. Kuroda and P. Hartogh)

### Study on winter polar warmings and the meridional transport on Mars simulated with a general circulation model

Winter polar warmings in the middle atmosphere of Mars occur due to the adiabatic heating associated with the downward branch of the cross-equatorial meridional circulation. Thus, they are the manifestation of the global meridional transport rather than of local radiative effects. We made a series of numerical experiments with our recently developed general circulation model of the Martian atmosphere (MAOAM, Hartogh *et al.*, 2005) to examine the relative roles of the mechanical and thermal forcing in the meridional circulation. The strength and the poleward extent of this circulation, rather than the direct radiative heating effects, determine the magnitude and the location of the winter polar warmings observed in the atmosphere of Mars. Partly, this work was motivated by findings that onsets of global dust storms enhance the winter polar temperature maxima. In this regard, it is important to answer the question if the meridional circulation in the middle atmosphere of Mars is consistent with the thermally driven almost inviscid Hadley cell, as argued by Wilson (1997) and Forget *et al.* (1999), or primarily driven by eddies (planetary and gravity waves, solar tide) similarly to the so-called "extratropical pump" mechanism (Holton *et al.*, 1995), as on Earth. We ran four sensitivity tests: a control run, one with the artificial damping of non-zonal disturbances, an experiment with no topography and diurnally averaged solar heating to inhibit the generation of eddies, and a run with increased dust load imitating a global dust storm. In all but the experiment with no planetary waves and tides (weak planetary waves generated by instabilities were still present), we found that the circulation is forced to a large degree by the mechanical effects of dissipating eddies. The strength and location of winter polar warmings are related to the divergence of wave action fluxes (Eliassen-Palm fluxes) in the manner consistent with the mechanism of the "extratropical pump", at least in the middle atmosphere. Only in the run with severely reduced eddies, the meridional transport was reminiscent of the thermally-induced Hadley cell.

In agreement with earlier arguments of Haberle *et al.* (1982), this circulation was confined to low latitudes. The run with an increased dust revealed that the magnification of the winter polar warming is not the direct result of heating due to the increased absorption of the solar radiation by the aerosol, but is caused by the extension of the meridional transport cell poleward. This conclusion corroborates the result of Wilson (1997), although in his experiment the dust was allowed to be transported, and, thus, to potentially magnify the effect. A closer examination has shown the mechanism of the poleward extension of the meridional cell. A strengthened westerly polar jet (prograde winds) forces planetary waves and tides propagate more vertically, and preventing them from dissipating at lower levels. Then, the Eliassen-Palm fluxes converge stronger near the upper edge of the polar vortex, and magnify the poleward transport. Correspondingly, the air descent over the pole intensifies, and the temperature maximum increases as well.

Additional numerical experiments have shown that insufficient model resolution, increased numerical dissipation, and, especially, neglect of non-LTE effects for the 15 $\mu$m $CO_2$ band radiative cooling could weaken the simulated meridional transport, and, as the result, decrease the magnitude of winter polar warmings in GCMs.

High sensitivity of the circulation above $\approx 80$ km may be an indication of missing effects in our and other contemporary GCMs. A potential candidate is the gravity wave drag exerted by broad-spectrum harmonics. Further measurements of large scale wind and temperature fields in the upper atmosphere as well as the statistics for small scale fluctuations will help to constrain the models and verify the nature of the meridional circulation.

(A. Medvedev and P. Hartogh)

### Temperature inversion during the 2001 global dust storm on Mars: Observation with SWAS and modelling with MAOAM

The Earth-orbiting Submillimeter Wave Astronomy Satellite (SWAS) observed the global mean surface and atmosphere temperature on Mars as a function of altitude. Unlike for infrared spectrometers, the temperature retrievals from submillimeter instruments can be performed in the presence of atmospheric dust. During the 2001 global dust storm on Mars, SWAS measured the atmosphere and surface temperature for aerocentric longitudes from $L_S$ = 166° to 233°, and observed the temperature inversion during the global dust storm. We used the General Circulation Model of the Martian Atmosphere (MAOAM) to simulate the temperature and other atmospheric fields under the conditions corresponding to those during the SWAS measurements. The model takes into account the radiative transfer by the atmospheric dust. Simulations show an overall agreement with the SWAS measurements. In particular, the model reproduces the inversion of the global mean temperature and the surface cooling detected by SWAS. Time series of the globally averaged surface and atmospheric temperature at

0.05 hPa (∼ 49 km, Fig. 162) are also in a good agreement with the measurements. Without the dust, the model cannot reproduce these features.

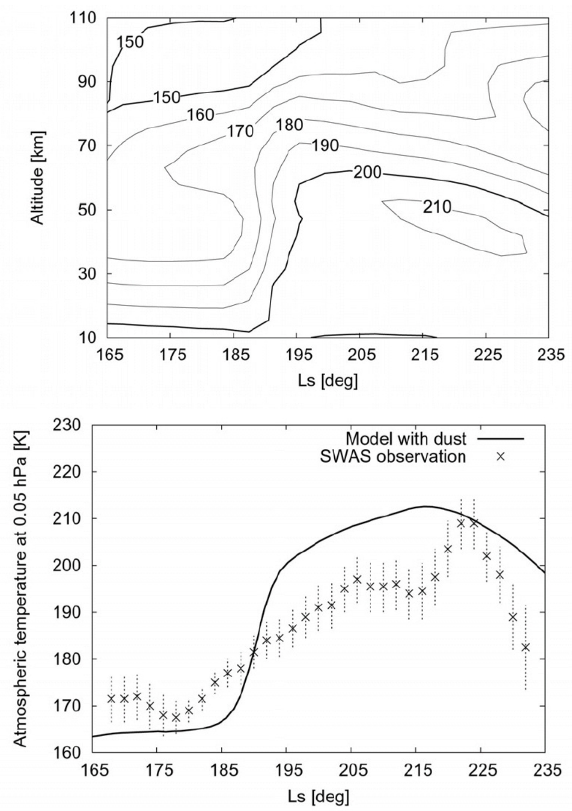


Fig. 162: Top: Vertical distribution of the global-mean atmospheric temperature simulated in the MAOAM-GCM with the dust radiation. Bottom: The time series of the global mean atmospheric temperature at 0.05 hPa from the model (the solid line) and from the SWAS observations (crosses and dotted error bars).

(T. Kuroda, A. S. Medvedev, and P. Hartogh)

### Middle atmosphere polar warmings on Mars: Simulations and study on the validation with sub-millimeter observations

Temperature inversions above 30 – 40 km and the associated warmings in the Martian polar winter atmosphere are caused by the adiabatic heating due to the descending branch of the poleward Hadley circulation. Using our recently developed Martian GCM (MAOAM), we demonstrate that global meridional transport in the middle atmosphere of Mars is driven primarily by the eddies (planetary waves and tides) through the mechanism called "extratropical pump", similar to the one in the terrestrial atmosphere. Existing observations cannot definitely validate the magnitude and location of the Martian winter polar warmings, and therefore cannot constrain general circulation models. We evaluated the capabilities of ground-based observations using a sub-millimeter wave interferometer, and performed radiative transfer and retrieval simulations for a low circular Mars orbit sub-mm wave limb sounder. The results show that the very good atmospheric transmission at Chajnantor (the ALMA site) will allow observations of the CO 6-5 rotational transition in the Martian atmosphere (Fig. 163). This line can be used to retrieve wind and temperature profiles from the surface up to about 80 km and higher, depending on the solar longitude. According to the simulation results, the sub-mm limb sounder provides high quality wind and temperature data up to at least 100 km (Figs. 164 and 165), which is very well suited for the validation of our GCM calculations.

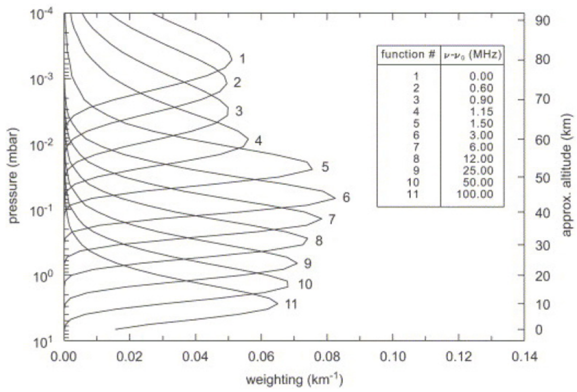


Fig. 163: Weighting functions for the CO 6-5 line in the Martian atmosphere (ground-based measurement, integrated over the whole disc with 32 rings in nadir and 32 rings covering the limb contributions). For the frequency offset zero, the weighting function peaks at 80 km.

(P. Hartogh, C. Jarchow, and A. Medvedev)

### New dynamical core for MAOAM

Implementation of a new spectral dynamical core into MAOAM GCM represents a major development of the model. The Martian atmosphere is thin, and Martian winds are strong. This puts strong constraints on the model in order to maintain numerical stability. The former grid dynamical core was specially designed for use in the middle atmosphere of Earth and Mars, but was not effective in the lower atmosphere. We implemented a new spectral dynamical core developed in IAP (Kühlungsborn). This dynamical engine is equally efficient in both lower and middle atmospheres. Adaptation to the Martian GCM included several major updates. They are: 1) Inclusion of the variable mass of the atmosphere; 2) Inclusion of the dry convective adjustment scheme suit-

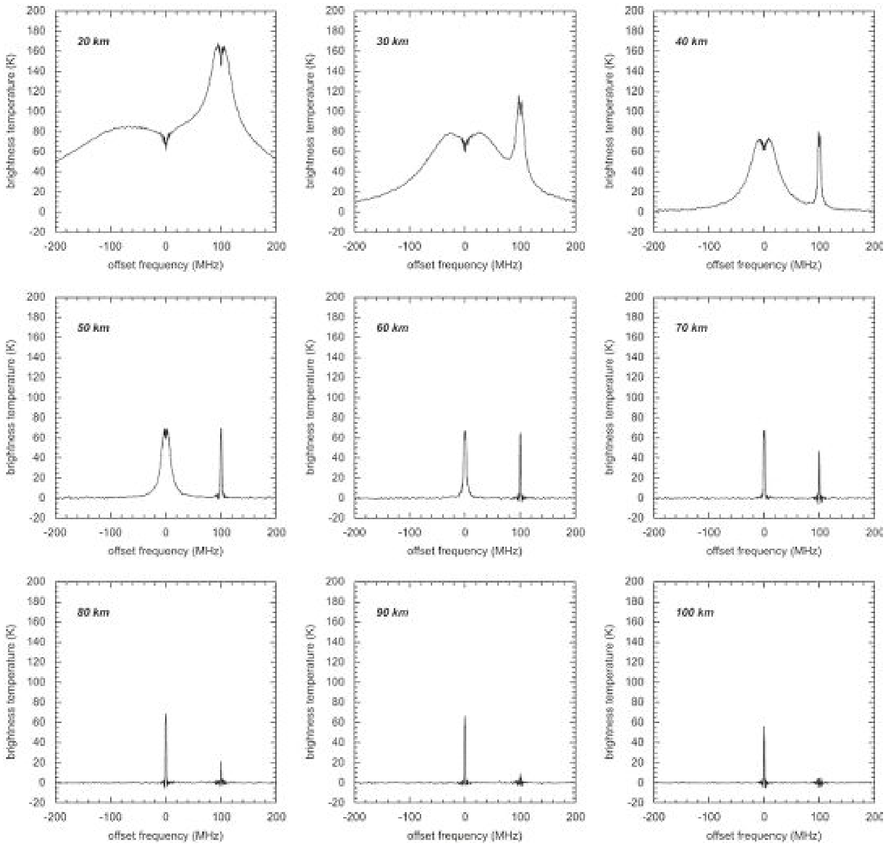


Fig. 164: Simulated limb sounding spectra of 12-CO (576 GHz) and 13-CO (551 GHz) for tangential altitudes between 20 and 100 km observed from 500 km altitude. Retrieval of these spectra provides high quality temperature profiles.

able for Mars; 3) Implementation of the $CO_2$ condensation/sublimation scheme; 4) Inclusion of multi-processing capabilities. The model with a new dynamical core was rigorously tested. It now adequately describes low level eddy variability (Held-Suarez tests), and maintains all the advantages of the former grid core in the upper atmosphere. The redesigned MAOAM is now approximately 2 times faster. This allows us to increase the resolution and realistically describe near-surface processes, which were shown to provide extremely strong response in the upper atmosphere (thesis of R. Saito, see also Fig. 166).

(A. Medvedev and P. Hartogh)

**MARSIS on Mars Express**

The Mars Express spacecraft carries a low-frequency radar called MARSIS (Mars Advanced Radar for Subsurface and Ionosphere Sounding) that is designed to study the subsurface and ionosphere of Mars. MARSIS was ready to make observations after deployment of the large dipole antenna (40 m tip-to-tip) in the summer of 2005 and started measurements the following August.

*Ionosphere*

Several types of ionosphere echoes are observed, ranging from vertical echoes caused by specular reflections from the horizontally stratified ionosphere to a wide variety of oblique and diffuse echoes. Echoes at the electron plasma frequency and the cyclotron period also provide measurements of the local electron density and magnetic field strength.

*Chapman layers*

The sounder spectrograms typically have a single trace of echoes controlled by nadir reflections. With the local density at the spacecraft derived from the measurements and using the lamination technique the spectrograms are inverted to electron density profiles. The observations yield density profiles from the sub-solar region to past the terminator. It is the first time the Martian ionosphere has been observed for solar zenith angles $< 48$ degrees, a limit imposed by the radio occultation technique yielding earlier measurements. The maximum density was shown to be controlled by the intensity of solar ionizing radiation (Fig. 167). Density increases associated with solar flares were

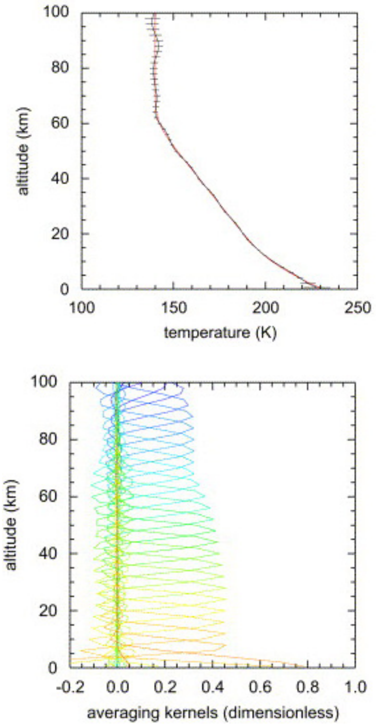


Fig. 165: Temperature limb scan retrieval simulation of the Martian atmosphere. Compare with the averaging kernel functions (a measure of the observation sensitivity to a certain altitude).

observed. The density variations around the density maximum is well accounted for by the Chapman theory, and the maximum density varies with solar zenith angle as predicted by the theory. The neutral scale height is from 10 to 14 km. The densities above the exobase tends to be larger than the extrapolation of the Chapman fit to the profile near the density maximum, implying effective upward diffusion above the collision dominated photo equilibrium region.

(E. Nielsen and H. Zou)

*Stationary reflectors in magnetic cusps*

The oblique echoes are believed to arise mainly from ionosphere structures associated with the complex crustal magnetic fields of Mars. At times two traces are present in the spectrograms. One of these traces corresponds to reflections from nadir, while the other oblique trace is shown (correcting for spacecraft dynamics) to be associated with the cusp like regions of near-vertical crustal magnetic fields (Fig. 168). In these regions the ionosphere appears to swell upward to form spatial density variations that allow for reflections in large off-vertical directions. On occasions the oblique trace is consistent with horizontal propagation implying vertical density structures. This points to

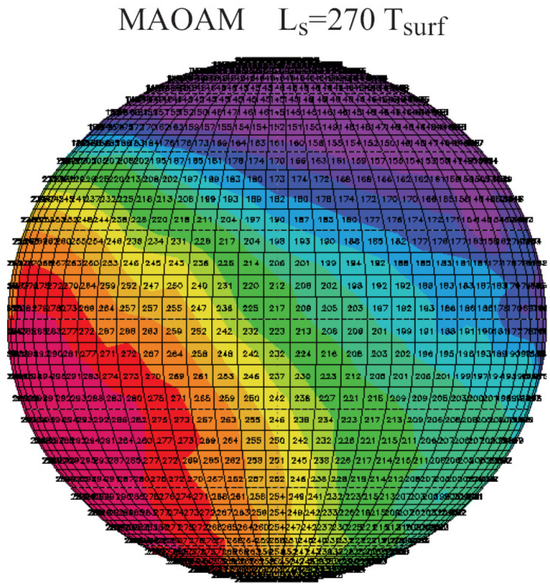


Fig. 166: MAOAM surface temperatures: result of Ryu Saito's PhD thesis.

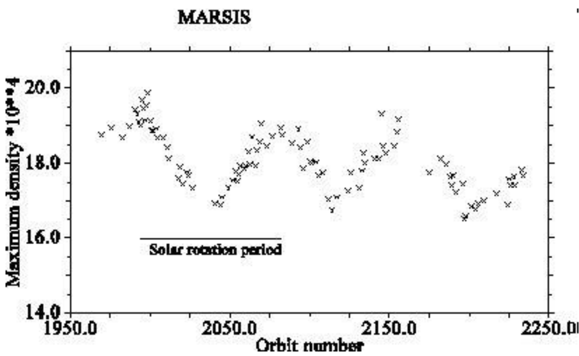


Fig. 167: Time variation of the maximum sub-solar electron density over a three month period with the solar rotation period marked. It reveals control of the Martian ionosphere densities by solar ionizing radiation.

steep gradient in the isodensity contours. Such gradients may arise owing to preferential access of solar wind energy to the cusp like regions or to precipitation of energetic electrons from acceleration regions located on cusp magnetic field lines high above the ionosphere.

(E. Nielsen and X. D. Wang)

*Absorption and reflections*

Radio wave absorption and reflection in the Martian ionosphere has been predicted on the basis of models and the results were tested against MARSIS radar observations. Models of electron densities and of absorption in a $CO_2$ dominated neutral atmosphere were used. The appearance of ground reflections in the

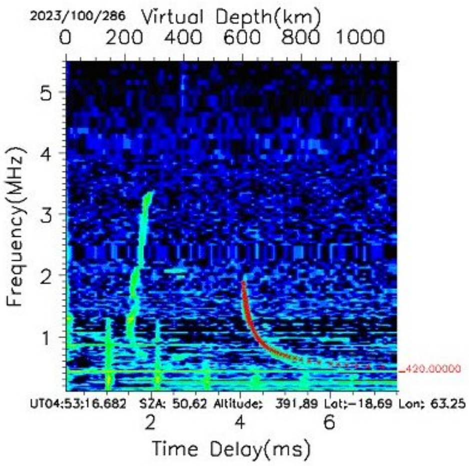


Fig. 168: Nadir echo trace (left) and oblique trace characterized by a strongly increasing delay time as the frequency decreases toward 0.4 MHz. The red data points are the predicted delay time for a signal propagating horizontally in a 0.4 MHz dense plasma to and from a vertical reflector. The good agreement between observation and prediction is a strong argument for near vertical reflecting structure in the ionosphere.

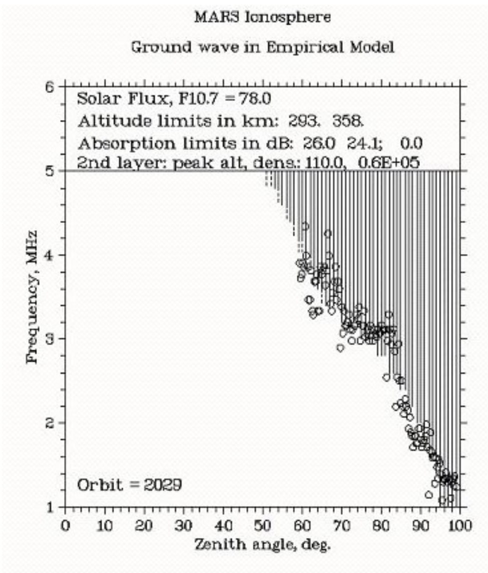


Fig. 169: The minimum frequency for ground reflections are plotted versus solar zenith angle (round sign). The cross-hatched region denote where ground reflections are predicted to occur. Combining absorption calculations in both the primary and secondary density maxima brings the observations in good agreement with prediction.

observations is shown to be consistent with predictions of reflection and absorption in the ionosphere (Fig. 169). It is concluded that the secondary density maximum, known to be typically present below the primary density peak, contributes considerably to the absorption and thus to the appearance of ground

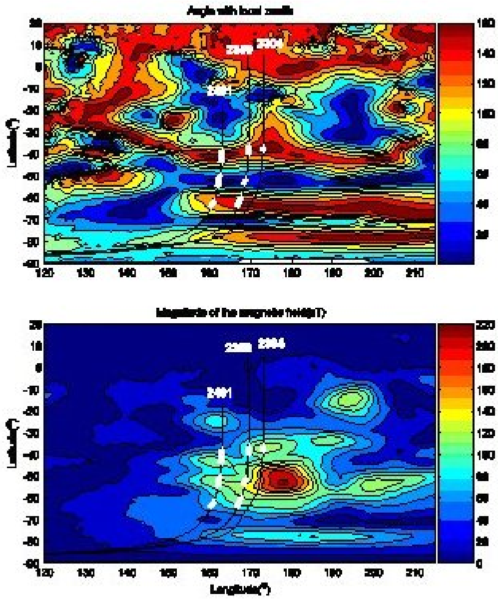

Fig. 170: Spatial maps of the inclination (top panel) and magnitude (lower panel) of the Martian crustal magnetic fields. Superposed on both maps are the ground tracks of the relevant orbits with location marked where peak density enhancement were observed. There is clear relation of the enhanced density events and with vertical and strong magnetic fields.

reflections. It is the first time predicted radio wave absorption in a $CO_2$ planetary atmosphere has been tested against actual observations.

(E. Nielsen)

*Local plasma processes*

Joint observations of MARSIS and ASPERA-3 have shown that events of intense ionospheric density enhancements occur in the lower ionosphere of magnetic crust regions (Fig. 170), and that these enhancements are not associated with precipitation of charged particles above a few hundred electron volts, much too low to account for the observed enhancement. No ionizing radiation, neither energetic particles nor X-rays, could be identified, which could explain the observed events. Actually, no increase in ionizing radiation, localized or not, was observed. It is argued that the process causing the increase in density is controlled mainly by convection of ionosphere plasma driven by the interaction between the solar wind and crustal magnetic field lines leading to excitation of two-stream instability in the cusp ionosphere. The result is to heat the plasma, reduce the electron-ion recombination coefficient and thereby increase ethe equilibrium electron density.

(E. Nielsen, M. Fraenz, and H. Zou)

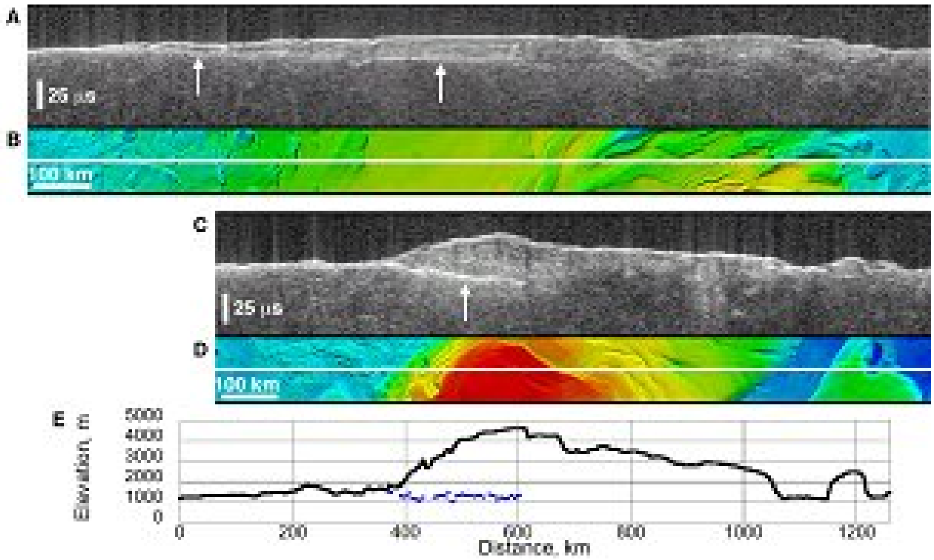


Fig. 171: (A) MARSIS data showing typical features of the SPLD. (B) MOLA topography along the ground tract. The lower interface (arrows) is interpreted as the SPLD interface with the substrate. (C) and (D) MARSIS data and MOLA topography. (E) MOLA surface elevation and MARSIS measured basal elevation (blue), assuming refractive index of ice.

*Subsurface*

The Martian subsurface has been probed with low frequency radio waves to a depth of several kilometers. Signals penetrating the polar layered deposits have imaged the base of the deposits. Observations in the northern lowlands of Chryse Planitia have revealed a shallow-buries, quasi-circular structure of about 250 km in diameter, that is interpreted as an impact basin.

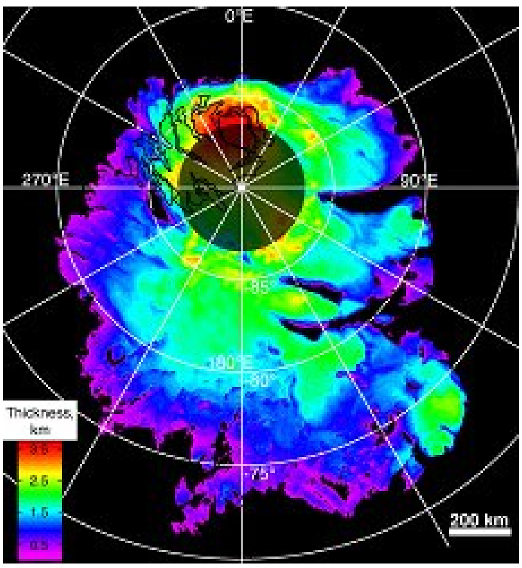


Fig. 172: Map of SPLD thickness based on MARSIS measurements and MOLA topography, equivalent to 11 m global water depth.

*Water revealed*

The radar signals penetrate deep into the ice-rich south polar layered deposits (SPLD) to a depth of more than 3.7 km. For most of the area a reflection is detected at a time delay consistent with an interface between the deposits and the substrate (Fig. 171). The reflected power from this substrate indicates minimal attenuation of the signal suggesting a composition of nearly pure water ice. Maps were generated of the thickness of the layered deposits (Fig. 172). The thickness map shows an asymmetric thickness. The total volume is estimated to be 1.6 × 106 km3, equivalent to a global water layer approximately 11 meters thick.

(E. Nielsen and T. Hagfors)

**Solar wind/ionosphere interface on Mars from comparative analysis of MEX-ASPERA-3 and MEX-MARSIS observations**

In-situ plasma and magnetic field measurements by the ASPERA-3 and MARSIS instruments complement each other and for the first time provide us with the parameters of cold ionospheric and hot solar wind components, and allow us to determine the pressure components and their balance in the solar wind/ionosphere interface. The MARSIS sounding experiment on MEX can trace not only ionospheric height profiles below the spacecraft from remote radio sounding, but also can infer the local plasma number density and the magnetic field strength from locally generated plasma echoes It is shown that the structure of the interface region can vary a lot. In some

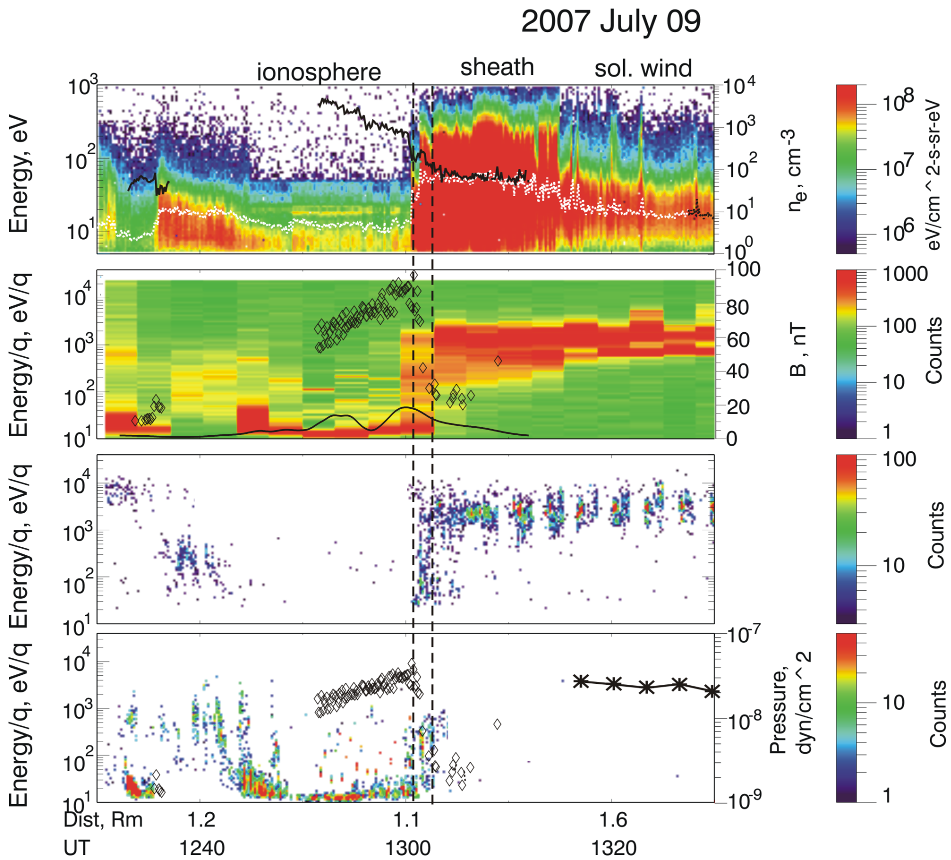


Fig. 173: Energy-time spectrogram of the electrons (top panel) with the imposed curves of $n_e$ from ASPERA (white) and MARSIS (black). The ionosphere is well recognized from the appearance of the energy peaks in the range between 20 and 30 eV on the electron spectrograms due to absorption of the strong HeII line at 30.4 nm in the carbon dioxide dominated atmosphere on Mars. The curves of the total electron density inferred from MARSIS and solar wind electrons ($E_e > 5$) (ASPERA-3) begin to diverge closer to Mars indicating a dropout of the solar wind and a dominance of a cold ionospheric component inside the magnetosphere. This transition is very sharp ($\sim$ 25 km in the normal direction to the boundary) and accompanied by a sudden jump of the magnetic field value inferred from MARSIS and depicted on the second panel by diamonds. This abrupt jump corresponds to the magnetic pile-up boundary (MPB). Energy time spectrograms of ions are on the lower panels: all ion species, $He^{++}$, and heavy ($m/q > 16$) ions. Imposed curves on the bottom panel are the magnetic pressure (diamonds), solar wind ram pressure (asterisks). The induced magnetic field balances the solar wind dynamic pressure.

cases, the main agent providing the solar wind termination at 450 – 500 km is the piled-up IMF. The magnetic field raises up to the value sufficient to balance the solar wind pressure. The solar wind ram pressure varies by a factor 5 – 6 although the position of the magnetospheric boundary almost does not change. This implies a strong coupling between the process of the formation of the magnetospheric cavity, ion extraction and solar wind. Probably we deal with a regime of 'heavy mass-loading' when the load by a planetary plasma becomes so strong that the ambient flow is completely stopped. The width of this region estimated in the assumption of the stationary picture can also be different varying from 25 to 800 km. There are also cases when the magnetic field almost does not change across the magnetospheric boundary. Such a configuration is built in the hemisphere out of which the motional electric field of the solar wind points. Our observations also for the first time show that the transition from the magnetospheric boundary (MB) to the ionospheric boundary (PEB) is accompanied by an increase in the plasma density. A density increase is also observed across the magnetic pile-up boundary. This region contains a mixture of different plasmas and forms the transition from solar wind to the ionospheric plasma. The magnetic field frozen to the electrons is transported through the magnetospheric boundary while the composition and origin of plasma changes drastically (Fig. 173). An important feature is the existence of a rather sharp ionospheric boundary (PEB). Although this boundary was previously tentatively identified from the drop of $CO_2$ photoelectrons only the MARSIS observations showed that the electron number density abruptly increases on this boundary up to $\sim 10^3$ cm$^{-3}$. Its existence can be maintained by the inward directed ambipolar electric field driven by a strong increase in the draping of the field lines at and behind the MB – central parts of the field lines are anchored in a dense ionosphere while their ends are carried by solar wind. Another possible mechanism suggests that the ionospheric plasma is 'pierced' by the induced magnetic field generated by the ionospheric currents which strongly reduces the characteristic plasma scale height.

(E. Dubinin, M. Fränz, and J. Woch in collaboration with Iowa University, USA)

### Pickup protons at Mars and their acceleration at the bow shock

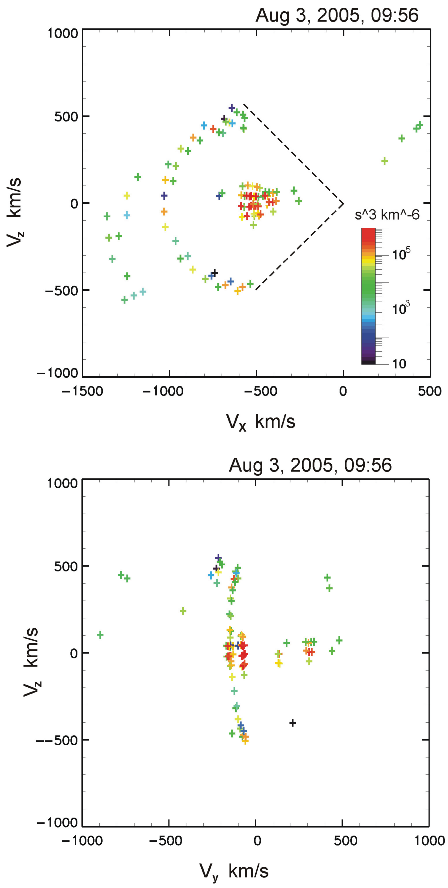


Fig. 174: Two slices of typical distribution functions of pickup protons in the $V_x V_z$ and $V_y V_z$ planes, which are close to the $\boldsymbol{V}_{sw}$ $\boldsymbol{E}_{IMF}$ and $\boldsymbol{B}_{IMF}$ $\boldsymbol{E}_{IMF}$ planes, respectively (only solar wind and primary pickup protons are shown in the bottom panel). Colours represent the values of distribution functions. Dashed curves bound the field of view of the instrument in the sunward hemisphere.

Pickup protons (PIs) with a ring-beam distribution originating from the extended hydrogen exosphere of Mars are observed by the ASPERA-3 experiment onboard the Mars Express spacecraft at solar minimum conditions (Fig. 174). PIs can contribute $\sim 1$ % to the solar wind number density at close distances to the flank bow shock. At the bow shock, pickup protons experience an efficient reflection accompanied by ion energization in the motional electric field. Despite the small scale of the Martian bow shock the acceleration of PIs is rather effective and can operate for injection of pre-energized ions into a subsequent acceleration process (Fig. 175). The injection efficiency is derived to be about $\geq 20$ %. These results imply that similar processes at shocks with much larger scales (e.g. the termination shock) can be important for ion acceleration.

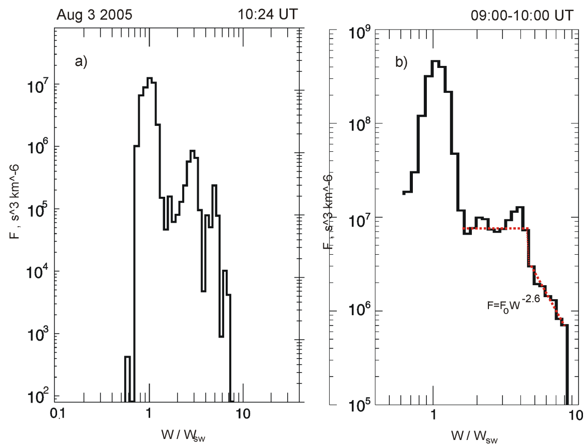


Fig. 175: Distribution functions of the proton component upstream from the bow shock averaged over all azimuth and elevation angles during one scan (a) and during one hour (b). Multiple peaks on panel (a) correspond to multiple reflections of pickup protons. (b) Above $W/W_{sw} \sim 4$ the $H^+$ spectrum is fitted by a power law spectrum with $W^{-2.6}$.

(E. Dubinin, M. Fränz, and J. Woch)

### Suprathermal Electrons as a Source of Aurora on Mars

Recently aurora-type UV emissions were discovered on the nightside of Mars (*Bertaux et al.,* 2005). It was suggested that these emissions are produced by suprathermal electrons with energies of tens of eV, rather than by the electrons with spectra peaked above 100 eV (*Leblanc et al.,* 2006). Observations of fluxes of suprathermal electrons ($E_e \approx 30 - 100$ eV) on the Martian nightside by the ASPERA-3 experiment onboard the Mars Express spacecraft show the existence of narrow spikes in energy-time spectrograms at altitudes between 250 – 600 km. These spikes are spatially well organized and form narrow strips in regions with strong upward and downward vertical com-

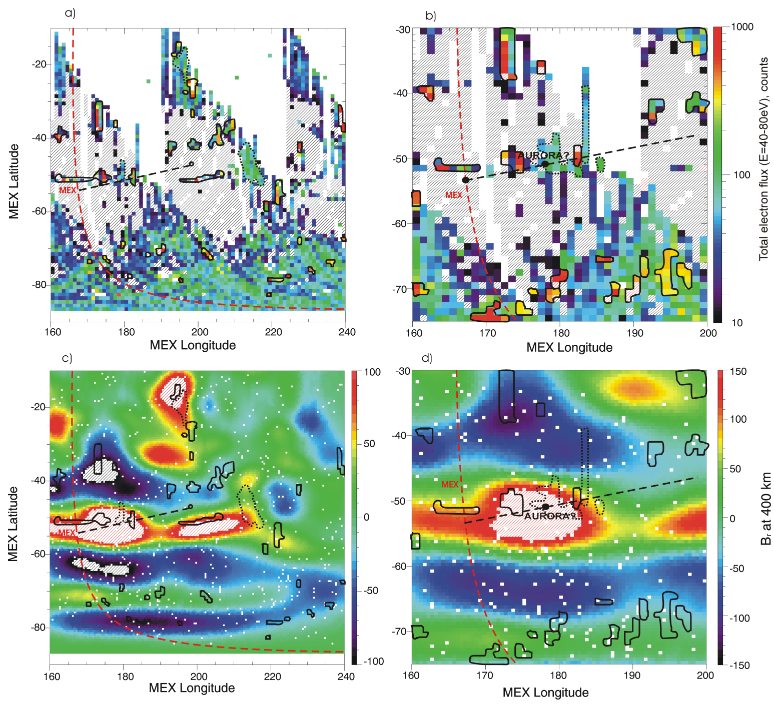


Fig. 176: Maps of mean (panel a) and max (panel b) values of the electron fluxes ($E_e = 40 - 80$ eV) measured at altitudes of 250 – 600 km in the regions of strong crustal field on the nightside of Mars. The MEX trajectory and the line of sight (LOS) of the SPICAM instrument on the orbit when SPICAM has detected aurora-type emissions are shown by the red and black dashed curves, respectively. On panel (b) the different scales are used to enlarge the region of the SPICAM measurements. (c, d) Vertical component of the magnetic field at 400 km. It is observed that the regions with strong crustal fields in the latitude range $-65°$ to $-30°$ are almost void of electron fluxes excepting narrow bands, stretched in longitude, in which the fluxes of suprathermal electrons are enhanced (these bands are bounded by black curves). The vertical crustal magnetic field in these bands can focus electrons to the altitudes $\sim$150 km where aurora-type emissions are produced.

ponents of the crustal magnetic field (Fig. 176). The values of electron fluxes in such events generally could explain the observed auroral UV emissions.

(E. Dubinin, M. Fränz, and J. Woch)

### Inflations of the magnetospheric cavity on Mars due to crustal magnetization

Due to a local origin of crustal magnetic sources on Mars and their additional contribution to the total ionospheric pressure which balances the solar wind pressure peculiar bulges on the magnetospheric surface can arise. Fig. 177 presents the example of the ASPERA-3 measurements carried out on 18 October 2005. The upper panel shows the spectrogram of electron fluxes. The Mars Express (MEX) spacecraft moving along the outbound trajectory at the dayside exited the magnetosphere at $\sim$2252 UT. The exit is accompanied by the appearance of magnetosheath electrons. The solar zenith angle (SZA) and the MEX altitude were $\sim 10°$ and $\sim 300$ km, respectively. At $\sim$2256 UT (SZA $\sim 25°$, ALT $\sim 400$ km) MEX suddenly again occurs in the ionosphere that is observed by a drop of the solar wind electrons and appearance of typical $CO_2$ ionospheric peaks of photoelectrons at 22 – 25 eV. At last, at $\sim$2301 UT (ALT $\sim 650$ km) the spacecraft finally exited the magnetosphere. The region of a sudden inflation of the magnetosphere coincides with the strong local magnetic field source. The second panel depicts the crustal magnetic field at an altitude of 400 km. The magnetic field value reaches $\sim 60$ nT and therefore can deflect the magnetosheath flow and produce a corrugated shape of the boundary.

(E. Dubinin, M. Fränz, and J. Woch)

### Influence of crustal magnetization on solar wind induced escape

The crustal magnetic fields on Mars influence the pattern of escape fluxes of planetary ions. Scavenging of planetary ions is less efficient in the regions of strong crustal magnetization and therefore the solar wind induced losses of atmospheric and ionospheric matter in the southern hemisphere are smaller. Fig. 178 shows the map of the oxygen ion number densities measured in the altitude range of 250 – 2000 km for solar zenith angle $> 90°$ as a function of planetocentric latitude and longitude. The bottom panel depicts the inverse

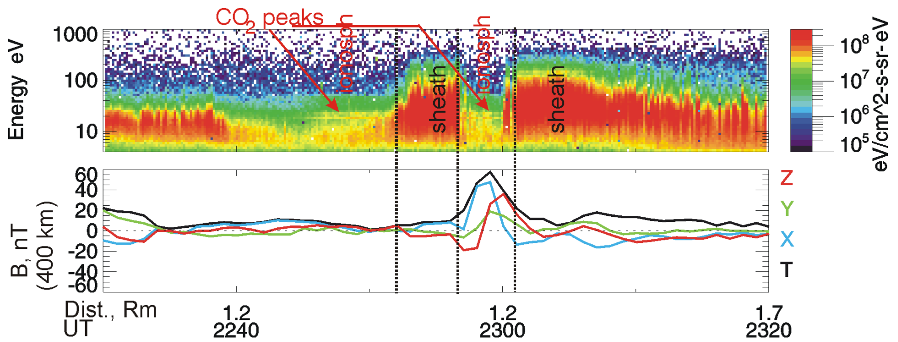


Fig. 177: Spectrogram of electron fluxes and the crustal magnetic field at the altitude 400 km, along the MEX orbit on 18 September 2005.

of the total crustal field strength at 400 km from Connerney *et al.* (2001). It is observed that the northern hemisphere is a stronger source of planetary ions escaping to the tail. The southern part of the magnetosphere, especially the regions with strongest crustal fields are better protected from the solar wind induced escape.

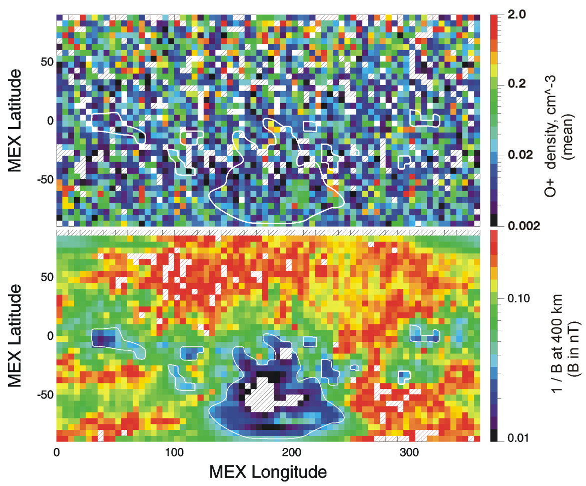


Fig. 178: Top: Map of the mean values of the oxygen ion density ($O^+$) as a function of planetocentric eastern longitude and latitude. Bottom: Inverse of the total crustal field strength (1/nT) at 400 km altitude. The regions of the strongest crustal sources are bounded by the white curves.

(E. Dubinin, M. Fränz, and J. Woch)

## Field-aligned currents and parallel electric field potential drops on Mars

The observations of electron inverted 'V' structures by the MGS and MEX spacecraft, their resemblance to similar events in the auroral regions of the Earth, and the discovery of strong localized magnetic field sources of the crustal origin on Mars raised hypotheses on the existence of Martian aurora produced by electron acceleration in parallel electric fields. Similar to the Earth, upward field-aligned currents necessary for the generation of parallel potential drops and peaked electron distributions can arise, for example, on the boundary between 'closed' and 'open' crustal field lines due to shears of the flow velocity of the magnetosheath or magnetospheric plasmas. A steady-state configuration assumes a closure of these currents in the Martian ionosphere. Due to much smaller magnetic fields as compared to the Earth case, the ionospheric Pedersen conductivity is much higher on Mars and the distribution of field-aligned currents and parallel potential drops on Mars can be different. Fig. 179 shows the results of the numerical solution of a current closure equation

$$j_\parallel = -\frac{\partial I_p}{\partial x} \tag{1}$$

using the Knight's relation between $j_\parallel$ and $\varphi_\parallel$, and assuming symmetrical boundary conditions $\varphi_{bp_{-\infty}} = \varphi_{bp_{+\infty}}$ and $\varphi_i \to \varphi_{bp}$ as $x \to \pm\infty$. The curves (a) of the potential $\varphi_i$ are plotted for the magnetospheric electric field $E_{b\infty} = \pm 0.5, 1, 2$ mV/m ($E_{i\infty} = \sqrt{(B_i/B_t)}E_{b\infty}$, $B_i/B_t = 10$, $n_e = 1$ cm$^{-3}$, $T_e = 50$ eV, $\Sigma_p = 20$ mho). The parallel potential drop increases with the ionospheric electric fields and varies between $\sim 150$ and 600 V which yields the kinetic energies of oxygen ions in the range 50 – 750 eV. Panels (b,c) depict also how $\varphi_i$ and $j_\parallel$ vary with $\Sigma_p$. The potential drop $\varphi_\parallel$ and field-aligned current increase with $\Sigma_p$. However for large values of $\Sigma_p$ structures become very broad and do not adjust to the characteristic scales of the crustal patches. Then a total field-aligned current is not able to supply a large Pedersen current in the ionosphere and a parallel potential voltage becomes comparable to a total voltage of the magnetospheric generator. Generally, two different scenarios may work. A perfectly conductive ionosphere can 'short-circuit' the magnetospheric electric field with a subsequent relief of magnetic field shear stresses in the generator region. In this case, a stationary model is not applied and one may expect, for example, a periodic storage and relief of the magnetic field tangential stresses. In another scenario, the field-aligned

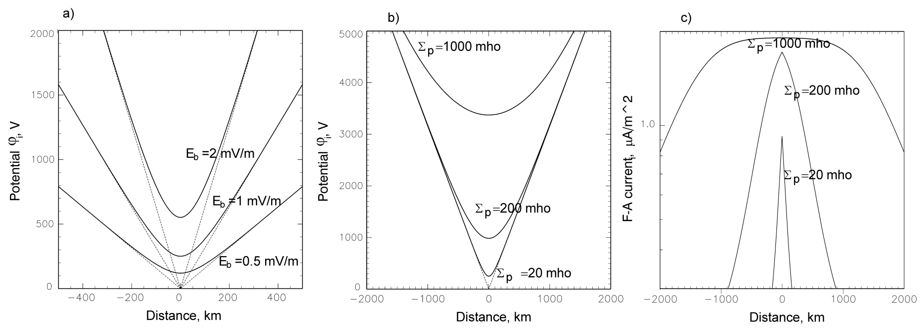


Fig. 179: (a) The ionospheric potential as a function of horizontal distance across the 'auroral' field tube on Mars at the nightside. The dashed curves correspond to the assumed boundary potentials. The field-aligned potential drop is a difference between these two curves. (b, c) The ionospheric potential and field-aligned current as a function of the distance for different $\Sigma_p$.

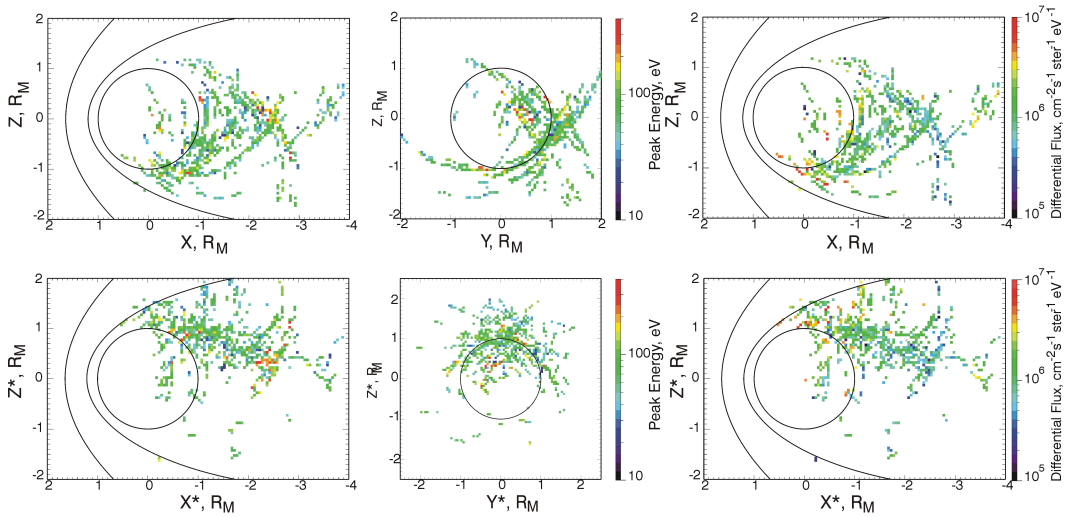


Fig. 180: (top) Maps of the events with peaked electron spectra in MSO coordinates, (bottom) maps in the coordinate system determined by the IMF direction. Colour shows the peak energy of electrons (left and middle panels) and the differential flux corresponding to the peak energies (right panels).

parallel potential drop decouples the stressed field in the generator region from the ionosphere and allows fast magnetospheric motions. The ionosphere is almost shielded from the magnetospheric electric field and the inverted 'V' structures arise at high altitudes.

(E. Dubinin, M. Fränz, and J. Woch)

### Peaked Electron distributions on Mars

Peaked electron distributions on Mars were observed at different altitudes on MGS and MEX. Analogy with inverted V structures in the Earth magnetosphere raised the questions whether aurora on Mars exist and whether there are significant field-aligned electric potential drops on the crustal field lines. More than 1500 events during two years of the MEX operation with peaks on differential flux spectra which could be candidates for aurora on Mars were analyzed. Fig. 180 (the top panels) presents a spatial distribution of all events in the XZ and YZ (MSO) coordinates. Events are observed in both hemispheres, not only in the southern one where crustal sources are localized, and at different distances from the planet. The maximum peak energies are measured at a large distance from Mars. There is also no clear trend of a peak energy increase with decreasing altitude as would be expected if we exploit a simple analogy with auroral processes on the Earth. On the other hand, fluxes are stronger in the southern hemisphere, closer to the planet. It is worth noting that in aurora on Earth both values, namely, the number flux of electrons and parallel potential voltage which can be inferred from the peaks in the energy spectra are equally responsible for the energy deposition in the atmosphere.

The bottom panels show spatial distributions of the 'inverted V' events in the coordinates determined by the IMF orientation (this system has the $X^*$ axis antiparallel with the upstream solar wind flow, the $Y^*$

axis along the cross-flow magnetic field component of the IMF, and the $Z^*$ axis is along the direction of the motional electric field $E = -\boldsymbol{V} \times \boldsymbol{B}_{IMF}$, where $\boldsymbol{B}_{IMF}$ has been taken from the MGS observations). Almost all peaked distributions are observed in the hemisphere into which the motional electric field is pointing. A map of planetary ion beams (not shown here), which often accompany the electron events with a peaked distribution, is similar. Peaked electron distributions can appear as the result of a coherent action of a combination of electrostatic potential and mirror-like magnetic field configuration. Since heavy planetary ions ($O^+$, $O_2^+$, $CO_2^+$) moving in the electric field driven by solar wind are not magnetized, ion and electron trajectories do not coincide. This can lead to the appearance of positive potential spikes and, correspondingly, to field-aligned fluxes of sheath electrons to supply a quasi-neutrality and provide $div\, \boldsymbol{j} = 0$, where $\boldsymbol{j}$ is the current density. Conservation of the electron magnetic moment in the piled up region of the Martian magnetosphere where the magnetic field strength increases results in a more isotropic distribution of the peaked electrons.

(E. Dubinin, M. Fränz, and J. Woch)

### Plasma moments in the environment of Mars

The Phobos-2 and Mars Global Surveyor missions to Mars gave us only a very limited view of the Martian plasma environment. For the first time we are now able to produce electron and ion moment maps (density, velocity and temperature) of this environment, using data from the ELS and IMA sensors of the ASPERA-3 experiment onboard Mars Express. Moments are calculated by integration and by Gaussian fits to the phase space distribution of thermal electrons and ions. The estimation of ionospheric electron densities assumes that the thermal electron temperature can be determined by the instrument – despite a cutoff by a negative spacecraft potential. The spacecraft potential is estimated by the location of photoelectron peaks in the energy spectrum. For the magnetosheath we can separate the low energy part of the electron spectrum – presumably spacecraft photoelectrons and the high energy part. For ions, we calculated maps for solar wind protons and alpha particles. Protons with energies below 500 eV which may play an important role in the ionosphere are not measured by the instrument. Similarly, the low speed solar wind protons are not sampled very well. The maps reveal all the boundaries of the Mars-solar wind interaction and give a good qualitative description of the plasma behaviour at the different interaction regions. Fig. 181 shows how electrons are heated in the region between bow shock and magnetic barrier around Mars and how the ion flow is deflected around this barrier. It is the first time that the magnetosphere of another planet than Earth has been mapped in this detail.

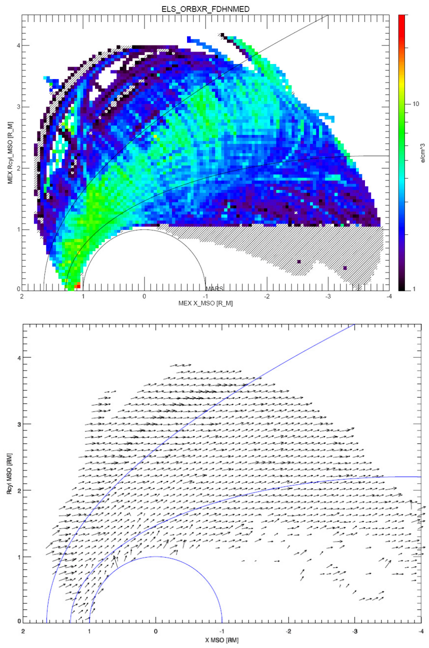


Fig. 181: Top: Median density of electrons with energies above 30 eV measured by the electron sensor of the Mars Express ASPERA-3 instrument for all orbits between 1 February 2004 and 1 March 2006 binned on a coordinate grid whose X-axis points toward the Sun and whose Y-axis is perpendicular to the Mars-Sun line. Bottom: Median ion velocity vector orientation in the same coordinate grid taken from alpha particle measurements of the ASPERA-3 instrument. Overplotted are the locations of the bow shock and magnetic pile-up boundary determined from magnetic field observations onboard Mars Global Surveyor.

(M. Fränz, E. Roussos, E. Dubinin, and J. Woch)

### Energetic electron asymmetries in the Martian magnetosphere

The interaction of Mars with the solar wind is primarily determined by the presence of the planet's dayside ionosphere. Still, it is difficult to establish the individual influence of all the different factors that control the global configuration of the Martian magnetospheric cavity. Complications could come from the presence of the strong crustal fields, their rotation with the planet, their continuously changing orientation with Martian season, and with respect to the interplanetary magnetic field (IMF) direction. In order to establish the origin of the various magnetospheric features that we observe, it was necessary to subtract the influence of all these complicating factors.

Using more than two years of observations with the

ASPERA-3 ELS electron sensor of Mars Express, we have organized electron densities and temperatures in various coordinate systems for the investigation of possible asymmetries in the formation and the origin of hot electron events that are observed in the Martian magnetotail. The data we used was obtained in different geometries with respect to the crustal magnetic fields and therefore their effect was averaged out to a large extent.

By binning the data with respect to the direction of the solar wind convective electric field, it was realized that magnetosheath electrons leak more effectively towards the magnetotail, in a region close to the terminator of the planet and in the hemisphere that the convective electric field points to $E^+$ sector (Fig. 182). This asymmetry is also visible in the magnetotail of the planet, where the occurrence of these hot electron events in the $E^+$ sector is also more frequent.

It is therefore concluded that a definite source region of hot electrons in the Martian tail is the magnetosheath at the terminator. These events seem to be transient rather than steady-state, as they appeared only when we plotted the maximum of the spatial distribution and not when we used a median average filter in our data. Physically, this asymmetric leaking probably occurs due to modulation of the magnetic pile-up boundary strength by the direction of the convective electric field, as hybrid plasma simulations of the Mars-solar wind interaction have shown.

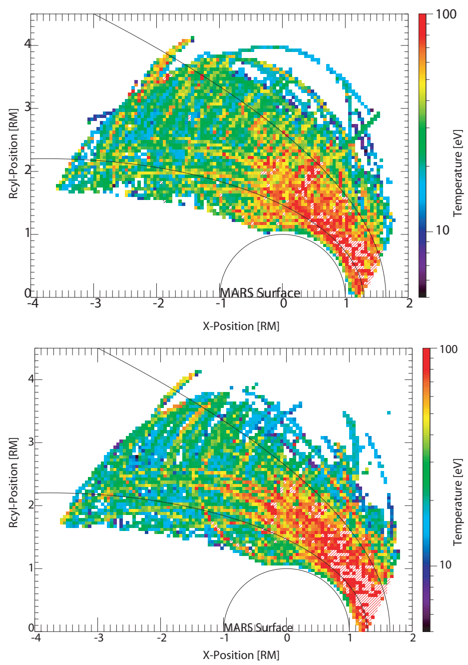


Fig. 182: Maximum electron temperatures (eV) in the Martian magnetosheath. The temperatures are separated in the $E^+$ and $E^-$ sectors (top and bottom panels, respectively).

(E. Roussos, M. Fränz, E. Dubinin, C. Martinecz, J. Woch, and U. Motschmann in collaboration with Southwest Research Institute, USA; University of Braunschweig, Germany; Swedish Institute of Space Physics, Sweden)

**Project MOMA**

*Introduction*

MOMA, the Martian Organic Molecule Analyser, is one of the instruments of the Pasteur payload of the European ExoMars mission which is scheduled to launch in 2013. The instrument team comprises members from Europe as well as the USA. It is part of a group of instruments for the detection of organic molecules. While the other instruments look for specific molecules with extremely high sensitivity, MOMA can, in principle, detect the presence of any organic molecule and identify it, although with lower sensitivity. The central part of the instrument is an ion-trap mass-spectrometer. It is used for the identification and quantification of molecules. Two major ion sources for the MS are envisaged: The first is the classical gas-chromatography/ mass-spectrometry (GC-MS) approach where solid soil samples are pyrolysed and the volatile fraction is separated by a GC and analysed by the MS. This channel also allows for chiral separation of enantiomers. The second is Laser Desorption (LD-MS) where larger and likely less volatile molecules are ionized via short Laser flashes, transferred to the MS and analysed. In order to aid the identification of intricate molecular mixtures it is possible to run the ion-trap in an MS-MS mode where a particular mass can be pre-selected and its fragments investigated further. Direct atmospheric sampling is also intended.

*Team and responsibilities*

The hardware team of MOMA comprises groups from three countries. The system lead and the team coordinator are located at MPS. The American group has members from the John Hopkins University, department of Physics and Astronomy, the Applied Physics Laboratory, and the Johns Hopkins School of Medicine in Baltimore (grouped as APL). The French contribution is supplied by the Service d'Aeronomie (SA) and the Laboratoire Interuniversitaire des Systèmes Atmosphériques (LISA) in Paris. The envisaged responsibilities for the hardware components of MOMA are as follows:

| component | responsible |
|---|---|
| Gas chromatograph | SA and LISA with MPS |
| Carrier gas system | SA with MPS and APL |
| Pyrolysis oven | MPS and APL |
| Vacuum system | APL with MPS |
| Electronics | MPS and APL |
| Mass spectrometer | APL and MPS |
| Laser | MPS with APL |
| Laser desorption head | APL with MPS |

*MPS activities in 2006 and 2007*

During 2006 and 2007 the project considerably gained momentum. DLR funding for four additional members of staff was secured at MPS. The project is funded under contract number 50QX0601.

An ESA funded study was the first opportunity for hardware development. In this study a commercial laser desorption source is interfaced to an ion trap mass spectrometer.

A laser study was started in cooperation with the company von Hoerner & Sulger (vHS) and the Laser Zentrum Hannover (LZH) in order to select the optimum laser design and to build a first breadboard model. This study ends in April 2007 and the results will be the basis of the following laser prototype development.

Since the instrument is under extreme pressure to reduce mass, the GC heritage concepts of COSAC on Rosetta and SAM on MSL09 are currently critically evaluated at MPS for further mass reduction.

The miniature valves used in COSAC but not available commercially are procured again as a special lot for MOMA under a DLR funded contract.

A special test chamber was currently built at MPS in order to perform tests under Martian atmosphere conditions of temperature, pressure, and gas composition. The size of the chamber will allow tests from simple components and sub-assemblies up to the complete flight instrument. The chamber is in use.

A first breadboard model of the laser was delivered by vH & S to MPS in early 2008.

Prototypes of GC column units were delivered by SA to MPS.

(F. Goesmann)

## Outer planets research – Jupiter and Saturn

### Comparison of periodic substorms at Jupiter and Earth

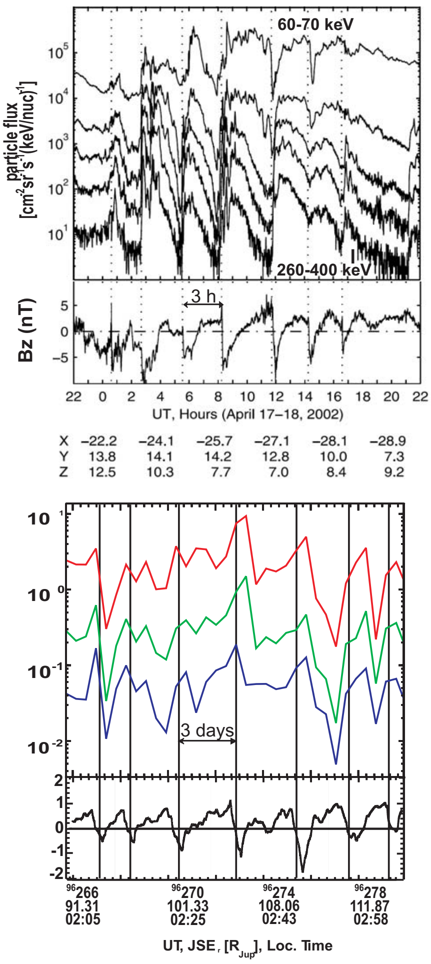


Fig. 183: A comparison of the proton fluxes and the meridional component of the magnetic field of the periodic magnetospheric substorms at Earth (17 – 18 April, 2002), left; and at Jupiter (day 266 – 282, 1996), right. The data for Jupiter are presented with 10 hour averaging, at 80, 220 and 540 keV. The plot for the terrestrial case is taken from Huang *et al.* (2003).

The Energetic Particles Detector and magnetometer measurements on Galileo showed that the Jovian magnetosphere undergoes reconfiguration processes which are very similar to the characteristics of a terrestrial substorm. At Jupiter the reconfiguration process occurs quasi-periodically with a repetition period of several days. In the terrestrial magnetosphere periodic substorms have been occasionally observed. The comparison of these periodic magnetospheric disturbances shows that they are similar in dynamic features as well as in spatial distribution, but have different energy sources. In the case of the Earth, the well established energy source is the solar wind. In the case of the Jovian magnetosphere, it is believed that the internal energy is supplied by mass loading of fast rotating flux tubes. The energy accumulation and release leads to similar features: in the particle data we observed periodic "sawtooth" intensity fluctuations, plasma pressure and bulk velocity variations (Fig. 183). Reoccurring signatures of stretching and dipolarization are observed in the magnetic field. Furthermore, the release process is associated with an intensification of auroral emissions. The periodic reconfiguration process in the Jovian magnetotail consists of a transition from a "quiet" (loading) state to a "disturbed" state. In analogy with the terrestrial substorm process the initial "loading" phase resembles the growth phase and the "disturbed" phase resembles the expansion phase of periodic terrestrial substorms. A closer look at the substorm-like processes in the Jovian magnetosphere also reveals further features similar to the terrestrial substorms, such as the onset of magnetic fluctuations with the frequency of an ion gyroperiod in the magnetotail, plasma sheet boundary layer formation, signatures of travelling compression regions (TCR) and the formation of a post plasmoid plasma sheet.

(E. Kronberg, J. Woch, N. Krupp, and A. Lagg in collaboration with Applied Physics Laboratory/The Johns Hopkins University, USA; Technical University Braunschweig, Imperial College London, UK)

### In-situ observations of the Saturnian magnetosphere and interaction of magnetospheric particles with moons

*Energetic particles in the Saturnian magnetosphere: MIMI/LEMMS results onboard Cassini after two years in orbit around Saturn*

In July 2004 the Cassini spacecraft began its orbital tour through the Saturnian system and performed orbits during the first two years of the mission (July 2004 – January 2007). One of the scientific instruments aboard Cassini is the Low Energy Magnetospheric Measurement System LEMMS, one out of three particle detectors of the Magnetospheric Imaging Instrument MIMI. This instrument measures the intensity, energy spectra, and pitch angle distributions of energetic ions ($E > 30$ keV) and electrons (20 keV $< E < 5$ MeV). Those measured energetic particles together with the measured magnetic field provide a very powerful tool to investigate the structure and dynamics of the Kronian magnetosphere over a variety of radial distances and local times. A statisical analysis shows that magnetospheric key regions such as plasma sheet, lobe, and radiation belts could have been determined and that they differ as a function of radial distance, local time, and partly latitude along the Cassini orbits.

An overview of energetic electron measurements from the first 36 orbits of the Cassini mission in the Kronian system is shown in Fig. 184.

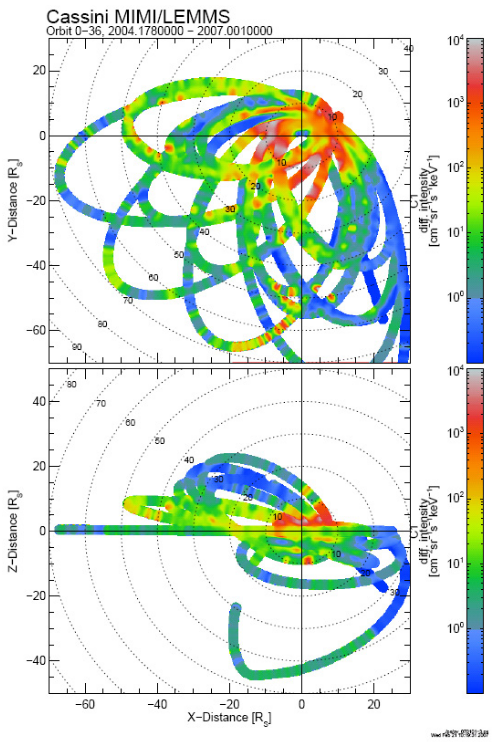


Fig. 184: Differential intensity of electrons as measured by the MIMI/LEMMS instrument onboard Cassini during the first 36 orbits of the mission (from day 178, 2004 to day 001, 2007). Shown is the colour-coded intensity of electrons (28 – 49 keV) along the Cassini orbits and projected into the equatorial plane (top) and perpendicular to it (bottom).

The data coverage in the Saturnian system after those orbits is already quite good, especially the local dawn to midnight sector in the equatorial plane. Highest intensities have been observed between 4 and 15 Saturn radii. At comparable distances the highest intensities were found in the midnight sector. Also the latitudinal data coverage has been getting better since the high inclination phase of the Cassini mission began in 2006. Further investigations are underway to classify and determine the differences in the particle fluxes with respect to local time, radial distance, and longitude inside the Saturnian system.

(N. Krupp, A. Lagg, E. Roussos, G. H. Jones, and J. Woch in collaboration with Applied Physics Laboratory/The Johns Hopkins University, USA)

*Anti-planetward auroral electron beams at Saturn*

Strong discrete aurorae on Earth are excited by electrons, which are accelerated along magnetic field lines towards the planet. Surprisingly, electrons accelerated in the opposite direction have been recently observed. The mechanisms and significance of this anti-earthward acceleration are highly uncertain because only earthward acceleration was traditionally considered, and observations remain limited. It is also unclear whether upward acceleration of the electrons is a necessary part of the auroral process or simply a special feature of Earth's complex space environment. Here we report anti-planetward acceleration of electron beams in Saturn's magnetosphere along field lines that statistically map into regions of aurora (Fig. 185). The energy spectrum of these beams is qualitatively similar to the ones observed at Earth, and the energy fluxes in the observed beams are comparable with the energies required to excite Saturn's aurora. These beams, along with the observations at Earth and the barely understood electron beams in Jupiter's magnetosphere, demonstrate that anti-planetward acceleration is a universal feature of aurorae. The energy contained in the beams shows that upward acceleration is an essential part of the overall auroral process.

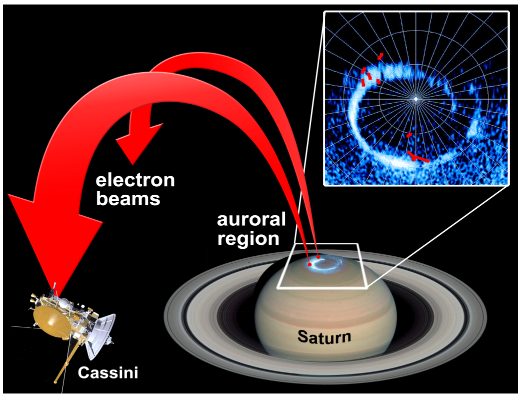


Fig. 185: Sketch of the electron beams mapping into the auroral zone of Saturn as observed by the Cassini MIMI/LEMMS instrument.

(N. Krupp, A. Lagg, and E. Roussos in collaboration with Applied Physics Laboratory/The Johns Hopkins University, USA)

*Formation of Saturn's ring spokes by lightning-induced electron beams*

Spokes are near-linear markings sometimes visible on Saturn's rings. They are widely accepted as being electrostatically-levitated sheets of 0.6 micron-radius charged grains. Previously-suggested causes of the grains' charging do not agree with all spoke characteristics, which include their rapid generation, localized formation primarily in Saturn's midnight-dawn sector, the seasonality of their apparitions, and, crucially, their morphologies. This study shows that spokes are caused by lightning-induced electron beams striking the rings at locations magnetically connected to thunderstorms (Fig. 186). This view is supported by a semi-quantitative spoke morphology simulation. Spokes' formation locations are further controlled by Saturn's ionospheric density, which reaches a near-dawn minimum where electron beams can most easily propagate to the rings. The beams may generate observed X-ray emission, supply particles to Saturn's radiation belts, and over time will modify the rings' constituents. Finally, we report Cassini MIMI instrument observations of an electron burst which displays some characteristics expected of a lightning induced event.

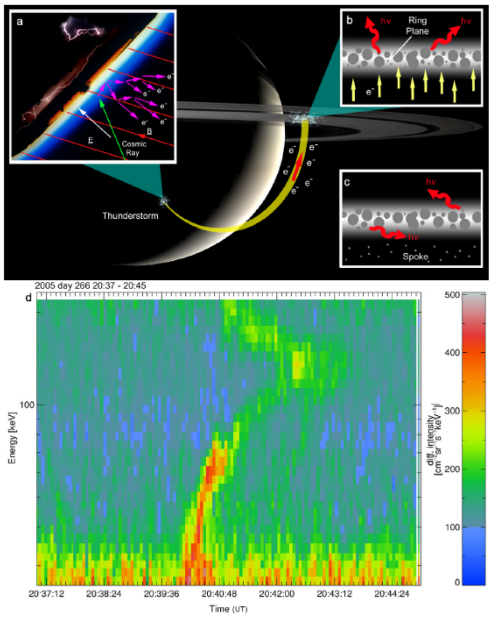


Fig. 186: The spoke formation process. (a) A cosmic ray particle triggers an upward electron avalanche above a thunderstorm. (b) The electrons propagate along Saturn's magnetic field lines, and on striking the rings induce rapid negative charging of ring grains and high-energy bremsstrahlung emission. The ring atmosphere is also ionized, dissociated, and excited by electron impact. Auroral emission emanates from excited gases, including in the X-ray range. (c) Large ring particles lose their small grain regoliths, which are repulsed by the ring to form a spoke. (d) A highly unusual electron burst consistent in some respects with a thunderstorm origin, observed at 17:48 local time (LT) by Cassini.

(G. H. Jones, N. Krupp, H. Krüger, E. Roussos, J. Woch, A. Lagg, and M. Fränz in collaboration with Applied Physics Laboratory/The Johns Hopkins University, USA; Imperial College London, UK; Mullard Space Science Laboratory, UK)

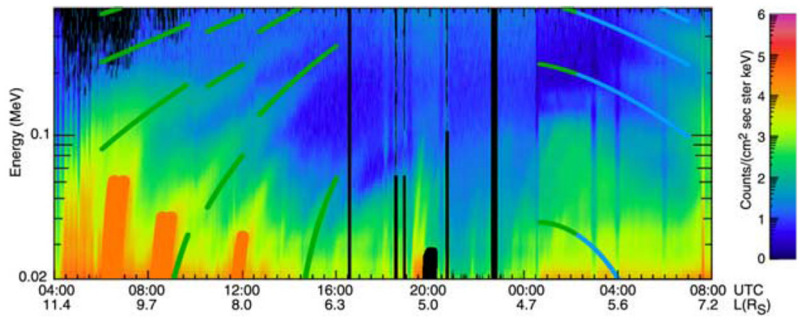


Fig. 187: Spectrogram of Cassini MIMI/LEMMS data showing electron fluxes detected over a wide range of energies. The intense injections at low energy are likely recent. At higher energies, older injection remnants can be seen. The hour of days 302 – 303 of 2005 and the dipole L shell are given. Superimposed on these data is a calculation of injection positions including several very recent intense injections and the remnants of an older injection as viewed by the LEMMS sensor.

*Energetic electrons injected into Saturn's neutral gas cloud*

The population of 20 – 410 keV electrons observed in Saturn's inner magnetosphere results principally from recent injections. Electrons at these energies appear to survive only up to a few days in the neutral gas cloud emitted by gas jets in Enceladus's southern hemisphere. Ions of similar energies have much shorter lifetimes in the gas cloud because of charge-exchange with the ambient neutrals. We have been able to associate fluxes at different energies and times with a single past injection based on the morphology of electron spectrograms from measurements made by Cassini's Magnetospheric Imaging Instrument (MIMI) (Fig. 187). Once injected, electrons disperse in longitude but the age of the initial injection and its approximate longitude can be reconstructed. Furthermore, the shape of time-dispersed features argues against rigid corotation of the magnetospheric plasma, or a fraction thereof, and instead favors L-dependent flow shear.

(N. Krupp in collaboration with Applied Physics Laboratory/The Johns Hopkins University, USA)

*Tracing Saturn's magnetospheric dynamics through the energetic electron absorption by the planet's icy moons*

Within 9 $R_s$ from the center of Saturn (1 $R_s$ = 60286 km) seven moons with a diameter greater than 100 km are orbiting the planet in almost circular and equatorial orbits, within Saturn's plasmasphere and radiation belts. With the exception of Enceladus, all other moons are electromagnetically inert (to a good approximation) and very effective absorbers of energetic electrons: practically, no electron above $\sim$5 keV can escape absorption by the large icy moons. A typical feature of this interaction is the formation of electron depletion regions, termed "microsignatures". Microsignatures "drift" in the magnetosphere with the properties of the pre-depletion plasma. Since the drift of the plasma is determined by the configuration of electromagnetic fields and currents in the magnetosphere, this information will be coded in the position of these signatures with respect to the position of the moon that caused them. In addition, the study of the microsignatures refilling gives us a direct estimate of the radial diffusion rates in the radiation belts.

Using data from the Low Energy Magnetospheric Measurement System of the MIMI instrument (MIMI/LEMMS), we studied electron (>20 keV) microsignatures of Saturn's moons, observed in the first 22 orbits of Cassini. Among the principal results of this study was the first ever derivation of the energetic electron radial diffusion rates as a function of dipole L-shell and electron energy, as well as the discovery of the high variability of these rates.

The L-dependence of the diffusion coefficient, $D_{LL} \sim L^9$ (Fig. 188), suggests that energetic electron diffusion is driven by magnetic field impulses. Most pre-Cassini studies assumed that the diffusion source was the ionospheric dynamo ($D_{LL} \sim L^3$). The $D_{LL}$ variability revealed that the source of these impulses is equally variable. Hot particle injections are then likely to be the actual source of electrons. These injection events might then have an important role in determining the energetic electron population of the inner radiation belts.

The absolute values of $D_{LL}$ for distances lower than 6.5 $R_s$ are consistent with very low net radial diffusion speeds and long lifetimes for electrons in fixed orbits within the radiation belts. This means that radially diffusing electrons would encounter Enceladus,

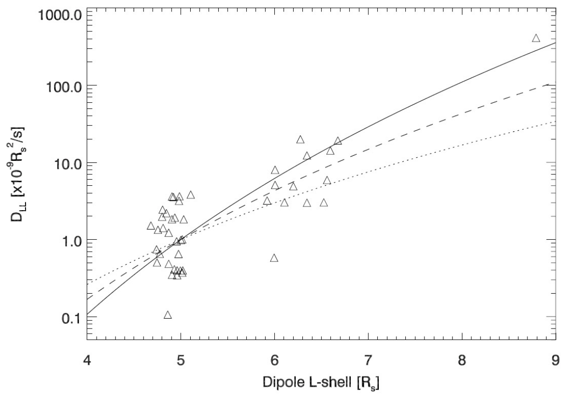


Fig. 188: L-dependence of the $D_{LL}$ for the electron energies of 28 – 49 keV. Three reference curves are shown that correspond to $D_{LL} \sim L^n$, for $n$ = 6,8 and 10 (dotted, dashed and solid curve, respectively).

Tethys and Dione at least once, if their azimuthal drift path is circular, and therefore be absorbed before they are transported in the inner belts. However, despite the low $D_{LL}$, diffusing electrons can escape absorption and be transported in the inner magnetosphere due to non-axisymmetric drift shells which can be detected even down to the orbit of Enceladus (3.89 $R_s$). These non-axisymmetric drift shells are revealed through the displacement of electron microsignatures from the expected circular orbits in dipole fields (Fig. 189).

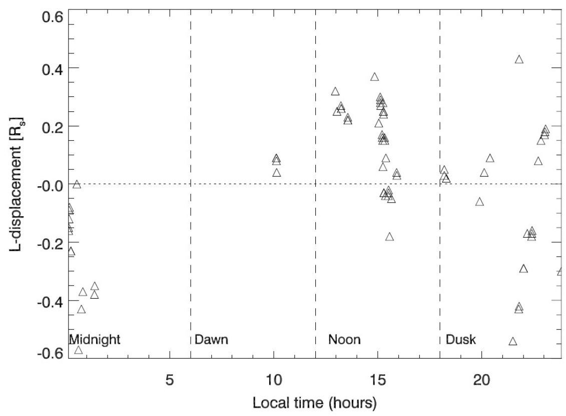


Fig. 189: Displacement of Tethys's 20 – 100 keV electron microsignatures from the expected dipole L-shell, as a function of local time. Positive displacements are away from Saturn, while negative displacements are towards Saturn.

The displacement of the microsignatures from the expected circular orbits also shows that magnetopause current disturbances and cross-tail electric fields might have a notable contribution in the radiation belt plasma circulation, despite the fact that Saturn's dipole field and fast rotation dominate the dynamics in the inner magnetosphere. This should have important implications for the global dynamics of the middle and outer Saturnian magnetosphere.

(E. Roussos, N. Krupp, G. H. Jones, A. Lagg, and J. Woch in collaborations with Applied Physics Laboratory/The Johns Hopkins University, USA; Technical University of Braunschweig; Imperial College London, UK)

*Detecting new ring structures in the Saturnian system with energetic particle measurements*

The first missions to the outer planets (Pioneer 10 & 11, and Voyager 1 & 2 missions) have led to the discovery of new moons and ring structures through the absorption of energetic particles. For example, Pioneer 11, the first spacecraft to flyby Saturn, revealed the presence of the F and G rings of the planet, as well as the presence of the moon Epimetheus.

Expectations for similar discoveries by the Cassini energetic particle instruments were not too high. It was most likely that optical observations with advanced instrumentation, currently available either on ground-based telescopes, the Hubble space telescope, and on the ISS cameras of Cassini, would be sufficient to detect previously unresolved features. Despite that, a series of surprising particle absorption events from unknown obstacles have been detected with the LEMMS electron sensor.

The first detection took place when Cassini was magnetically connected to Saturn's G-ring. The imprint of the G-ring in particle fluxes usually appears as a persistent, subtle decrease in the MeV proton fluxes (due to the mean encounter time of these particles with the G-ring material being faster than the diffusion timescales). On 5 September 2005, a sharp, 50 % decrease of MeV electron fluxes was also observed. Around the same period, Cassini's ISS camera resolved an arc-like structure on top of the G-ring. It was later realised that the electron depletion originated at this arc. However, the measured optical depth of the arc for the 1 – 10 $\mu$m sized particles that the ISS camera can detect, was about $10^{-5}$. That translates into mass that is about 2 orders of magnitude less than what is needed for energetic electron absorption to occur. Therefore the mass that absorbs the electrons has to be contained in a few larger particles, which, however, are not numerous enough to scatter light. Indeed their optical depth would be $10^{-7}$, beyond the Cassini's ISS camera remote sensing capabilities. These particles, that if added together, would form a body of 100 m radius, are the main source of material for Saturn's G-ring. Before Cassini, the presence of Saturn's G-ring was not possible to explain.

The second detection occurred around the orbit of the

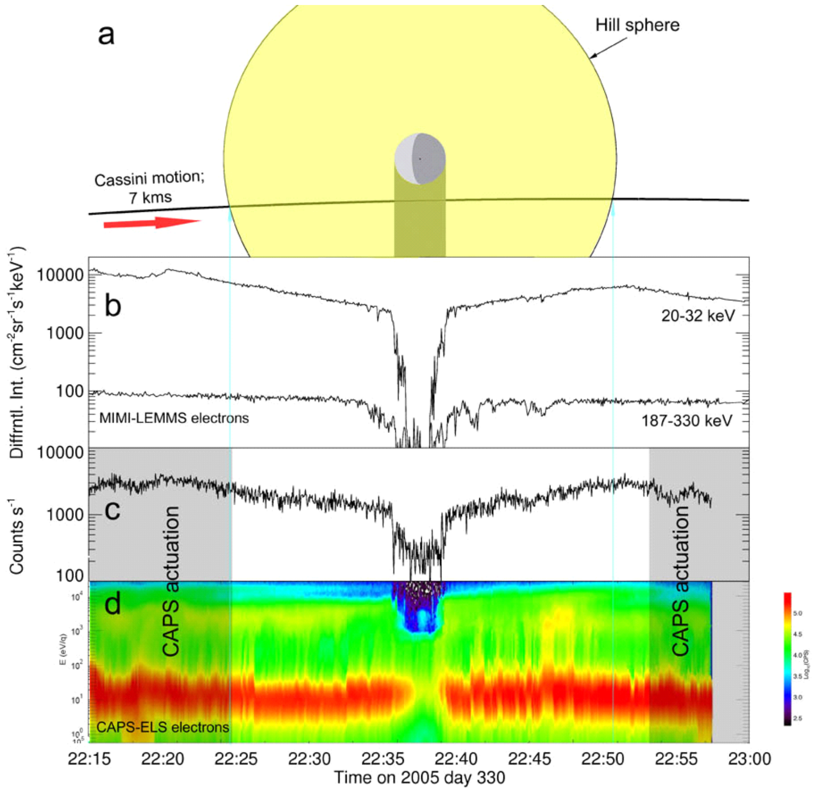


Fig. 191: Data returned during Cassini's flyby of Rhea. (a) Rhea and its Hill sphere to the same scale as the other panels, viewed from the north; Saturn is towards the right. (b) MIMI-LEMMS 20 – 32 keV electron fluxes. (c) CAPS-ELS 26 keV electron fluxes, and (d) for all energies and instrument anodes in spectrogram form. CAPS and MIMI reveal a broad, near-monotonic electron flux decrease between 22:21 and 22:52 UT, decreasing in depth with increasing energy. This decrease is interpreted as the signature of electron absorption by dust surrounding Rhea.

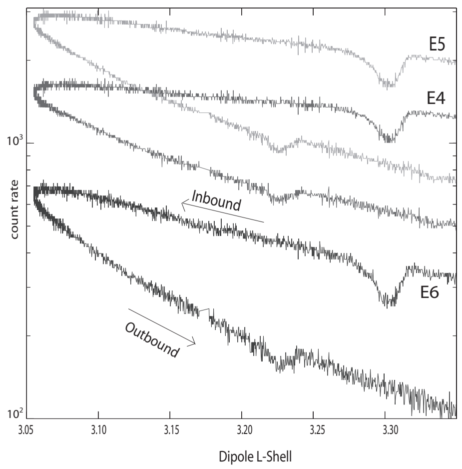


Fig. 190: Depletions around Methone's orbit recorded in LEMMS channels E4-E6, as a function of dipole L-shell. E4-E6 are sensitive to electrons above $\sim$800 keV. The outbound microsignature occurs exactly on Methone's L-shell.

newly-discovered moon, Methone, at $\sim$3.23 $R_s$ from Saturn, on 9 September 2006 (Fig. 190). Methone is a 3 km diameter moon and due to its small size with respect to characteristic scales of the electron and ion motion (gyration and bounce around the magnetic field lines), it is not an effective particle absorber. Despite that, the observed absorption signatures were thousands of kilometers wide. Comparing this observation with electron absorption theory for similar observations at other asteroid-sized moons of Saturn, it was realized that such depletion cannot have occurred directly at Methone's surface. The absorbing medium is possibly an arc of material that resides on a previously undetected ring of Saturn. Such a ring could be produced by micrometeoroid impacts on Methone that can easily release material from its surface (similar processes form the Gossamer rings of Jupiter). No optical detection has occurred so far, suggesting that this arc of material might consist of few large particles, which are difficult to observe.

(E. Roussos, N. Krupp, G. H. Jones, A. Lagg, and J. Woch in collaborations with Applied Physics Laboratory/The Johns Hopkins University, USA; Cornell University, USA; CICLOPS - Space Science Institute, USA)

*The dust halo of Saturn's moon Rhea*

The satellites of the outer planets provide key information on the history and evolution of their respective planetary systems. Moons with little or no atmosphere provide important constraints on the sputtering and erosion of bodies' and rings' surfaces by energetic particles and meteoroids. Rhea, the second-largest of Saturn's satellites, was considered massive enough to retain an externally-generated atmosphere capable of observably-affecting Saturn's magnetosphere. On 26 November 2005, the Cassini spacecraft encountered the moon at 500 km altitude. Data gathered by MIMI-LEMMS and other instruments reveal that Rhea's magnetospheric interaction region, rather than being dominated by sputtered gas and its products, is of a previously-unobserved type, dominated by dust grains (Fig. 191).

The grains absorb energetic magnetospheric particles, forming an electron-depleted region within Saturn's magnetosphere coincident with the region of dominance of Rhea's gravitational field. The study of Cassini data led by MPS members indicates that this dust population has two components. An approximately spherical distribution of grains lofted from the moon's surface by the impact of interplanetary dust was anticipated, and detected in situ by the CDA and RPWS instruments. Electron signatures suggest that an equatorial debris disk is also present. Collaborations with other groups based on our results have revealed that, surprisingly, large particles could indeed remain in suitable orbits around Rhea for considerable periods.

(G. H. Jones, E. Roussos, N. Krupp, H. Krüger, A. Lagg, and J. Woch in collaborations with Applied Physics Laboratory/The Johns Hopkins University, USA; Imperial College London, UK; Mullard Space Flight Laboratory, UK; Universität Potsdam, Germany; Max-Planck-Institut für Kernphysik, Heidelberg, Germany; Astronomical Institute of St. Petersburg, Russia; Southwest Research Institute, San Antonio, USA; Centre d'Etude Spatiale des Rayonnements, Toulouse, France; Jet Propulsion Laboratory, Pasadena, USA; University of Iowa, Iowa City, USA; University of Virginia, Charlottesville, USA; University of California, Los Angeles, USA; Institut für Geophysik und Meteorologie, Universität Köln, Germany; Los Alamos National Laboratory, Los Alamos, USA; The Johns Hopkins University, Baltimore, USA; Swedish Institute of Space Physics, Uppsala, Sweden)

## Outer planets research – Ice Giants

### A Deep Convection Model for the Zonal Flows on the Ice Giants

Previous numerical simulations of deep convection in planetary atmospheres have successfully modeled the zonal wind structure observed on Jupiter and Saturn. On these planets, the dominating equatorial jet blows in prograde direction, the direction of the planets rotation. We have now shown that deep convection simulations can also capture the flows observed on the ice giants where the equatorial jet blows in the opposite direction (Aurnou *et al.*, 2008).

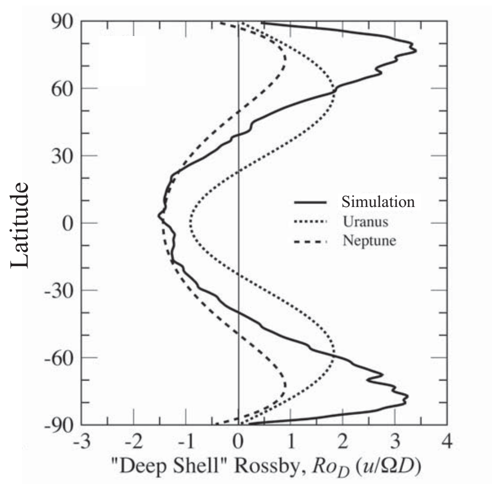


Fig. 192: Comparison of the surface flow observed on Uranus and Neptune with a numerical simulation. The Rossby number $Ro_D$ is a measure for the flow vigoure, $D$ is the depth of the convective outer shell (atmosphere).

Our numerical models solve for the 3D flow in a rotating spherical shell; convection is driven by an imposed temperature difference between the inner and outer boundaries, and stress-free flow boundary conditions are employed. The ice giants surface flow structure is replicated when the control parameter $Ra^\star$ is of order one or larger. $Ra^\star$ is a measure for the ratio of buoyancy to Coriolis force in the Navier-Stokes equation. The ordering action of the Coriolis force enforces a two-dimensionality where flow variations along the axis of rotation are negligible. Such a flow structure is likely present in Jupiter and Saturn and tends to produce prograde equatorial jets. When $Ra^\star$ is of order one, buoyancy forces overcome the ordering nature of the Coriolis force and destroy the two-dimensionality.

Our simulations show that the vigorous turbulent convection tends to homogenize the total angular momentum in this regime. Zonal flows balance the angular momentum associated with the planetary rotation, which leads to a retrograde flow in the equatorial region and prograde flows at higher latitudes (see Fig. 192).

(J. Wicht in collaboration with J. Aurnou (UCLA) and M. Heimpel (University of Alberta))

## Cometary research

### The recent mega-outburst of comet 17P/Holmes at millimeter wavelengths

Introduction: On 23/24 October 2007, the Jupiter family comet 17P/Holmes underwent an event which eventually raised its optical brightness by a factor of a million, making it an easy object to see with the naked eye. It was the greatest cometary outburst ever observed. The explosion occurred nearly half a year after the perihelion passage, at the helio- and geocentric distances of 2.4 and 1.7 AU respectively. At the same time the comet was perfectly placed in the Northern hemisphere, prompting several observing campaigns. High-resolution spectroscopy at millimeter wavelengths is a powerful tool for studying the gas environment in comets, thus it is ideal for characterizing the cometary explosions. Through the rotational transitions it allows investigation of the molecular composition and the physical conditions (such as a kinetic temperature, an expansion velocity, and a spatial density) within the coma observed.

Observations: We traced this astonishing event within the Arizona Radio Observatory in USA. The campaign was divided into two main parts:
Part I. Everyday between October 25.5 and 31.5, 2007 (UT), we were using the 12-m telescope on Kitt Peak. The highest spectral resolution was 24.4 kHz.
Part II. On 28 November, 5 December, 28 December 2007, and 13 – 16 March 2008, we monitored the HCN J(3-2) transition using the Submillimeter Telescope on Mount Graham. Because the target line was at best very faint, the highest useful resolution was equal to 1 MHz.

Results and discussion: During part I of the cam-paign the following molecules were detected: HCN, CS, $CH_3OH$, $H_2CO$, and $H_2S$. We also obtained a sensitive upper limit on CO. The follow-up observations of HCN, conducted as the part II, resulted in the last detection on 5 December 2007, and the last sensitive upper limit on 13 – 16 March 2008.
The early evolution of the outburst was traced through the J(1-0) transition of HCN and the J(3-2) transition of CS. We observed that the lines were continually fading until 28 October 2007, and then the intensities temporarily stabilized, and the spectral profiles underwent a dramatic change as presented in Fig. 193.
Furthermore, the early spectra are very informative concerning the physical conditions in the gas environment shortly after the outburst. Using the spectrum of $CH_3OH$ (Fig. 194) we determined a rotational temperature of $50 \pm 5$ K, whereas the HCN and CS line profiles suggest a gas-expansion velocity of about 1 km/s. The late monitoring shows that the comet was loosing its excessive activity very quickly. Only two months after the explosion, the detected HCN J(3-2) line was not much brighter from what should be expected for a typical nucleus of that size at that heliocentric distance. If we also assume that at least a part of this late activity was originating from the icy grains blown at the outburst, the scenario that the nucleus was behaving like nothing had happened two months before seems very realistic.

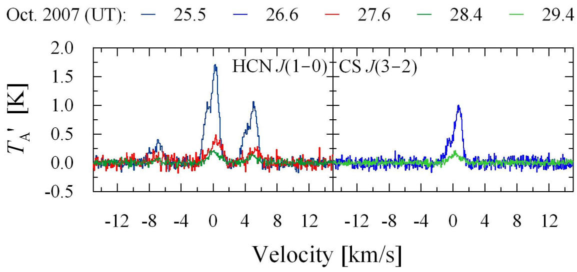


Fig. 193: The early evolution of the outburst.

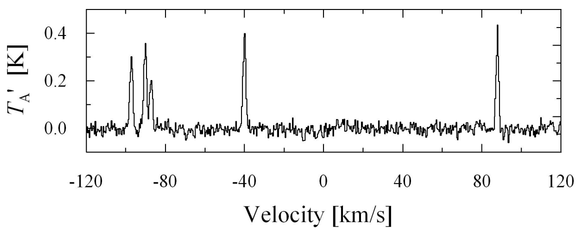


Fig. 194: $CH_3OH$ at 157.225 GHz. The spectrum was re-binned to the resolution of 195.2 kHz in order to increase the S/N ratio.

Conclusions and future work: By running our monitoring very quickly, within less than two days from the onset of the outburst, we could characterize the molecular environment in the very early stages of this event. With the further follow-up observations we witnessed the amazing speed at which the comet was returning to its regular activity. The next step is to retrieve the wealth of information from the spectral line profiles and intensities. Although it is a very challenging task, it can provide a detailed portrait of the outburst and its evolution – the unique clues to understand the processes occurring inside the nucleus which triggered this spectacular event.

(M. Drahus, L. Paganini, C. Jarchow, and P. Hartogh in collaboration with L. M. Ziurys and W. Peters (Arizona Radio Observatory, Tucson, USA))

### Millimeter-wavelength spectroscopy as a tool for studying the rotation of active comets: the case study of comet 8P/Tuttle

Introduction: Active cometary nuclei are expected to manifest their rotation by diurnal variability of the outgassing rate and direction of parent molecules. A natural observing tool for detecting and investigating these effects is millimeter-wavelength spectroscopy. It is sensitive to parent molecules through their rotational transitions, and offers spectral resolution of the order of 1 million or more (0.3 km/s or better). The unique resolving power provides a detailed spectral profile (or at least a position) of an individual line, which is controlled by an instantaneous outgassing pattern of the nucleus surface, whereas the integral sum of the line is a good indicator of an instantaneous total production rate. A critical condition for a successful detection of these effects is to restrict the observation to the molecules emitted at similar moments in time, which requires small beam sizes and short exposures. So far, such effects have been detected only for comet Hale-Bopp, Tempel 1, and recently Schwassmann-Wachmann 3. Comet 8P/Tuttle approached the Earth at a distance of only 0.25 AU in December 2007 and January 2008, providing a natural opportunity to investigate the effects related with the rotation of its nucleus. It is a Halley family comet with an orbital period of 13.6 years. Due to the very unfavorable geometric conditions around its previous perihelion passage in 1994, the last time it was widely observed was only during its return in 1980/1981.

Observations: Comet 8P/Tuttle was monitored through the J(3-2) transition of the HCN molecule using the Arizona Radio Observatory's Submillimeter Telescope on Mount Graham. The half-power radius of the beam was 14.5 arcsec, corresponding to 2600 km at the comet, and the spectral resolution was 0.28 km/s. The monitoring covered five hours of observation on 30 December 2007, three hours on 31 December 2007, and five hours on 1 January 2008, all under excellent weather conditions. As a result we acquired 27 spectra, each comprising a 30-min. time interval.

Results and discussion: On each night the line profile was evolving in an organized manner; in Fig. 195 we show two contrasting examples. At the same time the integral sum of the line was fairly constant. The repeatability of the spectral signatures is consistent with the rotation periods of 5.7 hr, 7.4 – 7.6 hr, and their multiplicities. Very similar results have been obtained

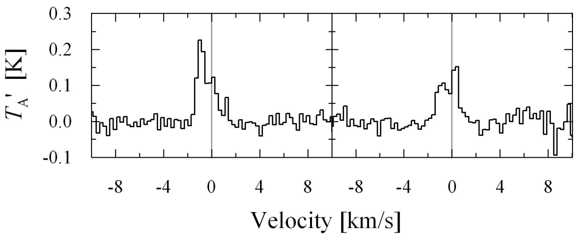


Fig. 195: An example of two individual spectra.

before. We should note, however, that the period of 7.4 hr links the spectra from different nights noticeably better than does the period of 5.7 hr. Multiplicities of both base periods cannot be excluded, though they are difficult to evaluate.
Our spectra suggest a gas-expansion velocity equal to 0.8 km/s, and a mean-diurnal production rate of log Q(HCN) = 25.45. Whereas the velocity is typical for a comet around the Earth's orbit, the production rate is significantly lower from what should be expected for a nucleus with a 7.3-km radius.

Conclusions and future work: We demonstrated that the millimeter-wavelength spectroscopy of parent molecules can be an effective tool for studying the rotation of active comets. As by-products of such observations, the gas-expansion velocity and the mean-diurnal production rate of the observed molecule can be easily retrieved. Furthermore, we will attempt to model the observed line profiles all together in order to obtain some constraints on the spin axis orientation and the location of active source(s).

(M. Drahus, C. Jarchow, and P. Hartogh in collaboration with W. Waniak (Astronomical Observatory of the Jagiellonian University, Krakow, Poland), T. Bonev and G. Borisov (Institute of Astronomy of the Bulgarian Academy of Sciences, Sofia, Bulgaria), K. Czart (Torun Centre for Astronomy of the Nicolaus Copernicus University, Torun, Poland), and M. Küppers (European Space Astronomy Centre, Madrid, Spain))

### Submillimeter monitoring of the HCN molecule in fragment C of the split comet 73P/Schwassmann-Wachmann 3

Comet SW3 is a short-period comet, belonging to the Jupiter family. In 1995 the comet broke-up into several fragments. After the unfavorable return in 2000/2001, it came back to the perihelion of its orbit in 2006. This time the comet passed very close to the Earth (below 0.1 AU). Simultaneously it was well situated on the sky, which provided the opportunity for several observing campaigns.

We observed this comet with the Heinrich-Herz submillimeter telescope at the Mt. Graham International

Observatory in Arizona. Our campaign covered the period from 1 May to 22 May 2006. In this work, however, we focus only on the best HCN data for fragment C, that were obtained on 10 May, 11 May, 12 May, 20 May, and 22 May 2006 with several different spectrometers. In total we got 124 measurements of the main-beam brightness temperature of the comet, resulting from 3-2 and 4-3 rotational transitions (at the ground vibrational state) of the HCN molecule.

Using a simplified model of gas coma and the observing instrument we could reconstruct the production rates $Q$ of the HCN molecule. We found $Q(r = 1\mathrm{AU}) = 2.7 \pm 0.1 \times 1025$ molec/s and the exponent of the power-law evolution with heliocentric distance equal to -8 ± 1. These results are very similar to the ones already published in the IAU Circulars and Electronic Telegrams both for HCN and CN (that is a photodissociation product of mainly HCN). For this derivation we used the expansion velocity of the molecules, equal to $\nu = 0.8$ km/s, that was obtained from our high-resolution CTS spectra. However, as we did not have enough data for deriving the kinetic temperature, we used the value of 80 K (Kawakita *et al.*, CBET 532).

Furthermore, we investigated the possibility that the production rate may exhibit short-term cyclic changes, induced by the rotation of the cometary nucleus. Although we did not receive a unique period solution, we are convinced that the true period is one of the 8 values that we report. The production rates (normalized to $r = 1$ AU) phased accordingly are shown in Fig. 196, and the period solutions themselves are listed in the following table.

| Solution | Period [hr] | Error [hr] | Harmonic |
|---|---|---|---|
| A | 13.567 | 0.007 | 4 |
| B | 11.868 | 0.009 | |
| C | 11.754 | 0.009 | |
| D | 10.174 | 0.006 | 3 |
| E | 06.780 | 0.006 | 2 |
| F | 03.392 | 0.002 | 1 |
| G | 03.349 | 0.002 | |
| H | 03.019 | 0.001 | |

As one can see, 4 of these solutions are connected in one system, thus the different solutions represent just a different harmonic of the base frequency, that is equal to 3.392 hr. The solutions of about 3 hr are very close to the value of 3.2 hr obtained with the use of the Hubble Space Telescope (Toth *et al.*, private communication) one month before our observations and 2.8 hr, that is one of the solutions reported by Farnham (presentation at the DPS meeting in 2001) from the previous return. Moreover, one of the periods claimed by Storm *et al.* (presentation at the DPS meeting in 2006), obtained just 2 weeks before the mid time-point of our dataset used for this work, is 13.2 hr. This is fairly close to our 4th harmonic of the system. If this is the case, than this claim would refer to the base frequency of 3.3 hr. However, there are also some other claims suggesting that the period is significantly longer than 3 hr.

Currently, we are investigating the possibility that the period may be indeed very short, and the nucleus is actually spinning-down. This would match most of the period claims. If this hypothesis would turn out to be true, several other properties of this comet may be derived (Drahus and Waniak, 2006). Moreover, this would support the hypothesis, that comets may break-up due to the fast rotation of their nuclei, and would also allow us to determine another set of properties, following the model of rotational break-up (Davidsson, 2001).

(M. Drahus, C. Jarchow, M. Küppers, and P. Hartogh)

### Deep Impact at comet 9P/Tempel 1: Exploring the Dust Component

Project and result description: The team of collaborators participated in the world-wide campaign to observe the Deep Impact target comet 9P/Tempel 1 in 2005. A regular monitoring programme was performed at the CalarAlto 2.2 m telescope over 6 months before the event and at the MPG/ESO 2.2 m for one month thereafter. The measurements characterize the dust and gas evolution of the comet that peaked about 60 – 80 days before perihelion. As of mid February 2005 a porcupine coma of several mostly straight jet-like features evolved in the coma that did not change much in geometry and relative intensity over the long orbit arc of the comet observed. The porcupine structure is interpreted as due to embedded fans produced by 3 – 4 active regions on the rotating nucleus requiring a rotation axis orientation close to perpendicular of the orbital plane of the comet. This result is in good agreement with the rotation axis analysis performed by the DeepImpact mission team. During the week of impact the comet was observed by the team with various telescopes at Calar Alto and at ESO Chile. The production rates of the CN, $C_2$ and $C_3$ gas remained unaffected by the event. However, changes (intensity, colours) in the dust ejecta cloud are identified. The imaging and spectropolarimetry (linear and circular) of the dust showed the expected behaviour. The data analysis is completed; 1 Science, 2 A&A and 1 proceedings papers are published, 2 A&A papers are submitted and 1 is in preparation.

(H. Boehnhardt)

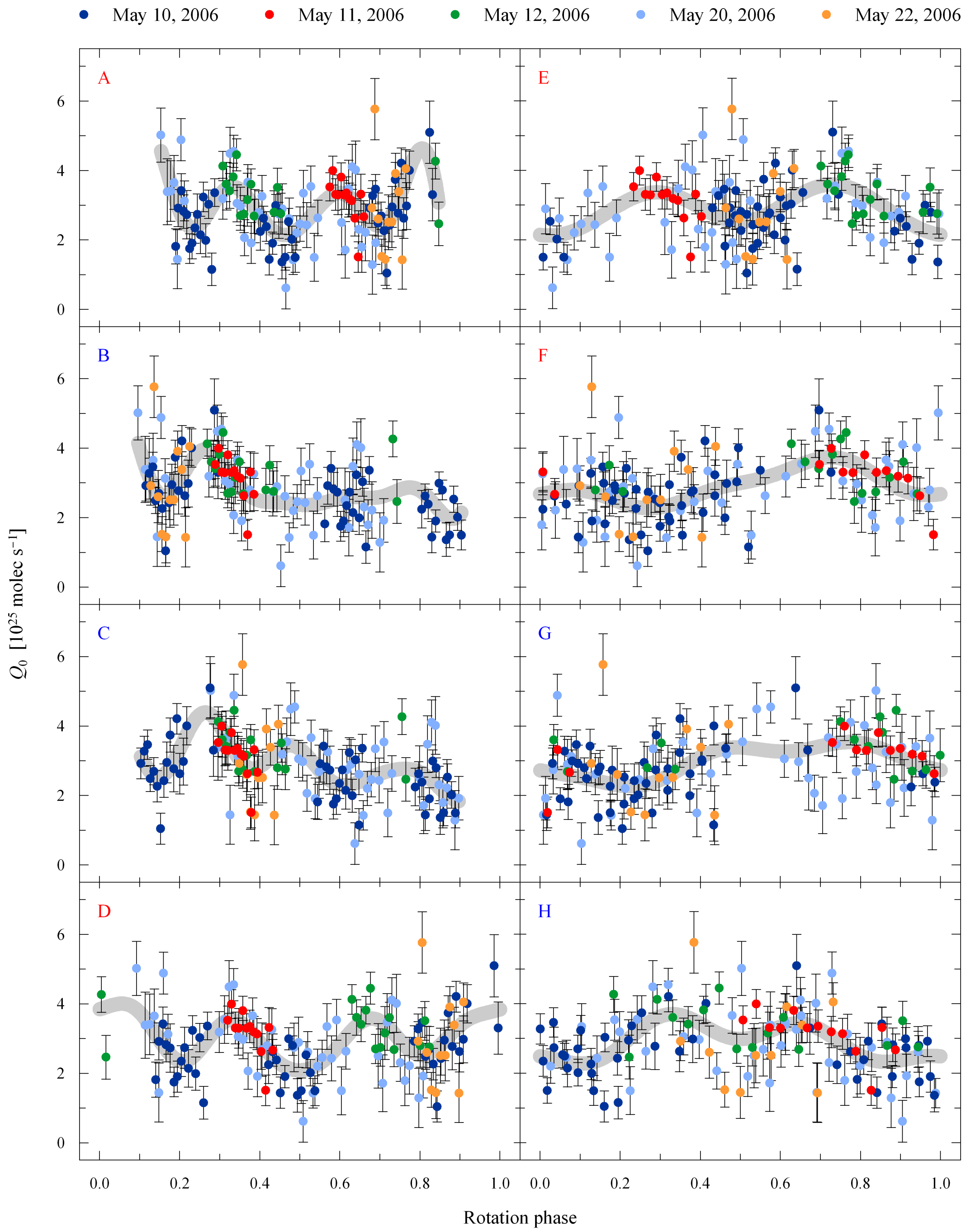


Fig. 196: The normalized production rates $Q_0(t)$ phased for 8 best solutions. The designations of solutions are given in the upper-left corners of the panels. Red and blue symbols are used for easy distinction between the "system" and the other solutions, respectively. The smooth fits were obtained with the $x^2$ minimization using harmonics, with $N_f = 5$ for the solutions at $f < 0.1h^{-1}$ (left panels) and $N_f = 3$ for the solutions at $f > 0.1h^{-1}$ (right panels). We used these fits for calculating individual errors of the discussed solutions.

**Physical and composition properties of short-periodic and Oort Cloud comets**

Project and result description: This programme investigates physical properties of the nuclei and of the coma dust as well as of the ice composition of comets through different observations and analysis techniques.

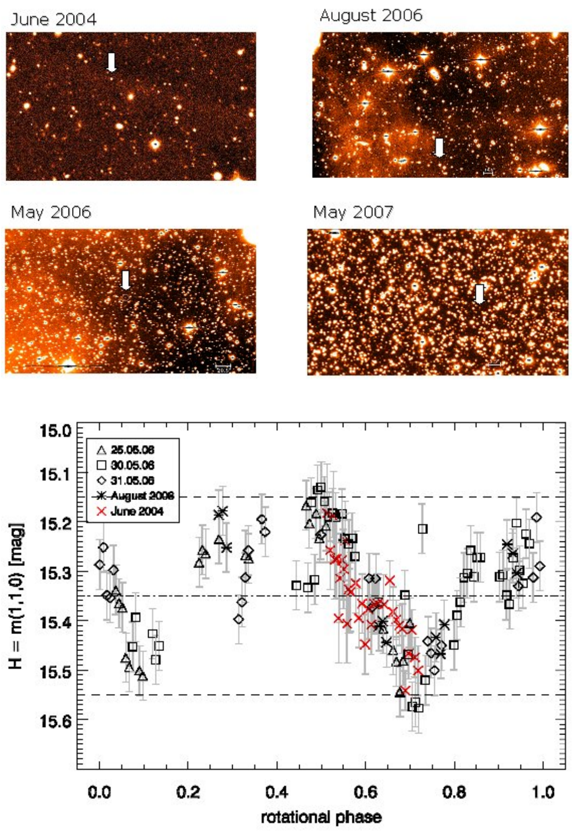


Fig. 197: Comet 67P/Churyumov-Gerasimenko in 2004–2007, imaged with the FORS2 instrument at the ESO VLT observatory. The comet, indicated by arrows, has stellar appearance indicating that the coma activity has ceased or is very low. The measured lightcurve of the nucleus is double-peaked suggesting non-spherical body shape of the nucleus and a rotation period of about 12.7 h.

Visible imaging and spectroscopy monitoring of the Rosetta target comet 67P/Churyumov-Gerasimenko during its aphelion passage revealed that the activity of the nucleus is extremely low if not absent at all (Fig. 197). The photometry of the nucleus allowed the confirmation of published size estimations and a significant refinement of the rotation period of the comet. The surface colours and spectra are found to be moderately red with no indications of variations with rotation phase. No absorption features could be identified. The nucleus phase function is only coarsely sampled by our observations so far, but it may have an atypical steep amplitude which we intend to verify by on-going observations over a wider and better sampled phase angle range. Quasi-simultaneous visible (VLT) and thermal IR (Spitzer satellite) measurements are currently analyzed to refine the albedo and size parameters of the comet. This part of the project is on-going, 1 A&A paper is published, 1 paper is submitted.

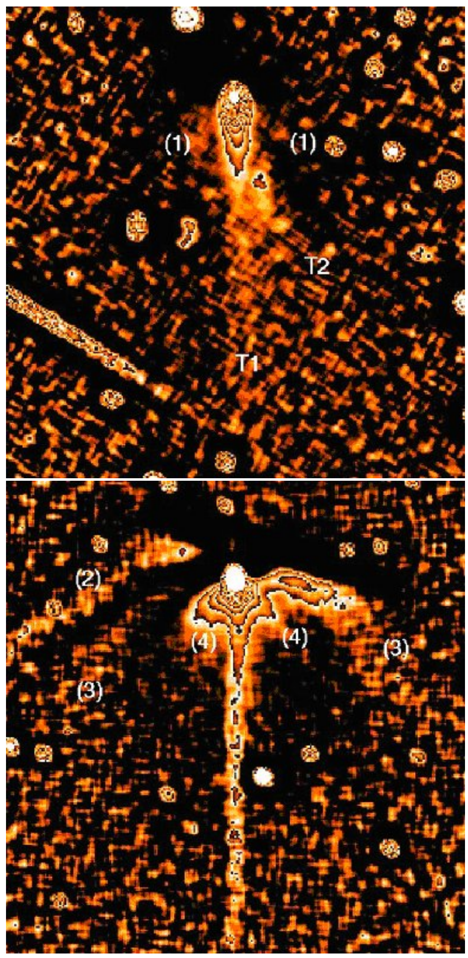


Fig. 198: Structures in the coma of component B of comet 73P/Churyumov-Gerasimenko, observed during the Earth approach in May 2006. The structures are enhanced by adaptive Laplace filtering. Numbered arclets are due to fragmentation events; two tail structures T1 and T2 are identified with T1 representing the normal dust tail of the comet and T2 a temporary dust tail produced by an earlier nucleus fragmentation event of the comet.

The split short-periodic comet 73P/Schwassmann-Wachmann 3 was measured through visible and near-IR imaging as well as through visible imaging and spectropolarimetry during its close approach to Earth in 2006 (Fig. 198). Structure analysis of the coma images of components B and C reveal the presence of isolated active regions on the nuclei and are currently modeled by a Monte-Carlo dust coma programme in order to constrain the rotation properties and the location of active regions on the nuclei. A number of temporary components and a dust streamer appeared in the coma of component B and could be related to an outburst event in late April 2006. The appearance of various short-term arclets in the coma of component B indicates a series of fragmentation events during May 2006. The linear polarimetry of component A and B indicates that both components are dust rich. Temporary distortion of the polarization degree of the dust in component B are found, probably related to the production of dust by on-going splitting events. The spectropolarimetry shows a constant linear polarization degree vs wavelength, modulated by attenuations in the emission band regions of the coma gases. The visible circular spectropolarimetry shows a neutral zero polarization degree of the components. Both spectropolarimetric measurements are unique and first-ever measurements for comets. Analysis is on-going, 1 A&A paper is published, 1 is submitted, and 1 in preparation.

High dispersion mid IR spectroscopy of the cometary coma is performed using CRIRES at the VLT observatory in Chile in order to detect parent gas species from supervolatile ices in cometary nuclei. In 2007 two comets (2P/Encke and C/2006 P1 McNaught) were tried unsuccessfully since too faint or in adverse atmospheric conditions. A data reduction pipeline for the spectrum analysis is set up and new observations of comet 8P/Tuttle in early 2008 are prepared. The observations will be analysed to determine production rates of the gases, to measure the spin temperature of the water ice as a proxy for the overall nucleus temperature and to assess the D/H ratio in cometary water. This part of the programme is on-going, no publication so far.

(H. Boehnhardt, M. Drahus, M. Lippi, C. Tubiana, and J.-P. Vincent)

## Cometary research – ROSETTA

### CONSERT on board ROSETTA

CONSERT (COmet Nucleus Sounding Experiment by Radio-wave Transmission) is a 90 MHz radio wave experiment to probe the interior of a comet to reveal its structure and electrical properties: permittivity, absorption, planetesimal size and volumne scattering coefficient (Fig. 199). The CONSERT experiment has equipment on both the orbiting spacecraft and on the lander, which will settle on the comet's surface. The radio waves will propagate between the two spacecrafts and through the comet. The relative position of the lander and orbiter will vary with time owing to motion of the orbiter and (possibly) owing to rotation of the comet. This allows the interior of the comet to be swept by radio waves revealing spatial inhomogeneities and internal structures. MPS contributed to definition of the experiment and designed, constructed and tested the antennas for the orbiter and the lander. The orbiter antenna was succesfully deployed shortly following launch; the lander antenna will first deploy when the lander is separated from the orbiter spacecraft to descent to the comet surface. The experiment was commisioned and operations verified. Since then every six months a status verification has been carried out. These tests have shown the experiment to be operational and to not have changed since commissioning.

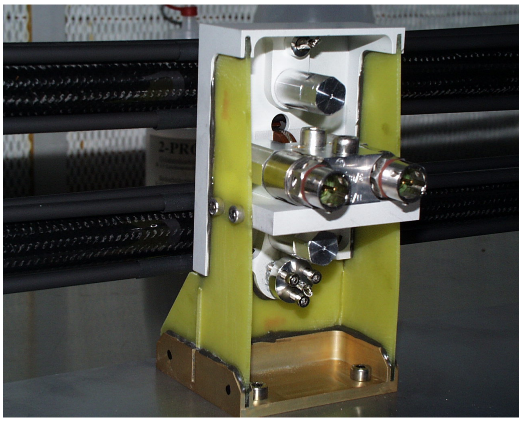

Fig. 199: Two-shot pyro mounted on thermally isolated support strucure. The orbiter antenna consists of ten spring loaded ~100 cm rods, which were bundeled together and lashed with a steel cable to the pyro support; the pyro cut the cable to deploy the antenna.

(E. Nielsen)

### Detailed report on COSAC (2006/07)

Following the successful launch and the commissioning phase several active payload check-outs were performed. COSAC is in good shape. As a result of these measurements the prediction of the necessary power for operation was further improved and is now available as a programme.

The mass spectra acquired during the check-out procedures can be interpreted assuming that water, which is the main constituent in the spectra, produces a total ion count proportional to its vapour pressure. Using these data it is possible to use the COSAC MS as a vacuum meter during the descent phase (Fig. 200).

A team meeting of the COSAC team took place from the 26th to the 27th of October 2006 in Lindau. Nine members of the team participated.

(F. Goesmann)

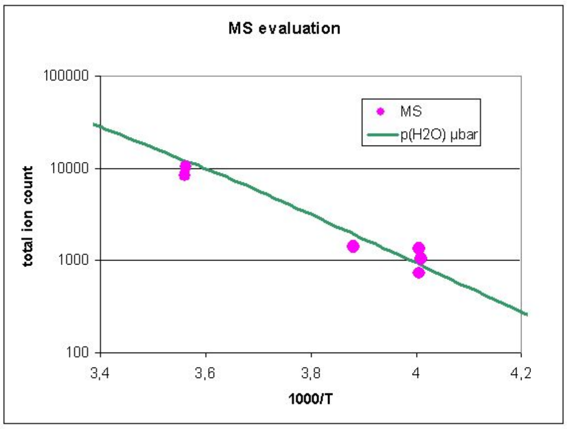


Fig. 200: The figure shows the total ion count of several mass spectra obtained in flight plotted versus the reciprocal temperature. In addition the vapour pressure of water is superimposed. Both curves follow the same trend. Hence the results can be explained by water and it is shown that the MS may be used for pressure measurement.

### The ROSETTA Lander PHILAE

Frequent testing of the spacecraft during flight shows that all subsystems supervised by the MPS work nominally. These tests have been performed since 2004, starting after launch with the commissioning followed by biyearly checkouts.

The subsystems under MPS responsibility are:

- Complex landing gear including damping mechanism
- Mechanical subsystem MSS device to separate lander and orbiter and to push PHILAE into the landing orbit
- Power subsystem PSS for handling of the electrical power generation and distribution
- Harpoon system to anchor the lander on the cometary surface
- Hardware for the command and data management system

Reference systems are available at MPS and DLR for each subsystem. Mission pre-tests of the PHILAE subsystems are generally performed at the PHILAE lander ground reference model at DLR Köln/Wahn. Fully functional reference systems at MPS are used for training, task planning, and verification. Support hardware and software allows detailed investigation of the subsystem behaviour, also under non nominal conditions. A long term thermal vacuum storage for some mechanisms provides reference systems to be operated shortly before use in mission. An expertise center is available at MPS to operate the subsystems and instruments as stand alone units or integrated to the command lines of the ROSETTA lander and ROSETTA orbiter.

(H. Boehnhardt, B. Chares, R. Enge, H. Fischer, O. Küchemann, W. Kühne, R. Roll, M. Sperling, and I. Szemerey)

### Retrieval Simulation for the MIRO Instrument on the Rosetta Orbiter

The Microwave Instrument for the Rosetta Orbiter (MIRO) is one of several instruments onboard the ESA Rosetta spacecraft headed for a rendezvous with comet 67P/Churyumov-Gerasimenko in 2014. It is a passive heterodyne receiver which measures next to the continuum emission of the nucleus especially the line emission of several key volatile species in a band centered at 562 GHz with a frequency resolution of 50 kHz. The instrument is fixed tuned to observe simultaneously eight transitions of the water and two of its isotopes, carbon monoxide, ammonia and methanol. The spectrally resolved line shapes allow to retrieve molecule abundance, expansion velocity, and coma temperature as a function of the distance to the nucleus. Describing the coma by a simple Haser model and assuming local thermodynamical equilibrium for the inner 1000 km we investigated with detailed simulations this retrieval task using the Optimal Estimation Technique. Especially the correlation between the eight profiles obtained with a combined retrieval from all measured spectral lines has been studied. In addition the influence of the observing geometry – nadir viewing vs. limb scanning – on the radial resolution of the profiles has been addressed. Fig. 201 shows the spectra of water vapour and two of its isotopes, methanol, ammonia and carbon monoxide in limb geometry for 5 tangential heights below the Rosetta spacecraft which is assumed to fly 20 km above the surface of the cometary nucleus. The retrieval algorithm almost perfectly fits the line shapes generated in a forward calculation (black lines within the colored lines). The retrieval provides not only the number density of the simultaneously observed molecules, but additionally the profiles of the coma temperature and outgassing speed of the molecules as illustrated in Fig. 202. For each of the 8 parameter the averaging kernels are plotted as well. They provide insight about the information gain of the observation. Looking at the averaging kernels the sensitivity to altitudes above the spacecraft height stands out. Since there is no geometrical information above the spacecraft altitude (in limb sounding generally most of the signal stems from the area around the tangential point of the measurement) it can be concluded that this information is retrieved from the molecular line shapes.

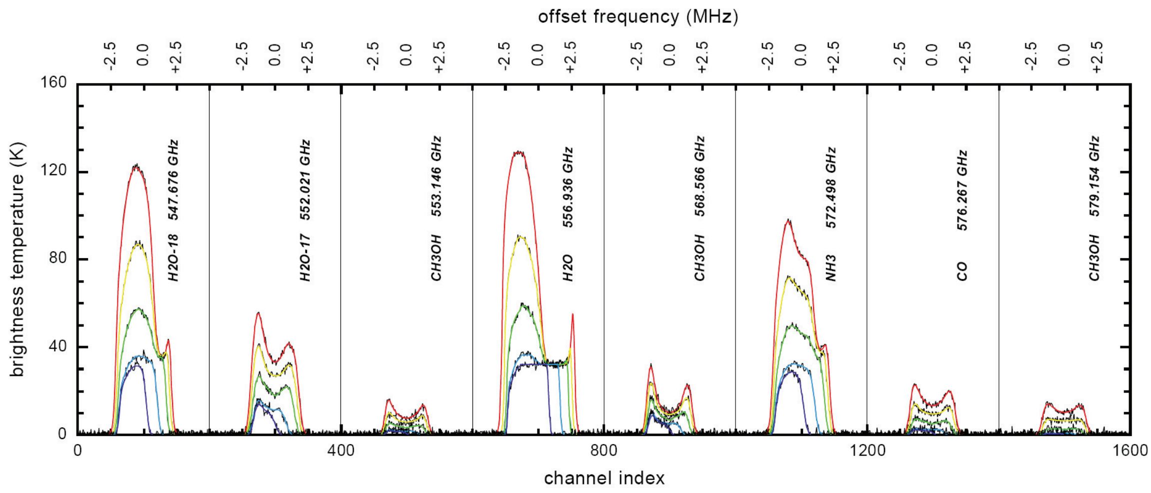


Fig. 201: Simulated limb spectra and almost perfect fits of the radiative transfer model for 5 tangential heights between 1 and 15 km above the surface of 67P.

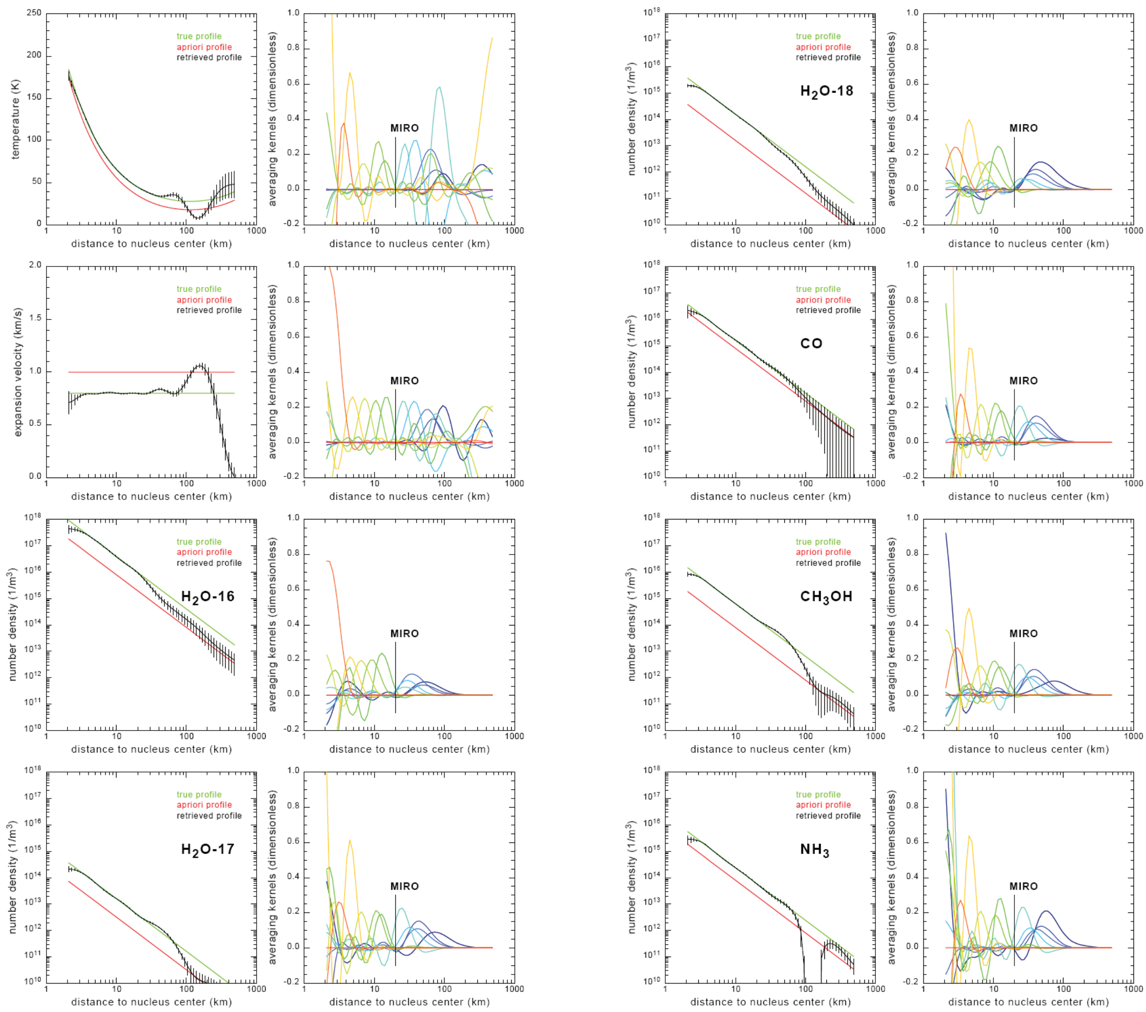


Fig. 202: The good reproduction of the true profiles by the retrieval algorithm in limb sounding geometry for altitudes below the Rosetta spacecraft.

The green lines in the plots on the left sides represent the so called true profiles which are the input profiles for the forward calculations. The red lines represent the apriori profiles which are required for the regularization of the retrieval. The black lines show the retrieved profiles. The upper retrieval altitudes are about: 40 km for the temperature, 50 km for the outgassing velocity, 25 km for water and its isotopes, 100 km for CO, 60 km for methanol and ammonia. The temperature information stems mainly from the methanol lines and the outgassing speed information from the Doppler shift of the lines. The same kind of simulation has been performed for nadir geometry, however the results were not that promising. The drawback was a correlation between the number density of the outgassing molecules and the temperature, i.e. one of the two parameters have to be assumed for a reasonable retrieval. A source of temperature profiles with good enough accuracy may be the VIRTIS experiment on the Rosetta spacecraft. Work for the MIRO retrieval problem is in progress. In the future we will try to retrieve information generated from hydrodynamical models (like the one of Crifo) which describe a more realistic inner coma of the Rosetta comet.

(C. Jarchow and P. Hartogh)

## Scientific observations with OSIRIS onboard Rosetta

The scientific observations of 2006 and early 2007 were observations of the Rosetta target asteroids 2867 Steins (flyby in September 2008) and 21 Lutetia (flyby in July 2010) and during the Rosetta Mars flyby in February 2007. Additionally, the instrument was found to be in good health during two passive checkouts in 2006 and the onboard software was updated in December 2006, greatly enhancing the image compression capabilities. Most of the observations during an active checkout in December 2006, foreseen for instrument calibration, were not executed. The instrument had been switched-off due to a software anomaly. The lost observations are now scheduled for the next active checkout in September 2007.

The efficient preparation of an asteroid flyby requires knowledge of some global properties of the asteroid like the approximate size, albedo, rotation period and the direction of its spin axis. Shortly after the selection of Rosetta's asteroidal flyby targets in 2004, an international observing campaign of the asteroids was initiated. OSIRIS participated in this campaign with continuous observations of Steins on 11 March 2006 and of Lutetia on 2 – 3 January 2007.

The Steins observations, performed over nearly 24 hours or four rotation periods without interruption, provided the best light curve of the asteroid so far (Fig. 203). The light curve shows that Steins rotates with a period of slightly more than 6 hours, in agreement with previous observations. The asymmetric light curve suggests an irregular shape of the asteroid. No evidence for complex rotation or the presence of a satellite of Steins was found (Küppers *et al.*, 2007).

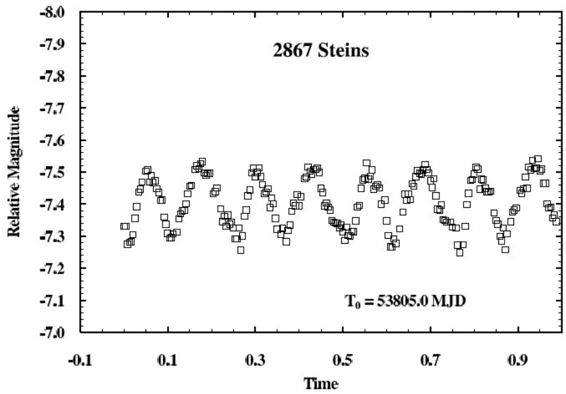


Fig. 203: Brightness of asteroid 21 Steins monitored over one day. The maximum brightness is about 23 percent higher than the minimum.

The determination of the direction of the spin axis of an asteroid requires observations from different viewing angles. Here the OSIRIS observations are particularly valuable because Steins was observed from a large phase angle of 42°, compared to a maximum of 30° that can be reached from Earth. The reconstruction of the spin axis of Steins from a combination of the OSIRIS results with various earth-based observations is in progress.

Asteroid Lutetia, larger and brighter than Steins, was observed during 12 hours through seven different optical filters, providing a rotationally resolved low resolution spectrum. The scientific analysis of the data is ongoing.

The detailed planning of the flyby of Asteroid Steins has started. We investigated different flyby strategies (closest approach distance and relative position of the Sun, Rosetta, and Steins at closest approach can be chosen) in terms of spatial resolution, surface coverage on the asteroid and phase angle coverage. An overall best strategy was found (flyby within the ecliptic plane and with a closest approach distance of 800 – 1000 km) that is in agreement with a suggestion by ESA.

The Mars flyby (closest approach on 25 February 2007) provided the first opportunity to observe a bright, extended object with OSIRIS. The images show the excellent performance of the cameras. It can be seen that a substantial fraction of the Martian surface was covered by clouds (Fig. 204). The images are currently being interpreted scientifically.

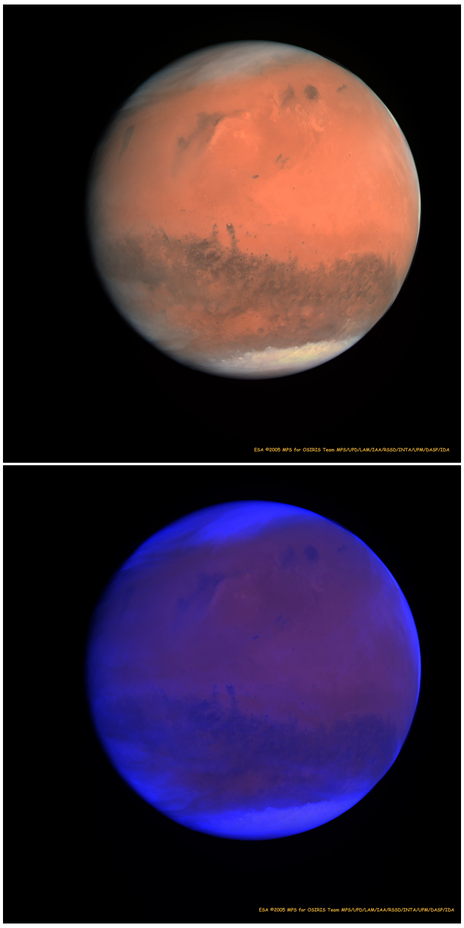

Fig. 204: True colour image of Mars (top) and colour composite with the blue channel replaced by enhanced near-ultraviolet to show the presence of cloud structures over most of the martian disk (bottom). The images were obtained on 24 February 2007 from a distance to Mars of about 240000 km. Image resolution is approximately 5 km.

The analysis of the OSIRIS observations of comet 9P/Tempel 1 around the impact of the projectile of the Deep Impact mission on 4 July 2005 has continued. Apart from the impact, temporal variations of the brightness of the comet during the two weeks of observations could be associated with the rotation of Tempel 1. No permanent new structures in the coma of the comet were created by the impact. The steep increase of the brightness of the comet after the impact suggests that the impact ejecta were quickly accelerated by collisions with gas molecules. Therefore, the ejecta motion cannot be described by ballistic trajectories, casting doubts on determinations of the density and tensile strength of the comet with models using ballistic ejection of particles (Keller *et al.*, 2007).

The motion of the expanding dust cloud ejected from the impact is influenced by solar radiation pressure. Since radiation pressure depends on particle size, the analysis of the motion of the cloud allows us to derive the size and velocity distribution of the dust particles. The cross section and brightness of the dust ejected by the impact is dominated by small (a few microns and smaller) particles, while most of the dust mass is contributed by larger grains. The velocity distribution shows a broad maximum at 190 m/s with a width of 150 m/s. The overall size- and velocity distribution of the impact ejected dust is similar to that typically seen in cometary comae (Jorda *et al.*, 2007).

The next target for Rosetta and OSIRIS is the Earth, with a flyby in November 2007. Another Earth flyby in 2009 and the asteroid flybys provide additional observing opportunities for OSIRIS before Rosetta will arrive at comet 67P/Churyumov-Gerasimenko in 2014.

(H. U. Keller, I. Büttner, S. F. Hviid, R. Kramm, O. Küchemann, M. Küppers, M. Rengel, H. Sierks, and S. Spjuth)

### OSIRIS images from Rosetta Earth swing-by

During its 10 year cruise to comet Churyumov-Gerasimenko the Rosetta spacecraft performs four planetary (3 times Earth, once Mars) and 2 asteroid flybys. After the successful Mars swing-by in February 2007, the second Earth swing-by took place in the evening of 13 November 2007.

The scientific camera system OSIRIS, built by an European consortium lead by MPS, observed the earth during the swing-by of the Rosetta spacecraft.

Earth swing-by images are shown in Fig. 205 to Fig. 208. The approach came from the night side, leaving Earth day side and imaging Moon outbound in various colour filters.

Fig. 205: Composite of four WAC images which shows both, the city lights in the Northern hemisphere and the illuminated crescent around Antarctica.

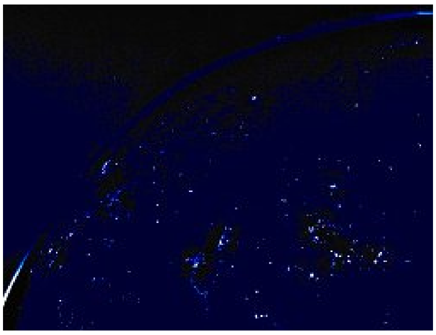

Fig. 206: Image taken with the OSIRIS Wide Angle Camera (WAC) at 18:45 UTC, about 2 h before the closest approach of the spacecraft to the Earth. At that time Rosetta was about 80,000 km above the Indian Ocean where the local time approached midnight (phase angle sun-earth-Rosetta ca. 160°). Islands of artificial lights of human habitations are sparsely distributed over the globe. The WAC image through its red filter was exposed for 5 s.

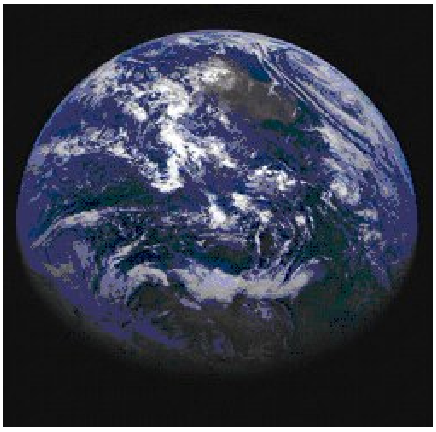

Fig. 207: Image of the Earth taken by the NAC in true colour representation.

Credit for all Figures:
ESA ©2007 MPS for OSIRIS Team
MPS/UPD/LAM/IAA/RSSD/INTA/UPM/DASP/IDA

(H. Sierks)

## Other small bodies

### Pluto-Charon and Triton:

The IR spectra, taken at the ESO Very Large Telescope VLT in 2005 using the adaptive optics instrument NACO, showed for the first time separate spectra of Pluto (1 – 5 $\mu$m), Charon (1 – 4 $\mu$m) and Triton (1 – 5 $\mu$m). In Pluto strong $CH_4$ absorption bands are detected and modeled. Moreover, a so far unknown absorption at 4.6 $\mu$m is detected (possibly originating from CO ice). The Charon spectrum shows the

Fig. 208: Image of the Moon taken with the OSIRIS Narrow Angle Camera at 06:36 UTC about 9 h after Rosetta's closest approach to the Earth. The image has been acquired through the far focus red filter of the camera (750 nm). OSIRIS has been designed to image faint objects so a neutral density filter was placed in the optical path to reduce the sensitivity of the camera 50 times.

expected water ice absorptions between 2.9 – 4.0 $\mu$m. The Triton surface spectra resemble those of Pluto, although the $CH_4$ ice absorptions are less pronounced.

(H. Böhnhardt and S. Protopapa)

### Surface exploration of Kuiper Belt Objects and Cometary Nuclei

Project and result description: One part of the project explores – using FORS1 at the ESO VLT – the linear polarization and opposition surge of cometary nuclei over the phase angle range from 0 to about 30 deg (Fig. 209). In 2006 the linear polarization of a cometary nucleus, i.e. comet 2P/Encke, was measured successfully, for the first time worldwide. The results show a steep linear increase of the polarization degree between 4 and 28 deg phase angle and a parallel linear decrease of the absolute magnitude of the nucleus. The polarization curve appears to be unique among solar system objects. Application of the empirical polarization – albedo relationship for asteroids yields unusual albedo values that are not in agreement with the known albedo of the nucleus, suggesting that the surface constitution of this cometary nucleus is different from the usual regolith surfaces expected on asteroids. The photometry of 2P/Encke confirms – assuming the published albedo value – the radius estimation of the nucleus. Project is on-going, 1 A&A paper is submitted.

The other part of the project focuses on the detection of surface ices on Pluto, its moon Charon and on the Neptunian moon Triton (that is likely to be a captured Kuiper Belt object). L and M band observations have

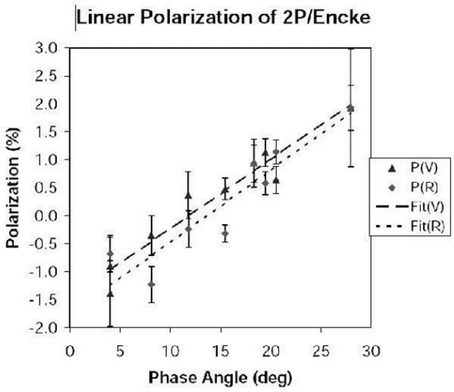


Fig. 209: The linear polarization degree of the nucleus of comet 2P/Encke, measured with the FORS1 instrument of the ESO VLT observatory.

been obtained in 2005 using the adaptive optics instrument NACO at the ESO VLT and resolving for the first time the spectra of Pluto and Charon in this wavelength region (Fig. 210). Apart from known absorptions of $CH_4$, $CH_4$ diluted in $N_2$ and water ice on the surfaces of the bodies, a new so far unknown absorption feature at 4.6 $\mu$m was identified in the Pluto spectra. It is interpreted as being due to CO ice and nitriles. A significant change of the $CH_4$ absorption band slope around 3 $\mu$m (compared to a published Pluto spectrum measured in 2001) suggests re-condensation of atmospheric gas on the surface. The surface ices are quantified through Hapke light scattering modelling of the spectra. The surface of Triton displays a very similar spectrum to that of Pluto. An on-going Large Programme at the ESO VLT measures the visible and JHK band spectra of about 50 Kuiper Belt objects for the identification and analysis of the surface composition of these primordial objects. Project is on-going, 1 proceedings paper is published, 2 A&A papers are submitted.

(H. Boehnhardt)

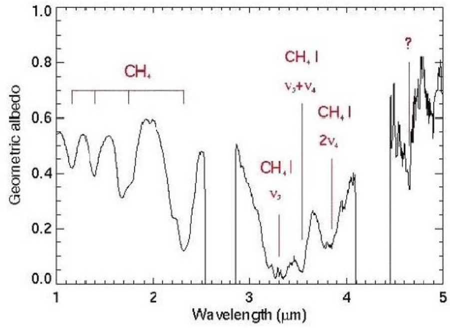


Fig. 210: Ices on the surface of Pluto. The plot shows the spectrum of the dwarf planet, obtained with the adaptive optics instrument at the ESO VLT observatory and undisturbed by the light of its close-by satellite Charon. Strong absorption bands of $CH_4$ ice are prominent between 1 and 4 $\mu$m and a so far unknown absorption around 4.6 $\mu$m is tentatively identified as being due to CO and nitrile ices. The gaps in the spectrum between about 2.5 to 2.8 and 4.1 to 4.5 $\mu$m are caused by opaque terrestrial atmospheric absorption bands.

## General studies

### Linearity Improvement of sub-millimeter heterodyne spectrometers

Up- and down looking sub-millimeter wave heterodyne spectrometers sounding planetary atmospheres provide the shapes of molecules observed. The shapes are characterized by the pressure broadening of the atmosphere. Using radiative transfer models and retrieval algorithms, the vertical profile of the observed molecule can be retrieved. This method requires the exact knowledge or the shape of the observed molecule. Systematic errors of the sub-millimeter heterodyne spectrometer can change the line shape in a way that the retrieved vertical profile is wrong. One error source is related to nonlinearities in the measurement setup and even very small deviations from the ideal linear transfer function of the system may lead to large retrieval errors. In the past, these deviations could be detected with an accuracy of about $1-2\,\%$. We developed a new, differential method which allows us to improve the accuracy on the linearity measurement by at least one order of magnitude. With this new test setup we were able to identify components causing the nonlinearities and replaced them by components with better linearity in a 400 MHz Chirp Transform Spectrometer with 100 KHz spectral resolution. In order to validate the result of the improvement we made an intercomparison campaign with a number of non-changed spectrometers at MPS (ground-based ozone heterodyne spectrometer) and at the Heinrich Hertz Telescope in Arizona. The preliminary results are promising and tests are on-going.

(L. Paganini and P. Hartogh)

### Improvement of instrument performance in ground-based (sub)millimeter observations

At millimeter and submillimeter wavelengths, spectra caused by rotational transitions of trace gases in planetary atmospheres yield essential characteristics such as vertical profiles, abundance, and temperature conditions. The large resolution provided by heterodyne spectroscopy ($\frac{f}{\Delta f} > 10^6$) allows to retrieve the chemical composition, thermal structure and winds of the atmosphere with very high accuracy. Nevertheless, on several observation campaigns unexpected differences are observed in the power spectral density (PSD) among heterodyne backend spectrometers. Since inversion methods compare the observed radiances with the corresponding retrievals, any inconsistency between the radiative transfer code and the measurement will lead to inaccurate results. Moreover, retrieval simulations of the Earth's middle atmosphere indicate that deviations in the line center of spectral information of trace gases may produce erratic results in the lower mesosphere and upper stratosphere, meanwhile deviations in the edges determine aberration in the lower stratosphere.

Intercomparison studies of ground-based observations of ozone in the Earth's atmosphere suggest that this discrepancy might be produced by small nonlinearities in microwave components composing the instruments. It is clear that nonlinearity in backend instruments may lead to significant degradation of the measurement accuracy. This motivated the construction of a method capable to detect and correct the effects of nonlinearity in heterodyne systems. Based on a differential approach, a novel experiment was conducted in order to analyze nonlinear behavior in backend spectrometers. As observed in Fig. 211, the results of this method confirm that the overall deviations introduced by nonlinearity in spectrometers have been decreased and thus the performance of the backend instruments has been successfully improved.

(L. Paganini and P. Hartogh)

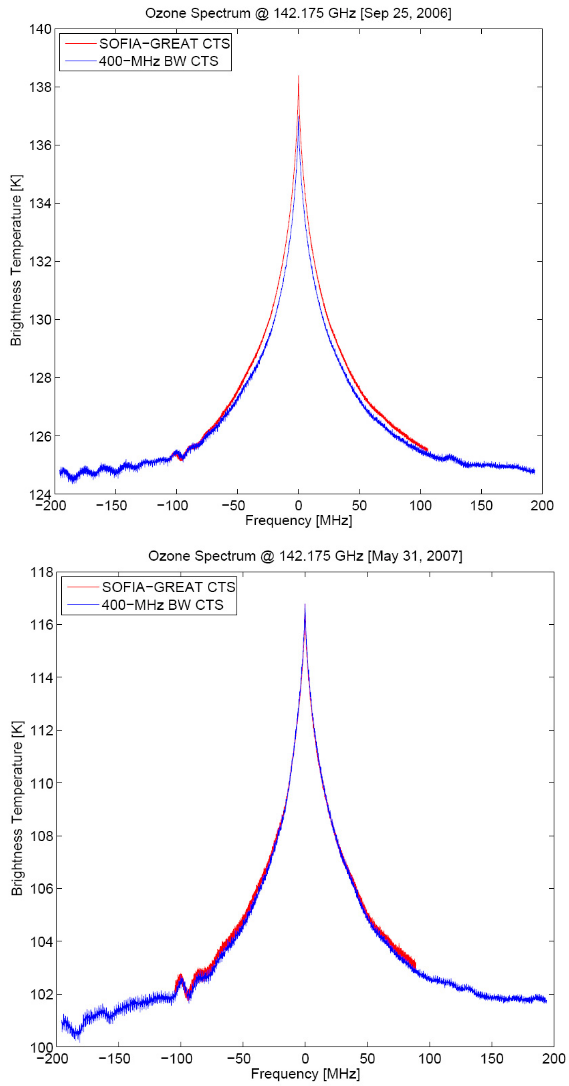


Fig. 211: Intercomparison studies of the rotational transition of ozone at 142.175 GHz from our institute. *Left:* backend nonlinearity produces discrepancies among the instruments. *Right:* the diminution of nonlinear behaviour is translated into a better agreement.

**Herschel Solar System Observations (HSSO)**

MPS is leading the Herschel Key Program for solar system observations with 48 participating scientists from 24 institutes in 10 countries. One unique feature of Herschel is its capability to observe water with extremely high sensitivity. Thus the project is focusing on water and related chemistry. Water is ubiquitous in the Solar System, being present in gaseous form in all planetary and cometary atmospheres, as ice on the surface and subsurface of Mars, comets, most planetary satellites and distant bodies, and in the liquid phase on Earth. Water plays an important or dominant role in the chemistry of planetary and cometary atmospheres. Comets are sources of water for planets through episodic collisions and continuous production of ice-dust grains. This proposal addresses the broad topic of water and its isotopologues in planetary and cometary atmospheres. The nature of cometary activity and the thermodynamics of cometary comae will be investigated by studying water excitation in a sample of comets. The D/H ratio, the key for constraining the origin and evolution of Solar System species (see Fig. 212), will be measured for the first time in a Jupiter-family comet. A comparison with existing and new measurements of D/H in Oort-cloud comets will constrain the composition of pre-solar cometary grains and possibly the dynamics of the protosolar nebula. New measurements of D/H in Giant Planets, similarly constraining the composition of proto-planetary ices, will be obtained. The D/H and other isotopic ratios, diagnostic of Mars' atmosphere evolution, will be accurately measured in $H_2O$ and CO. The role of water vapor in Mars' atmospheric chemistry will be studied by monitoring vertical profiles of $H_2O$ and HDO and by searching for several other species. A detailed

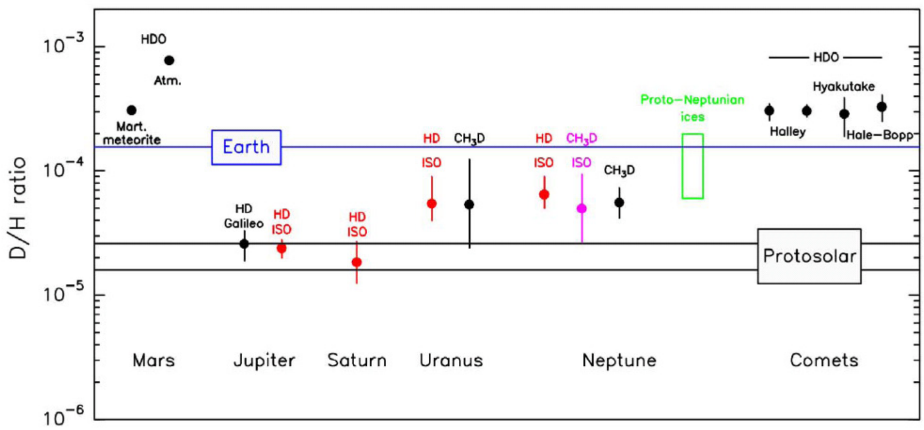


Fig. 212: D/H ratios. Its more accurate determination by Herschel will help to understand the evolution of the solar system.

study of the source of water in the upper atmosphere of the Giant Planets and Titan will be performed. By monitoring the water abundance, vertical profile, and input fluxes in the various objects, and when possible with the help of mapping observations, the project HSSO will discriminate between the possible sources of water in the outer planets (interplanetary dust particles, cometary impacts, and local sources). In addition to these inter-connected objectives, serendipitous searches will enhance our knowledge of the composition of planetary and cometary atmospheres.

(P. Hartogh)

### HIFI absolute flux calibration using opaque molecular spectra in the Martian atmosphere

The European Space Agency's cornerstone project HERSCHEL is a space based 3.5 m-telescope for exploration of the Universe in the spectral range from far-infrared to sub-millimeter wavelength (57 – 670 $\mu$m). The science payload consists of three instruments:
1. PACS, a bolometer detector array camera and a low- to medium-resolution spectrometer to perform imaging photometry and imaging line spectroscopy in the 60 – 210 $\mu$m wavelength band,
2. SPIRE, an imaging photometer covering the 250 – 500 $\mu$m range, and an imaging Fourier Transform Spectrometer covering 200 – 670 $\mu$m, and
3. HIFI, a high resolution heterodyne receiver covering the frequency range 480 – 1910 GHz with a resolving power of up to $10^7$.
In order to achieve an absolute flux calibration accuracy of better than 5 percent for HIFI, it is intended to use Uranus and Mars as primary flux standards for continuum radiation. But especially Mars seems to be a challenging calibration source, because numerous rotational absorption lines – caused by CO and $H_2O$ in Mars' tenuous atmosphere – disturb the continuum radiation emitted by the surface. So usually these wavelength regions are omitted for an accurate instrument calibration. However, we have studied the emitted radiation especially in the deep core of the CO absorption lines, because the spectral lines are optically thick at these frequencies and Mars can be treated as a pure gas planet without any need to model the surface emission. Using a detailed radiation transfer model and our MAOAM general circulation model to predict the seasonal variation of Mars' atmosphere we found for several CO lines a variability of Mars' brightness temperature of less than $\pm$ 5 percent. The model has been constraint against observations of the thermal emission spectrometer (TES) on Mars Global Surveyor (MGS). The globally averaged errors between model and TES observations are smaller than 2 % over the seasons. The simulation is characterized by three steps:
1) MAOAM seasonal grid point temperatures are selected and weighted according to the visibility of the Martian disk from Herschel (at L2). Fig. 213 shows only the lowest of 110 altitude layers (for one date only). Fig. 214 represents the temperature profiles above each grid point shown in Fig. 213 (above and including).
2) Calculation of submm spectra of CO for two frequencies (Fig. 215) and each grid point over the season and determination of the weighted average. Herschel will see only the weighted average, since it will not resolve the Martian disk in the HIFI frequency range.
3) Calculation of the annually averaged spectrum and the deviation from the annual average (Fig. 216). Except for northern winter, the flux deviation of the CO lines is smaller than 5 % over the season.
So we suggest not to avoid the rotational CO absorption lines of Mars, but to observe especially the line center of all observable CO lines in order to increase the accuracy of the absolute flux calibration of HIFI.

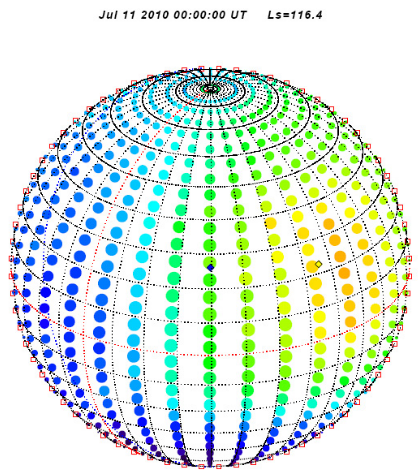


Fig. 213: Visible temperature grid points representing the lowest atmospheric layer for 11 July 2010 simulated with our MAOAM model. The size of the grid points represent their weight as observed from the Herschel Space Observatory. The red boxes represent the limb contribution. Blue and yellow diamonds are sub-Herschel and sub-solar points. For the simulation of the CO-spectra to be observed by Herschel, 110 atmospheric layers of 1 km thickness have been considered.

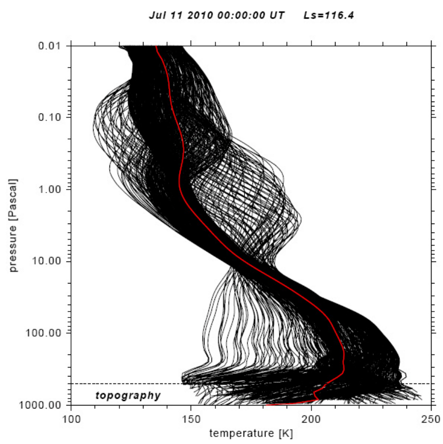


Fig. 214: Temperature profiles from the MAOAM GCM corresponding to the grid points visible by Herschel.

(P. Hartogh, C. Jarchow, and A. Medvedev)

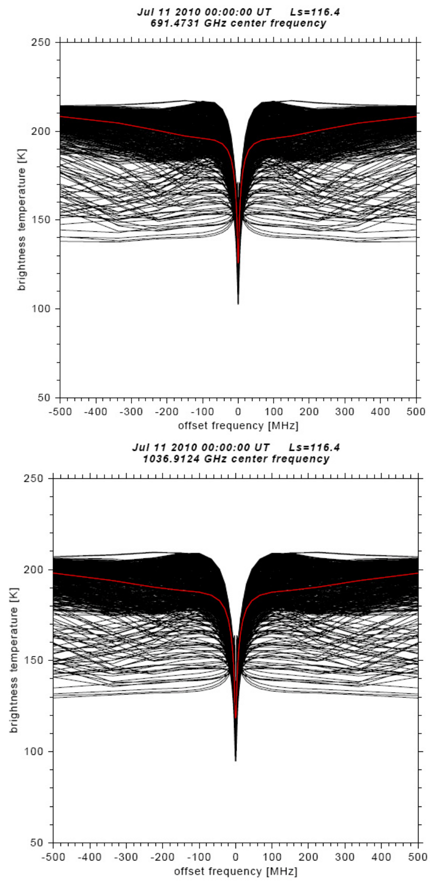


Fig. 215: Submm spectra (691 GHz and 1027 GHz) of CO for the given temperature profiles. The red line represents the averaged weighted spectrum as it would be detected by Herschel.

## Development of Wide Bandwidth SAW Chirp Filters with Improved Magnitude Response

Dispersive delay lines (DDLs) are key elements in Chirp Transform Spectrometers used as real-time backends in heterodyne spectrometers. The so-called reflective array compressor (RAC) design based on the coherent reflection of surface acoustic wave forms propagating on a crystal is the best choice generating large time-bandwidth product impulse responses of DDLs. While long dispersion times have been reported since the mid 1980s, the design and production of large bandwidths is a major challenge, because on the one hand the propagation loss of surface acoustic waves increase with the third power of the center frequency of the DDL and structure sizes of the interdigital transducers (IDTs) and the reflective array get very small. New photo- and electron beam lithographic techniques and improved design tools make it possible to increase the bandwidth step by step. The Microwave Instrument for the Rosetta Orbiter (MIRO) used DDLs with 180 MHz bandwidth. Meanwhile we finished the development for 400 and 600 MHz bandwith and got promising results for 800 MHz.

Fig. 217 shows a drawing of the new DDL design including a new type of phase error reduction. Fig. 218 shows the magnitude response for the 600 MHz bandwidth DDL operating at a center frequency of 1500 MHz. The structures of the IDT fingers are below 500 nm in diameter.

The following table 1 shows more details about the

Table 1: The specifications of 3 wide bandwidth SAW chirp filters

| Chirp filter | Central Frequency | Bandwidth | Chirp Duration | Insertion Loss | Magnitude Ripple | Phase Error |
|---|---|---|---|---|---|---|
| I | 1.0 GHz | 400 MHz | 10 $\mu$s | $\sim$ 37 dB | $\pm$ 0.5 dB | $<$ 2° (RMS) |
| II | 1.5 GHz | 600 MHz | 10 $\mu$s | $\sim$ 46 dB | $\pm$ 1.5 dB | $<$ 3° (RMS) |
| III | 2.0 GHz | 800 MHz | 6 $\mu$s | $\sim$ 54 dB | | |

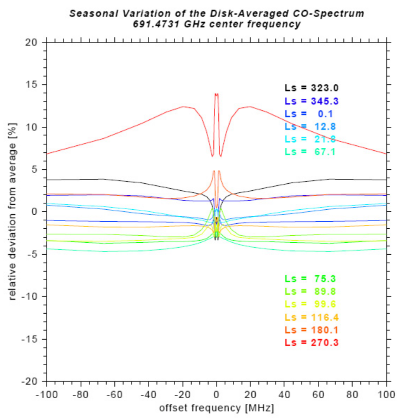


Fig. 216: Relative deviation of spectra over a Martian year. Except for northern winter (solar longitude = 270), the variation of the 691 GHz CO line flux is smaller than 5 % (applies for the 1097 GHz line, too).

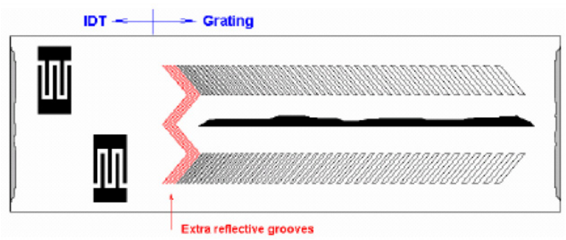


Fig. 217: RAC with IDTs and reflective array (grating). The additional reflective grooves reduce the cubic phase error to less than 6 degrees rms.

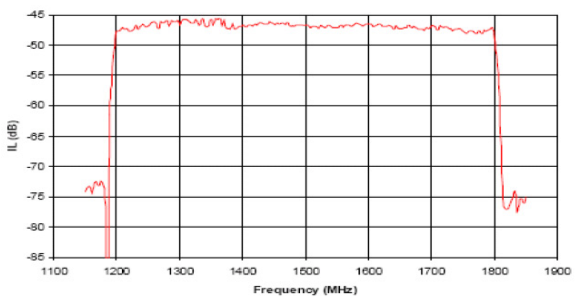


Fig. 218: Scattering parameter 21 for the 600 MHz DDL.

achieved specifications of the three DDL designs.

All three filters have been produced using lithium niobate wavers. This material provides good results up to about 2 GHz, however for higher bandwidths the SAW propagation loss gets too high. Using new materials (e.g. sapphire, rutil, etc.) with potentially lower propagation losses at high frequencies we hope to increase the DDL bandwidth to far more than 1 GHz in the near future. The development and production is done in collaboration with Physikalisch-Technische Bundesanstalt (PTB) in Braunschweig.

(P. Hartogh)

### A tool to study rings around satellites

The Cassini spacecraft flight by the Saturnian moon Rhea revealed signatures in the electron flux that can be interpreted as the electron absorption on rings around this satellite of Saturn. In order to assess the plausibility of such structures inside the Hill sphere of Rhea and simulate their possible origin and evolution scenarios, a computer programme is necessary to simulate the dynamics of dust particles near planetary satellites. The problem is peculiar since conventional N-body integrators fail to solve accurately the system of equations of the motion of the Sun, planet, satellite and particle in orbit around the satellite: the orbital periods are tremendously different! The exact Kepler solution should therefore be used for the motion of the planet about the Sun, and of the satellite about the planet, and the particle motion should be integrated in the rest frame of the satellite. This was done by using an existing computer programme to simulate the particle dynamics around a planet, by changing the reference frame to that of the satellite, accounting for its non-inertiality. The new programme has been applied to find the regions of stability of particle orbits about a satellite taking only gravity into account, and can be used to take the non-gravitational perturbations into account, including the Solar radiation pressure and the Poynting-Robertson effect, plasma drag and Lorentz force.

(V. Dikarev, H. Krüger, and G. Jones)

### Modelling the photoelectron distribution in planetary ionospheres

Solar EUV photons entering the upper layers of a planetary atmosphere will ionize neutral atoms and molecules, thus creating the planet's ionosphere with

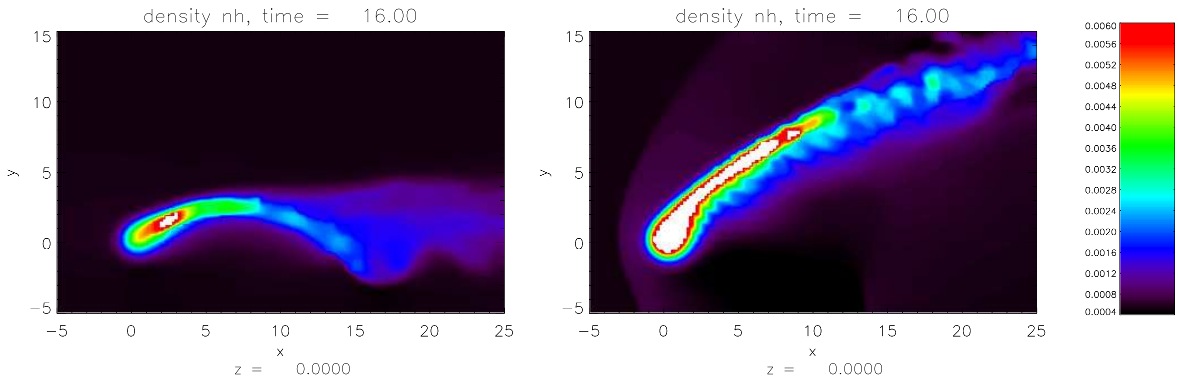


Fig. 220: Examples of cometary ion tails for different values of mass loading $\dot{q}$ and atomic mass number $A$ of cometary ions, shown as colour-coded contour plots in the plane perpendicular to the magnetic field. Left: $\dot{q} = 1.0$, $A = 10$, right: $\dot{q} = 2.0$ and $A = 2$. The solar wind is incident from the left at twice the Alfvén velocity. A corresponding one-fluid run would not exhibit these characteristic cycloidal particle trajectories, but rather a symmetric, cone-shaped distribution of ions. As the mass loading increases, clump-like instabilities begin to form in the tail, the dynamic of which is not fully evident from these static illustrations. (MPEG movies of these simulations may be viewed on the web page `http://www.mps.mpg.de/homes/kleimann/science/num-mhd.html`.)

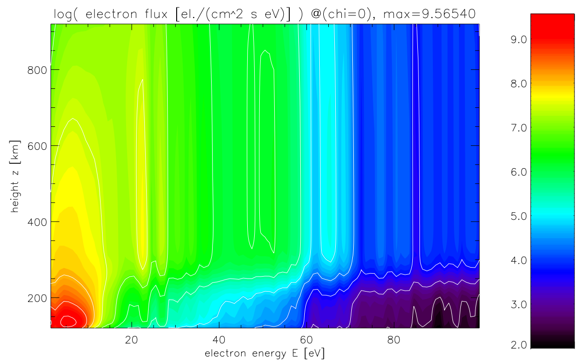


Fig. 219: Change of the photoelectron flux spectrum with height above the Martian surface for solar zenith angle $\chi = 0$ (i.e., at the subsolar point). The two peaks at $\sim 22$ eV and $\sim 26$ eV resulting from the ionization of atmospheric $CO_2$ by the Solar 30.4 nm He-line are clearly discernible. Above $\sim 600$ km, the spectrum apparently varies only little with height.

its population of energetic ($E \approx 1 \ldots 100$ eV) electrons. These photoelectrons may subsequently undergo further ionizing collisions with neutral particles, leading to a redistribution of kinetic energy within the population.

For Mars and Venus, the resulting spectral distribution of photoelectrons is currently measured by the ASPERA 3 and 4 instruments on-board MarsExpress and VenusExpress, respectively.

In order to interpret these recent measurements, we have implemented a simplified transport model developed by Mantas & Hanson (1979) using more recent data for the relevant atomic absorption and ionization properties, as well as an improved solar irradiance model. Starting form a given solar EUV spectrum, the model first computes the available photon flux at height $z$ and solar zenith angle $\chi$, then deduces the 'primary' electron spectrum resulting from direct photoionization. Finally, a simplified Boltzmann equation is solved for the electron flux (defined as distribution function $f(v, z)$ times the particle velocity $v \equiv \sqrt{2E/m_e}$) to compute the equilibrium photoelectron distribution resulting from elastic, inelastic, and ionizing scattering events involving the constituents of the neutral background atmosphere.

Resulting spectra for Mars (at $\chi = 0$) are shown in Fig. 219. (Note that, since the dependence on $\chi$ only enters via the absorption of photons occurring at atmospheric layers above $z$, it is negligible at heights $\leq 500$ km covered by MarsExpress data.)

(J. Kleimann and M. Fränz)

### Multi-fluid modelling of solar wind interaction with planetary bodies

When studying the interaction of the solar wind (SW) with solid obstacles, three cases need to be distinguished. Objects lacking both an atmosphere and an intrinsic magnetic field (such as Earth's moon) will cause the SW particles to simply hit the surface and be absorbed, leaving a wake behind the obstacle. The SW flow around planets with a strong magnetosphere (such as Earth or Jupiter) can usually be studied using standard one-fluid magnetohydrodynamics (MHD), since the solar wind particles will tend to deform the magnetosphere but will generally not be able to penetrate down to the planet, such that the atmosphere is shielded from direct SW contact. This treatment, however, is clearly not appropriate for objects which lack a magnetosphere but either possess an atmosphere (like Mars and Venus) or exhibit *mass load-*

*ing* (such as outgassing comets or moons with volcanic activity). In order to adequately treat such settings, we have set up a multi-fluid MHD model, which allows us to distinguish between SW protons and heavy planetary ions: both are characterized by their own density distributions, can move at their own respective velocity, and only interact via their common electric field. This approach allows us to capture important gyro effects (as seen in Fig. 220) not present in standard one-fluid MHD at only mildly increased numerical expenditure.

(J. Kleimann and K. Sauer in collaboration with A. Kopp (Ruhr-Universität Bochum))

**DAWN Framing Camera**

DAWN has started its mission to study the two largest asteroids in our solar system. On board is the Framing Camera, developed at the MPS with contributions from DLR (Berlin) and IDA (Braunschweig). The spacecraft was launched on 27 September 2007, and is scheduled to rendezvous with Vesta in 2011 and Ceres in 2015.

The Framing Camera, which consists of two redundant units (FC1 and FC2), is a multispectral imager that will also serve as optical navigation camera. Light enters the camera through a door at the top, shown in Fig. 221, passes through the baffle (designed to minimize stray light), and the lens barrel to reach the Camera Head (CH). Baffle and lens barrel are supported by two struts. The CH contains the CCD with the associated Front End Electronics and a filter wheel, featuring a clear filter and 7 narrow-band filters that cover the visible and near-IR wavelength range. Two radiators, one for the CCD and one for the CH, cool the instrument. The CCD is of the frame-transfer type and front illuminated. It has an active area of $1024 \times 1024$ pixels and a field-of-view of 5.46° squared.

At Vesta and Ceres the FC will create global topography, albedo, and colour maps to map the asteroid topograpy and mineralogical composition. To achieve this plans call for obtaining images of more than 80 % of Vesta's surface at a resolution of better than 100 m per pixel (200 m per pixel at Ceres), and a $S/N \geq 50$ in the clear filter and at least 3 colour filters. However, selected regions on Vesta (Ceres) will be imaged at 17 (66) m per pixel resolution.

In December 2007 the FC successfully passed the initial checkout phase (ICO). Characteristics like responsivity, geometric distortion, Point Spread Function (PSF), and dark current were determined for both units. The FC optical performance was found to be excellent, with very little distortion and a narrow PSF.

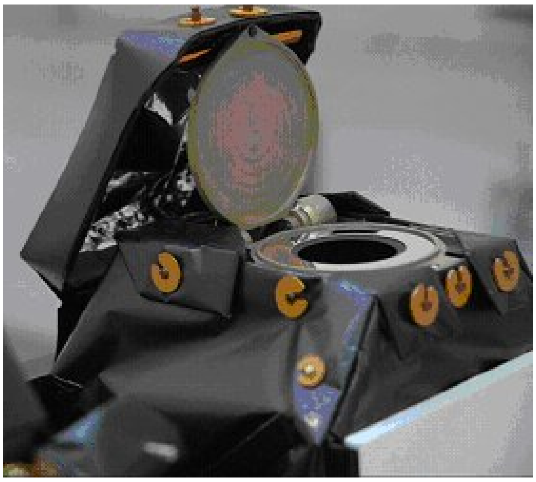

Fig. 221: The Framing Camera, wrapped in Multi Layer Insulation has opened its door. A radiator is visible in white at bottom right.

Fig. 222: The Eta Carinae nebula, captured by FC2 during the ICO phase (clear filter, 600 s exposure).

The FC concluded ICO by acquiring a grand $3\times3$ image mosaic of NGC 3532 and the Eta Carinae nebula, part of which is shown in Fig. 222. Next on the agenda is a Mars Gravity Assist in February 2009, a good opportunity to test FC performance.

(H. Sierks)

# 3. *Atmosphäre, Ionosphäre und Magnetosphäre der Erde/ Terrestrial Atmosphere, Ionosphere, Magnetosphere*

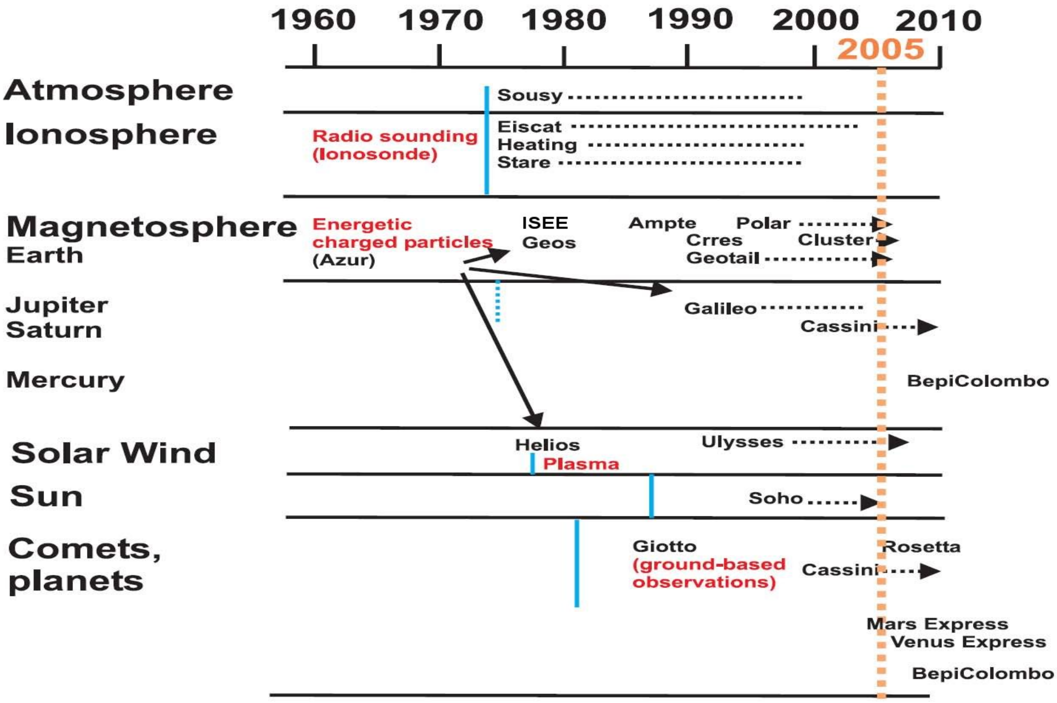


Fig. 223: Historical development of particle instruments in magnetospheric research and of project involvement at the Institute for the last 45 years.

## Overview of Magnetospheric research

Magnetospheric research at what was then the Max Planck Institute for Aeronomy (MPAe) began as a natural extension of the two original directions, stratospheric physics (including efforts at *in situ* measurements at high altitudes, particularly of cosmic rays) and ionospheric physics. Beginning in the early 1960s with an energetic particles instrument on the first German satellite AZUR, magnetospheric research at the Institute received a particularly strong boost in 1974 when Prof. W. Ian Axford (arguably one of the world's greatest magnetospheric physicists) was called to become Director at MPAe, with the mandate to revitalize, reorient, and expand the Institute. Under his leadership, emphasis was placed on cutting-edge research, concentrating on interesting fundamental questions, making use of all opportunities both of technical development and of mission availability.

The Institute has been particularly successful in the development and analysis of state-of-the-art particle instruments aboard spacecraft – the backbone of the Institute's international reputation to this day. These instruments were flown on a great variety of space missions (including GEOS, ISEE, AMPTE, GEOTAIL, HELIOS, CRRESS, POLAR, GALILEO, ULYSSES, CLUSTER) to investigate the magnetosphere of Earth and of other planets, their interactions with the solar wind, and the properties of the solar wind itself. Built partly at the Institute, within a framework of extensive international collaborations, these instruments were highly successful and stimulated hundreds of publications in the respective research areas.

Beginning in the 1980s, the Institute expanded into new research areas, applying its technical expertise (both with existing instrument types and with new developments) as well as the ideas of its scientists (who played a key role in the conception and design of the relevant missions): these areas were comets (the GIOTTO Mission to Comet Halley, with interest in both the comet itself and in its plasma environment) and the Sun (the SUMER experiment on board SOHO). An overview of the participation in various missions, along with developments in ionospheric and atmospheric research, is shown in Fig. 223.

Despite the brilliant scientific successes, the required level of effort proved ultimately to be incompatible with the shrinking available resources. The result was a decision by the Max Planck Society (formally made in 1996, but discussed already a year or so earlier) to phase out terrestrial research (atmosphere, ionosphere, magnetosphere) at MPAe. This decision was based not on scientific grounds (i.e. it was *not* a judgment that this research was no longer worth pursuing at MPAe) but rather on grounds of resources (research at MPAe was judged too broad for the available resources). The choice of future research areas was made primarily on the basis of

1. priority for the fields most recent at MPAe (comets/planets and Sun)
2. age distribution of scientists (particularly in the research areas of ionosphere and atmosphere, most scientists reached retirement age within a few years on either side of 2000).

This process of reorientation was completed on 30 September 2007, with the retirement of Prof. Vytenis M. Vasyliūnas as Director at MPS and the official closure of the division headed by him for research on magnetospheres – ending an era in the history of the Institute.

Ongoing magnetospheric/plasma research projects, however, together with new projects at planets other than Earth, are to be integrated into the planetary department of the Institute. In part as the result of its past successes, MPS is currently involved in the following particle instrumentation projects, either in flight or in preparation:

- Mercury: Bepi Colombo SERENA/PICAM and MPPE/MSA
- Venus: Venus Express ASPERA 4
- Sun-Earth: SOHO Celias, STEREO IMPACT
- Earth: Cluster RAPID and CIS
- Mars: Mars Express ASPERA 3
- Saturn: Cassini MIMI/LEMMS
- Comets: Rosetta ROSINA/RTOF and COSAC

### Future Exploration of Planetary Magnetospheres

In the near future, MPS with its reputation in magnetospheric research will still play a key role in the important missions to come. The investigation of planetary magnetospheres other than Earth's is currently being done at Saturn with the Cassini spacecraft, orbiting the ring planet since 2004 with a particle instrument MIMI/LEMMS developed in the laboratories of MPS. In addition, the Mercury space probes of the Bepi Colombo project are currently in preparation to be launched in the next decade; the Institute is involved in two particle instruments, one on each spacecraft. The planning of new missions to Jupiter or Saturn, including magnetospheric research proposed for ESA's cosmic vision theme, will proceed with participation from the planetary department of MPS.

### The Earth's magnetosphere and the Cluster Mission

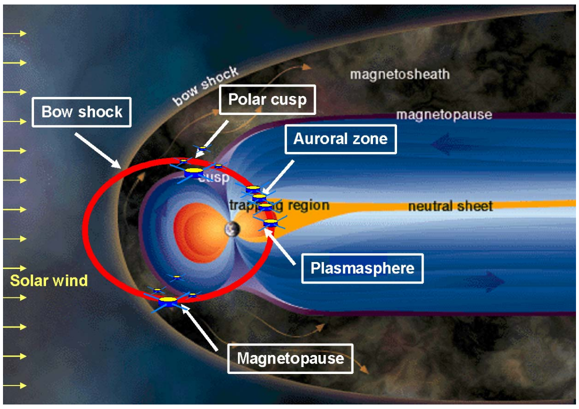


Fig. 224: Regions of the Earth magnetosphere investigated by the Cluster satellites: Solar wind, bowshock, magnetosheath, magnetopause, polar cusp, plasmasphere and aurora region.

The solar corona is heated up to a temperature of more than 1 million kelvin. This heating causes ions to be blown continuously into the vacuum of interplanetary space. This ion outflow is called the *solar wind* and has a density of only a few thousand particles per $m^3$, but a velocity of more than 300 km/s and a thermal energy of more than $10^5$ K.

The solar wind ions carry with them the magnetic structure of the solar chromosphere, thus causing the *interplanetary magnetic field*. An ionized gas is called a *collisionless plasma* if collisions between ions are so rare that acoustic waves cannot propagate. This is the case for the solar wind. Electromagnetic waves on the other hand can propagate through the plasma, as well as waves which propagate as changes in density and direction of the magnetic field which is bound to the plasma. The latter are called *magneto-acoustic* and Alfvén waves. They have a typical velocity of 30 – 100 km/s in the solar wind.

Solar wind ions are deflected by the Earth's magnetic field. The terrestrial magnetosphere, defined by the interaction of solar wind and Earth's magnetic field, is shown in Fig. 224. The boundary at which the pressure of the Earth's magnetic field equalizes the pressure of the inflowing wind is called *magnetopause*. This boundary is observed at distances between 30 000 – 60 000 km depending on solar wind pressure.

Since the solar wind streams relative to Earth with a speed which is higher than the speed of waves in the plasma, a *bow shock* builds up upstream of the magnetosphere similar to that of a supersonic aircraft. At the bow shock the energy of the bulk motion of the solar wind is converted to thermal energy such that the bulk motion becomes less than the wave velocity. While the plasma is heated it is also compressed in the region between bow shock and magnetopause. This region is called *magnetosheath*.

Inside the magnetopause the magnetosphere is essentially dominated by the dipolar magnetic field of the Earth. But even here plasma escapes from the *ionosphere* (at a height of about 200 km above the atmosphere) and builds the corotating *plasmasphere*. At the magnetospheric equator plasma can escape further to build the equatorial *neutral sheet*. This can stretch anti-sunward into the *magnetotail*. At the *polar cusp* magnetosheath ions can intrude down to the ionosphere causing the aurora, or polar lights. However, ionospheric ions can as well escape through the cusp.

While this global structure of the magnetosphere can be described fairly accurately by a magnetized fluid model (*magneto-hydrodynamics, MHD*), such a model already breaks down if we try to describe the temporal change or the plasma interaction at the boundaries. Here the distribution of energy and propagation directions of the ions plays an essential role and linear fluid models are misleading.

It was for this reason that the European Space Agency, ESA, developed the *Cluster Mission*, to allow the separation of temporal and spatial changes of the magnetospheric plasma. Consisting of four satellites orbiting the Earth since August 2000, it flys in a tetrahedral formation on a polar orbit with a period of 56 hours and at distances of 4 – 20 Earth radii (25 000 – 120 000 km). A typical initial orbit is shown in red in Fig. 224. One can see that the satellites cover the most important regions of plasma interaction in the magnetosphere.

More on this Mission including its current status, MPS participation, and some recent results, can be found in the individual reports starting on page 179.

### The Galileo Mission, new insights about planetary magnetospheres

A new era in the exploration of the outer solar system began with the Galileo mission to Jupiter. For the first time ever a manmade space probe was put in orbit around a gas giant in our solar system (Fig. 225).

Fig. 225: Artistic view of the Galileo spacecraft approaching Jupiter after a 6 year journey through the interplanetary space.

Galileo orbited Jupiter, the largest planet in our solar system, between 1995 and 2003. Fascinating data were received on Earth from Jupiter itself, from the Galilean satellites, and from the Jovian magnetosphere. Galileo was approved at the end of the 1970's by NASA together with the German space agency DLR. Originally a launch was foreseen for 1982 but technical difficulties caused a delay by almost 4 years. Then in 1986 Galileo was scheduled for lift-off by one of the space shuttles but the Challenger catastrophe put the project again on hold for 3 additional years. Finally the spacecraft was launched in October 1989 onboard the space shuttle Atlantis. The delay caused also a change in the trajectory of the spacecraft. Three planetary swing-bys were necessary to reach the final target Jupiter. Galileo flew past Venus and twice at Earth to gain energy by gravitational assists from those planets. In December 1995 Galileo was put into orbit around the largest planet in our solar system. Soon after, the scientists and engineers were faced with another problem. The high-gain antenna, built as a large umbrella, did not open and only the small low-gain antenna could be used for data transmission and communications. A complete reconfiguration of the spacecraft's flight software and an enormous effort of all instrument teams were necessary to save the mission.

Galileo consisted of the main spacecraft (Galileo orbiter) and a small atmospheric probe (Galileo Probe) which was dropped into Jupiter's atmosphere to measure the cloud structure, chemical composition and other parameters as well as their variability. One of the scientific instruments onboard the probe was a lightning detector with significant contributions from MPS. The outstanding results and health of the space-

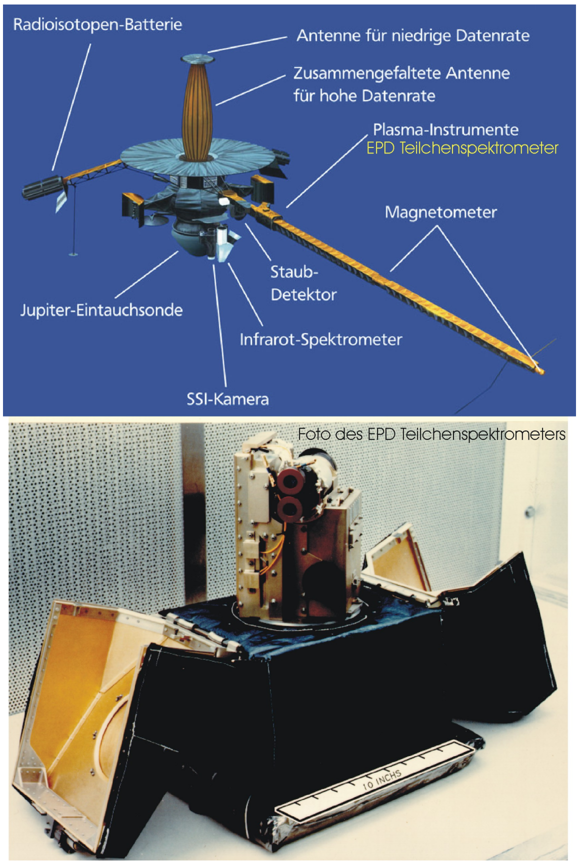


Fig. 226: Scientific payload of the Galileo spacecraft (top) and a picture of the Energetic Particles Detector (EPD) at the bottom.

craft led to several mission extensions between 1997 and 2003. Although the spacecraft has accumulated 4 times more radiation than it was designed for, everything was working and the data quality was excellent until the final plunge into Jupiter in September 2003.

The scientific payload of the Galileo orbiter (Fig. 226) consisted of a whole variety of camera systems for different wavelengths and sometimes spectrometric and interferometric capabilities to study the planet and its moons.

In addition particles and fields measurements were performed to study Jupiter's magnetosphere as a whole, and to study the interaction between magnetospheric plasma and the Galilean moons. One of the more complex sensors onboard was partly built at MPS. The Energetic Particles Detector (EPD) was designed to measure the three-dimensional distributions of electrons and ions, separately, in the energy range between 10 keV and several MeV. These ions which have velocities of several 1000 to several 10 000 km/s are very important for understanding the dynamics in Jupiter's magnetosphere. Electrons with such energies reach a significant fraction of the speed of light. It is not easy to measure these particles in space and a well-designed detector is necessary to distinguish not only the energy but also their mass and their incidence direction. The separation of different ion species and their three-dimensional distributions are indeed very important in Jupiter's magnetosphere; this has been described in previous *Tätigkeitsberichten*.

(V. M. Vasyliūnas, P. Daly and N. Krupp)

## Wissenschaftliche Einzelberichte/
*Individual scientific reports*

(nur in Englisch)

### The 5-day signal in the mesospheric water vapour concentration in high latitudes in 2003 – a comparison between observations in ALOMAR and calculations

The analysis of the water vapour measurements in 2003 by means of the microwave technique in high latitudes at ALOMAR, Norway, revealed the signature of a quasi 5-day wave in the mesosphere beginning in May and lasting with decreasing amplitude until July/August. The period varies between about 5 and 7 days. Real-date calculations on the basis of our GCM brought evidence that the 5-day wave is a global phenomenon occurring particularly in high and middle latitudes during the summer season. The agreement of the calculations with the observations is good. These waves were theoretically predicted in 1984 and were identified as normal (1,1) mode Rossby wave. The dynamical wind components and temperatures are able to modulate the transport of relatively inert minor constituents such as water vapour in the whole middle atmosphere and atomic hydrogen and atomic oxygen in the lower thermosphere. They also impact the chemistry of constituents marked by characteristic times noticeably smaller than 5 days. The variation of both the temperature and the water vapour mixing ratio influence the occurrence rates of NLCs and PMSEs. The calculations show a strong influence of the night-to-day-ratio of ozone in heights of the secondary ozone maximum whereas the impact on the mesospheric ozone is relatively small. The year 2003 was marked by a strong outbreak of the quasi 5-day wave. The analysis of further years of water vapour measurements at ALOMAR has still to be done.

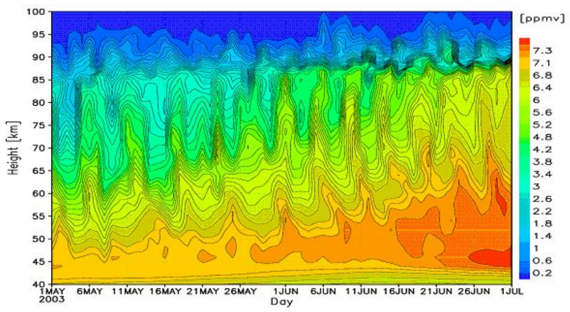


Fig. 227: Seven-day sliding average of the water vapor mixing ratio at ALOMAR (69.29° N, 16.03° E), Norway in 2003.

(G. Sonnemann, P. Hartogh and L. Song, in collaboration with M. Grygylashvyly and U. Berger (IAP Kühlungsborn))

### Long-term trends of the concentration of the minor constituents in the mesosphere – a model study

We investigated the influence of the rising concentrations of methane, dinitrogen oxide and carbon dioxide since the pre-industrial era upon the chemistry of the mesosphere. In order to get approximated data of the solar Lyman-$\alpha$ flux back to the pre-industrial time, we derived a quadratic fit using the sunspot number available since 1749 as the only solar proxy for the Lyman-$\alpha$ flux before 1947. The Lyman-$\alpha$ flux values are employed to determine the water vapour dissociation rate. The water vapour trend analysis utilizes estimated methane trends since the pre-industrial era. An unsolved problem for the model calculations consists of the water vapour mixing ratio at the hygropause during the time range of trend calculation. We assume that the hygropause was dryer at the pre-industrial time than currently. As a consequence of the methane oxidation, the middle atmosphere became more humid according to the rising methane concentration, but depending on height and with a small time delay of few years. The solar influence on the water vapour mixing ratio is insignificant below about 80 km (see Fig. 228) within summer high latitudes, but it becomes increasingly more important above this altitude. The growing water vapour concentration increases the hydrogen radical concentration and reduces the mesospheric ozone. A second region of stronger ozone decrease is located in the vicinity of the stratopause. Increasing $CO_2$ concentration enhances slightly the concentration of CO in the mesosphere, but its influence upon the chemistry is small and its main effect is connected with a cooling of the upper atmosphere.

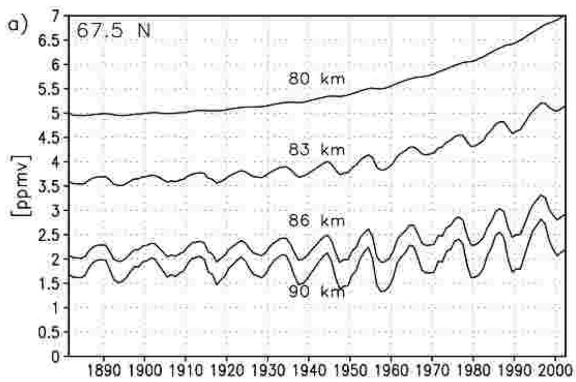


Fig. 228: Modelled mesosphere/mesopause water vapour trend at ALOMAR since 1880.

(P. Hartogh in collaboration with G. Sonnemann and M. Grygalashvyly (IAP Kühlungsborn))

**A new 22 GHz water vapour heterodyne spectrometer**

We developed a new 22 GHz water vapour heterodyne spectrometer. It has been funded by the Deutsche Forschungsgemeinschaft (DFG) within the research priority program CAWSES (Climate and Weather in the Sun Earth System) and will replace the old WASPAM spectrometer in the Artic Lidar Observatory of middle atmospheric research (ALOMAR, Northern Norway) in order to understand short term phenomena related to solar input, atmospheric dynamics and noctilucent clouds. In order to achieve this goal, extremely low noise Indium Phosphite (InP) High Electron Mobility Transistor (HEMT) amplifiers, especially designed for this purpose have been used as frontend components. At the same time the system observes the atmosphere in vertical and horizontal polarization in order to double the throughput. HEMT amplifiers and important parts of the optics are cooled to temperatures around 12 K using a closed cycle refrigerator. The external optics consists of one rotational and two fixed parabolic mirrors. The fixed mirrors reflect radiation from hot and cold black bodies. The loads are mounted into the same dewar than the HEMTs and are operating at temperatures of about 50 K and 120 K. The rotating mirror is pointing alternately too the load mirrors and the atmosphere. Combining the HEMTs an effective receiver noise temperature of 15 K has been achieved (compare old WASPAM system: 110 K), which presently is the world record for this kind of system. The spectrum analysis is performed by two high resolution (13 kHz) chirp transform spectrometers with 40 MHz bandwidth. Figs. 229 and 230 show the front- and backend of the new system. From spring 2008 on the system is planned to operate from the (ALOMAR) in Northern Norway. The PhD student Kristofer Hallgren was heavily involved in putting the new water vapour system together and he intends to use it in order to search for diurnal or semi-diurnal tides in the upper mesosphere water vapour.

(P. Hartogh, K. Hallgren, and C. Jarchow)

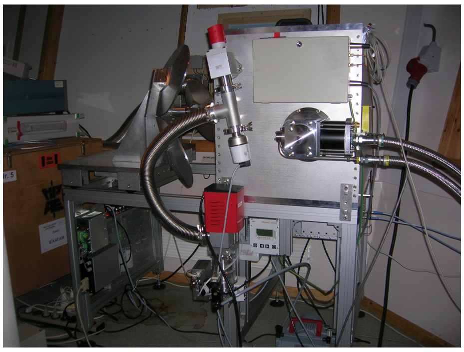

Fig. 229: Frontend of cooled 22 GHz heterodyne spectrometer. Right: dewar with helium supply and return, left: parabolic mirrors mounted on moving table. The table moves by about a quarter wavelength per measurement interval. This movement is called “wobbling”. The purpose of the wobbler is to cancel out reflections in the system, also known as baseline ripple removal. The baseline wobbler transfer function is described by a Bessel function. For effective baseline removal the wobbling amplitude as to be very accurate ($< 5\ \mu$m error) in order to hit the first zero of the Bessel function.

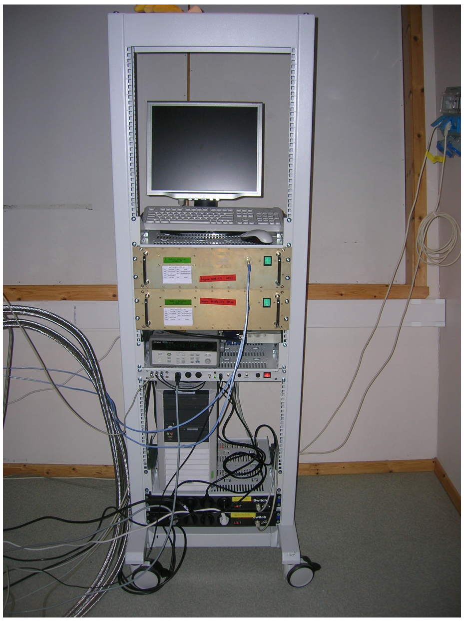

Fig. 230: Backend rack with chirp transform spectrometer, measurement computer and housekeeping processor.

**Forces in the magnetosphere-ionosphere-Earth system**

Magnetosphere-ionosphere interactions involve electric currents that circulate between the two regions; the associated Lorentz forces, existing in both regions as matched opposite pairs, are generally viewed as the primary mechanism by which linear momentum, derived ultimately from solar wind flow, is transferred from the magnetosphere to the ionosphere, where it is further transferred by collisions to the neutral atmosphere. For a given total amount of current, however, the total force is proportional to $\mathcal{L}B$ and in general, since $\mathcal{L}^2 B \sim$ constant by flux conservation, is much larger in the ionosphere than in the magnetosphere ($\mathcal{L}$ = effective length, $B$ = magnetic field). The magnetosphere may be described as possessing a mechanical advantage: the Lorentz force in it is coupled with a Lorentz force in the ionosphere that has been amplified by a factor given approximately by the square root of magnetic field magnitude ratio ($\sim$ 20 to 40 on field lines connected to the outer magnetosphere). The linear momentum transferred to the ionosphere (and thence to the atmosphere) as the result of magnetic stresses applied by the magnetosphere can thus be much larger than the momentum supplied by the solar wind through tangential stress. The added linear momentum comes from within the Earth, extracted by the Lorentz force on currents that arise as a consequence of magnetic perturbation fields from the ionosphere (specifically, the shielding currents within the Earth that keep out the time-varying external fields). This implies at once that Fukushima's theorem on the vanishing of ground-level magnetic perturbations cannot be fully applicable, a conclusion confirmed by reexamining the assumptions from which the theorem is derived. To balance the inferred Lorentz force within the Earth's interior, there must exist an anti-sunward mechanical stress there, only a small part of which is the acceleration of the entire Earth system by the net force exerted on it by the solar wind. The solar-wind interaction can thus give rise to internal forces, significantly larger than the force exerted by the solar wind itself, between the ionosphere and the neutral atmosphere as well as within the current-carrying regions of the Earth's interior. (This work has been published by Vasyliūnas, 2007.)

(V. M. Vasyliūnas)

### Rotationally driven interchange instability

We derive the dispersion relation for the rotationally driven interchange instability, using the same basic equations as in our previous work but taking care to keep some terms that had been overlooked, and show that inclusion of the Coriolis force does modify the dispersion relation, reducing the growth rate of the instability and adding an oscillating component. Its effect becomes negligible only in the limit of azimuthal wavelength very short in comparison to radial distance, in the limit of plasma acceleration time very short in comparison to rotation period, and in the singular case of flux tube content proportional to equatorial field strength. Some authors had found no effect of the Coriolis force because they assumed all wavelengths to be short. For plasma acceleration time longer than the rotation period, the effect of the Coriolis force can restrict the range of radial gradients that are unstable. Although not a generally valid result, neglect of the Coriolis force effects is in practice applicable as long as the fastest-growing (hence presumably the most significant) instabilities are those with very short wavelengths. (This work is published by Vasyliūnas and Pontius, 2007.)

(V. M. Vasyliūnas)

## The Cluster Mission

The Cluster Mission to the Earth's magnetosphere was launched in 2000 from Baikonur and started its initial two-year operation phase in February 2001. A first extension was later granted to last until the end of 2005. At the beginning of 2005, the ESA approved a second extension, so that Cluster operations will now continue, pending spacecraft and instrument health, until the end of 2009. Further extensions (1–2 years) are being considered.

Each of the four spacecraft carries an identical payload of 11 experiments for measuring plasma and energetic particles, electric and magnetic fields, as well as wave phenomena. During the first $4\frac{1}{2}$ years, the spacecraft were in a tetrahedron configuration of size varying from 100 to 5000 km, in order to investigate events at different scale sizes. The separation distances were altered first twice, and then later once a year.

The latest extension provides new possibilities for this already successful mission. After the manoeuvres in June–July 2005, a totally new concept was implemented: 3 of the 4 spacecraft form a large triangle of size 10 000 km, while the 4th spacecraft is in an orbit such that its distance from one of the others is adjustable between 30 km and 10 000 km. Furthermore, the orientation of the large triangle can be rotated to be parallel to the geomagnetic tail during the months when the apogee is in the nightside, or perpendicular to the solar wind when the apogee is on the dayside. All these manoeuvres can be achieved with small changes to the spacecraft's phases within the orbits, with very little fuel consumption. This new aspect of the Cluster constellation is called *multi-scaling*.

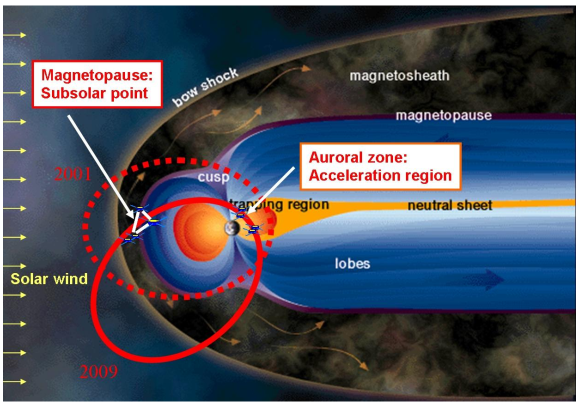


Fig. 231: The Cluster orbit as it will be early 2009; the apogee will have moved far to the south and three spacecraft form a large triangle with the fourth one at variable distances

Furthermore, as seen in Fig. 231, the Cluster orbit will have evolved such that its apogee is no longer over the equator but far in the southern hemisphere. This permits new regions to be investigated, such as the auroral zones and the subsolar magnetopause.

MPS has two major contributions to Cluster: the CIS ion spectrometer (up to ~40 keV/e) and the RAPID ion and electron imager (from ~30 keV). These instruments will be able to exploit the multi-spacecraft feature of the mission at best with the large separations which approximate the typical ion gyroradii.

(P. W. Daly and A. Korth)

### Multipoint observations of ions in the energy range 30–235 keV upstream of Earth's bow shock

We used multipoint observations by the Cluster spacecraft to study diffusive transport in the upstream region and the efficiency of Fermi acceleration of ions at the quasi-parallel bow shock. The time periods with appropriate spacecraft separations along the upstream magnetic field together with the stable solar wind conditions are rather rare cases. For these unique events we determined spatial gradients by measuring partial proton intensities in the energy range 27.7 keV to 159.7 keV and partial helium intensities in the energy range 29.9 keV to 235.1 keV as a function of distance from the bow shock along the magnetic field, using data from the RAPID experiments onboard the Cluster spacecraft. Combining RAPID data with CIS data at lower energies from 10 to 32 keV, we find that the e-folding distance increases from lower energies approximately linear with energy, confirming that particles could be affected by the Fermi acceleration (Fig. 232). This effect is also seen in the hardening of the particle spectra with the distance from the bow shock. The partial oxygen intensities from the energy 274 to 638 keV do not produce gradients along the magnetic field. Assuming that upstream diffusion is balanced by downstream convection we determine the spatial diffusion mean free path parallel to the magnetic field as a function of energy. Several upstream events under different solar wind conditions undergo this study.

(E. Kronberg, P. W. Daly in collaboration with A. Kis, B. Klecker, and E. Lucek)

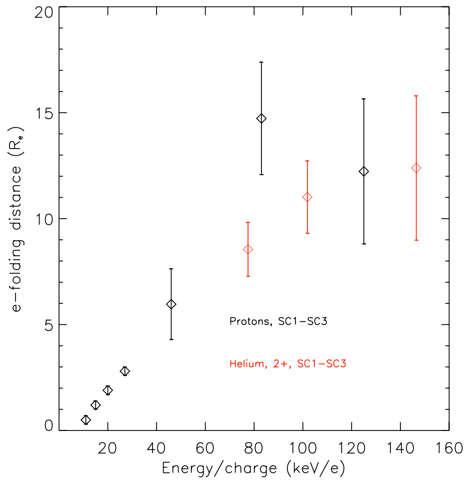


Fig. 232: The e-folding distance versus energy during the ion upstream event on 18 February 2008 using the data from the Cluster spacecraft 1 and 3. Black points are protons and red are helium ions. First four black points at low energy ranges are obtained from an earlier work using the CIS instrument, for comparison. The approximately linear growth of the e-folding distance with the energy implies that particles can be affected by the Fermi acceleration.

### Cluster encounter with an electron beam during a substorm

On August 11, 2002, the electron spectrometers PEACE and RAPID on board Cluster observed a beam of energetic electrons with energies up to 400 keV (Taylor *et al.*, 2006). The entire event lasted only 20 s, but within this time the flow direction of the particles changed radically, in an energy-dependent manner (Fig. 233). This allows the internal structure of the beam to be reconstructed.

Although the four Cluster spacecraft were only 3700 km apart, the beam was observed exclusively on Cluster 3. This indicates that it is sharply limited in both time and space. Such events are extremely difficult to observe. It is shown, that the beam is associated with a magnetospheric substorm; the consequences for various theories of particle acceleration are discussed.

(P. W. Daly, in collaboration with colleagues from the Cluster RAPID and PEACE teams)

### Motion of flux transfer events

FTEs (*flux transfer events* result from localize field line reconnection at the magnetopause and play a key role in the transfer of magnetic flux from the solar wind to the Earth's magnetosphere. An important factor during the analysis of FTEs is to which hemisphere, north or south, the field lines are connected. This question can be answered by examining the pitch angle distribution of energetic ions.

Although the central ion sensor on all four RAPID instruments failed early in the mission, it is still possible to observe strong anisotropies in the ion distributions in order to determine FTE "connectivity", as seen in Fig. 234. A thorough investigation of over 200 FTEs (Fear *et al.*, 2007) exploited this possibility to support a simplified model for the creation of FTEs.

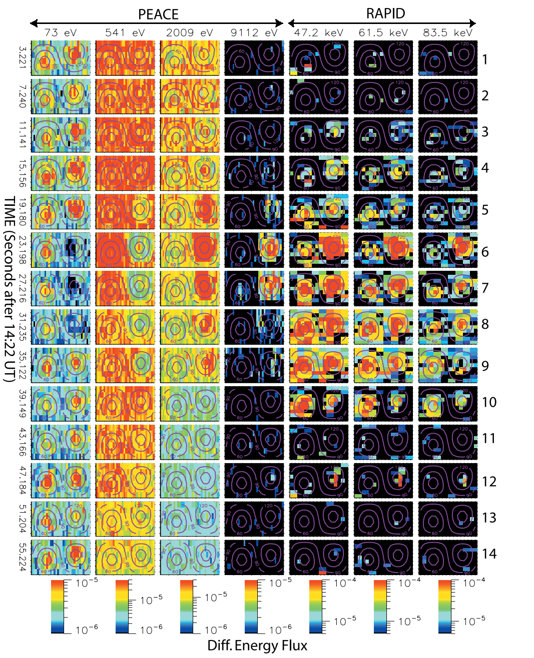


Fig. 233: Electron data from PEACE and RAPID with high resolution in time and direction. Each panel shows the particle flux distribution in 2 directions (polar and azimuth). Time runs from top to bottom, with 4 s between each row; energy increases from left to right, the three right-hand columns contain RAPID data.

(P. W. Daly in collaboration with colleagues from the Cluster RAPID and CIS teams)

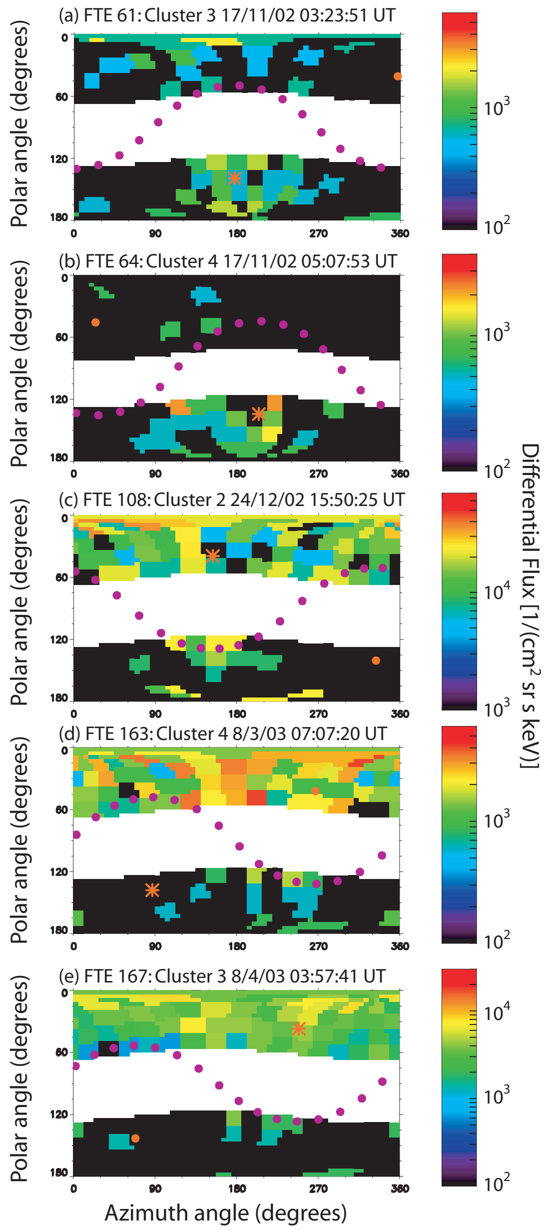


Fig. 234: RAPID ion data, as particle flux in 2 angular dimensions; the red points indicate the direction 90° to the magnetic field, the orange dot and cross are the magnetic field vector itself (0° and 180° respectively). The white band in the middle arises from the missing data in the non-functioning central ion sensor. Each panel corresponds to a separate event.

## Substorm observations in the magnetotail with Cluster during high-speed plasma streaming from the Sun

In recent times, there have been many discussions on constantly repeating substorm activities and their causes. In this investigation, we carry out a "cross-wavelet" analysis between solar wind and plasmasheet parameters at 20 and 6.6 (geostationary orbit) Earth radii. For this analysis, we make use of data from ACE (*Advanced Composition Explorer*), Cluster, and the Los Alamos geostationary satellites. We could demonstrate that the plasmasheet periods agree very well with the structure of the Alfvén waves embedded in the fast plasma streams from the Sun. They have a period of 2 – 4 hours. This indicates that the solar activity directly affects the plasmasheet activity. See Fig. 235 taken from Korth *et al.* (2007).

(A. Korth and M. Fränz in collaboration with colleagues from the Cluster CIS team)

## The non-cusp Earth's magnetopause observed by Cluster

The ambient plasma and magnetic field conditions on two sides of the magnetopause, as well as the proper parameters of the magnetopause current sheet are investigated using plasma and magnetic field data collected by the four Cluster spacecrafts at inter-

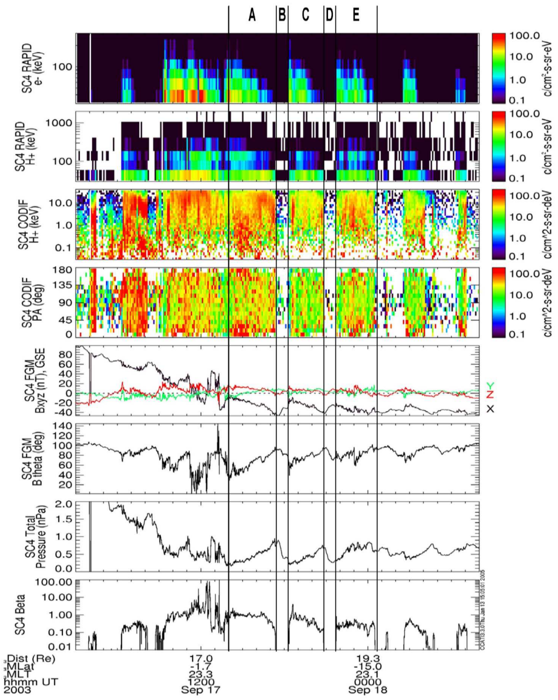


Fig. 235: Plasmasheet crossing by Cluster during a high-speed plasma stream an September 17/18, 2003. The panels show from top to bottom: energy spectrograms of electrons and ions from RAPID, energy and pitch angle distributions of protons from CIS, magnetic $x$, $y$, $z$ components, and the $\theta$ angle from the magnetometer, the plasma pressure, and the beta parameter from CIS.

spacecraft distances less than 300 km based on all available 154 magnetosheath-magnetosphere transitions more and less probable ambient plasma and magnetic field configurations are found, depending on the sort of the magnetospheric boundary. The transitions through the low-latitude boundary layer, transitions through the plasma mantle and cusps-associated transitions are distinguished (see Fig. 236). The maximal amplitude of the magnetopause flapping is demonstrated. The sub-Alfvénic magnetosheath flows, required for stabilizing the magnetopause reconnection, are shown just above the plasma mantle on a statistical basis. The analysis of the magnetopause pressure balance revealed a group of 24 transitions when both thermal and magnetic magnetosheath pressures exceeded the magnetospheric ones providing exotic conditions for a non-stationary way of the magnetopause formation. Furthermore, the orientation of the magnetopause is shown and distribution functions of the magnetopause speed, thickness and current density are provided based on 52 magnetopause crossings. The magnetopause with the attached plasma mantle was slower and thinner than the one with the adjacent low-latitude boundary layer. A comparison with observations at low latitudes revealed that the magnetopause

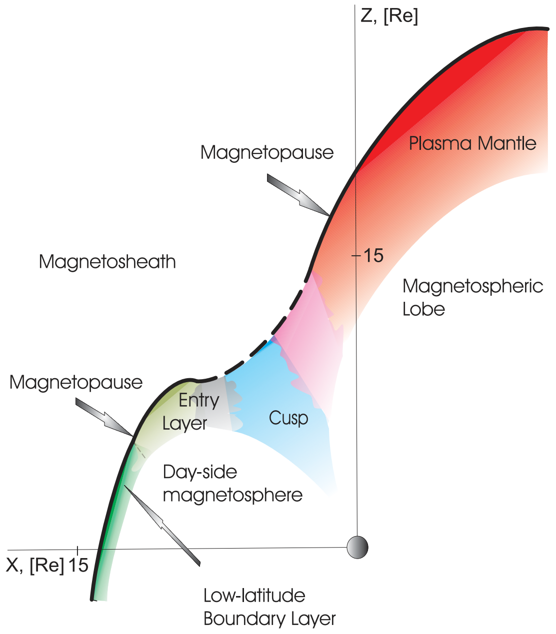


Fig. 236: Sketch of the noon-meridian slice of the Earth's magnetosphere in the vicinity of the polar cusp (only northern magnetospheric hemisphere is shown). The thick solid line corresponds to the magnetopause where proper current sheet signatures are observed, while thick dashed line indicates the probable magnetopause location where the proper magnetopause current sheet cannot be formed continuously.

at high and middle latitudes is, on average, about two times thicker. The magnetopause current densities are defined by both the magnetopause thickness and the change in the maximum variance magnetic field component across the magnetopause current sheet.

(E. V. Panov and J. Büchner et al.)

## RAPID contribution to the Cluster Active Archive

The Cluster Active Archive (CAA) is the ESA contribution to the NASA *Living with a Star* Project. It is a depository of processed and validated high-resolution Cluster data, raw data, processing software, calibration data, documentation and other value added products. During the remaining Cluster operation phase (currently until the end of 2009) plus one year, the archive is *active*, meaning it is being regularly populated with new and/or upgraded data, directly from the instrument teams. After that, it will become the long-term archive for the invaluable Cluster data set, making processed data available to the world long after the instrument teams have been dissolved and direct knowledge of the experiments is no longer at hand.

Fig. 237 shows the CAA home page at `http://caa.estec.esa.int/caa/`.


Fig. 237: The CAA home page

As one of 11 instruments per spacecraft RAPID (Research with Adaptive Particle Imaging Detectors) detects counts of electrons with its Imaging Electron Spectrometer (IES) and protons, helium and heavier ions with the Imaging Ion Mass Spectrometer (IIMS). The RAPID instrument is able to provide 3-D particle measurements in an energy range of 28 to 1500 keV. For CAA, RAPID delivers count rates and differential fluxes of omnidirectional and 3-D data products and their standard deviations, particle flow directions and pitch angles, useful diagnostic products for expert users, caveat and instrument mode files and 6-hour overview plots.

Following the delivery schedule, the data for the first five years of operation (2001 – 2005) have been ingested by the end of 2007. Afterwards, two years of data are to be delivered per year. Because of on-going improvements in the calibration and processing algorithms, a reprocessing of the existing data will be undertaken.

In addition, a RAPID data analysis software is developed as well as summary plots, which are produced at the MPS and delivered to CAA.

(P. W. Daly, E. Kronberg, and S. Mühlbachler)

### The German Cluster Data Centre

As part of the Cluster Mission, the *Cluster Science Data System*, has been operating well since the first Cluster data have been available in 2001. Intended as a means by which Cluster investigators could quickly access online a subset of the data from other Cluster instruments, it consists of national data centres in the UK, Sweden, Austria, Hungary, France, and Germany, each processing the data sets for the PI instruments in their respective countries. By mirroring every night, each national data centre has a full set of data for all experiments, for distribution within that country.

American investigators obtain the data from the NSSDC at Goddard, through the UK Data Centre; Chinese associates through a copy via the Austrian Centre in Graz.

Fig. 238 shows the CSDS distribution as shown on the Web page at `http://sci2.estec.esa.nl/cluster/csds/ring.html`.

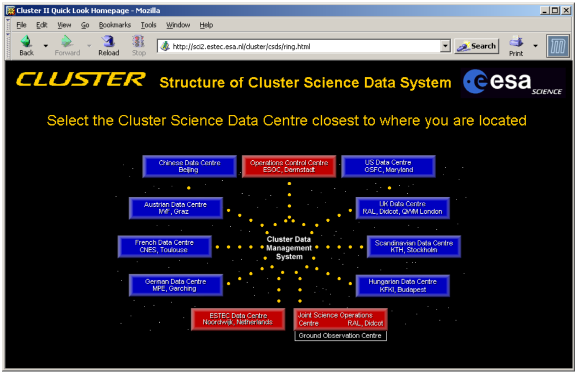


Fig. 238: The CSDS National Data Centres and data flow

The *German Cluster Data Centre*, GCDC, is responsible for the two German-led Cluster instrument: RAPID and EDI (*Electron Drift Instrument*, PI originally G. Paschmann at MPE, now retired). GCDC has been housed at MPE, the Max-Planck-Institut für extraterrestrische Physik in Garching, but due to restructuring at that Institute, it was necessary to find a new location and responsible person for the time period 2008 and beyond. Since the RAPID PI at MPS has long collaborated with GCDC from its inception, the most logical new home should be in Lindau.

During the course of 2007, a parallel system has been set up at Lindau, which as of 1 January 2008, became the official GCDC for the rest of CSDS.

Two new positions will come with this move: a data centre manager and data centre scientist.

Thus the German contributions to both the CSDS and the Cluster Active Archive will be coordinately together from one location.

(P. W. Daly and E. Georgescu)

# III. Selbständige Nachwuchsgruppe Helio- und Asteroseismologie / Independent Junior Research Group of the Max Planck Society "Helio- and Asteroseismology"

## Wissenschaftliche Einzelberichte/ *Individual scientific reports*

Research on solar and stellar oscillations is carried out at the Institute by the Independent Junior Research Group "Helio- and Asteroseismology" (Max Planck Society).

### Measurement of the meridional flow with Fourier-Hankel decomposition

On the solar surface a meridional flow of 10 – 20 m/s is observed. This flow is directed away from the equator towards the poles. Because of mass conservation an equatorward return flow is expected in the deeper layers of the convection zone. This meridional circulation might play an important role in the dynamo process which causes the solar magnetic cycle.

We used a technique called Fourier-Hankel decompositon to measure the meridional flow. In each solar hemisphere, the observed acoustic wavefield can be separated into waves propagating either polewards or equatorwards. The frequencies of the acoustic modes are Doppler shifted by the meridional flow: waves propagating with a flow have a higher frequency than waves propagating against it.

Depending on the spatial wavelength and the temporal frequency, acoustic modes probe different depths of the solar interior. This allows us to measure the Doppler shift due to the meridional circulation as function of mode penetration depths (Fig. 239). For such an analysis, we used a time series of 30 days of full-disk Doppler velocity maps recorded by the Michelson Doppler Imager aboard the Solar Heliospheric Observatory (SOHO-MDI) in April 1999. For modes probing the outer 40 Mm of the Sun, the meridional flow is measured to be poleward with an amplitude of about 15 m/s.

Our observations confirm that the Fourier-Hankel decomposition of the wavefield, originally developed by D. Braun, is a useful tool for local helioseismology.

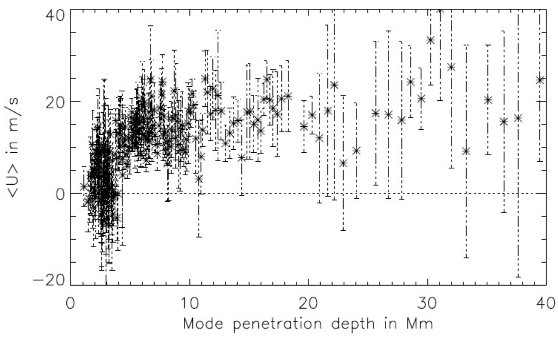


Fig. 239: Poleward meridional flow sensed by single acoustic modes as a function of mode penetration depth (northern hemisphere).

(M. Roth in collaboration with L. Krieger (KIS, Freiburg))

### Solar-cycle variation of rotation and meridional circulation

The temporal variations in rotation and meridional circulation have a long-term component with a period near eleven years. These are small variations of a few m/s, which are connected to the evolution of the large-scale magnetic field. We have made independent observations of the solar-cycle variation of large-scale flows at two different depths in the solar interior: near the solar surface and at a depth of about 60 Mm. The latitude range of the observations is $\pm 45°$.

For the near-surface layers, we used f-mode time-distance helioseismology to obtain a map of the convection pattern every 12 hour. The near-surface plasma flow was then estimated from these maps by observing the advection of the convection pattern. At 60 Mm depth, rotation and meridional circulation can be estimated directly from the difference in travel time for acoustic waves propagating in opposite directions between surface locations separated by about 17°.

Fig. 240 summarizes the results. Over the period 1996 – 2002, the time-varying components of the meridional flow at the surface and at a depth of 60 Mm

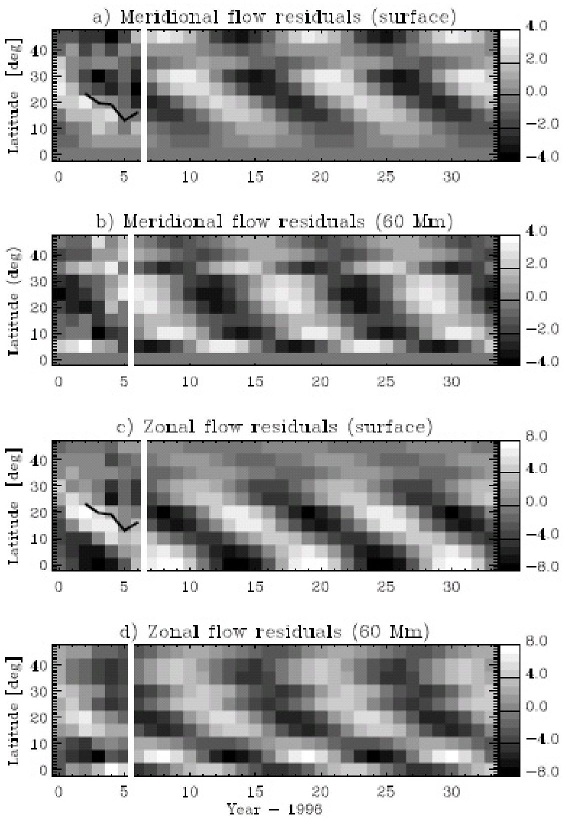


Fig. 240: Time-varying components of the meridional (a,b) and zonal (c,d) flows as a function of time. The colour bar is in units of m/s. Panels a) and c) are for the near solar surface, while panels b) and d) are for a depth of about 60 Mm below the surface. The black lines in panels a) and c) show the mean latitude of active regions. The eleven-year periodic component of the data is extrapolated into the future beyond the white vertical lines.

have opposite sign, while the time-varying components of the zonal flow are in phase. The solar-cycle variations with respect to the long-term average do not exceed $\pm$ 10 m/s.

We investigated a theoretical model based on a flux-transport dynamo combined with a geostrophic flow caused by increased radiative loss in the active region belt. The model is qualitatively consistent with the observations, in particular the phase of the solar-cycle variations of the flows near the surface and 60 Mm below is reproduced. Deeper in the interior, however, the model underestimates the amplitude of the time variations of the meridional flow by nearly an order of magnitude. Overall, it is fair to say that the model is encouraging.

(L. Gizon in collaboration with M. Rempel (HAO, Boulder))

**Accurate travel-time measurements**

We studied different methods for measuring helioseismic travel times. In particular, these methods were compared for robustness with respect to noise. In order to demonstrate the sensitivity of the measurements to small-amplitude flows, we repeated observations by Beck et al. (2005) of the cross-equator meridional flow as a function of time using MDI Doppler velocity data. The results are shown in Fig. 241. The cross-equator meridional flow is southward on average (about 6 m/s), with an annual variation of about $\pm$ 5 m/s. Our measurements are consistent with those of Beck et al. (2005). The offset and the annual variation have been attributed to systematic errors in the determination of the direction of the rotation axis of the Sun.

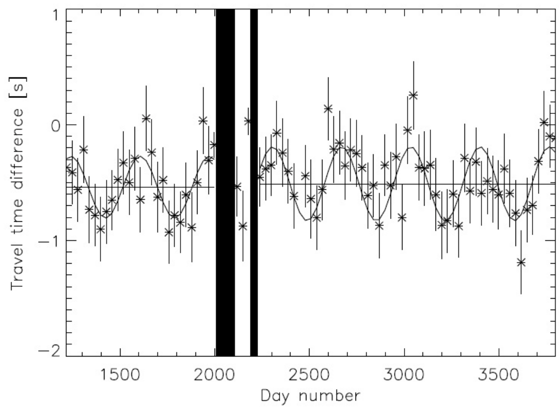


Fig. 241: MDI travel-time shifts for acoustic wave packets travelling in the south-north direction. The offset from zero and the annual variation are attributed to an error in the determination of the direction of the solar rotation axis. A travel-time shift of 1 s corresponds to about 10 m/s. The time intervals in black are for missing data.

(M. Roth and L. Gizon in collaboration with J. Beck (Stanford))

**High resolution time-distance helioseismology**

We are interested in using solar surface-gravity waves, or f modes, to probe flow structures in the upper layers of the Sun ($\sim$ 1 Mm depth). One goal, for instance, is to study supergranular flows at spatial resolutions close to the f-mode wavelength (5 Mm at 3 mHz). Another aim is to understand the behaviour of flows around magnetic active regions.

Achieving high spatial resolution requires two main steps. The first step is realistic modeling of solar wave propagation, sometimes called the forward problem. In time-distance helioseismology, we consider the wave travel-time difference between any two

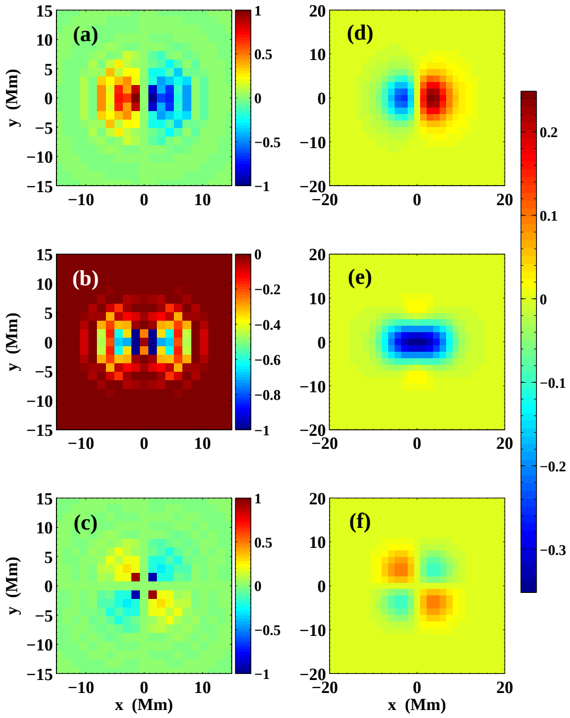


Fig. 242: Examples of kernel functions (panels a,b,c) that give the linear sensitivity of f-mode travel times (quadrant averaging) to horizontal flows in the $x$ direction. The radius of the annulus is 8.7 Mm. The units of the colour scales are s $(\mathrm{km/s})^{-1}$ $\mathrm{Mm}^{-2}$. (Panels d,e,f) Optimal inversion coefficients computed using the kernels on the left (see text). These inversion coefficients are combined with the travel-time measurements to give local estimates of the $x$-component of the flow. The colorscale is in units of $\mathrm{m/s}^2$.

points on the solar surface. Travel-time differences convey information about the underlying flows. To extract this information, it is necessary to model how f-mode travel times are affected by flows. For small-amplitude flows, this procedure can be carried out accurately in the first Born approximation, which is a single-scattering approximation. From here one can derive two-dimensional linear sensitivity functions, called travel-time kernels. Some examples of theoretical kernels are shown in the column on the left in Fig. 242. The travel times we consider here are various combinations of the travel times for waves propagating between the center of an annulus and its perimeter (called quadrant averaging).

The second step involves using the computed sensitivity kernels along with measured travel times to infer the solar flows. The inversion procedure may be done in a number of ways. We chose a method known as Optimally Localized Averaging (OLA), whereby one seeks a set of coefficients to form a linear combination of the sensitivity kernels (an averaging kernel) that resembles a Gaussian target function. The inversion coefficients are then used to average the travel-time measurements and invert the local flow with a spatial resolution given by the width of the averaging kernel. A full inversion uses as input many types of kernels, including those shown in Fig. 242.

There are various subtleties with this method that need to be considered, such as the trade off between having a well-localized averaging kernel, and minimizing the measurement noise that propagates through the inversion. A characteristic set of inversion coefficients is shown in the right column of Fig. 242. These inversion coefficients, when convolved with the sensitivity kernels, give an averaging kernel that is well localized in space.

Fig. 243 shows an OLA intersion of f-mode travel times around a sunspot. The data are averaged over one day. The outflow around the sunspot (the moat flow) is clearly seen, as well as neighboring supergranules. This is perhaps the first example of a fully consistent procedure to infer flows in time-distance helioseismology.

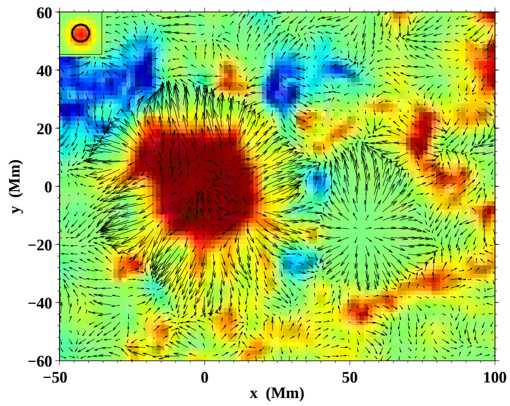


Fig. 243: Map of horizontal flows around a sunspot (arrows) using one day of MDI full-disk data. The spatial resolution is determined by the width of the averaging kernel (FWHM 7 Mm) shown in the top-left corner. The longest arrow corresponds to a flow of 450 m/s. The surface line-of-sight magnetic field is displayed in red and blue shades (saturated at $\pm 350$ G).

We are in the process of extending the inversion procedure to measure flows in three spatial dimensions, using p-mode travel times and the sensitivity kernels discussed below.

(J. Jackiewicz and L. Gizon in collaboration with A. C. Birch (CoRA, Boulder) and M. J. Thompson (Sheffield))

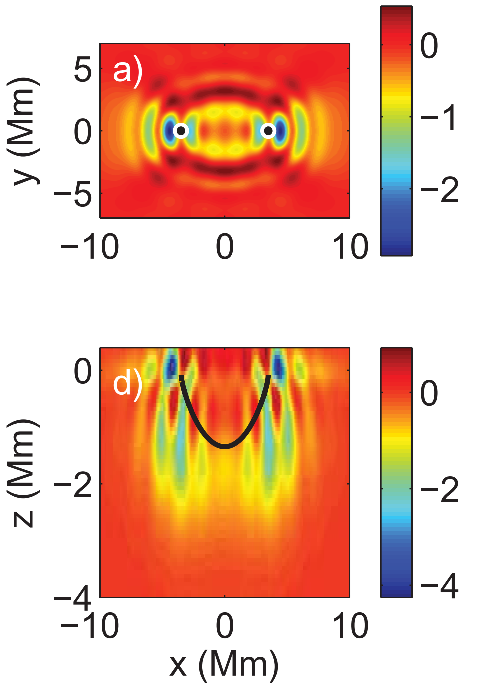


Fig. 244: Slices through a kernel function that gives the sensitivity of a $p_1$ travel-time measurement to the $x$-component of a local flow. The top panel shows a horizontal slice at the photosphere. The black dots at ($x = -5$ Mm, $y = 0$) and ($x = 5$ Mm, $y = 0$) indicate the two points between which the travel time is measured. The colour bar is in units of s $\mathrm{Mm}^{-3}$/(km/s). The bottom panel shows a vertical slice through the kernel along $y = 0$. The black curve shows the ray path (infinite frequency limit). Notice that the sentivity extends much beyond the ray path.

### Travel-time sensitivity kernels for vector flows

In time-distance helioseismology, inferences of plasma flows depend critically on the ability to accurately model the effects of subsurface flows on the travel-time measurements. Using the first Born approximation, we have computed the sensitivity of travel times to weak, steady, inhomogeneous subsurface flows. Three sensitivity functions are obtained, one for each component of the 3D vector flow. Fig. 244 shows slices through an example kernel function computed for $p_1$ acoustic modes. We have shown that the depth sensitivity of travel times to horizontally uniform flows is given approximately by the kinetic energy density of the oscillation modes which contribute to the travel times. For flows with strong depth dependence, the Born approximation can give substantially different results than the ray approximation.

(L. Gizon in collaboration with A. C. Birch (CoRA, Boulder))

### Three-dimensional sensitivity kernels for ring-diagram analysis

Ring-diagram analysis is a technique of local helioseismology used to infer plasma flows in the solar convection zone. It generates intermediate data products known as ring-fitting parameters. Knowing the sensitivity of ring-fitting parameters to actual flows in the Sun is important for interpreting these measurements. Working in plane-parallel geometry, we have computed the linear sensitivity of ring-fitting parameters to small changes in the local power spectrum of solar oscillations and then the sensitivity of the power spectrum to time-independent weak local flows. We combined these two results to obtain the three-dimensional Frechet kernels that give the linear sensitivity of ring-fitting parameters to both vertical and horizontal local flows. An example kernel is shown in Fig. 245. We found that ring measurements are essentially only sensitive to flows that are within the spatial region for which the ring diagram is computed. In addition, we found that the depth dependence of the sensitivity is essentially given by the mode kinetic energy density, as has traditionally been assumed. We showed that the exact form of the sensitivity of ring measurements depends on the details of the fitting procedure.

(L. Gizon in collaboration with A. C. Birch (CoRA, Boulder), B. W. Hindman, and D. A. Haber (JILA, Boulder))

### Solar supergranular structure from local helioseismology

Maps of the horizontal divergence of the near-surface velocity field have been calculated using local helioseismology and SOHO/MDI full-disk Dopplergrams. These maps provide a continuous coverage for two to three months each year with a cadence of 12 hours and a spatial sampling rate of 0.24° in longitude ($\lambda$) and latitude ($\phi$). The maps are interpolated onto a longitude-latitude grid and structures with spherical harmonics degrees $l > 250$ are filtered out.

By applying 2D and 3D Fourier segmentation algorithms as well as feature tracking procedures large samples of individual supergranular cell structures (Fig. 246) and evolutionary histories have been extracted.

Geometrical and evolutional properties of more than $10^5$ single supergranular cells and almost 5000 lifetime histories have been studied. Supergranular cells have sizes in a range around 650 $\mathrm{Mm}^2$ (circular diameter of 28.77 Mm) with lifetimes of up to 4.5 days. A clear trend for larger cells to have stronger divergence values and larger lifetimes than smaller ones has been

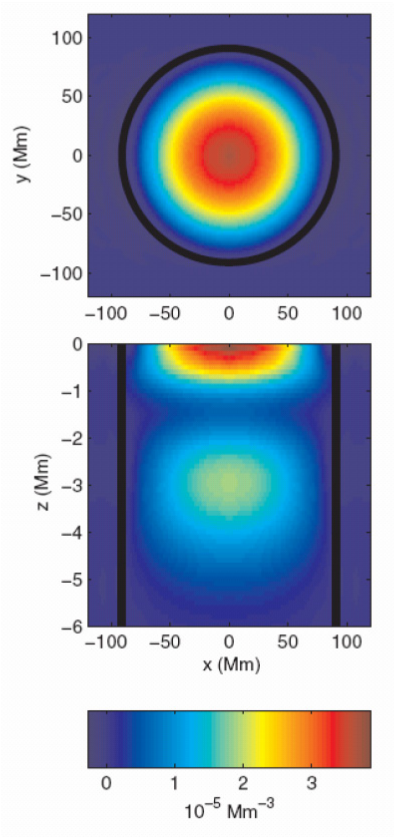


Fig. 245: An example kernel for the sensitivity of a ring-fitting parameter to a flow in the $x$ direction for the $p_1$ mode at spherical harmonic degree $l = 716$. The top panel shows a horizontal slice at $z = -200$ km below the surface. The black circle outlines the outer edge of the apodization region. The lower panel shows a vertical slice in the plane $y = 0$.

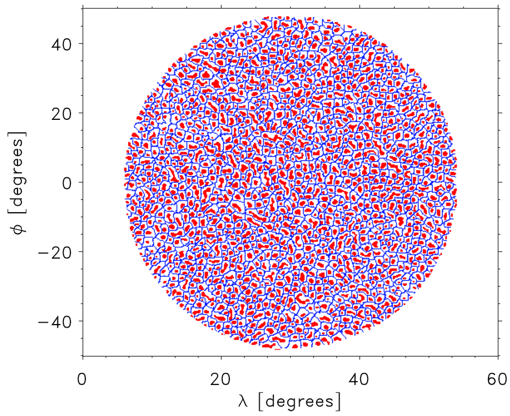


Fig. 246: Centers of positive divergence of the horizontal flow velocities in a depth of approximately 1 Mm below the solar surface as detected with a Fourier segmentation algorithm (red areas). The blue mesh shows a dilation of each supergranular area towards its surrounding local divergence minima.

observed. In addition, no indication for a regular arrangement of supergranules on the solar surface has been found.

(J. Hirzberger, L. Gizon, and S. K. Solanki)

### Surface magnetic field effects in local helioseismology

Helioseismology is used to image the solar interior using observed photospheric Doppler velocities. A matter of interest is to image subsurface active regions. It is thought that the phase of the acoustic waves is altered in the shallow layers (less than a few Mm) inside active regions. This needs to be treated with care, as the phase changes could wrongly be interpreted as subsurface phenomena. This effect is called the ‘showerglass effect’.

We study the ‘showerglass effect’ by computing the so-called ingression correlation phase. The ingression is defined to be the forward propagated wavefield at a particular point on the surface. The ingression correlation phase, $\delta\phi$, is the phase of the correlation between the ingression and the observed wavefield (by construction, $\delta\phi$ is zero in the quiet Sun). We have computed maps of the ingression correlation phase around an active region for waves with frequencies around 3, 4 and 5 mHz. Our analysis shows that the high-frequency waves are more affected by the presence of the magnetic field than the low-frequency waves. In all cases the ingression correlation phase is larger in absolute value for strong magnetic fields moderately inclined from the vertical. This is illustrated in the penumbra of a sunspot in Fig. 247. Another important aspect is that the ingression correlation phase also varies with the angle from which the magnetic field is viewed (the variation is as much as 100° around the penumbra) because the observed MDI seismic signal is the line-of-sight component of velocity. We conclude that the showerglass effect cannot be ignored and depends on the magnetic field direction and its strength.

(H. Schunker in collaboration with D. C. Braun (CoRA, Boulder) and P. S. Cally (Monash))

### Penumbral acoustic anomaly

The ‘penumbral acoustic anomaly’ is an enhancement of the local phase shift of acoustic waves in the penumbra which depends on the line of sight. In Fig. 248 it can be seen that, for a sunspot near the limb, the ingression correlation phase depends on position in the penumbra, with an enhancement toward the limb. Such an effect is, however, absent when the sunspot is close to disk center.

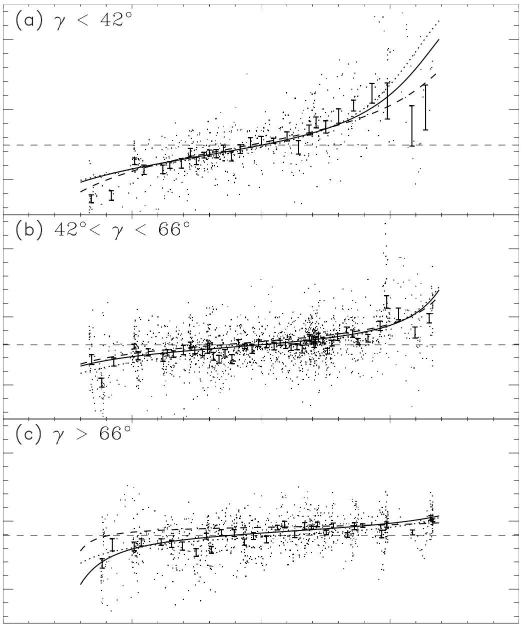


Fig. 247: Ingression correlation phase ($\delta\phi$) at 4 mHz in the penumbra of the sunspot in AR9026. Panel (a) shows the variation of the ingression correlation phase for strong magnetic fields inclined from the vertical (angle $\gamma$) by less than 42°, panel (b) for an intermediate strength magnetic fields with an inclination between 42° and 66°, and panel (c) for weaker magnetic fields inclined greater than 66°. The abscissa is the angle $\theta_p$ defined as the angle from vertical of the line-of-sight vector projected onto the plane containing the magnetic field and the vector normal to the Sun's surface. In each panel, the horizontal dashed line is the value of $\delta\phi$ averaged over $\theta_\mathrm{p}$. The error bars indicate the standard deviation of the mean over bins of 20 measurements in $\theta_\mathrm{p}$. The solid line is a fit to the data. Notice that the variations of $\delta\phi$ are larger as $\gamma$ decreases.

A possible explanation is the conversion of acoustic waves into magneto-acoustic waves as they encounter the magnetic field. Waves in magnetic regions travel preferentially in the direction of the magnetic field lines. In a spreading sunspot field an asymmetry in the ingression correlation phase is thus expected since the MDI observable is the line-of-sight component of velocity. This study reinforces the fact that interactions near the surface make a very significant contribution to seismic travel times in magnetic active regions.

(H. Schunker in collaboration with C. Lindsey (CoRA, Boulder) and P. S. Cally (Monash))

### Imaging the interaction of solar waves with a sunspot

The physical conditions (temperature, density, magnetic field) underneath a sunspot imprint their signature on the waves that go through the sunspot. Sunspots are known to absorb, scatter, and phase

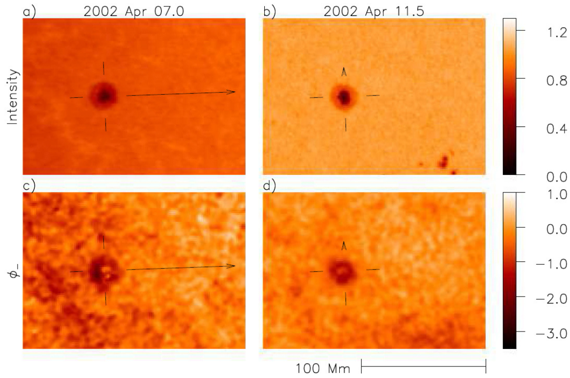


Fig. 248: Penumbral acoustic anomaly. The top panels show MDI intensity maps of sunspot AR9896 close to the east limb (panel a) and near disk center (panel b, 4.5 days later). The bottom panels show the corresponding maps of the ingression correlation phase (denoted here by $\phi_-$) for acoustic waves with frequencies around 5 mHz. Notice in panel c (sunspot close to the east limb) the enhanced phase perturbation on the east (left) side of the penumbra compared to the west side. When the sunspot is near disk center, however, no such azimuthal dependence in the ingression correlation phase is observed (panel d). In each panel, the arrows indicate direction and distance toward disk center from the center of the sunspot.

shift seismic waves. As shown in Fig. 249, these effects can be observed directly by cross-correlating the wave field between points situated on each side of the sunspot. The interpretation of the observations is, however, extremely challenging. Indeed, incoming acoustic or surface-gravity waves change nature at the sunspot boundary and convert into magnetoacoustic waves. This cannot easily be studied with standard perturbation methods. In order to better understand helioseismic observations, the propagation of waves in sunspots must be studied using numerical simulations.

(L. Gizon)

### Simulations of wave propagation: The Semi-spectral Linear MHD (SLiM) code

We have developed a numerical code for treating the evolution of small (linear) perturbations through an inhomogeneous stratified atmosphere. The inhomogeneities can include magnetic fields, density, velocity, pressure, and $\Gamma_1$ perturbations of arbitrarily large magnitude. Specific examples of intended applications include sunspots, granulation, and slender flux tubes.

The code is called SLiM (Semi-spectral Linear MHD) and uses a spectral treatment in the two horizontal directions and a Lax-Wendroff scheme in the vertical. The evolution is assumed to be ideal, with all diffusivities assumed to be negligible for the propagation clip,width=6cm]seismo11-neu

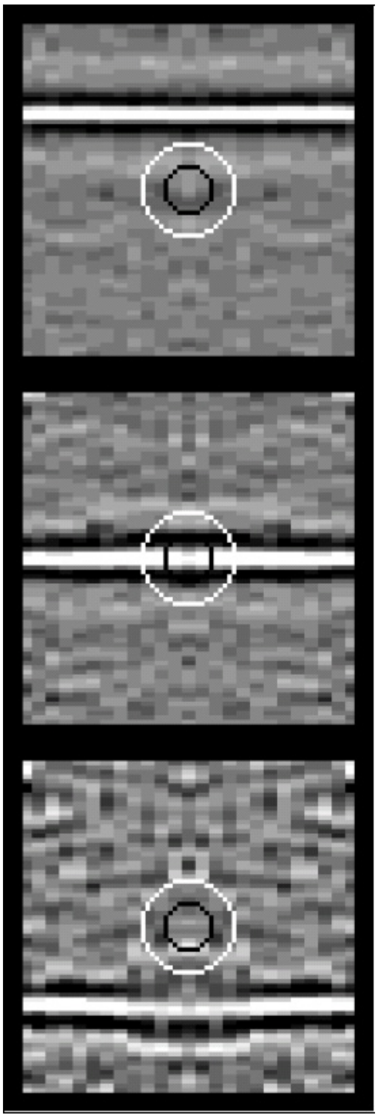

Fig. 249: MDI observations of the deformation of a wave packet (f modes) traversing a sunspot. Plotted is the cross-correlation between a line (above the sunspot) and any other point in the map. The three frames correspond to three different correlation time lags, increasing from top to bottom. White shades correspond to the positions where the amplitude of the cross-correlation is large. A dispersion correction was applied. The location of the sunspot is given by the black (umbra) and white (penumbra) circles. The bottom frame clearly shows that the wave packet sped up as it went through the sunspot.

of the waves. Currently the background is assumed to be fixed, although this restriction will eventually be relaxed. As a simple illustrative example, Fig. 250 shows the effect of a flow jet on wave propagation.

(R. Cameron)

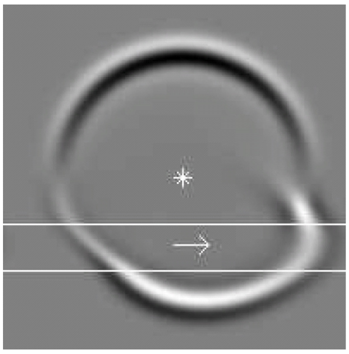

Fig. 250: A snapshot from a calculation showing the effect of a jet on wave propagation. An acoustic wave packet was generated from a source, a displacement in the y-direction, centred on the asterisk. The background atmosphere has a uniform sound speed of 11 km/s. The jet, which has a profile consisting of a half-cycle of a cosine and a peak amplitude of 10 km/s is indicated by the arrow and the white lines which indicate where the jet's speed is 5 km/s.

### Testing the SLiM code

The SLiM code that we developed has now been tested against various analytic solutions and has been parallelised. These two steps allow us to begin using the code for its intended purpose: to better understand the action of large-amplitude inhomogeneities on the waves propagating through the solar atmosphere. The tests consisted of comparing the numerical solutions against analytic solutions. The analytic solutions chosen consisted of cylinders containing magnetic, density, pressure or velocity fields embedded in a uniform medium. The properties inside the tube are also assumed to be uniform, giving rise to a discontinuity at the interface between the tube and its surroundings; in practice we created a layer several grid points thick to resolve the boundary. The results are pleasing, as is shown in Fig. 251.

We have also made the code parallel using MPI-1. Since the code uses a finite difference scheme in the vertical and a spectral scheme in the horizontal directions, the parallelisation has been implemented for the vertical direction. We anticipate typically using at least 500 grid points in this direction which means that we should be reasonably efficient using up to 50 nodes.

(R. Cameron, L. Gizon, and K. Daiffallah)

### Three-dimensional numerical simulation of wave propagation through model sunspots

The interaction of waves with sunspots is being studied in a fully 3-D geometry using numerical simulations and the SLiM code. Currently we are study-

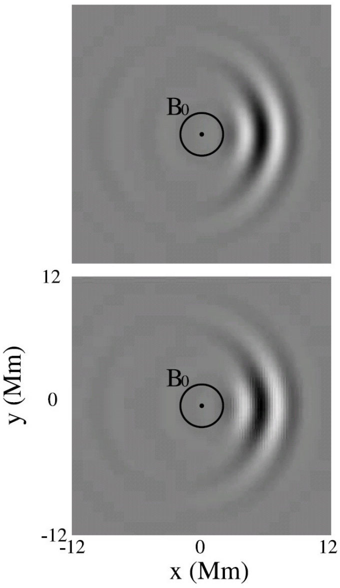


Fig. 251: A snapshot of the scattered wave field from a wavepacket interacting with a 1 kG vertical fluxtube of radius 2 Mm. The background atmosphere is uniform with a sound speed of 11 km/s and a density of $5 \times 10^7$ g/cm$^3$. The wavepacket has a gaussian envelope centred on 3 mHz with a standard deviation of 1 mHz. The bottom panel shows the pressure perturbation in the $x - y$ plane of the exact result and the top panel that of the numerical result.

ing the behaviour of incoming f-modes, as shown in Fig. 252.

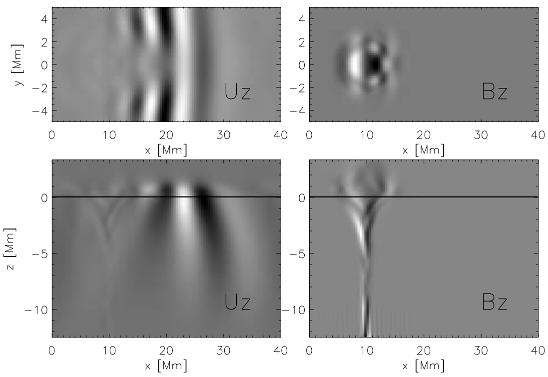


Fig. 252: A snapshot showing the perturbations to the vertical velocity and magnetic field components after an f-mode wave packet travelling in the $x$ direction has passed through a model sunspot. The sunspot axis is at $x = y = 0$. The upper two panels show a horizontal slice near the surface, the lower two show a vertical cut taken through the sunspot. High-frequency incoming f modes are partially converted into downward propagating magneto-acoustic waves.

A model sunspot was supplied to us by Manfred Schüssler and Matthias Rempel. The model is a similarity solution for the magnetohydrostatic problem of an untwisted tube embedded in a stratified atmosphere. In the present case, the magnetic field strength at the centre of the spot is 3500 G. The external atmosphere for the calculation of the field is that of Kiefer, Grabowski, Mattig and Stix (2000, A&A 355, 381). We modified the atmosphere to make it convectively stable. The atmosphere was also extended in height with a damping region so that outward propagating waves are removed from the calculation.

A preliminary qualitative comparison with observations appears to be very encouraging.

(R. Cameron, L. Gizon, and K. Daiffallah)

### Asteroseismology of K Giants

K giants are cool, low and intermediate mass stars evolved off the main sequence occupying the Red Giant Branch (RGB). Quite recently very precise measurements of radial velocity variations of these red giants have allowed to establish that K giants are pulsating stars showing low amplitude oscillations with periods of about 2 – 10 days. The main oscillations of these stars possibly have the same nature as the oscillations of the Sun, which are excited by turbulent convection. Theoretical calculations of solar-like oscillations in K Giants carried out by M. Di Mauro show an expected excess in oscillation power at frequencies below 5 $\mu$Hz.

We studied, in particular, the occurrence of solar-like oscillations in K giants, by considering the stars $\epsilon$ Lep and $\alpha$ Hya. These stars were observed with FEROS (ESO's Fiber fed Extended Range Optical Spectrograph) at the 2.2 m MPG/ESO telescope in La Silla observatory in November 2004 and in March and April 2005. We found pulsations in these stars with periods of 3 – 4 days (Fig. 253). This is in good agreement with the theoretical expectations for solar-like oscillations. However, the high-frequency part of the spectrum that we observe can not be explained by solar-like oscillations. It is possible that at least part of the observed modes could be self-excited Mira-like pulsations.

Longer time series on K Giants will be available in the next few years. They will allow to finally conclude on the nature of the observed oscillations. This will give us the possibility to infer information on the structure of these stars.

(M. Roth in collaboration with J. Setiawan (MPI für Astronomie))

### Beyond mean-field theories of atomic Fermi gases

Fermi liquid theory is a powerful tool for studying strongly-correlated electron systems. It is essentially

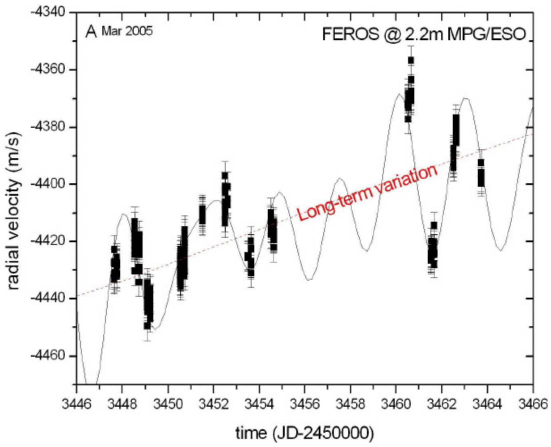


Fig. 253: Radial velocity measurements of the K Giant $\alpha$ Hya. The plot shows as an examplary part of the whole data twelve days in March 2005. The solid line gives a fit of 5 superposed sine functions with periods 7.96, 3.6, 2.95, 2.48, and 2.29 days. Besides the periodic behaviour, a long term variation is visible.

a way to formalize the strong interparticle interactions of degenerate fermions into an effective low energy theory of weakly interacting *quasi*particles.

A Fermi liquid in an attractive potential and at sufficiently low temperatures tends to superfluidity (or superconductivity, if the particles carry charge). This implies a negative scattering length of the two-body interactions that lead to coherent attractive pairing. Typically, this problem is solved with some mean-field theory which predicts the negative scattering length to diverge at the resonant energy (Feshbach resonance). It also predicts the ensemble of paired fermions to have a wavefunction that is spatially spherically symmetric (s wave) and spin antisymmetric (singlet), like a normal BCS superconductor.

We have instead formulated a theory that goes beyond mean field and considers a feedback effect of induced quantum fluctuations on the pairing interactions arising from the exchange of quasiparticles and quasiholes Gaudio *et al.* (2007). The equations we derive that describe the many-body physics are non perturbative (and therefore are valid for any interaction strength) and conserve the Pauli principle rigorously (mean-field theories do not). When solved for an input attractive interaction, this theory predicts a non-divergent scattering length as well as a competing p-wave triplet superfluid component. Experiments on the atomic Fermi gases $^{40}$K and $^{6}$Li confirm the finiteness of the s-wave scattering length at resonance. The critical temperature of this new state is slightly below the s-wave one, and indeed, experiments on the same systems have shown evidence of a double superfluid transition nearby the predicted temperatures.

Similarly, on the repulsive side of the Feshbach resonance, where Bose-Einstein condensation of molecules is energetically favorable, our theory agrees remarkably well with the experimentally obtained binding energies and finite scattering lengths.

The next step of this research is to consider spin-polarized systems to determine self-consistenetly how the preferred states change when magnetic interactions are present, and to map out a low-temperature phase diagram.

(J. Jackiewicz in collaboration with S. Gaudio (University of Rome, Italy) and K. S. Bedell (Boston College, USA)).

### Initial-value formalism for spherically symmetric matter distributions in General Relativity

A new method for solving Einstein's Field equations is established, which utilizes the 1+3 initial-value formalism for general relativity. This method is well suited for learning about gravitational effects of spherically symmetric matter distributions. In traditional methods, a common complication arises whereby the coordinate system must be separated into two parts; one contains the matter distribution, whereas the other contains a vacuum region. It is then an arduous task to apply matching conditions, on the two coordinate systems, at the interface between the matter and vacuum regions. The method developed here alleviates this complication by expressing the space-time using a single coordinate system. This paper outlines the derivation of the new method and solves for the specific example of collapsing dust balls. Furthermore, this paper laid the foundation for subsequent generalizations to include other matter quantities such as pressure, temperature and fluxes. Summarily, this method is useful for modeling any spherically symmetric object, such as the Sun, within the realm of full general relativity.

(R. Burston in collaboration with P. Lasky and A. Lun (Monash University, Australia))

### HELAS local helioseismology database

The European Helioseismology and Asteroseismology Network (HELAS) is a Coordination Action funded by the European Union under the Sixth Framework Programme. The MPS hosts the HELAS data web page for local helioseismology at `http://www.mps.mpg.de/projects/seismo/data.html`. This dedicated web page was created to make observational data accessible to the community (840 Gigabytes in total). It gives details about how the data were obtained and provides thorough information about the datasets. The navigation of the website has been simplified by a site map linked to every page. The best data set available for local helioseismology on this web site is that of Active Region 9787: a complete 9-day data set including not only MDI Doppler, magnetic and intensity data but also, for instance, the extrapolated vector components of the magnetic field. Sunspot AR9787 was selected because it is perhaps the best example of a "theorist's sunspot". This data web page is a significant and unique achievement.

(L. Gizon, H. Schunker, M. Roth, and HELAS collaboration)

### German Data Center for the Solar Dynamics Observatory

The German Data Center (GDC) for the Solar Dynamics Observatory (SDO), hosted by the Max Planck Institute for Solar System Research in Germany, will provide access to SDO data for the German solar physics community. The GDC-SDO will make available all the relevant Helioseismic and Magnetic Imager (HMI) data for helioseismology and smaller selected Atmospheric Imaging Assembly (AIA) data sets. This project commenced in August 2007 and is funded by the German Aerospace Center (Deutsches zentrum fuer Luft- und Raumfahrt/DLR) until December 2012. An important component of the GDC-SDO is the Data Record Management System (DRMS), developed and distributed by the Stanford/Lockheed Joint Science Operations Center (JSOC). Additional information about the GDC-SDO can be found at `http://www.mps.mpg.de/projects/seismo/GDC1/index.html`.

(R. Burston, L. Gizon, Y. Saidi, and S. K. Solanki)

### Helioseismology with Solar Orbiter

Solar Orbiter, ESA's next mission to study the Sun, is scheduled to be launched in May 2015 according to the current baseline (Dec 2006). The extended mission will be completed in January 2024. The most interesting aspects of the mission for helioseismology reside in the unique vantage points from which the Sun will be viewed (Gizon 2007; Woch & Gizon 2007). The spacecraft will use multiple gravity assist manoeuvres at Venus and Earth to reach its science orbit after a cruise phase of about 3.4 years. The orbit design will include two main characteristics, both of which offer novel perspectives for helioseismology. First, Solar Orbiter will make observations away from the ecliptic plane to provide views of the Sun's polar regions. The inclination of the spacecraft's orbit to the ecliptic will incrementally increase at each Venus swing-by manoeuvre to reach at least 30° toward the end of the mission. Second, Solar Orbiter will cover a large range of spacecraft-Sun-Earth angles. In combination with data collected from the ground or near-Earth orbit, Solar orbiter will thus mark the advent of stereoscopic helioseismology. One important goal is to gain a better understanding of solar activity and variability by probing the solar interior at higher latitudes and larger depths, well beyond what can be achieved with Earth-side observations alone.

(L. Gizon and J. Woch)

# IV. International Max Planck Research School on Physical Processes in the Solar System and Beyond at the Universities of Braunschweig and Göttingen

## **Übersicht** / Overview

Die "International Max Planck Research School on Physical Processes in the Solar System and Beyond at the Universities of Braunschweig and Göttingen" wurde 2002 als gemeinsame Inititative des Max-Planck-Instituts für Sonnensystemforschung in Katlenburg-Lindau und der physikalischen Fakultäten der Universität Göttingen (Institut für Astrophysik, Institut für Geophysik) und der Technischen Universität Braunschweig (Institut für Geophysik und Extraterrestrische Physik, Institut für Theoretische Physik) gegründet. Sie bietet in- und ausländischen Studenten Gelegenheiten, auf dem Gebiet der Physik des Sonnensystems zu promovieren.

Die Schule bietet ein forschungsintensives dreijähriges Promotionsstudium. Voraussetzung ist ein Diplom oder ein Master of Science in Physik. Der Doktorgrad kann an den beteiligten Universitäten Braunschweig oder Göttingen oder an der Heimatuniversität angestrebt werden.

Das Lehrprogramm beinhaltet die gesamte Physik des Sonnensystems von der Geophysik über Planetenphysik zur Sonnenphysik. Es garantiert eine breite, interdisziplinäre und fundierte wissenschaftliche Ausbildung. Das wissenschaftliche Programm wird durch Kurse in numerischer Physik, Weltraumtechnologie und Projektmanagement ergänzt. Das Lehrangebot ist in englischer Sprache.

Die Forschungsmöglichkeiten für Doktoranden reichen von Instrumentierung und Beobachtung über Datenanalyse und -interpretation zu numerischen Simulationen und theoretischer Modellierung.

In den Jahren 2006 und 2007 nahmen insgesamt 75 Doktoranden an der Schule teil, davon haben 20 ihre Promotion erfolgreich abgeschlossen. Die Teilnehmer kamen aus insgesamt 26 Ländern, 73% sind ausländischer Nationalität, 32% sind weiblich. Über 1200 Bewerbungen in den ersten sechs Jahren der Research School zeigen die Attraktivität dieses internationalen Programms für junge Wissenschaftler.

Am 11. November 2005 wurde die IMPRS von einer externen wissenschaftlichen Kommission begutachtet und ihre Weiterführung empfohlen. Aufgrund der uneingeschränkt positiven Einschätzung der Gutachter wurden am 16. März 2007 die Mittel für die Fortführung der IMPRS bis 2013 bewilligt.

---

The "International Max Planck Research School on Physical Processes in the Solar System and Beyond at the Universities of Braunschweig and Göttingen" was founded in 2002 as a joint venture of the Max Planck Institute for Solar System Research with the University of Göttingen (Institute of Astrophysics, Institute of Geophysics) and the Technical University Braunschweig (Institute of Geophysics and Extraterrestrial Physics, Institute of Theoretical Physics). The participating institutes are uniquely positioned in the fields of solar system physics and together form a center of scientific excellence in an innovative and interdisciplinary research area.

The school offers graduate students from many countries attractive conditions for education and research. A prerequisite is a diploma or masters degree in physics. The PhD degree can be obtained either from the Universities of Braunschweig or Göttingen or the home university of the student.

The program covers the full range of physics inherent in the rapidly growing field of solar system science from geophysics and planetary science to solar physics, as well as the underlying fundamental physics. It ensures a broad, interdisciplinary, and well-founded education for a career in science. The science program is complemented by training in computational physics, space technology, and project management, which considerably widens the career opportunities for the students.

High-profile space missions and projects for ground-based instruments, data analysis as well as theoretical and large-scale numerical modeling provide a wide range of research possibilities for PhD students.

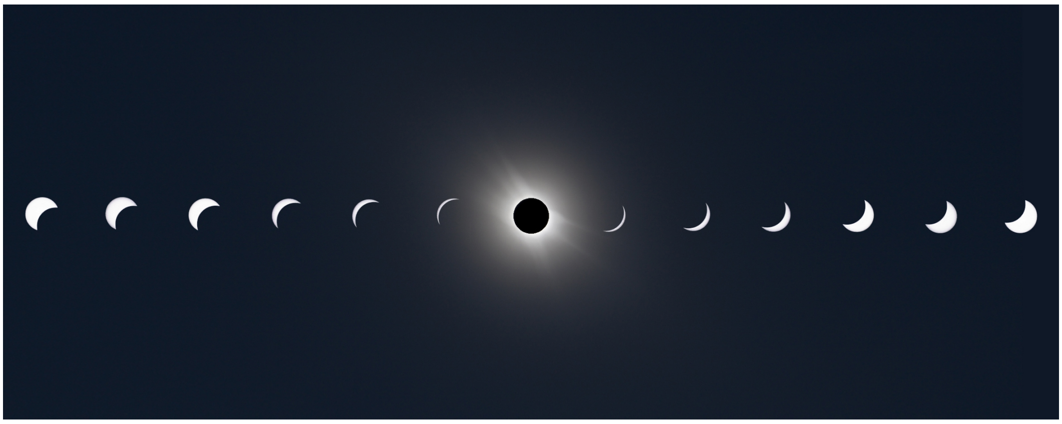

Fig. 254: Totale Sonnenfinsternis vom 29. März 2006, aufgenommen von Vasily Zakharov während einer Schulung der IMPRS-Studenten in Antalya, Türkei / Total solar eclipse of 29 March 2006, recorded by Vasily Zakharov during the IMPRS retreat in Antalya, Turkey

In 2006 and 2007 altogether 75 students took part in the program, from which 20 successfully finished their PhD in these two years. The students came from 26 countries, 73% were of foreign nationality, 32% were female. More than 1200 applications in the first six years of operation of the Research School show the attraction of this international program for young scientists.

On 11 November 2005, an external scientific committee evaluated the IMPRS and recommended its continuation. Based on the very positive evaluation report, the IMPRS grant was extended until 2013 on 16 March 2007.

http://www.solar-system-school.de

## Vorstand / *Chair*

U. Christensen (MPS), J. Blum (Technische Universität Braunschweig), S. Dreizler (Universität Göttingen), K.-H. Glassmeier Technische Universität Braunschweig), F. Kneer (Universität Göttingen), U. Motschmann (Technische Universität Braunschweig), D. Schmitt (MPS, Koordinator/Coordinator), S. K. Solanki (MPS, Vorsitz/Chair), A. Tilgner (Universität Göttingen)

## Lehrveranstaltungen / *Lectures*

Origin of solar systems, 13 – 15 February 2006 (Jockers)

The solar corona, 27 – 28 March 2006 (Marsch, Peter)

Research ethics, 28 March 2006 (Schüssler)

Job application, 30 March 2006 (Schmitt)

Magnetohydrodynamics, 9 – 13 October 2006 (Ferriz Mas)

Space instrumentation, 4 – 7 December 2006 (Woch et al.)

Helioseismology, 5 – 16 February 2007 (Gizon)

Minor bodies in the planetary system, 19 – 20 March 2007 (Böhnhardt)

Stellar structure and evolution, 23 – April 2007 (Glatzel)

Space plasma physics, 11 – 15 June 2007 (Marsch)

Planetary interiors and surfaces, 11 – 15 June 2007 (Christensen et al.)

How to write a research paper, 6 November 2007 (Solanki)

How to write a grant proposal, 7 November 2007 (Glassmeier)

Presentation skills, 8 – 9 November 2007 (Meyer-Ross)

Astrobiology Lecture Course Network, 30 October 2007 – 18 March 2008 (Brack et al.)

Solar System Seminar, 26 seminar days with 78 talks by students and 12 tutorial talks by guests (Schmitt)

## Abgeschlossene Dissertationen / *Finished PhDs*

*Laura Balmaceda:* Solar variability and solar irradiance reconstructions on time scales of decades to centuries. Technische Universität Braunschweig, April 2007.

Fig. 255: Ausflug der Studenten nach Phaselis während der IMPRS Schulung in Antalya, Türkei / Excursion to Phaselis during the IMPRS retreat in Antalya, Turkey

*Nazaret Bello González:* Spectropolarimetry of sunspot penumbrae. Institut für Astrophysik, Universität Göttingen, June 2006.

*Monika Buske:* Dreidimensionale thermische Evolutionsmodelle für das Innere von Mars und Merkur. Universität Göttingen, April 2006.

*Mark Cheung:* Magnetic flux emergence in the solar photosphere. Universität Göttingen, February 2006.

*Dragos Constantinescu:* Wave sources and structures in the Earth's magnetosheath and adjacent regions. Institut für Geophysik und Extraterrestrische Physik, Technische Universität Braunschweig, March 2007.

*Jean-Mathias Grießmeier:* Aspects of the magnetosphere-stellar wind interaction of close-in extrasolar planets. Institut für Theoretische Physik, Technische Universität Braunschweig, February 2006.

*Elena Kronberg:* Dynamics of the Jovian magnetotail. Technische Universität Braunschweig, May 2006.

*Takeshi Kuroda:* Study of the effects of dust in the Martian meterology using a general circulation model. University of Tokio, Japan, November 2006.

*Redouane Mecheri:* Coronal waves and instabilities within the multi-fluid description. Universität Göttingen, February 2007.

*Yasuhito Narita:* Low frequency waves upstream and downstream of the terrestrial bow shock. Institut für Geophysik und Extraterrestrische Physik, Technische Universität Braunschweig, February 2006.

*Evgeny Panov:* Investigation of the current sheets at the outer boundary of the Earth's magnetosphere using the four CLUSTER spacecraft. Space Research Institute Moscow, April 2007.

*Aikaterini Radioti:* Energetic ion composition and acceleration mechanisms in the magnetosphere of Jupiter. Technische Universität Braunschweig, May 2006.

*Michael Rost:* Aggregation magnetischer Staubpartikel unter Mikrogravitation und unter variablen Magnetfeldbedingungen. Institut für Geophysik und Extraterrestrische Physik, Technische Universität Braunschweig, May 2006.

*Markus Sailer:* Simulationsrechnungen anisoplanatischer Übertragungsfunktionen für solare Adaptive Optik. Institut für Astrophysik, Universität Göttingen, August 2006.

*Ryu Saito:* Influence of the surface on the atmospheric circulation of Mars: Study with a general circulation model. Technische Universität Braunschweig, July 2006.

*Stefan Schröder:* Investigating the surface of Titan with the Descent Imager/Spectral Radiometer onboard Huygens. Universität Göttingen, April 2007.

*Alina Semenova:* Doppler imaging of starspots: A study of the RS CVn Star $\sigma$ Geminorium. Universität Göttingen, November 2006.

*Sven Simon:* Titan's highly variable plasma environment: A 3D hybrid simulation study. Institut für Theoretische Physik, Technische Universität Braunschweig, Oktober 2007.

*Martin Tschimmel:* Investigation of the atmospheric water cycle on Mars by the Planetary Fourier Spectrometer onboard Mars Express. Universität Göttingen, February 2007.

*Vasily Zakharov:* Diagnostic of the solar photosphere with high spatial resolution using CH, CN and continuum spectral bands. Universität Göttingen, March 2006.

## Laufende Dissertationen / *Ongoing PhDs*

### MPS:

Akhtar, Naseem: Solar coronal plasma simulation (Büchner/Motschmann).

Attie, Raphael: Explosive events in the transition regions and coronal heating (Solanki/Innes).

Bourouaine, Sofiane: Kinetic models including collisions and wave-particle interactions for magnetic structures in the solar corona (Marsch/Glatzel).

Danilovic, Sanja: The fine structure of photospheric magnetic fields: analysis of high resolution spectropolarimetric observations and MHD simulations (Solanki/Lagg/Kneer).

Drahus, Michal: Submillimeter radiative transfer and retrieval simulations of cometary atmospheres in the vicinity of the nucleus (Jarchow/Hartogh/Christensen/Dreizler).

Feng, Li: Stereoscopy of the solar corona (Wiegelmann/Inhester/Solanki/Dreizler).

Guo, Jingnan: Particle acceleration by 3D solar magnetic reconnection (Büchner/Marsch/Fang).

Hallgren, Kristofer: Mesospheric water vapour: detection of short term variability by ground-based microwave spectroscopy (Hartogh/Lübken).

Işık, Emre: Magnetic flux generation and transport in cool stars (Schüssler/Kneer).

Javadi Dogaheh, Setareh: Simulation of solar coronal reconnection (Büchner/Glatzel).

Kobel, Philippe: Imaging of photospheric magnetic features and SUNRISE filtergraph instrumentation development (Solanki/Gandorfer/Kneer).

Koch, Christian: Extraction of Mercury's topography and its time dependent variations from laser altimetry data (Christensen/Müller).

Lee, Kuang Wu: Linear theory and nonlinear saturation of solar beam plasma instabilities (Büchner).

Li, Xianyi: Wideband-CTS development (Hartogh/Reindl/Ahlers).

Li, Xiaobo: Tracking of magnetic features in the solar photosphere (Büchner).

Lippi, Manuela: The composition of comets as inferred from measured production rates of volatiles (Böhnhardt/Blum).

deLucas, Aline: Study of interplanetary shock waves propagation by using Helios 1 and 2 data (Marsch/Schwenn).

Maltagliati, Luca: Investigation of the Martian atmospheric water cycle by the OMEGA mapping spectrometer onboard Mars Express (Titov/Keller/Blum).

Maneva, Yana: Generation, propagation and dissipation of Alfvénic turbulence in the solar corona and its role in coronal heating and solar wind acceleration (Marsch/Glatzel).

Martinecz, Cornelia: Investigations of the plasma environment of Venus using data of the ASPERA-4 experiment on the Venus Express spacecraft (Fränz/Woch/Krupp/Motschmann).

Matloch, Lukasz: Modeling of solar mesogranulation (Schüssler/Schmitt/Kneer).

Meling, Martin: Ground- and space-based observation of solar magnetism (Solanki/Gandorfer/Lagg/Dreizler).

Moissl, Richard: Energy transport in the upper Venus mesosphere (Markiewicz/Titov/Keller/Blum).

Oklay, Nilda: Investigations of solar surface magnetism by high resolution imaging and spectroscopy (Solanki/Gandorfer/Kneer).

Paganini, Lucas: Accuracy characterization and improvement of real-time spectrometer for remote-sensing applications in radio astronomy and planets atmosphere sounding (Hartogh/Reindl).

Piccialli, Arianna: Investigation of the dynamics of the Venus mesosphere from the Venus Express observations (Titov/Hördt).

Protopapa, Silvia: Surface ice characterization of Pluto and Charon and other Kuiper Belt objects (Böhnhardt/Blum).

Riethmüller, Tino: The SUNRISE filter imager SUFI (Solanki/Gandorfer).

Roussos, Elias: Plasma environment of Mars, Venus and Saturn (Krupp/Woch/Fränz/Motschmann).

Ruan, Peng: Modeling large-scale coronal structures with advanced models (Wiegelmann/Inhester/Solanki/Marsch/Dreizler).

Saidi, Yacine: Computing and data management systems for helioseismology (Gizon/Appourchaux).

Santos, Jean: Investigation of solar eruptions using numerical simulations (Büchner).

Sasso, Clementina: Spectro-polarimetry of the solar chromosphere in He I 1083nm (Solanki/Lagg/Kneer).

Spjuth, Sofie: Generation of a 3D shape model from OSIRIS images (Küppers/Keller/Glassmeier).

Stahn, Thorsten: Helioseismic probing of solar structure and activity (Gizon/Dreizler/Schmitt).

Thalmann, Julia: Evolution of coronal magnetic fields (Wiegelmann/Solanki).

Tian, Hui: Solar transition region and solar wind origin (Marsch/Tu).

Tòthová, Danica: Spectroscopic observations of soft X-ray loops (Innes/Solanki/Kneer).

Tubiana, Cecilia: Characterization of the Rosetta Target Comet 67P/Churyumov-Gerasimenko (Böhnhardt/Blum).

Vilenius, Esa: Analysis of near infrared data from lunar dayside using the SIR point spectrometer onboard the SMART-1 spacecraft (Mall/Kappas).

Vincent, Jean-Baptiste: From observations and measurements to realistic modeling of cometary nuclei (Böhnhardt/Blum).

Wang, Mingyuan: The Mars ionospheric research based on radar sounding (Nielsen).

Wiese, Manuela Maria: Lunar mineralogy (Mall/Stalder/van den Kerkhof).

Yelles Chaouche, Lotfi: Spectro-polarimetric diagnostics of magnetic fields in solar and stellar atmospheres (Solanki/Schüssler/Kneer).

**Universität Göttingen:**

Blanco Rodriguez, Julian: Magnetic activity at the poles of the Sun (Kneer).

Lutz, Ronny: Key objects in subdwarf B asteroseismology (Dreizler).

Sánchez-Andrade Nuño, Bruno: Observations, analysis and interpretation with non-LTE of chromospheric structures on the Sun (Kneer).

**Technische Universität Braunschweig:**

Bößwetter, Alexander: Solar wind – Mars interaction (Motschmann).

von Borstel, Ingo: Dust-dust interaction processes studied in dense aerosols using a paul trap (Blum).

Guicking, Lars: Low-frequency waves and the dynamics of the Venusian solar wind interaction region (Glassmeier).

Johansson, Erik: Interaction of extrasolar planets with stellar winds (Motschmann).

Kleindienst, Gero: ULF waves in the Kronian magnetosphere (Glassmeier).

Müller, Joachim: Development of an adaptive grid code for particle-in-cell simulations in plasma physics (Motschmann).

Plaschke, Ferdinand: Dynamic response of the magnetosphere to solar wind variations (Glassmeier).

Schäfer, Sebastian: Correlated observations of magnetohydrodynamic waves as seen by Cluster and from the ground (Glassmeier).

## Preise / *Awards* 2006 – 2007

Fünf ehemalige Studenten der Research School erhielten in 2006 – 2007 Preise für ihre ausgezeichneten Dissertationen: / Five former students of the Research School received awards for their outstanding PhD theses:

Dr. Laura Balmaceda, Max-Planck-Institut für Sonnensystemforschung: AGU 2007 Joint Assembly Outstanding Student Paper Award, 2007.

Dr. Mark Cheung, Max-Planck-Institut für Sonnensystemforschung: Otto-Hahn-Medaille, Max-Planck-Gesellschaft, 2007.

Dr. Yasuhito Narita, Institut für Geophysik und Extraterrestrische Physik, TU Braunschweig: Heinrich-Büssing-Preis, Braunschweigischer Hochschulbund, 2007.

Dr. Markus Sailer, Institut für Astrophysik, Universität Göttingen: Berliner-Ungewitter-Preis, Fakultät für Physik, Universität Göttingen, 2007.

Dr. Martin Schrinner, Max-Planck-Institut für Sonnensystemforschung: Berliner-Ungewitter-Preis, Fakultät für Physik, Universität Göttingen, 2006.

(D. Schmitt)

# V. Rechenzentrum, Elektroniklabor, Mechanik, Haustechnik und Ausbildung / Computer Centre, Electronic Laboratory, Mechanics, Physical Plant and Education

## Rechenzentrum

(I. Pardowitz und Mitarbeiter)

*Neue Server und Datenzentren*

Im zweiten Halbjahr 2006 wurden zwei Rechnersysteme für die Nachwuchsgruppe Helioseismologie (Gizon) und eines für die "Ground Based Solar Observation" Gruppe zur Verarbeitung und Speicherung von "high resolution solar observation" Daten aufgrund einer Ausschreibung beschafft und in Betrieb genommen. Dabei handelt es sich um Linux Server mit je 4 AMD Opteron dual core CPUs, mit 32 GB Hauptspeicher und je 20 500 GB Datenplatten die mittels internem Hardware-Raid-6 angeschlossen sind.

Ende 2007 wurden für die Nachwuchsgruppe Helioseismologie aus DLR Mitteln zwei weitere Datenserver mit je 40 TB (netto) Datenkapazität beschafft und in Betrieb genommen. Es handelt sich um ein Sun X4500 Server mit je 2 AMD Opteron dual core CPUs, 16 GB Hauptspeicher und 48 1 TB Datenplatten die mittels Solaris ZFS, einem speziellen Dateisystem verwaltet werden. Ziel ist die Einrichtung eines German Data Centers (GDC) für SDO am MPS, um Zugriff auf alle relevanten SDO Daten zu erhalten. Das GDC wird ein Datenverwaltungssystem zur Abfrage von Daten aus einer relationalen Datenbank bereitstellen. Das Solar Dynamics Observatory (SDO) der NASA soll 2009 gestartet werden.

Das German Cluster Data Centre (GCDC), wurde im Laufe des Jahres 2007 vom MPI für extraterrestrische Physik an das MPI für Sonnensystemforschung verlegt, ab 1. Januar 2008 ist das Lindauer System offizieller GCDC im ESA-Verbund des Cluster Science Data System (CSDS). Dieser Verbund besteht seit 2001 aus Datenzentren in Großbritanien, Schweden, Österreich, Ungarn, Frankreich und Deutschland, wobei jedes nationale Zentrum für die Prozessierung der Daten der Instrumente verantwortlich ist, deren PI aus dem entsprechenden Land kommt. Die prozessierten Daten werden jede Nacht zwischen den Datenzentren ausgetauscht und erlauben somit den an Cluster-Daten interessierten Wissenschaftlern aus den entsprechenden Ländern einen schnellen online-Zugang zu den Daten. Die hardwaremäßige Implementierung besteht aus zwei Maschinen vom Typ Dell PowerEdge 2900 mit je 2 Xeon 2 GHz Prozessoren und je 900 GB netto Plattenkapazität.

*Tivoli Storage Manager (TSM)*

Da sich die im Jahre 2003 eingeführte Backup- und Archivlösung auf Basis des Tivoli Storage Managers (TSM), an die zunächst ausschließlich Windows-Server angebunden waren, außerordentlich bewährt hat, wurde ab 2006 auch die Sicherung und Archivierung der Sun- und Linux-Server über dieses System in Angriff genommen. Die auf diesen Maschinen gespeicherten Datenmengen betragen ein Vielfaches der auf den Windows-Servern vorgehaltenen Daten, sodass eine Migration der TSM-Installation auf eine erheblich leistungsfähigere Hardware unumgänglich war. Das neue System, das ebenfalls unter Windows Server 2003 läuft, verfügt jetzt über einen Plattencache von 15 TB sowie eine DLT-S4-Bandbibliothek mit 4 Laufwerken und Stellplätzen für 384 Bandkassetten. Im Vergleich zum Vorläufer kann mit einer nativen Gesamtkapazität von ca. 300 TB damit jetzt die 75-fache Datenmenge im Direktzugriff gehalten werden, ein Ausbau mit weiteren Laufwerken und Stellplätzen ist möglich.

*Servervirtualisierung*

Bei der Virtualisierungsplattform VMware ESX Server wurden die Hostrechner Ende 2006 durch 2 Quadprozessor-Server vom Typ Fujitsu-Siemens RX600-S3 mit jeweils 32 GB Hauptspeicher ersetzt. Die Software wurde um eine Lastverteilungs-, eine dedizierte Backup- und um eine Hochverfügbarkeitskomponente erweitert, die bei Ausfall eines Hosts die darauf laufenden virtuellen Maschinen automatisch auf dem anderen Host neu startet. Neben inzwischen ca. 15 Produktions- und Management-Servern unter Windows sowie der Test- und Entwicklungsumgebung werden seit einiger Zeit auch eine Reihe von Solaris-und Linux-Serverdiensten wie Cups, MySQL und LDAP auf ESX gehostet.

*Windows SharePoint Services*

Die Windows SharePoint Services (WSS) stellen eine Webapplikation dar, die als spezielles Werkzeug für die Zusammenarbeit in Projekt-Teams gedacht ist. Der Name “SharePoint” leitet sich dabei von dem Grundgedanken ab, dass alle wichtigen Informationen an einem Punkt zusammengeführt und dort von den Mitgliedern eines Teams geteilt werden sollen. In einem Webportal wird einer Benutzergruppe bspw. ein Instrument zur Verwaltung der gemeinsamen Dokumente (einschließlich Mechanismen zum Ein- und Auschecken sowie zur Versionskontrolle) an die Hand gegeben, darüber hinaus gibt es gemeinsame Kalender, Diskussionsrunden, Möglichkeiten der Aufgabenzuweisung und -verfolgung und typische “Web 2.0”-Anwendungen wie Blogs und Wikis. Viele diese Komponenten sind transparent in Microsoft Office integrierbar, können aber auch etwa mit Firefox von einem Linux- oder Macintosh-Client aus genutzt werden. Sie sind “out-of-box” verwendbar, bieten jedoch auch Möglichkeiten, sie mit entsprechenden Programmier- und Designwerkzeugen an individuelle Anforderungen anzupassen und Arbeitsabläufe abzubilden.

Die Einführung der WSS befindet sich derzeit noch in der Pilotphase. Die SharePoint-Seite der PC-Gruppe wird in erster Linie intern zur Dokumentation und für den Aufbau einer Wissensdatenbank genutzt. Weitere Pilotseiten, auf die auch externe Team-Mitglieder Zugriff haben, werden von den Projekten PHI und MOMA betrieben.

(G. Kettmann)

*Entwicklung von Spammails*

Im Oktober 2006 wurde unser bisheriges Mailgateway ‘unix1’ durch einen leistungsfähigeren Sun Fire X4100 Server mit zwei Opteron Doppelkern-Prozessoren ersetzt, um die zunehmende Spamflut besser bewältigen zu können. Von Anfang 2003 bis Ende 2006 war die Anzahl der täglichen Spammails von 2000 – 3000 auf über 10000 angestiegen. Abb. 256 zeigt das Spamaufkommen am MPI Lindau in den letzten 12 Monaten, in denen sich allein die Anzahl der Spammails nahezu verdreifacht hat und inzwischen Spitzenwerte von mehr als 40000 Spammails pro Tag erreicht. Der Anteil der Spammails an den gesamten Mails beträgt dabei mehr als 90 Prozent.

Für die Analyse von eintreffenden Mails werden auf dem Mailgateway die Produkte MailScanner, Spamassassin, Sophos Antivirensoftware und Sendmail eingesetzt. Erkannte Viren werden aus den Mails entfernt und temporär für einige Tage gespeichert. Als Spam

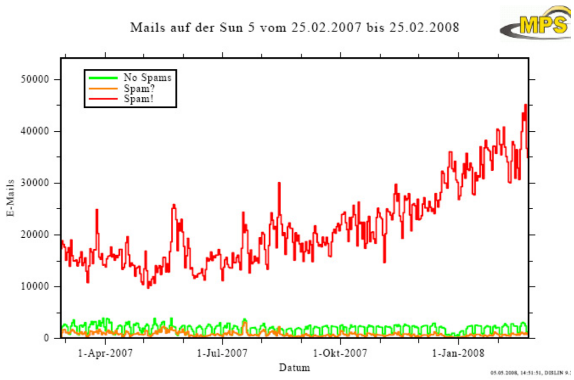


Abb. 256: Spamaufkommen am MPS Lindau in den letzten 12 Monaten.

identifizierte Mails werden als solche gekennzeichnet und können so vom Adressaten leichter gefiltert werden. Auf einen schriftlichen Antrag hin können Spammails auch direkt für einen Benutzer am Mailgateway gelöscht werden, wobei sich Spammails mit hoher und geringer Punktezahl unterscheiden lassen.

(H. Michels)

## Elektroniklabor

(I. Pardowitz)

SUNRISE Power Distribution Unit: Für das Ballon Projekt SUNRISE wurde eine Kontroll- und Schalteinheit (PPD = Power Distribution Unit) entwickelt, die 16 Schaltkanäle mit einer Gesamtleistung von bis zu 1200 W besitzt. Ein elektrisch isoliertes Microcontroller Board nimmt Daten von über 50 Temperatursensoren auf und misst Spannungen und Ströme. Die Einheit ist qualifiziert für Betrieb in Vakuum und im Temperaturbereich von -40°C bis +40°C. Zwei dieser "Power Controller" wurden auf einem Ballon Testflug im September 2007 erfolgreich eingesetzt und dienten zur Versorgung der Post Focus Instrumente und der Gondel Subsysteme. Abb. 257 zeigt die Einheit bei geöffnetem Gehäusedeckel.

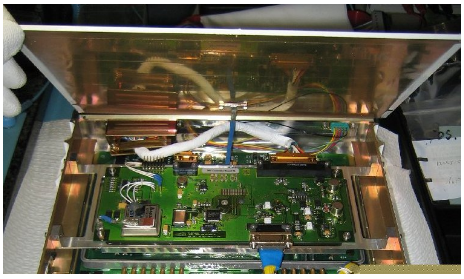

Abb. 257: SUNRISE PPD Elektronik / SUNRISE PPD Electronics.

## Abteilung Mechanik

(B. Chares)

Zu der Abteilung Mechanik gehören die Konstruktion, die Feinmechanik mit der Schlosserei und die Lehrwerkstatt für die Ausbildungsberufe im Industriemechaniker- und Metallbauerbereich. Die Beteiligung unseres Institutes an mehreren laufenden oder geplanten Missionen beinhaltet auch die Entwicklung, den Bau und Test von Instrumenten oder Teilen davon. Neben direkten Missionsbeteiligungen werden Zuarbeiten für Missionsunterhaltungen, Laborexperimente und Testreihen abgedeckt. Weiterhin wird der Bereich zu Reparatur- und Instandsetzungsarbeiten herangeführt. Für die Jahre 2006 und 2007 können folgende Schwerpunkte genannt werden.

*Konstruktion*

Unsere Konstruktionsabteilung, im Berichtszeitraum aus 6 Voll- und Teilzeitmitarbeitern bestehend, entwickelt und konstruiert mit 3D-CAD Software der Marke Pro-Engineer in enger Zusammenarbeit mit den Wissenschaftlern mechanische Komponenten für laufende Projekte. Die mechanisch-konstruktive Betreuung unserer laufenden und zukünftigen Projekte gehört ebenso zur Abteilung wie die Erstellung von Graphiken für wissenschaftliche Veröffentlichungen.

*Feinmechanik*

In der Feinmechanik-Werkstatt wurden für viele verschiedene Experimente bzw. Missionen mechanische Arbeiten geleistet. Weitestgehend abgeschlossen, weil mittlerweile gestartet oder kurz vor dem Start, sind die Projekte Phoenix, DAWN und SIR-II zu nennen. Abb. 258 zeigt als Beispiel die für DAWN entwickelten Türmechanismen.

Die DAWN-Kameras sind mit großer mechanischer Beteiligung aus unserer Institutswerkstatt entstanden. Vom Weltraumbahnhof Cape Canaveral in Florida ist am 27. September 2007 eine Delta Rakete erfolgreich gestartet. Mit an Bord waren die beiden Kameras.

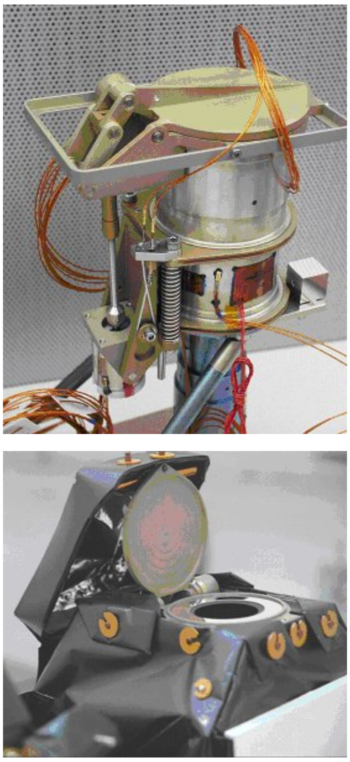

Abb. 258: DAWN Türmechanismus / DAWN Door mechanism .

Für das Frühjahr 2008 ist der Start der indischen Mondsonde Chandrayaan-1 vorgesehen. Eines der wissenschaftlichen Instrumente ist ein Infrarotspektrometer, das als Weiterentwicklung des auf SMART-1 geflogenen SIR-1 Instruments gilt (Abb. 259).

Ein großes Etappenziel für das Projekt "SUNRISE" ist mit dem erfolgten Testflug im Oktober 2007 erreicht. Die vom MPS dazu beigestellten Systeme sind mit großer Beteiligung der Konstruktion/Feinmechanik

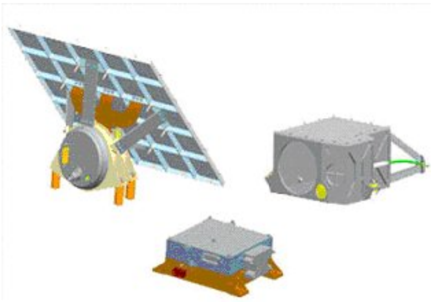

Abb. 259: CAD Darstellung der SIR-II Instrumentes.

entstanden (Abb. 260).

Abb. 260: Aufhängung und Behälter zur Datenspeicherung der gewonnenen Bilddaten.

In einem relativ frühen Entwicklungsstadium befinden sich derzeit die Beteiligungen für eine Merkurmission und die ExoMars Mission zum Planeten Mars. Ein Teilinstrument des **M**ercury **P**lasma **P**article **E**xperiments ist ein **M**ass **S**pectrum **A**nalyzer, der mit Kapazitäten der Konstruktionsabteilung und der Werkstätten entwickelt und gebaut wird. Bei weiteren Instrumenten liegt die Beteiligung des Bereiches Mechanik in der Unterstützung bei und Durchführung von Schwingungsbelastungstests.

Für ExoMars laufen Entwicklungsarbeiten für ein Instrument zur Detektierung von organischen Molekülen auf dem Mars (Abb. 261).

Ebenfalls für ExoMars ist der Bereich Mechanik an der Entwicklung eines Subsystems für ein Seismometer beteiligt. Dabei handelt es sich um den wichtigen Teil der Startverriegelung, der Nivellierung nach der Landung und der Möglichkeit das Seismometer in der Höhe über der Marsoberfläche anzupassen (Abb. 262).

Für sämtliche mechanischen Arbeiten stehen den Mitarbeitern der Feinmechanikwerkstatt konventionelle Bearbeitungsmaschinen sowie CNC-gesteuerte

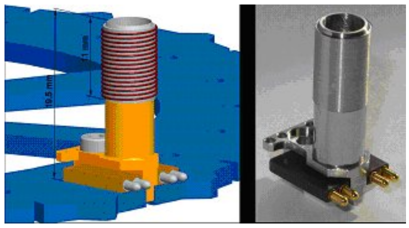

Abb. 261: CAD Abbildung und Foto eines sogenannten Öfchens zur Detektierung von organischen Molekülen innerhalb des Instrumentes.

Abb. 262: CAD Darstellungen der Seismometeraufhängung.

Dreh- und Fräsmaschinen zur Verfügung. Außerdem verfügt die Feinmechanikwerkstatt über eine Erodiermaschine, mit der im Senkerodierverfahren Oberflächenstrukturen erzeugt werden können. Über eine 3D-Messmaschine kann die Maßhaltigkeit und Qualität der Fertigung verifiziert und protokolliert werden. Weiterhin steht ein Multifunktionslaser zur Verfügung. Mit diesem können aus dünnen Werkstücken Konturen in hoher Qualität geschnitten werden, so zum Beispiel Masken für optische Sensoren.

*Schlosserei*

Die Aufgabe der Mitarbeiter in der Schlosserei umfasst neben den Wartungs- und Reparaturarbeiten an unseren Großgeräten auch Spezialanfertigungen für wissenschaftliche Projekte. Zu dem Wartungs- und Reparaturbereich gehören sämtliche Vakuumanlagen inklusive Peripherie. Außerdem werden die Mitarbeiter der Schlosserei bei Reparatur- und Umbaumaßnahmen innerhalb des Instituts herangezogen.

## Verwaltung – Teilbereich Haustechnik

(A. Poprawa)

Im Jahr 2006 waren insgesamt 12 Mitarbeiter verschiedener Handwerksberufe beschäftigt, gegen Ende 2007 nur noch 9. Hier zeigen sich auch die Auswirkungen des Sozialplans. Um so erfreulicher ist es, dass trotzdem weiterhin einem jungen Mann eine Ausbildung angeboten werden konnte.

Neben den traditionellen Tätigkeitsfeldern, die in jedem Institut notwendig sind, um die Infrastruktur für wissenschaftliche Forschung sicherzustellen und die bauliche Substanz zu erhalten, haben die Mitarbeiter auch bei Umbaumaßnahmen, Modellen für wissenschaftliche Experimente und der Öffentlichkeitsarbeit ihr Können unter Beweis gestellt.

Im S-Gebäude wichen die alten Holzdecken einer modernen Brandschutzdecke. Viele Büroräume wurden neu gestrichen, mit neuen Heizkörpern und Regalwänden ausgestattet und erhielten hohe, helle Decken.

Eine weitere Aufgabe, die in letzter Zeit verstä´rkt wurde, ist der Modellbau für die Öffentlichkeitsarbeit. Bedingt durch die wissenschaftlichen Erfolge steigt die Nachfrage nach Ausstellungen und Führungen, und so wurden verschiedene Modelle angefertigt und im gesamten Bundesgebiet gezeigt.

## Ausbildung

*Rechenzentrum*

Im Berichtszeitraum hat das Thema Ausbildung weiterhin eine wichtige Bedeutung eingenommen. Insgesamt haben Praktikanten im Rechenzentrum im Jahr 2006 *87* und 2007 *65* Praktikumswochen absolviert. Es sind teils Schüler-Praktikanten aus Haupt-, Realschulen oder Gymnasien, teils Praktikanten im Rahmen eines Fachhochschul-Studiums, die während ihres 2 bis 22 Wochen langen Aufenthalts im Institut allgemein den Betriebsalltag in einem Rechenzentrum kennen lernen oder anhand von konkreten Projekten praktische Erfahrungen für ihren späteren Beruf erwerben.
Seit dem Jahre 2002 wurde im Rechenzentrum ein Ausbildungsplatz zum Fachinformatiker für Systemintegration eingerichtet. Im Herbst 2003 hat der erste Jugendliche im Rechenzentrum seine 3-jährige Ausbildung als Fachinformatiker, Fachrichtung Systemintegration, begonnen und erfolgreich beendet. 2005 wurde ein weiterer Ausbildungsplatz zum Fachinformatiker geschaffen, und ein zweiter Jugendlicher hat seine Ausbildung aufgenommen, die er im Juni 2008 mit der Abschlussprüfung erfolgreich beendet. Im September 2009 wird der mittlerweile dritte Jugendliche seine Ausbildung in diesem Beruf beginnen.

(G. Monecke)

*Elektroniklabor*

Im Bereich Elektronik Lehrwerkstatt lernen acht Elektroniker für Geräte und Systeme. Sie werden in den Grundlagen der Analog- und Digital-Technik ausgebildet und erhalten zusätzlich noch Betriebsunterricht. Sie werden an allen dafür erforderlichen Messgeräten und Maschinen unterwiesen. Im Jahr 2008 haben zwei Lehrlinge mit sehr gutem Erfolg ihre Prüfung bestanden. Alle jungen Gesellen fanden in den letzten Jahren im Anschluss eine Beschäftigung. Es wurden zahlreiche Schülerpraktika absolviert, sodass sie den ersten Eindruck in dem Beruf des Elektronikers für Geräte und Systeme bekommen konnten. Auch ein Hochschulpraktikant hat im Rahmen seines Studiums die Arbeitswelt eines Elektronikers kennen gelernt.

(O. Matuschek)

*Mechanik*

In der Feinmechanikwerkstatt und der Schlosserei am MPS wurden in den Jahren 2006 und 2007 bis zu 14 Lehrlinge gleichzeitig in den Berufen Industriemechaniker oder Metallbauer ausgebildet. Für beide Lehrberufe bestehen Lehrwerkstätten für die je ein Meister zuständig ist. Den Auszubildenden stehen sowohl herkömmliche Bearbeitungsmaschinen wie CNC-gesteuerte Maschinen zur Verfügung, und sie erhalten Grundkenntnisse in allen ihrem Berufsbild entsprechenden gängigen Metallbearbeitungsverfahren. Außerdem haben in dem Berichtszeitraum 34 Schülerpraktikanten und 5 Hochschulpraktikanten bei uns ein Praktikum absolviert. Vor der Industrie- und Handelskammer haben folgende Mitarbeiter ihre Facharbeiterprüfung erfolgreich bestanden:

Industriemechaniker: 2006: Arno Kiefert, Oliver Kliemand, Alexander Schmidt, Christian Risch.
2007: André Bode, Fabian Maulhardt, Martin Hildebrand, Christoph Ressel (ausgezeichnet als Innungsbester im Metallbauberuf).

(B. Chares)

*Haustechnik und Verwaltung*

Im Bereich der Verwaltung wurden im Jahr 2006 insgesamt 4 Lehrlinge ausgebildet, davon 3 Kaufleute für Bürokommunikation und ein Elektroniker für Energie- und Gebäudetechnik.
Im Jahr 2007 wurden 4 Lehrlinge ausgebildet, davon 3 Kaufleute für Bürokommunikation und 1 Elektroniker für Energie- und Gebäudetechnik.
Eine Kauffrau wurde aufgrund der sehr guten Leistungen in ein Beschäftigungsverhältnis übernommen, und einer Kauffrau wurde ein weitergehendes berufsbegleitendes Studium zum Bachelor an der VWA Göttingen ermöglicht.

(A. Poprawa)

# VI. Personelle Gliederung / Personnel

## Kollegium, wissenschaftliche Mitglieder / Board of directors, scientific members

**Direktoren /** Directors:

Prof. Dr. Ulrich R. Christensen
(Geschäftsführender Direktor/Managing director), 01.01.2005 – 31.12.2007
Prof. Dr. Sami K. Solanki
Prof. Dr. Vytenis M. Vasyliūnas (bis 30.09.2007)

**Leiter der Selbständigen Nachwuchsgruppe Helio- und Asteroseismologie /**
Head, Independent Junior Research Group of the Max Planck Society "Helio- and Asteroseismology":

Dr. Laurent Gizon

**Emeritierte wissenschaftliche Mitglieder /** Emeritus scientific members:

*Prof. Sir Ian Axford, FRS*
*Prof. Dr. Tor Hagfors* († 17.01.2007)
*Dr. Helmut Rosenbauer*
Prof. Dr. Vytenis M. Vasyliūnas

**Auswärtige wissenschaftliche Mitglieder /** External scientific members:

*Prof. Dr. Albert A. Galeev*, Moskau
*Prof. Dr. Johannes Geiss*, Universität Bern
*Prof. Dr. Karl-Heinz Glaßmeier*, Technische Universität Braunschweig
*Prof. Dr. Erwin Schopper*, Bad Soden

**Technischer Geschäftsführer /** Technical Manager:

*Dr. Iancu Pardowitz*

## Wissenschaftliche und wissenschaftlich-technische Mitarbeiter / Scientific staff

**Angestellte /** Permanent staff

Dr. Klaus-Michael Aye
Dr. Peter Barthol
Dr. Hermann Böhnhardt
Prof. Dr. Jörg Büchner
Dr. Raymond Burston (seit 01.08.2007)
Dr. Robert Cameron
Dr. Werner Curdt
Dr. Patrick W. Daly
Prof. Dr. Eduard Dubinin
Dr. Nina Elkina (seit 22.02.2006)
Dr. Alex Feller (seit 01.12.2007)
Dr. Markus Fränz
Dr. Achim Gandorfer
Dr. Maya Garcia-Comas (bis 28.02.2007)
Dr. Laurent Gizon
Dr. Fred Goesmann
Dr. Walter Goetz
Dr. Björn Grieger (bis 31.03.2007)
Pablo Gutierrez-Marques
Dr. Paul Hartogh
Dipl.-Phys. Hermann Hartwig (bis 31.12.2007)
Dr. Martin Hilchenbach
Dr. Johann Hirzberger
Dr. Nico Hoekzema
Dr. Volkmar Holzwarth (seit 01.06.2006)
Dr. Stubbe Hviid
Dr. Bernd Inhester
Dr. Christopher Jarchow
Dr. Geraint Jones (bis 15.03.2007)
Dr. Rainald Kallenbach (seit 01.12.2006)
Dr. habil. Horst Uwe Keller (bis 31.01.2006)
Dr. Georg Kettmann
Dr. Jochen Kissel
Dr. Jens Kleimann (bis 31.12.2007)
Christian Koch (bis 03.07.2006)
Dr. Axel Korth (bis 31.10.2007)
Dr. Jörg-Rainer Kramm (bis 30.09.2006)
Dipl.-Ing. Ivor Krause (seit 01.07.2007)

Dr. Natalie Krivova
Dr. Elena Kronberg (seit 01.11.2006)
Dr. Harald Krüger
Dr. Norbert Krupp
Dipl.-Inf. Oliver Küchemann
Dr. Michael Küppers (bis 31.08.2007)
Dr. Andreas Lagg
Dr. Urs Mall
Dr. Wojcieck Markiewicz
Dr. Davina Markiewicz-Innes
Prof. Dr. Eckart Marsch
Dipl.-Ing. Thorsten Maue (seit 01.03.2007)
Dr. Alexandre Medvedev
Dipl.-Math. Helmut Michels
Dr. Stefan Mühlbachler (bis 31.09.2006)
Dr. Andreas Nathues
Dr. Bernd Nikutowski (bis 16.03.2006)
Dr. Iancu Pardowitz
Dipl.-Ing. Borut Podlipnik
Dipl.-Ing. Hendrik Raasch (seit 01.01.2006)
Dr. Arne K. Richter (bis 31.05.2006)
Dipl.-Phys. Tino Riethmüller
Dr. Olaf Roders (seit 01.04.2007)
Dr. Reinhard Roll
Dr. Markus Roth
Dr. Jon Rotvig (bis 30.06.2006)
Dr. Dieter Schmitt
Dr. Stefan Schröder (seit 15.05.2007)
Dr. Udo Schühle
Prof. Dr. Manfred Schüssler
Prof. Dr. Rainer Schwenn (bis 30.04.2006)
Dr. Holger Sierks
Dipl.-Ing. Li Song
Dr. Harald Steininger (seit 19.04.2006)
Dr. Oliver Stenzel
Dipl.-Ing. Istvan Szemerey
Dr. Luca Teriaca
Dr. Armin Theißen (seit 06.04.2006)
Dr. Hellmuth Timpl
Dr. Dmitri Titov
Dipl.-Ing. Georg Tomasch
Dipl.-Ing. Stephan Werner (seit 01.01.2006)
Dr. Johannes Wicht
Dr. Thomas Wiegelmann
Dr. Joachim Woch
Dr. Bernd Wöbke

**Wissenschaftliche Stipendiaten /** Postdocs

Dr. Regina Aznar Cuadrado
Dr. Laura Antonia Balmaceda (bis 11.10.2007)
Dr. David Bloomfield (bis 30.09.2007)
Dr. Radoslav Bucik (seit 05.02.2007)
Dr. Monika Buske (bis 31.12.2006)
Dr. Chun Ming Mark Cheung (bis 31.08.2006)
Dr. Borys Dabrowski (bis 10.07.2006)
Dr. Valery Dikarev (seit 01.11.2006)
Dr. Rene Damian Duffard (bis 31.01.2007)
Dr. Nina Elkina (bis 21.02.2006)
Dr. Michael Heuer (bis 31.03.2006)
Dr. Yuichi Ito (bis 11.12.2006)
Dr. Jason Jackiewicz
Dr. Maxim Kramar (bis 31.03.2006)
Dr. Elena Kronberg (03.05.-31.10.2006)
Dr. Takeshi Kuroda
Dr. Maria Loukitcheva (01.01.–30.06.2007)
Dr. Maria Madjarska
Dr. Rupali Mahajan (bis 12.03.2006)
Dr. Ajay Manglik (01.04.–30.09.2007)
Dr. Redouane Mecheri (bis 30.09.2007)
Dr. Evgeny Panov (bis 16.12.2007)
Dr. Anna Pietarila Graham (seit 15.08.2007)
Dr. Jonathan Pietarila Graham (seit 15.08.2007
Dr. Ganna Portyankina
Dr. Oliver Preuss (bis 16.08.2006)
Dr. Sabine Preusse (bis 31.02.2006)
Dr. Aikaterini Radioti (bis 01.09.2006)
Dr. Miriam Rengel (bis 31.12.2007)
Dr. Hideo Sagawa (seit 06.08.2007)
Dr. Hannah Schunker (seit 18.09.2006)
Dr. Alina Semenova (bis 17.05.2007)
Dr. Iouri Skorov (bis 31.12.2007)
Dr. Martin Tschimmel (02.02.-15.07.2007)
Dr. Neeharika Verma (01.11.–31.12.2007)
Dr. Luis Vieira
Dr. Alexander Vögler (bis 31.12.2006)
Dr. Zhi Xu
Dr. Vasily Zakharov (bis 04.01.2006)
Prof. Dr. Zhenfei Zhang (bis 28.03.2007)

**Doktoranden und Diplomanden /** PhD students

Naseem Akhtar (seit 01.05.2007)
Vladislav Sashev Alexandrov (26.01.-18.12.2006)
Raphael Attie (seit 16.03.2007)
Laura Antonia Balmaceda (bis 02.03.2007)
Megha Upendra Bhatt (seit 03.12.2007)
Julian Blanco Rodriguez
Sofiane Bourouaine (seit 06.02.2006)
Nazaret Bello Gonzalez (bis 28.02.2006)
Monika Buske (bis 31.01.2006)
Chun Ming Mark Cheung (bis 27.02.2006)
Khalil Daifallah (04.10.06–17.08.07)
Sanja Danilovic (seit 06.02.2006)
Prasanta Das (seit 06.08.2007)
Michal Drahus (seit 01.02.2006)
Li Feng (seit 10.01.2006)
Jingnan Guo (seit 01.09.2007)
Kristofer Hallgren (seit 07.11.2007)
Tom-Oliver Husser (01.05.–31.07.07)
Emre Ishik
Setareh Javadi Dogaheh (seit 22.02.2007)
Erik Johansson (seit 15.01.2007)
Philippe Kobel (seit 21.03.2006)
Christian Koch (seit 01.08.2006)
Elena Kronberg (bis 04.01.2006)
Takeshi Kuroda (bis 30.11.2006)
Kuang Wu Lee (seit 11.2007)
Xianyi Li (01.09.2006)
Xiaobo Li (seit 11.2006)
Manuela Lippi (seit 15.01.2007)
Aline deLucas (15.01.-31.12.2007)
Ronny Lutz (seit 01.12.2007)
Luca Maltagliati
Yana Maneva (seit 28.02.2007)
Cornelia Martinecz (seit 09.01.2006)
Lukasz Matloch (bis 15.01.2007)
Redouane Mecheri (bis 28.02.2007)
Martin Meling (seit 01.12.2006)
Maria Laura Merenda (seit 29.10.2007)
Richard Moissl
Nilda Oklay (seit 04.12.2006)
Roman Orlik (seit 09.01.2006)
Lucas Paganini (bis 30.11.2007)
Evgeny Panov (bis 06.04.2007)
Arianna Piccialli (seit 08.01.2007)
Silvia Protopapa (seit 15.01.2006)
Aikaterini Radioti (bis 22.01.2006)
Tino Riethmüller
Pedro Rodrigues dos Santos Russo(02.06–07.07)
Elias Roussos
Peng Ruan (seit 10.01.2006)
Yacine Saidi (seit 02.04.2007)
Markus Sailer (bis 31.07.2006)
Ryu Saito (bis 31.03.2006)
Bruno Sánchez-Andrade Nuño
Jean Carlo Santos
Clementina Sasso
Stefan Schröder (bis 11.04.2007)
Alina Semenova (bis 28.02.2006)
Piotr Sitek (seit 01.08.2006)
Sofie Spjuth (seit 21.02.2006)
Thorsten Stahn (seit 06.02.2006)
Cedric St-Jean-Leblanc (09.01.–02.11.07)
Julia Thalmann (seit 08.01.2007)
Hui Tian (seit 03.09.2007)
Danica Tòthová (seit 01.02.2006)
Martin Tschimmel (bis 31.01.2007)
Cecilia Tubiana
Esa Vilenius
Jean-Baptiste Vincent (seit 15.01.2007)
Mingyuan Wang (seit 29.11.2007)
Piotr Wawer (seit 01.06.2007)
Manuela Maria Wiese (seit 01.02.2006)
Lotfi Yelles Chaouche

**Abteilung EDV /** Computing department

Leitung/Management: Dr. Iancu Pardowitz

Jens Aigner (seit 01.01.2006)
Andreas Blome (bis 31.12.2007)
Michael Bruns
Alexander Forsch (14.07.–13.09.06)
Lothar Graf
Terrance Ho
Dr. Georg Kettmann
Christine Ludwieg
Helmut Michels
Godehard Monecke
Adolf Piepenbrink
Jürgen Wallbrecht

*Auszubildende / Apprentices:*

Alexander Forsch (bis 13.07.2006), Daniel Maase

**Laboratorien /** Laboratories

Leitung/Management: Dr. Iancu Pardowitz
Ausbilder Elektrotechnik: Olaf Matuschek
Sekretariat: Christiane Heise (bis 30.04.2007), Helga Oberländer (seit 01.05.2007)

Günther Auckthun
Walter Böker
Ulrich Bührke
Dipl.-Ing. Irene Büttner
Dipl.-Ing. Arne Dannenberg
Dipl.-Ing. Werner Deutsch
Dipl.-Ing. Rainer Enge
Fabian Ernst (bis 31.08.2007)
Andreas Fischer
Dipl.-Ing. Henning Fischer
Dipl.-Ing. Dietmar Germerott
Klaus-Dieter Gräbig
Dipl.-Ing. Bianca Grauf
Manfred Güll (bis 30.06.2007)
Dipl.-Ing. Klaus Heerlein
Heinz Günter Kellner
Tobias Kleindienst (seit 01.06.2007)
Martin Kolleck
Alexander Kornehl (bis 15.08.2006)
Wolfgang Kühn
Wolfgang Kühne
Dipl.-Ing. Alexander Loose
Olaf Matuschek
Dipl.-Ing. Reinhard Meller
Markus Monecke
Dipl.-Ing. Reinhard Müller
Jürgen Nitsch (bis 31.03.2007)
Helga Oberländer
Dipl.-Ing. Henry Perplies
Klaus-Dieter Preschel (bis 30.11.2007)
Marianne Pulst (seit 04.10.2006)
Dipl.-Ing. Claudius Römer (bis 31.10.2006)
Rolf Schäfer
Helmut Schüddekopf (bis 31.12.2007)
Dipl.-Ing. Hartmut Sommer (bis 31.03.2006)
Michael Sperling
Dipl.-Ing. Eckhard Steinmetz
Dipl.-Ing. Christoph Stucke
Jan Hendrik Wagner
Alex Weber (27.01.-31.03.2007)
Wolfgang Wunderlich

*Auszubildende / Apprentices:*

Philip Brakel (seit 01.09.2006), Julian Ifland (seit 01.09.2007), Manuel-Roland Jünemann, Tobias Napp (seit 01.09.2007), Nicholas Unger, Dustin Vogel (seit 01.09.2006), Stefan Wagner, Alex Weber (bis 26.01.2007), Jens Wegner

**Mechanik** / Mechanics

Leitung/Management: Bernd Chares
Stellvertreter Feinmechanik: Norbert Meyer
Stellvertreter mechanische Konstruktion: Anita Dullinger
Ausbilder Feinmechanik und Metallbau: Roland Mende
Sekretariat: Beatrix Hartung

*Feinmechanik:*

Hermann Arnemann, André Bode (27.01.-31.07.2007), Robert Burkhardt (01.02.-30.04.2007), Ernst-Reinhold Heinrichs, Dietmar Hennecke (bis 28.02.2007), Martin Hildebrand (01.07.–22.08.06), Detlef Jünemann, Arno Kiefer (21.01.–30.04.06), Fabian Maulhardt (seit 27.01.2007), Roland Mende, Norbert Meyer, Egon Pinnecke (bis 31.08.2006), Alexander Schmidt (21.01.06–30.04.07), Werner Steinberg

*Schlosserei:*

Hans-Joachim Heinemeier, Christoph Ressel (27.01.–30.04.07)

*Siebdruck / Laser:*

Mathias Schwarz

*Dokumentation, Konstruktion / Documentation, mechanical design:*

Leitung: Bernd Chares
Anita Brandt (bis 31.05.2007), Dipl.-Ing. Anita Dullinger (seit 08.05.2007), Steffen Ebert, Jan Heinrichs (seit 27.08.2007), Angelika Hilz, Marianne Krause, Dietmar Oberdorfer (seit 01.04.2006), Mona Wedemeier

*Auszubildende / Apprentices:*

Sascha Adamski, André Bode (bis 26.01.2007), Robert Burkhardt (bis 31.01.2007), André Echtermeyer (seit 01.09.2006), Timo Effler, Fabian Ernst (bis 27.01.2006), Christina Fahlbusch (seit 01.09.2006), Nils Henne, Martin Hildebrand (bis 30.06.2006), Sven Hilz (seit 01.09.2007), Dennis Hirche (seit 13.02.2006), Arno Kiefert (bis 20.01.2006), Sascha Kirchhoff (seit 01.09.2006), Oliver Kliemand (bis 17.02.2006), Fabian Maulhardt, (bis 26.01.2007), Hendrik Meller, David Otto, Christoph Ressel (bis 26.01.2007), Marius Rinkleff, David Römermann, Patrick Schenke (seit 01.09.2007), Alexander Schmidt (bis 20.01.2006), Martin Sieber (seit 01.09.2007), Peer Strogies, Björn Wemheuer (seit 01.09.2006), Sebastian Westphal (seit 01.09.2007), Marcus Wolf

**Verwaltung** / Administration:

Verwaltungsleiter: Andreas Poprawa
Andrea Macke, Swetlana Alekseenko (seit 05.07.2007), Petra Fahlbusch, Roswitha Komossa (bis 30.06.2006), Dorothee Schreiber (bis 31.05.2006), Christina Thomitzek

*Personalbüro / Personell office:*

Edith Deisel, Christiane Neu

*Buchhaltung / Book-keeping:*

Martina Heinemeier, Nadine Teichmann, Andrea Werner

*Einkauf / Goods received:*

Nadine Ehbrecht, Carina Huchthausen (01.02.-31.03.2007), Ilse Schwarz (bis 31.12.2007), Bernhard Vogt

*Bibliothek / Library:*

Dr. Bernd Inhester (wissenschaftlicher Bibliotheksbeauftragter)
Simone Dietrich (seit 01.09.2007), Inge Kraeter (bis 25.08.2007), Margit Steinmetz

*Direktionssekretärinnen / Secretaries of the directors:*

Sabine Deutsch, Karin Peschke, Barbara Wieser

*Sekretärinnen / Secretaries:*

Gerlinde Bierwirth, Carmen Braun (seit 03.07.2006), Jacqueline Bukatz, Kerstin Gebhardt (01.06.06-31.12.07), Elke Hartmann (bis 31.01.2006), Susanne Kaufmann, Julia Müller (seit 19.11.2007), Sibylla Siebert-Rust, Ute Spilker, Sabine Stelzer (bis 31.01.2006), Andrea Vogt, Anja Walowsky, Helga Washausen

*Auszubildende / Apprentices:*

Swetlana Alekseenko (bis 04.07.2007), Jennifer Bartels (seit 01.09.2007), Carina Huchthausen (bis 31.01.2007), Jennifer Raabe (seit 01.09.2007), Michaela Schmalstieg (bis 08.01.2007), Aris Thieme (bis 02.07.2007)

**Technische Dienste:** / Technical services

Leitung: Andreas Poprawa

*Elektro:*

Michael Hilz, Peter Mutio (bis 28.02.2006), Mario Reich, Mario Strecker

*Auszubildende / Apprentices:*

Matthias Franke (bis 31.08.2007), Denis Wirt (seit 01.09.2006)

*Heizung-Sanitär:*

Karl-Heinrich Deisel, Werner Hundertmark (bis 31.07.2006)

*Tischlerei:*

Helge Aue, Martin Heinrich

*Gärtner:*

Martin Schröter

*Reinigung / Wäscherei:*

Ngow Heine (bis 31.12.2007), Maria Müller (bis 31.12.2007), Rosemarie Poppe

*Küche:*

Johannes Kohlrautz, Sylvia Aue, Lilli Dargel, Diana Meyenkoth (20.08.-14.09.2007), Beate Meyer

*Sonstige Dienste / Other services:*

Jürgen Bethe, Inge Reuter (bis 31.12.2007), Robert Uhde (bis 28.02.2006)

**Öffentlichkeitsarbeit** / Public relations:

Dr. Norbert Krupp, Dr. Bernd Wöbke

*Redaktion der Instituts-Informationen / Editor of the institute newsletter:*

Dr. Martin Hilchenbach

**Studentische Hilfskräfte und Praktikanten** / Student assistant and traineeship:

Benjamin Beeck (01.07.06-30.06.07), Marc Cornwell (25.05.-10.08.2007), Annika Freyberg (01.07.-31.08.2007), Sebastian Glahn (01.02.-30.04.2007), Marius Hellmold (01.07.-31.08.2006), Pau Jordi Jesus de Bras (15.05.-31.07.2007), Petra Kluth (bis 31.01.2006), Manuel Mielenz (01.-31.08.2006)

# VII. Wissenschaftliche Zusammenarbeit / Scientific Collaboration

## **Wissenschaftler, die als Gäste längere Zeit am MPS tätig waren** / Long-term scientific visitors at MPS

*(Stipendiaten der MPG, des DAAD, der DFG, der Alexander von Humboldt-Stiftung/Friedrich-Wilhelm-Bessel-Preisträger, Postdocs und Honorarempfänger/ Stipend holders of the MPG, the DAAD, the DFG, the Alexander von Humboldt Foundation/Friedrich Wilhelm Bessel Research Award and Postdocs)*

*Dr. Jaime Araneda*, Facultad de Ciencias Fisicas y Matematicas, Universidad de Concepcion, Chile, 1. Juli – 5. August 2006 und 19. Juli – 18. August 2007. Zusammenarbeit mit Prof. E. Marsch.

*Dr. K. Bamert*, Universität Kiel, Universität Bern, Schweiz, 1. – 30. September 2006 und 9. März – 9. April 2007. Zusammenarbeit mit Dr. M. Hilchenbach.

*Dr. Miroslav Barta*, Ondrejov Astronomical Institute, Czech Republic, 12. November – 21. Dezember 2007. Zusammenarbeit mit Prof. J. Büchner.

*Prof. Alexander Basilevsky*, Vernadsky Institute for Analitical Chemistry and Geochemistry (GEOKHI), Russia, 1. – 30. August 2006. Zusammenarbeit mit Dr. D. Titov.

*Dr. Tanyu Bonev*, Bulgarian Academy of Sciences, Sofia, Bulgaria, 10. Juli – 11. August 2006 und 15. Juli – 14. August 2007. Zusammenarbeit mit Dr. H. Boehnhardt.

*Prof. Nikolai Borisov*, Institute of Terrestrial Magnetism, Ionosphere and Radio Waves Propagation, (IZMIRAN), Russia, 7. Juli – 5. August 2007. Zusammenarbeit mit Dr. U. Mall.

*Dr. Juan Manuel Borrero*, High Altitude Observatory, Boulder, CO, USA, 8. Juni – 5. Juli 2006. Zusammenarbeit mit Prof. S. K. Solanki.

*Prof. Dr. Peng-Fei Chen*, Nanjing Department of Astronomy, University Nanjing, China, 28. Oktober -– 28. November 2006. Zusammenarbeit mit Prof. S. K. Solanki.

*Dr. A. Czechowski*, Space Research Center, Polish Academy of Sciences, Warsaw, Poland, 6. September – 31. Oktober 2006 und 1. März – 30. April 2007. Zusammenarbeit mit Dr. M. Hilchenbach.

*Dr. Allison DalLago*, Institute for Space Research, San Jose Dos Campos, Brazil, 4. Mai – 8. Juli 2007. Zusammenarbeit mit Dr. B. Inhester.

*Dr. Alberto Flandes*, Instituto de Geofisica, UNAM, Mexico, 12. Mai – 1. August 2007. Zusammenarbeit mit Dr. H. Krüger.

*Ms. Tania Marcela Penuela Gomez*, St. Petersburg University, St. Petersburg, Russia, 12. Februar – 12. Juli 2007 (Master Thesis). Zusammenarbeit mit N. Krivova und S. K. Solanki.

*Dr. Douglas P. Hamilton*, University of Maryland, USA, 3. – 30. August 2006. Zusammenarbeit mit Dr. H. Krüger.

*Dr. Nikolay Ignatiev*, Institute for Space Research (IKI), Moscow, Russia, 11. März – 25. Mai 2007. Zusammenarbeit mit Dr. D. Titov.

*Dr. Hiroaki Isobe*, University Kyoto, Japan, 29. Juni -– 8. September 2006. Zusammenarbeit mit Prof. M. Schüssler und Prof. S. K. Solanki.

*Prof. Dr. Michael Knölker*, High Altitude Observatory, Boulder, CO, USA, 9. Juni -– 9. Juli 2006. Zusammenarbeit mit Prof. M. Schüssler und Prof. S. K. Solanki.

*Dr. Maria Loukitcheva*, Astronomical Institute, St. Petersburg State University, Russia, 1. Januar 2006 — 31. Dezember 2007. Zusammenarbeit mit Prof. S. K. Solanki.

*Dr. Ajay Manglik*, National Geophysical Research Institute, Hyderabad, India, 2. April – 30. September 2007. Zusammenarbeit mit Prof. U. Christensen.

*Dr. Maria J. Martínez González*, Instituto de Astrofisica de Canarias, La Laguna, Teneriffa, Spain, 24. Juli -– 31. Dezember 2006. Zusammenarbeit mit Prof. S. K. Solanki und Dr. A. Lagg.

*Dr. Shibu K. Mathew*, Udaipur Solar Observatory, India, 12. Januar -– 11. Februar 2006 und 20. November -– 11. Dezember 2006. Zusammenarbeit mit Prof. S. K. Solanki.

*Dr. Marilena Mierla*, Rumanian Academy of Sciences, 8. Oktober – 10. November 2007. Zusammenarbeit mit Dr. B. Inhester.

*Dr. Ansgar Reiners*, University of California, Berkeley, USA, 1. April 2006 –- 30. September 2006. Zusammenarbeit mit Prof. S. K. Solanki und Prof. M. Schüssler.

*Dr. Anatoly Remizov*, Space Science Institute (IKI) of the Russian Academy of Sciences, Moscow, Russia, 1. Dezember 2005 – 31. März 2006 und 1. – 31. Juli 2007. Zusammenarbeit mit Dr. H. Boehnhardt.
1. September – 31. Oktober 2006. Zusammenarbeit mit Dr. F. Goesmann.
1. Mai – 30. September 2007. Zusammenarbeit mit Dr. M. Hilchenbach.

*Mr. Eugene Shalygin*, Kharkov State University, Ukraine, 15. Juni – 15. Juli 2007. Zusammenarbeit mit Dr. D. Titov.

*Dr. Nandita Srivastava*, Solar Observatory Udaipur, India, 7. August – 31. Oktober 2007. Zusammenarbeit mit Dr. B. Inhester.

*Tilaye Tadesse*, Addis Ababa University, Ethopia, 4. Juli – 27. September 2007. Zusammenarbeit mit Dr. T. Wiegelmann.

*Dr. Gian Paolo Tozzi*, INAF Arcetri Observatory, Firenze, Italy, 6. November – 2. Dezember 2006. Zusammenarbeit mit Dr. H. Boehnhardt.

*Prof. Chuanyi Tu*, Peking University, Beijing, China, 14. Oktober – 30. November 2006 und 15. November – 15. Dezember 2007. Zusammenarbeit mit Prof. E. Marsch.

*Neeharika Verma*, Dipartimento di Fisica Generale, University Turin, Italy, 1. November –- 31. Dezember 2007. Zusammenarbeit mit Prof. S. K. Solanki.

*Maria-Jesus Vidal-Nunez*, Institute Astrofisico de Andalucia, Granada, Spain, 29. März – 30. Mai 2006. Zusammenarbeit mit Dr. H. Boehnhardt.

*Dr. Jun Zhang*, National Astronomical Observatory, Beijing, China, 25. Oktober –- 20. Dezember 2006 und 1. –- 22. Juni 2007. Zusammenarbeit mit Prof. S. K. Solanki und Dr. J. Woch.

## **Wissenschaftler, die als Gäste nur kurzzeitig am MPS tätig waren** / Scientific guests with short-term visits to MPS

*Dr. Nancy Ageorges*, European Southern Observatory, Santiago, Chile, 12. – 21. Oktober 2006. Zusammenarbeit mit Dr. H. Boehnhardt.

*Prof. Maria Virigina Alves*, INPE, Sao Jose Dos Santos, Brazil, 15. – 22. Oktober 2007. Zusammenarbeit mit Prof. J. Büchner.

*Dr. Hagay Amit*, Institut de Physique du Globe, Paris, France, 13. Juni – 9. Juli 2006. Zusammenarbeit mit Prof. U. Christensen.

*Dr. Vincenzo Andretta*, NAF-Osservatorio Astronomico di Capodimonte, Napoli, Italy, 3. – 10. März 2007. Zusammenarbeit mit Dr. L. Teriaca.

*Dr. Miroslav Barta*, Ondrejov Astronomical Institute, Czech Republic, 1. – 8. November 2006. Zusammenarbeit mit Prof. J. Büchner.

*Dr. Aaron C. Birch*, Colorado Research Associates, Boulder, CO, USA, 29. November –- 15. Dezember 2006, 8. –- 15. März 2007 und 23. –- 27. April 2007. Zusammenarbeit mit Dr. L. Gizon.

*Prof. D. Breitschwerdt*, Institut für Astronomie der Universität Wien, Austria, 9. – 14. Juli 2006 und 19. – 26. Juli 2007. Zusammenarbeit mit Dr. M. Rengel.

*Dr. Raymond Burston*, Monash University, School of Mathematical Sciences, Clayton, Victoria, Australia, 15. –- 28. Januar 2007. Zusammenarbeit mit Dr. L. Gizon.

*Prof. Paul Cally*, Monash University, Centre for Stellar and Planetary Astrophysics, School of Mathematical Sciences, Clayton, Victoria, Australia, 6. –- 10. November 2006 und 10. –- 19. August 2007. Zusammenarbeit mit Dr. L. Gizon.

*Prof. Dr. Gerard Chanteur*, CETP, Paris, France, 16. – 31. Juli 2007. Zusammenarbeit mit Dr. M. Fränz.

*Prof. Dr. Debi Prasad Choudhary*, California State University Northridge, USA, 4. –- 14. Juni 2007. Zusammenarbeit mit Prof. S. K. Solanki.

*Dr. Vania Dadeppo*, University of Padova, Italy, 19. Februar – 2. März 2007. Zusammenarbeit mit Dr. H. Sierks.

*Dr. Alicia Della Stella*, University of Padova, Italy, 19. Februar – 2. März 2007. Zusammenarbeit mit Dr. H. Sierks.

*Dr. Bhola N. Dwivedi*, Institute of Technology, Banaras Hindu University, Varanasi, India, 13. – 28. Juni 2007. Zusammenarbeit mit Dr. W. Curdt.

*Dr. I. Ermolli*, INAF Osservatorio Astronomico di Roma, Italy, 28. Mai – 1. Juni 2007. Zusammenarbeit mit S. K. Solanki und N. A. Krivova.

*Dr. Theresa Evans-Nguyen*, John Hopkins University, School of Medicine, Baltimore, USA, 5. – 16. November 2007. Zusammenarbeit mit Dr. H. Steininger.

*Dr. Sonia Fornasier*, Observatoire de Paris, France, 19. Februar – 2. März 2007. Zusammenarbeit mit Dr. H. Sierks.

*Dr. Olivier Groussin*, Observatoire d'Astrophysique de Marseille, France, 19. Februar – 2. März 2007. Zusammenarbeit mit Dr. H. Sierks.

*Marcin Gruszecki*, Universität Lublin, Polen, 20. November -– 1. Dezember 2006. Zusammenarbeit mit Prof. S. K. Solanki.

*Mr. Girjesh Gupta*, Indian Institute of Astrophysics, Bangalore, India, 24. August – 13. September 2007. Zusammenarbeit mit Prof. S. K. Solanki und Dr. L. Teriaca. Stay supported by DAAD project D/07/03045.

*Dr. Pedro Gutierrez*, Instituto de Astrofisica, Spain, 19. Februar – 2. März 2007. Zusammenarbeit mit Dr. H. Sierks.

*Dr. Peter Hoyng*, SRON, Utrecht, Netherlands, 1 Woche 2006 und 4 mal 1 Woche 2007. Zusammenarbeit mit Dr. D. Schmitt.

*Dr. Laurent Jorda*, Observatoire d'Astrophysique de Marseille, France, 19. Februar – 2. März 2007. Zusammenarbeit mit Dr. H. Sierks.

*Prof. Marian Karlicky*, Ondrejov Astronomical Institute, Czech Republic, 1. – 8. November 2006. Zusammenarbeit mit Prof. J. Büchner.

*Satoshi Kasahara*, Solar-Terrestrial Physics Group, Institute for Space and Astronautical Science, Japan Aerospace Exploration Agency, Japan, 8. – 28. Juli 2007. Zusammenarbeit mit Dr. N. Krupp und Dr. E. Kronberg.

*Mr. Igor Khatuntsev*, Institute for Space Research (IKI), Russia, 1. – 15. September 2007. Zusammenarbeit mit Dr. D. Titov.

*Prof. Hedda E. Kolm*, Centro do Estudos do Mar - UFPR, Pontal du Sul, Brazil, 11. August – 3. September 2006. Zusammenarbeit mit Dr. M. Hilchenbach.

*Dr. Detlef Koschny*, ESTEC, The Netherlands, 19. Februar – 2. März 2007. Zusammenarbeit mit Dr. H. Sierks.

*Dipl.-Phys. Lars Krieger*, Kiepenheuer–Institut für Sonnenphysik, Freiburg, 18. -– 20. Mai 2006, 23. -– 25. Mai 2006 und 30. Mai — 2. Juni 2006. Zusammenarbeit mit Dr. M. Roth.

*Romain Lapole*, École Centrale Paris, Châtenay–Malabry, France, 18. Juni -– 27. Juli 2007. Zusammenarbeit mit Dr. L. Gizon.

*Dr. Luisa Lara*, Instituto Astrofisico de Andalucia, Granada, Spain, 12. – 19. Februar 2006. Zusammenarbeit mit Dr. H. Boehnhardt.
19. Februar – 2. März 2007. Zusammenarbeit mit Dr. H. Sierks.

*Zhong Yi Lin*, University of Taipeh, Taiwan, 14. September – 3. Oktober 2006. Zusammenarbeit mit Dr. H. Boehnhardt.

*Ms. Eva Malecore*, Istituto Vanoni Menaggio, Tremezzo, Italy, 17. Juli – 28. Juli 2006. Zusammenarbeit mit Dr. M. Rengel.

*Dr. Antonio Ferriz Mass*, University of Vigo, Spain, 6. – 23. Oktober 2006. Zusammenarbeit mit Dr. D. Schmitt.

*Dr. Travis Metcalfe*, National Center for Atmospheric Research (NCAR), Boulder, CO, USA, 22. -– 25. April 2007. Zusammenarbeit mit Dr. L. Gizon.

*Dr. H. Müller*, Dartmouth College, Hanover, NH, USA, 23. Juli – 16. August 2007. Zusammenarbeit mit Dr. M. Hilchenbach.

*Dr. Thomas Neukirch* Solar Group, University of St. Andrews, UK 18. – 22. Juni 2007. Zusammenarbeit mit Dr. T. Wiegelmann.

*Rafal Ogrodowczyk*, Universität Lublin, Polen, 20. November -– 1. Dezember 2006. Zusammenarbeit mit Prof. S. K. Solanki.

*Dr. Nour-Eddine Raouafi*, National Solar Observatory, Tucson, AZ, USA, 7. -– 14. November 2007. Zusammenarbeit mit Prof. S. K. Solanki.

*Dr. Johann Reiter*, Technische Universität München, Zentrum Mathematik, 7. – 10. November 2006. Zusammenarbeit mit Dr. L. Gizon.

*Dr. Ilan Roth*, Space Sciences Laboratory, University Berkeley, USA, 24. April -– 5. Mai 2007. Zusammenarbeit mit Prof. S. K. Solanki.

*Dipl.-Phys. Ariane Schad*, Albert-Ludwigs-Universität, Freiburg, 24. – 31. August 2007. Zusammenarbeit mit Dr. M. Roth.

*Prof. Dr. Werner Schmutz*, World Climate Centre, Davos, Schweiz, 10. April — 4. Mai 2007. Zusammenarbeit mit Prof. S. K. Solanki.

*Mag Selwa*, Universität Lublin, Polen, 23. Januar -– 4. Februar 2006 und 31. August -– 9. September 2006. Zusammenarbeit mit Prof. S. K. Solanki.

*Ms. S. Subramanian*, PhD student at Armagh Observatory, Northern Ireland, 28. Januar – 11. Februar 2007. Zusammenarbeit mit M. Madjarska.

*Dr. Nicolas Thomas*, Universität Bern, Schweiz, 19. Februar – 2. März 2007. Zusammenarbeit mit Dr. H. Sierks.

*Prof. Michael Thompson*, University of Sheffield, Great Britain, 26. -– 29. Juni 2006. Zusammenarbeit mit Dr. L. Gizon.

*Dr. Andrey Tlatov*, Pulkovo Observatory, Kislovodsk, Russia, 28. Mai – 20. Juni 2007. Zusammenarbeit mit Prof. S. K. Solanki und Dr. N. A. Krivova.

*Dr. Gian Paolo Tozzi*, INAF Arcetri Observatory, Firenze, Italy, 24. November – 11. Dezember 2007. Zusammenarbeit mit Dr. H. Boehnhardt.

*Clement Trosseille*, Institute d'Astrophysique Spatiale (IAS), Orsay, France, 30. -– 31. Oktober 2006. Zusammenarbeit mit Dr. L. Gizon.

*Dr. Vaclav Waniak*, Krakow University, Krakow, Poland, 20. November – 4. Dezember 2007. Zusammenarbeit mit Dr. H. Boehnhardt.

*Prof. H. Zhang*, Chinese Academy of Sciences, 21. – 28. November 2007. Zusammenarbeit mit Prof. J. Büchner.

*Prof. Dr. Honqi Zhang*, Huairou Solar Observing Station, Beijing, China, 17. -– 24. November 2007. Zusammenarbeit mit Prof. S. K. Solanki.

*Dr. Sergei Zharkov*, University of Sheffield, Great Britain, 10. -– 15. Dezember 2006. Zusammenarbeit mit Dr. L. Gizon.

## **Längere Aufenthalte von Wissenschaftlern des MPS an anderen Instituten** / Long-term visits of MPS scientists to other institutes

*Dr. Hermann Böhnhardt*, National Astronomical Observatory, Rozhen, Bulgaria, 1. – 15. Mai 2006. ESO Chile, Paranal Observatory, 22. – 27. Mai 2006. ESO Chile, La Silla Observatory, 21. – 28. Oktober 2006. ESO Chile, Santiago, research stay, 3. – 12. März 2007. ESO Chile, Paranal Observatory, 15. – 26. Juni 2007. ESO Chile, Santiago, research fellowship, 12. Oktober – 19. November 2007.

*Prof. Dr. Jörg Büchner*, Chinese Academy of Sciences, 23. September – 3. Oktober 2006.

*Dr. Johann Hirzberger*, Observing campaigns at the Swedish Solar Telescope (SST) La Palma, Spain, 7. – 16. August 2006 und 8. – 17. August 2007.

*Dr. Rainald Kallenbach*, Visiting Scientist at the Institute for Geophysics and Planetary Physics, University of California, Riverside, CA, USA, 6. Juli – 6. August 2007.

*Dr. Norbert Krupp*, ISAS, Tokio, Japan, 9. – 17. Januar 2007.

*Dr. Urs Mall*, Space Application Center ISRO, Ahmedabad, India, 28. September – 9. Oktober 2007.

*Nilda Oklay* IRSOL (Istituto Ricerche Solari Locarno), Switzerland, 1. – 8. Juni 2007.

*Dr. Hannah Schunker*, Monash University, Clayton, Victoria, Australia, 15. – 25. Juli 2007.

*Dr. Holger Sierks*, Orbital Science Corperation, Washington DC, USA; NRL, Washington DC, USA; UCLA, Los Angeles, USA, 31. Januar – 11. Februar 2007.

*Dr. Udo Schühle*, Space Sciences Laboratory, University of California, Berkeley, CA, USA, 19. März – 20. April 2007.

*Dr. Luca Teriaca*, Indian Institute of Astrophysics, Bangalore, India, 6. – 15. November 2007.

*Dr. Thomas Wiegelmann* Solar Group, University of St. Andrews, UK, 28. Februar – 10. März 2006 und 11. – 19. Dezember 2006.

## **Projekte in Zusammenarbeit mit anderen Institutionen** / Projects in collaboration with other institutions

*Die Art der Zusammenarbeit des MPS mit anderen Institutionen ist im einzelnen ziemlich unterschiedlich. Die folgende Aufzählung soll nur einen kurzen Überblick geben./The cooperation of MPS with other institutions is extensive and varied. The following list only provides a brief overview.*

**Asteroseismology of K Giants.-** M. Roth in Zusammenarbeit mit J. Setiawan (MPI für Astronomie, Heidelberg).

**ASTROD I (Astrodynamical Space Test of Relativity using Optical Devices I), a class-M fundamental physics mission proposal submitted to ESA's Cosmic Vision Programme.-** R. Burston und L. Gizon in Zusammenarbeit mit T. Appourchaux (IAS, Orsay, France); Y.-T. Ni (Purple Mountain Observatory, Nanjing, China).

**Astronomical tests of gravitation theory.-** S. K. Solanki in Zusammenarbeit mit O. Preuss (Bielefeld); F. W. Hehl (Universität Köln).

**Astrophysical spectropolarimetry.-** A. Gandorfer in Zusammenarbeit mit J. O. Stenflo (Institute of Astronomy, ETH Zürich, Schweiz).

**Advanced Composition Explorer (ACE).-** R. Kallenbach in Zusammenarbeit mit G. Gloeckler (University of Michigan, USA); J. Geiss (International Space Science Institute, Bern, Schweiz).

**BepiColombo – BELA (Laser Altimeter).-** M. Hilchenbach, U. Christensen, R. Kallenbach, R. Roll, H. Fischer und C. Koch in Zusammenarbeit mit N. Thomas, W. Benz, K. Gunderson, K. Seiferlin (Physikalisches Institut, Universität Bern, Schweiz); T. Spohn, E. Hauber, H. Michaelis, J. Oberst (DLR - Institut für Planetenforschung, Berlin); G. Beutler (Astronomy Institute, Universität Bern, Schweiz); C. Fallnich (Laser Zentrum Hannover); D. Giardini (Institute of Geophysics/Swiss Seismological Service, Swiss Federal Institute of Technology, (ETHZ), Zürich, Schweiz); O. Groussin (Department of Astronomy, University of Maryland, College Park, USA); L. Jorda, P. Lamy (Laboratoire d'Astrophysique de Marseille, Marseille, France); L.-M. Lara, J. J. Lopez-Moreno, R. Rodrigo (Instituto de Astrofisica de Andalucia, Granada, Spain); P. Lognonné (Département de Géophysique Spatiale et Planétaire/UMR7096-CNRS, Saint Maur des Fossé, France); D. Resendes (Instituto Superior Técnico, Universidade Técnica de Lisboa, Lisboa, Portugal).

**BepiColombo — MERMAG (Magnetic Field Investigation).-** U. Christensen in Zusammenarbeit mit K.-H. Glaßmeier (PI) (Institut für Geophysik und Extraterrestrische Physik, Braunschweig).

**BepiColombo – MIXS.-** M. Hilchenbach in Zusammenarbeit mit Fraser (PI) (Leicester, UK).

**BepiColombo – MMO (Mercury Magnetospheric Orbiter).-** *MPPE-MSA: Spektrometer zur Messung von geladenen und neutralen Teilchen in der Merkurmagnetosphäre (Bauphase).* N. Krupp, J. Woch, M. Fränz, A. Loose, H. Fischer und U. Bührke in Zusammenarbeit mit D. Delcourt (Centre d'Etude Terrestre et Planetaire (CETP), Paris, France); Y. Saito (Jaxa/ISAS, Tokio, Japan).

**BepiColombo – MPO (Mercury Planetary Orbiter).-** *PICAM (Planetary Ion CAMera) - Detektoreinheit des Neutral and Charge Particle Analyzers SERENA (Search for Exospheric Refilling and Emitted Natural Abundances).* J. Woch, A. Loose, N. Krupp und M. Fränz in Zusammenarbeit mit S. Orsini (PI) (IFSI, Roma, Italy); K. Torkar (Co-PI) (SRI, Graz, Austria); J.-J. Berthelier (CETP-CNRS, St Maur des Fosses, France); P. Escoubet (ESTEC, Noordwijk, Niederlande); F. Leblanc (IPSL Verrieres-Le-Buisson, France); D. Nevejans (BIRA, Brusseles, Belgium); K. Szego (KFKI, Budapest, Hungary); O. Vaisberg (IKI, Moscow, Russia).

**CASSINI – DISR.-** B. Grieger und M. Küppers in Zusammenarbeit mit M. Tomasko und Mitarbeiter (Lunar and Planetary Laboratory, University of Arizona, USA).

**CASSINI – MIMI/LEMMS.-** *Spektrometer zur Messung von geladenen und neutralen energiereichen Teilchen in der Saturnmagnetosphäre (Datenauswertung).* N. Krupp, J. Woch und A. Lagg in Zusammenarbeit mit S. M. Krimigis, S. Livi, D. G. Mitchell (Johns Hopkins University, Applied Physics Laboratory, USA); D. Hamilton (University of Maryland, USA); I. Dandouras (CESR, Toulouse, France); T. P. Armstrong (Fundamental Technologies, Kansas, USA).

**CASSINI – UVIS (Ultraviolet Imaging Spectrometer), CASSINI/HUYGENS Mission.-** H. U. Keller und A. Korth in Zusammenarbeit mit L. W. Esposito (PI), LASP, University of Colorado, Boulder, USA; University of Southern California, Los Angeles, USA; Jet Propulsion Laboratory, Pasadena, USA; California Institute of Technology, Pasadena, USA; Southwest Research Institute, Boulder, USA.

**Chandrayaan-1, ISRO.-** U. Mall in Zusammenarbeit mit N. Goswami (PRL, India).

**Cluster II – CIS (Cluster Ion Spectrometer).-** A. Korth, M. Fränz, P. W. Daly, E. Panov und E. Kronberg in Zusammenarbeit mit H. Rème (PI), CESR (Toulouse, France); MPI für extraterrestrische Physik (Garching); Universities of New Hampshire (Washington, Seattle, Berkeley, USA); IFSI/CNR (Frascati, Italy); Lockheed (Palo Alto, USA); SISP (Kiruna, Sweden).

**Cluster II – RAPID.-** *Das Teilchen-Spektrometer RAPID.* Principle Investigator: P. W. Daly; Co-Investigators: U. Mall, J. Büchner, A. Korth, J. Woch, E. Kronberg, Sir Ian Axford und V. M. Vasyliūnas in Zusammenarbeit mit J. B. Blake, J. F. Fennell, J. Roeder (AC, Los Angeles, USA); Z. Y. Pu, S. Y. Fu (Beijing University, Beijing, China); T. A. Fritz, Q.-G. Zong (BU, Boston, USA); F. Gliem (IDA, Braunschweig); I. Sandahl, M. Yamauchi (IRF, Kiruna, Sweden); H. Borg (Univ. Umea, Sweden); K. Kecskemety (KFKI, Budapest, Hungary); G. D. Reeves, R.H.W. Friedel (LANL, Los Alamos, USA); D. N. Baker (LASP, Boulder, USA); M. Grande, M. Carter, C. H. Perry, J. Davies, M. Dunlop (RAL, Chilton, UK); M.G.G.T. Taylor (ESTEC, Niederlande); S. McKenna-Lawlor (SPC, Maynooth, USA); F. Søraas, K. Aarsnes, K. Oksavik (University Bergen, Norway); K. Mursula, P. Tanskanen (University Oulu, Finland); E. T. Sarris (University Thrace, Greece); A.T.Y. Lui (APL, USA).

**Cluster Active Archive (CAA).-** *Archivierung der RAPID-Daten.* P. W. Daly, S. Mühlbachler und E. Kronberg in Zusammenarbeit mit C. H. Perry, J. Davies (RAL, Chilton, UK).

**CME driven shock wave.-** B. Inhester, N.-E. Raouafi, S. K. Solanki und M. Mierla in Zusammenarbeit mit S. Manusco, C. Benna (Osservatorio Astronomico di Torino, Torino, Italy); J. P. Delaboudinière (Institut d'Astrophysique Spatiale, Orsay, France).

**Computational Acoustics in a Spherical Shell.-** M. Roth in Zusammenarbeit mit S. Hanasoge (Stanford University, Stanford, USA) und anderen.

**Coronal downflows.-** S.K. Solanki in Zusammenarbeit mit H. Mason, D. Tripathi (University of Cambridge, UK); D. F. Webb (Boston College, USA).

**Coronal holes studied with UVCS.-** S. K. Solanki in Zusammenarbeit mit N.-E. Raouafi, J. W. Harvey (NSO, Tucson, USA).

**Coronal MHD-equilibria.-** T. Wiegelmann in Zusammenarbeit mit T. Neukirch (University St. Andrews, UK).

**COROT additional program (AP).-** *"Stellar variability and microvariability – III: convection and short term evolution of photospheric active regions"*. S. K. Solanki und N. A. Krivova in Zusammenarbeit mit Institute of Astronomy, University of Cambridge, UK; School of Physics and Astronomy, University of St. Andrews, UK; Astrophysics Group, Imperial College, London, UK.

**DAWN.-** H. U. Keller, H. Sierks, H. Hartwig, A. Nathues und U. Christensen in Zusammenarbeit mit R. Jaumann, S. Mottola (DLR/Institut für Planetenforschung, Berlin); H. Michalik, B. Fiethe (Institut für Datentechnik und Kommunikationsnetze, Braunschweig); C. Russell, C. Raymond (University of California, Los Angeles, USA); K. C. Patel, E. Miller (Jet Propulsion Laboratory, Pasadena, USA).

**Deep Impact at comet 9P/Tempel 1: Exploring the Dust Component.-** H. Böhnhardt (PI) in Zusammenarbeit mit N. Ageorges, S. Bagnulo, O. Hainaut, E. Jehin, H. U. Kaeufl, F. Kerber, G. LoCurto, E. Pompei, O. Marco, F. Selmann (ESO Garching & Santiago de Chile); L. Barrera (UMCE, Santiago de Chile); T. Bonev (University Sofia, Bulgaria); R. Gredel (MPI Astronomie, Heidelberg); L. Lara, J. L. Ortiz (Inst. Astrof. Andalucia, Granada, Spain); K. Meech (University Hawaii, Honolulu, USA); E. Pantin (CNRS Paris, France); H. Rauer (DLR Berlin); G. P. Tozzi (INAF Arcetri Observatory, Florence, Italy).

**DFG Schwerpunktprogramm 1176: Climate and Weather of the Sun-Earth-System (CAWSES).-** *Influence of the mean circulation on gravity wave generation* P. Hartogh, A. Medvedev und T. Kuroda in Zusammenarbeit mit E. Yigit (University College London, UK).

**DFG Schwerpunktprogramm 1176: Climate and Weather of the Sun-Earth-System (CAWSES).-** *Investigation of the solar influence on middle atmospheric water vapour and ozone during the last solar cycle – analysis of the MPS data set* P. Hartogh, C. Jarchow und G. Sonnemann in Zusammenarbeit mit U. Berger und M. Grygalashvyly (Leibniz-Institut für Atmosphärenphysik, Kühlungsborn).

**DFG Schwerpunktprogramm 1176: Climate and Weather of the Sun-Earth-System (CAWSES).-** *Support proposal for refurbishment and replacement of a microwave spectrometer to be used in the priority programme CAWSES* P. Hartogh und K. Hallgren in Zusammenarbeit mit F.-J. Lübken (Leibniz-Institut für Atmosphärenphysik, Kühlungsborn).

**DFG Schwerpunktprogramm 1176: Climate and Weather of the Sun-Earth-System (CAWSES).-** N. A. Krivova und S. K. Solanki in Zusammenarbeit mit Freie Universität Berlin; Institut für Umweltphysik, Universität Bremen; MPI für Meteorologie, Hamburg.

**DFG-Schwerpunktprogramm 1115 – MAOAM (The Martian Atmosphere: Observing And Modelling).-** P. Hartogh, C. Jarchow, T. Kuroda, und A. Medvedev in Zusammenarbeit mit U. Berger, G. Sonnemann, M. Grygalashvyly (IAP Kühlungsborn); A. Feofilov, A. Kutepov (IAA München); H. Elbern (Institut für Geophysik und Meteorologie, Köln); M. Allen (JPL, Pasadena, USA); Gordon Chin (GSFC, Greenbelt, USA).

**DFG-Schwerpunktprogramm 1115.-** *Mars und die terrestrischen Planeten – Plasma induced atmospheric escape on Mars.* J. Woch, E. Dubinin und M. Fränz in Zusammenarbeit mit TU Braunschweig.

**Diagnostics of magnetoconvection.-** M. Schüssler und S. K. Solanki in Zusammenarbeit mit S. Shelyag (University of Sheffield, UK); A. Vögler (Universität Utrecht, Niederlande).

**Dust from the $\beta$ Pictoris disk.-** N. A. Krivova und S. K. Solanki in Zusammenarbeit mit A. V. Krivov (Universität Potsdam); V. B. Titov (Universität St. Petersburg, Russland).

**EUROPLANET (European Planetology Network).-** *Aufbau eines Netzwerks in Europa zur Optimierung der Forschungsaktivitäten im Bereich Planeten.* N. Krupp in Zusammenarbeit mit CESR (Toulouse, France); FMI Helsinki (Finland); University Nantes (France); Observatoire Paris (France); University Grenoble (France); Imperial College (London, UK); KFKI (Budapest, Hungary).

**ExoMars – MOMA.-** F. Goesmann (PI), M. Hilchenbach und O. Roders in Zusammenarbeit mit Dr. L.

Becker (John Hopkins University, Department of Physics and Astronomy, Baltimore, USA); Dr. T. Cornish (Applied Physics Laboratory, Baltimore, USA); Dr. R. Cotter (Johns Hopkins School of Medicine , Baltimore, USA); Dr. C. Szopa (Service d'Aeronomie (SA), Paris, France); Dr. F. Raulin (Laboratoire Interuniverstaire des Systemes Atmospheriques (LISA), Paris, France).

**ExoMars – RAMAN – LIBS.-** M. Hilchenbach in Zusammenarbeit mit Rull (PI) (Madrid, Spanien).

**ExoMars – SEIS.-** U. Christensen und R. Roll in Zusammenarbeit mit P. Lognonné (IPGP, Paris, France).

**Galileo – EPD (Energetic Particles Detector).-** *Spektrometer zur Messung von geladenen energiereichen Teilchen in der Jupitermagnetosphäre (Datenauswertung).* N. Krupp, J. Woch, A. Lagg und E. Kronberg in Zusammenarbeit mit D. J. Williams, R. McEntire (Johns Hopkins University, Applied Physics Laboratory, USA); S. Kasahara (Institute of Space and Astronautical Science, Sagamihara, Kanagawa, Japan).

**GBSO – Ground Based Solar Observations.-** A. Lagg, J. Woch, A. Gandorfer, J. Hirzberger, S. K. Solanki, Z. Xu, S. Danilovic, C. Sasso, M. Meling, V. Zakharov, R. Aznar-Cuadrado, T. Riethmüller in Zusammenarbeit mit M. Collados (IAC, La Laguna, Tenerife, Spain); A. López Ariste (THEMIS, La Laguna, Tenerife, Spain); R. Wachter (University of Stanford, USA); D. Fluri, N. Afram (ETH Zürich, Schweiz); K. Puschman, E. Wiehr (Institut für Astrophysik, Universität Göttingen); S. Stangl (Institut für Physik, Universität Graz, Austria); Kiepenheuer-Institut für Sonnenphysik, Freiburg; Instituto de Astrofísica de Canarias, Spain; Institute for Solar Physics of the Royal Swedish Society, Stockholm, Sweden.

**German Data Center for the Solar Dynamics Observatory.-** R. Burston und L. Gizon in Zusammenarbeit mit H. Peter (Kiepenheuer-Institut für Sonnenphysik, Freiburg); G. Mann (Astrophysikalisches Institut Potsdam).

**HELAS (European HELio- and ASteroseismology network).-** L. Gizon, M. Roth, Y. Saidi, H. Schunker in Zusammenarbeit mit O. von der Lühe (Kiepenheuer-Institut für Sonnenphysik, Freiburg); P. Pallé (IAC, La Laguna, Tenerife, Spain); M. Thompson (University Sheffield, UK); J. Christensen-Dalsgaard (Universität Aarhus, Dänemark); M. Monteiro (Center for Astrophysics, University Porto, Portugal); M. P. Di Mauro (INAF, Roma, Italy); C. Aerts (Katholische Universität Leuven, Belgien); J. Daszyńska-Daskiewicz (Uniwersytet Wroclawski, Polen); T. Corbard (CNRS, Nizza, Frankreich).

**HIFI–WBS (Heterodyne Instrument for FIRST – Wideband Spectrometer).-** P. Hartogh, C. Jarchow, M. Rengel und M. Küppers in Zusammenarbeit mit T. de Graauw, H. J. Aarts, D. A. Beintema, J. Gao, H. Jacobs, W. Jellema, W. Luinge, P. R. Roelfsema, X. Tielens, H. van de Stadt, B. van Leeuwen, N. D. Whyborn, K. J. Wildeman (SRON, Utrecht, Niederlande); E. Van Dishoeck (Universität Leiden, Niederlande); R. Güsten, K. Menten (Max-Planck-Institut für Radioastronomie, Bonn); C. H. Honingh, K. Jacobs, R. Schieder, J. Stutzki (Universität Köln); A. Emrich (Omnisys, Göteborg, Schweden); S. Torchinsky (Chalmers, Göteborg, Schweden); M. Larsson (Universität Stockholm, Schweden); C. Rosolen (Arpeges, Observatoire de Paris, Meudon, Frankreich); G. Beaudin (LERMA, Meudon, Frankreich); E. Caux, A. Cros (CESR, Toulouse, Frankreich); P. Cais (Bordeaux Observatory, Frankreich); E. Lellouch, T. Encrenaz (DESPA, Paris, Frankreich); C. Gry (LAS Marseille, Frankreich); N. Maurun (Graal, Montpellier, Frankreich); K. Schuster (IRAM, Grenoble, Frankreich); F. Boulanger (IAS, Orsay, Frankreich); L. T. Little (Kent University, UK); T. Miller (UMIST, UK); T.J.T. Moore (Liverpool-J. Moures, UK); S. Withington (MRAO Cambridge, UK); G. J. White (QMW London, UK); R. Cerrulli, R. Orfei (IFSI Frascati, Italien); V. Natale (CAISMI Florenz, Italien); J. Martin-Pintado (OAN, Alcala, Spanien); J.D.G. Puyol (Obs. Yebes, Spanien); M. J. Sarna, R. Szczerba (Copernicus AC, Warschau, Polen); W. R. McGrath, J. C. Pearson, T. C. Gaier (JPL, Pasadena, USA); T. G. Phillips, J. Zmuidzinas (Caltech, Pasadena, USA); A. I. Harris (Maryland University, USA); E. Herbst (Ohio State University, USA); D. A. Neufeld (Johns Hopkins University, USA); N. R. Erickson (FCRAO, Amherst, MA, USA); S. Verghese (Lincoln Lab., MIT, USA); S. Kwok (Calgary University, Canada); D. A. Naylor (Lethbridge University, Canada); F. Lo (IAA Taiwan); H. Wang (NTU, Taipeh, Taiwan); P. Zimmermann (RPG, Meckenheim).

**Hinode.-** A. Lagg, T. Riethmüller, S. Danilovic, S. K. Solanki, J. Hirzberger, M. Madjarska in Zusammenarbeit mit National Astronomical Observatory of Japan (NAOJ); Armagh Observatory, Northern Ireland.

**INTAS-Projekt 2003-51-4872.-** *Ion and electron scales in mass and energy transfer: magnetospheric mapping, modelling and future missions.* J. Büchner in Zusammenarbeit mit Partnerteilnehmerländern: Belarus, Frankreich, Italien, Polen, Russland.

**INTAS Project WP 01-270.-** *Physics of the Heliosheath Plasma Flow and Structure of the Termination Shock.* R. Kallenbach in Zusammenarbeit mit V. Izmodenov (Moscow State University, Russia).

**Interaction of Acoustic Waves with a Magnetic Cylinder.-** L. Gizon in Zusammenarbeit mit A. C. Birch (CoRA, NorthWest Research Associates, Boulder, USA); S. Hanasoge (Stanford University, Stanford, USA).

**Interpretation of Interball and Cluster data.-** J. Büchner in Zusammenarbeit mit L. Zelenyi, S. Savin, E. Panov (Space Research Institute of the Russian Academy of Sciences, Moscow, Russia).

**Inversion of helioseismic traveltimes.-** J. Jackiewicz und L. Gizon in Zusammenarbeit mit A. C. Birch (CoRA, Boulder, USA).

**Investigation of kinetic plasma processes in the solar corona.-** J. Büchner in Zusammenarbeit mit L. Hau, K. W. Lee (National Central University of Taiwan).

**ISSI team "Interpretation and modelling of Solar Spectral Irradiance measurements".-** N. A. Krivova und S. K. Solanki in Zusammenarbeit mit INAF Osservatorio Astronomico di Roma, Italy; Astrophysics Group, Imperial College, London, UK; PMOD WRC, Davos, Switzerland; LASP, University of Colorado, Boulder, USA; Institut für Umweltphysik, Universität Bremen; Interferometrics Inc., Herndon, USA.

**Kinetische Physik des Sonnenwinds.-** *Forschung auf dem Gebiet der Plasma-Beam Instabilitäten im Sonnenwind und in der Sonnenkorona. Numerische Simulationen zum Zerfall und der parametrischen Entwicklung von Alfvén Wellen großer Amplitude.* E. Marsch in Zusammenarbeit mit J. Araneda (Universität Concepcion, Chile).

**Kinetic simulation techniques in space physics.-** J. Büchner in Zusammenarbeit mit N. Elkina (Keldysh Institute of the Russian Academy of Sciences, Moscow, Russia).

**KuaFu – "Space Weather Explorer".-** R. Schwenn, U. Schühle und E. Marsch in Zusammenarbeit mit Chuanyi Tu (PI), J.-S. Wang (Peking University, Beijing, China); E. Donavan (Department of Physics and Astronomy, University of Calgary, Canada); L.-D. Xia (School of Earth and Space Sciences, University of Science and Technology of China, Hefei, Anhui, China); Y.-W. Zhang (China Academy of Space Technology and DFH Satellite Co. Ltd, Beijing, China).

**Local Helioseismology of Small Magnetic Features.-** L. Gizon in Zusammenarbeit mit T. L. Duvall (NASA, GSFC, Greenbelt, USA); A. C. Birch (CoRA, NorthWest Research Associates, Boulder, USA); S. Hanasoge (Stanford University, USA).

**LYman-Alpha Orbiting Telescopes (LYOT) on board SMESE (Small Explorer for the study of Solar Eruptions).-** U. Schühle in Zusammenarbeit mit J.-C. Vial (PI) (Institut d'Astrophysique Spatiale, Orsay, France).

**Magnetic Activity in Cool Stars.-** R. Aznar Cuadrado in Zusammenarbeit mit I. Busà, L. Terranegra, V. Andretta, M. T. Gomez (INAF/Osservatorio Astronomico di Capodimonte, Italy).

**Mars Climate Simulator.-** B. Grieger in Zusammenarbeit mit K. Fraedrich und Mitarbeiter (Meteorologisches Institut der Universität Hamburg); R. Greve (Institute of Low Temperature Science, Hokkaido University, Japan).

**Mars Express.-** Nick Hoekzema in Zusammenarbeit mit K. Gwinner, T. Roatch, H. Hofmann (DLR, Berlin); G. Neukum (FU, Berlin); A. Inada (CalTech, Los Angeles, CA, USA); L. Petrova (IKI, Moskau, Russland).

**Mars Express – ASPERA-3 (Analyzer of Space Plasmas and EneRgetic Atoms).-** M. Fränz, J. Woch, N. Krupp, E. Dubinin, E. Roussos, C. Martinecz und J. Kleimann in Zusammenarbeit mit R. Lundin (PI), S. Barabash (IRF, Kiruna, Sweden); D. Winningham, R. Frahm (SWRI, San Antonio, USA); P. Wurz (Universität Bern, Schweiz); A. Coates (MSSL, London, UK); M. Grande (RAL, Chilton, UK); J. A. Sauvaud, A. Fedorov (CESR, Toulouse, France); E. Kallio (FMI, Helsinki, Finland); S. Orsini (IFSI, Roma, Italy); C. C. Curtis (UoA, Tuscon, USA).

**Mars Express – OMEGA.-** D. Titov in Zusammenarbeit mit J.-P. Bibring, Y. Langevin, B. Gondet (Institut d'Astrophysique Spatiale (IAS), Orsay, France); P. Drossart (Observatoire de Paris, Meudon, France); N. Ignatiev (Space Research Institute (IKI), Moscow, Russia).

**Mars Express – PFS.-** D. Titov in Zusammenarbeit mit V. Formisano (Institute of Physics of Interplanetary Space (IFSI-INAF), Roma, Italy); N. Ignatiev, A. Fedorova (Space Research Institute (IKI), Moscow, Russia); E. Lellouch, T. Fouchet, Th. Encrenaz (Observatoire de Paris, Meudon, France).

**MARSIS.-** E. Nielsen in Zusammenarbeit mit Department of Physics and Astronomy, University of Iowa, Iowa City, Iowa, USA; Jet Propulsion Laboratory, California Institute of Technology, Pasadena, CA 91109, USA; Istituto di Fisica dello Spazio Interplanetario, Istituto Nazionale di Astrofisica, Rome, Italy; Infocom Department, "La Sapienza" University of Rome, Rome, Italy; School of Earth and Space sciences, Peking University, Beijing, P.R. China.

**MARVEL – Mars Volcanic Emission and Life Scout.-** P. Hartogh in Zusammenarbeit mit M. Allen

(JPL, Pasadena, USA); G. Chin (GSFC, Greenbelt, USA).

**Measurement of the meridional flow with Fourier–Hankel decomposition.-** M. Roth in Zusammenarbeit mit L. Krieger (Kiepenheuer-Institut für Sonnenphysik, Freiburg).

**Meteorites, cosmogenic nuclides and past solar activity.-** S. K. Solanki in Zusammenarbeit mit I. G. Usoskin (Sodankylä Geophysical Observatory, Finland); C. Taricco (University Turin, Italy); N. Bhandari (Basic Sciences Research Institute, Ahmedabad, India); G. A. Kovaltsov (Ioffe Physical-Technical Institute, St. Petersburg, Russia).

**MICA – Mirror Coronagraph for Argentina.-** R. Schwenn in Zusammenarbeit mit Instituto de Astronomia y Fisica del Espacio (IAFE), Buenos Aires, Argentinien; Observatorio Astronomico Felix Aguilar (OAFA), University Juan, Argentinien; MPE, Garching.

**Microflares and the solar emission distribution.-** S. K. Solanki in Zusammenarbeit mit A. Pauluhn (Paul Scherrer Institut, Villingen, Schweiz).

**Millennium – climate simulations for the last millennium using the Earth System Model (ESM).-** N. A. Krivova und S. K. Solanki in Zusammenarbeit mit Max-Planck-Institut für Meteorologie, Hamburg; Freie Universität Berlin.

**Molecular Zeeman effect.-** S. K. Solanki in Zusammenarbeit mit N. Afram, S. Berdyugina, D. M. Fluri (ETH Zürich, Schweiz).

**Moving magnetic features in and around sunspots.-** S. K. Solanki und J. Woch in Zusammenarbeit mit J. Wang, J. Zhang (National Astronomical Observatories, Beijing, VR China).

**NERC consortium: "SOLCLI: Solar Influence on Climate".-** N. A. Krivova und S. K. Solanki in Zusammenarbeit mit Astrophysics Group, Imperial College London, UK.

**Nonlinear force-free coronal magnetic fields (NLFFF-consortium).-** T. Wiegelmann in Zusammenarbeit mit C. J. Schrijver (LMSAL, Palo Alto, USA).

**Numerical simulations of coronal loop oscillations.-** S. K. Solanki in Zusammenarbeit mit L. Ofman, M. Selwa, T. J. Wang (NASA GSFC Greenbelt, USA); K. Murawski, M. Gruszecki (UMCS Lublin, Polen).

**Phobos Grunt.-** F. Goesmann in Zusammenarbeit mit Dr. M. Gerasimov (IKI, Moskau, Russia).

**Plasmawechselwirkungen extrasolarer Planeten mit ihrem Stern.-** J. Büchner in Zusammenarbeit mit U. Motschmann (Technische Universität Braunschweig).

**POLARIS (POLar Investigation of the Sun), a class-L mission submitted to ESA's Cosmic Vision Programme.-** L. Gizon in Zusammenarbeit mit T. Appourchaux (IAS, Orsay, France).

**PROBA II – LYRA (Large Yield Radiometer).-** U. Schühle in Zusammanarbeit mit: J.-F. Hochedez (PI), A. BenMoussa, D. Berghmans, A. Theissen, V. Delouille, B. Nicula, L. Wauters, R. Van der Linden, A. Zhukov, F. Clette (Royal Observatory of Belgium (ROB), Brussels, Belgium); W. Schmutz, S. Koller, H. Roth, E. Rozanov, I. Rüedi, C. Wehrli (Physikalisch-Meteorologisches Observatorium Davos (PMOD) and World Radiation Center, Davos, Schweiz); K. Haenen, V. Mortet, Z. Remes, M. Nesládek, M. D'Olieslaeger (Institute for Materials Research, Diepenbeek, Belgium); Y. Stockman, J.-M. Defise, J.-P. Halain, P. Rochus (Centre Spatial de Liège (CSL), Angleur, Belgium); D. Gillotay, D. Fussen, M. Dominique, F. Vanhellemont (Belgian Institute for Space Aeronomy, Brussels, Belgium); V. Slemzin, A. Mitrofanov (Lebedev Physical Institute, Moscow, Russia); D. McMullin (Naval Research Laboratory (NRL), Washington, DC, USA); M. Kretzschmar, (Istituto Fisica dello Spazio Interplanetario (IFSI), Roma, Italy); R. Petersen, M. Nesládek, M. D'Olieslaeger (IMEC, Division IMOMEC, Diepenbeek, Belgium); J. Roggen (IMEC, Louvain, Belgium); S. Koizumi (Advanced Materials Laboratory, National Institute for Materials Science, Tsukuba, Japan); H. Amano (Department of Materials Science and Engineering, Meijo University, Nagoya, Japan); A. Soltani (Institut d'Electronique, de Microélectronique et de Nanotechnologie, Villeneuve d'Ascq, France).

**PROBA II – SWAP (Sun Watcher using APS Detectors).-** U. Schühle in Zusammenarbeit mit D. Berghmans, J. F. Hochedez, B. Nicula, G. Lawrence, A. C. Katsyiannis, R. Van der Linden, A. Zhukov, F. Clette (Royal Observatory of Belgium, Solar Physics, Brussels, Belgium); J. M. Defise (PI), J. H. Lecat, P. Rochus, E. Mazy, T. Thibert (Centre Spatial de Liège, Angleur, Belgium); P. Nicolosi, M. G. Pelizzo (University of Padova, Padova, Italy); V. Slemzin (Lebedev Physical Institute, Moscow, Russia).

**Physical and composition properties of short-periodic and Oort Cloud comets.-** H. Boehnhardt, M. Drahus, M. Lippi, C. Tubiana und J.-P. Vincent in Zusammenarbeit mit S. Bagnulo (ESO Santiago de Chile, Armagh Observatory Northern Ireland); L. Barrera (UMCE, Santiago de Chile); D. Harker (University San Diego, USA); M. Kelley (Joint Astronomy

Center, USA); S. Kolokolova (University Maryland, College Park, USA); L. Lara (IAA Granada, Spain); M. Mumma, M. DiSanti, B. Bonev (NASA Goddard, Greenbelt, USA); D. Prialnik, E. Beer-Harari (University Tel Aviv, Israel); G. P. Tozzi (INAF Arcetri Observatory, Florence, Italy); D. Wooden (PI) (NASA Ames Res. Center, Moffett Fields, USA) C. Woodward (University Minnesota, USA).

**RAISE – Rapid Imaging Spectrograph Experiment.-** U. Schühle in Zusammenarbeit mit D. Hassler (PI), D. Slater, C. DeForest, S. McIntosh (Southwest Research Institute, San Antonio, USA); T. Ayres (University of Colorado, Boulder, USA); R. Thomas (NASA GSFC, Greenbelt, USA); H. Michaelis (Institut für Planetenforschung, DLR, Berlin).

**Rosetta – CONSERT (Radio Tomography Project).-** E. Nielsen und T. Hagfors in Zusammenarbeit mit Laboratoire de Planétologie, University of Grenoble, France; ESA.

**Rosetta – COSAC (PHILAE).-** F. Goesmann, R. Roll in Zusammenarbeit mit F. Raulin (LISA - UMR 7583, Universités Paris 12 & Paris 7, Faculté des Sciences, Créteil, France); U. J. Meierhenrich (Université Nice-Sophia Antipolis L.C.M.B.A. et UMR 6001 CNRS, Nice, France); C. Szopa (Service d'Aéronomie (SA), UMR CNRS 7620, IPSL, Verrières le Buisson, France).

**Rosetta – COSIMA.-** J. Kissel (PI bis 15. Mai 2005), M. Hilchenbach (Co-PI, PI seit 15. Mai 2005), H. Krüger (Co-I), H. Böhnhardt (Co-I) und H. Fischer (engineer) in Zusammenarbeit mit K. Altwegg (Physikalisches Institut, Universität Bern, Schweiz); B. C. Clark (Lockheed Martin Astronautics, Denver, USA); L. Colangeli (Istituto Nazionale di Astrofisica - Osservatorio Astronomico di Capodimonte, Napoli, Italy); H. Cottin, F. Raulin (LISA, Universites Paris 12 & 7, Creteil Cedex, France); S. Czempiel, J. Eibl, G. Haerendel, H. Höfner, P. Parigger (MPI für extraterrestrische Physik, Garching); C. Engrand (Centre de Spectrométrie Nucléaire et de Spectrométrie de Masse (CSNSM), Orsay, France); H. M. Fehringer, R. Schulz (ESA/ESTEC, Noordwijk, Niederlande); B. Feuerbacher (DLR, Köln); M. Fomenkova (Center for Astrophysics and Space Sciences, University of California, La Jolla, USA); A. Glasmachers (Universität Wuppertal, Lehrstuhl für Messtechnik, Wuppertal); J. M. Greenberg (Raymond and Beverly Sackler Laboratory for Astrophysics, Leiden, Niederlande); E. Grün (MPI für Kernphysik, Heidelberg); H. Henkel, H. von Hoerner, A. Koch (von Hoerner und Sulger, Schwetzingen); K. Hornung (Universität der Bundeswehr LRT-7, Neubiberg); E. K. Jessberger, T. Stephan (Institut für Planetologie, Münster); F. R. Krueger (Ingenieurbüro Krueger, Darmstadt); G. Kurat (Naturhistorisches Museum, Wien, Austria); Y. Langevin (Institut d'Astrophysique, Orsay, France); F. Rüdenauer (Institut für Physik, Seibersdorf, Austria); J. Rynö, J. Silén (Finnish Meteorological Institute, Helsinki, Finland); E. R. Schmid, W. Werther (Department of Analytical and Food Chemistry, Universität Wien, Austria); W. Steiger (ARC Seibersdorf Research GmbH Business Field Aerospace Technology, Seibersdorf, Austria); T. Stephan (Univ. of Chicago, Dept. of the Geophys. Sciences, USA); L. Thirkell, R. Thomas, C. Briois (Laboratoire de Phys. & Chim. de L'Environnement, Orléans, France); K. Torkar (Institut für Weltraumforschung, Graz, Austria); M. Trieloff (Mineralogisches Institut der Universität Heidelberg); N. G. Utterback (Consultant, Sta. Barbara, USA); K. Varmuza (Institut für Verfahrenstechnik, Umwelttechnik und Techn. Biowissenschaften, TU Wien, Austria); K. P. Wanczek (Institut für Anorganische und Physikalische Chemie, Universität Bremen); E. Zinner (Laboratory for Space Sciences, Washington University, St. Louis, MO, USA); H. Zscheeg (Abbott Laboratories Vascular Devices Ltd., Beringen, Schweiz).

**Rosetta – MIRO (Mirowave Instrument for the Rosetta-Orbiter).-** P. Hartogh, W. Ip und I. Mann in Zusammenarbeit mit S. Gulkis, M. Allen, M. Frerking, M. Hofstadter, M. Janssen, T. Spilker (JPL, Pasadena, USA); D. Muhleman (Caltech, Pasadena, USA); G. Beaudin, D. Bockelee-Morvan, J. Crovisier, P. Encrenaz, T. Encrenaz, E. Lellouch (Observatoire de Paris-Meudon, France); D. Despois (Observatoire de Bordeaux, France); H. Rauer (DLR, Berlin); P. Schloerb (University of Massachusetts, Amherst, USA).

**Rosetta – OSIRIS.-** H. U. Keller, H. Sierks, S. F. Hviid, R. Kramm und M. Küppers in Zusammenarbeit mit C. Barbieri, F. Angrilli (CISAS, University of Padova, Padova, Italy); P. Lamy, L. Jorda (Laboratoire d'Astrophysique de Marseille, Marseille, France); H. Rickmann (Department of Astronomy and Space Physics, Uppsala, Sweden); R. Rodrigo, L. M. Lara (Instituto de Astrofísica de Andalucía – CSIC, Granada, Spain); D. Koschny (Research and Scientific Support Department, ESTEC, Noordwijk, Niederlande); M. F. A'Hearn (Department of Astronomy University of Maryland, USA); L. Sabau (Instituto Nacional de Técnica Aersospacial, Torrejon de Ardoz, Spain); M. E. Bailey (Armagh Observatory College Hill, Armagh, Northern Ireland); M. A. Barucci (Observatoire de Paris, Meudon, France); J.-L. Bertaux (Service d'Aéronomie du CNRS, Verrière-le-Buisson, France); J. A. Burns (Cornell University, Ithaca, USA); M. Fulle (Osservatorio Astronomica de Trieste, Trieste, Italy); F. Gliem, H. Michalik (Institut für Datentechnik und Kommunikationsnetze, Braunschweig); W.-H. Ip (Institute of Space Science, National Central University, Chung Li, Taiwan); E. Kührt (DLR/Institut für Planetenforschung, Braunschweig); A. Sanz (Universidad Politécnica de Madrid, Madrid, Spain); N. Thomas (Physikalisches Institut der Universität Bern, Bern, Schweiz); G. Cremonese, R. Ragazzoni (INAF, Osservatorio Astronomico, Padova, Italy).

**Rosetta – PHILAE (Rosetta Lander).-** H. Böhnhardt, R. Roll, B. Chares, R. Enge, H. Fischer, O. Küchemann, W. Kühne, M. Sperling und I. Szemerey in Zusammenarbeit mit DLR Köln-Wahn; J. P. Bibring (IAS, Paris, France).

**Rosetta – PHILAE – ROMAP.-** M. Hilchenbach in Zusammenarbeit mit U. Auster (Braunschweig).

**Rosetta – RTOF/ROSINA.-** *Bau der Elektronik für das Massenspektrometer RTOF (Reflection Time-of-Flight).* A. Korth und U. Mall in Zusammenarbeit mit H. Balsiger (PI), Universität Bern, Schweiz; BIRA, Brussels, Belgium; CESR, Toulouse, France; IPSL, Saint Maur, France; IDA, Technische Universität Braunschweig; University of Michigan, Ann Arbor, USA; Southwest Research Institute, San Antonio, USA; Universität Giessen.

**Secular evolution of solar activity.-** M. Schüssler und S. K. Solanki in Zusammenarbeit mit I. Usoskin (University Oulu, Finland).

**Simulation of the dynamics of the solar corona.-** J. Büchner in Zusammenarbeit mit A. Otto (University of Alaska, Fairbanks, USA); M. Karlicky, M. Barta (Astronomical Observatory Ondrejov, Czech Republic).

**Simulation of the kinetics of space plasmas.-** J. Büchner in Zusammenarbeit mit N. Elkina (Keldysh Institute of the Russian Academy of Sciences, Moscow, Russia).

**SMART-1 SIR.-** U. Mall in Zusammenarbeit mit M. Banaszkiewicz (Polish Academy of Science, Poland).

**SOFIA–GREAT (SOFIA – German Receiver for Astronomy at THz frequencies).-** P. Hartogh in Zusammenarbeit mit R. Guesten, K. Menten, P. v. d. Wal (MPI für Radioastronomie, Bonn); R. Schieder, J. Stutzki (Universität Köln); H. W. Hübers (DLR-Berlin); H. P. Röser (Institut für Raumfahrtsysteme, Universität Stuttgart).

**SOHO – CELIAS (Charge, Element and Isotope Analysis System onboard SOHO).-** M. Hilchenbach (Lead Co-I STOF), R. Kallenbach und E. Marsch in Zusammenarbeit mit P. Bochsler (PI), H. Balsiger, A. Bürgi, J. Fischer, P. Wurz, B. Klecker (Physikalisches Institut, Universität Bern, Schweiz); D. Hovestadt (PI hardware phase), B. Klecker (Deputy PI), P. Laeverenz, M. Scholer (MPI für Extraterrestrische Physik, Garching); F. M. Ipavich (Lead Co-I MTOF), M. A. Coplan, G. Gloeckler, S. E. Lasley, J. A. Paquette (Department of Physics and Astronomy and IPST, University of Maryland, College Park, USA); R. Wimmer-Schweingruber, Karin Bamert (Extraterrestrische Physik, Universität Kiel); J. Geiss (International Space Science Institute, Bern, Schweiz); F. Gliem (Lead Co-I DPU), K.-U. Reiche (Institut für Datentechnik und Kommunikationsnetze, TU Braunschweig); D. L. Judge, H. S. Ogawa (Space Science Center, University of Southern California, Los Angeles, USA); G. G. Managadze, M. I. Verigin (Institute for Space Physics, Moscow, Russia); A. B. Galvin, H. Kucharek, M. A. Lee, Y. Litvinenko, E. Möbius (EOS, University of New Hampshire, Durham, USA); M. Neugebauer (Jet Propulsion Laboratory, Pasadena, USA); K. C. Hsieh (Department of Physics, University of Arizona, Tucson, USA); D. McMullin (Space Science Division, Naval Research Laboratory, Washington, USA); A. Czechowski (Space Research Center, Polish Academy of Sciences, Warsaw, Poland).

**SOHO – LASCO (Large Angle and Spectrometric Coronagraph).-** R. Schwenn und B. Inhester in Zusammenarbeit mit R. Howard (PI) (Naval Research Laboratory, Washington, USA); Laboratoire d'Astronomie Spatiale, Marseille, France; University of Paris, France; Observatoire de Paris, France; University of Birmingham, UK.

**SOHO – SUMER.-** *Solar and Heliospheric Observatory – Solar Ultraviolet Measurements of Emitted Radiation.* W. Curdt, D. E. Innes, E. Marsch, U. Schühle, S. K. Solanki, T. Wang, L. Teriaca und M. Madjarska in Zusammenarbeit mit E. Landi, U. Feldman, G. A. Doschek, J. T. Mariska (Naval Research Laboratory (NRL), Washington, USA); P. Lemaire, A. H. Gabriel, J.-C. Vial (Institut d'Astrophysique Spatiale (IAS), Orsay, France); A. I. Poland (GSFC, Greenbelt, USA); M.C.E. Huber (Schweiz); J. Hollandt (PTB, Berlin); O. Siegmund (SSL, Berkeley, USA); D. Hassler (SWRI, Boulder, USA); P. G. Judge (HAO, Boulder, USA); N. Brynildsen, M. Carlsson, P. Maltby, O. Kjeldseth-Moe (ITA, Oslo, Norway); P. Brekke (ESA/GSFC, Greenbelt, USA); H. P. Warren (HSCA, Cambridge, USA); B. N. Dwivedi (DAP, Varanasi, India); C.-Y. Tu (DG, Peking, China); H. Peter (KIS, Freiburg); J. G. Doyle (Armagh Observatory, Ireland); P. Heinzel (Czech Academy); A. Pauluhn (ISSI Bern, Schweiz).

**SOLAIRE – Solar Atmospheric and Interplanetary Reasearch.-** Dieses Research Training Network ist ein Projekt der EU im Rahmen der Marie Curie Actions, umfasst 10 Forschungsgruppen in Europa aus verschiedenen Ländern. Die chinesische Doktorandin Frau J. Guo wird davon finanziert. Beginn von SOLAIRE am 1. Juni 2007, Dauer 4 Jahre.

**Solar coronal numerical simulation results comparison with flare magnetic field observations.-** J. Büchner in Zusammenarbeit mit H. Zhang, X. Li, S. Yang (Chinese Academy of Sciences, Bejing, China).

**Solar–cycle variation of rotation and meridional circulation.-** L. Gizon in Zusammenarbeit mit M. Rempel (HAO, Boulder, USA).

**Solar Dynamics Observatory.-** L. Gizon und S. K. Solanki in Zusammenarbeit mit P. H. Scherrer (Stanford University, Palo Alto, USA); A. M. Title (Lockheed-Martin Solar and Astrophysics Laboratory, Palo Alto, USA).

**Solar Flare Telescope.-** T. Wiegelmann in Zusammenarbeit mit T. Sakurai (National Astronomical Observatory, Japan).

**Solar infrared spectropolarimetry.-** A. Lagg, C. Sasso, S. K. Solanki, J. Woch und Z. Xu in Zusammenarbeit mit M. Collados (Instituto de Astrofisica de Canarias, Tenerife, Spain).

**Solar irradiance variations.-** S. K. Solanki und N. Krivova in Zusammenarbeit mit Y. Unruh (Imperial College, London, UK); J. Harder (Univ. of Colorado, Boulder, USA); T. Wenzler (ETH Zürich, Schweiz).

**Solar Orbiter: COR.-** U. Schühle in Zusammenarbeit mit E. Antonucci (PI) (INAF Osservatorio Astronomico di Torino, Italy).

**Solar Orbiter: EUI.-** U. Schühle, W. Curdt, L. Teriaca, E. Marsch und S. K. Solanki in Zusammenarbeit mit T. Apporchaux, J.-C. Vial, F. Auchere (Institut d'Astrophysique Spatiale, Paris, France); J.-F. Hochedez (PI), A. BenMoussa (Royal Observatory of Belgium, Brussels, Belgium); J. M. Defise (Centre Spatial de Liege, Liege, Belgium); L. Harra, J. Sun, D. Williams (Mullard Space Science Laboratories, London, UK).

**Solar Orbiter: PHI (formally VIM).-** S. K. Solanki, W. Curdt, A. Gandorfer, L. Gizon, H. Hartwig, J. Hirzberger, A. Lagg, U. Schühle, G. Tomasch, J. Woch und H. Raasch in Zusammenarbeit mit V. Martinez Pillet (Instituto de Astrofísica de Canarias, IAC, La Laguna, Spain); T. Appourchaux (Institut d'Astrophysique Spatiale, IAS, Paris, France); M. Sigwarth, (Kiepenheuer-Institut für Sonnenphysik, KIS, Freiburg); G. Scharmer (Institute for Solar Physics, Stockholm, Sweden); M. Carlsson, (Institutt for teoretisk astrofysikk, Oslo, Norway).

**Solar Orbiter: SPICE (formally EUS).-** W. Curdt und U. Schühle in Zusammenarbeit mit D. Hassler, C. DeForest, D. Slater (Southwest Research Institute, San Antonio, USA); Davila, Antiochos, Kucera, R. Thomas (GSFC, NASA, Washington, USA); H. P. Warren, Mariska (NRL, Washington, USA); Schrijver (Lockheed, USA); S. Habbal, Roussev (University of Hawaii, USA); T. Zurbuchen (University of Michigan, USA); Longcope (Montana State University, USA); T. Appourchaux, Buchlin, F. Auchere, J.-C. Vial (IAS, Paris, France); Harrison, Young (RAL, Chilton, UK); Mathews (MSSL, London, UK); H. Peter (KIS, Freiburg); M. Carlsson, V. Hansteen (ITA, Oslo, Norway).

**Solar plasma dynamics.-** J. Büchner in Zusammenarbeit mit M. V. Alves, J. Santos (INPE, Sao Jose dos Santos, Brazil).

**Solare Stereoskopie.-** B. Inhester in Zusammenarbeit mit ISSI Bern; T. Dudoc de Witt (CNRS, Orleans, France); A. Vouridas (NRL, Washington, USA); J.-F. Hochedez (ROB, Brussels, Belgium); A. Llebaria (LAS, Marseille, France); J. P. Wuelser (LMSAL, Palo Alto, USA); F. Auchere (IAS, Orsay, France).

**Spitzer and ESO observations of Oort Cloud Comets during their sojourns through the Solar Systems.-** H. Böhnhardt in Zusammenarbeit mit N. Biver (Observatory Paris-Meudon, France); P. Ehrenfreund (University Leiden, Niederlande); D. Harker (University San Diego, USA); M. Kelley (Joint Astronomy Center, USA); S. Lederer (University San Bernardino, USA); D. Prialnik, E. Beer-Harari (University Tel Aviv, Israel); D. Wooden (PI) (NASA Ames Res. Center, Moffett Fields, USA); C. Woodward (University Minnesota, USA).

**Star-exo-planet plasma interaction.-** J. Büchner in Zusammenarbeit mit U. Motschmann (Technische Universität Braunschweig).

**Starspots.-** S. K. Solanki und A. Semenova in Zusammenarbeit mit S. Berdyugina (ETH Zürich, Schweiz); P. Petit (Observatoire Midi-Pyrénées, Toulouse, France).

**STEREO – IMPACT/SIT.-** *Bau einer Flugzeit-Elektronik für das SIT-Instrument (Suprathermal Ion Telescope).* A. Korth, U. Mall und V. M. Vasyliūnas in Zusammenarbeit mit J. Luhmann (PI), UC Berkeley Space Science Laboratory, USA; NASA GSFC, USA; California Institute of Technology, USA; University of Maryland, USA; Centre d'Etude Spatiale des Rayonnements, France; Los Alamos National Laboratory, USA; Jet Propulsion Laboratory, USA; ESA/ESTEC - European Space and Technology Center, Niederlande; CNRS Observatoire Midi-Pyrenees and Observatoire de Paris, France; University of California, Los Angeles, USA; SAIC, Science Applications, USA; International Corporation, USA; NOAA Space Environment Center, USA; University of Michigan, USA.

**STEREO – SECCHI (Sun Earth Connections Coronal and Heliospheric Investigation).-** R. Schwenn und B. Inhester in Zusammenarbeit mit R. Howard (PI), Naval Research Laboratory, Washington, USA; University of Michigan, USA; Applied Physics Laboratory, Johns Hopkins University, Laurel, USA; GSFC, Greenbelt, USA; Lockheed Martin Palo Alto Research Laboratory, Stanford, USA; Stanford University, Stanford, USA; Boston College, Boston, USA; Jet Propulsion Laboratory, Pasadena, USA; SAIC, San Diego, USA; Mullard Space Science Center, UK; University of Birmingham, UK; Laboratoire d'Astronomie Spatiale, Marseille, France; University of Paris, France; Observatoire de Paris, France; Universität Lüttich, Belgien; Universität Kiel.

**Structure of sunspots.-** J. M. Borrero, A. Lagg, S. K. Mathew, S. K. Solanki und N. A. Krivova in Zusammenarbeit mit L. Bellot Rubio (Instituto de Astrofísica de Andalucía, Granada, Spain); M. Collados (Instituto de Astrofisica de Canarias, Tenerife, Spain); H. Socas Navarro, B. Lites (High Altitude Observatory, Boulder, USA).

**Structure of the solar chromosphere.-** S. K. Solanki in Zusammenarbeit mit M. Loukitcheva (University St. Petersburg, Russia); S. White (University of Maryland, Greenbelt, USA); M. Carlssson (University of Oslo, Norway).

**SUNRISE.-** *Ballongetragenes 1-m Sonnenteleskop für hochauflösende spektro-polarimetrische Beobachtungen der Sonnenatmosphäre.* S. K. Solanki, P. Barthol, A. Gandorfer und M. Schüssler in Zusammenarbeit mit V. Martinez-Pillet (Instituto de Astrofisica de Canarias, Tenerife, Spain), W. Schmidt (Kiepenheuer-Institut für Sonnenphysik, Freiburg), B. W. Lites (High Altitude Observatory, NCAR, Boulder, USA); Lockheed Martin Solar and Astrophysical Lab, Palo Alto, USA.

**Sunspots.-** A. Lagg, S.K. Solanki and N.A. Krivova in Zusammenarbeit mit V. Martínez Pillet (Instituto de Astrofisica de Canarias, Tenerife, Spain); J. M. Borrero, B. Lites (High Altitude Observatory, Boulder, USA); S. K. Mathew (Udaipur Solar Observatory, India).

**Surface exploration of Kuiper Belt Objects and Cometary Nuclei.-** H. Böhnhardt (PI) und S. Protopapa in Zusammenarbeit mit S. Bagnulo (ESO, Santiago de Chile, Armagh Observatory, Northern Ireland); A. Barucci (Observatory Paris-Meudon, France); D. Cruikshank (NASA Ames, USA); W. Grundy (University Flagstaff, USA); T. Herbst (MPI für Astronomie, Heidelberg); K. Muinonen (University Helsinki, Finland) C. Olkin (SWRI Boulder, USA); G. P. Tozzi (INAF Arcetri Observatory, Florence, Italy).

**Surface magnetic field effects in local helioseismology.-** H. Schunker in Zusammenarbeit mit D.C. Braun (CoRA, Boulder, USA); P.S. Cally (Monash University, Victoria, Australia).

**The YORP effect in asteroid (54509) 2000PH5.-** H. Böhnhardt in Zusammenarbeit mit A. Fitzsimmons (PI), S. Lowry (University Belfast, Great Britain); P. Pravec (Ondrejov Observatory, Slovakia).

**Three–dimensional sensitivity kernels for ring–diagram analysis.-** L. Gizon in Zusammenarbeit mit A.C. Birch (CoRA, Boulder, USA); B. W. Hindman, D. A. Haber (JILA, Boulder, USA).

**Time-Distance Helioseismology with Data from the MDI Structure Program.-** L. Gizon und M. Roth in Zusammenarbeit mit J. G. Beck (Stanford University, Stanford, USA).

**Topological investigations and applications to the solar atmosphere.-** J. Büchner in Zusammenarbeit mit E. Priest (University of St. Andrews, Scotland, UK).

**Topology of coronal magnetic fields.-** T. Wiegelmann in Zusammenarbeit mit E. Priest, S. Régnier (University St. Andrews, UK).

**Travel–time sensitivity kernels for vector flows.-** L. Gizon in Zusammenarbeit mit A.C. Birch (CoRA, Boulder, USA).

**Ulysses – DUST.-** H. Krüger (PI) und J. Kissel in Zusammenarbeit mit N. Altobelli, C. Polanskey (Jet Propulsion Laboratory, Pasadena, USA); B. Anweiler, D. Linkert, G. Linkert, R. Srama (MPI für Kernphysik, Heidelberg); E. Grün, R. Srama (MPI für Kernphysik, Heidelberg und Hawaii Institute of Geophysics and Planetology, Honolulu, USA); S. F. Dermott, B. A. Gustafson (University of Florida, Gainesville, USA); A. Flandes (Instituto de Geofisica, UNAM, Mexico); A. L. Graps (INAF-Istituto di Fisica dello Spazio Interplanetario, CNR - ARTOV, Roma, Italy); D. P. Hamilton (University of Maryland, College Park, USA); M. S. Hanner (Jet Propulsion Laboratory, Pasadena, USA); M. Horany (Laboratory for Atmospheric and Space Physics, Univ. of Colorado, Boulder, USA); M. Landgraf (ESA/ESOC, Darmstadt); B. A. Lindblad (Lund Observatory, Lund, Sweden); I. Mann (Institut für Planetologie, Universität Münster); J.A.M. McDonnell (Planetary and Space Science Research Institute, Milton Keynes, UK); G. E. Morfill (MPI für Extraterrestrische Physik, Garching); G. Schwehm

(ESTEC, Noordwijk, Niederlande).

**Ulysses – EPAC/GAS.-** *Teilchenspektrometer zur Messung energiereicher geladener Teilchen im interplanetaren Raum und zur Messung interstellaren neutralen Heliums (Datenauswertung).* N. Krupp, J. Woch, M. Witte und M. Fränz in Zusammenarbeit mit B. Blake (Aerospace Corporation, USA); J. Quenby (Imperial College London, UK); M. Yamauchi (IRF, Sweden).

**Ulysses – SWICS (Solar Wind Ion Composition Spectrometer).-** J. Woch und M. Fränz in Zusammenarbeit mit L. Rodriguez (Royal Observatory of Belgium, Brussels, Belgium); R. von Steiger (ISSI, Bern, Schweiz).

**Venus Express – ASPERA-4 (Analyzer of Space Plasmas and EneRgetic Atoms).-** M. Fränz, J. Woch, N. Krupp, E. Dubinin, E. Roussos, C. Martinecz und J. Kleimann in Zusammenarbeit mit S. Barabash (PI), R. Lundin (IRF, Kiruna, Sweden); D. Winningham, R. Frahm (SWRI, San Antonio, USA); P. Wurz (Universität Bern, Schweiz); A. Coates (MSSL, London, UK); M. Grande (RAL, Chilton, UK); C. C. Curtis (UoA, Tuscon, USA); J. A. Sauvaud, A. Fedorov (CESR, Toulouse, France); E. Kallio (FMI, Helsinki, Finland); S. Orsini (IFSI, Roma, Italy).

**Venus Express Scientific Support.-** D. Titov in Zusammenarbeit mit H. Svedhem, O. Witasse (ESTEC-ESA, Noordwijk, Niederlande); R. Hoofs, D. Meritt, M. Almeida (ESAC-ESA, Madrid, Spain).

**Venus Express – VIRTIS.-** D. Titov in Zusammenarbeit mit P. Drossart (Observatoire de Paris, Meudon, France); G. Piccioni, D. Grassi (Institute for Space Astrophysics (IAS-INAF), Roma, Italy).

**Venus Express – VMC (Venus Monitoring Camera).-** D. Titov in Zusammenarbeit mit H. Michalik, B. Fiethe, C. Dierker, B. Osterloh (Institut für Datentechnik und Kommunikationsnetze (IDA), TU Braunschweig); R. Jaumann, Th. Behnke, Th. Roatsch, K.-D. Matz, F. Scholten (Institut für Planetenforschung); N. Ignatiev, D. Belyaev, I. Khatuntsev (Space Research Institute (IKI), Moscow, Russia); E. Shalygin (Kharkov University, Ukraine); A. Basilevsky (Vernadsky Institute for Analytical Chemistry and Geochemistry (GEOKHI), Moscow, Russia); S. Limaye (University of Wisconsin, USA).

**VESPER – Venus Atmosphere Chemistry and Dynamics Orbiter.-** P. Hartogh in Zusammenarbeit mit G. Chin (GSFC, Greenbelt, USA); M. Allen (JPL, Pasadena, USA).

**WASPAM / CAWSES.-** P. Hartogh, C. Jarchow und L. Song in Zusammenarbeit mit G. Hansen (NILU, Tromsö, Norwegen); U. P. Hoppe (FFI, Kjeller, Norwegen); M. Gausa (ALOMAR, Andenes, Norwegen); U. von Zahn, F. J. Lübken, U. Berger, G. Sonnemann (IAP Kühlungsborn); G. Nedoluha, M. Stevens (NRL, Washington, USA); P. Espy (British Antarctic Survey, Cambridge, UK); Y. Kasai (NICT, Applied Research and Standards Department, Tokyo, Japan).

**White dwarf magnetic fields.-** R. Aznar Cuadrado und S. K. Solanki in Zusammenarbeit mit S. Jordan (Universität Heidelberg); R. Napiwotzki (University of Leicester, UK); H. M. Schmid (ETH Zürich, Schweiz).

## Projektförderungen durch das Bundesministerium für Bildung und Forschung (BMBF) und andere Institutionen / Project grants provided by BMBF and other institutions

**BMBF / DLR:** ASTEX (DLR-Studie zu Near-Earth Asteroid Mission), BepiColombo-BELA, BepiColombo MMO MPPE-MSA, BepiColombo MPO SERENA-PICAM, Cassini MIMI-LEMMS, Cluster Active Archive (50%), Cluster-CIS, DAWN, ExoMars-SEIS, HIFI/WBS, Mars Express ASPERA-3, MOMA, Phoenix, RAPID, Rosetta/COSAC, Rosetta/COSIMA, Rosetta/MIRO, Rosetta/OSIRIS, Rosetta/PHILAE (Rosetta lander), Rosetta/RTOF, SECCHI, SOHO-SUMER, SOHO-LASCO, STEREO, SUNRISE, ULYGAL (Galileo EPD and Ulysses EPAC/GAS+SWICS).

**DFG:** DFG-Projekt: Evolution of Coronal Magnetic Fields, DFG Schwerpunktprogramm 1115 “Mars und die terrestrischen Planeten”: Plasma induced atmospheric escape on Mars und MAOAM (Martian Atmosphere: Observing And Modelling).

**ESA:** BepiColombo-BELA, Chandrayaan-1, Cluster Active Archive (50%), Exomars, PROBA2/LYRA, PROBA2/SWAP, Venus Express/ASPERA-4, Venus Express/VIRTIS, VEXCEL, Wide Band Spectrometer.

**EU:** Belarus, EuroPlaNet, HELAS, Solaire.

**NASA:** RAISE.

## **Lehrtätigkeiten** / Teaching

*Von Mitgliedern des MPS wurden an mehreren, inländischen und ausländischen Universitäten verschiedene Vorlesungen gehalten:/ MPS scientists have lectured at a number of German and foreign universities:*

**Georg-August-Universität zu Göttingen**

*Prof. Dr. J. Büchner*
WS 2005/2006: Physikalische Grundlagen des Weltraumwetters
SS 2006: Numerical Methods in Astrophysics
WS 2006/2007: Heliophysics and Space Weather I and A window to Space: The Sun-Earth system, STEREO & SOHO SS 2007: Heliophysics and Space Weather II (Master-course Wahlpflichtmodul M.phy.505 "Advanced topics in Astro- and Geophysics") WS 2007/2008: Heliophysics and Space Weather I (Master-course Wahlpflichtmodul M.phy.505 "Advanced topics in Astro- and Geophysics")

*Prof. Dr. J. Büchner, Prof. S. Dreizler und Prof. F. Kneer*
Public (Ring-) Lectures SS 2007: Numerical Methods in Astrophysics for PHD- and Erasmus-exchange students
Unsere Sonne, Feuer des Lebens

*Prof. Dr. J. Büchner und Dr. L. Gizon*
WS 2005/2006: Physikalische Grundlagen des Weltraumwetters

*Dr. L. Gizon und Prof. S. Dreizler*
WS 2006/2007: Helioseismology

*Ms. N. Oklay*
SS 2007: Teaching Assistant for the F-Praktikum Astrophysik: "Enge bedeckende Doppelsterne"
WS 2007/2008: Teaching Assistant for the F-Praktikum Astrophysik: "Enge bedeckende Doppelsterne"

**Universität Heidelberg**

*Dr. H. Krüger, gemeinsam mit 3 weiteren Dozenten*
SS 2006: Seminar für mittlere Semester "Neuere Ergebnisse der Planetenphysik"

**University Bern, Switzerland**

*Dr. R. Kallenbach*
WS 2006/2007: Radioastronomie, zweistündige Spezialvorlesung
HS 2007: Physics of Collisionless Plasmas, zweistündig, Graduate Course Masters in Physics

## **IMPRS Vorlesungen** / IMPRS lectures

Origin of solar systems, 13 – 15 February 2006 (Jockers)

The solar corona, 27 – 28 March 2006 (Marsch, Peter)

Research ethics, 28 March 2006 (Schüssler)

Job application, 30 March 2006 (Schmitt)

Magnetohydrodynamics, 9 – 13 October 2006 (Ferriz Mas)

Space instrumentation, 4 – 7 December 2006 (Woch et al.)

Helioseismology, 5 – 16 February 2007 (Gizon)

Minor bodies in the planetary system, 19 – 20 March 2007 (Böhnhardt)

Stellar structure and evolution, 23 – April 2007 (Glatzel)

Space plasma physics, 11 – 15 June 2007 (Marsch)

Planetary interiors and surfaces, 11 – 15 June 2007 (Christensen et al.)

How to write a research paper, 6 November 2007 (Solanki)

How to write a grant proposal, 7 November 2007 (Glassmeier)

Presentation skills, 8 – 9 November 2007 (Meyer-Ross)

Astrobiology Lecture Course Network, 30 October 2007 – 18 March 2008 (Brack et al.)

## **Weitere Lehrtätigkeiten oder Kurse** / Other lectures or courses

*Prof. Dr. J. Büchner*
Course "Flares, CMEs and Space Weather"
Course "Numerical Simulation approaches to Space and Solar Plasma Problems, Peking-University and Chinese Academy of Science, 2006.

*Dr. M. Madjarska*
Supervisor for approximately 3 months of internship student Celine Boutry from University of Orsay, France.

*Dr. M. Roth*
Öffentliche Vorlesungsreihe in der Paulinerkirche, Göttingen: Sonne – Feuer des Lebens.

*Prof. R. Schwenn*
Vorlesungsreihe: "Physics of the Heliosphere, and Introduction", Peking University, China, 24. – 30. Oktober 2006. Blockvorlesung: "Space Weather" im Rahmen der ELAGE-School in Merida, Mexico, 11. – 17. Juli 2007.

*Dr. H. Sierks*
Educators Public Outreach, Dawn Science Symposium, Cocoa Beach, USA, 29. Juni 2007.

*Dr. D. Titov*
Lecture course "Space Science and Instrumentation" at Lulea Technical University, Kiruna, Sweden, 2006 and 2007. Lecture "Is Venus the Earth's twin" at the International Space University (ISU), Beijing, China, 2007.

## **Mitgliedschaften in wissenschaftlichen Gremien** / Memberships in scientific councils

*Büchner, J.*: Scientific Committee of the International School for Plasma-Astrophysics Varenna-Abastumani; Scientific Committee of the World Institute for Space Environmental Research (WISER); member of the Scientific Board of the International School of Space Plasma Simulation.

*Christensen, U.*: Advisory board / Center of Dynamics of Complex Systems, Universität Potsdam; American Geophysical Union; Deutsche Akademie der Naturforscher Leopoldina; ESA Solar System Working Group; Executive Committee der International Association of Seismology and Physics of the Earth's Interior (IASPEI); Göttinger Akademie der Wissenschaften und Kommission für Geowissenschaftliche Hochdruckforschung der Bayerischen Akademie der Wissenschaften.

*Curdt, W.*: German JOSO representative.

*Gizon, L.*: Chairman of the local helioseismology network activity of the European Helio- and Asteroseismology Network (HELAS), HELAS Board Member.

*Hartogh, P.*: Alomar Scientific Advisory Committee; International Commission on Planetary Atmospheres and their Evolution (ICPAE).

*Lagg, A.*: Telescope Allocation Committee (TAC) for the German Vacuum Tower Telescope.

*Marsch, E.*: Vorsitzender des Joint Science Technology Definition Team des HELEX (Heliophysical Explorers) Wissenschafts- und Missions-Programms der ESA und NASA (mit drei Treffen in Paris, Washington und London im Jahre 2007); Mitglied (seit 2001) im Gutachterausschuss Extraterrestrik des DLR.

*Roth, M.:* HELAS Board Member; HELAS Project Scientist.

*Schmitt, D.*: Studienkommission Physik der Universität Göttingen.

*Solanki, S. K.*: Stellvertretender Vorsitzender und Mitglied des Senatsausschusses des DLR; Mitglied des Berufungsausschusses und des Dreierausschusses des Senats des DLR; Vorsitzender und Mitglied des Programmausschusses Extraterrestrik des DLR; Mitglied der Perspektivenkommission der Chemisch-Physikalisch-Technischen Sektion der MPG; Mitglied des wissenschaftlichen Beirats des High Altitude Observatory in Boulder, Colorado/USA, und des Istituto Ricerche Solari Locarno (IRSOL); Stellvertretender Vorsitzender und Mitglied des Beirats der Gesellschaft für Wissenschaftliche Datenverarbeitung Göttingen.

*Titov, D.*: Vice-Chair of the International Committee on the Planetary Atmospheres and Evolution (ICPAE).

## **Gutachtertätigkeiten** / Review reports

*Gutachtertätigkeiten für wissenschaftliche Zeitschriften/Reviews for scientific journals*
(Die folgende Aufstellung soll nur eine kurze Übersicht über die Gutachtertätigkeiten von Wissenschaftlern des MPS für wissenschaftliche Zeitschriften geben. Angeführt sind die Namen der Gutachter (alphabetisch) und die Zeitschriften./*In the following the names of the reviewers and the journals.*)

*Gutachter/Reviewers:*

H. Boehnhardt, J. Büchner, U. Christensen, W. Curdt, P. W. Daly, M. Fränz, L. Gizon, P. Hartogh, M. Hilchenbach, J. Hirzberger, B. Inhester, N. Krivova, E.

Kronberg, H. Krüger, N. Krupp, A. Lagg, M. Madjarska, U. Mall, E. Marsch, A. Pietarila Graham, K. Schlegel, D. Schmitt, U. Schühle, R. Schwenn, H. Sierks, S. K. Solanki, D. Titov, J. Wicht, T. Wiegelmann, J. Woch.

*Zeitschriften/Journals:*

Advance of Radio Science, Advances in Geosciences, Advances in Space Research, Annales Geophysicae, Astra, Astronomische Nachrichten, Astronomy and Astrophysics, Astrophysical Journal, Atmospheric Chemistry and Physics (ACP), COSPAR Proceedings, Earth, Moon and Planets, Earth Planets and Space, Earth & Planetary Science Letters, Encyclopedia of Life Support Systems (EOLSS), Geology, Geophysical & Astrophysical Fluid Dynamics, Geophysical Journal International, Geophysical Research Letters, Icarus, Journal of Applied Sciences Research, Journal of Atmospheric and Solar-Terrestrial Physics, Journal of Geophysical Research, Living Reviews in Solar Physics, Monthly Notices of the Royal Astronomical Society, Nature, Nonlinear Processes in Geophysics, Particle Physics and Astronomy Council, Publications of the Astronomical Society of the Pacific (PASP), Physics of Plasmas, Physics of the Earth and Planetary Deep Interiors, Physical Review Letters, Physik und Didaktik in Schule und Hochschule, Planetary and Space Science, Publications of the Astronomical Society of Japan, Radio Science, Science, Solar Physics, Space Science Reviews, Space Weather, The Rosetta Mission (ESA book), The solar system beyond Neptune (University Arizona book),

*Gutachtertätigkeiten anderer Art/Other types of reviews:*

*Böhnhardt, H.*: Observing Program Committee – Main board and Panel C, European Southern Observatory (2005/2006/2007); Advisor for Time Allocation Committee of Canada-France-Hawaii Observatory (2005/2006); Advisor for application to the German-Israeli Foundation for Scientific and Technical development (2007/2008); Member of the Science Study Definition team for ESA's Marco Polo Mission Study (2007/2008); 2 PhD thesis reviews; 8 Personengutachten.

*Büchner, J.*: NASA Peer review panel member (2006/2007); mehrere Projektgutachten für DFG; mehrere Promotionsgutachten.

*Christensen, U.*: Fachgutachter der DFG für Physik des Erdkörpers; Begutachtung von Projektanträgen beim DLR, Helmholtzgesellschaft, NSF, NERC, SNF und Gutachten in verschiedenen Berufungsverfahren.

*Gizon, L.*: Review panelist for NASA Living with a Star program.

*Hartogh, P.*: Gutachten für die DFG; National Roads Authority (NRA).

*Kallenbach, R.*: Member of the NASA review panel for proposals submitted to NASA Research Announcement (NRA) NNH06ZDA001N, Research Opportunities in Space and Earth Sciences 2006, and the Solar and Heliospheric Physics' Supporting Research and Technology (SR&T) and Low Cost Access to Space Program in the competition for Fiscal Year 2008 funds.

*Krivova, N.*: Swedish National Space Board; Portugese Science and Technology Foundation (FCT).

*Schlegel, K.*: 2 Gutachten für Promotionen (2006), 3 Gutachten für Bewerbungen (2006), 3 Gutachten für die Alexander-von-Humboldt Stiftung (2007), 1 Gutachten für eine Professorenstelle an der Universität Kreta (2007), 1 Gutachten für das KFZ Jülich (2007), 1 Gutachten für die Universität Potsdam (2007).

*Schwenn, R.*: 4 Gutachten für Proposals für ESA Cosmic Vision, 4 Gutachten für Proposals für NASA Solar HelioPanel.

*Solanki, S. K.*: Je 1 Gutachten für Alexander von Humboldt, Deutsche Forschungsgemeinschaft, International Space Science Institute, Leibniz-Gemeinschaft, Royal Society, 4 Gutachten für Schweizerischer Nationalfonds.

*Wiegelmann, T.*: Grant Proposal Reviewer for Academy of Science of the Czech Republic (1).

## Tätigkeiten als Convener bei wissenschaftlichen Tagungen / Converierships during scientific meetings

*Büchner, J.*: Convenor des Fachverbandstreffen Extraterrestrische Physik, Annual Meeting of the German Physical Society Society, Heidelberg, Germany, March 2006; Co-convenor, EGU, Symposium "Theory and simulations of solar system plasmas", Vienna, Austria, 2 – 7 April 2006; Main Scienitific organizer (Convenor) COSPAR, Symposium "Magnetic Coupling in Solar and Stellar Atmospheres", Bejing, China, July 2006; Co-convenor 8th International School for Space Simulations (ISSS-8), Kauai, Hawaii, USA, February 2007; Convenor des Fachverbandstreffen Extraterrestrische Physik, Annual Meeting of the German Physical Society Society, Regensburg, Germany, April 2007; Co-convenor, EGU, Symposium "Theory and simulations of solar system plasmas" Vienna, Austria, 15 – 20 April 2007.

*Christensen, U.*: Co-Convener, Session GP23A "Geodynamics and Statistical Properties of Terrestrial and Planetary Magnetic Fields I", AGU Fall Meeting, San Francisco, USA, 10 -– 14 December 2007.

*Curdt, W.*: SOC "Coimbra Solar Physics Meeting", Coimbra, Portugal, 9 – 13 October 2006.

*Gizon, L.*: Co-convener, Session ST5 "Magnetic variability of the Sun and heliospheric consequences", EGU, General Assembly, Vienna, Austria, 2 – 7 April 2006; Member of the scientific organizing committee, First HELAS Local Helioseismology Workshop, Nice, France, 25 – 27 September 2006; Co-convener, Session ST4 "Oscillations of the solar interior and atmosphere", EGU, General Assembly, Vienna, Austria, 15 – 20 April 2007.

*Hartogh P.*: AOGS 3rd Annual Meeting, Singapore, 10 – 14 July 2006; AOGS 4th Annual Meeting, Bangkok, 31 July – 4 August 2007.

*Hilchenbach, M.*: Convener, EGU Session "Solar variation", Vienna, Austria, 2 – 7 April 2006.

*Krüger, H.*: Sitzungen über "Comets, asteroids and dust" bei der EGU, Vienna, Austria, 2 – 7 April 2006 und Vienna, Austria, 15 – 20 April 2007.

*Marsch, E.*: Member of the SOC for the "SOHO 10th Anniversary Symposium" (SOHO-17), Sicily, Italy, 8 – 14 May 2006; Member of the SOC for "The Second International Symposium on KuaFu Project", Sanya, Hainan, China, 15 – 19 January 2007.

*Titov, D.*: Convener of the EGU Symposium on Venus Express results in 2007. Convener of the COSPAR-2008 Symposium C3.1 "Planetary Atmospheres" Convener of the COSPAR-2008 Symposium C3.3 "Venus Express: two years of observations" Convener of the Europlanet-2 Symposium on Venus Express Convener of the IAMAS-2007 Symposium "Atmospheres of terrestrial planets"

## Organisation von Workshops / Workshop organisation

*Böhnhardt, H.*: 2nd Philae post-launch scientific workshop, Helsinki, Finland, 3 – 6 September 2006; 3rd Philae post-launch scientific workshop, Budapest, Hungary, 17 – 19 December 2007; Third Kuiper Belt workshop "Transneptunian Objects -– Dynamical and physical properties", Catania, Italy, 3 – 10 July 2006; "DeepImpact as a world observatory event -– Synergies in space, time and wavelengths", Brusseles, Belgium, 4 – 8 August 2006; ESO workshop on "Observing Planetary Systems", Santiago de Chile, 5 – 8 March 2007; ESA workshop on "Rosetta Asteroid Flyby Preparation Workshop", Athens, Greece, 22 – 25 October 2007.

*Büchner, J.*: Annual Meeting of the German Extraterrestrial Society, Heidelberg, Germany, March 2006; Annual Meeting of the German Extraterrestrial Society, Regensburg, Germany, March 2007.

*Christensen, U. and Wicht, J.*: Deutscher Geodynamik Workshop, MPS, Katlenburg-Lindau, Germany, 27 – 28 September 2006.

*Gizon, L. and Roth, M.*: Members of the scientific organizing committee, First HELAS Local Helioseismology Workshop “Roadmap for European Local Helioseismology”, Nice, France, 25 – 27 September 2006.

*Gizon, L. (Chair), M. Roth, M. Schüssler, A. Blome, R. Burston, R. Cameron, S. Deutsch, J. Jackiewicz, A. Lagg, Y. Saidi, H. Schunker, T. Stahn, and others*: Members of the scientific organizing committee, HELAS II International Conference “Helioseismology, Asteroseismology and MHD Connection”, Göttingen, Germany, 20 – 24 August 2007.

*Hilchenbach, M.*: COSIMA Workshop, MPS, Katlenburg-Lindau, Germany, November 2006.

*Krüger, H.*: Mitorganisation des Workshops “Dusty Visions”, Heidelberg, Germany, 10 – 13 April 2007.

*Marsch, E.*: Co-chair of the Scientific Organising Committee (SOC) of the “Second Solar Orbiter Workshop”, Athens, Greece, 16 – 20 October 2006.

*Oklay, N.*: Solar Polarization Workshop 5, Poster Presentation: Spectropolarimetric Investigations of the deep photospheric layers of solar magnetic structures.

*Schmitt, D.*: IMPRS Retreat, Antalya, Turkey, 25 March – 1 April 2006; IMPRS Retreat, Burg Bodenstein, 5 – 9 November 2007.

*Solanki, S. K.*: SOC Member of: “MHD waves and oscillations in solar magnetic structures”, Palma de Mallorca, Spain, 29 May -— 1 June 2006; COSPAR “E2.4 Solar Magnetic Field and Activities”, 36th COSPAR SA, Beijing, China, 16 – 23 July 2006; 2nd International Symposium on Space Climate (ISSC-2), Sinaia, Romania, 13 – 16 September 2006; 2nd Solar Orbiter Workshop, Athens, Greece, 16 – 20 October 2006; The 2nd International Symposium on KuaFu Project (ISKP-II), Sanya, PR China, 15 – 19 January 2007; “Challenges for Solar Cycle 24”, Diamond Jubilee PRL, Ahmedabad, India, 22 – 25 January 2007; “Living With a Star — From the Sun towards the Earth”, Boulder, CO, USA, 10 – 13 September 2007; 5th Solar Polarization Workshop, Ascona, Switzerland, 17 – 21 September 2007; SCOSTEP International Symposium on CAWSES, Kyoto, Japan, 23 – 27 October 2007.

*Titov, D.*: Co-convener of the Venus Express Workshop, La Thuile, 2007.

## **Öffentlichkeitsarbeit** / Public relations

Dr. N. Krupp (Verantwortlicher für die Presse- und Öffentlichkeitsarbeit des MPS)

Presse- und Öffentlichkeitsarbeit am MPS setzt sich aus der Erstellung von Pressenotizen, Organisation und Durchführung von Besuchen von Radio- und Fernsehteams, Führungen durch das Institut, Vorlesungsreihen, Ausstellungen, sowie von speziellen Events.

### **TV- und Hörfunkauftritte** / Media coverage

Der Besuch von Radio- und TV-Teams am MPS hat sich in den Jahren 2006/2007 weiterhin verstärkt. Der Bekanntheitsgrad des MPS konnte weiter gesteigert werden. Eine Übersicht aller uns bekannten Sendungen 2006/2007 ist in nachfolgender Tabelle 2 (siehe Seite 238) zusammengefasst.

### **Pressenotizen** / Press releases

Im Berichtszeitraum wurden die folgenden Pressenotizen herausgegeben:

- “Verkehrte” Elektronen am Saturnhimmel. 9. Februar 2006.
- Aurora über dem Mars. 17. Februar 2006.
- Lindauer Max-Planck-Institut ist Ort im Land der Ideen. 7. März 2006.
- Kleiner Saturnmond ganz groß. Max-Planck Forscher detektieren Material aus den Tiefen des Mondes Enceladus. 10. März 2006.
- NASA Asteroidenmission Dawn wieder zum Leben erweckt. 30. März 2006.
- Die Sonde Venus Express “kreist” um die Venus. 11. April 2006.
- Erster Blick hinter den Schleier der Venus. 13. April 2006
- Odyssey im Weltall. 5. Mai 2006.
- Meteoriten zeichnen Sonnenaktivität der letzten Jahrhunderte auf. 26. September 2006
- Merkurs Magnetfeld erklärt? 21. Dezember 2006.
- Kameras auf Rosetta messen Lichtkurven der Rosetta-Asteroiden. 5. Februar 2007
- OSIRIS Kameras nehmen spektakuläre Bilder vom Mars auf. 26. Februar 2007

- Förderung der Solar System School am MPS verlängert. 27. März 2007
- Unsere Sonne - Feuer des Lebens. 16. April 2007
- Ausstellung anlässlich des Internationalen Heliophysikalischen Jahres 2007. Unsere Sonne – Feuer des Lebens. Geschichte und aktuelle Forschung. 26. April 2007
- START VERSCHOBEN – Neustart frühestens September 2007. MPS Kameras mit der NASA Discovery Mission DAWN unterwegs zu den Asteroiden Vesta und Ceres. 06. Juli 2007
- 60 Jahre Forschung in Lindau in einem Buch zusammengefasst. 30. Juli 2007
- MPS Kameras starten mit der NASA Mission Phoenix zum Mars. 1. August 2007.
- Raumsonde CASSINI/HUYGENS enthüllt den Ursprung des geheimnisvollen G-Staubrings um Saturn. 03. August 2007
- Weltweit führende Wissenschaftler sprechen in Göttingen über Wellenphänomene in Physik, Geophysik und Astrophysik. 15. August 2007
- Mission DAWN - neuer Starttermin. 19. September 2007.
- Prof. Dr. Vytenis M. Vasyliunas, Direktor am Max-Planck-Institut für Sonnensystemforschung, geht in Ruhestand. 11. Oktober 2007.
- Erfolgreicher Testflug für das Ballonexperiment SUNRISE. 16. Oktober 2007.
- VENUS EXPRESS lüftet den Wolkenschleier unseres Nachbarplaneten. Kamera aus dem Max-Planck-Institut für Sonnensystemforschung schaut durch dicke Wolkendecke. 9. November 2007.
- Erste OSIRIS-Bilder vom Erdvorbeiflug von Rosetta. 15. November 2007.
- Dr. habil. Horst Uwe Keller erhält die Christiaan-Huygens-Medaille. 27. November 2007.
- Die Venus – eine ungleiche Schwester der Erde. In der Atmosphäre des Nachbarplaneten toben Stürme mit doppelter Orkanstärke und Wasser entweicht in den Weltraum. 28. November 2007.
- Raumsonde Cassini beobachtet “unsichtbare” rotierende Stromsysteme um Saturn. 14. Dezember 2007.

**Erich-Regener-Vortragsreihe /**
Erich-Regener lecture series

Die Erich-Regener-Vortragsreihe wurde auch in 2006 und 2007 erfolgreich fortgesetzt. Alle Vorträge waren sehr gut besucht und konnten die Zuhörer begeistern:

- 9. Februar 2006
  Dr. Oliver Preuss (MPS, Katlenburg-Lindau): Gekrümmter Raum und gedehnte Zeit: Das Weltbild der Relativitätstheorie Ein Rückblick auf das Einsteinjahr 2005
- 24. April 2006
  Ansgar Korte (Essen): Die Walter-Hohmann-Sternwarte Essen.
- 26. Juni 2006
  Prof. Dr. Ralf Klessen (Heidelberg): Die turbulente Geburt der Sterne.
- 6. September 2006
  Thomas Weber (Sonneberg): Die Sternwarte Sonneberg und die Suche nach veränderlichen Sternen.
- 6. November 2006
  Dipl. Met. Franz Ossing (GeoForschungsZentrum Potsdam): Wissenschaft in der Kunst: Wolken und Wetter in der Malerei.
- 7. Dezember 2006
  Frank-E. Rietz (Aspach-Einöd): Rückkehr zum Mond.
- 15. Februar 2007
  Dr. Günther Oestmann (Deutsches Museum, München): Zur Geschichte der Ortsbestimmung auf See.
- 19. April 2007
  Dr. Markus Roth (MPS, Katlenburg-Lindau): Helioseismologie - Neues aus dem Innern der Sonne.
- 4. Juni 2007
  Prof. Dr. Karl-Heinz Glaßmeier (TU Braunschweig): Erdmagnetische Variationen.
- 4. September 2007
  Ulrich Uffrecht (Buxtehude): Die Messung kosmischer Entfernungen im Altertum und in der beginnenden Neuzeit.
- 29. Oktober 2007
  Christoph Förste (GeoForschungsZentrum Potsdam): CHAMP, GRACE und die ’Potsdamer Kartoffel’ - Die Erforschung des Erdschwerefeldes.

- 10. Dezember 2007
  Dr. Frank Jansen (Greifswald): Weltraumwetterforschung in Greifswald.

**Institutsführungen, Ausstellungen und spezielle Events /**
Guided tours, exhibitions, and special events

Ein wesentlicher Bestandteil der Öffentlichkeitsarbeit am MPS besteht in der Durchführung von Führungen durch das Institut und in der Organisation von Ausstellungen und speziellen Events zum Thema Weltraum.

Im Jahr 2007 fanden 10 Führungen für 222 Personen statt und 2006 wurden 931 Personen in 30 Gruppen durch das Institut geführt. Dabei handelte es sich um Besucher jeder Altersgruppe von Schülern bis Rentner, die großteils sehr starkes Interesse an unser Forschung gezeigt haben unbd gerne wieder kommen möchten.

Im Jahr 2006 wurde das Institut im Rahmen der bundesweiten Aktion "Ort im Land der Ideen" für den 13. März ausgewählt anlässlich des 20. Jahrestages des Vorbeiflugs der Raumonde Giotto am Kometen Halley. An dieser Mission war das Institut maßgeblich mit einer Kamera beteiligt, die das erste Bild eines Kometenkernes aufgenommen hat. An diesem Tag wurde eine Veranstaltung mit fachspezifischen Vorträgen und einem Empfang organisiert. Außerdem wurde eine Vorlesungsreihe und eine Ausstellung über Kometen eröffnet, die vom 13. März bis zum 9. April 2006 im MPS sehr viele Besucher anzog. Insgesamt acht "Kometenvorträge" wurden von externen Referenten und von MPS-Mitarbeitern gehalten:

- 13. März 2006, 19.00 Uhr: Prof. Dr. Karin Reich (Universität Hamburg, Institut für Geschichte der Naturwissenschaften, Mathematik und Technik): Legenden, Vermutungen, Fakten: ein Streifzug durch die Geschichte der Kometen von der Antike bis ins 19. Jahrhundert.
- 16. März 2006, 19.00 Uhr: Prof. Dr. Klaus Jockers (MPS): Beobachtungen von Kometen mit astronomischen Teleskopen.
- 23. März 2006, 19.00 Uhr: Lutz Clausnitzer (Niedercunnersdorf): Wilhelm Tempel – Entdecker von Planetoiden, Kometen und NGC-Objekten.
- 26. März 2006, 15.00 Uhr: Dr. Marion Gindhart (Universität Kiel): Altes und neues Wissen im Widerstreit – der Blick auf Kometen im frühen 17. Jahrhundert.
- 30. März 2006, 19.00 Uhr: Dr. Harald Krüger (MPS): Staubteilchen – Boten ferner Welten.
- 2. April 2006, 15.00 Uhr: Dr. Hermann Böhnhardt (MPS): Deep Impact und Rosetta: Kometenforschung jetzt und in 10 Jahren.
- 6. April 2006, 19.00 Uhr: Dr. Michael Küppers (MPS): Sungrazers: Kometen, die der Sonne zu nah kommen.
- 9. April 2006, 15.00 Uhr: Dr. Jürgen Hamel (Berlin): Kometenforschung am Kasseler Landgrafenhof. Wilhelm IV., Christoph Rothmann und Jost Bürgi – Arbeiten zur Grundlegung der neuen Astronomie in Kassel.

Weiterhin hat sich das MPS am Wissenschaftssommer 15. bis zum 21. Juli 2006 in München beteiligt. Thema war die Mission Cassini/Huygens zum Saturn und dem Mond Titan an der das Institut mit drei Instrumenten beteiligt ist.
Auch 2007 fanden drei größere Veranstaltungen statt, an denen das MPS beteiligt war: Im Rahmen des "Internationalen Heliophysikalischen Jahres" IHY 2007 organisierte das MPS zusammen mit dem Astrophysikalischen Institut Göttingen eine Ausstellung in der Universitätsbibliothek Göttingen mit dem Thema "Unsere Sonne – Feuer des Lebens", die vom 2. bis 29. Mai 2007 zu sehen war. Neben der Ausstellung wurde eine Vorlesungsreihe zum Thema Sonne angeboten, die sehr großen Zuhörerzuspruch fand.
Das zweite Event 2007, "Tag der Sonne und ihrer Erforschung", fand am MPS am 10. Juni 2007 statt. Diese Veranstaltung wurde von ca. 1000 Interessierten besucht und wurde allgemein als gelungene Veranstaltung registriert.
Eine dritte Veranstalung mit MPS-Teilnahme 2007 war die "Ideenexpo" vom 6. bis 14. Oktober 2007 auf dem Messegelände in Hannover. Dort stellte das MPS das 1:1 Modell des Rosetta-Landers Philae aus. Tausende von Besuchern informierten sich an diesem Stand über die vielen technischen und wissenschaftlichen Details der Kometenmission Rosetta, die 2014 erstmals ein Landegerät auf einem Kometenkern absetzen wird. Dieses Landegerät namens Philae wurde im wesentlichen am MPS in Zusammenarbeit mit dem DLR gebaut.

**Vorträge außerhalb des MPS /**
External presentations

Als Bestandteil der Presse- und Öffentlichkeitsarbeit wurden puiblikumswirksame, allgemeinverständliche Vorträge von Institutsmitarbeitern ausserhalb des

MPS gehalten:

- H. Boehnhardt, Deep Impact und Rosetta – Kometenforschung heute und in 10 Jahren, Seminar, Ministerium fuer Bau und Verkehr des Landes Thueringen, Erfurt, 25 January 2006. (Oral).
- J. Büchner, Der vierte Aggregatzustand: Heliophysikalische Plasmen, Ringvorlesung "Das Reich der Sonne—Heimat der Menschheit", Christian-Albrechts-Universität zu Kiel, 29 November 2007, eingeladene Vorlesung.
- J. Büchner, B. Heber, F. Jansen, H. Peter, and K. Scherer, The German contributions to the International Heliophysical Year, 1st European General Assembly on the International Heliophysical Year, Paris (France), 10-13 January 2006, invited talk. (Oral). [Online]
- U. Christensen, Internal dynamics and magnetism of planets, Integrated Geodynamics seminar, Delft and Utrecht, 14-15 November 2007. (Oral).
- W. Curdt, Das System Erde-Sonne, Göttinger Woche, Campe Gymnasium, Holzminden, 13 July 2006. (Oral).
- B. Grieger, Die Cassini-Huygens-Mission zum Saturn und seinem Mond Titan, 22. Hochschultage Physik, Astronomie heute, Fachbereich Physik der Universität Marburg, Germany, 12-13 February 2007. (Oral).
- N. A. Krivova, Solar variability of relevance for the Earth's climate, Workshop A contribuição do Sol para o problema do aquecimento global da Terra, Coimbra, Portugal, 3 March 2007, invited.
- H. Krüger, Extrasolare Planeten – Welten um andere Sonnen, Volkshochschule Mosbach, Aussenstelle Binau, Binau/Neckar, 12 May 2006. (Oral).
- H. Krüger, Staubteilchen – Boten ferner Welten, Abendvortrag zum Tag der Ideen, MPS Katlenburg-Lindau, 30 March 2006. (Oral).
- H. Krüger, 3 Jahre Cassini – Was haben wir gelernt?, Volkshochschule Mosbach (Baden), Binau, 30 November 2007. (Oral).
- H. Krüger, Stonehenge & Co. -— Astronomie in der Steinzeit, Volkshochschule Mosbach/Baden; Binau, Volkshochschule Mosbach/Baden; Binau, 15 June 2007. (Oral).
- H. Krüger, Astronomische Beobachtungsmethoden —- die Brille der Astronomen, Volkshochschule Mosbach/Baden, Binau am Neckar, 17 November 2006. (Oral).
- N. Krupp, Cassini/Huygens -— Ein Resümee nach zwei Jahren im Saturnsystem, Vortragreihe "Faszinierendes Weltall" des Förderkreises Planetarium Göttingen, Universität Göttingen, 14 November 2006. (Oral).
- N. Krupp, Die Mission Cassini/Huygens – Besuch beim Herrn der Ringe, Astronomie-AG der Volkshochschule Buxtehude, 22 November 2007 (Oral).
- U. Mall, From Technology to Science, SIR on ESAs SMART-1 Mission, Workshop on Space Technologies STW-2006, Polish Academy of Science, Krakow, Poland, 2006. (Oral).
- U. Mall, Weitere Mondmissionen?, DLR Workshop Exploration unseres Sonnensystems, Dresden, Germany, 2006. (Oral).
- M. Rengel, M. Küppers, H. U. Keller, P. Gutierrez, and S. F. Hviid, Impactando a un Cometa: La Misión Impacto Profundo, La Semana de la Astronomía en la Isla de Margarita, Isla de Margarita, Venezuela, 22-26 October 2007. (Oral).
- M. Roth, Der Puls der Sonne – Was Sonnenbeben über unser Zentralgestirn verraten, öffentliche Abendvorlesung, Paulinerkirche, Göttingen, Germany, 24 August 2007. (Oral).
- M. Roth, Helio- und Asteroseismologie: Die Musik der Sonne und Sterne, Helmholtz-Gymnasium Bielefeld, 31 October 2007. (Oral).
- K. Schlegel, Blitze -– Urgewalten am Himmel, Vortragsreihe des Förderkreis Planetarium Göttingen e.V., Göttingen, Germany, 6 February 2007. (Oral).
- D. Schmitt, Der Sternhimmel im Herbst, Wohnstift, Göttingen, 13 October 2007. (Oral).
- D. Schmitt, Die Sternbilder am Winterhimmel, Wohnstift Göttingen, Göttingen, 13 January 2007. (Oral).
- M. Schüssler, Feuer und Eis: Ein Reise vom Zentrum der Sonne bis nach Grönland, Feldbergschule, Oberursel/Taunus, 11 July 2006. (Oral).
- M. Schüssler, Steuert die Sonne das Erdklima?, Frühjahrstagung der Deutschen Physikalischen Gesellschaft, Heidelberg, 14 March 2006. (Oral).
- M. Schüssler, Steuert die Sonne das Erdklima?, Loge "Georg zu den drei Säulen", Einbeck, 20 April 2006. (Oral).

- R. Schwenn, Ein neues Bild der Sonne: 10 Jahre SOHO, Festkolloquium “10 Jahre SOHO”, Universität Kiel, 10 July 2006.
- R. Schwenn, Explosive events on the Sun and their effects on space weather near the Earth, IAU Symposium 233 on Solar Activity and its Magnetic Origin, Cairo, Egypt, 31 March – 3 April 2006, invited review.
- R. Schwenn, Giotto und der Halleysche Komet: 20 Jahre nach dem historischen Rendez-vous, Jubiläumsfeier “20 Jahre Giotto”, Max-Planck-Institut für Sonnensystemforschung, Lindau, 13 March 2006, Festvortrag.
- R. Schwenn, Space Weather: A New Science Discipline, Culture and Astronomy at the Bibliotheca Alexandrina, Alexandria, Egypt, 26 March 2006, invited review. (Oral).
- R. Schwenn, Coronal Mass Ejections —- the Open Questions, International Conference on “Challenges for Solar Cycle 24”, Ahmedabad, India, 22-25 January 2007, invited talk. (Oral).
- R. Schwenn, Coronal mass ejections: The open questions, VIII COLAGE meeting, Mérida, Mexico, 11-17 July 2007, invited Review. (Oral).
- R. Schwenn, Sonnenstürme brausen durchs Sonnensystem – wie funktioniert das Weltraumwetter?, XLAB Science Festival, Göttingen, 20 December 2007. (Oral).
- R. Schwenn, Sonne-Erde-Weltraumwetter, Öffentlicher Vortrag, Planetarium Bochum, 20 June 2007.
- R. Schwenn, Space storms are roaring through the solar system: why do we earthlings care?, 10th International Congress of the Brazilian Geophysical Society, Technical Program Committee, Rio de Janeiro, 19-23 November 2007, invited. (Oral).
- R. Schwenn, Space Weather, 2nd ELAGE school, Mérida, Mexico, 11-17 July 2007, lectures.
- R. Schwenn, Space weather – the open questions, 9th Brazilian Meeting on Plasma 9 Encontro Brasileiro de Física dos Plasmas, Sao Pedro, Brazil, 25-28 November 2007, invited.
- R. Schwenn, Space weather – the open questions, Seminar at INPE, Sao José dos Campos, Brazil, 29 November 2007, invited Seminar lecture.
- R. Schwenn, Space Weather Science and the KuaFu project, The Second International Symposium on KuaFu Project, Sany, China, 15-19 January 2007, invited paper. (Oral).
- S. K. Solanki, Sonnenaktivität und Klima, Forum Astronomie der Volkssternwarte Bonn, Bonn, 2 November 2006, invited.
- S. K. Solanki, Variations of the Sun’s activity and brightness: are they causing global climate change?, The Physics of Chromospheric Plasmas, Coimbra, Portugal, 9-13 October 2006, public lecture.
- S. K. Solanki, Was hat das Magnetfeld der Sonne mit Einstein und unserem Klima zu tun?, Öffentliche Vorlesungsreihe Physik am Samstagmorgen der Fakultät für Physik der TU Braunschweig, Braunschweig, 25 November 2006, invited.
- S. K. Solanki, Der Feuerball am Himmel und die Klimakatastrophe auf der Erde, Sonnenaktivität und Klimawandel, IHY 2007 Vortrag, Zeiss Planetarium Bochum, 16 May 2007, invited talk.
- J. Woch, Venus, Mars, Saturn: Neues aus der Planetenforschung, Helmholtz-Gymnasium Bielefeld, 8 March 2007.

**Auszeichnungen /** Awards

*Dr. habil. Horst Uwe Keller*
Auszeichnung mit der Christiaan-Huygens-Medaille, 27. November 2007.

*Prof. Dr. Rainer Schwenn*
Von EGU: Auszeichnung mit der Julius Bartels- Medaille im April 2007 in Wien, “for his outstanding and pioneering achievements towards our understanding of the solar corona and the solar wind”.

*Prof. Dr. Rainer Schwenn*
Von COLAGE: Auszeichnung mit dem “Ruth Gall Award”, for intense collaborations with institutions in several Latin American countries.

*Prof. Dr. Vytenis M. Vasyliūnas*
2007 Editors’ Citation for Excellence in Refereeing for the Journal of Geophysical Research – Space Physics.

Fünf ehemalige Studenten der Research School erhielten in 2006 – 2007 Preise für ihre ausgezeichneten Dissertationen: / Five former students of the Research School received awards for their outstanding PhD theses:

*Dr. Laura Balmaceda*
AGU 2007 Joint Assembly Outstanding Student Paper Award, 2007.

*Dr. Mark Cheung*
Otto-Hahn-Medaille, Max-Planck-Gesellschaft, 2007.

*Dr. Yasuhito Narita*
Heinrich-Büssing-Preis, Braunschweigischer Hochschulbund, 2007.

*Dr. Markus Sailer*
Berliner-Ungewitter-Preis, Fakultät für Physik, Universität Göttingen, 2007.

*Dr. Martin Schrinner*
Berliner-Ungewitter-Preis, Fakultät für Physik, Universität Göttingen, 2006.

### **Herausgebertätigkeiten /** Editorships

*Aznar Cuadrado, R.*: Technical editor of Living Reviews in Solar Physics.

*Böhnhardt, H.*: Member editorial board "Earth, Moon, and Planets", Scientific Journal of Springer-Kluwer Academic Publishers (since 1992); Guest co-editor of special issue on the Rosetta mission, Space Science Review, published in spring 2007 as SSR 128; Co-editor, "The solar system beyond Neptune", book project of the University of Arizona Press, to be published in 2008; Co-editor, "The Rosetta Book", book project of ESA on Rosetta mission following the SSR special issue on Rosetta, Springer Press, to be published in 2008; Invited contributor, "Handbook of Practical Astronomy", Editor R. Roth, Springer Press Heidelberg, to be published in 2008; Invited contributor, "Abriss der Astronomie", Editors V. Voigt, H. Roeser, Wissenschaftliche Verlagsanstalt, Mannheim, to be published in 2009.

*Büchner, J.*: Herausgeber (editor) "Nonlinear Processes in Geophysics"; Associate Editor for Solar and Heliophysics of "J. Advances in Space Research", Elsevier Publishers.

*Christensen, U.*: Advisory Editor: Physics of the Earth & Plantetary Interiors.

*Gizon, L.*: Guest editor, Astronomische Nachrichten, Vol. 328, Number 3–4, March 2007.

*Hartogh P.*: Editor: Atmospheric Chemistry and Physics (ACP) and ACP MIPAS Special Issue. Editor: Advances in Geosciences.

*Kallenbach, R.*: V. Izmodenov and R. Kallenbach (eds.), The Physics of the Heliospheric Boundaries, no. SR-005 in ISSI Scientific Reports, ESA Publ. Div., Noordwijk, Netherlands, 413 pp, 2007.

*Krüger, H.*: H. Krüger, A. L. Graps (eds.), Proceedings of the conference on "Dust in planetary systems" held at Kauai, Hawaii, USA, 26 – 30 September 2005, ESA SP-643, ISBN 92-9092-207-9, 250 p, 2007.

*Marsch, E.*: Mitherausgeber (seit 2003) der elektronischen Zeitschrift Living Reviews in Solar Physics.

*Roth, M.*: Guest editor, Astronomische Nachrichten, Vol. 328, Number 3–4, March 2007.

*Schlegel, K.*: Hauptredaktion: The URSI Board of Officers: URSI White Paper on Solar Power Satellite Systems (SPS), The Radio Science Bulletin, no. 321, 13-27, 2007.

*Schwenn, R.*: "Coronal Mass Ejections", H. Kunow, N.U. Crooker, J.A. Linker, R. Schwenn and R. von Steiger (Eds.), Space science series of ISSI, Volume 21, Springer, 2006; "Solar Dynamics and its Effects on the Heliosphere an Earth", D.N. Baker, B. Klecker, S.J. Schwartz, R. Schwenn, and R. von Steiger (Eds.), Space science series of ISSI, Volume 22, Springer, 2007; Mitherausgeber von "Living Reviews in Solar Physics"

*Solanki, S. K.*: 'Editor in chief' der elektronischen, referierten Review-Zeitschrift "Living Reviews in Solar Physics" http://solarphysics.livingreviews.org/; "Solar Physics" Editorial Board.

*Titov, D.*: Associated Editor of the special section of the Journal of Geophysical Research "Venus Express: results of the nominal mission".

### **Direktionsberaterkreis des MPS /** „Direktionsberaterkreis" at MPS

Gewählte Mitglieder des Direktionsberaterkreises für die Amtszeit 2006 waren:
*Dr. Fred Goesmann (Planeten),* als Ersatzmitglied *Dr. Hermann Böhnhardt, Prof. Eckart Marsch (Sonne),* als Ersatzmitglied *Dr. Udo Schühle, Irene Büttner (Zentrale Dienste),* als Ersatzmitglied *Bernd Chares.*

Gewählte Mitglieder des Direktionsberaterkreises für die Amtszeit 2007 waren:
*Dr. Paul Hartogh (Planeten),* als Ersatzmitglied *Dr. Holger Sierks, Dr. Udo Schühle (Sonne),* als Ersatzmitglied *Dr. Joachim Woch, Irene Büttner (Zentrale Dienste),* als Ersatzmitglied *Dr. Peter Barthol.*

### **40 Jahre in der MPG /** 40 years at MPG

- Dietmar Hennecke (4. Januar 2006)
- Egon Pinnecke (6. Januar 2006)
- Norbert Meyer (1. Oktober 2006)
- Lothar Graf (1. April 2007)
- Manfred Güll (5. April 2007)
- Anita Brandt (23. April 2007)

**25 Jahre in der MPG /** 25 years at MPG

- Dr. Iancu Pardowitz (1. April 2006)
- Hermann Hartwig (1. Juni 2006)
- Jürgen Bethe (15. Juli 2006)
- Dr. Patrick Daly (24. Juli 2006)
- Michael Hilz (7. Oktober 2006)
- Robert Uhde (24. November 2006)
- Christiane Heise (20. April 2007)
- Roland Mende (16. Mai 2007)

Tabelle 2: **Radio und TV Berichte über das Institut**

| **Tag der Aufnahme** | **Radio Sender** | **TV Sender** | **Sende-datum/zeit** | **Projekt Thema** |
|---|---|---|---|---|
| 25.01.2006 | NDR 2 Nachrichten | | 17.00 + 19.00 | MPS Umzug, Christensen |
| 25.01.2006 | | NDR Hallo Niedersachsen | 18.00 | MPS Umzug, Christensen |
| 08.02.2006 | | RTL Nachtjournal | 24.02.06: 00.00 | SOHO, Schwenn |
| 28.02.2006 | NDR Plattenkiste | | 12.00 - 13.00 | Allgemein, Krupp, Lagg, Gandorfer |
| 09.03.2006 | NDR 1 | | 13.03.06: 14.40 | Giotto, Keller, Krupp, Wöbke |
| 09.03.2006 | | SWR | | Stereo, Deutsch, Bothmer |
| 09.03.2006 | | SWR Tagesschau | 13.03.06: 17.00 | Sonne und Klima |
| | | Tagesschau | 13.03.06: 17.00 | Schüssler |
| 13.03.2006 | | NDR Hallo Niedersachsen | 18.00 + 19.30 | Giotto, Land der Ideen<br>Schwenn, Kramm |
| 15.03.2006 | | Deutsche Welle TV | 26.03.06: 21.30 (dt.)<br>27.03.06: 00.30 (engl.)<br>09.30 (dt.)<br>12.30 (engl.)<br>28.03.06: 03.30 (dt.)<br>06.30 (engl.) | Magnetfeld Sonne<br>Marsch, Gandorfer, Lagg,<br>Tomasch, Wiegelmann |
| | | ARD "W wie Wissen"<br>3 SAT "Nano"<br>SWR "Odysso" | 26.03.06: 17.00<br>29.03.06: 18.30<br>30.03.06: 22.00 | Sonnenforschung<br>Bothmer, Schwenn |
| 11.04.2006 | | RTL Welt der Wunder | 30.04.06: 19.00 | Venus Express<br>(VMC Kamera) Titov |
| | | N24 Forschen und Fliegen | 24.06.06: 16:30 | Sonnenforschung |
| | | Deutsche Welle TV<br>"<br>"<br>"<br>"<br>" | 27.08.06: 19.30<br>28.08.06: 07.30<br>29.08.06: 01.30<br>" 04.30<br>" 13.30<br>" 16.30 | Sonne Stereo<br>"<br>"<br>"<br>"<br>" |

| **Tag der Aufnahme** | **Radio Sender** | **TV Sender** | **Sende-datum/zeit** | **Projekt Thema** |
|---|---|---|---|---|
| | | Deutsche Welle<br>Video on Demand | Feb. 07 | Sonnenstürme,<br>Vorhersage für das Weltraumwetter |
| 24.02.07 | | NDR Hallo Niedersachsen | 25.02.07: 19.30 | Rosetta Mars Flyby, Küppers<br>Keller live um 19.30 |
| <br>16.03.07 | | RTL<br>NDR das Erste Tagesschau | 27.02.07<br>16.03.07: 20.00 | Rosetta Mars Flyby<br>Mars-Express, MARSIS, Nielsen |
| 30.04.07 | | History channel | Ende 2007 | Sonne und Klima, Aufnahmen<br>auf Teneriffa, Solanki, Lagg |
| | FFN | | 30.07.07 | 60 Jahre Forschung in Lindau<br>Czechowsky |
| | Stadtradio<br>Göttingen | | 30.07.07 | 60 Jahre Forschung in Lindau<br>Rüster |
| 30.07.07 | NDR1 | | 03.08.07: 17.00 | Phoenix Launch, Goetz |
| 31.07.07 | | Deutsche Welle TV<br>Journal/Tagesthema | 03.08.07: 11.17,<br>13.17, 17.17, 21.17 | Phoenix Launch, Goetz,<br>Kramm, Schüddekopf |
| 01.08.07 | | RTL | 01.08.07 | Phoenix, Goetz<br>Rosetta/Osiris, Küppers |
| 01.08.07 | FFN | | 03.08.07: 9.30, 11.30 | Phoenix, Goetz |
| 02.08.07 | Bayrischer Rundfunk<br>B5 Aktuell | | 05.08.07 | Phoenix, Goetz |
| 03.08.07 | | NDR Hallo Niedersachsen | 18.00 + 19.30 | Phoenix, Goetz |
| | | Guten Abend RTL<br>"Wissen Exakt" | 02.08.07 | Phoenix, Goetz<br>Rosetta, Küppers |
| | | Phoenix | 03.08.07 | "Auf zur Kometenjagd"<br>Film von Adrian Lehnigk<br>über Rosetta-Start 2004<br>WDR-Produktion im Rahmen<br>der Sendung "Hier und heute" |
| | | Bayrischer Rundfunk | 13.08.07 | Der Mensch und seine Erde (F4) -<br>Im Bann der Sonne |
| 04.08.07 | | N-TV | 04.08.07: 12.00 | Phoenix, Goetz |
| 27.09.07 | Inforadio rbb | | 09.07 | Reise zu den Ursprüngen<br>des Sonnensystems, H.U. Keller |
| 19.11.07 | MDR info | | zwischen 5-9.00 | Venus Express<br>Markiewicz, Fränz |

# VIII. Berichte, Vorträge und Veröffentlichungen / Reports, Talks and Publications

## Interne MPS-Berichte / Internal MPS reports

MPS-T-P028-06-01
*Kissel, J., K. Altwegg, B. C. Clark, L. Colangeli, H. Cottin, S. Czempiel, J. Eibl, C. Engrand, H. M. Fehringer, B. Feuerbacher, M. Fomenkova, A. Glasmachers, J. M. Greenberg, E. Grün, G. Haerendel, H. Henkel, M. Hilchenbach, H. von Hoerner, H. Höfner, K. Hornung, E. K. Jessberger, A. Koch, H. Krüger, Y. Langevin, P. Parigger, F. Raulin, F. Rüdenauer, J. Rynö, E. R. Schmid, R. Schulz, J. Silén, W. Steiger, T. Stephan, L. Thirkell, R. Thomas, K. Torkar, N. G. Utterback, K. Varmuza, K. P. Wanczek, W. Werther, and H. Zscheeg*
COSIMA – Secondary time-of-flight ion mass spectrometer (SIMS) onboard Rosetta: instrument overview.

MPS-W-S012-07-01
*Inhester, B.*
Stereoscopy basics for the STEREO mission.

MPS-W-aero804S-07-02
*Wilhelm, K., E. Marsch, B. Dwivedi, and U. Feldman*
Observations of the Sun at vacuum-ultraviolet wavelengths from space. Part II: Results and interpretations.

## Experimentvorschläge / Proposals

**Asteroseismological Determination of Stellar Rotation Axes**: Implications for Stellar Radii, Stellar Rotation, and Planetary System Formation. (L. Gizon, S. K. Solanki, MPS). Proposal in response to COROT Additional Program AO. (accepted)

**ASTEX** -– a 2 asteroid orbiter and lander exploration mission funded by DLR Bonn; PI: A. Nathues (MPS); co-investigators: H. Boehnhardt (MPS), A. Harris (DLR Berlin), 2007 – 2008.

**Cosmic Vision:**

**ASTROD I** (Astrodynamical Space Test of Relativity using Optical Devices I), a class-M fundamental physics mission proposal submitted to ESA's Cosmic Vision Programme: R. Burston und L. Gizon in Zusammenarbeit mit T. Appourchaux (IAS, Orsay, France) und Y.-T. Ni (Purple Mountain Observatory, Nanjing, China). Not selected.

**COMPASS** – Coronal Magnetism, Plasma and Activity Studies from Space, E. Marsch, Co-Investigator, (PIs Fineschi and Solanki). A class-M mission proposed to ESA for Cosmic Vision, 29 June 2007.

**European Venus Explorer** – D. Titov, Member of the Steering Committee of the European Venus Explorer Proposal for the ESA Cosmic Vision Programme.

**Laplace** – a mission to Europe and the Jupiter system for ESA's Cosmic Vision Programme. Laplace is a multi-platform mission aiming at an in-depth, quantitative study of the Jupiter system and its moons. (N. Krupp, P. Hartogh, C. Jarchow, H. Sagawa, M. Fränz, H. Boehnhardt)

**Marco Polo** – Near-Earth-Asteroid/Dead-Comet Mission. (H. Boehnhardt)

**Tandem** – a mission to Titan and the Saturn system for ESA's Cosmic Vision Programme. Tandem is a multi-platform mission. (N. Krupp, M. Küppers, P. Hartogh, M. Rengel)

**Triple F** – Comet Sample Return, Cosmic Vision Proposal, PI: M. Küppers. (H. U. Keller, M. Rengel, P. Hartogh, H. Sierks)

**Deutsches Datenzentrum für das Solar Dynamics Observatory**. L. Gizon (PI), S. K. Solanki, I. Pardowitz, MPS. Granted (2008 – 2012).

**EST** – European Solar Telescope, FP7, Design Study for a 4m class European solar telescope, A. Lagg, Co-I on EST Proposal, funded by EU.

**ExoMars** M. Hilchenbach, Co-I

**HELAS**: European Helio- and Asteroseismology Network. Proposal to the European Union (FP 6). L. Gizon (Chairman of Network Activity), M. Roth (Project Scientist). Granted 2006 – 2009).

**LEONARDO** -– an asteroid mission, CNES study of a lander and orbiter mission to primitive asteroid; PI: A. Barucci (Observatoire Meudon, France); co-investigators: H. Boehnhardt, A. Nathues (MPS); 2005 – 2006.

**Local Helioseismology of Small Magnetic Elements**. L. Gizon, MPS (Consultant) with Aaron Birch, CoRA, USA (PI). Proposal 0607604 submitted to the National Science Foundation.

**MAPSO** – Team of Herschel Open Time Key Programme proposal, entitled: "MAPSO: Mapping Sgr B2 and Orion Star-Forming Regions", PI: J. Cernicharo. (M. Rengel)

**MARVEL** – Mars Volcanic Emission and Life Scout: Mars Scout Proposal, PI: M. Allen (CoI: P. Hartogh)

**MIMO** – Team of MIMO (Mikrowellen-Instrument für einen Mondorbiter). PI: P. Hartogh. (M. Rengel)

**NASA Flagship mission** – D. Titov, Member of the Science and Technology Definition Team for the NASA Flagship mission to Venus.

**POLARIS** (POLar Investigation of the Sun), a class-L mission proposal submitted to ESA's Cosmic Vision Programme: L. Gizon in Zusammenarbeit mit T. Appourchaux (IAS, Orsay, France). Not selected.

**RAMAN/LIBS**. The ExoMars mission to the red planet, Mars, is part of the ESA Aurora programme. The combined Raman/LIBS instrument is being developed for the Pasteur rover payload on the ExoMars lander. Raman spectroscopy is dedicated to molecular analysis of organics (exobiology) and minerals (geochemistry) of Martian soil. Our institute is member of the Raman science team. (M. Hilchenbach)

**SISI** Seismic Imaging of the Solar Interior using space–based data. Starting Grant proposal to the European Research Council (ERC, FP7). L. Gizon (PI). Proposal ranked 243/9167, expected to be granted.

**Subphotospheric Dynamics of the Sun**. (L. Gizon, M. Schüssler, A. Vögler, R. Cameron, MPS). Proposal to the International Space Science Institute (ISSI, Bern). (accepted)

**The magnetism of the chromosphere: Combining theory and observations** PI of Marie Curie EU Proposal (FP7), European Integration Grant für Laura Merenda. (A. Lagg)

**TNOs are Cool** – Team of the Herschel Open Time Key Programme proposal, entitled: "TNOs are Cool: A survey of the Transneptunian Region", PI: Th. Müller. (CoIs: H. Boehnhardt, P. Hartogh, M. Rengel)

**T-Owl** –- A thermal and mid-infrared imager and spectrograph for the Overwhelmingly Large Telescope OWL, ESO study proposal of an astronomical instrument; PI: R. Lenzen (MPI for Astronomy, Heidelberg); contributor for science case of the study: H. Boehnhardt (MPS); 2006 – 2007.

**VESPER** – Venus Atmosphere Chemistry and Dynamics Orbiter: NASA Discovery Proposal, PI: G. Chin (CoI: P. Hartogh)

**VEXCEL/MICROSOFT**: E. Nielsen was in 2006 hired as a consultant to VEXCEL/MICROSOFT to advice on the next generation orbital radars to probe ice deposits on the Earth (Antarctic, Greenland), Mars and the icy Jovian moon Europa.

**VIS-NIR**: A proposal for LEO, the German Mission to the Moon. (U. Mall)

**Water and related chemistry in the solar system**: A guaranteed time key program proposed for Herschel. (PI: P. Hartogh, CoIs: C. Jarchow, A. Medvedev, M. Rengel, associated scientist: H. Boehnhardt)

### Sonstige

*Dr. H. Boehnhardt*: Mitarbeit bei Beobachtungsproposals: 2 approved Herschel Key Programs (associated scientist for guaranteed time proposal, co-PI for open time proposal); 30 approved ESO observing time proposals (13 PI, 17 Co-I); 3 approved Calar Alto observing time proposals (3 Co-I).

*Dr. M. Madjarska*: Co-leader of a proposal for an International team in Space Science at the International Space Science Institute, Bern, Switzerland.

*Prof. E. Marsch*: Koordinator für das Proposal to the President of the Max-Planck Society submitted by a team of scientists from MPS and IPP in response to the call for "Institutsübergreifende Forschungsinitiativen" mit dem Titel "Turbulent transport, plasma heating, particle acceleration, and magnetic reconnection in heliophysical and fusion plasmas", in Zusammenarbeit mit den MPIs in Lindau und Garching/Greifswald erstellt und eingereicht im Juni 2007.

## **Tee-Seminare** / Tea Seminars

### Leitung/Organizers: Dr. W. Curdt, Dr. C. Jarchow und Dr. W. Markiewicz

*In den Seminaren wird von Wissenschaftlern des MPS, aber auch von Gästen in unregelmäßigen Zeitabständen über laufende Arbeiten vorgetragen.*

*MPS scientists, as well as guests to the Institute, report on their current work in the informal seminars.*

*Dr. Matthieu Kretzschmar*, Center for the Study of the Variability of the Sun, Rome, Italy: Solar activity: EUV and UV irradiance variations and possible analysis tools.
10 January 2006.

*Prof. Ronglan Xu*, Center for Space Sciences, Beijing, China: Earth Plasmasphere EUV Imaging from the Chinese 2nd Chang E's Moon Lander.
13 January 2006.

*Christian Beck*, Kiepenheuer Institut für Sonnenphysik, Freiburg: The properties and topology of magnetic fields in sunspots and their surroundings.
17 January 2006.

*Dr. Wolfgang Wild*, SRON Groningen, Niederlande: Herschel-HIFI, TELIS and other Submm Activities at SRON Netherlands Institute for Space Research.
27 January 2006.

*Dr. Oskar Steiner*, Kiepenheuer-Institut, Freiburg: Magnetohydrodynamic simulation from the convection zone to the chromosphere.
16. Februar 2006.

*Dr. Wing Ip*, Institute of Astronomy, National Central University, Taiwan: Atmospheres of the Saturnian rings, Enceladus and Iapetus.
22 February 2006.

*Dr. Karl Schuster*, Institut de RadioAstronomie Millimetrique (IRAM), Grenoble, France: IRAM, a Vector for Space Research through Millimeter Wave Technology.
27 March 2006.

*Dr. Maxim Reshetnyak*, Research Computing Center of Moscow State University and Institute of the Physics of the Earth, Russian Academy of Science, Moscow, Russia: The control volume method in geodynamo simulations.
29 March 2006.

*Dr. Monika Korte*, GeoForschungsZentrum Potsdam: Global centennial to millennial geomagnetic field changes.
23 May 2006.

*Dr. Regina Soufli*, Lawrence Livermore National Laboratory: EUV multilayer optics for solar physics.
13 June 2006.

*Dr. Reinald Kallenbach*, ISSI, Bern, Schweiz: Isotopic abundance ratios as tracers for planetary formation processes.
21 June 2006.

*Dr. Eberhard Wiehr*, retired from Institut für Astrophysik der Universität Göttingen: The He/Balmer emission ratio in solar prominences.
22 June 2006.

*Dr. Valeri Dikarev*, Universität Jena: Dust Rings of Mars: Discovery is Close?
27 June 2006.

*Frank Postberg*, Max-Planck-Institut für Kernphysik: The Composition of the Jovian Dust Stream Particles and Implications for Io's Volcanism.
6 July 2006.

*Prof. Konrad Sauer*, retired from MPS: Kinetic Theory of Whistler Oscillitons.
10 July 2006.

*Dr. Eike Guenther*, Thüringer Landessternwarte Tautenburg: Extrasolar planets: "The Tautenburg search programme".
17 July 2006.

*Prof. Dr. Doug Hamilton*, University of Maryland, USA: What tilted Saturn? And how did Neptune capture Triton?
16 August 2006.

*Prof. Dr. H. Kolm*, Centro de Estudos do Mar, Pontal do Sul, Brazil: Was ist Leben?
23 August 2006.

*Dr. Günther Rüdiger*, AIP Potsdam: Magnetic instabilities of differential rotation and toroidal fields.
25 September 2006.

*Dr. Leonid Kitchatinov*, Institute for Solar-Terrestrial Physics, Irkutsk, Russia: Magnetic confinement of the solar tachocline.
26 September 2006.

*Dr. Robert Richter*, Elettra Synchrotron Light Source, Trieste, Italy: Spectroscopy in the Soft X-Ray Region: From Helium Atoms to Molecules.
25 October 2006.

*Prof. Dr. Mathieu Ossendrijver*, Universität Tübingen: Babylonian computational astronomy.
1 November 2006.

*Drs. Miroslav Barta & Marian Karlicky*, Ondrejov Observatory, Czech Academy of Sciences, Czech Republic: Solar flare reconnection and corresponding radio bursts: MHD and PIC simulations and examples of radio observations.
3 November 2006.

*Dr. Peng-Fei Chen*, Nanjing University (on leave), China: TR explosive events: magnetic reconnection modulated by p-mode waves.
6 November 2006.

*Prof. Paul Cally*, Monash University, Australia: Helioseismology of Magnetic Activity.

7 November 2006.

*Dr. Peng-Fei Chen*, Nanjing University (on leave), China: EIT waves: observations and modellings.
9 November 2006.

*Dr. Dolores Maravilla*, Universidad Nacional Autonoma de Mexico (UNAM): Dust streams from Saturn: Where do they come from?
22 November 2006.

*Prof. Takashi Sakurai*, National Astronomical Observatory of Japan: An Initial Glimpse of Hinode (Solar-B) Data.
7 December 2006.

*Prof. Alexander Lipatov*, TU Braunschweig: From Fluid/Particle Toward Complex Particle Kinetic Models: Particle acceleration by shock surfing.
8 December 2006.

*Dr. Eberhard Wiehr*, retired from Institut für Astrophysik, Universität Göttingen: Intergranular magnetic structures complementary to G-band bright points. 19 February 2007.

*Prof. Kai Sundmacher*, MPI of Dynamics of Complex Technical Systems, Physical and Chemical Process Engineering, Magdeburg: Fuel Cell Systems for Electrochemical Energy Conversion.
22 March 2007.

*Dr. Olga E. Malandraki*, ESA, ESTEC, Niederlande: Analysis and Interpretation of Energetic Particle Measurements in the Heliosphere.
4 April 2007.

*Dr. W.-C. Müller*, IPP München: Numerical magnetohydrodynamic studies of homogeneous turbulence and turbulent convection.
18 April 2007.

*Dr. Ilan Roth*, UC Berkeley, USA: Some new story about relativistic electron processes in solar plasmas.
26 April 2007.

*Dr. Michael J. S. Belton*, Astronomer Emeritus, National Optical Astronomy Observatories, USA: The accelerating spin of 9P/Tempel 1 and its implications for the Stardust-NExT mission.
7 May 2007.

*Dr. Timur Rashba*, Werner-Heisenberg-Institut, München: Probing the internal solar magnetic field through g-modes and neutrinos.
15 June 2007.

*Dr. Shinsuke Imada*, National Astronomical Observatory of Japan: Discovery of temperature dependent upflow in the plage region during the gradual phase of an X-class flare.
9 July 2007.

*Dr. Martin Breuer*, Institut für Geophysik, Westfälische-Wilhelms-Universität Münster: Numerical Study on Thermo-Chemically Driven Convection in Planetary Cores.
12. Juli 2007.

*Satoshi Kasahara*, ISAS/JAXA, Japan: Works on ring current electrons with Cluster/RAPID.
19 July 2007.

*Hans-Reinhard Mueller*, Dept. of Physics and Astronomy, Dartmouth College, NH, USA: Paleoheliospheres: Solar system and heliosphere reacting to different galactic environments.
13 August 2007.

*Dr. Marco Delbo*, Laboratoire Cassiopee, Nice, France: Recent results from observations and modelling of asteroids in the thermal infrared.
28 August 2007.

*Dr. Thais Mothè Diniz*, National Observatory Rio de Janeiro, Brazil: Spectroscopic study of the EOS Asteroid family from Visible and NIR-data: using and comparing three different tools.
15 October 2007.

*Dr. M. Virginia Alves*, Instituto National de Pesquisaa Espaciais, Brazil: The geoeffectiveness of solar wind interplanetary magnetic structures: statistical results.
17 October 2007.

*Dr. Stein Haaland*, University Bergen, Norway, MPE Garching: Propagation velocity and dimensions of plasmoids in the magnetotail.
7 November 2007.

*Prof. H. Zhang*, National Astronomical Observatories, Chinese Academy of Sciences (NAOC), Beijing, China: Progress of the 1 m Space Solar Telescope for High Spatial Resolution Solar Observation.
22 November 2007.

*Dr. Waclaw Waniak*, Astronomical Observatory of the Jagiellonian University, Cracow, Poland: Observations of Comet 73P/SW3 from Cracow Observatory.
30 November 2007.

*Prof. Zarko Cucej*, University of Maribor, Faculty of Electrical Enginering and Computer Science, Slovenia: Slovenian remote sensing center: research results and plans.
12 December 2007.

## **IMPRS Solar System Seminars /** IMPRS Solar System Seminars

*The Solar System Seminars ($S^3$) takes place every second Wednesday afternoon from 13:00 to 16:30. It consists of up to three talks by students on their PhD projects (each 20 min talk plus 10 min discussion), an extended coffee break for further discussion and a tutorial talk (60 min).*

*Sebastian Schäfer:*
Field line resonances in the terrestrial plasmasphere: Case studies from Cluster.
*Markus Sailer:*
Problems of Adaptive Optics induced anisotropy for Speckle Reconstruction.
*Alexander Bösswetter:*
Simulation of the evolution of the Martian water inventory.
*Rainer Schwenn:*
CMEs, solar wind, and Sun-Earth connections: unresolved issues.
18 January 2006.

*Jean Santos:*
Photospheric boundary conditions for the investigation of solar eruptions by numerical simulations.
*Stefan Schröder:*
Investigating the properties of Titan's surface with Huygens' Descent Imager / Spectral Radiometer.
*Lotfi Yelles:*
Spectropolarimetric diagnostcics of simulated mixed polarity surface fields.
*Klaus Strassmeier (Potsdam):*
Robotic astronomy – observing without observer.
2 February 2006.

*Luca Maltagliati:*
Water vapor retrieval in Mars atmosphere with OMEGA experiment onboard Mars Express.
*Redouane Mecheri:*
Waves and instabilities in coronal funnels within the multi-fluid description.
*Cecilia Tubiana:*
Physical parameters of the Rosetta target comet: 67P/Churyumov-Gerasimenko.
*Gerhard Wurm (Münster):*
Experiments on planet formation: from current concepts to new ideas.
15 February 2006.

*Bruno Sanchez-Andrade Nuno:*
Solar spicules: Speckle reconstruction in the limb.
*Emre Ishik:*
Magnetic flux transport on cool stars.
*Richard Moissl:*
Planned observations of the Venus Monitoring Camera.
*Dieter Schmitt / Emre Ishik:*
The solar eclipse of 29 March 2006 and the retreat in Antalya.
1 March 2006.

*Lucas Paganini:*
On the measurement accuracy of microwave heterodyne spectrometers.
*Lucasz Matloch:*
Modelling of solar mesogranulation.
*Esa Vilenius:*
Exploring the Moon using the SIR near infrared spectrometer onboard SMART-1.
*Willy Benz (Bern):*
The formation of giant planets: Confronting theory with observations.
15 March 2006.

*Dragos Constantinescu:*
Location of wave sources using Cluster as a sensor array.
*Sven Simon:*
Plasma environment of Titan: A 3D hybrid simulation study.
*Richard Moissl:*
Planned observations of the Venus Monitoring Camera.
*Karsten Danzmann (Hannover):*
Gravitational wave observatories on Earth and in space: The first detectors are in operation.
17 May 2006.

*Ganna Portyankina:*
Lee wave clouds in Martian atmosphere: observations with HRSC.
*Gero Kleindienst:*
ULF waves in the Kronian magnetosphere.
*Elias Roussos:*
The plasma environment of Mars: Mars Express ASPERA-3 observations.
31 May 2006.

Visit to the National Metrology Institute and the Technical University Braunschweig.
*Julian Blanco Rodriguez:*
First results on polar faculae with the new Göttingen FPI.
*Ryu Saito:*
Influence of the surface on the atmospheric circulation of Mars.
*Philippe Kobel:*
FLASH & SPLASH! 1500 seconds in weightlessness.
28 June 2006.

*Tino Riethmüller:*
SUNRISE: A balloon-borne 1m solar telescope.
*Ingo von Borstel:*

Photophoresis: application in astrophysics.
*Dieter Breitschwerdt (Vienna):*
The local bubble: Origin and evolution of our solar neighbourhood.
12 July 2006.

*Laura Balmaceda:*
Reconstruction of total solar irradiance since the end of Maunder Minimum.
*Cecilia Tubiana:*
Characterization of physical parameters of the Rosetta target comet 67P/Churyumov-Gerasimenko.
18 October 2006.

*Stefan Schröder:*
Spectral observations of the Huygens landing site.
*Sanja Danilovic:*
Spectropolarimetry.
*Mathieu Ossendrijver (Tübingen):*
Babylonian computational astronomy.
1 November 2006.

*Cornelia Martinecz:*
Solar wind interactions with magnetized and unmagnetized bodies.
*Luca Maltagliati:*
Behaviour of atmospheric water vapor on the Tharsis volcanoes.
*Clementina Sasso:*
Observations and analysis of the full Stokes vector in a flaring region in the He I 1083.0 nm multiplet.
*Reinhardt Genzel (Garching):*
Studying galaxy formation: dynamics of high-redshift galaxies.
15 November 2006.

*Michal Drahus:*
Research on comets at submillimeter wavelengths.
*Sofie Spjuth:*
Shape modelling of asteroids.
29 November 2006.

*Pedro Russo:*
Fundamentals of Venus science.
*Evgeny Panov:*
Characteristics of the near-cusp Earth's magnetopause and associated magnetic turbulence.
13 December 2006.

*Lotfi Yelles Chaouche:*
Spectropolarimetric diagnostics of a high latitude active region on the Sun.
*Sebastian Schäfer:*
Characteristics of an ULF pulsation observed by Cluster within the terrestrial plasmapause.
*Martin Tschimmel:*
Investigation of the atmospheric water cycle on Mars by the Planetary Fourier Spectrometer onboard Mars Express.
*Artie Hatzes (Tautenburg):*
Extrasolar Planets: Recent results and searches from deep in the heart of Germany.
17 January 2007.

*Thorsten Stahn:*
Introduction to the observation of pulsating stars.
*Khalil Daiffallah:*
Numerical simulation of wave propagation in the Sun.
*Sofiane Bourouaine:*
Introduction to the kinetic theory of the solar corona.
31 January 2007.

*Peng Ruan:*
Modelling large scale coronal structures.
*Li Feng:*
Introduction to stereoscopic reconstruction for the STEREO mission.
*Werner Tscharnuter (Heidelberg):*
Dynamical and chemical evolution of protoplanetary accretion disks.
14 February 2007.

*Silvia Protopapa:*
Trans Neptunian Objects: What are they? How to characterize them?.
*Danica Tothova:*
Spectroscopic observations of hot coronal loops.
*Alexander Bösswetter:*
Transport processes in the Martian plasma environment.
*Alina Semenova:*
Doppler imaging of starspots: Spectral diagnostics. A case study of sigma Geminorum.
14 March 2007.

*Manuela Wiese:*
The Moon, and what he's made of – Lunar mineralogy.
*Christian Koch:*
Introduction to laser altimetry in the frame of the Bepi-Colombo mission.
*Philippe Kobel:*
Small-scale radiative features in the solar photosphere.
28 March 2007.

*Sven Simon:*
Three-dimensional multi-species hybrid simulations of Titan's highly variable plasma environment: Comparison with Cassini data.
*Richard Moissl:*
Cloud tracking in VMC UV Images.
*Emre Isik:*
A coupled model of magnetic field generation and transport in solar-type stars.
9 May 2007.

*Jean Santos:*
MHD simulations of electric currents formation in the solar atmosphere due to photospheric horizontal motions.
*Lucas Paganini:*
Impact of nonlinearities on retrieved vertical profiles of atmospheric species in microwave remote sensing.
23 May 2007.

*Julian Blanco:*
Hidden properties of polar faculae.
*Bruno Sanchez:*
High resolution imaging of the solar chromosphere.
*Ingo von Borstel:*
A study of photophoresis of materials relevant to the early pre-planetary disc.
*Elias Roussos:*
The origin of Saturn's G-ring.
27 June 2007.

*Lukasz Matloch:*
Mesogranulation as a cellular automaton effect.
*Tino Riethmüller:*
Fine structure and dynamics of sunspot umbral dots.
*Kuang Wu Lee:*
High frequency electron/electron modes in solar plasmas: linear approach.
*Esa Vilenius:*
Data reduction of near infrared spectrometer SIR on board SMART-1.
11 July 2007.

*Christian Koch:*
Determination of time-dependent variations and the long wave-length topography of Mercury from BepiColombo laser altimeter data.
*Michal Drahus:*
Submillimeter monitoring of the HCN molecule in comet 73P-C/Schwassmann-Wachmann 3.
*Thorsten Stahn:*
Improved estimates of solar-like oscillation parameters.
24 October 2007.

*Sofie Spjuth:*
Determination of photometric properties of asteroid Steins.
*Martin Meling:*
Magnetic vector structure of active region plage fields – An analysis of VTT and HINODE data.
*Xiaobo Li:*
Tracking of moving magnetic flux concentrations around sunspots in the photosphere.
*Bruno Leibundgut (ESO, Garching):*
Supernova cosmology.
21 November 2007.

*Cornelia Martinecz:*
Plasma environment of Venus: a 3D simulation study.
*Luca Maltagliati:*
Behaviour of atmospheric water vapour in the Hellas region on Mars.
*Julia Thalmann:*
The coronal magnetic field.
28 November 2007.

*Jean-Baptiste Vincent:*
An introduction to comets.
*Cecilia Tubiana:*
67P/Churyumov-Gerasimenko at large heliocentric distance.
*Kristofer Hallgren:*
Detection of mesospheric water.
*Clementina Sasso:*
Complex supersonic flows in a filament during a flare.
12 December 2007.

## **Instituts-Seminare** / Institute seminars

**Leitung: Das Kollegium**

*In den Institutsseminaren wird hauptsächlich über die Fortführung laufender und die Aufnahme neuer Projekte berichtet, einschließlich der finanziellen und personellen Belange.*

*The Institute seminars report on the status of current projects as well as presentations of future projects, including questions of financing and personnel.*

*Dr. M. Hilchenbach*: MIXS auf BepiColombo.
19 December 2006.

*Dr. P. Hartogh*: VESPER – Venus Chemistry & Dynamics Orbiter.
19 December 2006.

*Dr. Joachim Bormann*: (MPI für biophysikalische Chemie, Göttingen, EU-Referat / EU Liaison Office)
How to write a competitive Framework 7 proposal.
24 May 2007.

*Dr. Joachim Bormann*: (MPI für biophysicalische Chemie, Göttingen, EU-Referat / EU Liaison Office)
Marie Curie Actions – next calls.
4 July 2007.

## **MPS-Kolloquien** / MPS Colloquia

**Leitung: Dr. Hermann Böhnhardt**

*Zu diesen Kolloquien werden meistens nur auswärtige Wissenschaftler eingeladen, um möglichst allgemein über ihr Arbeitsgebiet zu berichten.*

*Colloquia are usually given by external scientists invited to the Institute to report fairly broadly on their field of research.*

*Prof. Dr. Klaus Strassmeier*, Astrophysical Institute Potsdam: Robotic astronomy – Observing without observer.
2 February 2006.

*Dr. Gerhard Wurm*, Universität Münster: Experiments on planet formation: From current concepts to new ideas.
15 February 2006.

*Prof. Willy Benz*, Universität Bern, Schweiz: The formation of giant planets: Confronting Theory with observation.
15 March 2006.

*Prof. Hans Zinnecker*, Astrophysical Institute Potsdam: Giant exoplanets around white dwarfs?
4 April 2006.

*Prof. Jean-Pierre Bibring*, University of Paris-Sud, France: The history of water on Mars: The Mars Express view.
12 April 2006.

*Prof. Karsten Danzmann*, MPI Gravitational Physics Hannover: Gravitational wave observatories on Earth and in Space: The first detectors are in operations!
17 May 2006.

*Prof. Jochem Marotzke*, MPS Meteorology Hamburg: Atlantic Ocean circulation and abrupt climate change.
24 May 2006.

*Dr. Francois Raulin*, LISA, CNRS and Universities of Paris 7 & 12, France: The Astrobiological Importance of Tholins.
13 June 2006.

*Dr. Dirk Schulz-Makuch*, Washington State University Pullman, USA: Perspectives on extraterrestrial life in our Solar System and beyond.
5 July 2006.

*Prof. Dieter Breitschwerdt*, University of Vienna, Austria: The local bubble: Origin and Evolution of our Solar Neighbourhood.
12 July 2006.

*Prof. Dr. Javier Trujillo-Bueno*, Instituto de Astrofisica de Canarias, Spain: Scattering physics and the Sun's hidden magnetism.
9 August 2006.

*Prof. Dr. Luke Dones*, South West Research Institute Boulder, USA: Dynamics of Centaurs – The link between the Kuiper Belt and comets.
25 October 2006.

*Prof. Dr. David Southwood*, European Space Agency: The magnetic rotation of Saturn.
3 November 2006.

*Prof. Dr. Reinhardt Genzel*, MPI for Extraterrestrial Physics Garching: Studying galaxy formation: Dynamics of highredshift galaxies.
15 November 2006.

*Prof. Dr. Artie Hatzes*, State Observatory of Thuringia Tautenburg: Extrasolar Planets: Recent results and searches from deep in the heart of Germany.
17 January 2007.

*Prof. Dr. Joachim Reitner*, Universität Göttingen: Geobiology of methane – an exo-biological perspective.
7 February 2007.

*Prof. Dr. Werner Tscharnuter*, Universität Heidelberg: Dynamical and chemical evolution of protoplanetary accretion disks.
14 February 2007.

*Prof. Dr. Konstantin Zioutas*, University of Patras and CERN Geneva: The CERN Axion Solar Telescope CAST: Motivation, concept, results and potential implications.
21 February 2007.

*Prof. Dr. Andreas Eckart*, Universität Köln: The Massive Black Hole at the Center of the Milky Way: Tracing the Accretion through Variable and Polarized Emission.
21 March 2007.

*Prof. Dr. Sanjay Limaye*, University of Wisconsin, Madison, USA: Venus atmospheric circulation: Known and Unknown.
27 March 2007.

*Prof. Dr. Joachim Saur*, Universität Köln: Satellite plasma interactions at Jupiter and Saturn.
24 May 2007.

*Prof. Dr. Robert Wimmer-Schweingruber*, Universität Kiel: The heliosphere as astrophysical laboratory.
13 June 2007.

*Prof. Dr. Wolfgang Hampel*, MPI for Nuclear Physics, Heidelberg: The Significance of the GALLEX-GNO experiment for the solution of the solar neutrino problem.
20 June 2007.

*Prof. Dr. Karen Meech*, University of Hawaii, USA: Origin of Earth's Oceans.
17 August 2007.

*Prof. Dr. Henner Busemann*, Open University Milton Keynes: "Stardust", Interplanetary Dust Particles and Meteorites – Correlated Studies of Asteroids and Comets in the Laboratory.
29 August 2007.

*Prof. Dr. Lutz Wisotzki*, Astrophysical Institut Potsdam: Galaxy evolution and the growth of supermassive black holes.
19 September 2007.

*Dr. Bruno Leibundgut*, European Southern Observatory Garching: Supernovae cosmology.
21 November 2007.

*Prof. Dr. C.-Y. Tu*, Department of Geophysics, Peking University, Beijing, China: The Kuafu mission.
13 December 2007.

## **Vorträge 2006 /**
## Talks 2006

**Betreuung der Online-Veröffentlichungs- und Vortragsliste: P. W. Daly**

**Aleksandrov, V.**, J. Wicht, and U. R. Christensen: Influence of inner-core size on the onset of convection. Deutscher Geodynamik Workshop 2006, Max-Planck-Institut für Sonnensystemsforschung, Katlenburg-Lindau, Germany, September 27-28, 2006. (Oral).

**Andre, N.**, E. C. Sittler, M. Blanc, J. L. Burch, A. J. Coates, J. Goldstein, T. W. Hill, K. K. Khurana, N. Krupp, W. S. Kurth, J. S. Leiser, P. Louarn, B. H. Mauk, A. M. Persoon, C. T. Russell, A. M. Rymer, M. F. Thomsen, M. K. Dougherty, D. A. Gurnett, S. M. Krimigis, D. G. Mitchell, and D. T. Young: Plasma transport signatures at Saturn observed during Cassini inbound orbit insertion. General Assembly of the European Geosciences Union, Vienna, Austria, April 2-7, 2006. (Oral).

**Andretta, V.**, P. J. Mauas, A. Falchi, and L. Teriaca: Spectroscopic measurements of helium abundance in an active region. The Physics of Chromospheric Plasmas, Coimbra, Portugal, October 9-13, 2006. (Oral).

**Armstrong, T. P.**, S. Taherion, J. Manweiler, S. M. Krimigis, and N. Krupp: Observation of two components in the distribution of trapped protons at Saturn. AGU Fall Meeting, San Francisco, USA, December 11-14, 2006. (Poster).

**Arridge, C. S.**, M. K. Dougherty, G. Giampieri, E. J. Smith, K. K. Khurana, C. T. Russell, D. J. Southwood, S. W. H. Cowley, G. Kleindienst, G. H. Jones, N. Krupp, H. J. McAndrews, A. J. Coates, D. G. Mitchell, and A. M. Rymer: Cassini observations of periodic modulations in Saturn's magnetospheric current sheet. General Assembly of the European Geosciences Union, Vienna, Austria, April 2-7, 2006. (Oral).

**Aurnou, J.**, M. Heimpel, and J. Wicht: Deep convection models of zonal flows on the giant planets. 10th Symposium of SEDI (Study of the Earth's Deep Interior), Prague, Czech Republic, July 9-14, 2006. (Poster).

**Balmaceda, L.**, N. A. Krivova, S. K. Solanki, and M. Schüssler: Reconstruction of total solar irradiance variations since the Maunder Minimum. 2nd International Symposium on Space Climate, Sinaia, Romania, September 13-16, 2006. (Oral).

**Barabash, S.**, J.-A. Sauvaud, H. Gunell, H. Andersson, A. Grigoriev, K. Brinkfeldt, M. Holmström, R. Lundin, M. Yamauchi, K. Asamura, W. Baumjohann, T. Zhang, A. J. Coates, D. R. Lindner, D. O. Kataria, C. C. Curtis, K. C. Hsieh, B. R. Sandel, A. Fedorov, C. Mazelle, J.-J. Thocaven, M. Grande, H. E. J. Koskinen, E. Kallio, T. Säles, P. Riihela, J. Kozyra, N. Krupp, J. Woch, J. Luhmann, S. McKenna-Lawlor, S. Orsini, R. Cerulli-Irelli, M. Mura, M. Milillo, M. Maggi, E. Roelof, P. Brandt, C. T. Russel, K. Szegoe, J. D. Winningham, R. A. Frahm, J. Scherrer, J. R. Sharber, P. Wurz, and P. Bochsler: The latest results on the energetic neutral atoms and plasma of Venus from the ASPERA-4 instrument of Venus Express. 36th COSPAR Scientific Assembly, Beijing, China, July 16-23, 2006, invited. (Oral).

**Barthol, P.**, S. K. Solanki, A. Gandorfer, M. Schüssler, B. W. Lites, V. M. Pillet, W. Schmidt, and A. M. Title: SUNRISE: high-resolution UV/VIS observations of the Sun from the stratosphere. 36th COSPAR Scientific Assembly, Beijing, China, July 16-23, 2006, invited. (Oral).

**Bavassano-Cattaneo, M. B.**, M. F. Marcucci, H. Rème, L. M. Kistler, B. Klecker, C. W. Carlson, A. Korth, M. McCarthy, R. Lundin, and A. Balogh: Kelvin-Helmholtz instability on the dusk magnetopause: Cluster CIS observations. General Assembly of the European Geosciences Union, Vienna, Austria, April 2-7, 2006. (Oral).

**Birch, A. C.**, T. L. Duvall, L. Gizon, and S. Hanasoge: Local helioseismology of small magnetic elements. Conference: MHD Waves and oscillations in solar magnetic structures, Palma de Mallorca, Balearic Islands, Spain, May 29 - June 1, 2006, invited. (Oral).

Birch, A. C., T. L. Duvall, L. Gizon, and J. Jackiewicz: Helioseismology of the average supergranule. 37th Meeting of the AAS Solar Physics Division, Durham, NH, USA, June 25-30, 2006. (Poster).

**Bloomfield, D. S.**, A. Lagg, S. K. Solanki, and J. M. Borrero: Finding needles in magnetic haystacks: the necessity of spectral imaging for magnetic structure studies. Solar Image Processing Workshop III, Trinity College Dublin, Ireland, September 6-8, 2006. (Oral).

**Bloomfield, D. S.**, A. Lagg, S. K. Solanki, and J. M. Borrero: Modified p-modes in penumbral filaments. Modern Solar Facilities - Advanced Solar Science, Göttingen, Germany, September 27-29, 2006. (Poster).

**Bloomfield, D. S.**, A. Lagg, S. K. Solanki, R. Centeno, M. Collados, and J. T. Bueno: Observations of running waves in a sunspot chromosphere. The Physics of Chromospheric Plasmas, Coimbra, Portugal, October 9-13, 2006. (Oral).

**Boehnhardt, H.**: Deep Impact and Rosetta - cometary science today and in 10 years from now. Institute Colloquium, Physics Department, Universidad Metropolitana de Ciencias e Educacion, Santiago de Chile, May 22, 2006. (Oral).

**Boehnhardt, H.**: Deep Impact und Rosetta - Kometenforschung heute und in 10 Jahren. Seminar, Ministerium für Bau und Verkehr des Landes Thüringen, Erfurt, Germany, January 25, 2006. (Oral).

**Boehnhardt, H.**: Deep Impact und Rosetta: Kometenforschung jetzt und in 10 Jahren. Jubiläumsfeier "20 Jahre GIOTTO", Katlenburg-Lindau, Germany, April 2, 2006. (Oral).

**Boehnhardt, H.**: Ground-based observations: capabilities then and now (invited). ESA scientific workshop on "How Giotto changed our view of comets", ESTEC Noordwijk, The Netherlands, March 13, 2006. (Oral).

**Boehnhardt, H.**: The Kuiper Belt. Institute colloquium, Thüringische Landessternwarte Tautenburg/Jena, Germany, March 21, 2006. (Oral).

**Boehnhardt, H.**: The Kuiper Belt - Fridge at the edge of the planetary system. Institute Colloquium, Astrophysical Institute Potsdam, Germany, February 20, 2006. (Oral).

**Boehnhardt, H.**, L. Lara, P. Gutierrez, J. L. Ortiz, R. Rodrigo, M. J. Vidal-Nunez, and R. Gredel: The dust coma of 9P/Tempel 1 from January to August 2005. Deep Impact as a World Observatory Event, Brussels, Belgium, August 7-10, 2006. (Oral).

**Boehnhardt, H.**, K. Muinonen, A. Barucci, S. Bagnulo, I. Belskaya, and L. Kolokolova: Polarization measurements of TNOs and Centaurs. Transneptunian Objects - Dynamical and Physical Properties, Catania, Italy, July 3-7, 2006. (Oral).

**Boehnhardt, H.** and the ESO DI Dust Team: The dusty view of DI from ESO Chile. Deep Impact as a World Observatory Event, Brussels, Belgium, August 7-10, 2006. (Poster).

**Boesswetter, A.**, S. Simon, M. Fränz, N. Krupp, J. Woch, E. Roussos, T. Bagdonat, and U. Motschmann: The Martian plasma environment: Comparison of Mars-Express ASPERA-3 measurements with 3d hybrid simulations. European Planetary Science Congress 2006, Berlin, Germany, September 18-22, 2006. (Oral).

**Bonev, T.**, N. Ageorges, S. B. L. Barrera, H. Boehnhardt, and the ESO DI Dust Team: Dynamical modeling of the DI dust ejecta cloud. Deep Impact as a World Observatory Event, Brussels, Belgium, August 7-10, 2006. (Oral).

**Büchner, J.**: Anomalous resistivity - concept and new results. SFB 591 Symposium "Cosmic Plasma Physics", Ruhr-Universität Bochum, Germany, October 30, 2006, invited review talk.

**Büchner, J.**: Anomalous resistivity in space plasmas simulations and Cluster s/c observations. Wuhan University, Department of Space Physics, Wuhan, China, July 24, 2006, invited Lecture.

**Büchner, J.**: "Anomalous" resistivity in the solar corona. 3rd International "Cambridge" Workshop on Reconnection at Sun and in magnetospheres, Arcetri Observatory, Florence, Italy, August 28 - September 1, 2006, invited review talk.

**Büchner, J.**: Anomalous resistivity of collisionless space plasmas. Third Asia Oceania Geosciences Society (AOGS), Singapore, July 10-14, 2006, invited Review Talk.

**Büchner, J.**: Astrophysical particle acceleration by magnetic reconnection. International Conference "The Nonthermal Universe", Würzburg, Germany, August 9-12, 2006, invited Review Talk.

**Büchner, J.**: Collisionless dissipation beyond the limits of the quasilinear theory. 6th International Conference on Nonlinear Waves and Turbulence in Space Plasmas, Fukuoka, Japan, October 9-13, 2006, invited Lecture.

**Büchner, J.**: Current concentrations in the solar corona. Frühjahrstagung des Fachverbands Extraterrestrische Physik der Deutschen Physikalischen Gesellschaft, Heidelberg, Germany, March 13-16, 2006. (Oral).

**Büchner, J.**: Current sheet formation for reconnection in the solar atmosphere. 3rd International "Cambridge" Workshop on Reconnection at Sun and in magnetospheres, Arcetri Observatory, Florence, Italy, August 28 - September 1, 2006, invited talk.

**Büchner, J.**: Current sheets and reconnection at the Sun. Lectures on Solar Physics, National Astronomical Observatory of China, Beijing, China, September 28, 2006, invited Lecture.

**Büchner, J.**: Current sheets at Sun: theories of their role, formation, location. International Workshop on Current Sheets at Sun, Bern, Switzerland, October 23-26, 2006, invited review talk.

**Büchner, J.**: Die Physik geoeffizienter Sonneneruptionen. Geophysikalisches Kolloquium der Universität Köln, Köln, Germany, April 24, 2006.

**Büchner, J.**: Flares, CCMEs and space weather phenomena. Lectures on Solar Physics, National Astronomical Observatory of China, Beijing, China, September 25, 2006, invited Lecture.

**Büchner, J.**: Magnetic reconnection - a universal heliophysical process. European General Assembly on the International Heliophysical Year, Paris, France, January 10-13, 2006, invited review talk.

**Büchner, J.**: Numerical simulation approaches to space and solar plasma problems. Peking University, Lectures on Solar Physics, Beijing, China, September 27, 2006, invited review talk.

**Büchner, J.**: Physik des Weltraumwetters. Geophysikalisches Kolloquium, Georg-August-Universität Göttingen, Germany, May 2, 2006, kolloquiumsvortrag. (Oral).

**Büchner, J.**: Releasing energy from the Sun and the magnetosphere through magnetic reconnection to be observed by KuaFu A and B. 36th COSPAR Scientific Assembly, Beijing, China, July 16-23, 2006, invited Review Talk.

**Büchner, J.**: Simulation of the electric fields created by magnetic reconnection in the solar corona by combining large scale and plasma kinetic approaches. 36th COSPAR Scientific Assembly, Beijing, China, July 16-23, 2006. (Oral).

Büchner, J., **B. Heber**, F. Jansen, H. Peter, and K. Scherer: The German contributions to the International Heliophysical Year. 1st European General Assembly on the International Heliophysical Year, Paris, France, January 10-13, 2006, invited talk. (Oral).

**Büchner, J.**, B. Nikutowski, and A. Otto: Physical modelling of the relationship between local and global structures of solar magnetic fields. 36th COSPAR Scientific Assembly, Beijing, China, July 16-23, 2006. (Oral).

**Büchner, J.**, S. Preusse, U. Motschmann, and A. Kopp: Plasma interaction between extrasolar planets and their stars. 4th Planet Formation Workshop, Heidelberg, Germany, March 1-3, 2006. (Oral).

**Buske, M.** and U. Christensen: Erweiterte dreidimensionale Konvektionsmodelle zur thermischen Entwicklung des Marsinneren. Deutscher Geodynamik Workshop 2006, Max-Planck-Institut für Sonnensystemsforschung, Katlenburg-Lindau, Germany, September 27-28, 2006. (Oral).

**Buske, M.** and U. Christensen: Thermische Evolutionsmodelle für das Merkurinnere. Deutscher Geodynamik Workshop 2006, Max-Planck-Institut für Sonnensystemsforschung, Katlenburg-Lindau, Germany, September 27-28, 2006. (Poster).

**Buske, M.** and U. R. Christensen: Convection models for the thermal evolution of the Martian interior. 10th Symposium of SEDI (Study of the Earth's Deep Interior), University of Agriculture, Prague, Czech Republic, July 9-14, 2006. (Poster).

**Buske, M.** and U. R. Christensen: Thermische Evolutionsmodelle für die Konvektion im Marsmantel. 66. Jahrestagung der Deutschen Geophysikalischen Gesellschaft, Bremen, Germany, March 6-9, 2006. (Oral).

**Buske, M.** and U. R. Christensen: Three-dimensional convection models for the thermal evolution of the Martian interior. Seminar für Nachwuchswissenschaftler, DLR, Berlin, Germany, August 30, 2006, invited. (Oral).

**Cai, H. T.**, S. Y. Ma, Y. L. Zhou, L. Cai, G. Dang, and K. Schlegel: Comparison of POLAR UVI and EISCAT radar estimates. 36th COSPAR Scientific Assembly, Beijing, China, July 16-23, 2006. (Oral).

**Cameron, R.**: Experiences from implementing an open upper boundary condition for MURaM. CO5BOLD Workshop 2006, Kiepenheuer-Institut für Sonnenphysik, Freiburg, Germany, June 12-14, 2006.

Cameron, R. and L. Gizon: Simulation of wave propagation in the solar interior. Workshop "Modern Solar Facilities - Advanced Solar Science", Göttingen, Germany, September 27-29, 2006. (Poster).

Cameron, R. and L. Gizon: Three-dimensional numerical simulation of wave propagation through a model sunspot. SOHO 18 / GONG 2006 / HELAS-I conference, Sheffield, UK, August 7-11, 2006. (Poster).

**Cameron, R.**, L. Gizon, and K. Daiffallah: Numerical simulations of wave propagation in the upper part of the convection. First HELAS Local Helioseismology Workshop "Roadmap for European Local Helioseismology", Nice, France, September 25-27, 2006.

**Cameron, R.**, A. Vögler, and M. Schüssler: Photospheric magnetoconvection. IAU Symposium 239, Prague, Czech Republic, August 21-25, 2006.

**Carbary, J.**, D. G. Mitchell, S. M. Krimigis, and N. Krupp: Charged particle periodicities in Saturn's outer magnetosphere. AGU Fall Meeting, San Francisco, USA, December 11-14, 2006. (Poster).

Christensen, U., **C. Koch**, and M. Hilchenbach: Determining Mercurys tidal Love number $h_2$ with laser altimetry. General Assembly of the European Geosciences Union, Vienna, Austria, April 2-7, 2006.

**Christensen, U. R.**: A deep dynamo generating Mercury's magnetic field. Seminar, Ninth Workshop "Fluid Dynamics in Earth and Planetary Sciences", Kyoto, Japan, November 28 - December 1, 2006, invited. (Oral).

**Christensen, U. R.**: Convection-driven planetary dynamos. IAU XXVIth General Assembly, Prague, Czech Republic, August 14-25, 2006, invited.

**Christensen, U. R.**: Die Entstehung des Erdmagnetfeldes. Kolloquium, Universität Duisburg-Essen, Duisburg, Germany, November 8, 2006. (Oral).

**Christensen, U. R.**: Fluid dynamics of earth and planetary interiors. Intensive Lecture Series, Ninth Workshop "Fluid Dynamics in Earth and Planetary Sciences", Kyoto, Japan, November 28 - December 1, 2006, invited. (Oral).

**Christensen, U. R.**: Geodynamo modeling - successes and challenges. The 10th Symposium of SEDI (Study of the Earths Deep Interior), University of Agriculture, Prague, Czech Republic, July 9-14, 2006, invited keynote lecture. (Oral).

**Christensen, U. R.**: Geodynamo modeling: successes and challenges. General Assembly of the European Geosciences Union, Vienna, Austria, April 2-7, 2006, C. F. Gauss Lecture, invited. (Oral).

**Christensen, U. R.**: Numerical modeling of the geodynamo. LGIT - Laboratoire de géophysique interne et tectonophysique, University Grenoble, France, March 21, 2006. (Oral).

**Christensen, U. R.**: Scaling laws for dynamos in rotating spherical shells and application to planetary magnetic fields. CMG - Geophysical Turbulence Program Workshop "Modeling Magnetohydrodynamic Turbulence: Application to planetary and stellar dynamos", National Center for Atmospheric Research (NCAR), Boulder, Colorado, USA, 27-30 June, 2006. (Oral).

**Christensen, U. R.**: The geodynamo from the perspective of mantle convection modellers. Deutscher Geodynamik Workshop 2006, Max-Planck-Institut für Sonnensystemsforschung, Katlenburg-Lindau, Germany, September 27-28, 2006. (Oral).

Collados, M., **A. Lagg**, J. J. Díaz García, E. Hernández Suárez, R. López, E. Páez Mañá, and S. K. Solanki: Tenerife Infrared Polarimeter II. The Physics of Chromospheric Plasmas, Coimbra, Portugal, October 9-13, 2006. (Poster).

**Curdt, W.**: Das System Erde-Sonne. Göttinger Woche, Campe Gymnasium, Holzminden, Germany, July 13, 2006. (Oral).

**Curdt, W.** and E. Landi: On the unidirectionality of SUMER hot loop oscillation events: evidence for DC-heating. The Physics of Chromospheric Plasmas, Coimbra, Portugal, October 9-13, 2006. (Oral).

**Curdt, W.** and E. Landi: Sunspots - clouds on the Sun? The Physics of Chromospheric Plasmas, Coimbra, Portugal, October 9-13, 2006. (Poster).

**Curdt, W.** and E. Landi: The transition region above sunspots. Solar and Steller Physics through Eclipses, Side-Antalya, Turkey, March 26-29, 2006. (Oral).

**Curdt, W.** and E. Landi: The transition region above sunspots. SOHO-17: 10 Years of SOHO and Beyond, Gardini Naxos, Sicily, Italy, May 7-12, 2006. (Poster).

**Czechowski, A.** and M. Hilchenbach: Neutral solar wind and the inner source of the pick-up ions. Second Solar Orbiter Workshop, Athens, Greece, October 16-20, 2006. (Oral).

**Dal Lago, A.**, R. Schwenn, and W. D. Gonzalez: A study of the CME geometry. 36th COSPAR Scientific Assembly, Beijing, China, July 16-23, 2006. (Oral).

**D'Amicis, R.**, S. Orsini, E. Antonucci, A. M. Di Lellis, M. Hilchenbach, D. Telloni, S. Fineschi, R. Bruno, A. Milillo, and E. De Angelis: Neutral solar wind numerical simulations as expected at the Solar Orbiter position. Second Solar Orbiter Workshop, Athens, Greece, October 16-20, 2006. (Oral).

**Dang, G.**, S. Y. Ma, L. Huo, L. Xu, and K. Schlegel: Morphology of storm-time ionospheric $O^+$ ion upflow by FAST in situ observations. 36th COSPAR Scientific Assembly, Beijing, China, July 16-23, 2006. (Oral).

**Danilovic, S.**, S. K. Solanki, W. Livingston, N. A. Krivova, and I. Vince: Magnetic source of the solar cycle variation of the MnI 539.4 nm line. Workshop Modern Solar Facilities - Advanced Solar Sciences, Göttingen, Germany, September 27-29, 2006.

**DeRosa, M.**, K. Schrijver, T. Metcalf, G. Barnes, B. Kliem, Y. Liu, J. McTiernan, Z. Mikic,

S. Régnier, S. Titov, G. Valori, A. van Ballegooijen, B. Welsche, M. Wheatland, and T. Wiegelmann: Non-linear force-free field (NLFFF) modeling:applications to solar-like data. SPD Meeting, UNH, Durham, USA, June 25-30, 2006. (Oral).

Di Mauro, M. P., D. Cardini, F. D'Antona, C. Maceroni, M. Döllinger, J. Setiawan, M. Roth, and O. v. d. Lühe: Asteroseismology of K giants. SOHO 18 / GONG 2006 / HELAS I - Conference, Sheffield, UK, August 7-11, 2006. (Poster).

**Dubinin, E.**, M. Fränz, J. Woch, S. Barabash, and R. Lundin: Ion distributions upstream and downstream of the Martian bow shock. ASPERA-3 observations. 36th COSPAR Scientific Assembly, Beijing, China, July 16-23, 2006. (Oral).

**Dubinin, E.**, M. Fränz, J. Woch, S. Barabash, R. Lundin, and M. Yamauchi: Hydrogen exosphere at Mars. Pickup protons and their acceleration at the bow shock. European Planetary Science Congress 2006, Berlin, Germany, September 18-22, 2006. (Oral).

**Dubinin, E.**, M. Fränz, J. Woch, E. Roussos, S. Barabash, R. Lundin, D. Winningham, R. Frahm, and M. Acuna: Plasma domains at Mars. Their boundaries and solar wind and IMF control of them. 36th COSPAR Scientific Assembly, Beijing, China, July 16-23, 2006. (Poster).

**Dunlop, M. W.**, J. A. Davies, C. Perry, A. N. Fazakerley, M. A. Hapgood, M. G. G. Taylor, Y. Bogdanova, Z. Pu, O. Nailard, and P. W. Daly: Cluster observations of energetic particles in the Earth's magnetosphere. 36th COSPAR Scientific Assembly, Beijing, China, July 16-23, 2006, invited. (Oral).

Duvall, T. L., Jr., A. C. Birch, L. Gizon, and J. Jackiewicz: The structure of the average supergranule. SOHO 18 / GONG 2006 / HELAS I - Conference, Sheffield, UK, August 7-11, 2006. (Poster).

**Ermolli, I.**, A. Tlatov, S. Solanki, and N. Krivova: Solar activity and irradiance studies with Ca II spectroheliogram time series: Potential problems and possible solutions. The Physics of Chromospheric Plasmas, Coimbra, Portugal, October 9-13, 2006. (Oral).

Facskó, G., **K. Kecskeméty**, G. Erdõs, M. Tátrallyay, and P. W. Daly: Geometrical study of hot flow anomalies aboard Cluster. 36th COSPAR Scientific Assembly, Beijing, China, July 16-23, 2006. (Poster).

**Facskó, G.**, K. Kecskeméty, G. Erdös, M. Tátrallyay, and P. Daly: Comparision of hot flow anomaly observations aboard Cluster with hybrid simulations. General Assembly of the European Geosciences Union, Vienna, Austria, April 2-7, 2006. (Oral).

**Feng, L.**, T. Wiegelmann, and B. Inhester: Magnetic stereoscopy of AR 8891. Solar Image Processing Workshop, Trinity College Dublin, Ireland, September 6-8, 2006. (Oral).

**Feng, L.**, T. Wiegelmann, and B. Inhester: Magnetic stereoscopy of coronal loops in NOAA 8891. Workshop: Modern Solar Facilities - Advanced Solar Science, Göttingen, Germany, September 6-8, 2006. (Poster).

**Feng, L.**, T. Wiegelmann, B. Inhester, S. Solanki, E. Marsch, W. Q. Gan, and P. Ruan: Coronal stereoscopy of AR 8891. 36th COSPAR Scientific Assembly, Beijing, China, July 16-23, 2006. (Poster).

**Flandes, A.** and H. Krueger: The interplanetary medium and the Jovian dust streams. 36th COSPAR Scientific Assembly, Beijing, China, July 16-23, 2006. (Poster).

**Fränz, M.**, E. Dubinin, N. Krupp, E. Roussos, J. Woch, S. Barabash, R. Lundin, and the ASPERA-3 Team: Ion moments and pressure balance in Mars magnetosphere. European Planetary Science Congress 2006, Berlin, Germany, September 18-22, 2006. (Oral).

**Fränz, M.**, E. Dubinin, J. Woch, E. Roussos, and C. Martinecz: Plasma Moments at Mars - Mars Express ASPERA-3 Observations. European Planetary Science Congress 2006, Berlin, Germany, September 18-22, 2006. (Oral).

**Fu, S.**, Q.-G. Zong, Z. Y. Pu, A. Korth, and P. W. Daly: Preliminary study of energetic particles embedded in magnetic structures observed in the near Earth plasmasheet. 8th International Conference on Substorms, Banff, Canada, March 28-31, 2006. (Poster).

**Fu, S. Y.**, Q. G. Zong, A. Korth, Z. Y. Pu, and P. W. Daly: Preliminary study of energetic particles embedded in magnetic structures observed in the near Earth plasmasheet. 36th COSPAR Scientific Assembly, Beijing, China, July 16-23, 2006. (Oral).

**Futana, Y.**, S. Barabash, A. Grigoriev, R. Lundin, H. Andersson, J. Gimholt, M. Holmström, O. Norberg, M. Yamauchi, K. Asamura, A. J. Coates, D. R. Linder, D. O. Kataria, C. C. Curtis, K. C. Hsieh, B. R. Sandel, A. Fedorov, E. Budnik, M. Grande, M. Carter, D. H. Reading, H. Koskinen, E. Kallio, P. Riihela, T. Säles, J. Kozyra, N. Krupp, S. Livi, J. Woch, J. Luhmann, S. McKenna-Lawlor, S. Orsini, R. Cerulli-Irelli, A. Mura, A. Milillo,

E. Roelof, D. Williams, J. A. Sauvaud, J.-J. Thocaven, D. Winningham, R. Frahm, J. Scherrer, J. Sharber, P. Wurz, and P. Bochsler: Response of the subsolar ENA jet flux caused by an interplanetary shock. 36th COSPAR Scientific Assembly, Beijing, China, July 16-23, 2006. (Oral).

**Garnier, P.**, I. Dandouras, D. Toublanc, D. G. Mitchell, E. C. Roelof, P. C. Brandt, S. M. Krimigis, N. Krupp, D. C. Hamilton, and H. Waite: The interaction between Titan exosphere and the Kronian magnetosphere: MIMI observations, statistical analysis and modeling. AGU Fall Meeting, San Francisco, USA, December 11-14, 2006. (Oral).

Garnier, P., **I. Dandouras**, D. Toublanc, D. G. Mitchell, E. C. Roelof, P. C. Brandt, S. M. Krimigis, N. Krupp, D. C. Hamilton, and J. H. Waite: The interaction between the Titan exosphere and the Kronian magnetosphere: MIMI observations and modelling. European Planetary Science Congress 2006, Berlin, Germany, September 18-22, 2006. (Oral).

**Garnier, P.**, I. Dandouras, D. Toublanc, D. G. Mitchell, E. C. Roelof, P. C. Brandt, S. M. Krimigis, N. Krupp, D. C. Hamilton, and J. H. Waite: The interaction between Titan exosphere and the Kronian magnetosphere: MIMI observations and modeling. General Assembly of the European Geosciences Union, Vienna, Austria, April 2-7, 2006. (Oral).

**Gizon, L.**: European Local Helioseismology and HELAS. HMI/AIA Science Teams Meeting, Monterey, CA, USA, February 13-17, 2006, invited. (Oral).

**Gizon, L.**: HELAS NA4 deliverables. First HELAS Local Helioseismology Workshop "Roadmap for European Local Helioseismology", Nice, France, September 25-27, 2006. (Oral).

**Gizon, L.**: Helioseismology: Science requirements and observational strategies. Second Solar Orbiter Workshop, Athens, Greece, October 16-20, 2006, invited. (Oral).

**Gizon, L.**: Imaging the interaction of solar waves with a sunspot. General Assembly of the European Geosciences Union, Vienna, Austria, April 2-7, 2006. (Oral).

**Gizon, L.**: Local helioseismology at high spatial resolution. Meeting of ISSI working group "Subphotospheric Dynamics of the Sun", International Space Science Institute, Bern, Switzerland, June 9, 2006. (Oral).

**Gizon, L.**: Local Helioseismology, Magnetic Activity, and Mode Physics Helioseismology and Models: Introductory Overview. IAU XXVIth General Assembly, Prague, Czech Republic, August 14-25, 2006, invited review talk. (Oral).

**Gizon, L.**: Local Helioseismology: Status of NA4 Activity. 1st HELAS Board Meeting, Leuven University, Belgium, April 20-21, 2006, invited. (Oral).

**Gizon, L.**: Measurements of flows with time-distance helioseismology: Prospects for HMI. HMI/AIA Science Teams Meeting, Monterey, CA, USA, February 13-17, 2006, invited. (Oral).

**Gizon, L.**: Probing Solar Activity and Convection with Local Helioseimology. SOHO-17: 10 Years of SOHO and Beyond, Giardini Naxos, Sicily, Italy, May 7-12, 2006, invited. (Oral).

**Gizon, L.**: Time-distance helioseismology. Astrophysikalisches Kolloquium am Institut für Astrophysik der Georg-August-Universität Göttingen, Göttingen, Germany, January 5, 2006, invited. (Oral).

Gizon, L., R. Cameron, J. Jackiewicz, M. Roth, and T. Stahn: Helioseismology at MPS. Workshop "Modern Solar Facilities - Advanced Solar Science", Göttingen, Germany, September 27-29, 2006. (Poster).

Gizon, L., S. M. Hanasoge, and A. C. Birch: Acoustic scattering off flux tubes: Is the Born approximation valid? SOHO 18 / GONG 2006 / HELAS I - Conference, Sheffield, UK, August 7-11, 2006. (Poster).

Gizon, L. and M. Rempel: Solar-cycle variation of the meridional circulation. Workshop "Modern Solar Facilities - Advanced Solar Science", Göttingen, Germany, September 27-29, 2006. (Poster).

Gizon, L. and M. Rempel: Time-varying component of the meridional flow. SOHO 18 / GONG 2006 / HELAS I - Conference, Sheffield, UK, August 7-11, 2006. (Poster).

Gizon, L., T. Stahn, and G. Vauclair: Fourier Analysis of Gapped Time Series of Stellar Oscillations. 10th COROT week of CNES, Nice, France, June 5-9, 2006. (Poster).

**Gomez, N.**, J. Wicht, and M. Heimpel: Dynamo simulations with radially variable electrical conductivity. 10th Symposium of SEDI (Study of the Earth's Deep Interior), Prague, Czech Republic, July 9-14, 2006. (Poster).

**Gömöry, P.**, J. Rybak, A. Kucera, W. Curdt, and H. Wöhl: Downward propagating waves detected in the chromospheric network by SOHO/CDS. The Physics of Chromospheric Plasmas, Coimbra, Portugal, October 9-13, 2006. (Poster).

**Grieger, B.**: A science case on atmospheric circulation from DWG 1. Europlanet N2-N7 workshop, ESAC, Villafranca, Madrid, Spain, April 24-26, 2006. (Oral).

**Grieger, B.**: Modelling the circulation of Europa's ocean. 36th COSPAR Scientific Assembly, Beijing, China, July 16-23, 2006. (Poster).

**Grieger, B.**: Modelling the circulation of Europa's ocean. European Planetary Science Congress 2006, Berlin, Germany, September 18-22, 2006. (Oral).

**Grieger, B.**: The 8th sea - modelling the ocean of the Jovian moon Europa. DFG Priority Programme 1115 "Mars and the Terrestrial Planets", Subgroup Atmosphere and Surface Processes, Göttingen, Germany, March 23-24, 2006. (Oral).

**Grieger, B.**: The 8th sea: modelling the ocean of the Jovian moon, Europa. Seminar über Weltraumforschung, Physikalisches Institut, Universität Bern, Switzerland, May 31, 2006. (Oral).

**Grieger, B.**, L. Doose, E. Karkoschka, H. U. Keller, R. Kramm, Y. Skorov, M. G. Tomasko, and The DISR Team: Topographic shading in Huygens/DISR images of Titan's surface. General Assembly of the European Geosciences Union, Vienna, Austria, April 2-7, 2006. (Oral).

**Grieger, B.**, L. Doose, E. Karkoschka, H. U. Keller, R. Kramm, Y. Skorov, M. G. Tomasko, and The DISR Team: Topographic shading in Huygens/DISR images of Titan's surface. 36th COSPAR Scientific Assembly, Beijing, China, July 16-23, 2006. (Oral).

**Grieger, B.** and R. Greve: Modelling the circulation of Europa's ocean with the Hamburg Large Scale Geostrophic ocean general circulation model (LSG). Europa Focus Group Workshop, Moffet Field, CA, USA, February 27-28, 2006. (Oral).

**Grieger, B.** and R. Greve: Modelling the circulation of Europa's ocean with the Hamburg Large Scale Geostrophic ocean general circulation model (LSG). General Assembly of the European Geosciences Union, Vienna, Austria, April 2-7, 2006. (Poster).

**Grieger, B.**, R. Greve, and O. Stenzel: MAIC-2: A latitudinal model to estimate Martian surface temperature and atmospheric water transport. Seminar of the Experimental and Theoretical Glaciology Group, Hokkaido University, Sapporo, Japan, October 19, 2006. (Oral).

**Grieger, B.**, H. U. Keller, R. Kramm, and Y. Skorov: Topographic shading in Huygens/DISR images of Titan's surface. DISR Team Meeting, Nantes, France, June 21, 2006. (Oral).

**Grieger, B.**, H. U. Keller, M. G. Tomasko, and E. Karkoschka: DISR data analysis status and plans. Huygens Data Analysis Workshop, ESTEC, Noordwijk, Netherlands, May 15-17, 2006. (Oral).

Grieger, B. and **F. Leblanc**: DWG-1: High atmosphere and chemistry. Europlanet N2-N7 workshop, ESAC, Villafranca, Madrid, Spain, April 24-26, 2006. (Oral).

**Grieger, B.**, F. Leblanc, M. Fränz, H. Lammer, T. Siili, and T. Tokano: A science case on atmospheric circulation. European Planetary Science Congress 2006, Berlin, Germany, September 18-22, 2006. (Oral).

**Grynko, Ye.**, Yu. Shkuratov, and U. Mall: Computer modeling of bidirectional spectra: the role of geometry of illumination/observation. European Planetary Science Congress 2006, Berlin, Germany, September 18-22, 2006. (Oral).

Gunar, S., L. Teriaca, P. Heinzel, and U. Schühle: Prominence Parameters Derived from Hydrogen Lyman-Alpha Spectral Profiles Measured by SOHO/SUMER. SOHO-17: 10 Years of SOHO and Beyond, Gardini Naxos, Sicily, Italy, May 7-12, 2006. (Poster).

**Hartogh, P.**: Submm-wave sounding of the Venusian atmosphere. European Planetary Science Congress 2006, Berlin, Germany, September 18-22, 2006. (Poster).

**Hartogh, P.** and P. de Maagt: Submm Wave Instrument (SWI) on a potential ExoMars orbiter. European Planetary Science Congress 2006, Berlin, Germany, September 18-22, 2006. (Oral).

Hassler, D. M., C. E. DeForest, S. McIntosh, D. Slater, T. Ayres, R. Thomas, U. Schühle, H. Michaelis, and H. Mason: Developing Next Generation Spectrograph Technology for Solar Orbiter with the Rapid Acquisition Imaging Spectrograph (RAISE) Sounding Rocket Program. Second Solar Orbiter Workshop, Athens, Greece, October 16-20, 2006. (Poster).

**Heber, B.**, J. Büchner, R. Wimmer-Schweingruber, H. Peter, K. Scherer, and F. Jansen: The International Heliophysical Year 2007: Activities in Germany. Frühjahrstagung des Fachverbands Extraterrestrische Physik der Deutschen Physikalischen Gesellschaft, Heidelberg, Germany, March 13-16, 2006.

**Hedman, M. M.**, J. A. Burns, M. S. Tiscareno, P. D. Nicholson, C. C. Porco, G. H. Jones, E. Roussos,

N. Krupp, and C. Paranicas: Multi-instrument studies of an arc in Saturn's G ring. AGU Fall Meeting, San Francisco, USA, December 11-14, 2006, invited poster. (Poster).

**Heimpel, M.**, J. Aurnou, and J. Wicht: Scaling turbulent zonal flow in numerical simulations and on Jupiter and Saturn. 10th Symposium of SEDI (Study of the Earth's Deep Interior), Prague, Czech Republic, July 9-14, 2006. (Poster).

**Hilchenbach, M.**: Comets as imperfections in a nearly perfect solar system. General Assembly of the European Geosciences Union, Vienna, Austria, April 2-7, 2006. (Poster).

**Hilchenbach, M.**: Das Potential massenspektrometrischer Messungen an Kometenstaubpartikeln bei Rosetta COSIMA. 17. Massenspektrometrische Diskussionsveranstaltung, Wien, Österreich, Feb 14-15, 2006, invited. (Oral).

**Hilchenbach, M.**: Space weathering of comets and cometary dust in the heliosphere. 36th COSPAR Scientific Assembly, Beijing, China, July 16-23, 2006. (Oral).

**Hilchenbach, M.**, A. Czechowski, K. C. Hsieh, and R. Kallenbach: Heliospheric energetic neutral atoms observed with SOHO/CELIAS/HSTOF. 36th COSPAR Scientific Assembly, Beijing, China, July 16-23, 2006. (Oral).

**Hilchenbach, M.**, A. Czechowski, K. C. Hsieh, and R. Kallenbach: Observations of energetic neutral atoms and their implications on modeling the heliosheath. 5th Annual International Astrophysics Conference, The Physics of the Inner Heliosheath: Voyager Observations, Theory, and Future Prospects, Honolulu, Hawaii, US, March 3-9, 2006, invited. (Oral).

**Hilchenbach, M.**, A. Czechowski, K. C. Hsieh, and R. Kallenbach: One decade of observations of energetic neutral atoms with SOHO/CELIAS/HSTOF and their implications on modeling the heliosphere. SOHO-17: 10 Years of SOHO and Beyond, Gardini Naxos, Sicily, Italy, May 7-12, 2006. (Poster).

Hilchenbach, M., **S. Orsini**, K. C. Hsieh, E. Antonucci, S. Barabash, K. Bamert, R. Bruno, M. R. Collier, A. Czechowski, I. Dandouras, R. Esser, J. Giacalone, M. Gruntman, S. R. Habbal, J. R. Jokipii, E. Kallio, J. Kota, H. Kucharek, S. Livi, I. Mann, E. Marsch, E. Moebius, R. B. Sheldon, W. Schmidt, K. Szego, J. Woch, P. Wurz, and T. H. Zurbuchen: Solar Orbiter Neutral Solar-Wind Detector. Second Solar Orbiter Workshop, Athens, Greece, October 16-20, 2006. (Oral).

Hirzberger, J., L. Gizon, S. K. Solanki, and T. L. Duvall, Jr.: Structure and evolution of supergranulation from local helioseismology. Workshop "Modern Solar Facilities - Advanced Solar Science", Göttingen, Germany, September 27-29, 2006. (Poster).

Hirzberger, J., **E. Wiehr**, and G. Stellmacher: Two-dimensional imaging of the HeD3/H-beta emission ratio inquiescent solar prominences. The Physics of the Chromospheric Plasmas, Coimbra, Portugal, October 9-13, 2006. (Poster).

**Hochedez, J.-F.**, T. Appourchaux, J.-M. Defise, L. K. Harra, U. Schühle, and the EUI Team: EUI, the ultraviolet imaging telescopes of Solar Orbiter. Second Solar Orbiter Workshop, Athens, Greece, October 16-20, 2006. (Oral).

**Hoekzema, N. M.**, K. Gwinner, W. J. Markiewicz, B. Grieger, G. Portyankina, H. U. Keller, H. Hoffmann, J. A. Meima, and G. Neukum: The dust scale height of the Martian atmosphere around Pavonis Mons from HRSC stereo images. European Planetary Science Congress 2006, Berlin, Germany, September 18-22, 2006. (Oral).

**Hoekzema, N. M.**, K. Gwinner, W. J. Markiewicz, B. Grieger, G. Portyankina, H. U. Keller, H. Hoffmann, J. A. Meima, and G. Neukum: The dust scale height of the Martian atmosphere from HRSC stereo images. European Planetary Science Congress 2006, Berlin, Germany, September 18-22, 2006.

**Holzwarth, V.**: Magnetic activity of cool stars. Armagh Observatory, Armagh, Northern Ireland, October 25, 2006, invited talk.

**Holzwarth, V.**: Magnetic flux emergence in fast rotating stars. Coronae of Stars and Accretion Disks, Bonn, Germany, December 12-13, 2006, (invited review).

**Holzwarth, V.** and M. Jardine: Mass loss rates and wind ram pressures of cool stars. Kiepenheuer-Institut für Sonnenphysik, Freiburg/Brsg., Germany, September 21, 2006. (Oral).

**Holzwarth, V.** and M. Jardine: Mass loss rates and wind ram pressures of cool stars. Modern Solar Facilities - Advanced Solar Science, Göttingen, Germany, September 27-29, 2006. (Poster).

**Holzwarth, V.** and M. Jardine: Mass loss rates and wind ram pressures of cool stars. $14^{th}$ Cambridge workshop on Cool Stars, Stellar Systems, and the Sun, Pasadena, CA, USA, November 6-10, 2006. (Poster).

Innes, D., T. J. Wang, S. K. Solanki, and D. Tothova: Microflares and loop oscillations. SOHO-17: 10

Years of SOHO and Beyond, Gardini Naxos, Sicily, Italy, May 7-12, 2006. (Poster).

**Jackiewicz, J.** and L. Gizon: Helioseismic inversion of f-mode travel times for the study of near-surface flows. Workshop "Modern Solar Facilities - Advanced Solar Science", Göttingen, Germany, September 27-29, 2006. (Poster).

Jackiewicz, J. and L. Gizon: Inversion of f-mode travel times for flows. SOHO-18 / GONG 2006 /HELAS-I Conference, Sheffield, UK, August 7-11, 2006. (Poster).

Jackiewicz, J., L. Gizon, and A. Birch: Sensitivity of solar f-mode travel times to internal flows. SOHO-17: 10 Years of SOHO and Beyond, Giardini Naxos, Sicily, Italy, May 7-12, 2006. (Poster).

**Jackiewicz, J.**, Y. Saidi, A. Birch, L. Gizon, and M. Roth: Travel-time sensitivity kernels and calculating them on the web. First HELAS Local Helioseismology Workshop "Roadmap for European Local Helioseismology", Nice, France, September 25-27, 2006. (Oral).

**Jackiewicz, J. A.** and L. Gizon: Sensitivity of travel-times to flows on the solar surface. HMI/AIA Science Teams Meeting, Monterey, CA, USA, February 13-17, 2006. (Poster).

**Jones, G.**: Enceladus's varying imprint on the magnetosphere of Saturn. Seminar, Mullard Space Science Laboratory, University College London, Holmbury St. Mary, UK, February 7, 2006. (Oral).

**Jones, G. H.**, N. Krupp, H. Krüger, E. Roussos, W. Ip, D. G. Mitchell, S. M. Krimigis, J. Woch, A. Lagg, M. Fränz, M. K. Dougherty, C. Arridge, and H. J. McAndrews: A new spoke formation model. AGU Fall Meeting, San Francisco, USA, December 11-14, 2006. (Oral).

**Jones, G. H.**, E. Roussos, N. Krupp, A. Lagg, J. Woch, and the Cassini MIMI team: The interaction of Rhea with Saturn's magnetosphere. European Planetary Science Congress 2006, Berlin, Germany, September 18-22, 2006. (Oral).

Jones, G. H., E. Roussos, **N. Krupp**, C. Paranicas, W.-H. Ip, and H. J. McAndrews: The energetic particle signatures of Saturn's G ring. 36th COSPAR Scientific Assembly, Beijing, China, July 16-23, 2006. (Oral).

**Jones, G. H.**, E. Roussos, N. Krupp, C. Paranicas, D. G. Mitchell, S. M. Krimigis, J. Woch, and A. Lagg: The energetic charged particle environment of Saturn's rings. General Assembly of the European Geosciences Union, Vienna, Austria, April 2-7, 2006. (Poster).

**Kaeufl, H. U.**, I. Saviane, V. Ivanov, T. Bonev, H. Boehnhardt, and R. Siebenmorgen: First results from the analysis of the serendipitious occultation of a field-star by the inner coma of 9P/Tempel 1. Deep Impact as a World Observatory Event, Brussels, Belgium, August 7-10, 2006. (Oral).

**Kallenbach, R.** and M. Hilchenbach: The injection problem at the solar wind termination shock. 5th Annual International Astrophysics Conference, The Physics of the Inner Heliosheath: Voyager Observations, Theory, and Future Prospects, Honolulu, Hawaii, USA, March 3-9, 2006, invited. (Oral).

Kaydash, V., **U. Mall**, and E. Vilenius: Estimating the spectral slope of the lunar Reiner Gamma swirl feature using measurements made by the SMART-1 near-infrared spectrometer SIR. European Planetary Science Congress 2006, Berlin, Germany, September 18-22, 2006. (Oral).

**Keller, H. U.**: Comet observations by OSIRIS onboard the Rosetta spacecraft. IAU XXVIth General Assembly, Prague, Czech Republic, August 14-25, 2006. (Oral).

**Keller, H. U.**: Cometary nuclei - what have we learned from the flybys? Workshop "From Dust to Planetesimals", Ringberg Castle, Germany, September 11-15, 2006.

**Keller, H. U.**: Comparison of the 4 cometary nuclei imaged by space missions: recent observations of cometary nuclei by the various space missions. IAU XXVIth General Assembly, Prague, Czech Republic, August 14-25, 2006. (Oral).

**Keller, H. U.**: Nature and physics of cometary nuclei. Kobe University Planetary School 2006, Kobe, Japan, December 4-6, 2006. (Oral).

**Keller, H. U.**, B. Grieger, S. Schröder, M. Tomasko, and the DISR Team: Titan's surface - illumination and reflection function. Planetary Science: challenges and discoveries, Blois, France, May 28 - June 2, 2006. (Oral).

**Keller, H. U.**, P. Hartogh, and W. J. Markiewicz: Mars atmospheric explorer. DLR "Exploration unseres Sonnensystems", Dresden, Germany, November 21-22, 2006. (Oral).

**Keller, H. U.**, M. Küppers, M. Rengel, S. Fornasier, G. Cremonese, P. Gutierrez, W. H. Ip, J. Knollenberg, and L. Jorda: Observations of comet 9P/Tempel 1 around the Deep Impact event with the OSIRIS cameras on Rosetta. 36th COSPAR Scientific Assembly, Beijing, China, July 16-23, 2006. (Oral).

**Keller, H. U.**, M. Küppers, M. Rengel, P. Gutierrez, S. Hviid, and S. Lowry: Monitoring of Comet 9P/Tempel around the Deep Impact event with the OSIRIS NAC camera. IAU XXVIth General Assembly, Prague, Czech Republic, August 14-25, 2006. (Poster).

**Keller, H. U.**, U. Mall, and A. Nathues: SIR - a NIR spectrometer for studying the lunar mineralogy. 36th COSPAR Scientific Assembly, Beijing, China, July 16-23, 2006. (Oral).

**Keller, H. U.**, W. J. Markiewicz, S. Hviid, M. T. Lemmon, P. H. Smith, R. V. Morris, and P. S. Team: The Robotic Arm Camera (RAC). Fourth Mars Polar Science Conference 2006, Davos, Switzerland, October 2-6, 2006. (Oral).

Keller, H. U., **M. Rengel**, M. Küppers, P. Gutierrez, S. Hviid, and S. Lowry: Monitoring of Comet 9P/Tempel 1 around the Deep Impact event with the OSIRIS NAC camera. IAU XXVIth General Assembly, Prague, Czech Republic, August 14-25, 2006. (Poster).

**Keller, H. U.**, A. Rodin, Y. Skorov, B. Grieger, and M. Tomasko: Microphysical transition of tolin aerosols in Titan atmosphere. AGU Fall Meeting, San Francisco, USA, December 11-14, 2006. (Oral).

Keller, H. U., A. V. Rodin, **Yu. V. Skorov**, B. Grieger, and M. J. Tomasko: Microphysical transition of tholin aerosols below Titan tropopause. European Planetary Science Congress 2006, Berlin, Germany, September 18-22, 2006. (Oral).

**Kistler, L. M.**, B. Klecker, C. W. Carlson, A. Korth, M. McCarthy, R. Lundin, and A. Balogh: Kelvin-Helmholtz instability on the dusk magnetopause. Cluster CIS observations. General Assembly of the European Geosciences Union, Vienna, Austria, April 2-7, 2006. (Poster).

**Koch, C.**, U. Christensen, and M. Hilchenbach: Determining Mercury's tidal love number and libration with laser altimetry. European Planetary Science Congress 2006, Berlin, Germany, September 18-22, 2006. (Oral).

**Koch, C.**, U. R. Christensen, and M. Hilchenbach: Determining Mercury's tidal love number and libration with laser altimetry. Deutscher Geodynamik Workshop 2006, Max-Planck-Institut für Sonnensystemsforschung, Katlenburg-Lindau, Germany, September 27-28, 2006. (Oral).

**Korokhin, V. V.**, Yu. G. Shkuratov, D. G. Stankevich, C. Pieters, and U. Mall: Artificial neural networks as a tool for prognosis of chemical and mineral composition of lunar soils from spectral measurements. 37th Lunar and Planetary Science Conference, League City, TX, USA, March 13-17, 2006. (Oral).

**Korth, A.**: Complex organic molecules in the coma of comet Halley. Measurements with the RPA-2/PICCA instrument onboard Giotto. 20 years Giotto flyby at comet Halley, ESTEC, The Netherlands, March 13, 2006. (Oral).

**Korth, A.**: Respective substorms during corotating interaction events. Workshop on Storm-Substorm Relations, Banff, Canada, March 24-25, 2006. (Oral).

**Korth, A.**, E. Echer, Q.-G. Zong, M. Fränz, W. D. Gonzalez, F. L. Guarnieri, S. Y. Fu, and H. Rème: Cluster observations of $O^+$ escape into the magnetotail in comparison with the ring current input rate during an intense magnetic storm. General Assembly of the European Geosciences Union, Vienna, Austria, April 2-7, 2006. (Poster).

**Korth, A.**, M. Fränz, E. Echer, F. Guarnieri, R. Friedel, and H. Rème: Cluster plasma sheet observations and injections at geosynchronous orbit during corotating high speed streams. 8th International Conference on Substorms, Banff, Canada, March 28-31, 2006. (Poster).

**Kossacki, K. J.**, W. J. Markiewicz, G. Portyankina, and G. Neukum: Conditions for water ice accumulation within craters on Mars. Fourth International Conference on Mars Polar Science and Exploration, Davos, Switzerland, October 2-6, 2006. (Oral).

**Krieger, L.**, M. Roth, and O. v. d. Lühe: Estimation of the meridional circulation via Fourier-Hankel. First HELAS Local Helioseismology Workshop "Roadmap for European Local Helioseismology", Nice, France, September 25-27, 2006. (Oral).

**Krivova, N.**: Solar irradiance variability of relevance for climate studies. AWI/IUP Blockseminar "Solar variability - climate interaction", Bremen, Germany, February 13, 2006, invited.

**Krivova, N.**: Solar magnetism and irradiance variability. Colloquium, Astrophysikalisches Institut Potsdam, Germany, April 7, 2006, invited.

**Krivova, N. A.**: MILLENNIUM project: Solar forcing. The 4th Annual COSMOS Meeting 2006, Lüneburg, Germany, May 29-31, 2006, invited.

**Krivova, N. A.**, S. K. Solanki, and T. Wenzler: Reconstruction of solar UV irradiance since 1974. 2nd International Symposium on Space Climate, Sinaia, Romania, September 13-16, 2006. (Poster).

**Kronberg, E.**, J. Woch, K.-H. Glassmeir, N. Krupp, and A. Lagg: The Magnetospheric dynamics: Periodic substorms at Jupiter and Earth. European Planetary Science Congress 2006, Berlin, Germany, September 18-22, 2006. (Oral).

**Kronberg, E. A.**, J. Woch, K.-H. Glassmeier, N. Krupp, and A. Lagg: The magnetospheric dynamics: Periodic substorms and Jupiter and Earth. 36th COSPAR Scientific Assembly, Beijing, China, July 16-23, 2006. (Oral).

**Kronberg, E. A.**, J. Woch, N. Krupp, A. Lagg, and H.-K. Glassmeier: Comparison of the mass-release processes at Jupiter and Earth. 36th COSPAR Scientific Assembly, Beijing, China, July 16-23, 2006. (Poster).

**Kronberg, E. A.**, J. Woch, N. Krupp, A. Lagg, and K.-H. Glassmeier: Comparison periodic substorms at Jupiter and Earth. European Planetary Science Congress 2006, Berlin, Germany, September 18-22, 2006. (Oral).

**Krueger, H.**: Astronomische Beobachtungsmethoden - die Brille der Astronomen. Volkshochschule Mosbach/Baden, Germany, Binau am Neckar, November 17, 2006. (Oral).

**Krueger, H.**: Cosmic dust - a tool to study astrophysical processes. Astrophysikalisches Kolloquium, Astrophysikalisches Institut der Universität Göttingen, Germany, February 16, 2006. (Oral).

**Krueger, H.**: Dust streams emanating from the volcanoes of Jupiter's moon Io. Geophysics Institute of the Autonomous National University of Mexico (UNAM), Mexico-City, October 19, 2006. (Oral).

**Krueger, H.**: Extrasolare Planeten - Welten um andere Sonnen. Volkshochschule Mosbach, Aussenstelle Binau, Binau/Neckar, Germany, May 12, 2006. (Oral).

**Krueger, H.**: In-situ spacecraft monitoring of the interstellar dust stream in the solar system. COSMIC DUNE Workshop, ESA/ESTEC Noordwijk, The Netherlands, February 23, 2006. (Oral).

**Krueger, H.**: Staubteilchen - Boten ferner Welten. Abendvortrag zum Tag der Ideen, MPS Katlenburg-Lindau, Germany, March 30, 2006. (Oral).

**Krueger, H.**, N. Altobelli, E. Gruen, S. Kempf, M. Landgraf, R. Srama, S. Helfert, and G. Moragas-Klostermeyer: In-situ monitoring of interstellar dust in the solar system. European Planetary Science Congress 2006, Berlin, Germany, September 18-22, 2006. (Oral).

**Krueger, H.**, N. Altobelli, E. Grün, S. Kempf, M. Landgraf, R. Srama, S. Helfert, and G. Moragas-Klostermeyer: Interstellar dust in the solar system. Symposium "Composition of Matter" held in honour of Johannes Geiss's 80th birthday, Grindelwald, Switzerland, September 11-15, 2006. (Oral).

**Krueger, H.**, C. Engrand, H. Fischer, M. Hilchenbach, K. Hornung, J. Kissel, T. Stephan, L. Thirkell, M. Trieloff, R. Thomas, C. Tubiana, and K. Varmuza: Rosetta/COSIMA: high resolution in-situ dust analysis at comet 67P/Churyumov-Gerasimenkov. Annual Meeting of the Division for Planetary Sciences of the American Astronomical Society, Pasadena, CA, USA, October 08-13, 2006. (Poster).

**Krueger, H.**, A. L. Graps, D. P. Hamilton, A. Flandes, and E. Gruen: Ulysses Jovian latitude scan of high-velocity dust streams originating from the Jovian system. 36th COSPAR Scientific Assembly, Beijing, China, July 16-23, 2006. (Poster).

**Krueger, H.**, A. L. Graps, M. Landgraf, D. P. Hamilton, A. Flandes, E. Gruen, and the Ulysses Dust Science Team: In-situ dust measurements from Ulysses' second solar orbit. EGU General Assembly 2006, Vienna, Austria, April 02-07, 2006. (Oral).

**Krueger, H.**, S. Kempf, A. Graps, D. P. Hamilton, A. Flandes, and E. Gruen: High-velocity electromagnetically interacting dust streams at Jupiter: the Ulysses perspective. Annual Meeting of the Division for Planetary Sciences of the American Astronomical Society, Pasadena, CA, USA, October 08-13, 2006. (Oral).

**Krupp, N.**: Cassini/Huygens - Ein Resümee nach zwei Jahren im Saturnsystem. Vortragsreihe "Faszinierendes Weltall" des Förderkreises Planetarium Göttingen, Universität Göttingen, Germany, November 14, 2006. (Oral).

**Krupp, N.**: Jupiter's magnetosphere after Galileo, Saturn's magnetosphere after 2 years of Cassini in orbit: Highlights and open questions? European Planetary Science Congress 2006, Berlin, Germany, September 18-22, 2006. (Oral).

**Krupp, N.**: Key science objectives and measurements for magnetospheric science. ESA-NASA Joint working group on a Europa-Jupiter mission, Meeting #3, ESA headquarters, Paris, France, April 10-12, 2006. (Oral).

**Krupp, N.**: Planetary auroae and their electrodynamic drivers: Solar wind vs. internal processes. European Planetary Science Congress 2006, Berlin, Germany, September 18-22, 2006. (Oral).

**Krupp, N.**: Science cases for the Europlanet discipline working group #2: Magnetospheres and plasmas. Europlanet N2-N7 workshop, ESAC, Villafranca, Madrid, Spain, April 24-26, 2006. (Oral).

**Krupp, N.**: The magnetospheres of Jupiter and Saturn after Galileo and 2 years of Cassini: Highlights and open questions. AGU Fall Meeting, San Francisco, USA, December 11-14, 2006, invited. (Oral).

**Krupp, N.** and M. Blanc: Saturn's magnetosphere: a comparative planetology perspective. 36th COSPAR Scientific Assembly, Beijing, China, July 16-23, 2006, invited. (Oral).

**Krupp, N.**, A.-M. Harri, and B. Grieger: Europlanet activity N2 (Discipline Working Groups) status report. Europlanet Coordinator Meeting, ESA Headquarters, Paris, France, May 22-23, 2006. (Oral).

**Krupp, N.**, G. H. Jones, E. Roussos, A. J. Coates, M. K. Dougherty, D. A. Gurnett, C. J. Hansen, A. Hendrix, K. Khurana, S. M. Krimigis, W. Kurth, H. Krüger, H. J. McAndrews, D. G. Mitchell, C. Paranicas, J. Saur, D. F. Strobel, and J. Wahlund: The interaction of Rhea with Saturn's magnetosphere. AGU Fall Meeting, San Francisco, USA, December 11-14, 2006. (Oral).

**Krupp, N.**, G. H. Jones, E. Roussos, A. Lagg, D. G. Mitchell, S. M. Krimigis, H. McAndrews, C. Arridge, M. K. Dougherty, and W. Kurth: The Saturnian magnetosphere after two years of Cassini in situ results. European Planetary Science Congress 2006, Berlin, Germany, September 18-22, 2006. (Oral).

**Krupp, N.**, G. H. Jones, E. Roussos, A. Lagg, J. Woch, D. G. Mitchell, S. M. Krimigis, C. Arridge, H. McAndrews, and W. Kurth: Particles and fields in Saturn's magnetosphere: Cassini results after 2 years in orbit. 36th COSPAR Scientific Assembly, Beijing, China, July 16-23, 2006. (Oral).

**Küppers, M.**: Neues von Tempel 1: Deep Impact und Rosetta. Erweitertes Abteilungsseminar, Abteilung Asteroiden und Kometen, DLR, Berlin, Germany, Sep 29, 2006. (Oral).

**Küppers, M.**: Sungrazers: Kometen, die der Sonne zu nah kommen. Jubiläumsfeier "20 Jahre Giotto", Max-Planck-Institut für Sonnensystemforschung, Katlenburg-Lindau, Germany, April 6, 2006. (Oral).

**Küppers, M.**: Surfaces in the solar system. Institut für Weltraumforschung, Österreichische Akademie der Wissenschaften, Graz, Österreich, November 14, 2006. (Oral).

**Küppers, M.**, M. Drahus, P. Hartogh, C. Jarchow, L. Paganini, and G. Villanueva: Observations of split comet 73P/Schwassmann-Wachmann with the Submillimeter Telescope (SMT). Asia Oceania Geosciences Society, 3rd annual meeting, Singapore, July 10-14, 2006. (Oral).

**Küppers, M.**, H. U. Keller, S. F. Hviid, S. Mottola, S. Fornasier, C. Barbieri, M. A. Barucci, P. Gutiérrez, P. Lamy, and The OSIRIS Team: Determination of the light curve of Rosetta target asteroid 2867 Steins with the OSIRIS Narrow Angle Camera onboard Rosetta. Division of Planetary Sciences of the American Astronomical Society, Pasadena, CA, USA, October 8-13, 2006. (Poster).

**Küppers, M.**, H. U. Keller, and the OSIRIS Team: Observations of comet 9P/Tempel 1 around the Deep Impact event by the OSIRIS cameras onboard Rosetta. Deep Impact as a world observatory event, Brussels, Belgium, August 7-10, 2006. (Oral).

**Kuroda, T.**, A. S. Medvedev, P. Hartogh, and M. Takahashi: Seasonal changes in baroclinic wave activity simulated with a general circulation model of the Martian atmosphere. European Planetary Science Congress 2006, Berlin, Germany, September 18-22, 2006.

**Lagg, A.**: Chromospheric and coronal magnetic field measurements. IAUS 233 - Solar Activity and its Magnetic Origin, Cairo, Egypt, March 31 - April 4, 2006, invited review. (Oral).

**Lagg, A.**: New insights into chromospheric structures from vector magnetic field measurements. 36th COSPAR Scientific Assembly, Beijing, China, July 16-23, 2006, invited. (Oral).

**Lara, L. M.**, H. Boehnhardt, P. J. Gutierrez, M. J. Vidal-Nunez, and R. Rodrigo: Eight months spying comet 9P/Tempel 1, the Deep Impact Target. Deep Impact as a World Observatory Event, Brussels, Belgium, August 7-10, 2006. (Oral).

Loukitcheva, M. A., S. K. Solanki, and S. White: Chromospheric oscillations from millimeter observations. SOHO-17: 10 Years of SOHO and Beyond, Gardini Naxos, Sicily, Italy, May 7-12, 2006. (Poster).

**Mall, U.**: From Technology to Science, SIR on ESAs SMART-1 Mission. Workshop on Space Technologies STW-2006, Polish Academy of Science, Krakow, Poland, 2006. (Oral).

**Mall, U.**: Weitere Mondmissionen? DLR Workshop Exploration unseres Sonnensystems, Dresden, Germany, 2006. (Oral).

**Mall, U.**, A. Nathues, H. U. Keller, E. Vilenius, V. Kaydash, and the SIR collaboration: The near-infrared spectrometer SIR and SIR-2 on SMART-1 and Chandrayaan-1. European Planetary Science Congress 2006, Berlin, Germany, September 18-22, 2006. (Oral).

**Maltagliati, L.**, D. Titov, T. Encrenaz, R. Melchiorri, J.-P. Bibring, H. U. Keller, and M. Garcia-Comas: Atmospheric water in the vicinity of Tharsis volcanoes from OMEGA/MEx. European Planetary Science Congress 2006, Berlin, Germany, September 18-22, 2006. (Oral).

Markiewicz, W. J., **H. U. Keller**, and The VMC Team: First results from Venus Monitoring Camera on Venus Express. 36th COSPAR Scientific Assembly, Beijing, China, July 16-23, 2006.

**Markiewicz, W. J.**, K. J. Kossacki, G. Portyankina, M. Garcia-Comas, H. U. Keller, and G. Neukum: Conditions for water ice accumulation within craters on Mars. European Planetary Science Congress 2006, Berlin, Germany, September 18-22, 2006. (Oral).

**Markiewicz, W. J.**, K. J. Kossacki, G. Portyankina, M. Garcia-Comas, H. U. Keller, G. Neukum, and J. P. Bibring: Conditions for water ice accumulation within craters on Mars. 36th COSPAR Scientific Assembly, Beijing, China, July 16-23, 2006.

Markiewicz, W. J., K. J. Kossacki, G. Portyankina, **H. U. Keller**, and G. Neukum: Conditions for water ice accumulation within craters on Mars. 36th COSPAR Scientific Assembly, Beijing, China, July 16-23, 2006. (Oral).

**Markiewicz, W. J.** and the VMC Team: First Results from Venus Monitoring Camera on Venus Express. European Planetary Science Congress 2006, Berlin, Germany, September 18-22, 2006.

**Markiewicz, W. J.** and the VMC Team: First Results from Venus Monitoring Camera on Venus Express. 36th COSPAR Scientific Assembly, Beijing, China, July 16-23, 2006.

**Marsch, E.**: Coronal origins of the solar wind - sources of steady streams and transient flows caused by solar magnetic eruptions. International Living With a Star Workshop, Goa, India, February 19 - 24, 2006. (Oral).

**Marsch, E.**: Diffusion plateaus and temperature anisotropies of proton velocity distributions in fast solar wind. Schloss Ringberg Theory Meeting of the Max Planck Institute for Plasma Physics, Schloss Ringberg, Tegernsee, Germany, November 13-17, 2006, invited. (Oral).

**Marsch, E.**: Origin and evolution of the solar wind. Solar Activity and its Magnetic Origin, International Astronomical Union, IAU Symposium 233, Cairo, Egypt, March 31 - April 4, 2006, invited. (Oral).

**Marsch, E.**: Origin and evolution of the solar wind and solar storms driven by magnetic eruptions. International Symposium on Recent Observations and Simulations of the Sun-Earth System (ISROSES), Varna, Bulgaria, September 17 - 22, 2006, invited. (Oral).

**Marsch, E.**: Status of knowledge after Helios, Ulysses and SOHO of the microstate of the coronal and solar-wind plasma. Second Solar Orbiter Workshop, Athens, Greece, October 16-20, 2006. (Oral).

Marsch, E. and **R. Schwenn**: KuaFu: A observations of mass supply to and loss from the solar corona. 36th COSPAR Scientific Assembly, Beijing, China, July 16-23, 2006. (Oral).

**Marsch, E.**, C.-Y. Tu, and J.-S. He: Study on plasma outflows and open magnetic field lines in a quiet-Sun region. SOHO 17: 10 Years of SOHO and Beyond, Giardini Naxos Sicily, Italy, 7-12 May, 2006. (Poster).

**Marsch, E.**, C.-Y. Tu, G.-Q. Zhou, and J.-S. He: On the structure of the solar transition region. SOHO 17: 10 Years of SOHO and Beyond, Giardini Naxos Sicily, Italy, 7-12 May, 2006. (Poster).

Marsch, E., L. Zhao, and **C.-Y. Tu**: Limits on the proton temperature anisotropy in the solar wind. 36th COSPAR Scientific Assembly, Beijing, China, July 16-23, 2006. (Oral).

Marsch, E., G.-Q. Zhou, J.-S. He, and **C.-Y. Tu**: Magnetic structure of the solar transition region as observed in various ultraviolet lines emitted at different temperatures. 36th COSPAR Scientific Assembly, Beijing, China, July 16-23, 2006. (Oral).

**Martinecz, C.**, M. Fraenz, E. Dubinin, E. Roussos, J. Woch, and the ASPERA Team: Plasma boundaries at Mars and Venus. Mars Workshop: Solar wind interaction and atmospheric evolution, IRF, Kiruna, Sweden, February 27 - March 1, 2006. (Poster).

**Martinecz, C.**, M. Fraenz, J. Woch, N. Krupp, E. Dubinin, E. Roussos, U. Motschmann, S. Barabash, R. Lundin, and the ASPERA-4 Team: Plasma boundaries around Venus. European Planetary Science Congress 2006, Berlin, Germany, September 18-22, 2006. (Oral).

**Martinecz, C.**, M. Fränz, J. Woch, N. Krupp, E. Dubinin, E. Roussos, U. Motschmann, S. Barabash, R. Lundin, and the ASPERA-4 Team: Bow shock and ion composition boundary fits at Venus. $15^{th}$ ASPERA-3 and $5^{th}$ ASPERA-4 project meeting, Kiruna, Sweden, October 8-10, 2006. (Oral).

**Martinecz, C.**, M. Fränz, J. Woch, N. Krupp, E. Dubinin, E. Roussos, U. Motschmann, S. Barabash, R. Lundin, and the ASPERA-4 Team: Plasma boundaries at Venus. European Planetary Science Congress 2006, Berlin, Germany, September 18-22, 2006. (Oral).

**Martinecz, C.**, M. Fränz, J. Woch, N. Krupp, E. Dubinin, E. Roussos, and the ASPERA Team: Plasma boundaries at Mars and Venus. Kiruna Mars Workshop, Kiruna, Sweden, February 27 - March 1, 2006. (Poster).

Mathew, S. K., V. Martinez Pillet, S. K. Solanki, and N. A. Krivova: Does the umbral brightness really change with solar cycle? SOHO-17: 10 Years of SOHO and Beyond, Gardini Naxos, Sicily, Italy, May 7-12, 2006. (Poster).

McComas, D. J., **M. I. Desai**, F. Allegrini, N. A. Schwadron, M. Berthomier, R. Bruno, and E. Marsch: The solar wind proton and alpha sensor for the Solar Orbiter. Second Solar Orbiter Workshop, Athens, Greece, October 16-20, 2006. (Oral).

**Medvedev, A. S.**, P. Hartogh, and T. Kuroda: Winter polar warmings and the meridional transport on Mars simulated with a general circulation model. EGU General Assembly, Vienna, Austria, April 2-7, 2006. (Oral).

**Medvedev, A. S.**, P. Hartogh, T. Kuroda, and R. Saito: Winter polar warmings and the meridional transport on Mars simulated with MAOAM. 4th MATSUP Workshop - Atmosphere and Surface Processes, Göttingen, Germany, March 23-24, 2006. (Oral).

**Medvedev, A. S.**, P. Hartogh, T. Kuroda, R. Saito, A. Feofilov, and A. Kutepov: A new general circulation model of the Martian atmosphere: description and first results. Second Mars Atmosphere Modelling and Observations Workshop, Granada, Spain, February 27 - March 3, 2006. (Oral).

**Middleton, K.**, V. Da Deppo, L. Poletto, U. Schühle, R. J. Thomas, and P. R. Young: Optical Design of the Extreme Ultravioletspectrometer (EUS) on Board Solar Orbiter. Second Solar Orbiter Workshop, Athens, Greece, October 16-20, 2006. (Poster).

**Mitchell, D. G.**, P. C. Brandt, J. F. Carbary, S. M. Krimigis, B. H. Mauk, C. P. Paranicas, and N. Krupp: Comparison of rotation-driven modulation of trapped energetic particles in Saturn's and Jupiter's magnetosphere. AGU Fall Meeting, San Francisco, USA, December 11-14, 2006. (Oral).

**Moissl, R.**, W. Markiewicz, D. Titov, P. Russo, H.-U. Keller, N. Ignatiev, and S. Limae: Observations of the global dynamics in the Venus upper cloud deck by the Venus Monitoring Camera onboard Venus Express. European Planetary Science Congress 2006, Berlin, Germany, September 18-22, 2006. (Oral).

**Moissl, R.**, W. J. Markiewicz, D. V. Titov, P. Russo, H. U. Keller, N. I. Ignatiev, and S. S. Limaye: Observations of global dynamics in the Venus upper cloud deck by Venus Monitoring Camera. European Planetary Science Congress 2006, Berlin, Germany, September 18-22, 2006.

Mühlbachler, S., **L. Chen**, S. Imada, P. Puhl-Quinn, B. Lefebvre, A. Bhattacharjee, P. Daly, and E. Georgescu: Electron acceleration by impulsive reconnection near separatrices: Cluster observations. AGU Fall Meeting, San Francisco, USA, December 11-14, 2006.

**Mühlbachler, S.**, D. Langmayr, A. T. Y. Lui, N. V. Erkaev, I. V. Alexeev, P. W. Daly, and H. K. Biernat: Cluster observations showing the indication of the formation of a modified-two-stream instability in the geomagnetic tail. 36th COSPAR Scientific Assembly, Beijing, China, July 16-23, 2006. (Poster).

**Mulligan, T.**, J. F. Fennell, J. L. Roeder, R. Friedel, T. A. Fritz, and P. Daly: Cluster/RAPID high energy particle observations within non-force-free flux ropes in the plasma sheet. General Assembly of the European Geosciences Union, Vienna, Austria, April 2-7, 2006. (Poster).

**Muñoz, G.** and R. Schwenn: Radial speed for slow CMEs. 36th COSPAR Scientific Assembly, Beijing, China, July 16-23, 2006. (Oral).

**Paganini, L.**, P. Hartogh, and C. Jarchow: Description of a new 400 MHz bandwidth chirp transform sprectrometer. Asia Oceania Geosciences Society, 3rd Annual Meeting, Singapore, July 10-14, 2006. (Oral).

**Panov, E. V.**, J. Büchner, M. Fränz, A. Korth, K.-H. Fornaçon, I. Dandouras, and H. Rème: Cluster spacecraft observations of current sheets at the Earths magnetopause. Frühjahrstagung des Fachverbands Extraterrestrische Physik der Deutschen Physikalischen Gesellschaft, Heidelberg, Germany, March 13-16, 2006. (Poster).

Panov, E. V., **J. Büchner**, M. Fränz, A. Korth, S. P. Savin, K.-H. Fornaçon, I. Dandouras, and H. Rème: Macroscopic properties of current sheets at the high-latitude Earth's magnetopause. 36th COSPAR Scientific Assembly, Beijing, China, July 16-23, 2006. (Poster).

Panov, E. V., **J. Büchner**, M. Fränz, A. Korth, S. P. Savin, K.-H. Fornaçon, I. Dandouras, and H. Rème: Magnetopause transport due to electromagnetic plasma waves near the ion-cyclotron frequency. 36th COSPAR Scientific Assembly, Beijing, China, July 16-23, 2006. (Oral).

**Paranicas, C.**, D. G. Mitchell, S. M. Krimigis, D. C. Hamilton, S. Christon, T. P. Armstrong, N. Krupp, E. Roussos, G. Jones, and R. E. Johnson: Charged particle weathering of Saturns satellites. Joint Assembly of the AGU, GS, MB, MSA, SEG, Baltimore, USA, May 23-26, 2006. (Oral).

**Paranicas, C.**, D. G. Mitchell, E. C. Roelof, B. H. Mauk, N. Krupp, S. M. Krimigis, P. C. Brandt, and F. S. Turner: Source mechanism for energetic electrons at Saturn. AGU Fall Meeting, San Francisco, USA, December 11-14, 2006. (Oral).

**Portyankina, G.**, W. J. Markiewicz, M. Garcia-Comas, H. U. Keller, J. P. Bibring, and G. Neukum: Simulations of Geyser-type Eruptions in cryptic Region of Martian South Polar Cap. Fourth Mars Polar Science Conference 2006, Davos, Switzerland, October 2-6, 2006. (Oral).

**Portyankina, G.**, W. J. Markiewicz, A. Inada, K. Gwinner, H. U. Keller, and G. Neukum: Altitudes of lee wave clouds as estimated from HRSC stereo images. European Planetary Science Congress 2006, Berlin, Germany, September 18-22, 2006. (Oral).

Preusse, S., **A. Kopp**, J. Büchner, and U. Motschmann: Interaction between hot Jupiters and their central stars. Frühjahrstagung des Fachverbands Extraterrestrische Physik der Deutschen Physikalischen Gesellschaft, Heidelberg, Germany, March 13-16, 2006. (Poster).

**Protopapa, S.**, T. Herbst, H. Boehnhardt, E. Gruen, W. M. Grundy, J. A. Spencer, and A. Stern: J to M band spectroscopy of Pluto and Charon. Transneptunian Objects - Dynamical and Physical Properties, Catania, Italy, July 3-7, 2006. (Oral).

**Radioti, A.**, N. Krupp, J. Woch, A. Lagg, and K.-H. Glassmeier: Temporal variability of the ion abundance ratios in the Jovian magnetosphere. 36th COSPAR Scientific Assembly, Beijing, China, July 16-23, 2006. (Oral).

**Radioti, A.**, J. Woch, E. Kronberg, N. Krupp, K.-H. Glassmeier, and A. Lagg: Energetic particle composition during substorm-like events in the Jovian magnetosphere. 36th COSPAR Scientific Assembly, Beijing, China, July 16-23, 2006. (Poster).

Raouafi, N.-E. and S. K. Solanki: Large temperature anisotropies in polar coronal holes: How reliable are they? SOHO-17: 10 Years of SOHO and Beyond, Gardini Naxos, Sicily, Italy, May 7-12, 2006. (Poster).

**Remizov, A.**, I. Apathy, H. U. Auster, M. Hilchenbach, H. Rosenbauer, and G. Berghofer: Capabilities of the plasma monitor onboard the Rosetta Lander. General Assembly of the European Geosciences Union, Vienna, Austria, April 2-7, 2006. (Poster).

**Rengel, M.**, K. Hodapp, and J. Eislöffel: SK 1: a possible case of trigerred star formation in Perseus. IAU XXVIth General Assembly, Prague, Czech Republic, August 14-25, 2006. (Oral).

**Rengel, M.**, M. Küppers, H.-U. Keller, and P. Gutierrez: Analysing the post Deep Impact brightness distribution of the cometary dust of the comet 9P/Tempel 1 with OSIRIS. General Assembly of the European Geosciences Union, Vienna, Austria, April 2-7, 2006. (Oral).

**Rengel, M.**, M. Küppers, H. U. Keller, and P. Gutierrez: Modeling of the terminal velocities of the dust ejected material by the impact. Deep Impact as a world observatoty event, Brussels, Belgium, August 7-10, 2006. (Oral).

**Rengel, M.**, M. Küppers, H.-U. Keller, P. Gutierrez, and S. Hviid: A study of the velocities of the ejected dust and of the rotational variability of comet 9P/Tempel 1 around the Deep Impact event. DPS Meeting #38, Pasadena, CA, USA, October 8-13, 2006. (Oral).

Rodin, A. V., Y. V. Skorov, **B. Grieger**, S. Schröder, H. U. Keller, and M. G. Tomasko: Charging and coagulation processes in Titan tholin haze as inferred from Huygens/DISR spectrophotometry data. General Assembly of the European Geosciences Union, Vienna, Austria, April 2-7, 2006. (Poster).

**Roeder, J.**, J. Fennell, R. Friedel, M. Grande, and P. W. Daly: Energetic electron distributions at the dusk and dawn magnetotail flanks: Cluster RAPID observations. 36th COSPAR Scientific Assembly, Beijing, China, July 16-23, 2006. (Oral).

**Roeder, J. L.**, J. F. Fennell, T. L. Mulligan, and A. Korth: Field-aligned energetic electrons during the storm of July 24, 2004: Cluster RAPID observations. AGU Fall Meeting, San Francisco, USA, December 11-14, 2006. (Oral).

**Roth, M.**: HELAS - European Helio- and Asteroseismology Network. HELAS-Workshop "Future of Asteroseismology", Vienna, Austria, September 20-22, 2006, invited talk. (Oral).

**Roth, M.**: HELAS - European Helio- and Asteroseismology Network. First HELAS Local Helioseismology Workshop "Roadmap for European Local Helioseismology", Nice, France, September 25-27, 2006, invited talk. (Oral).

**Roth, M.**: Helioseismologie - Einblicke ins Innere der Sonne. Lehrerfortbildung auf dem Schauinsland Observatorium, Hofsgrund, Germany, October 7, 2006, invited talk. (Oral).

**Roth, M.**: Helioseismologie: Einblicke ins Innere der Sonne. Physik-Kolloquium der Universität Marburg, Marburg, Germany, December 12, 2006, invited talk. (Oral).

**Roth, M.**: Helioseismology at high resolution. Workshop "Modern Solar Facilities - Advanced Solar Science", Göttingen, Germany, September 27-29, 2006, invited talk. (Oral).

**Roth, M.**: New measurements of meridional circulation. ISSI Team Meeting, Bern, Switzerland, October 31, 2006, invited talk. (Oral).

**Roth, M.**: Report of the HELAS Project Scientist. 1st HELAS Board Meeting, Leuven University, Belgium, April 20-21, 2006. (Oral).

Roth, M., J. Beck, and L. Gizon: Helioseismic travel times from the MDI structure programme. SOHO-17: 10 Years of SOHO and Beyond, Giardini Naxos, Sicily, Italy, May 7-12, 2006. (Poster).

**Roth, M.**, J. G. Beck, and L. Gizon: Noise in helioseismic travel times. General Assembly of the European Geosciences Union, Vienna, Austria, April 2-7, 2006, invited. (Oral).

Roth, M., L. Gizon, and J. G. Beck: Helioseismic travel time measurements. Workshop "Modern Solar Facilities - Advanced Solar Science", Göttingen, Germany, September 27-29, 2006. (Poster).

**Roth, M.**, L. Gizon, and J. G. Beck: Travel time measurements. First HELAS Local Helioseismology Workshop "Roadmap for European Local Helioseismology", Nice, France, September 25-27, 2006, invited talk. (Oral).

Roth, M., L. Gizon, and A. C. Birch: Sensitivity kernels for helioseismic travel times in spherical geometry. SOHO 18 / GONG 2006 /HELAS I - Conference, Sheffield, UK, August 7-11, 2006. (Poster).

**Roth, M.**, O. v. d. Lühe, P. Pallé, M. Thompson, J. Christensen-Dalsgaard, M. Monteiro, L. Gizon, M. P. Di Mauro, C. Aerts, J. Daszynska, and T. Corbard: HELAS - European Helio- and Asteroseismology Network. SOHO-17: 10 Years of SOHO and Beyond, Giardini Naxos, Sicily, Italy, May 7-12, 2006, also given as a Poster. (Oral).

**Roth, M.**, O. v. d. Lühe, P. Pallé, M. Thompson, J. Christensen-Dalsgaard, M. Monteiro, L. Gizon, M. P. Di Mauro, C. Aerts, J. Daszynska, and T. Corbard: HELAS - European Helio- and Asteroseismology Network. SOHO 18 / GONG 2006 / HELAS I - Conference, Sheffield, UK, August 7-11, 2006, also given as a Project Report. (Poster).

Rother, M., K. Schlegel, **H. Lühr**, G. Lee, and M. Purucker: Statistical Properties of Intense, Small-Scaled Field-Aligned Currents at Auroral Latitudes. AGU Fall Meeting, San Francisco, USA, December 11-14, 2006. (Oral).

**Roussos, E.**: Interaction of weakly or non-magnetized bodies with their surrounding plasma environment: observations at Mars with Mars Express/ASPERA-3 and at the moons of Saturn with Cassini/MIMI-LEMMS experiments. Space physics course - seminar talk, University of Athens, Physics Department, December 20, 2006, (invited). (Oral).

**Roussos, E.**, M. Fränz, E. Dubinin, J. Woch, C. Martinecz, S. Barabash, R. Lundin, and the ASPERA-3 Team: Asymmetries in the Mars-solar wind interaction: MarsExpress ASPERA-3 observations. European Planetary Science Congress 2006, Berlin, Germany, September 18-22, 2006. (Oral).

**Roussos, E.**, N. Krupp, G. H. Jones, C. Paranicas, A. Lagg, J. Woch, D. G. Mitchell, S. M. Krimigies, and M. K. Dougherty: Icy moon absorption signatures reveal non-axisymmetric drift shells in the Saturnian radiation belts: implications for a magnetospheric electric field? European Planetary Science Congress 2006, Berlin, Germany, September 18-22, 2006. (Oral).

**Roussos, E.**, N. Krupp, G. H. Jones, C. Paranicas, D. G. Mitchell, S. M. Krimigis, U. Motschmann, M. K. Dougherty, A. Lagg, and J. Woch: Icy moon absorption signatures: Probes of Saturnian magnetospheric dynamics and moon activity. AGU Fall Meeting, San Francisco, USA, December 11-14, 2006, invited. (Oral).

**Roussos, E.**, N. Krupp, G. H. Jones, C. Paranicas, D. G. Mitchell, A. Lagg, J. Woch, and S. M. Krimigis: The inner Saturnian magnetosphere as revealed by Cassini/LEMMS moon absorption signature observations. General Assembly of the European Geosciences Union, Vienna, Austria, April 2-7, 2006. (Oral).

**Roussos, E.**, S. Simon, A. Bößwetter, U. Motschmann, M. Fränz, N. Krupp, J. Woch, and G. H. Jones: Interaction scenarios between Rhea and Saturn's magnetospheric plasma: a hybrid simulation approach. AGU Fall Meeting, San Francisco, USA, December 11-14, 2006. (Poster).

**Ruan, P.**, T. Wiegelmann, and B. Inhester: Modeling large scale coronal structures. Seminar, St. Andrews, Scotland, December 18, 2006. (Oral).

**Ruan, P.**, T. Wiegelmann, B. Inhester, S. Solanki, E. Marsch, and L. Feng: Modeling large scale coronal structures. 36th COSPAR Scientific Assembly, Beijing, China, July 16-23, 2006. (Poster).

**Russo, P.**, D. V. Titov, W. J. Markiewicz, R. Moissl, N. Ignatiev, H. U. Keller, D. Crisp, A. T. Basilevsky, and the VMC Team: Imaging of the Venus night side with the Venus Monitoring Camera onboard Venus Express. European Planetary Science Congress 2006, Berlin, Germany, September 18-22, 2006.

**Santolik, O.**, E. Macusova, D. A. Gurnett, J. S. Pickett, N. Cornilleau-Wehrlin, Y. de Conchy, K. H. Yearby, and P. W. Daly: Variability of amplitudes, polarization and propagation of whistler-mode chorus emissions measured by the Cluster and Double Star spacecraft. 36th COSPAR Scientific Assembly, Beijing, China, July 16-23, 2006. (Oral).

**Santolik, O.**, N. P. Meredith, P. W. Daly, D. A. Gurnett, J. S. Pickett, V. Y. Trakhtengerts, D. Winningham, A. Fazakerley, and N. Cornilleau-Wehrlin: Stability analysis of whistler-mode chorus using measurements of waves and particles on board the Cluster spacecraft. General Assembly of the European Geosciences Union, Vienna, Austria, April 2-7, 2006. (Oral).

**Santos, J.** and J. Büchner: Current concentrations above an active region before flare eruptions and CME release. CAWSES International Workshop on Space Weather Modeling, Yokohama, Japan, November 13-16, 2006. (Poster).

**Santos, J.** and J. Büchner: Determining the plasma flow from simulated photospheric magnetic fields. CAWSES International Workshop on Space Weather Modeling, Yokohama, Japan, November 13-16, 2006. (Poster).

Santos, J., **J. Büchner**, and H. Zhang: Physical modelling of the relationship between local and global structures of solar magnetic fields. 36th COSPAR Scientific Assembly, Beijing, China, July 16-23, 2006. (Poster).

**Sasso, C.**, A. Lagg, and S. Solanki: Observations and analysis of the full Stokes vector in a flaring region in the He I 1083.0 nm multiplet. The Physics of Chromospheric Plasmas, Coimbra, Portugal, October 9-13, 2006. (Oral).

**Sasso, C.**, A. Lagg, S. K. Solanki, R. Aznar Cuadrado, and M. Collados: Observations and analysis of the full Stokes vector in a flaring region in the HeI 1083.0 nm multiplet. Astromeeting, INAF - Osservatorio di Capodimonte, Italy, October 31, 2006. (Oral).

**Sasso, C.**, A. Lagg, S. K. Solanki, M. Collados, and R. Aznar Cuadrado: Multi-component analysis of a flaring region in the chromospheric He I 1083.0 nm triplet. IAU XXVIth General Assembly, Prague, Czech Republic, August 14-25, 2006. (Oral).

**Sasso, C.**, A. Lagg, S. K. Solanki, M. Collados, and R. Aznar Cuadrado: Spectropolarimetric observations of the flaring active region NOAA 10763 in the He I 10830 Å multiplet. Modern Solar Facilities - Advanced Solar Science, Göttingen, Germany, September 27-29, 2006. (Poster).

**Savin, S.**, E. Amata, J. Blecki, J. Büchner, E. Lucek, T. Passot, P. L. Sulem, and L. Zelenyi: Nonlinear structures in magnetosheath plasma jets with anomalous dynamic pressure. 36th COSPAR Scientific Assembly, Beijing, China, July 16-23, 2006. (Oral).

**Schippers, P.**, N. Andre, M. Blanc, S. Livi, I. Dandouras, L. K. Gilbert, A. J. Coates, G. R. Lewis, S. Maurice, A. M. Rymer, E. C. Sittler, N. Krupp, B. H. Mauk, F. J. Crary, D. T. Young, S. M. Krimigis, D. Santos-Costa, and S. Bolton: Analysis of inter-calibrated electron observations in Saturn's inner magnetosphere. General Assembly of the European Geosciences Union, Vienna, Austria, April 2-7, 2006. (Poster).

**Schlegel, K.**: URSI science in the humanosphere. Radio Science Symposium for A Sustainable Humanosphere, Kyoto University, Kyoto, Japan, March 20-21, 2006. (Oral).

**Schlegel, K.**: URSI Science in the Humanosphere . Radio Science Symposium for a Sustainable Humanosphere, Kyoto University, Japan, March 20-21, 2006.

**Schröder, S.**, S. Douté, H. U. Keller, and M. Tomasko: Reflectance properties of Titan's surface as determined by DISR. 36th COSPAR Scientific Assembly, Beijing, China, July 16-23, 2006. (Oral).

**Schröder, S.** and H. U. Keller: The reflectance spectrum of Titan's surface as determined by DISR. European Planetary Science Congress 2006, Berlin, Germany, September 18-22, 2006. (Oral).

**Schroeder, P.**, J. Luhmann, and R. Schwenn: In-situ data from Helios 1 and 2 on the web in preparation for STEREO. 36th COSPAR Scientific Assembly, Beijing, China, July 16-23, 2006.

**Schühle, U.**: Instrumental Approaches to achieve the measurements required for exploring the energetics, dynamics, and fine-scale structure of the Sun's magnetized atmosphere. Second Solar Orbiter Workshop, Athens, Greece, October 16-20, 2006. (Oral).

Schühle, U., S. K. Mathew, S. K. Solanki, and V. Martinez-Pillet: Space qualification of a thin wafer lithium niobate etalon for the Visible light Imager and Magnetograph (VIM). Second Solar Orbiter Workshop, Athens, Greece, October 16-20, 2006. (Poster).

Schühle, U., S. K. Mathew, M. Wedemeier, H. Hartwig, E. Ballesteros, V. Martinez Pillet, and S. K. Solanki: Space qualification of a thin wafer lithium niobate etalon for the Visible light Imager and Magnetograph (VIM). Second Solar Orbiter Workshop, Athens, Greece, October 16-20, 2006. (Poster).

Schühle, U., L. Teriaca, and W. Curdt: Design and expected efficiency of an imager and a spectrograph at the H I Lyman alpha line. Modern Solar Facilities - Advanced Solar Science, Göttingen, September 27-29, 2006. (Poster).

Schühle, U., H. Uhlig, W. Curdt, T. Feigl, A. Theissen, and L. Teriaca: Thin silicon carbide coating of the primary mirror of VUV imaging instruments for Solar Orbiter. Second Solar Orbiter Workshop, Athens, Greece, October 16-20, 2006. (Poster).

**Schunker, H.**, P. S. Cally, and D. C. Braun: Surface magnetic effects in helioseismology. First HELAS Local Helioseismology Workshop "Roadmap for European Local Helioseismology", Nice, France, September 25-27, 2006, invited talk. (Oral).

**Schüssler, M.**: Feuer und Eis: Ein Reise vom Zentrum der Sonne bis nach Grönland. Feldbergschule, Oberursel/Taunus, Germany, July 11, 2006. (Oral).

**Schüssler, M.**: Steuert die Sonne das Erdklima? Frühjahrstagung der Deutschen Physikalischen Gesellschaft, Heidelberg, Germany, March 14, 2006. (Oral).

**Schüssler, M.**: Steuert die Sonne das Erdklima? Loge "Georg zu den drei Säulen", Einbeck, Germany, April 20, 2006. (Oral).

**Schüssler, M.**, A. Vögler, and B. Beeck: Simulations of magneto-convection in a sunspot umbra. Modern Solar Facilities - Advanced Solar Science, Göttingen, Germany, September 27-29, 2006. (Oral).

**Schwenn, R.**: Ein neues Bild der Sonne: 10 Jahre SOHO. Festkolloquium "10 Jahre SOHO", Universität Kiel, Germany, July 10, 2006.

**Schwenn, R.**: Explosive events on the Sun and their effects on space weather near the Earth. IAU Symposium 233 on Solar Activity and its Magnetic Origin, Cairo, Egypt, March 31-April 3, 2006, invited review.

**Schwenn, R.**: Forecasting space weather KuaFu and the missing links in understanding Sun-Earth connections. Western Pacific Geophysics Meeting (WPGM), Beijing, China, July 24-27, 2006, invited.

**Schwenn, R.**: Giotto und der Halleysche Komet: 20 Jahre nach dem historischen Rendezvous. Jubiläumsfeier "20 Jahre Giotto", Max-Planck-Institut für Sonnensystemforschung, Katlenburg-Lindau, Germany, March 13, 2006, festvortrag.

**Schwenn, R.**: Space weather a new science discipline. Culture and Astronomy at the Bibliotheca Alexandrina, Alexandria, Egypt, March 26, 2006, invited review. (Oral).

**Schwenn, R.**: Why KuaFu? The missing links in understanding Sun-Earth connections. 36th COSPAR Scientific Assembly, Beijing, China, July 16-23, 2006, invited. (Oral).

**Schwenn, R.** and S. Martin: Space weather research: theory, modeling, and prediction II. Western Pacific Geophysics Meeting (WPGM), Beijing, China, July 24-27, 2006.

**Sergis, N.**, S. M. Krimigis, D. G. Mitchell, D. C. Hamilton, N. Krupp, B. H. Mauk, E. C. Roelof, and M. K. Dougherty: Ring current at Saturn; energetic particle pressures in Saturn's equatorial magnetosphere measured with Cassini/MIMI. AGU Fall Meeting, San Francisco, USA, December 11-14, 2006. (Poster).

**Skorov, Yu. V.**, H. U. Keller, and G. N. Markelov: Kinetic model of dusty atmosphere around cometary nucleus with topography. European Planetary Science Congress 2006, Berlin, Germany, September 18-22, 2006. (Poster).

**Solanki, S. K.**: Der Feuerball am Himmel und die Klimakatastrophe auf der Erde. 8. Ärztefortbildungskurs der Lungenliga Zürich, Lugano, Switzerland, September 28-30, 2006, invited.

**Solanki, S. K.**: Die Sonne - unser lebenspendender Stern. 19. Raumfahrt-Kolloquium der FH Aachen, Aachen, Germany, November 16, 2006, invited.

**Solanki, S. K.**: Global variations of the chromospheric irradiance. The Physics of Chromospheric Plasmas, Coimbra, Portugal, October 9-13, 2006, invited review.

**Solanki, S. K.**: How is the Suns magnetic field related to Einstein and climate? Kolloquium MPI für Dynamik komplexer technischer Systeme, Magdeburg, Germany, September 21, 2006.

**Solanki, S. K.**: Measured solar magnetic field and irradiance connection. STP-11 "Sun, Space Physics and Climate", Rio de Janeiro, Brazil, March 6-10, 2006, invited review.

**Solanki, S. K.**: Modelling the variability of solar irradiance. 2nd International Symposium on Space Climate, Sinaia, Romania, 13-16 September, 2006, invited review.

**Solanki, S. K.**: New directions in solar outer atmospheric diagnostics. ESF Workshop on Large Aperture Solar Telescopes, Monte Porzio Catone, Italy, April 10-12, 2006, invited review.

**Solanki, S. K.**: Quiet Sun magnetic fields. IAU XXVIth General Assembly, Prague, Czech Republic, August 14-25, 2006, invited.

**Solanki, S. K.**: Secular variations of solar activity and irradiance. AGU Fall Meeting, San Francisco, USA, December 11-14, 2006, invited.

**Solanki, S. K.**: Small-scale solar magnetic fields, Sunrise and solar irradiance variations. Kolloquium High Altitude Observatory, Boulder, USA, February 10, 2006, invited.

**Solanki, S. K.**: Sonnenaktivität und Klima. Forum Astronomie der Volkssternwarte Bonn, Bonn, Germany, November 2, 2006, invited.

**Solanki, S. K.**: Variations of solar irradiance. IAU XXVIth General Assembly, Prague, Czech Republic, August 14-25, 2006, invited.

**Solanki, S. K.**: Variations of the Sun's activity and brightness: are they causing global climate change? The Physics of Chromospheric Plasmas, Coimbra, Portugal, October 9-13, 2006, public lecture.

**Solanki, S. K.**: Was hat das Magnetfeld der Sonne mit Einstein und unserem Klima zu tun? Öffentliche Vorlesungsreihe Physik am Samstagmorgen der Fakultät für Physik der TU Braunschweig, Braunschweig, Germany, November 25, 2006, invited.

**Solanki, S. K.**: Was hat das solare Magnetfeld mit Einstein und dem Klima zu tun? Physikkolloquium der Universität Jena, Jena, Germany, January 16, 2006.

**Solanki, S. K.**: What happened to the Sun during the last 100 years? 2nd International Symposium on Space Climate, Sinaia, Romania, 13-16 September, 2006, invited talk.

**Solanki, S. K.** and N. A. Krivova: Modelling the variability of solar irradiance. 2nd International Symposium on Space Climate, Sinaia, Romania, September 13-16, 2006, invited.

**Solanki, S. K.**, N. A. Krivova, L. Balmaceda, and T. Wenzler: The solar total and spectral irradiance since the Maunder Minimum. International Symposium on Recent Observations and Simulations of the Sun-Earth System, Varna, Bulgaria, 17-22 September, 2006. (Oral).

Solanki, S. K. and **A. Lagg**: Magnetic field measurements at different levels in the solar atmosphere and magnetic coupling. 36th COSPAR Scientific Assembly, Beijing, China, July 16-23, 2006, invited. (Oral).

Solanki, S. K. and **E. Marsch**: Solar Microscopy: Unveiling the Sun's basic physical processes at their intrinsic scales. SOHO 17: 10 Years of SOHO and Beyond, Giardini Naxos Sicily, Italy, 7-12 May, 2006. (Oral).

Solanki, S. K. and A. Pauluhn: Are nanoflares responsible for coronal heating? Results of a simple statistical model. SOHO-17: 10 Years of SOHO and Beyond, Gardini Naxos, Sicily, Italy, May 7-12, 2006. (Poster).

Solanki, S. K., V. M. Pillet, and the VIM Team: A possible configuration of the Visible-light Imager and Magnetograph on Solar Orbiter. Second Solar Orbiter Workshop, Athens, Greece, October 16-20, 2006. (Poster).

Solanki, S. K., N.-E. Raouafi, A. Gandorfer, U. Schühle, A. Lagg, T. Wiegelmann, B. Inhester, and M. Kramar: Measuring the coronal magnetic field using the Hanle effect. SOHO-17: 10 Years of SOHO and Beyond, Gardini Naxos, Sicily, Italy, May 7-12, 2006. (Poster).

**Song, L.**, P. Hartogh, and C. Jarchow: A new water vapour heterodyne spectrometer for sounding the stratosphere. 36th COSPAR Scientific Assembly, Beijing, China, July 16-23, 2006. (Poster).

Sonnemann, G. R., **P. Hartogh**, M. Grygalashvyly, A. S. Medvedev, and U. Berger: A new coupled 3D-model of the dynamics and chemistry of the Martian atmosphere. European Planetary Science Congress 2006, Berlin, Germany, September 18-22, 2006. (Poster).

**Spanswick, E.**, E. Donovan, R. Friedel, and A. Korth: Ground based observations of dispersionless electron injections. 8th International Conference on Substorms, Banff, Canada, March 28-31, 2006. (Oral).

Stellmacher, G., **E. Wiehr**, and J. Hirzberger: Two-dimensional imaging of the HeD3/H-beta emission ratios in quiescent solar prominences. Solar Magnetism and Dynamics & THEMIS Users Meeting, Meudon, France, November 15-17, 2006. (Poster).

**Stenzel, O.**, B. Grieger, and H. U. Keller: Suggesting a new Exo-Planet Atmosphere Modelling Project. ISSI Team Meeting on Habitable Zones, Bern, Switzerland, February 20-23, 2006. (Oral).

**Stenzel, O. J.**, B. Grieger, H. U. Keller, K. F. R. Greve, E. Kirk, and F. Lunkeit: Mars climate simulation project - atmosphere and ice-cap climate interaction. Seminar of the Experimental and Theoretical Glaciology Group, Hokkaido University, Sapporo, Japan, October 19, 2006.

**Stenzel, O. J.**, R. A. Mahajan, B. Grieger, H. U. Keller, R. Greve, K. Fraedrich, E. Kirk, and F. Lunkeit: Mars atmosphere and ice sheet modelling. Second Mars Atmosphere Modelling and Observations Workshop, Granada, Spain, February 27-28, March 1-3, 2006. (Oral).

**Štverák, Š.**, P. Trávniček, M. Maksimovic, E. Marsch, A. Fazakerley, and E. E. Scime: Electron anisotropy constraint in the solar wind. Second Solar Orbiter Workshop, Athens, Greece, October 16-20, 2006. (Poster).

**Svedhem, H.**, D. Titov, S. Barabash, J.-L. Bertaux, P. Drossart, V. Formisano, B. Haeusler, W. J. Markiewicz, G. Piccini, T. Zhang, and the Venus Express Team: Venus Express first reuslts - an overview. 36th COSPAR Scientific Assembly, Beijing, China, July 16-23, 2006.

**Taylor, M. G.**, Y. V. Bogdanova, M. W. Dunlop, B. Lavraud, A. Asnes, P. Escoubet, H. Laakso, R. H. Friedel, G. D. Reeves, C. H. Perry, A. Masson, H. J. Opgenoorth, C. Vallat, P. Daly, A. N. Fazakerley, H. Rème, E. A. Lucek, and T. A. Fritz: The dayside plasma sheet at high-altitude, mid-latitudes: the view from within the (magnetic) bottle? AGU Fall Meeting, San Francisco, USA, December 11-14, 2006.

Teriaca, L., A. Lagg, R. Aznar Cuadrado, C. Sasso, and S. K. Solanki: The dynamics and structure of the solar atmosphere as obtained from combined SUMER/SOHO and TIP2/VTT observations alpha line. SOHO-17: 10 Years of SOHO and Beyond, Gardini Naxos, Sicily, Italy, May 7-12, 2006. (Poster).

Teriaca, L., U. Schühle, and W. Curdt: Imaging and spectroscopy around the H I Lyman alpha line: expected radiometric performances. Second Solar Orbiter Workshop, Athens, Greece, October 16-20, 2006. (Poster).

Teriaca, L., U. Schühle, S. K. Solanki, W. Curdt, and E. Marsch: The dynamic nature of the lower transition region as revealed by spectroscopy of the hydrogen Lyman alpha line. SOHO-17: 10 Years of SOHO and Beyond, Gardini Naxos, Sicily, Italy, May 7-12, 2006. (Poster).

**Teriaca, L.**, U. Schühle, S. K. Solanki, W. Curdt, and E. Marsch: The lower transition region as seen in the H I Lyman Alpha line. Second Solar Orbiter Workshop, Athens, Greece, October 16-20, 2006. (Oral).

Theissen, A., A. BenMoussa, U. Schühle, and J.-F. Hochedez: LYRA, a solar UV radiometer using diamond detectors. Modern Solar Facilities - Advanced Solar Science, Göttingen, Germany, September 27-29, 2006. (Poster).

**Thomas, N.**, K. Seiferlin, T. Spohn, J. Oberst, K. Gunderson, J. Whitby, H. Michaelis, U. Christensen, and M. Hilchenbach: BELA: The first European laser altimeter for planetary exploration. General Assembly of the European Geosciences Union, Vienna, Austria, April 2-7, 2006. (Oral).

**Tian, H.**, C.-Y. Tu, J.-S. He, and E. Marsch: A Study on the heights of coronal bright points on Fe XII radiance map. 36th COSPAR Scientific Assembly, Beijing, China, July 16-23, 2006. (Poster).

Tishkovets, V. P. and **K. Jockers**: Light scattering by densely packed random media. Dense media vector radiative transfer equation. 9th international conference on electromagnetic and light scattering by non-spherical particles: Theory, measurements, and applications, St. Petersburg, Russia, June 5-9, 2006. (Oral).

Tomás, A. T., J. Woch, **N. Krupp**, A. Lagg, G. H. Jones, and K.-H. Glassmeier: Energetic electrons in the inner part of the Jovian magnetosphere and their relation to auroral emissions. EUROPLANET strategic workshop on comparative planetary aurorae, UCL, London, UK, November 10-11, 2006. (Poster).

**Tozzi, G. P.**, H. Boehnhardt, and the ESO DI Dust Team: Solid particle activity from the visible to the near-IR in comet 9P/Tempel 1 around the DI event. Deep Impact as a World Observatory Event, Brussels, Belgium, August 7-10, 2006. (Poster).

Tripathi, D., S. K. Solanki, R. Schwenn, V. Bothmer, M. Mierla, and G. Stenborg: SOHO/EIT observation of a bright coronal downflow. SOHO-17: 10 Years of SOHO and Beyond, Gardini Naxos, Sicily, Italy, May 7-12, 2006. (Poster).

**Tschimmel, M.**, N. I. Ignatiev, D. V. Titov, E. Lellouch, T. Fouchet, V. Formisano, M. Giuranna, and A. Maturilli: Atmospheric water vapour from the PFS/Mars Express observations. 36th COSPAR Scientific Assembly, Beijing, China, July 16-23, 2006.

**Tschimmel, M.**, N. I. Ignatiev, D. V. Titov, E. Lellouch, T. Fouchet, V. Formisano, M. Giuranna, and A. Maturilli: The latest on atmospheric water vapour from the PFS shortwavelength observations. European Planetary Science Congress 2006, Berlin, Germany, September 18-22, 2006. (Oral).

**Tu, C.-Y.**, J.-S. He, and E. Marsch: Can solar wind originate in the quiet-Sun region? 36th COSPAR Scientific Assembly, Beijing, China, July 16-23, 2006.

**Tu, C.-Y.** and E. Marsch: Ion-cyclotron resonance and non-thermal features of solar wind ions. Western Pacific Geophysics Meeting (WPGM), Beijing, China, July 24-27, 2006. (Oral).

**Tu, C.-Y.**, R. Schwenn, E. Donovan, J.-S. Wang, L.-D. Xia, Y.-W. Zhang, and The KuaFu Study Team: An introduction to KuaFu project (scientific goals, scientific payloads, historical events, present status and perspectives). 36th COSPAR Scientific Assembly, Beijing, China, July 16-23, 2006, invited. (Oral).

**Tubiana, C.**, H. Böhnhardt, L. Barrera, J. L. Ortiz, G. Schwehm, R. Schulz, and J. Stuewe: Characterization of physical parameters of the Rosetta target comet 67P/Churyumov-Gerasimenko. European Planetary Science Congress 2006, Berlin, Germany, September 18-22, 2006. (Oral).

**Vaisberg, O.**, J.-J. Berthelier, K. Torkar, F. Leblanc, J. Woch, L. Avanov, A. Skalski, D. Delcourt, V. Smirnov, and G. Koinash: Panoramic imaging mass-spectrometer for planetary studies. European Planetary Science Congress 2006, Berlin, Germany, September 18-22, 2006. (Oral).

**Vasyliūnas, V. M.**: Harry Petschek and the universality of magnetic reconnection. Harry Petschek Symposium on Magnetic Reconnection, University of Maryland, College Park, Maryland, USA, March 21-23, 2006, invited paper. (Oral).

**Vasyliūnas, V. M.**: History of magnetic reconnection. Seminar, Applied Physics Laboratory, Laurel, Maryland, USA, March 20, 2006. (Oral).

**Vasyliūnas, V. M.**: Impossibility of calculating magnetic field change from current disruption. 8th International Conference on Substorms, Banff, Canada, March 28-31, 2006. (Oral).

**Vasyliūnas, V. M.**: Physical origin of magnetospheric convection flow on closed field lines. Space Physics Seminar, Rice University, Houston, Texas, USA, March 17, 2006. (Oral).

**Vasyliūnas, V. M.**: Physical origin of pickup currents. European Planetary Science Congress 2006, Berlin, Germany, September 18-22, 2006. (Oral).

**Vasyliūnas, V. M.**: Prompt penetration of magnetospheric convection to low latitudes: what is the physical mechanism? AGU Fall Meeting, San Francisco, USA, December 11-15, 2006. (Oral).

**Vasyliūnas, V. M.**: Review of conclusions of storm-substorm workshop. 8th International Conference on Substorms, Banff, Canada, March 28-31, 2006. (Oral).

**Vasyliūnas, V. M.**: The paradoxical role of the displacement current in cosmic plasmas. Symposium "Cosmic Plasma Physics" in honor of Karl Schindler on the occasion of his 75th birthday, Bochum, Germany, October 30-31, 2006, invited paper. (Oral).

**Vilenius, E.**, U. Mall, and V. Kaydash: In-flight calibration of SIR near infrared spectrometer onboard SMART-1. European Planetary Science Congress 2006, Berlin, Germany, September 18-22, 2006. (Oral).

**Wang, J.**, C. Tu, R. Schwenn, E. Donovan, L. Xia, and Y. Zhang: KuaFu mission: from myth to mission. Western Pacific Geophysics Meeting (WPGM), Beijing, China, July 24-27, 2006, invited. (Oral).

**Wang, X.**, K. Bamert, P. Bochsler, M. Hilchenbach, F. Ipavich, B. Klecker, E. Moebius, and P. Wurz: Stream-limited transport of solar energetic particles. 36th COSPAR Scientific Assembly, Beijing, China, July 16-23, 2006. (Oral).

**Wicht, J.**: Diversity of planetary dynamos: A new challenge for numerical modelling. 10th Symposium of SEDI (Study of the Earth's Deep Interior), Prague, Czech Republic, July 9-14, 2006, invited. (Oral).

**Wicht, J.**: Modelling Mercurys dynamo. Mercury Workshop, ISSI (International Space Science Institute), Bern, Switzerland, June 26-30, 2006, invited. (Oral).

**Wicht, J.**: Saturns Dynamo ist anders. Deutscher Geodynamik Workshop 2006, Max-Planck-Institut für Sonnensystemsforschung, Katlenburg-Lindau, Germany, September 27-28, 2006. (Oral).

**Wicht, J.**: The geomagnetic dynamo - virtual lab vs. reality as seen in polarity reversal data. International Final Colloquium of the German Science Foundation Priority Programm 1097 "Geomagnetic Field Variations: Space-Time Structure, Processes, and Effects on System Earth", TU Braunschweig, Germany, October 4-5, 2006. (Oral).

**Wicht, J.**: Warum polt sich das Erdmagnetfeld um? 66. Jahrestagung der Deutschen Geophysikalischen Gesellschaft, Bremen, Germany, March 6-9, 2006, invited. (Oral).

**Wicht, J.** and U. Christensen: Torsional oscillations in dynamo simulations. 10th Symposium of SEDI (Study of the Earth's Deep Interior), Prague, Czech Republic, July 9-14, 2006. (Poster).

**Wicht, J.** and C. Constable: Reversal rate in a dynamo model. 10th Symposium of SEDI (Study of the Earth's Deep Interior), Prague, Czech Republic, July 9-14, 2006. (Poster).

**Wicht, J.** and C. Constable: Variation der Umkehrhäufikeit in Dynamosimulationen. 66. Jahrestagung der Deutschen Geophysikalischen Gesellschaft, Bremen, Germany, March 6-9, 2006.

**Wiegelmann, T.**: Can we use nonlinear and selfconsistent models for data analysis? SFB 591 Symposium "Cosmic Plasma Physics", Bochum, Germany, October 30-31, 2006. (Oral).

**Wiegelmann, T.**: Coronal stereoscopy. Solar Group Seminar, Katlenburg-Lindau, Germany, April 25, 2006. (Oral).

**Wiegelmann, T.**: Nonlinear force-free field modeling of the solar coronal magnetic field. CAWSES International Workshop on Space Weather Modeling (CSWM), Yokohama, Japan, November 14-17, 2006, invited review talk. (Oral).

**Wiegelmann, T.**: Nonlinear force-free fields: Aads magnetofrictional model case. Nonlinear force-free coronal magnetic field workshop, Stanford, Palo Alto, USA, June 05-07, 2006. (Oral).

**Wiegelmann, T.**: Nonlinear force-free fields: First tests in spherical coordinates. Nonlinear force-free coronal magnetic field workshop, Stanford, Palo Alto, USA, June 05-07, 2006, invited. (Oral).

**Wiegelmann, T.**: Nonlinear force-free fields: Non-force-free boundary conditions and preprocessing. Nonlinear force-free coronal magnetic field workshop, Stanford, Palo Alto, USA, June 05-07, 2006, invited. (Oral).

**Wiegelmann, T.** and B. Inhester: Coupling of photospheric and coronal magnetic fields. 36th COSPAR Scientific Assembly, Beijing, China, July 16-23, 2006. (Oral).

**Wiegelmann, T.**, B. Podlipnik, B. Inhester, L. Feng, and P. Ruan: 3D visualization techniques for the STEREO-mission. 36th COSPAR Scientific Assembly, Beijing, China, July 16-23, 2006. (Poster).

Wiegelmann, T., **S. K. Solanki**, L. Yelles, A. Lagg, A. Vögler, R. Cameron, and M. Schüssler: Nonlinear force-free magnetic field modelling for VIM on SO. Second Solar Orbiter Workshop, Athens, Greece, October 16-20, 2006. (Oral).

**Wiehr, E.**, J. Hirzberger, and G. Stellmacher: The He-D3 to H-beta emission ratio in prominences. The Physics of Chromospheric Plasmas, Coimbra, Portugal, October 9-13, 2006. (Poster).

**Wilhelm, K.**: Lessons from SUMER/SOHO Solar Ultraviolet Spectrograph. 2nd UN/NASA Workshop on International Heliophysical Year and Basic Space Science, Indian Institute of Astrophysics, Bangalore, India, November 27 - December 1, 2006, invited. (Oral).

**Wilhelm, K.**: Solar coronal-hole plasma densities and temperatures. SOHO-17: 10 Years of SOHO and Beyond, Gardini Naxos, Sicily, Italy, May 7-12, 2006. (Oral).

**Xia, L.-D.**, C.-Y. Tu, R. Schwenn, E. Donovan, J.-S. Wang, and Y.-W. Zhang: KuaFu mission: the scientific payload of KuaFu-A. 36th COSPAR Scientific Assembly, Beijing, China, July 16-23, 2006. (Poster).

**Xiao, C.**, X. Wang, Z. Pu, H. Zhao, J. Wang, Z. Ma, S. Fu, M. Kivelson, Z. Liu, Q. Zong, K. Glassmeier, A. Balogh, A. Korth, H. Réme, and C. Escoubet: In situ evidence for the structure of the magnetic null in a 3D reconnection event in the Earth's magnetotail. AGU Fall Meeting, San Francisco, USA, December 11-14, 2006, invited. (Oral).

**Xiao, C. J.**, L. T. Song, Z. Y. Pu, Z. X. Liu, P. W. Daly, A. Balogh, and H. Rème: Magnetic field diffusion during the CME-magnetosphere interaction with Cluster measurement on 6 November 2001. 36th COSPAR Scientific Assembly, Beijing, China, July 16-23, 2006. (Poster).

Yelles, L., A. Lagg, **J. Hirzberger**, J. Woch, S. K. Solanki, and A. Vögler: Simulations of science data of the SO-VIM instrument. Second Solar Orbiter Workshop, Athens, Greece, October 16-20, 2006. (Oral).

**Zhang, H.**, T. Fritz, Q. Zong, S. Schaefer, K. Glassmeier, P. Daly, H. Rème, and A. Balogh: Energetic particle flux enhancement at the high latitude boundaries. AGU Fall Meeting, San Francisco, USA, December 11-14, 2006.

Zhang, H., Q. Zong, **T. Fritz**, S. Fu, M. Taylor, S. Schaefer, K. Glassmeier, P. Daly, H. Rème, and A. Balogh: High latitude magnetopause current sheet during an IMF by dominated period. General Assembly of the European Geosciences Union, Vienna, Austria, April 2-7, 2006. (Poster).

**Zhang, H.**, Q. Zong, T. Fritz, S. Fu, M. Taylor, S. Schaefer, K. Glassmeier, P. Daly, H. Rème, and A. Balogh: High latitude magnetopause current sheet during an IMF By dominated period. 36th COSPAR Scientific Assembly, Beijing, China, July 16-23, 2006. (Poster).

**Zhanghui, H.**, Z. Y. Pu, Z. X. Liu, A. Korth, M. Frazen, R. Friedel, Q.-G. Zong, H. Rème, and K.-H. Glassmeier: Magnetic flux pileup and magnetic field dipolarization during substorm. 36th COSPAR Scientific Assembly, Beijing, China, July 16-23, 2006. (Poster).

**Zong, Q.**, H. Alleyne, N. Cornilleau-Wehrlin, P. Daly, P. Decreau, A. Fazakerley, D. Gurnette, G. Gustafsson, E. Lucek, G. Paschmann, H. Rème, and K. Torkar: Multiple cusps during an extended northward IMF. General Assembly of the European Geosciences Union, Vienna, Austria, April 2-7, 2006. (Oral).

**Zong, Q.**, T. Fritz, S. Fu, P. Song, Z. Pu, G. Parks, A. Korth, P. Daly, M. Dunlop, and H. Rème: BBF plasmoid observed by Cluster and Double Star constellation. AGU Fall Meeting, San Francisco, USA, December 11-14, 2006. (Oral).

**Zong, Q.-G.**, H. Zhang, T. A. Fritz, S. Wing, M. L. Goldstein, W. Keith, J. D. Winningham, R. Frahm, M. W. Dunlop, A. Korth, P. W. Daly, H. Rème, A. Balogh, and A. N. Fazakerley: Multiple cusps during an extended northward IMF period observed by Cluster. General Assembly of the European Geosciences Union, Vienna, Austria, April 2-7, 2006. (Oral).

## **Vorträge 2007 /**
## Talks 2007

Araneda, J., E. Marsch, and **A. Vinas**: Collisionless damping of parametrically unstable Alfvén waves in the solar wind. European Geosciences Union General Assembly 2007, Vienna, Austria, April 16 - 20, 2007. (Poster).

Arridge, C., A. Rymer, A. Coates, **N. Krupp**, M. Blanc, J. Richardson, N. Andre, M. Thomson, M. Henderson, J. F. Cooper, M. Burger, D. Simpson, K. K. Khurana, M. Dougherty, and D. T. Young: Cassini observations of Saturns dawn-magnetotail region: preliminary results. European Planetary Science Congress 2007, Potsdam, Germany, August 19-24, 2007. (Oral).

**Asnes, A.**, A. L. Borg, M. G. Taylor, P. Escoubet, R. W. Friedel, G. D. Reeves, P. Daly, A. Fazakerley, and E. A. Lucek: High resolution measurements of electron distributions in the proximity of near Earth neutral lines by Cluster. European Geosciences Union General Assembly, Vienna, Austria, April 15-20, 2007. (Poster).

**Åsnes, A.**, M. G. Taylor, A. L. Borg, C. P. Escoubet, H. Laakso, A. Masson, N. Østgaard, R. Friedel, P. Daly, and A. N. Fazakerley: Cluster observations of electron acceleration in near-Earth reconnection events. AGU Fall Meeting, San Francisco, USA, December 10-14, 2007. (Oral).

**Balmaceda, L.**, N. A. Krivova, and S. K. Solanki: Reconstruction of the long-term irradiance variations. AGU Joint Assembly, Acapulco, Mexico, May 22-25, 2007, invited.

Barucci, M. A., **F. Merlin**, A. Guilbert, S. Fornasier, C. de Bergh, A. Doressoundiram, A. Alvarez, C. Dumas, O. Hainaut, I. Belskaya, S. Bagnulo, A. Delsanti, S. Protopapa, G. P. Tozzi, K. Muinonen, D. Perna, and N. Peixinho: Characterization of TNOs' surface properties: preliminary results of a large VLT programme. DPS 2007, Orlando, Florida, USA, October 7-12, 2007. (Oral).

Birch, A., T. L. Duvall, S. Hanasoge, L. Gizon, and J. Jackiewicz: Local Helioseismology of Supergranulation. 210th meeting AAS/SPD, Honolulu, Hawaii, USA, May 27-31, 2007. (Poster).

**Birch, A.** and L. Gizon: Sensitivity of helioseismic travel times to internal flows. HELAS II International Conference "Helioseismology, Asteroseismology and MHD Connections", Göttingen, Germany, August 20-24, 2007. (Poster).

**Birch, A. C.**, L. Gizon, B. W. Hindman, and D. A. Haber: Sensitivity of ring diagrams to weak local flows. HELAS II International Conference "Helioseismology, Asteroseismology and MHD Connections", Göttingen, Germany, August 20-24, 2007. (Poster).

**Bloomfield, D. S.**, A. Lagg, and S. K. Solanki: The nature of running penumbral waves revealed. International Astronomical Union Symposium 247 "Waves & Oscillations in the Solar Atmosphere: Heating and Magneto-seismology", Porlamar, Isla de Margarita, Venezuela, September 17-22, 2007. (Oral).

**Bloomfield, D. S.**, A. Lagg, and S. K. Solanki: The nature of running waves in sunspot penumbrae. HELAS II International Conference "Helioseismology, Asteroseismology and MHD Connections", Göttingen, Germany, August 20-24, 2007. (Oral).

**Bloomfield, D. S.**, A. Lagg, S. K. Solanki, R. Centeno, M. Collados, and J. T. Bueno: The nature of running penumbral waves revealed. 5th Solar Polarization Workshop, Ascona, Switzerland, September 17-21, 2007. (Poster).

**Boehnhardt, H.**: Deep Impact and Rosetta - cometary science today and in 7 years from now. Seminar, European Southern Observatory Santiago de Chile, October 17, 2007. (Oral).

**Boehnhardt, H.**: News from the Kuiper Belt. Seminar, European Southern Observatory Santiago de Chile, October 31, 2007. (Oral).

**Boehnhardt, H.**: Weiche Landung auf einem kosmischen Vagabunden - die Weltraummission Rosetta. Öffentlicher Vortrag, Goslar, Germany, December 11, 2007. (Oral).

**Boehnhardt, H.**, F. Goesmann, S. Bagnulo, L. Kolokolova, and G. P. Tozzi: Comets and life. ESO Workshop on "Observing Planetary Systems", Santiago de Chile, March 5-8, 2007. (Oral).

**Boehnhardt, H.**, S. Lowry, A. Fitzsimmons, *et al.*: The YORP effect at asteroid 2000 PH5. European Southern Observatory, institute seminar, Santiago de Chile, March 9, 2007. (Oral).

**Büchner, J.**: Astrophysical reconnection. 34th Plasma Physics Conference of the European Physical Society, Warsaw, Poland, July 2-6, 2007, invited Lecture.

**Büchner, J.**: Connecting local and global physics of reconnection. Fourth International "Cambridge" Workshop on Magnetic Reconnection, St. Michaels, Maryland, USA, September 10-14, 2007, invited Talk.

**Büchner, J.**: Currents and current sheets in the solar atmosphere. IGPP Colloquium, University of Riverside, USA, March 13, 2007, invited Lecture.

**Büchner, J.**: Der vierte Aggregatzustand: Heliophysikalische Plasmen. Ringvorlesung "Das Reich der Sonne - Heimat der Menschheit", Christian-Albrechts-Universität zu Kiel, November 29, 2007, eingeladene Vorlesung.

**Büchner, J.**: Macro- and microphysics of three-dimensional reconnection. First Solaire network-wide meeting, Katholieke Universiteit Leuven, Belgium, December 17-19, 2007, invited Lecture.

**Büchner, J.**: Magnetic reconnection a universal heliophysical process. International Heliophysical Conference, Bad Honeff, Germany, May 15, 2007, invited Talk.

**Büchner, J.**: Magneto-plasmaphysics of the Sun, stars and galaxies. 3rd DFG and NSF Research Conference: Astrophysics, Washington DC, USA, June 12, 2007, invited Talk.

**Büchner, J.**: Magnetospheres as plasma laboratories. 71. Jahrestagung der Deutschen Physikalischen Gesellschaft, Regensburg, Germany, March 28, 2007, invited Lecture.

**Büchner, J.**: Numerical solution of the Vlasov equation in astrophysical problems. 2nd International Conference on Numerical Modeling of Space Plasma Flows ASTRONUM-2, Paris, France, June 15, 2007, invited Talk.

**Büchner, J.**: Parametrization of anomalous resistivity for large scale resistive MHD models. IGPP Space Plasma Simulation Colloquium, University of California, Los Angeles, USA, March 12, 2007, colloquium Talk.

**Büchner, J.**: Physical - forward - simulation of the magnetic field in the solar atmosphere. Coronal Magnetic Mapping Prepration Meeting, MPS Katlenburg-Lindau, Germany, February 5-7, 2007. (Oral).

**Büchner, J.**: Simulation of Anomalous Resistivity. 8th International School for Space Plasma Simulation, Kauai, USA, January 28, 2007, invited Lecture.

**Büchner, J.**: Space Plasma - Investigation of complex systems. Topical conference and symposium on "Solar system exploration", Moscow, October 2-5, 2007, invited talk.

**Büchner, J.**, V. Bothmer, and D. Tripathi: The role of reconnection in solar eruptions. SOHO 20 - Transient Events on the Sun and in the Heliosphere, Gent, Belgium, August 27-31, 2007. (Oral).

**Büchner, J.**, N. Elkina, K. W. Lee, B. Nikutowski, and J. Santos: Simulation of turbulence, structuring, transport and reconnection in astrophysical plasmas. Third Joint HLRB and KONWIHR Result and Reviewing Workshop, Garching bei München, Germany, December 3-4, 2007, invited Review Talk.

**Büchner, J.**, R. MacLean, and E. Priest: Structure of reconnection regions in the solar atmosphere - derived from observations of X-ray bright points. Fourth International "Cambridge" Workshop on Magnetic Reconnection, St. Michaels, Maryland, USA, September 10-14, 2007, invited Talk. (Oral).

**Bucik, R.**, A. Korth, U. Mall, and G. M. Mason: Simulation of time-of-flight telescope for suprathermal ions in heliosphere. 10th ICATPP Conference, Como, Italy, October 8-12, 2007. (Oral).

Bucik, R. and **K. Kudela**: Hard X-ray observations of electron precipitation in January 2005. European Geosciences Union General Assembly, Vienna, Austria, April 15-20, 2007. (Poster).

Bucik, R., **K. Kudela**, and D. Smith: Simulations of hard X ray and gamma ray response in CsI(Tl) scintillator detector. 30th International Cosmic Ray Conference, Merida, Mexico, July 3-11, 2007. (Poster).

**Burston, R. B.**, L. Gizon, T. Appourchaux, and the Cosmic Vision 2015-2025 Team: Detecting solar g modes and gravitational waves with ASTROD. HELAS II International Conference "Helioseismology, Asteroseismology and MHD Connections", Göttingen, Germany, August 20-24, 2007. (Poster).

**Cameron, R.**: 3-D Simulations of wave propagation and sunspots. SOHO 19 / GONG 2007 Seismology of Magnetic Activity, Melbourne, Australia, July 9-13, 2007, invited. (Oral).

**Cameron, R.**, K. Daiffallah, and L. Gizon: Three-dimensional numerical simulation of wave propagation through model sunspots. European Geosciences Union General Assembly, Vienna, Austria, April 15-20, 2007, invited. (Oral).

**Cameron, R.** and L. Gizon: Simulations of wave propagation through model sunspots. HELAS II International Conference "Helioseismology, Asteroseismology and MHD Connections", Göttingen, Germany, August 20-24, 2007, invited. (Oral).

**Chanteur, G.**, R. Modolo, E. Dubinin, and M. Fraenz: Capture of solar wind alpha-particles by the Martian atmosphere. European Geosciences Union General Assembly, Vienna, Austria, April 15-20, 2007. (Poster).

**Christensen, U.**: Internal dynamics and magnetism of planets. Integrated Geodynamics seminar, Delft and Utrecht, The Netherlands, November 14-15, 2007. (Oral).

**Christensen, U.** and J. Wicht: A dynamo operating in the partly stable and core of Mercury. IUGG XXIV General Assembly, Perugia, Italy, July 2-13, 2007. (Oral).

**Christensen, U. R.**: A deep dynamo explaining Mercury's weak magnetic field. European Geosciences Union General Assembly, Vienna, Austria, April 15-20, 2007. (Oral).

**Christensen, U. R.**: Das Magnetfeld des Merkur. Planetenseminar, DLR - Institut für Planetenforschung, Berlin, Germany, May 30, 2007, invited. (Oral).

**Christensen, U. R.** and J. Wicht: A quadrupolar magnetic field for Mercury? AGU Fall Meeting, San Francisco, USA, December 10-14, 2007. (Oral).

**Curdt, W.**: High-resolution solar EUV spectroscopy. HINODE-SUMER workshop, NAOJ, Tokyo, Japan, October 8-12, 2007. (Oral).

**Curdt, W.**: The solar transition region as seen by EUV spectroscopes. HINODE-SUMER workshop, University of Kyoto, Japan, October 5, 2007. (Oral).

**Curdt, W.**, K. Wilhelm, L. Feng, and S. Kamio: Multi-spacecraft observations of polar coronal plumes. HINODE First Results, Dublin, Ireland, August 20-24, 2007. (Oral).

**Czechowski, A.**, M. Hilchenbach, K. C. Hsieh, and J. Kota: Comparing the ENA data to Voyager 1 ion measurements in the heliosheath: the puzzle of H/He ratio. 30th International Cosmic Ray Conference - ICRC, Merida, Yucatan, Mexico, July 3-11, 2007. (Poster).

**Daiffallah, K.**, R. Cameron, and L. Gizon: Helioseismology of small magnetic flux tubes: Three dimensional simulations. HELAS II International Conference "Helioseismology, Asteroseismology and MHD Connections", Göttingen, Germany, August 20-24, 2007. (Poster).

**Dal Lago, A.**, R. Schwenn, and W. D. Gonzalez: Limb CME geometry using LASCO observations. European Geosciences Union General Assembly, Vienna, Austria, April 15-20, 2007. (Poster).

**Daly, P.**: Cluster/RAPID instrument status report. RAPID/PEACE Joint Team Meeting, Abingdon, UK, September 5-7, 2007.

**Daly, P.**: Strömende energiereiche Teilchen im Schweif der Magnetosphäre: Beobachtungen von RAPID/Cluster. MPE Workshop on Solar System Plasmas, Schloß Ringberg, Tegernsee, Germany, January 29-31, 2007. (Oral).

**Daly, P. W.**: RAPID instrument overview. CIS/HIA Cluster and Double Star Team Meeting, Starnberg, Germany, June 19-21, 2007. (Oral).

**D'Amicis, R.**, D. Telloni, S. Orsini, A. Mura, A. Milillo, A. di Lellis, E. Antonucci, and M. Hilchenbach: Numerical studies on neutral solar wind generated at high and low solar latitudes. AGU Fall Meeting, San Francisco, USA, December 10-14, 2007. (Oral).

Dammasch, I., W. Curdt, B. Dwivedi, and S. Parenti: The redshifted footpoints of coronal loops. SOHO 20 Workshop, Gent, Belgium, August 27-31, 2007. (Poster).

**Dubinin, E.**, G. Chanteur, M. Fraenz, R. Modolo, J. Woch, E. Roussos, S. Barabash, and R. Lundin: Asymmetry of plasma fluxes at Mars. ASPERA-3 observations and hybrid simulations. European Geosciences Union General Assembly, Vienna, Austria, April 15-20, 2007. (Poster).

**Dubinin, E.**, M. Fraenz, G. Chanteur, J. Woch, J. D. Winningham, R. Frahm, R. Lundin, and S. Barabash: Peaked electron distributions on Mars and possible mechanisms of their generation. European Geosciences Union General Assembly, Vienna, Austria, April 16-20, 2007. (Oral).

**Dubinin, E.**, M. Fraenz, and J. Woch: Martian plasma environment. Overview of ASPERA-3 observations on MEX. DFG Priority Colloquium "Mars and the Terrestrial Planets", Berlin, Germany, February 19-20, 2007. (Oral).

**Dubinin, E.**, M. Fraenz, J. Woch, G. Chanteur, J. D. Winningham, R. Frahm, R. Lundin, and S. Barabash: Field-aligned currents, parallel electric field potentials and aurora on Mars. IUGG, Perugia, Italy, July 2-7, 2007, invited. (Oral).

**Dubinin, E.**, M. Fraenz, J. Woch, C. Martinecz, S. Barabash, and T. Zhang: Venus plasma environment. Comparative magnetospheres of Venus and Mars. Venus Express Workshop, La Thuile, Italy, March, 18-24, 2007. (Oral).

Dubinin, E., **M. Fränz**, J. Woch, E. Roussos, J. D. Winningham, R. Frahm, G. Chanteur, A. Coates, R. Lundin, and S. Barabash: Electrons as tracers of physical processes within the Martian magnetosphere. European Planetary Science Congress 2007, Potsdam, Germany, August 19-24, 2007. (Oral).

**Elkina, N.** and J. Büchner: The momentum transfer rate due to current-driven turbulence in magnetized plasma. European Geosciences Union General Assembly, Vienna, Austria, April 15-20, 2007. (Oral).

Elkina, N. V. and **J. Büchner**: Interaction of a dense electron-positron jet with a dilute galactic plasma. 71. Jahrestagung der Deutschen Physikalischen Gesellschaft, Regensburg, Germany, March 28, 2007. (Poster).

**Elkina, N. V.** and J. Büchner: The momentum transfer rate due to current-driven turbulence in magnetized plasma. DPG Frühjahrstagung des Arbeitskreises Atome, Moleküle, Quantenoptik und Plasmen, Düsseldorf, Germany, March 19-23, 2007. (Poster).

**Escoubet, C.**, J. Berchem, J. Bosqued, M. G. Taylor, K. Trattner, F. Pitout, H. Laakso, A. Masson, M. Dunlop, I. Dandouras, H. Rème, A. Fazakerley, and P. Daly: Cusp particle precipitation before and after an abrupt change of direction of the IMF. AGU Fall Meeting, San Francisco, USA, December 10-14, 2007. (Oral).

**Facskó, G.**, K. Kecskeméty, M. Tátrallyay, G. Erdös, P. W. Daly, and I. Dandouras: An extended global study of hot flow anomalies using Cluster multi-spacecraft measurements. European Geosciences Union General Assembly, Vienna, Austria, April 15-20, 2007. (Oral).

Feng, L., B. Inhester, S. K. Solanki, **T. Wiegelmann**, B. Podlipnik, and R. A. Howard: First stereoscopic coronal loop reconstructions from STEREO/SECCHI images. AGU Fall Meeting, San Francisco, USA, December 10-14, 2007. (Oral).

**Feng, L.**, T. Wiegelmann, B. Inhester, S. Solanki, and P. Ruan: Magnetic stereoscopy of coronal loops for SECCHI. 5th SECCHI Consortium Meeting, Orsay, France, March 5-8, 2007.

**Foing, B. H.**, M. Grande, J. Huovelin, J.-L. Josset, H. U. Keller, A. Nathues, A. Malkki, G. Noci, B. Kellett, S. Beauvivre, P. Cerroni, P. Pinet, H. Makkinen, U. Mall, M. Almeida, D. Frew, J. Volp, M. Sarkarati, D. Heather, and D. Koschny: SMART-1 mission: highlights of lunar results. 38th Lunar and Planetary Science Conference, (Lunar and Planetary Science XXXVIII), League City, TX, USA, March 12-16, 2007. (Oral).

**Fraenz, M.**, E. Dubinin, C. Martinecz, E. Roussos, J. Woch, R. Frahm, J. D. Winningham, A. Coates, Y. Soobiah, and R. Lundin: Photo-electron boundaries at Mars and Venus. European Geosciences Union General Assembly, Vienna, Austria, April 15-20, 2007. (Poster).

**Fraenz, M.**, E. Dubinin, C. Martinecz, and J. Woch: The plasma environment of Venus. Venus Express first results and prospects. DFG Priority Colloquium "Mars and the Terrestrial Planets", Berlin, Germany, February 19-20, 2007. (Oral).

**Fraenz, M.**, E. Dubinin, J. Woch, E. Roussos, and C. Martinez: Plasma boundaries on Mars and Venus. IUGG, Perugia, Italy, July 2-7, 2007. (Oral).

**Fränz, M.**, E. Dubinin, C. Martinecz, E. Roussos, J. Woch, S. Barabash, A. Coates, A. Fedorov, R. Frahm, and R. Lundin: Plasma moments in the environment of Mars and Venus. European Planetary Science Congress 2007, Potsdam, Germany, August 19-24, 2007. (Oral).

**Fu, S.**, Q. Zong, Z. Pu, A. Korth, and P. Daly: Magnetic structures with rich ionospheric oxygen ions observed in the near Earth plasmasheet. AGU Fall Meeting, San Francisco, USA, December 10-14, 2007. (Poster).

**Gizon, L.**: German Data Center for SDO. 1st Heliophysics Knowledge Base Workshop, Royal Observatory of Belgium, Brussels, Belgium, June 20-22, 2007, invited. (Oral).

**Gizon, L.**: Helioseismology: learning to map solar subsurface magnetic fields. Living with a Star 2007 conference, Boulder, CO, USA, September 10-13, 2007, invited review. (Oral).

**Gizon, L.**: Local helioseismology. Cargèse Workshop 2007: Acoustical Imaging of Complex Media: Applications in Medicine, Seismology and Oceanography, Cargèse, France, October 15-20, 2007, invited review. (Oral).

**Gizon, L.**: Recent progress in helioseismic tomography. Physik-Kolloquium am II. Physikalischen Institut der Georg-August-Universität Göttingen, Göttingen, Germany, April 30, 2007, invited. (Oral).

**Gizon, L.**: Solar oscillations. Institutskolloquium am Albert-Einstein-Institut (AEI), Potsdam-Golm, Germany, March 15, 2007, invited. (Oral).

**Gizon, L.**: Theoretical aspects of helioseismology. IUGG XXIV General Assembly, Perugia, Italy, July 2-13, 2007, invited. (Oral).

**Gizon, L.**: Tomography of the solar interior. Séminaire, Institut de Physique du Globe de Paris (IPGP), Paris, France, April 3, 2007, invited. (Oral).

**Gizon, L.**, T. L. Duvall Jr., and H. Schunker: A remarkable dataset for local helioseismology: active region AR9787. HELAS II International Conference “Helioseismology, Asteroseismology and MHD Connections”, Göttingen, Germany, August 20-24, 2007. (Poster).

**Gizon, L.** and J. Jackiewicz: OLA inversion of helioseismic traveltimes. European Geosciences Union General Assembly, Vienna, Austria, April 15-20, 2007. (Oral).

**Gizon, L.** and J. Woch: Solar Orbiter: prospects for helioseismology. HELAS II International Conference “Helioseismology, Asteroseismology and MHD Connections”, Göttingen, Germany, August 20-24, 2007. (Poster).

**Goetz, W.**, M. B. Madsen, S. F. Hviid, H. P. Geller, K. M. Gunnlaugsson, G. Klingelhöfer, K. Leer, M. Olsen, and the Athena Science Team: The nature of Martian airborne dust. Indication of long-lasting drz periods on the surface of Mars. Seventh International Conference on Mars, Pasadena, CA, USA, July 10, 2007. (Oral).

**Graham, J. P.**, D. Holm, P. Mininni, and A. Pouquet: Lagrangian-averaged modeling for hydrodynamics and MHD. 10. MHD-Tage, Max-Planck-Institut für Plasmaphysik, Garching, Germany, November 26-28, 2007. (Oral).

**Grieger, B.**: Die Cassini-Huygens-Mission zum Saturn und seinem Mond Titan. 22. Hochschultage Physik, Astronomie heute, Fachbereich Physik der Universität Marburg, Germany, February 12-13, 2007. (Oral).

Han, D., T. Araki, H. Yang, K. Schlegel, and H. Lühr: Geomagnetic Sudden Commencements (SCs) observed by low altitude satellites. Japan Geoscience Union Meeting, Makuhari, Japan, May 19-24, 2007. (Poster).

**Heimpel, M.**, J. Aurnou, and J. Wicht: Turbulent deep convection at low Rossby number: a model for zonal flow and thermal emission of Jupiter and Saturn. AGU Fall Meeting, San Francisco, USA, December 10-14, 2007. (Oral).

**Hilchenbach, M.**: Cometary matter interaction with the local interstellar medium. Bioastronomy 2007, San Juan, Puerto Rico, July 16-20, 2007. (Poster).

**Hilchenbach, M.**: Die Dicke der Heliosheath. 71. Jahrestagung der Deutschen Physikalischen Gesellschaft, Regensburg, Germany, March 23-30, 2007, invited. (Oral).

**Hilchenbach, M.**: Estimates of minimum levels of organic molecules on Mars. European Geosciences Union General Assembly, Vienna, Austria, April 15-20, 2007. (Oral).

**Hilchenbach, M.**, A. Czechowski, and R. Kallenbach: Energetic neutral atoms in the heliosphere. European Geosciences Union General Assembly, Vienna, Austria, April 15-20, 2007. (Poster).

**Hilchenbach, M.**, R. Kallenbach, A. Czechowski, and K. C. Hsieh: Energetic neutral atom observations and their implications on modeling the heliosheath. 30th International Cosmic Ray Conference - ICRC, Merida, Yucatan, Mexico, July 3-11, 2007. (Oral).

Hirzberger, J., **L. Gizon**, S. K. Solanki, and T. L. Duvall Jr.: Structure and evolution of supergranulation from local helioseismology. HELAS II International Conference “Helioseismology, Asteroseismology and MHD Connections”, Göttingen, Germany, August 20-24, 2007. (Poster).

**Hoekzema, N.**, N. Thomas, W. J. Markiewicz, H. U. Keller, A. Inada, W. A. Delamere, K. E. Herkenhoff, M. Millazo, A. McEwen, and H. Team: Optical depth retrievals from shadows in HiRISE images. 39th Annual DPS Meeting, Orlando, Florida, USA, October 7-12, 2007. (Oral).

**Hoekzema, N. M.**, M. Garcia-Comas, K. Gwinner, B. Grieger, W. J. Markiewicz, and H. U. Keller: The Scale-height of dust around Pavonis Mons from HRSC stereo images. Seventh International Conference on Mars, Pasadena, CA, USA, July 9-13, 2007. (Oral).

**Hoekzema, N. M.**, N. Thomas, H. U. Keller, W. J. Markiewicz, A. Inada, W. A. Delamere, K. E. Herkenhoff, M. Milazzo, A. McEwen, and the HiRISE Team: Optical Depth Retrievals From Shadows in HiRISE images. Seventh International Conference Mars, Pasadena, CA, USA, July 9-13, 2007. (Oral).

**Holzwarth, V.**: Magnetic activity of cool stars. Astronomisches Seminar, Sternwarte Hamburg, Germany, January 11, 2007. (Oral).

**Holzwarth, V.**, D. H. Mackay, and M. Jardine: Impact of meridional circualtion on stellar butterfly diagrams and polar caps. 5th Potsdam Thinkshop “Meridional flow, differential rotation, solar and stellar activity”, Potsdam, Germany, June 24-29, 2007. (Oral).

**Holzwarth, V.** and M. Schüssler: Friction-induced instabilities of magnetic flux tubes. 10th MHD Days, Garching, Germany, November 26-28, 2007. (Oral).

**Inhester, B.**, L. Feng, and B. Podlipnik: A SECCHI EUVI ridge and loop detection tool. 5 SECCHI Consortium Meeting, Orsay, France, March 5-8, 2007. (Oral).

**Isik, E.**: A coupled model of magnetic field generation and transport in stars. 5th Potsdam Thinkshop: "Meridional Flow, Differential Rotation, Solar and Stellar Activity", Potsdam, Germany, June 24-29, 2007. (Oral).

**Jackiewicz, J.**: The forward and inverse problems in local helioseismology. HELAS II International Conference "Helioseismology, Asteroseismology and MHD Connections", Göttingen, Germany, August 20-24, 2007, invited. (Oral).

**Jackiewicz, J.**, L. Gizon, and A. C. Birch: 2+1 dimensional inversion of helioseismic travel times to infer solar flows. HELAS II International Conference "Helioseismology, Asteroseismology and MHD Connections", Göttingen, Germany, August 20-24, 2007. (Poster).

**Jones, G.**: Saturn's ring spokes: A link with atmospheric thunderstorms? Group Seminar, Institut für Geophysik und Meteorologie der Universität zu Köln, Köln, Germany, January 16, 2007. (Oral).

Jones, G. H., **N. Krupp**, E. Roussos, and the MIMI team: Rhea's interaction with the Saturnian magnetosphere. Cassini PSG meeting, JPL, Pasadena, CA, USA, January 30 - February 5, 2007. (Oral).

Jones, G. H., E. Roussos, **N. Krupp**, A. J. Coates, M. K. Dougherty, S. M. Krimigis, H. J. McAndrews, D. G. Mitchell, C. Paranicas, and D. T. Young: Rhea's magnetospheric environment as determined by Cassini MIMI and CAPS electron observations. European Planetary Science Congress 2007, Potsdam, Germany, August 19-24, 2007. (Oral).

**Kallenbach, R.**, C. Koch, U. Christensen, M. Hilchenbach, H. Michaelis, and D. Kracht: Laser altimetry at the centimeter level. European Planetary Science Congress 2007, Potsdam, Germany, August 19-24, 2007. (Oral).

**Keller, H. U.**: Properties of cometary nuclei. XII Latin American Regional IAU Meeting, Isla Margarita, Venezuela, October 22-26, 2007. (Oral).

**Keller, H. U.**, B. Grieger, M. Küppers, S. Schröder, and Y. Skorov: Titan's surface near the Huygens landing site. 2007 Joint AGU Assembly, Acapulco, Mexico, May 22-25, 2007. (Oral).

**Keller, H. U.** and E. Kührt: Sampling organic molecules from a cometary nucleus. Bioastronomy 2007, San Juan, Puerto Rico, July 16-20, 2007. (Oral).

**Keller, H. U.** and H. Sierks: Cometary physics observed by OSIRIS during the Rosetta rendezvous. European Geosciences Union General Assembly, Vienna, Austria, April 15-20, 2007. (Oral).

**Keller, H. U.**, Y. V. Skorov, and E. Kührt: Where is the water ice on cometary nuclei? 39th Annual DPS Meeting, Orlando, Florida, USA, October 7-12, 2007. (Oral).

**Khurana, K. K.** and N. Krupp: Evidence for Solar Wind Driven Reconnection in Jupiters Magnetosphere. Magnetospheres of the Outer Planets (MOP) Meeting, San Antonio, Texas, USA, June 25-29, 2007. (Oral).

**Klecker, B.**, A. B. Galvin, H. Kucharek, L. M. Kistler, M. A. Popecki, C. Mouikis, C. Farrugia, E. Möbius, M. A. Lee, L. Ellis, K. Simunac, K. Singer, L. M. Blush, P. Bochsler, P. Wurz, H. Daoudi, C. Giammanco, R. Karrer, A. Opitz, R. F. Wimmer-Schweingruber, M. Koeten, M. Hilchenbach, B. Thompson, M. Acuna, and J. Luhman: Pickup helium in the inner heliosphere: an overview. AGU Fall Meeting, San Francisco, USA, December 10-14, 2007. (Oral).

**Klecker, B.**, E. Moebius, M. A. Popecki, L. M. Kistler, and M. Hilchenbach: Ionic charge states of low energy ions in solar energetic particle events: an overview. AGU Fall Meeting, San Francisco, USA, December 10-14, 2007. (Oral).

**Kleimann, J.**, M. Fränz, J. Woch, R. A. Frahm, and J. D. Winningham: Modeling of photoelectron spectra observed in the Martian ionosphere. European Geosciences Union General Assembly, Vienna, Austria, April 15-20, 2007. (Poster).

**Koch, C.**: Geodäten in den planetaren Wissenschaften. Deutscher Geodätentag, Braunschweig, Germany, June 08-09, 2007, invited. (Oral).

**Koch, C.**, U. R. Christensen, M. Hilchenbach, and R. Kallenbach: Extraction of time-dependent variations from BepiColombo laser altimeter data. European Geosciences Union General Assembly, Vienna, Austria, April 15-20, 2007. (Poster).

**Koch, C.**, U. R. Christensen, and R. Kallenbach: Extraction of time-dependent topography variations from BepiColombo laser altimeter data for different realizations of topography. European Planetary Science Congress 2007, Potsdam, Germany, August 19-24, 2007. (Oral).

**Krivova, N.**: Models of solar irradiance variations. International Conference on "Challenges for Solar Cycle 24", Ahmedabad, India, January 22-25, 2007, invited talk. (Oral).

**Krivova, N. A.**: Modelling solar total and spectral irradiance. IUGG XXIV General Assembly, Perugia, Italy, July 2-13, 2007, invited.

**Krivova, N. A.**: Solar-terrestrial relations: Sun & climate. Heliophysics: The Sun, the Heliosphere and the Earth, Bad Honeff, Germany, May 14-18, 2007, invited.

**Krivova, N. A.**: Solar variability of relevance for the Earth's climate. Workshop A contribuição do Sol para o problema do aquecimento global da Terra, Coimbra, Portugal, March 3, 2007, invited.

**Krivova, N. A.**: Variations of solar irradiance on time scales of days to millennia. European Meteorological Society: 7th EMS Annual Meeting/ 8th European Conference on Applications of Meteorology, San Lorenzo de El Escorial, Spain, October 1-5, 2007, invited.

**Kronberg, E.** and P. Daly: RAPID report for the 2nd CAA operations review. Cluster Active Archive 2nd Operations Review, Noordwijk, The Netherlands, May 15, 2007. (Oral).

**Kronberg, E.** and P. Daly: RAPID/IIMS and CIS/CODIF cross-calibration. 5th Cluster Cross-calibration Meeting, Noordwijk, The Netherlands, May 14, 2007. (Oral).

**Kronberg, E.**, P. W. Daly, and I. Dandouras: RAPID/IIMS & CIS/CODIF cross-calibration. CIS/HIA Cluster and Double Star Team Meeting, Starnberg, Germany, June 19-21, 2007. (Oral).

Kronberg, E., S. Mühlbachler, and **P. Daly**: RAPID visualization software and its applications. RAPID/PEACE Joint Team Meeting, Abingdon, UK, September 5-7, 2007.

**Kronberg, E. A.**, A. Kis, B. Klecker, P. W. Daly, and E. A. Lucek: Multipoint observations of ions in the energy range 30 - 90 KeV upstream of Earth's bow shock. AGU Fall Meeting, San Francisco, USA, December 10-14, 2007. (Poster).

**Krueger, H.**: 3 Jahre Cassini - Was haben wir gelernt? Volkshochschule Mosbach (Baden), Binau, Germany, November 30, 2007. (Oral).

**Krueger, H.**: Dust inside and outside the heliosphere. ISSI-Workshop "From the Outer Heliosphere to the Local Bubble: Comparison of New Observations with Theory", Bern, Switzerland, October 15-19, 2007, invited. (Oral).

**Krueger, H.**: Stonehenge & Co. - Astronomie in der Steinzeit. Volkshochschule Mosbach/Baden; Binau, Germany, June 15, 2007. (Oral).

**Krueger, H.**, C. Engrand, H. Fischer, M. Hilchenbach, K. Hornung, J. Kissel, T. Stephan, L. Thirkell, R. Thomas, M. Trieloff, K. Varmuza, and the COSIMA science team: Laboratory calibration of Rosetta/COSIMA - Preparation for Comet 67P/Churyumov-Gerasimenko. European Geosciences Union General Assembly, Vienna, Austria, April 15-20, 2007. (Poster).

**Krueger, H.**, C. Engrand, H. Fischer, M. Hilchenbach, K. Hornung, J. Kissel, T. Stephan, L. Thirkell, R. Thomas, M. Trieloff, K. Varmuza, and the COSIMA science team: Laboratory calibration of Rosetta/COSIMA - preparation for comet 67P/Churyumov-Gerasimenko. Workshop "Dusty Visions", Heidelberg, Germany, April 10-13, 2007. (Oral).

**Krupp, N.**: An update on field-aligned energetic electron beams in the Saturnian magnetosphere. Cassini MAPS Workshop, Iowa City, Iowa, USA, May 17-18, 2007. (Oral).

**Krupp, N.**: Review of plasma dynamics in the magnetospheres of Jupiter and Saturn. Magnetospheres of the Outer Planets (MOP) Meeting, San Antonio, Texas, USA, June 25-29, 2007. (Oral).

**Krupp, N.**: The magnetosphere of Jupiter after Galileo. Bepi Colombo MMO SOWG, ISAS, Tokyo, Japan, January 12, 2007. (Oral).

**Krupp, N.**, A.-M. Harri, and B. Grieger: Europlanet activity N2 (Discipline Working Groups) annual report 2006. Europlanet Coordinator Meeting, CNES office, Brussels, Belgium, January 25-26, 2007. (Oral).

**Krupp, N.** and P. Louarn: The magnetospheres theme for the Europa/Jupiter mission (in response to ESA Cosmic vision proposal). Juno Team Meeting, Caltech, Pasadena, CA, USA, February 5, 2007. (Oral).

**Krupp, N.**, E. Roussos, D. G. Mitchell, K. K. Khurana, and S. M. Krimigis: Energetic electron beams in the magnetosphere of Saturn: Cassini MIMI results. European Planetary Science Congress 2007, Potsdam, Germany, August 19-24, 2007. (Oral).

**Kudela, K.**, R. Bucik, and P. Bobik: Transmissivity predictions for cosmic rays in disturbed magnetosphere: a case study. European Geosciences Union General Assembly, Vienna, Austria, April 15-20, 2007. (Poster).

Kulyk, I. and **K. Jockers**: Icy satellites of Saturn: disk-integrated observations of the brightness opposition surge at low phase angles. European Planetary Science Congress 2007, Potsdam, Germany, August 19-24, 2007. (Poster).

**Küppers, M.**: Cometas. Inauguration of the new facilities of the observatory of the University of Nariño, Pasto, Colombia (participation by video conference), March 16, 2007. (Oral).

**Küppers, M.**, H. U. Keller, and the OSIRIS team: OSIRIS science during Rosetta cruise. European Geosciences Union General Assembly, Vienna, Austria, April 15-20, 2007. (Oral).

Küppers, M., **M. Rengel**, H. U. Keller, P. J. Gutierrez, and S. F. Hviid: The light curve of the dust cloud ejected by the collision between the Deep Impact projectile and the nucleus of comet 9P/Tempel 1. 39th Annual Meeting of the Division of Planetary Sciences (DPS), Florida, USA, October 7-12, 2007. (Poster).

**Lagg, A.**, S. K. Solanki, J. Woch, and A. Gandorfer: Measurements of Canopy Fields at Chromospheric Heights. 5th Solar Polarization Workshop, Ascona, Switzerland, September 17-21, 2007. (Oral).

**Lee, K. W.**, N. V. Elkina, and J. Büchner: High frequency electron/electron modes in solar coronal plasma. 71. Jahrestagung der Deutschen Physikalischen Gesellschaft, Regensburg, Germany, March 23-30, 2007. (Poster).

**Lee, K. W.**, N. V. Elkina, and J. Büchner: High frequency electron/electron modes in solar coronal plasma. European Geosciences Union General Assembly, Vienna, Austria, April 15-20, 2007. (Oral).

**Lee, K. W.**, N. V. Elkina, and J. Büchner: Linearly unstable modes in coronal current-driven plasma. 71. Jahrestagung der Deutschen Physikalischen Gesellschaft, Regensburg, Germany, March 23-30, 2007. (Oral).

**Lee, K. W.**, N. V. Elkina, and J. Büchner: Linearly unstable modes in coronal current-driven plasma. European Geosciences Union General Assembly, Vienna, Austria, April 15-20, 2007. (Poster).

**Li, X.** and J. Büchner: Tracing moving magnetic flux concentrations around sunspots. 71. Jahrestagung der Deutschen Physikalischen Gesellschaft, Regensburg, Germany, March 28, 2007. (Oral).

**Li, X.**, J. Büchner, and J. Zhang: Tracing moving flux concentrations around sunspots. Conference on International Heliophysical Year, Bad Honnef, Germany, May 14-18, 2007. (Oral).

**Lühr, H.**, M. Rother, and K. Schlegel: Observation of intense kilometre-scale field-aligned currents: Evidence for an Alfvén resonator? AGU Fall Meeting, San Francisco, USA, December 10-14, 2007. (Oral).

Maltagliati, L., D. Titov, T. Encrenaz, F. Forget, R. Melchiorri, and J.-P. Bibring: Atmospheric water vapour in the vicinity of Hellas Basin by OMEGA/MEx. European Mars Science & Exploration Conference: Mars Express & ExoMars, ESA-ESTEC, Noordwijk, The Netherlands, November 12-16, 2007. (Poster).

**Maltagliati, L.**, M. Tschimmel, D. Titov, T. Encrenaz, R. Melchiorri, T. Fouchet, N. Ignatiev, J.-P. Bibring, and V. Formisano: Seasonal water cycle of Mars observed by OMEGA and PFS. European Mars Science & Exploration Conference: Mars Express & ExoMars, ESA-ESTEC, Noordwijk, The Netherlands, November 12-16, 2007. (Oral).

**Maltagliati, L.**, M. Tschimmel, D. V. Titov, N. I. Ignatiev, T. Fouchet, E. Lellouch, J.-P. Bibring, Y. Langevin, V. Formisano, and M. Giuranna: Atmospheric water behavior from the observations by the PFS and OMEGA spectrometers onboard Mars Express. European Planetary Science Congress 2007, Potsdam, Germany, August 19-24, 2007. (Oral).

**Marsch, E.**: Connections between magnetic fields and plasma flows in transition region and corona. First Solaire network-wide meeting at KU Leuven, Leuven, Belgium, December 17-19, 2007. (Oral).

**Marsch, E.**: Introduction to Solar Orbiter and its synergies with Kuafu. The Second International Symposium on KuaFu Project (ISKP-II), Sanya, Hainan, China, January 15-19, 2007. (Oral).

**Marsch, E.**: Kinetic physics of the solar wind. Conference on International Heliophysical Year, Bad Honnef, Germany, May 14-18, 2007, invited. (Oral).

**Marsch, E.**: Kinetic Physics of the Solar Wind. International School of Space Science "Turbulence and Waves in Space Plasmas", l'Aquila, Italy, September 9-14, 2007, invited lecture. (Oral).

**Marsch, E.**: Solar wind orgin in the solar transition region and possible Kuafu observations. The Second International Symposium on KuaFu Project (ISKP-II), Sanya, Hainan, China, January 15-19, 2007. (Oral).

**Marsch, E.**: The combined science program of the Solar Orbiter and Sentinels missions for exploration of the Sun-Heliosphere connections. SOHO 20 Transient Events on the Sun and in the Heliosphere, Gent, Belgium, August 27-31, 2007, invited. (Oral).

**Marsch, E.**, M. Heuer, L. Zhao, and C. Tu: Diffusion plateaus and temperature anisotropies of proton velocity distributions in fast solar wind. 71 Annual Meeting of the DPG and Spring Meeting of the Extraterrestrial Physics Division, und Frühjahrstagung der Arbeitsgemeinschaft Extraterrestrische Forschung, Regensburg, Germany, March 26-30, 2007. (Poster).

**Marsch, E.** and C. Tu: Magnetic structure of the solar transition region as observed in various ultraviolet lines emitted at different temperatures. 71 Annual Meeting of the DPG and Spring Meeting of the Extraterrestrial Physics Division, und Frühjahrstagung der Arbeitsgemeinschaft Extraterrestrische Forschung, Regensburg, Germany, March 26-30, 2007. (Oral).

Martinecz, C., M. Fraenz, J. Woch, **N. Krupp**, E. Roussos, E. Dubinin, U. Motschmann, A. Boesswetter, S. Simon, and S. Barabash: The plasma environment of Venus: comparison of Venus Express ASPERA-4 measurements with 3D hybrid simulation. European Planetary Science Congress 2007, Potsdam, Germany, August 19-24, 2007. (Oral).

**Martinecz, C.**, M. Fränz, J. Woch, N. Krupp, E. Dubinin, E. Roussos, U. Motschmann, S. Barabash, R. Lundin, and the ASPERA-4 Team: Location of the bow shock and the ion composition boundary at Venus - initial determinations from Venus Express ASPERA-4. Venus Express Workshop, La Thuile, Italy, March 18-24, 2007. (Oral).

**Martinecz, C.**, M. Fränz, J. Woch, N. Krupp, E. Dubinin, E. Roussos, U. Motschmann, S. Barabash, R. Lundin, and the ASPERA-4 Team: Location of the bow shock and the ion composition boundary at Venus - initial determinations from Venus Express ASPERA-4. $16^{th}$ ASPERA-3 and $6^{th}$ ASPERA-4 project meeting, Stockholm, Sweden, May 9-11, 2007. (Oral).

**Martinecz, C.**, M. Fränz, J. Woch, N. Krupp, E. Dubinin, E. Roussos, U. Motschmann, A. Bößwetter, S. Simon, S. Barabash, H. Lammer, H. Lichtenegger, T. L. Zhang, Y. Kulikov, M. Pätzold, M. K. Bird, and the ASPERA-4 Team: The plasma environment of Venus: Comparison of Venus Express ASPERA-4 measurements with 3D hybrid simulations. European Planetary Science Congress 2007, Potsdam, Germany, August 20-24, 2007. (Poster).

**Martinecz, C.**, M. Fränz, J. Woch, N. Krupp, E. Dubinin, E. Roussos, U. Motschmann, A. Bößwetter, S. Simon, S. Barabash, and the ASPERA-4 Team: Location of the bow shock and the ion composition boundary at Venus and initial 3D hybrid simulations results of the plasma environment of Venus. European Geosciences Union General Assembly, Vienna, Austria, April 15-20, 2007. (Poster).

**Mierla, M.**, R. Schwenn, L. Teriaca, G. Stenborg, and B. Podlipnik: On the dynamics of the solar corona. International Conference on “Challenges for Solar Cycle 24”, Ahmedabad, India, January 22-25, 2007. (Oral).

**Mitchell, D. G.**, S. M. Krimigis, B. E. Mauk, J. Saur, W. S. Kurth, D. A. Gurnet, M. K. Dougherty, W. R. Pryor, L. W. Esposito, and N. Krupp: Saturns aurora: its relationship to energetic particles in the middle and outer magnetosphere. Magnetospheres of the Outer Planets (MOP) Meeting, San Antonio, Texas, USA, June 25-29, 2007. (Oral).

**Modolo, R.**, G. Chanteur, E. Dubinin, A. P. Matthews, and J.-E. Wahlund: Global hybrid simulations of planetary plasma environment. European Geosciences Union General Assembly, Vienna, Austria, April 15-20, 2007. (Oral).

**Nakamura, R.**, K. Keika, W. Baumjohann, A. Runov, W. Magnes, H. Eichelberger, V. Angelopoulos, J. McFadden, C. W. Carlson, D. Larson, K. H. Glassmeier, U. Auster, K. H. Fornaçon, E. A. Lucek, C. M. Carr, O. Amm, A. N. Fazakerley, H. Rème, I. Dandouras, B. Klecker, and P. Daly: Relationship between tail-current sheet activation and dayside magnetosphere. AGU Fall Meeting, San Francisco, USA, December 10-14, 2007. (Poster).

Neukirch, T., **T. Wiegelmann**, P. Ruan, and B. Inhester: Optimization approach for the computation of 3D magnetohydrostatic coronal equilibria from multi-spacecraft observations. AGU Fall Meeting, San Francisco, USA, December 10-14, 2007. (Oral).

**Nutto, C.**, M. Roth, Y. Zhugzhda, J. Bruls, and O. von der Lühe: Calculation of spectral darkening functions for solar and stellar oscillations. HELAS II International Conference “Helioseismology, Asteroseismology and MHD Connections”, Göttingen, Germany, August 20-24, 2007. (Poster).

**Ondrej, S.**, D. A. Gurnett, J. S. Pickett, M. Parrot, N. Cornilleau-Wehrlin, and P. W. Daly: Storm-time dynamics of whistler-mode chorus at different scales. IUGG XXIV General Assembly, Perugia, Italy, July 2-13, 2007. (Oral).

**Protopapa, S.**, H. Boehnhardt, T. Herbst, F. Merlin, D. Cruikshank, and W. Grundy: Surface ice spectroscopy of Pluto and Charon resolved. DPS 2007, Orlando, Florida, USA, October 7-12, 2007. (Oral).

**Protopapa, S.**, T. Herbst, and H. Boehnhardt: Surface ice spectroscopy of Pluto, Charon and Triton. European Planetary Science Congress 2007, Potsdam, Germany, August 19-24, 2007. (Oral).

**Raouafi, N.-E.**, S. K. Solanki, and T. Wiegelmann: Diagnostics of the solar coronal magnetic field using the Hanle effect: a test using realistic magnetic field configurations. 5th Solar Polarization Workshop, Ascona, Switzerland, September 17-21, 2007. (Oral).

**Rengel, M.**: Observations and modelling of stellar embryos. Seminar, Centro de Investigaciones de Astronomia F. J. Duarte, Merida, Venezuela, February 1, 2007. (Oral).

**Rengel, M.**, P. Hartogh, and C. Jarchow: Mesospheric winds, thermal structure, and CO distribution in Venus around the messenger flyby. 39th Annual Meeting of the Division of Planetary Sciences (DPS), Florida, USA, October 7-12, 2007. (Oral).

**Rengel, M.**, P. Hartogh, and C. Jarchow: Mesospheric Winds, Thermal Structure, and CO Distribution on Venus from SMT Observations. Venus Express Ground-based observation Workshop, Noordwijk, The Netherlands, December 17-10, 2007. (Oral).

**Rengel, M.**, P. Hartogh, and C. Jarchow: SMT Observations of the Venusian temperature and winds around the messenger flyby. Asia Oceania Geosciences Society 2007, 4th Annual Meeting, Bangkok, Thailand, July 31 - August 4, 2007. (Oral).

**Rengel, M.**, G. H. Jones, M. Küppers, H. U. Keller, and M. Owens: The ion tail of comet Machholz observed by OSIRIS as a tracer of the solar wind velocity. European Geosciences Union General Assembly, Vienna, Austria, April 15-20, 2007. (Poster).

**Rengel, M.**, M. Küppers, H. U. Keller, P. Gutierrez, and S. Hviid: The terminal velocity of the Deep Impact dust ejecta. Oberseminar in Sommersemester 2007, Institute for Geophysics and Extraterrestial Physics, Braunschweig, Germany, July 10, 2007, invited talk. (Oral).

**Rengel, M.**, M. Küppers, H. U. Keller, P. Gutierrez, and S. F. Hviid: Impactando a un Cometa: La Misión Impacto Profundo. La Semana de la Astronomía en la Isla de Margarita, Isla de Margarita, Venezuela, October 22-26, 2007. (Oral).

**Rengel, M.**, M. Küppers, H. U. Keller, P. Gutierrez, and S. F. Hviid: The terminal velocity of the Deep Impact dust ejecta. 12th Latin-American Regional IAU Meeting, Isla de Margarita, Venezuela, October 22-26, 2007. (Oral).

**Roth, M.**: Der Puls der Sonne - helioseismische Untersuchungen des Sonneninnern. Öffentliche Vortragsreihe "Aus Naturwissenschaft und Technik", Physikalischer Verein, Universität Frankfurt, Frankfurt a.M., Germany, May 16, 2007, invited talk. (Oral).

**Roth, M.**: Der Puls der Sonne - Was Sonnenbeben über unser Zentralgestirn verraten. Öffentliche Abendvorlesung, Paulinerkirche, Göttingen, Germany, August 24, 2007. (Oral).

**Roth, M.**: Helioseismic measurements of the meridional circulation. 5th Potsdam Thinkshop "Meridional flow, differential rotation, solar and stellar activity", Astrophysikalisches Institut Potsdam, Germany, June 24-29, 2007. (Oral).

**Roth, M.**: Helioseismologie. Veranstaltung der Sternfreunde Freiburg i.Br. e.V., Freiburg, Germany, February 28, 2007, invited talk. (Oral).

**Roth, M.**, L. Gizon, and J. G. Beck: Measurements of helioseismic travel times. HELAS II International Conference "Helioseismology, Asteroseismology and MHD Connections", Göttingen, Germany, August 20-24, 2007. (Poster).

**Roth, M.**, L. Gizon, and A. C. Birch: Sensitivity kernels for flows in spherical geometry. HELAS II International Conference "Helioseismology, Asteroseismology and MHD Connections", Göttingen, Germany, August 20-24, 2007. (Poster).

**Roussos, E.**: Saturn's rings through magnetospheric measurements. Space physics lectures, University of Athens, Greece, June 12, 2007. (Oral).

**Roussos, E.**: The origin of Saturn's G-ring. Solar System Seminar, Max Planck Institute for Solar System Research, Katlenburg-Lindau, Germany, June 27, 2007. (Oral).

Roussos, E., **M. Fraenz**, E. Dubinin, C. Martinecz, U. Motschmann, S. Barabash, J. Woch, R. Lundin, R. Frahm, and J. D. Winningham: Energetic electron asymmetries at Mars: Mars Express ASPERA-3 observations. European Planetary Science Congress 2007, Potsdam, Germany, August 19-24, 2007. (Oral).

Roussos, E., G. H. Jones, **N. Krupp**, C. Paranicas, D. G. Mitchell, M. M. Hedman, J. A. Burns, and U. Motschmann: Detection and physical characterization of dust structures at Saturn, through energetic charged particle data: new results from Cassini. European Planetary Science Congress 2007, Potsdam, Germany, August 19-24, 2007. (Oral).

**Roussos, E.**, N. Krupp, G. H. Jones, C. Paranicas, D. G. Mitchell, and S. M. Krimigis: Determining the timing of injections at Saturn: prospects from energetic electron absorption by the icy moons. Magnetospheres of the Outer Planets (MOP) Meeting, San Antonio, Texas, USA, June 25-29, 2007. (Poster).

Roussos, E., **N. Krupp**, G. H. Jones, C. Paranicas, D. G. Mitchell, S. M. Krimigis, U. Motschmann, A. Lagg, and J. Woch: Energetic charged particle absorption by Saturn's icy moons: future studies and new applications. European Planetary Science Congress 2007, Potsdam, Germany, August 19-24, 2007. (Oral).

Roussos, E., J. Mueller, S. Simon, A. Boesswetter, U. Motschmann, M. Fränz, and **N. Krupp**: The magnetic and plasma wake of Rhea: results from hybrid plasma simulations. European Planetary Science Congress 2007, Potsdam, Germany, August 19-24, 2007. (Oral).

**Roussos, E.**, J. Müller, S. Simon, A. Bößwetter, U. Motschmann, N. Krupp, M. Fränz, and J. Woch: Rhea's interaction with Saturn's magnetospheric plasma: a combined data-simulation approach. Planetary seminar, University of Braunschweig, Germany, June 28, 2007.

**Ruan, P.**, T. Wiegelmann, B. Inhester, S. Solanki, and L. Feng: Modeling the 3D coronal plasma and magnetic field from STEREO/SECCHI and magnetic surface data. SECCHI workshop, Paris, France, March 5-8, 2007. (Oral).

**Saidi, Y. M.**, A. C. Birch, and L. Gizon: Distant computation of travel-time sensitivity kernels over the internet. HELAS II International Conference "Helioseismology, Asteroseismology and MHD Connections", Göttingen, Germany, August 20-24, 2007. (Poster).

**Santolik, O.**, D. A. Gurnett, J. S. Pickett, V. Y. Trakhtengerts, A. G. Demekhov, N. Cornilleau-Wehrlin, P. W. Daly, and A. Fazakerley: Hiss and chorus emissions: loss and source mechanisms for energetic particles. European Geosciences Union General Assembly, Vienna, Austria, April 15-20, 2007, invited. (Oral).

**Santos, J.** and J. Büchner: Inferring photospheric velocities from a sequence of photospheric magnetograms. 71. Jahrestagung der Deutschen Physikalischen Gesellschaft, Regensburg, Germany, March 28, 2007. (Poster).

**Sasso, C.**, A. Lagg, S. K. Solanki, R. Aznar Cuadrado, L. Teriaca, and M. Collados: The He I 10830 Å multiplet: analysis of the Stokes vector in a filament during a flare. 5th Solar Polarization Workshop, Ascona, Switzerland,, September 17-21, 2007. (Poster).

**Schad, A.**, M. Roth, B. Schelter, O. von der Lühe, and J. Timmer: Cross-spectral analysis of global solar oscillations. HELAS II International Conference "Helioseismology, Asteroseismology and MHD Connections", Göttingen, Germany, August 20-24, 2007. (Poster).

**Schlegel, K.**: Blitze - Urgewalten am Himmel. Vortragsreihe des Förderkreis Planetarium Göttingen e.V., Göttingen, Germany, February 06, 2007. (Oral).

**Schmitt, D.**: Das Magnetfeld der Sonne. Kolloquium, TU Ilmenau, Germany, June 12, 2007. (Oral).

**Schmitt, D.**: Der Sternhimmel im Herbst. Wohnstift, Göttingen, Germany, October 13, 2007. (Oral).

**Schmitt, D.**: Die Sternbilder am Winterhimmel. Wohnstift Göttingen, Göttingen, Germany, January 13, 2007. (Oral).

Schrijver, C. J., **M. L. DeRosa**, T. Metcalf, G. Barnes, B. Lites, T. Tarbell, J. McTiernan, G. Valori, T. Wiegelmann, M. Wheatland, T. Amari, G. Aulanier, P. Demoulin, M. Fuhrmann, K. Kusano, S. Regnier, M. Smith, and J. Thalmann.: Nonlinear force-free field modelling of a large, flaring active region observed with the Hinode Solar Optical Telescope. Hinode Science Meeting, Trinity College Dublin, Dublin, Ireland, August 20-24, 2007. (Oral).

**Schühle, U.**: A Lyman-Alpha telescope for KuaFu-A. The Second International Symposium on KuaFu Project (ISKP-II), Sanya, Hainan, China, January 15-19, 2007. (Oral).

**Schunker, H.**: The search for evidence of mode conversion. SOHO 19 / GONG 2007 Seismology of Magnetic Activity, Melbourne, Australia, July 9-13, 2007, invited. (Oral).

**Schunker, H.** and L. Gizon: HELAS local helioseismology data webpage. HELAS II International Conference "Helioseismology, Asteroseismology and MHD Connections", Göttingen, Germany, August 20-24, 2007. (Poster).

**Schüssler, M.**: Simulation of solar magnetoconvection. Astrophysikalisches Kolloquium, Astrophysikalisches Institut Potsdam (AIP), Germany, December 15, 2007. (Oral).

**Schwenn, R.**: Coronal mass ejections - the open questions. International Conference on "Challenges for

Solar Cycle 24", Ahmedabad, India, January 22-25, 2007, invited talk. (Oral).

**Schwenn, R.**: Coronal mass ejections: The open questions. VIII COLAGE meeting, Mérida, Mexico, July 11-17, 2007, invited Review. (Oral).

**Schwenn, R.**: Sonne-Erde-Weltraumwetter. Öffentlicher Vortrag, Planetarium Bochum, Germany, June 20, 2007.

**Schwenn, R.**: Sonnenstürme brausen durchs Sonnensystem - wie funktioniert das Weltraumwetter? XLAB Science Festival, Göttingen, Germany, December 20, 2007. (Oral).

**Schwenn, R.**: Space storms are roaring through the solar system: why do we earthlings care? European Geosciences Union General Assembly, Vienna, Austria, April 15-20, 2007, invited Medal Lecture (Julius Bartels Medal). (Oral).

**Schwenn, R.**: Space storms are roaring through the solar system: why do we earthlings care? 10th International Congress of the Brazilian Geophysical Society, Rio de Janeiro, Brazil, November 19-23, 2007, invited. (Oral).

**Schwenn, R.**: Space weather. 2nd ELAGE school, Mérida, Mexico, July 11-17, 2007, lectures.

**Schwenn, R.**: Space weather - the open questions. 9th. Brazilian Meeting on Plasma 9 Encontro Brasileiro de Física dos Plasmas, Sao Pedro, Brazil, November 25-28, 2007, invited.

**Schwenn, R.**: Space weather - the open questions. Seminar at INPE, Sao José dos Campos, Brazil, November 29, 2007, invited Seminar lecture.

**Schwenn, R.**: Space weather science and the KuaFu project. The Second International Symposium on KuaFu Project, Sany, China, January 15-19, 2007, invited paper. (Oral).

**Shinsuke, I.**, R. Nakamura, P. Daly, M. Hoshino, W. Baumjohann, S. Mühlbachler, A. Balogh, and H. Rème: Energetic electron acceleration in the downstream reconnection outflow region. IUGG XXIV General Assembly, Perugia, Italy, July 2-13, 2007. (Oral).

**Sittler, E. C., Jr.**, C. Arridge, A. Rymer, A. Coates, N. Krupp, M. Blanc, J. Richardson, N. Andre, M. Thomsen, M. Henderson, J. F. Cooper, M. Burger, D. Simpson, K. K. Khurana, M. Dougherty, and D. T. Young: Cassini observations of Saturns dawn-magnetotail region: preliminary results. Magnetospheres of the Outer Planets (MOP) Meeting, San Antonio, Texas, USA, June 25-29, 2007. (Oral).

**Skorov, Y. U.** and H. U. Keller: Where is the ice in comets? Twenty years after. European Planetary Science Congress 2007, Potsdam, Germany, August 19-24, 2007. (Oral).

**Solanki, S. K.**: Der Feuerball am Himmel und die Klimakatastrophe auf der Erde. Sonnenaktivität und Klimawandel, IHY 2007 Vortrag, Zeiss Planetarium Bochum, Germany, May 16, 2007, invited talk.

**Solanki, S. K.**: Jan Stenflo's contributions to solar physics. 5th Solar Polarization Workshop, Ascona, Switzerland, September 17-21, 2007, invited talk.

**Solanki, S. K.**: Magnetic active regions and sunspots. HELAS II International Conference, Göttingen, Germany, August 20-24, 2007, invited talk.

**Solanki, S. K.**: Photospheric magnetic fields. 5th Solar Polarization Workshop, Ascona, Switzerland, September 17-21, 2007, invited review.

**Solanki, S. K.**: The International Max Planck Research School. Seminar Space Physics Department, University of Helsinki, Helsinki, Finland, March 14, 2007, invited.

**Solanki, S. K.**: The Suns magnetic field and global climate change. Physik-Kolloquium ETH Zürich, Zürich, Switzerland, January 10, 2007, invited.

**Solanki, S. K.**: The Suns magnetic field and global climate change. Seminar, Finnish Meteorological Institute, Helsinki, Finland, March 14, 2007, invited.

**Solanki, S. K.**: The Suns magnetic field and global climate change. XVI Annual Meeting Finnish Physical Society, Tallin, Estland, March 14-17, 2007, invited.

**Solanki, S. K.**: The Suns magnetic field and global climate change. Kolloquium MPI für Biogeochemie, Jena, Germany, June 7, 2007, invited talk.

**Solanki, S. K.**: The Suns magnetic field and global climate change. Kolloquium, Gesellschaft für Schwerionenforschung mbH, Darmstadt, Germany, October 30, 2007.

**Solanki, S. K.**: The Suns magnetic field from core to corona. 3rd Joint ILIAS-CERN-DESY Axion-WIMPs Workshop, Patras, Greece, June 19-25, 2007, invited talk.

**Solanki, S. K.**: The Sun's magnetic field, irradiance variations and global climate change. Osservatorio Astronomico di Capodimonte, Napoli, Italy, July 4, 2007, invited talk.

**Solanki, S. K.**: Was hat das Magnetfeld der Sonne mit Einstein und dem Klima zu tun? Greifswalder Physikalisches Kolloquium, MPI für Plasmaphysik, Greifswald, Germany, June 28, 2007, invited talk.

**Stahn, T.** and L. Gizon: Improved estimates of solar and stellar oscillation parameters. HELAS II International Conference "Helioseismology, Asteroseismology and MHD Connections", Göttingen, Germany, August 20-24, 2007. (Poster).

Stenzel, O., B. Grieger, H. U. Keller, **R. Greve**, K. Fraedrich, E. Kirk, and F. Lunkeit: North polar ice cap of Mars at varying obliquities, simulated with coupled ice and atmosphere models. IUGG XXIV General Assembly, Perugia, Italy, July 2-13, 2007. (Oral).

**Stenzel, O. J.**, B. Grieger, H. U. Keller, R. Greve, K. Fraedrich, E. Kirk, and F. Lunkeit: Results from the Mars climate simulation project. DFG Priority Colloquium "Mars and the Terrestrial Planets", Berlin, Germany, February 19-20, 2007. (Oral).

**Stenzel, O. J.**, N. Hoekzema, W. J. Markiewicz, H. U. Keller, and the HRSC Co-Investigator Team: A Simple scheme for batch processing atmospheric corrections of HRSC colour images. European Mars Science and Exploration Conference: Mars Express & ExoMars, ESTEC, Noordwijk, The Netherlands, November 12-16, 2007. (Poster).

**Stenzel, O. J.**, N. Hoekzema, W. J. Markiewicz, H. U. Keller, and the HRSC Co-Investigator Team: Simple scheme for batch processing atmospheric corrections of HRSC colour images. HRSC Team Meeting, ESTEC, Noordwijk, The Netherlands, November 16-17, 2007. (Oral).

**Teriaca, L.**: Polar plumes as seen in the vacuum ultraviolet. IIA Colloquia, Indian Institute of Astrophysics, November 13, 2007. (Oral).

**Teriaca, L.**: Search for photospheric footpoints of quiet Sun transition region loops. Catania Astrophysical Observatory, Catania, Italy, September, 17, 2007. (Oral).

**Teriaca, L.**, T. Wiegelmann, A. Lagg, S. K. Solanki, W. Curdt, T. Sekii, and the HINODE/SOT team: Loop morphology and flows and their relation with the magnetic field. Hinode Science Meeting, Trinity College Dublin, Dublin, Ireland, August 20-24, 2007. (Poster).

**Thalmann, J. K.** and T. Wiegelmann: Nonlinear force-free field extrapolation of NOAA AR 0696. AGU Fall Meeting, San Francisco, USA, December 10-14, 2007. (Poster).

**Thalmann, J. K.** and T. Wiegelmann: Testing of H-Alpha preprocessing. Nonlinear force-free workshop 4, Paris, France, June 12-14, 2007, invited. (Oral).

**Timo, A.**, K. Mursula, and P. Daly: Energetic particle signatures in association with flux transfer events in the exterior cusp. IUGG XXIV General Assembly, Perugia, Italy, July 2-13, 2007. (Oral).

**Tubiana, C.**, H. Boehnhardt, L. Barrera, M. Drahus, J. L. Ortiz, G. Schwehm, and R. Schulz: VLT observations of 67P/Churyumov-Gerasimenko at large heliocentric distance. Coordination of ground-based observations of Rosetta target comet 67P/Churyumov-Gerasimenko, Orlando, Florida, USA, October 7, 2007.

**Tubiana, C.**, H. Boehnhardt, L. Barrera, M. Drahus, J. L. Ortiz, G. Schwehm, R. Schulz, J. Stuewe, and M. Lippi: Photometry and spectroscopy of 67P/Churyumov-Gerasimenko at large heliocentric distance. EPSC 2007, Potsdam, Germany, August 19-24, 2007. (Oral).

**Tubiana, C.**, H. Boehnhardt, L. Barrera, J. Ortiz, G. Schwehm, and R. Schulz: 67P/Churyumov-Gerasimenko: photometry and spectroscopy of the Rosetta target comet at large heliocentric distance. DPS meeting, Orlando, Florida, USA, October 7-12, 2007. (Oral).

**Tubiana, C.**, R. Duffard, L. Barrera, and H. Boehnhardt: Photometric and spectroscopic observations of (132524) 2002 JF56: fly-by target of the New Horizons mission. EPSC 2007, Potsdam, Germany, August 19-24, 2007. (Poster).

**Vasyliūnas, V. M.**: Comparative Magnetospheres. LWS-IHY Heliophysics Summer School, Boulder, Colorado, USA, July 30 - August 7, 2007, invited lecture.

**Vasyliūnas, V. M.**: How to distinguish different types of periodicities. Cassini MAPS Workshop, Iowa City, Iowa, USA, May 17-18, 2007. (Oral).

**Vasyliūnas, V. M.**: Meaning and time evolution of the Dst index II: Does the tail wag the dog? Space Physics Seminar, Rice University, Houston, Texas, USA, December 5, 2007. (Oral).

**Vasyliūnas, V. M.**: Periodicities in the magnetosphere of Saturn: making the distinctions. European Geosciences Union General Assembly, Vienna, Austria, April 15-20, 2007. (Oral).

**Vasyliūnas, V. M.**: The plasma frequency as the boundary between plasma physics and single-particle electrodynamics. Prof. Bodo W. Rheinisch 70th Birthday Honorary Symposium "Radio

Sounding and Plasma Physics", Lowell, Massachusetts, USA, April 29, 2007, invited. (Oral).

**Vasyliūnas, V. M.**: Topology of plasma flow: Intertwining of the Dungey and the Vasyliūnas cycles. AGU Fall Meeting, San Francisco, USA, December 10-14, 2007. (Oral).

**Wicht, J.**: Simulating geomagnetic reversals. Colloquium, University of Liverpool, UK, March 9, 2007. (Oral).

**Wicht, J.** and U. R. Christensen: Torsional oscillations in dynamo simulations. IUGG XXIV General Assembly, Perugia, Italy, July 2-13, 2007. (Oral).

**Wicht, J.** and U. R. Christensen: Torsional oscillations in numerical dynamo simulations. IUGG XXIV General Assembly, Perugia, Italy, July 2-13, 2007. (Oral).

**Wiegelmann, T.**: Optimization code for nonlinear force-free modeling: First application to Hinode data. Nonlinear Force-Free Workshop 4, Paris, France, June 12-14, 2007. (Oral).

**Wiegelmann, T.**, L. Feng, and B. Inhester: Reconstruction of the solar corona in 3D with STEREO. Invited seminar talk, MSSL, Dorking, UK, May 10, 2007. (Oral).

**Wiegelmann, T.**, B. Inhester, L. Feng, P. Ruan, J. Thalmann, and B. Podlipnik: SECCHI-3D reconstruction software. 5th SECCHI Consortium Meeting, Orsay, France, March 5-8, 2007. (Oral).

**Wiegelmann, T.** and J. Thalmann: Towards the next generation active region model: What can nonlinear force-free extrapolation codes provide? Active Region Evolution Model Development Meeting, Goddard Space Flight Center, USA, October 29-30, 2007, invited, Telecon. (Oral).

Wiegelmann, T., J. K. Thalmann, C. J. Schrijver, **M. L. DeRosa**, and T. Metcalf: Can we improve the preprocessing of photospheric vector magnetograms by inclusion of chromospheric observations? Hinode Science Meeting, Trinity College Dublin, Dublin, Ireland, August 20-24, 2007. (Poster).

**Wiegelmann, T.**, J. K. Thalmann, C. J. Schrijver, M. L. Derosa, and T. R. Metcalf: Can we improve the preprocessing of photospheric vectormagnetograms by the inclusion of chromospheric observations? AGU Fall Meeting, San Francisco, USA, December 10-14, 2007. (Oral).

**Wiegelmann, T.**, J. K. Thalmann, K. Schrijver, M. DeRosa, and T. Metcalf: Preprocessing using H-alpha images. Nonlinear Force-Free Workshop 4, Paris, France, June 12-14, 2007, invited. (Oral).

**Yamauchi, M.**, Y. Futana, A. Fedorov, E. Dubinin, R. Lundin, R. Frahm, S. Barabash, and J. D. Winningham: IMF direction derived from cycloid-like ion distribution observed by Mars Express. European Geosciences Union General Assembly, Vienna, Austria, April 15-20, 2007. (Poster).

Yushkov, B., S. N. Kuznetsov, **K. Kudela**, and R. Bucik: CORONAS-F measurements of high-energy solar proton spectra. 30th International Cosmic Ray Conference, Merida, Mexico, July 3-11, 2007. (Poster).

**Zaatri, A.**, T. Corbard, M. Roth, and I. Gonzalez Hernandez: Geometric mapping comparisons for ring diagram analysis. HELAS II International Conference "Helioseismology, Asteroseismology and MHD Connections", Göttingen, Germany, August 20-24, 2007. (Poster).

**Zhang, H.**, G. Siscoe, T. A. Fritz, Q. Zong, P. W. Daly, H. Rème, A. Balogh, A. J. Ridley, and J. Raeder: Multiple cusps under northward IMF conditions: observations and MHD simulations compared. AGU Fall Meeting, San Francisco, USA, December 10-14, 2007. (Oral).

Zong, Q. G., **S. Y. Fu**, A. Korth, and P. Daly: BBFs with rich ionospheric oxygen ions observed by Cluster and Double Star. European Geosciences Union General Assembly, Vienna, Austria, April 15-20, 2007. (Oral).

## **Veröffentlichungen 2006 /** Publications 2006

*Afram, N., S. V. Berdyugina, D. M. Fluri, S. K. Solanki, A. Lagg, P. Petit, and J. Arnaud*: Molecular diagnostics of the internal structure of starspots and sunspots. In: Solar Polarization 4, eds. R. Casini and B. W. Lites, *ASP Conference Series*, vol. 358, pp. 375–380 (2006).

*Agarwal, J., M. Müller, H. Boehnhardt, and E. Grün*: Modelling the large particle environment of comet 67P/Churyumov-Gerasimenko. Adv. Space Res. **38**, 2049–2053 (2006), doi:10.1016/j.asr.2005.04.046.

*Ahn, H. S., E. S. Seo, J. H. Adams, G. Bashindzhagyan, K. E. Batkov, J. Chang, M. Christl, A. R. Fazely, O. Ganel, R. M. Gunasingha, T. G. Guzik, J. Isbert, K. C. Kim, E. Kouznetsov, M. Panasyuk, A. Panov, W. K. H. Schmidt, R. Sina, N. V. Sokolskaya, J. Z. Wang, J. P. Wefel, J. Wu, and V. Zatsepin*: The energy spectra of protons and helium measured with the ATIC experiment. Adv. Space Res. **37**, 1950–1954 (2006), doi:10.1016/j.asr.2005.09.031.

*Amata, E., S. Savin, M. André, M. Dunlop, Y. Khotyaintsev, M. F. Marcucci, A. Fazakerley, Y. V. Bogdanova, P. M. E. Décréau, J. L. Rauch, J. G. Trotignon, A. Skalsky, S. Romanov, J. Büchner, J. Blecki, and H. Rème*: Experimental study of nonlinear interaction of plasma flow with charged thin current sheets: 1. Boundary structure and motion. Nonlin. Proc. Geophys. **13**, 365–376 (2006).

*Arnaud, J., S. V. Berdyugina, D. M. Fluri, N. Afram, S. K. Solanki, and N.-E. Raouafi*: Spectropolarimetry of a sunspot in atomic and molecular lines with THEMIS. In: Solar Polarization 4, eds. R. Casini and B. W. Lites, *ASP Conference Series*, vol. 358, pp. 319–322 (2006).

*Arvelius, S., M. Yamauchi, H. Nilsson, R. Lundin, H. Rème, M. B. Bavassano-Cattaneo, G. Paschmann, A. Korth, L. M. Kistler, and G. K. Parks*: Statistical study of relationships between dayside high-altitude/-latitude $O^+$ outflows, solar winds, and geomagnetic activity. In: Proceedings Cluster and Double Star Symposium – 5th Anniversary of Cluster in Space, Noordwijk, The Netherlands, 19–23 September 2005, eds. P. Escoubet, H. Laakso, M. Taylor, and A. Masson, ESA SP-598, ESA Publ. Div., Noordwijk (2006), on CD.

*Arvidson, R. E., S. W. Squyres, R. C. Anderson, J. F. Bell, D. Blaney, J. Brückner, N. A. Cabrol, W. M. Calvin, M. H. Carr, P. R. Christensen, B. C. Clark, L. Crumpler, D. J. Des Marais, P. A. de Souza, C. d'Uston, T. Economou, J. Farmer, W. H. Farrand, W. Folkner, M. Golombek, S. Gorevan, J. A. Grant, R. Greeley, J. Grotzinger, E. Guinness, B. C. Hahn, L. Haskin, K. E. Herkenhoff, J. A. Hurowitz, S. Hviid, J. R. Johnson, G. Klingelhofer, A. H. Knoll, G. Landis, C. Leff, M. Lemmon, R. Li, M. B. Madsen, M. C. Malin, S. M. McLennan, H. Y. McSween, D. W. Ming, J. Moersch, R. V. Morris, T. Parker, J. W. Rice, L. Richter, R. Rieder, D. S. Rodionov, C. Schroder, M. Sims, M. Smith, P. Smith, L. A. Soderblom, R. Sullivan, S. D. Thompson, N. J. Tosca, A. Wang, H. Wanke, J. Ward, T. Wdowiak, M. Wolff, and A. Yen*: Overview of the Spirit Mars Exploration Rover Mission to Gusev Crater: Landing site to Backstay Rock in the Columbia Hills. J. Geophys. Res. **111**, E02S01 (2006), doi:10.1029/2005JE002499.

*Aschwanden, M. J., L. F. Burlaga, M. L. Kaiser, C. K. Ng, D. V. Reames, M. J. Reiner, T. I. Gombosi, N. Lugaz, W. Manchester, I. I. Roussev, T. H. Zurbuchen, C. J. Farrugia, A. B. Galvin, M. A. Lee, J. A. Linker, Z. Mikić, P. Riley, D. Alexander, A. W. Sandman, J. W. Cook, R. A. Howard, D. Odstrčil, V. J. Pizzo, J. Kóta, P. C. Liewer, J. G. Luhmann, B. Inhester, R. W. Schwenn, S. K. Solanki, V. M. Vasyliūnas, T. Wiegelmann, L. Blush, P. Bochsler, I. H. Cairns, P. A. Robinson, V. Bothmer, K. Kecskemety, A. Llebaria, M. Maksimovic, M. Scholer, and R. F. Wimmer-Schweingruber*: Theoretical Modeling for the Stereo Mission. Space Sci. Rev. **136**, 565–604 (2008), doi:10.1007/s11214-006-9027-8.

*Åsnes, A., R. W. H. Friedel, B. Lavraud, G. Reeves, P. Daly, H. Rème, and A. Balogh*: A statistical survey of tail plasma sheet energetic electrons. In: Proceedings Cluster and Double Star Symposium – 5th Anniversary of Cluster in Space, Noordwijk, The Netherlands, 19–23 September 2005, eds. P. Escoubet, H. Laakso, M. Taylor, and A. Masson, ESA SP-598, ESA Publ. Div., Noordwijk (2006), on CD.

*Bagnulo, S., H. Boehnhardt, K. Muinonen, L. Kolokolova, I. Belskaya, and A. Barucci*: Exploring the surface properties of transneptunian objects and Centaurs with polarimetric FORS1/VLT observations. Astron. & Astrophys. **450**, 1239–1248 (2006), doi:10.1051/0004-6361:20054518.

*Baines, K. H., S. Atreya, R. W. Carlson, D. Crisp, P. Drossart, V. Formisano, S. S. Limaye, W. J. Markiewicz, and G. Piccioni*: To the depths of Venus: Exploring the deep atmosphere and surface of our sister world with Venus Express. Planet. Space Sci. **54**, 1263–1278 (2006), doi:10.1016/j.pss.2006.04.034.

*Balan, N., H. Alleyne, S. Walker, H. Rème, P. M. E. Décréau, A. Balogh, M. André, A. N. Fazakerley, N. Cornilleau-Wehrlin, D. Gurnett, and M. Fraenz*: Cluster observations of a structured magnetospheric cusp. Ann. Geophys. **24**, 1015–1027 (2006).

*Barabash, S., R. Lundin, H. Andersson, K. Brinkfeldt, A. Grigoriev, H. Gunell, M. Holmström, M. Yamauchi, K. Asamura, P. Bochsler, P. Wurz, R. Cerulli-Irelli, A. Mura, A. Milillo, M. Maggi, S. Orsini, A. J. Coates, D. R. Linder, D. O. Kataria, C. C. Curtis, K. C. Hsieh, B. R. Sandel, R. A. Frahm, J. R. Sharber, J. D. Winningham, M. Grande, E. Kallio, H. Koskinen, P. Riihelä, W. Schmidt, T. Säles, J. U. Kozyra, N. Krupp, J. Woch, S. Livi, J. G. Luhmann, S. McKenna-Lawlor, E. C. Roelof, D. J. Williams, J.-A. Sauvaud, A. Fedorov, and J.-J. Thocaven*: The Analyzer of Space Plasmas and Energetic Atoms (ASPERA-3) for the Mars Express Mission. Space Sci. Rev. **126**, 113–164 (2006), doi:10.1007/s11214-006-9124-8.

*Basilevsky, A. T. and H. U. Keller*: Comet nuclei: Morphology and implied processes of surface modification. Planet. Space Sci. **54**, 808–829 (2006), doi:10.1016/j.pss.2006.05.001.

*Baumann, I., D. Schmidt, and M. Schüssler*: A necessary extension of the surface flux transport model. Astron. & Astrophys. **446**, 307–314 (2006), doi:10.1051/0004-6361:20053488.

*Bavassano-Cattaneo, M. B., M. F. Marcucci, A. Retinò, G. Pallocchia, H. Rème, I. Dandouras, L. M. Kistler, B. Klecker, C. W. Carlson, A. Korth, M. McCarthy, R. Lundin, and A. Balogh*: Kinetic signatures during a quasi-continuous lobe reconnection event: Cluster Ion Spectrometer (CIS) observations. J. Geophys. Res. **111**, A09212 (2006), doi:10.1029/2006JA011623.

*Bavassano-Cattaneo, M. B., M. F. Marcucci, A. Retinò, G. Pallocchia, H. Rème, I. Dandouras, E. Moebius, B. Klecker, C. W. Carlson, A. Korth, R. Lundin, and A. Balogh*: Ion kinetic features around a lobe reconnection site. In: Proceedings Cluster and Double Star Symposium – 5th Anniversary of Cluster in Space, Noordwijk, The Netherlands, 19–23 September 2005, eds. P. Escoubet, H. Laakso, M. Taylor, and A. Masson, ESA SP-598, ESA Publ. Div., Noordwijk (2006), on CD.

*BenMoussa, A., J.-F. Hochedez, U. Schühle, W. Schmutz, K. Haenen, Y. Stockman, A. Soltani, F. Scholze, U. Kroth, V. Mortet, A. Theissen, C. Laubis, M. Richter, S. Koller, J.-M. Defise, and S. Koizumi*: Diamond detectors for LYRA, the solar VUV radiometer on board PROBA2. Diamond and Related Materials **15**, 802–806 (2006), doi:10.1016/j.diamond.2005.10.024.

*BenMoussa, A., U. Schühle, F. Scholze, U. Kroth, K. Haenen, T. Saito, J. Campos, S. Koizumi, C. Laubis, M. Richter, V. Mortet, A. Theissen, and J.-F. Hochedez*: Radiometric characteristics of new diamond PIN photodiodes. Meas. Sci. Technol. **17**, 913–917 (2006), doi:10.1088/0957-0233/17/4/042.

*BenMoussa, A., A. Theissen, F. Scholze, J.-F. Hochedez, U. Schühle, W. Schmutz, K. Haenen, Y. Stockman, A. Soltani, D. McMullin, R. E. Vest, U. Kroth, C. Laubis, M. Richter, V. Mortet, S. Gissot, V. Delouille, M. Dominique, S. Koller, J. P. Halain, Z. Remes, R. Petersen, M. D'Olieslaeger, and J.-M. Defise*: Performance of diamond detectors for VUV applications. Nucl. Instr. Methods Phys. A **568**, 398–405 (2006), doi:10.1016/j.nima.2006.06.007.

*Berdyugina, S. V., D. M. Fluri, and S. K. Solanki*: The molecular Paschen-Back effect. In: Solar Polarization 4, eds. R. Casini and B. W. Lites, *ASP Conference Series*, vol. 358, pp. 329–332 (2006).

*Bertelsen, P., M. B. Madsen, C. S. Binau, W. Goetz, H. P. Gunnlaugsson, S. F. Hviid, K. M. Kinch, G. Klingelhofer, K. Leer, D. E. Madsen, J. Merrison, M. Olsen, S. W. Squyres, and The Athena Team*: Backscattering Mossbauer spectroscopy of Martian dust. Hyperfine Interact. **166**, 523–527 (2006), doi:10.1007/s10751-006-9320-7.

*Bloomfield, D. S., R. T. J. McAteer, M. Mathioudakis, and F. P. Keenan*: The influence of magnetic field on oscillations in the solar chromosphere. Astrophys. J. **652**, 812–819 (2006), doi:10.1086/508409.

*Bodewits, D., R. Hoekstra, B. Seredyuk, R. W. McCullough, G. H. Jones, and A. G. G. M. Tielens*: Charge exchange emission from solar wind helium ions. Astrophys. J. **642**, 593–605 (2006), doi:10.1086/500731.

*Borisov, N. and U. Mall*: Charging and motion of dust grains near the terminator of the moon. Planet. Space Sci. **54**, 572–580 (2006), doi:10.1016/j.pss.2006.01.005.

*Borrero, J. M., M. Rempel, and S. K. Solanki*: The uncombed penumbra. In: Solar Polarization 4, eds. R. Casini and B. W. Lites, *ASP Conference Series*, vol. 358, pp. 19–24 (2006).

*Borrero, J. M., S. K. Solanki, A. Lagg, H. Socas-Navarro, and B. Lites*: On the fine structure of sunspot penumbrae: III. The vertical extension of penumbral filaments. Astron. & Astrophys. **450**, 383–393 (2006), doi:10.1051/0004-6361:20054378.

*Boswell, R. W., E. Marsch, and C. Charles*: The current-free electric double layer in a coronal magnetic funnel. Astrophys. J. **640**, L199–L202 (2006), doi:10.1086/503155.

*Brinkfeldt, K., H. Gunell, P. C. Brandt, S. Barabash, R. A. Frahm, J. D. Winningham, E. Kallio, M. Holmstrom, Y. Futaana, A. Ekenback, R. Lundin, H. Andersson, M. Yamauchi, A. Grigoriev, J. R. Sharber, J. R. Scherrer, A. J. Coates, D. R. Linder, D. O. Kataria, H. Koskinen, T. Sales, P. Riihela, W. Schmidt, J. Kozyra, J. Luhmann, E. Roelof, D. Williams, S. Livi, C. C. Curtis, K. C. Hsieh, B. R. Sandel, M. Grande, M. Carter, J. A. Sauvaud, A. Fedorov, J. J. Thocaven, S. McKenna-Lawler, S. Orsini, R. Cerulli-Irelli, M. Maggi, P. Wurz, P. Bochsler, N. Krupp, J. Woch, M. Fränz, K. Asamura, and C. Dierker*: First ENA observations at Mars: Solar-wind ENAs on the nightside. Icarus **182**, 439–447 (2006), doi:10.1016/j.icarus.2005.12.023.

*Brownlee, D., P. Tsou, J. Aleon, C. M. O. Alexander, T. Araki, S. Bajt, G. A. Baratta, R. Bastien, P. Bland, P. Bleuet, J. Borg, J. P. Bradley, A. Brearley, F. Brenker, S. Brennan, J. C. Bridges, N. D. Browning, J. R. Brucato, E. Bullock, M. J. Burchell, H. Busemann, A. Butterworth, M. Chaussidon, A. Cheuvront, M. F. Chi, M. J. Cintala, B. C. Clark, S. J. Clemett, G. Cody, L. Colangeli, G. Cooper, P. Cordier, C. Daghlian, Z. R. Dai, L. D'Hendecourt, Z. Djouadi, G. Dominguez, T. Duxbury, J. P. Dworkin, D. S. Ebel, T. E. Economou, S. Fakra, S. A. J. Fairey, S. Fallon, G. Ferrini, T. Ferroir, H. Fleckenstein, C. Floss, G. Flynn, I. A. Franchi, M. Fries, Z. Gainsforth, J. P. Gallien, M. Genge, M. K. Gilles, P. Gillet, J. Gilmour, D. P. Glavin, M. Gounelle, M. M. Grady, G. A. Graham, P. G. Grant, S. F. Green, F. Grossemy, L. Grossman, J. N. Grossman, Y. Guan, K. Hagiya, R. Harvey, P. Heck, G. F. Herzog, P. Hoppe, F. Horz, J. Huth, I. D. Hutcheon, K. Ignatyev, H. Ishii, M. Ito, D. Jacob, C. Jacobsen, S. Jacobsen, S. Jones, D. Joswiak, A. Jurewicz, A. T. Kearsley, L. P. Keller, H. Khodja, A. L. D. Kilcoyne, J. Kissel, A. Krot, F. Langenhorst, A. Lanzarotti, L. Le, L. A. Leshin, J. Leitner, L. Lemelle, H. Leroux, M. C. Liu, K. Luening, I. Lyon, G. MacPherson, M. A. Marcus, K. Marhas, B. Marty, G. Matrajt, K. McKeegan, A. Meibom, V. Mennella, K. Messenger, S. Messenger, T. Mikouchi, S. Mostefaoui, T. Nakamura, T. Nakano, M. Newville, L. R. Nittler, I. Ohnishi, K. Ohsumi, K. Okudaira, D. A. Papanastassiou, R. Palma, M. E. Palumbo, R. O. Pepin, D. Perkins, M. Perronnet, P. Pianetta, W. Rao, F. J. M. Rietmeijer, F. Robert, D. Rost, A. Rotundi, R. Ryan, S. A. Sandford, C. S. Schwandt, T. H. See, D. Schlutter, J. Sheffield-Parker, A. Simionovici, S. Simon, I. Sitnitsky, C. J. Snead, M. K. Spencer, F. J. Stadermann, A. Steele, T. Stephan, R. Stroud, J. Susini, S. R. Sutton, Y. Suzuki, M. Taheri, S. Taylor, N. Teslich, K. Tomeoka, N. Tomioka, A. Toppani, J. M. Trigo-Rodriguez, D. Troadec, A. Tsuchiyama, A. J. Tuzzolino, T. Tyliszczak, K. Uesugi, M. Velbel, J. Vellenga, E. Vicenzi, L. Vincze, J. Warren, I. Weber, M. Weisberg, A. J. Westphal, S. Wirick, D. Wooden, B. Wopenka, P. Wozniakiewicz, I. Wright, H. Yabuta, H. Yano, E. D. Young, R. N. Zare, T. Zega, K. Ziegler, L. Zimmerman, E. Zinner, and M. Zolensky*: Research article – Comet 81P/Wild 2 under a microscope. Science **314**, 1711–1716 (2006), doi:10.1126/science.1135840.

*Buchert, S. C., T. Hagfors, and J. F. McKenzie*: Effect of electrojet irregularities on DC current flow. J. Geophys. Res. **111**, A02305 (2006), doi:10.1029/2004JA010788.

*Büchner, J.*: Locating current sheets in the solar corona. Space Sci. Rev. **122**, 149–160 (2006), doi:10.1007/s11214-006-8213-z.

*Büchner, J.*: Locating reconnection sites in the solar atmosphere. In: Proc. of the 11th European Solar Physics Meeting The Dynamic Sun: Challenges for Theory and Observations, 11-16 September 2005, Leuven, Belgium, eds. D. Danesy, K. U. Poedts, A. De Groof, and J. Andries, ESA SP-600, ESA Publ. Div., Noordwijk (2006), on CD.

*Büchner, J.*: Magnetic reconnection - a universal heliophysical process. In: Proc. International Heliophysical Year, First European General Assembly, ed. C. Briand, p. 10 (2006).

*Büchner, J.*: Theory and Simulation of Reconnection. Space Sci. Rev. **124**, 345–360 (2006), doi:10.1007/s11214-006-9094-x.

*Büchner, J. and X. Deng*: Reconnection at Sun and in magnetospheres. Adv. Space Res. **37**, 1267–1268 (2006), doi:10.1016/j.asr.2006.04.008.

*Büchner, J. and N. Elkina*: Anomalous resistivity of current-driven isothermal plasmas due to phase space structuring. Phys. Plasmas **13**, 082304 (2006), doi:10.1063/1.2209611.

*Büchner, J. and N. Elkina*: Vlasov code simulation of anomalous resistivity. Space Sci. Rev. **121**, 237–252 (2006), doi:10.1007/s11214-006-6542-6.

*Budding, E., C. Bembrick, B. D. Carter, N. Erkan, M. Jardine, S. C. Marsden, R. Osten, P. Petit, M. Semel, O. B. Slee, and I. Waite*: Multisite, multiwavelength studies of the active cool binary CC

Eri. Astrophys. Space Sci. **304**, 13–16 (2006), doi:10.1007/s10509-006-9086-z.

*Busà, I., V. Andretta, M. T. Gomez, L. Terranegra, and R. Aznar Cuadrado*: SARG observations of 40 stars with different activity level: test for the $R_{IRT}$ chromospheric activity indicator. Memorie della Societa Astronomica Italiana Supplement **9**, 229–231 (2006).

*Cameron, R. and D. Galloway*: High field strength modified ABC and rotor dynamos. Mon. Not. Roy. Astron. Soc. **367**, 1163–1169 (2006).

*Cameron, R. and D. Galloway*: Saturation properties of the Archontis dynamo. Mon. Not. Roy. Astron. Soc. **365**, 735–746 (2006), doi:10.1111/j.1365-2966.2006.10012.x.

*Cameron, R. and L. Gizon*: Three-dimensional numerical simulation of wave propagation through a model sunspot. In: Proceedings of SOHO 18 / GONG 2006 / HELAS I - Beyond the spherical Sun, 7-11 August 2006, Sheffield, UK, ed. K. Fletcher, ESA SP-624, ESA Publ. Div., Noordwijk, The Netherlands (2006), on CD.

*Carlsson, E., A. Fedorov, S. Barabash, E. Budnik, A. Grigoriev, H. Gunell, H. Nilsson, J. A. Sauvaud, R. Lundin, Y. Futaana, M. Holmstrom, H. Andersson, M. Yamauchi, J. D. Winningham, R. A. Frahm, J. R. Sharber, J. Scherrer, A. J. Coates, D. R. Linder, D. O. Kataria, E. Kallio, H. Koskinen, T. Sales, P. Riihela, W. Schmidt, J. Kozyra, J. Luhmann, E. Roelof, D. Williams, S. Livi, C. C. Curtis, K. C. Hsieh, B. R. Sandel, M. Grande, M. Carter, J. J. Thocaven, S. McKenna-Lawler, S. Orsini, R. Cerulli-Irelli, M. Maggi, P. Wurz, P. Bochsler, N. Krupp, J. Woch, M. Fränz, K. Asamura, and C. Dierker*: Mass composition of the escaping plasma at Mars. Icarus **182**, 320–328 (2006), doi:10.1016/j.icarus.2005.09.020.

*Cheung, M. C. M., F. Moreno-Insertis, and M. Schüssler*: Moving magnetic tubes: fragmentation, vortex streets and the limit of the approximation of thin flux tubes. Astron. & Astrophys. **451**, 303–317 (2006), doi:10.1051/0004-6361:20054499.

*Cheung, M. C. M., M. Schuessler, and F. Moreno-Insertis*: 3D magneto-convection and flux emergence in the photosphere. In: Proceedings of the International Scientific Conference on Chromospheric and Coronal Magnetic Fields, eds. D. Innes, A. Lagg, S. K. Solanki, and D. Danesy, ESA SP-596, ESA Publ. Div., Noordwijk (2006), on CD.

*Cheung, M. C. M., M. Schuessler, and F. Moreno-Insertis*: Flux emergence at the photosphere. In: Proceedings of the Conference Held 18-22 July, 2005, at the National Solar Observatory, Sacramento Peak, Sunspot, New Mexico, USA, eds. J. Leibacher, R. F. Stein, and H. Uitenbroek, vol. 356, p. 97, Astronomical Society of the Pacific, San Francisco (2006).

*Christensen, U. R.*: A deep dynamo generating Mercury's magnetic field. Nature **444**, 1056–1058 (2006), doi:10.1038/nature05342.

*Christensen, U. R. and J. Aubert*: Scaling properties of convection-driven dynamos in rotating spherical shells and application to planetary magnetic fields. Geophys. J. Int. **166**, 97–114 (2006), doi:10.1111/j.1365-246X.2006.03009.x.

*Christensen, U. R., J. Aubert, and P. Olson*: Convection-driven planetary dynamos. In: Convection in Astrophysics, eds. F. Kupka, I. W. Roxburgh, and K. L. Chan, no. 239 in Proceedings IAU Symposium, pp. 188–195 (2006), doi:10.1017/S1743921307000403.

*Constantinescu, O. D., K.-H. Glassmeier, U. Motschmann, R. A. Treumann, K.-H. Fornaçon, and M. Fränz*: Plasma wave source location using Cluster as a spherical wave telescope. J. Geophys. Res. **111**, A09221 (2006), doi:10.1029/2005JA011550.

*Cremades, H., V. Bothmer, and D. Tripathi*: Properties of structured coronal mass ejections in solar cycle 23. Adv. Space Res. **38**, 461–465 (2006), doi:10.1016/j.asr.2005.01.095.

*Czechowski, A., M. Hilchenbach, and K. C. Hsieh*: Anomalous cosmic ray properties deduced from ENA measurements. In: Physics of the Inner Heliosheath: Voyager Observations, Theory, and Future Prospects; 5th Annual IGPP International Astrophysics Conference, vol. 858, pp. 282–287 (2006).

*Czechowski, A., M. Hilchenbach, K. C. Hsieh, R. Kallenbach, and J. Kota*: Estimating the thickness of the heliosheath from CELIAS/HSTOF and Voyager 1 data. Astrophys. J. **647**, L69–L72 (2006), doi:10.1086/507148.

*Czechowsky, P. and F. Dahl*: Raumfahrtmedaillen — Zwei Medaillen eines Max-Planck-Instituts. Münzen und Papiergeld **12/2006**, B99 118 (2006).

*Dal Lago, A., W. D. Gonzalez, L. A. Balmaceda, L. E. A. Vieira, E. Echer, F. L. Guarnieri, J. Santos, M. R. da Silva, A. de Lucas, A. L. C. de Gonzalez, R. Schwenn, and N. J. Schuch*: The 1722 October (1999) solar-interplanetary-geomagnetic event: Very intense geomagnetic storm associated with a pressure balance between interplanetary coronal mass ejection and a high-speed stream. J. Geophys. Res. **111**, A07S14 (2006), doi:10.1029/2005JA011394.

*Daly, P. W. and S. Mühlbachler*: The Cluster Active Archive – The RAPID contribution. In: Proceedings Cluster and Double Star Symposium – 5th Anniversary of Cluster in Space, Noordwijk, The Netherlands, 19–23 September 2005, eds. P. Escoubet, H. Laakso, M. Taylor, and A. Masson, ESA SP-598, ESA Publ. Div., Noordwijk (2006), on CD.

*Dandouras, I., V. Pierrard, J. Goldstein, C. Vallat, G. K. Parks, H. Rème, M. McCarthy, L. M. Kistler, B. Klecker, A. Korth, M. B. Bavassano-Cattaneo, P. Escoubet, and A. Masson*: Cluster multipoint observations of ionic structures in the plasmasphere by CIS and comparison with IMAGE-EUV observations and with model simulations. In: Proceedings Cluster and Double Star Symposium – 5th Anniversary of Cluster in Space, Noordwijk, The Netherlands, 19–23 September 2005, eds. P. Escoubet, H. Laakso, M. Taylor, and A. Masson, ESA SP-598, ESA Publ. Div., Noordwijk (2006), on CD.

*Davies, J. A., M. W. Dunlop, C. H. Perry, M. Lockwood, I. Alexeev, M. G. G. T. Taylor, A. N. Fazakerley, C. J. Owen, A. Marchaudon, R. H. W. Friedel, X. H. Deng, M. Grande, and P. W. Daly*: Energetic electron signatures in an active magnetotail plasma sheet. Adv. Space Res. **38**, 1608–1614 (2006), doi:10.1016/j.asr.2006.02.012.

*Delsanti, A., N. Peixinho, H. Boehnhardt, A. Barucci, F. Merlin, A. Doressoundiram, and J. K. Davies*: Near-infrared color properties of Kuiper Belt objects and Centaurs: Final results from the ESO Large Program. Astron. J. **131**, 1851–1863 (2006), doi:10.1086/499402.

*Di Mauro, M. P., D. Cardini, F. D'Antona, A. Weiss, M. P. Döllinger, L. Pasquini, L. Girardi, A. Hatzes, O. von der Lühe, J. R. de Medeiros, M. Roth, J. Setiawan, and L. da Silva*: Asteroseismology of K Giants. In: Proceedings of SOHO 18 / GONG 2006 / HELAS I - Beyond the spherical Sun, 7-11 August 2006, Sheffield, UK, ed. K. Fletcher, ESA SP-624, ESA Publ. Div., Noordwijk, The Netherlands (2006), on CD.

*Dotto, E., S. Fornasier, M. A. Barucci, J. Licandro, H. Boehnhardt, O. Hainaut, F. Marzari, C. de Bergh, and F. de Luise*: The surface composition of Jupiter Trojans: Visible and near-infrared survey of dynamical families. Icarus **183**, 420–434 (2006), doi:10.1016/j.icarus.2006.02.012.

*Dubinin, E., M. Fraenz, J. Woch, S. Barabash, R. Lundin, and M. Yamauchi*: Hydrogen exosphere at Mars: Pickup protons and their acceleration at the bow shock. Geophys. Res. Lett. **33**, L22103 (2006), doi:10.1029/2006GL027799.

*Dubinin, E., M. Fränz, J. Woch, E. Roussos, S. Barabash, R. Lundin, J. D. Winningham, R. A. Frahm, and M. Acuña*: Plasma Morphology at Mars. ASPERA-3 Observations. Space Sci. Rev. **126**, 209–238 (2006), doi:10.1007/s11214-006-9039-4.

*Dubinin, E., R. Lundin, M. Fränz, J. Woch, S. Barabash, A. Fedorov, D. Winningham, N. Krupp, J.-A. Sauvaud, M. Holmström, H. Andersson, M. Yamauchi, A. Grigoriev, J.-J. Thocaven, R. Frahm, J. Sharber, K. Asamura, A. Coates, C. Curtis, K. S. Hsieh, B. Sandel, H. Koskinen, E. Kallio, P. Riihelä, W. Schmidt, T. Säles, J. Kozyra, J. Luhmann, S. McKenna-Lawler, R. Cerulli-Irelli, S. Orsini, M. Maggi, E. Roelof, D. Williams, S. Livi, P. Wurz, P. Bochsler, C. Dierker, M. Grande, and M. Carter*: Electric fields within the Martian magnetosphere and ion extraction: ASPERA-3 observations. Icarus **182**, 337–342 (2006), doi:10.1016/j.icarus.2005.05.022.

*Dubinin, E., K. Sauer, and J. F. McKenzie*: Nonlinear 1-D stationary flows in multi-ion plasmas-sonic and critical loci-solitary and oscillatory waves. Ann. Geophys. **24**, 3041–3057 (2006).

*Dubinin, E., D. Winningham, M. Fränz, J. Woch, R. Lundin, S. Barabash, A. Fedorov, R. Frahm, J. R. Sharber, A. J. Coates, N. Krupp, J.-A. Sauvaud, M. Holmström, H. Andersson, M. Yamauchi, A. Grigoriev, J.-J. Thocaven, K. Asamura, C. Curtis, K. S. Hsieh, B. Sandel, H. Koskinen, E. Kallio, P. Riihelä, W. Schmidt, T. Säles, J. Kozyra, J. Luhmann, S. McKenna-Lawler, R. Cerulli-Irelli, S. Orsini, M. Maggi, E. Roelof, D. Williams, S. Livi, P. Wurz, P. Bochsler, C. Dierker, M. Grande, and M. Carter*: Solar wind plasma protrusion into the Martian magnetosphere: ASPERA-3 observations. Icarus **182**, 343–349 (2006), doi:10.1016/j.icarus.2005.05.023.

*Duvall, T. L., A. C. Birch, and L. Gizon*: Direct measurement of travel-time sensitivity kernels for helioseismology. Astrophys. J. **646**, 553–559 (2006), doi:10.1086/504792.

*Dyrud, L., B. Krane, M. Oppenheim, H. L. Pecseli, K. Schlegel, J. Trulsen, and A. W. Wernik*: Low-frequency electrostatic waves in the ionospheric E-region: a comparison of rocket observations and numerical simulations. Ann. Geophys. **24**, 2959–2979 (2006).

*Elkina, N. V. and J. Büchner*: A new conservative unsplit method for the solution of the Vlasov equation. Journal of Computational Physics **213**, 862–875 (2006), doi:10.1016/j.jcp.2005.09.023.

*Engrand, C., J. Kissel, F. R. Krueger, P. Martin, J. Silen, L. Thirkel, R. Thomas, and K. Varmuza*: Chemometric evaluation of time-of-flight secondary ion mass spectrometry data of minerals in the frame of future in situ analyses of cometary material by COSIMA onboard ROSETTA. Rapid Commun. Mass Spectrom. **20**, 1361–1368 (2006).

*Espy, P. J., P. Hartogh, and K. Holmen*: A microwave radiometer for the remote sensing of nitric oxide and ozone in the middle atmosphere. In: Remote Sensing of Clouds and the Atmosphere XI, eds. J. R. Slusser, K. Schaefer, and A. Comeron, *Proceedings of the SPIE*, vol. 6362 (2006), doi:10.1117/12.688953.

*Falchi, A., L. Teriaca, and L. Maltagliati*: The evaporation regime in a confined flare. Solar Phys. **239**, 193–216 (2006), doi:10.1007/s11207-006-0273-4.

*Fedorov, A., E. Budnik, J. A. Sauvaud, C. Mazelle, S. Barabash, R. Lundin, M. Acuna, M. Holmstrom, A. Grigoriev, M. Yamauchi, H. Andersson, J. J. Thocaven, D. Winningham, R. Frahm, J. R. Sharber, J. Scherrer, A. J. Coates, D. R. Linder, D. O. Kataria, E. Kallio, H. Koskinen, T. Sales, P. Riihela, W. Schmidt, J. Kozyra, J. Luhmann, E. Roelof, D. Williams, S. Livi, C. C. Curtis, K. C. Hsieh, B. R. Sandel, M. Grande, M. Carter, S. McKenna-Lawler, S. Orsini, R. Cerulli-Irelli, M. Maggi, P. Wurz, P. Bochsler, N. Krupp, J. Woch, M. Fränz, K. Asamura, and C. Dierker*: Structure of the Martian wake. Icarus **182**, 329–336 (2006), doi:10.1016/j.icarus.2005.09.021.

*Feng, L. and W. Q. Gan*: An impulsive heating model for the evolution of coronal loops. Chin. J. Astron. Astrophys. **6**, 608–616 (2006).

*Foing, B. H., G. D. Racca, A. Marini, E. Evrard, L. Stagnaro, M. Almeida, D. Koschny, D. Frew, J. Zender, J. Heather, M. Grande, J. Huovelin, H. U. Keller, A. Nathues, J. L. Josset, A. Malkki, W. Schmidt, G. Noci, R. Birkl, L. Iess, Z. Sodnik, and P. McManamon*: SMART-1 mission to the Moon: Status, first results and goals. Adv. Space Res. **37**, 6–13 (2006), doi:10.1016/j.asr.2005.12.016.

*Formisano, V., F. Angrilli, G. Arnold, S. Atreya, K. H. Baines, G. Bellucci, B. Bezard, F. Billebaud, D. Biondi, M. I. Blecka, L. Colangeli, L. Comolli, D. Crisp, M. D'Amore, T. Encrenaz, A. Ekonomov, F. Esposito, C. Fiorenza, S. Fonti, M. Giuranna, D. Grassi, B. Grieger, A. Grigoriev, J. Helbert, H. Hirsch, N. Ignatiev, A. Jurewicz, I. Khatuntsev, S. Lebonnois, E. Lellouch, A. Mattana, A. Maturilli, E. Mencarelli, M. Michalska, J. L. Moreno, B. Moshkin, F. Nespoli, Y. Nikolsky, F. Nuccilli, P. Orleanski, E. Palomba, G. Piccioni, M. Rataj, G. Rinaldi, M. Rossi, B. Saggin, D. Stam, D. Titov, G. Visconti, and L. Zasova*: The planetary fourier spectrometer (PFS) onboard the European Venus Express mission. Planet. Space Sci. **54**, 1298–1314 (2006), doi:10.1016/j.pss.2006.04.033.

*Frahm, R. A., J. D. Winningham, J. R. Sharber, J. R. Scherrer, S. J. Jeffers, A. J. Coates, D. R. Linder, D. O. Kataria, R. Lundin, S. Barabash, M. Holmstrom, H. Andersson, M. Yamauchi, A. Grigoriev, E. Kallio, T. Sales, P. Riihela, W. Schmidt, H. Koskinen, J. U. Kozyra, J. G. Luhmann, E. C. Roelof, D. J. Williams, S. Livi, C. C. Curtis, K. C. Hsieh, B. R. Sandel, M. Grande, M. Carter, J. A. Sauvaud, A. Fedorov, J. J. Thocaven, S. McKenna-Lawler, S. Orsini, R. Cerulli-Irelli, M. Maggi, P. Wurz, P. Bochsler, N. Krupp, J. Woch, M. Fränz, K. Asamura, and C. Dierker*: Carbon dioxide photoelectron energy peaks at Mars. Icarus **182**, 371–382 (2006), doi:10.1016/j.icarus.2006.01.014.

*Fränz, M., E. Dubinin, E. Roussos, J. Woch, J. D. Winningham, R. Frahm, A. J. Coates, A. Fedorov, S. Barabash, and R. Lundin*: Plasma Moments in the Environment of Mars. Space Sci. Rev. **126**, 165–207 (2006), doi:10.1007/s11214-006-9115-9.

*Fränz, M., J. D. Winningham, E. Dubinin, E. Roussos, J. Woch, S. Barabash, R. Lundin, M. Holmström, H. Andersson, M. Yamauchi, A. Grigoriev, R. A. Frahm, J. R. Sharber, J. R. Scherrer, A. J. Coates, Y. Soobiah, D. R. Linder, D. O. Kataria, E. Kallio, T. Säles, P. Riihelä, W. Schmidt, H. E. J. Koskinen, J. Kozyra, J. Luhmann, E. Roelof, D. Williams, S. Livi, C. C. Curtis, K. C. Hsieh, B. R. Sandel, M. Grande, M. Carter, J.-A. Sauvaud, A. Fedorov, J.-J. Thocaven, S. McKenna-Lawler, S. Orsini, R. Cerulli-Irelli, M. Maggi, P. Wurz, P. Bochsler, N. Krupp, K. Asamura, and C. Dierker*: Plasma intrusion above Mars crustal fields – Mars Express ASPERA-3 observations. Icarus **182**, 406–412 (2006), doi:10.1016/j.icarus.2005.11.016.

*Frische, M., K. Garofalo, T. H. Hansteen, and R. Borchers*: Fluxes and origin of halogenated organic trace gases from Momotombo volcano (Nicaragua). Geochem. Geophys. Geosyst. **7**, Q05020 (2006), doi:10.1029/2005GC001162.

*Futaana, Y., S. Barabash, A. Grigoriev, M. Holmstrom, E. Kallio, P. C. Brandt, H. Gunell, K. Brinkfeldt, R. Lundin, H. Andersson, M. Yamauchi, S. McKenna-Lawler, J. D. Winningham, R. A.*

*Frahm, J. R. Sharber, J. R. Scherrer, A. J. Coates, D. R. Linder, D. O. Kataria, T. Sales, P. Riihela, W. Schmidt, H. Koskinen, J. Kozyra, J. Luhmann, E. Roelof, D. Williams, S. Livi, C. C. Curtis, K. C. Hsieh, B. R. Sandel, M. Grande, M. Carter, J. A. Sauvaud, A. Fedorov, J. J. Thocaven, S. Orsini, R. Cerulli-Irelli, M. Maggi, P. Wurz, P. Bochsler, N. Krupp, J. Woch, M. Fränz, K. Asamura, and C. Dierker*: First ENA observations at Mars: Subsolar ENA jet. Icarus **182**, 413–423 (2006), doi:10.1016/j.icarus.2005.08.024.

*Futaana, Y., S. Barabash, A. Grigoriev, M. Holmstrom, E. Kallio, P. C. Brandt, H. Gunell, K. Brinkfeldt, R. Lundin, H. Andersson, M. Yamauchi, S. McKenna-Lawler, J. D. Winningham, R. A. Frahm, J. R. Sharber, J. R. Scherrer, A. J. Coates, D. R. Linder, D. O. Kataria, T. Sales, P. Riihela, W. Schmidt, H. Koskinen, J. Kozyra, J. Luhmann, E. Roelof, D. Williams, S. Livi, C. C. Curtis, K. C. Hsieh, B. R. Sandel, M. Grande, M. Carter, J. A. Sauvaud, A. Fedorov, J. J. Thocaven, S. Orsini, R. Cerulli-Irelli, M. Maggi, P. Wurz, P. Bochsler, A. Galli, N. Krupp, J. Woch, M. Fränz, K. Asamura, and C. Dierker*: First ENA observations at Mars: ENA emissions from the Martian upper atmosphere. Icarus **182**, 424–430 (2006), doi:10.1016/j.icarus.2005.09.019.

*Galli, A., P. Wurz, S. Barabash, A. Grigoriev, R. Lundin, Y. Futaana, H. Gunell, M. Holmstrom, E. C. Roelof, C. C. Curtis, K. C. Hsieh, A. Fedorov, D. Winningham, R. A. Frahm, R. Cerulli-Irelli, P. Bochsler, N. Krupp, J. Woch, and M. Fränz*: Direct measurements of energetic neutral hydrogen in the interplanetary medium. Astrophys. J. **644**, 1317–1325 (2006), doi:10.1086/503765.

*Gandorfer, A.*: What can we learn about the Sun from observations in the near ultraviolet? Ground based polarimetry and the role of SUNRISE . In: The Many Scales in the Universe - JENAM 2004 Astrophysics Reviews, eds. J. C. del Toro Iniesta, E. J. Alfaro, J. G. Gorgas, E. Salvador-Sole, and H. Butcher, Springer, Doordrecht, The Netherlands (2006).

*Gandorfer, A. M., S. K. Solanki, P. Barthol, B. W. Lites, V. Martínez Pillet, W. Schmidt, D. Soltau, and A. M. Title*: SUNRISE: High resolution UV/VIS observations of the Sun from the stratosphere. In: Ground-based and Airborne Telescopes, ed. L. M. Stepp, Proceedings of SPIE 6267, p. 62670S, SPIE, Bellingham (2006), doi:10.1117/12.672828.

*Gazis, P. R., A. Balogh, S. Dalla, R. Decker, B. Heber, T. Horbury, A. Kilchenmann, J. Kota, H. Kucharek, H. Kunow, D. Lario, M. S. Potgieter, J. D. Richardson, P. Riley, L. Rodriguez, G. Siscoe, and R. von Steiger*: ICMEs at high latitudes and in the outer heliosphere. Space Sci. Rev. **123**, 417–451 (2006), doi:10.1007/s11214-006-9023-z.

*Gizon, L.*: De toekomst van de helio- en asteroseismologie. Zenit **33**, 511–515 (2006).

*Gizon, L.*: Line profiles of fundamental modes of solar oscillation. In: Central European Astrophysical Bulletin, vol. 30, pp. 1–9, Zagreb, Croatia (2006).

*Gizon, L.*: Probing convection and solar activity with local helioseismology. In: Proceedings of SOHO 17 - 10 Years of SOHO and Beyond, 7-12 May 2006, Giardini Naxos, Sicily, Italy, ed. H. Lacoste, ESA SP-617, ESA Publ. Div., Noordwijk (2006), on CD.

*Gizon, L.*: Tomography of the solar interior. Mod. Phys. Lett. A **21**, 1701–1715 (2006), doi:10.1142/S0217732306021207.

*Gizon, L., S. M. Hanasoge, and A. C. Birch*: Acoustic scattering by flux tubes: Is the Born approximation valid? In: Proceedings of SOHO 18 / GONG 2006 / HELAS I - Beyond the spherical Sun, 7-11 August 2006, Sheffield, UK, ed. K. Fletcher, ESA SP-624, ESA Publ. Div., Noordwijk, The Netherlands (2006), on CD.

*Gizon, L., S. M. Hanasoge, and A. C. Birch*: Scattering of acoustic waves by a magnetic cylinder: accuracy of the Born approximation. Astrophys. J. **643**, 549–555 (2006), doi:10.1086/502623.

*Gizon, L. and M. Rempel*: Time-varying component of the solar meridional flow. In: Proceedings of SOHO 18 / GONG 2006 / HELAS I - Beyond the spherical Sun, 7-11 August 2006, Sheffield, UK, ed. K. Fletcher, ESA SP-624, ESA Publ. Div., Noordwijk, The Netherlands (2006), on CD.

*Goetz, W., S. F. Hviid, M. B. Madsen, K. M. Kinch, K. Leer, and H. P. Gunnlaugsson*: Results from the RAT Magnet Experiment on Spirit and Opportunity. In: Proceedings of the 38th Annual DPS Meeting, American Astronomical Society, Oct. 8-13, 2006 (2006).

*Gomory, P., J. Rybak, A. Kucera, W. Curdt, and H. Wohl*: SOHO/CDS observations of waves above the network. Astron. & Astrophys. **448**, 1169–1175 (2006), doi:10.1051/0004-6361:20053779.

*Gong, J., Y. Zhang, X. Zhou, and P. Hartogh*: Wide Bandwidth SAW Chirp Filters with Improved Magnitude Response. In: 2006 IEEE Ultrasonics Symposium, pp. 1895–1898, IEEE Operations Center, P.O. Box 1331, 445 Hoes Lane, Piscataway, NJ 08855-1331, USA (2006).

*Gopalswamy, N., Z. Mikic, D. Maia, D. Alexander, H. Cremades, P. Kaufmann, D. Tripathi, and Y. M. Wang*: The Pre-CME Sun. Space Sci. Rev. **123**, 303–339 (2006), doi:10.1007/s11214-006-9020-2.

*Gosling, J. T., S. Eriksson, and R. Schwenn*: Petschek-type magnetic reconnection exhausts in the solar wind well inside 1 AU: Helios. J. Geophys. Res. **111**, A10102 (2006), doi:10.1029/2006JA011863.

*Graf, U., S. Heyminck, R. Güsten, P. Hartogh, H.-W. Hübers, K. Jacobs, M. Phillip, D. Rabanus, H.-P. Röser, J. Stutzki, P. van der Wal, and A. Wagner-Gentner*: GREAT: the German first light heterodyne instrument for SOFIA. In: Millimeter and Submillimeter Detectors and Instrumentation for Astronomy III., eds. J. Zmuidzinas, W. S. Holland, S. Withington, and W. D. Duncan, *Proceedings of the SPIE*, vol. 6275, p. 627509 (2006), doi:10.1117/12.673168.

*Grynko, Y., Y. Shkuratov, and G. Videen*: Polarization of near-forward-scattered light from particulate substrates illuminated at near-grazing angles. J. Quant. Spectrosc. Radiat. Transf. **101**, 522–526 (2006).

*Gulkis, S., M. Frerking, J. Crovisier, G. Beaudin, P. Hartogh, P. Encrenaz, T. Koch, C. Kahn, Y. Salinas, N. Nowicki, R. Irigoyen, M. Jansen, P. Stek, M. Hofstadter, M. Allen, C. Backus, L. Kamp, C. Jarchow, E. Steinmetz, A. Deschamps, J. Krieg, M. Gheudin, N. Bockelee-Morvan, N. Biver, T. Encrenaz, D. Despois, W. Ip, E. Lellouch, I. Mann, D. Muhleman, H. Rauer, P. Schloerb, and T. Spilker*: MIRO: Microwave Instrument for Rosetta Orbiter. Space Sci. Rev. pp. 561–597 (2006), doi:10.1007/s11214-006-9032-y.

*Gunar, S., L. Teriaca, P. Heinzel, and U. Schühle*: Prominence Parameters Derived from Hydrogen Lyman-Alpha Spectral Profiles Measured by SOHO/SUMER. In: Proceedings of SOHO 17 - 10 Years of SOHO and Beyond, 7-12 May 2006, Giardini Naxos, Sicily, Italy, ed. H. Lacoste, vol. 617, ESA Publ. Div., Noordwijk (2006), on CD.

*Gunell, H., K. Brinkfeldt, M. Holmstrom, P. C. Brandt, S. Barabash, E. Kallio, A. Ekenback, Y. Futaana, R. Lundin, H. Andersson, M. Yamauchi, A. Grigoriev, J. D. Winningham, R. A. Frahm, J. R. Sharber, J. R. Scherrer, A. J. Coates, D. R. Linder, D. O. Kataria, T. Sales, P. Riihela, W. Schmidt, H. Koskinen, J. Kozyra, J. Luhmann, E. Roelof, D. Williams, S. Livi, C. C. Curtis, K. C. Hsieh, B. R. Sandel, M. Grande, M. Carter, J. A. Sauvaud, A. Fedorov, J. J. Thocaven, S. McKenna-Lawler, S. Orsini, R. Cerulli-Irelli, M. Maggi, P. Wurz, P. Bochsler, N. Krupp, J. Woch, M. Fränz, K. Asamura, and C. Dierker*: First ENA observations at Mars: Charge exchange ENAs produced in the magnetosheath. Icarus **182**, 431–438 (2006), doi:10.1016/j.icarus.2005.10.027.

*Gunnlaugsson, H. P., E. S. Worm, P. Bertelsen, W. Goetz, K. Kinch, M. B. Madsen, J. P. Merrison, and P. Nornberg*: Simulations of the magnetic properties experiment on Mars Exploration Rovers. Hyperfine Interact. **166**, 555–560 (2006), doi:10.1007/s10751-006-9334-1.

*Hanasoge, S. M., R. M. Larsen, T. L. Duvall, Jr., M. L. DeRosa, N. E. Hurlburt, J. Schou, M. Roth, J. Christensen-Dalsgaard, and S. K. Lele*: Computational acoustics in spherical geometry: Steps toward validating helioseismology. Astrophys. J. **648**, 1268–1275 (2006), doi:10.1086/505927.

*Hartogh, P.*: Multi-channel spectrometer developments at MPAE/MPS. In: Proceedings of ICSST04, pp. 112–126, Allied publishers Pvt. Ltd, New Dehli, India (2006).

*Hartogh, P. and C. Jarchow*: Microwave brightness temperature modelling of planetary atmospheres in preparation of GREAT and HIFI. In: Proceedings of ICSST04, pp. 24–29, Allied publishers Pvt. Ltd, New Dehli, India (2006).

*Hartogh, P. and L. Song*: Microwave detection of rocket exhaust plumes in the lower thermosphere. In: Proceedings of ICSST04, pp. 35–39, Allied publishers Pvt. Ltd, New Dehli, India (2006).

*Hilchenbach, M., A. Czechowski, K. C. Hsieh, and R. Kallenbach*: Observations of energetic neutral atoms and their implications on modeling the heliosheath. In: Physics of the Inner Heliosheath: Voyager Observations, Theory, and Future Prospects; 5th Annual IGPP International Astrophysics Conference, vol. 858, pp. 276–281 (2006).

*Hochedez, J.-F., W. Schmutz, Y. Stockman, U. Schühle, A. BenMoussa, S. Koller, K. Haenen, D. Berghmans, J.-M. Defise, J.-P. Halain, A. Theissen, V. Delouille, V. Slemzin, D. Gillotay, D. Fussen, M. Dominique, F. Vanhellemont, D. McMullin, M. Kretzschmar, A. Mitrofanov, B. Nicula, L. Wauters, H. Roth, E. Rozanov, I. Rüedi, C. Wehrli, A. Soltani, H. Amano, R. van der Linden, A. Zhukov, F. Clette, S. Koizumi, V. Mortet, Z. Remes, R. Petersen, M. Nesládek, M. D'Olieslaeger, J. Roggen, and P. Rochus*: LYRA, a solar UV radiometer on Proba2. Adv. Space Res. **37**, 303–312 (2006), doi:10.1016/j.asr.2005.10.041.

*Horz, F., R. Bastien, J. Borg, J. P. Bradley, J. C. Bridges, D. E. Brownlee, M. J. Burchell, M. F. Chi, M. J. Cintala, Z. R. Dai, Z. Djouadi, G. Dominguez, T. E. Economou, S. A. J. Fairey, C. Floss, I. A. Franchi, G. A. Graham, S. F. Green, P. Heck, P. Hoppe, J. Huth, H. Ishii, A. T. Kearsley, J. Kissel, J. Leitner, H. Leroux, K. Marhas, K. Messenger, C. S. Schwandt, T. H. See, C. Snead, F. J. Stadermann, T. Stephan, R. Stroud, N. Teslich, J. M. Trigo-Rodriguez, A. J. Tuzzolino, D. Troadec, P. Tsou, J. Warren, A. Westphal, P. Wozniakiewicz, I. Wright, and E. Zinner*: Impact features on Stardust: Implications for comet 81P/Wild 2 dust. Science **314**, 1716–1719 (2006), doi:10.1126/science.1135705.

*Inhester, B. and T. Wiegelmann*: Nonlinear force-free magnetic field extrapolations: comparisonof the Grad-Rubin and Wheatland-Sturrock-Roumeliotis algorithm. Solar Phys. **235**, 201–221 (2006), doi:10.1007/s11207-006-0065-x.

*Innes, D. E., T. J. Wang, S. K. Solanki, and D. Tothova*: Microflares and loop oscillations. In: SOHO-17: 10 Years of SOHO and Beyond, ed. H. Lacoste, ESA SP-617, ESA Publ. Div., Noordwijk (2006), on CD.

*Ip, W.-H., I.-G. Jiang, D. Kinoshita, L. N. Hau, A. Fujiwara, Y. Saito, F. Yoshida, K. W. Min, A. Bhardwaj, H. Boehnhardt, P. Hartogh, T. M. Capria, G. Cremonese, A. Milillo, S. Orisini, D. Gautier, D. Jewitt, and T. Owen*: A Mission Called SAPPORO. In: Advances in Geosciences, Volume 3, Planetary Sciences (PS), eds. W. Ip, A. Bhardwaj, F. Leblanc, Y. Kasaba, P. Hartogh, and I. Mann, pp. 241–254, World Scientific Publishing Co., Singapore (2006).

*Jäckel, A., M. Rubin, K. Altwegg, P. Wurz, H. Balsiger, U. Mall, and H. Rème*: Neutral gas and ion measurements with the Reflectron-type Time of Flight mass spectrometer ROSINA-RTOF. Meteorit. Planet. Sci. **41**, A86–A86 (2006).

*Jackiewicz, J., L. Gizon, and A. C. Birch*: F-mode sensitivity kernels for flows. In: Proceedings of SOHO 18 / GONG 2006 / HELAS I - Beyond the spherical Sun, 7-11 August 2006, Sheffield, UK, ed. K. Fletcher, ESA SP-624, ESA Publ. Div., Noordwijk, The Netherlands (2006), on CD.

*Jackiewicz, J., L. Gizon, and A. C. Birch*: Sensitivity of solar f-mode travel times to internal flows. In: Proceedings of SOHO 17 - 10 Years of SOHO and Beyond, 7-12 May 2006, Giardini Naxos, Sicily, Italy, ed. H. Lacoste, ESA SP-617, ESA Publ. Div., Noordwijk (2006), on CD.

*Jones, G. H., N. Krupp, H. Krüger, E. Roussos, W.-H. Ip, D. G. Mitchell, S. M. Krimigis, J. Woch, A. Lagg, M. Fränz, M. K. Dougherty, C. S. Arridge, and H. J. McAndrews*: Formation of Saturns ring spokes by lightning-induced electron beams. Geophys. Res. Lett. **33**, L21202 (2006), doi:10.1029/2006GL028146.

*Jones, G. H., E. Roussos, N. Krupp, C. Paranicas, J. Woch, A. Lagg, D. G. Mitchell, S. M. Krimigis, and M. K. Dougherty*: Enceladus' varying imprint on the magnetosphere of Saturn. Science **311**, 1412–1415 (2006), doi:10.1126/science.1121011.

*Jordan, S., R. Aznar Cuadrado, R. Napiwotzki, H. M. Schmid, and S. K. Solanki*: The fraction of DA white dwarfs with kilo-Gauss magnetic fields. In: Proceedings of the 15 European Workshop on White Dwarfs, pp. 10 881–10 884 (2006).

*Kaiser, J., A. Engel, R. Borchers, and T. Rockmann*: Probing stratospheric transport and chemistry with new balloon and aircraft observations of the meridional and vertical N2O isotope distribution. Atmos. Chem. Phys. **6**, 3535–3556 (2006).

*Kallenbach, R. and M. Hilchenbach*: Is the solar wind termination shock a cosmic-ray mediated shock? In: Physics of the Inner Heliosheath: Voyager Observations, Theory, and Future Prospects; 5th Annual IGPP International Astrophysics Conference, vol. 858, pp. 177–182 (2006).

*Kallio, E., S. Barabash, K. Brinkfeldt, H. Gunell, M. Holmstrom, Y. Futaana, W. Schmidt, T. Sales, H. Koskinen, P. Riihela, R. Lundin, H. Andersson, M. Yamauchi, A. Grigoriev, J. D. Winningham, R. A. Frahm, J. R. Sharber, J. R. Scherrer, A. J. Coates, D. R. Linder, D. O. Kataria, J. Kozyra, J. G. Luhmann, E. Roelof, D. Williams, S. Livi, P. C. Brandt, C. C. Curtis, K. C. Hsieh, B. R. Sandel, M. Grande, M. Carter, J. A. Sauvaud, A. Fedorov, J. J. Thocaven, S. McKenna-Lawler, S. Orsini, R. Cerulli-Irelli, M. Maggi, P. Wurz, P. Bochsler, N. Krupp, J. Woch, M. Fränz, K. Asamura, and C. Dierker*: Energetic Neutral Atoms (ENA) at Mars: Properties of the hydrogen atoms produced upstream of the Martian bow shock and implications for ENA sounding technique around non-magnetized planets. Icarus **182**, 448–463 (2006), doi:10.1016/j.icarus.2005.12.019.

*Kallio, E., A. Fedorov, E. Budnik, T. Sales, P. Janhunen, W. Schmidt, H. Koskinen, P. Riihela, S. Barabash, R. Lundin, M. Holmstrom, H. Gunell, K. Brinkfeldt, Y. Futaana, H. Andersson, A. Yamauchi, A. Grigoriev, J. A. Sauvaud, J. J. Thocaven, J. D. Winningham, R. A. Frahm, J. R. Sharber, J. R. Scherrer, A. J. Coates, D. R. Linder, D. O. Kataria, J. Kozyra, J. G. Luhmann, E. Roelof, D. Williams, S. Livi, C. C. Curtis, K. C. Hsieh, B. R. Sandel, A. Grande, M. Carter, *S. McKenna-Lawler, S. Orsini, R. Cerulli-Irelli, M. Maggi, P. Wurz, P. Bochsler, N. Krupp, J. Woch, M. Fränz, K. Asamura, and C. Dierker*: Ion escape at Mars: Comparison of a 3-D hybrid simulation with Mars Express IMA/ASPERA-3 measurements. Icarus **182**, 350–359 (2006), doi:10.1016/j.icarus.2005.09.018.

*Kecskeméty, K., G. Erdős, G. Facskó, M. Tátrallyay, I. Dandouras, P. Daly, and K. Kudela*: Distributions of suprathermal ions near hot flow anomalies observed by RAPID aboard Cluster. Adv. Space Res. **38**, 1587–1594 (2006), doi:10.1016/j.asr.2005.09.027.

*Keppler, F., R. Borchers, J. T. G. Hamilton, G. Kilian, J. Pracht, and H. F. Scholer*: De novo formation of chloroethyne in soil. Environmental Science & Technology **40**, 130–134 (2006), doi:10.1021/es0513279.

*Kistler, L. M., C. G. Mouikis, X. Cao, H. Frey, B. Klecker, I. Dandouras, A. Korth, M. F. Marcucci, R. Lundin, M. McCarthy, R. Friedel, and E. Lucek*: Ion composition and pressure changes in storm time and nonstorm substorms in the vicinity of the near-Earth neutral line. J. Geophys. Res. **111**, A11222 (2006), doi:10.1029/2006JA011939.

*Klecker, B., E. Möbius, M. A. Popecki, L. M. Kistler, H. Kucharek, and M. Hilchenbach*: Observation of energy-dependent ionic charge states in impulsive solar energetic particle events. Adv. Space Res. **38**, 493–497 (2006), doi:10.1016/j.asr.2005.04.042.

*Kossacki, K. J., W. J. Markiewicz, M. D. Smith, D. Page, and J. Murray*: Possible remnants of a frozen mud lake in southern Elysium, Mars. Icarus **181**, 363–374 (2006), doi:10.1016/j.icarus.2005.11.018.

*Kossacki, K. J. and S. Szutowicz*: Comet 67P/Churyumov-Gerasimenko: Modeling of orientation and structure. Planet. Space Sci. **54**, 15–27 (2006), doi:10.1016/j.pss.2005.09.001.

*Kramar, M., B. Inhester, and S. K. Solanki*: Vector tomography for the coronal magnetic field. I. Longitudinal Zeeman effect measurements. Astron. & Astrophys. **456**, 665–673 (2006), doi:10.1051/0004-6361:20064865.

*Kramm, J. R., H. U. Keller, R. Bredthauer, and M. Tomasko*: Imaging technique of the DISR camera on the Huygens lander. In: Scientific Detectors for Astronomy 2005, eds. J. E. Beletic, J. W. Beletic, and P. Amico, pp. 199–204, Springer, Dordrecht, The Netherlands (2006).

*Krivova, N. A., S. K. Solanki, and L. Floyd*: Reconstruction of solar UV irradiance in cycle 23. Astron. & Astrophys. **452**, 631–639 (2006), doi:10.1051/0004-6361:20064809.

*Krüger, H., N. Altobelli, B. Anweiler, S. F. Dermott, V. Dikarev, A. L. Graps, E. Grün, B. A. Gustafson, D. P. Hamilton, M. S. Hanner, M. Horanyi, J. Kissel, M. Landgraf, B. A. Lindblad, D. Linkert, G. Linkert, I. Mann, J. A. M. McDonnell, G. E. Morfill, C. Polanskey, G. Schwehm, R. Srama, and H. A. Zook*: Five years of Ulysses dust data: 2000–2004. Planet. Space Sci. **54**, 932–956 (2006), doi:10.1016/j.pss.2006.04.015.

*Krüger, H., D. Bindschadler, S. F. Dermott, A. L. Graps, E. Grün, B. A. Gustafson, D. P. Hamilton, M. S. Hanner, M. Horanyi, J. Kissel, B. A. Lindblad, D. Linkert, G. Linkert, I. Mann, J. A. M. McDonnell, R. Moissl, G. E. Morfill, C. Polanskey, G. Schwehm, R. Srama, and H. A. Zook*: Galileo dust data from the Jovian system: 1997-1999. Planet. Space Sci. **54**, 879–910 (2006), doi:10.1016/j.pss.2006.04.010.

*Krüger, H., A. L. Graps, D. P. Hamilton, A. Flandes, R. J. Forsyth, M. Horanyi, and E. Grün*: Ulysses jovian latitude scan of high-velocity dust streams originating from the Jovian system. Planet. Space Sci. **54**, 919–931 (2006), doi:10.1016/j.pss.2006.05.010.

*Kunow, H., N. U. Crooker, J. A. Linker, R. Schwenn, and R. von Steiger*: Forward. Space Sci. Rev. **123**, 1–2 (2006), doi:10.1007/s11214-006-9007-z, Forward to special issue on Coronal Mass Ejections.

*Kuo, F. S. and J. Röttger*: A wave packet analysis method for vertical energy flux measured by VHF radar. Chin. J. Phys. **44**, 243–256 (2006).

*Küppers, M. and H. Krüger*: Boten aus der Frühzeit des Sonnensystems—Neues über Kometen. Sterne und Weltraum **5**, 24–32 (2006).

*Kuroda, T., A. Medvedev, and P. Hartogh*: The Martian Atmosphere During the 2001 Global Dust Storm: Observations with SWAS and Simulations with a General Circulation Model . In: Advances in Geosciences, Volume 3, Planetary Sciences (PS), eds. W. Ip, A. Bhardwaj, F. Leblanc, Y. Kasaba, P. Hartogh, and I. Mann, pp. 154–155, World Scientific Publishing Co., Singapore (2006).

*Laemmerzahl, C., O. Preuss, and H. Dittus*: Is the physics within the Solar system really understood? In: Lasers, Clocks, and Drag-Free: Technologies for Future Exploration in Space and Tests of Gravity, ed. C. Laemmerzahl, Proceedings of the 359th WE-Heraeus Seminar (2006).

*Lagg, A., J. Woch, S. K. Solanki, and A. Gandorfer*: Supersonic downflows in the vicinity of a solar pore. In: Solar Polarization 4, eds. R. Casini and B. W. Lites, *ASP Conference Series*, vol. 358, pp. 437–442 (2006).

*Lara, L., H. Boehnhardt, R. Gredel, P. Gutiérrez, J.-L. Ortiz, R. Rodrigo, and M.-J. Vidal-Nuñez*: Pre-impact monitoring of Comet 9P/Tempel 1, the Deep Impact target. Astron. & Astrophys. **445**, 1151–1157 (2006), doi:10.1051/0004-6361:20053833.

*Liemohn, M. W., R. A. Frahm, J. D. Winningham, Y. Ma, S. B. Barabash, R. Lundin, J. U. Kozyra, A. F. Nagy, S. M. Bougher, J. Bell, D. Brain, D. Mitchell, J. Luhmann, M. Holmstrom, H. Andersson, M. Yamauchi, A. Grigoriev, S. McKennna-Lawler, J. R. Sharber, J. R. Scherrer, S. J. Jeffers, A. J. Coates, D. R. Linder, D. O. Kataria, E. Kallio, H. Koskinen, T. Sales, P. Riihela, W. Schmidt, E. Roelof, D. Williams, S. Livi, C. C. Curtis, K. C. Hsieh, B. R. Sandel, M. Grande, M. Carter, J. A. Sauvaud, A. Fedorov, J. J. Thocaven, S. Orsini, R. Cerulli-Irelli, M. Maggi, P. Wurz, P. Bochsler, N. Krupp, J. Woch, M. Fränz, K. Asamura, and C. Dierker*: Numerical interpretation of high-altitude photoelectron observations. Icarus **182**, 383–395 (2006), doi:10.1016/j.icarus.2005.10.036.

*Loukitcheva, M., S. K. Solanki, and S. White*: The dynamics of the solar chromosphere: comparison of model predictions with millimeter-interferometer observations. Astron. & Astrophys. **456**, 713–723 (2006), doi:10.1051/0004-6361:20053171.

*Loukitcheva, M. A., S. K. Solanki, and S. White*: Acoustic shock waves in the solar chromosphere from millimeter observations. In: Solar Activity and its Magnetic Origin, Proc. IAU Symp. 233, eds. V. Bothmer and A. A. Hady, pp. 104–107, Cambridge University Press, Cambridge (2006), doi:10.1017/S174392130600158X.

*Lui, A. T. Y., Y. Zheng, A. Balogh, P. W. Daly, M. W. Dunlop, T. A. Fritz, G. Gustafsson, S. Livi, S. B. Mende, C. J. Owen, R. F. Pfaff, H. Rème, Y. Zhang, and Q. Zong*: Magnetotail substorm features from multi-point observations. In: Proceedings Cluster and Double Star Symposium – 5th Anniversary of Cluster in Space, Noordwijk, The Netherlands, 19–23 September 2005, eds. P. Escoubet, H. Laakso, M. Taylor, and A. Masson, ESA SP-598, ESA Publ. Div., Noordwijk (2006), on CD.

*Lundin, R., D. Winningham, S. Barabash, R. Frahm, D. Brain, H. Nilsson, M. Holmström, M. Yamauchi, J. R. Sharber, J.-A. Sauvaud, A. Fedorov, K. Asamura, H. Hayakawa, A. J. Coates, Y. Soobiah, C. Curtis, K. C. Hsieh, M. Grande, H. Koskinen, E. Kallio, J. Kozyra, J. Woch, M. Fraenz, J. Luhmann, S. McKenna-Lawler, S. Orsini, P. Brandt, and P. Wurz*: Auroral Plasma Acceleration Above Martian Magnetic Anomalies. Space Sci. Rev. **126**, 333–354 (2006), doi:10.1007/s11214-006-9086-x.

*Lundin, R., D. Winningham, S. Barabash, R. Frahm, M. Holmstrom, J. A. Sauvaud, A. Fedorov, K. Asamura, A. J. Coates, Y. Soobiah, K. C. Hsieh, M. Grande, H. Koskinen, E. Kallio, J. Kozyra, J. Woch, M. Fraenz, D. Brain, J. Luhmann, S. McKenna-Lawler, R. S. Orsini, P. Brandt, and P. Wurz*: Plasma acceleration above Martian magnetic anomalies. Science **311**, 980–983 (2006), doi:10.1126/science.1122071.

*Lundin, R., D. Winningham, S. Barabash, R. A. Frahm, H. Andersson, M. Holmstrom, A. Grigoriev, M. Yamauchi, H. Borg, J. R. Sharber, J. A. Sauvaud, A. Fedorov, E. Budnik, J. J. Thocaven, K. Asamura, H. Hayakawa, A. J. Coates, D. R. Linder, D. O. Kataria, C. Curtis, K. C. Hsieh, B. R. Sandel, M. Grande, M. Carter, D. H. Reading, H. Koskinen, E. Kallio, P. Riihela, W. Schmidt, T. Sales, J. Kozyra, N. Krupp, J. Woch, M. Fränz, J. Luhmann, S. McKenna-Lawler, R. Cerulli-Irelli, S. Orsini, M. Maggi, E. Roelof, D. Williams, S. Livi, P. C. Brandt, P. Wurz, and P. Bochsler*: Ionospheric plasma acceleration at Mars: ASPERA-3 results. Icarus **182**, 308–319 (2006), doi:10.1016/j.icarus.2005.10.035.

*Mall, U. and T. Althaus*: Die SMART-1 Mission geht zu Ende. Sterne und Weltraum **11**, 36–42 (2006).

*Maltagliati, L., A. Falchi, and L. Teriaca*: Rhessi Images and Spectra of Two Small Flares. Solar Phys. **235**, 125–146 (2006), doi:10.1007/s11207-006-1977-1.

*Manglik, A. and U. R. Christensen*: Effect of lithospheric root on decompression melting in plume-lithosphere interaction models. Geophys. J. Int. **164**, 259–270 (2006), doi:10.1111/j.1365-246X.2005.02811.x.

*Marsch, E.*: Addendum and erratum, The relativistic energy spectrum of hydrogen [Ann.Phys.(Leipzig) 14, 324(2005)]. Annalen der Physik **15**, 434–437 (2006), doi:10.1002/andp.200510183.

*Marsch, E.*: Coronal origins of the solar wind - sources of steady streams and transient flows caused by solar magnetic eruptions. In: Solar Influence on the Heliosphere and Earth's Environment: Recent Progress and Prospects, eds. N. Gopalswamy and A. Bhattacharyya, pp. 111–118, Quest Publications for ILWS and Indian Institute of Geomagnetism (2006), proceedings of the ILWS Workshop Goa, India: February 19-24, 2006.

*Marsch, E.*: Kinetic physics of the solar corona and solar wind. Living Rev. Solar Phys. **3**, 1 (2006).

*Marsch, E.*: Origin and evolution of the solar wind. In: Solar Activity and its Magnetic Origin, Proceedings of the International Astronomical Union, Symposium S233, eds. V. Bothmer and A. Hady, vol. 2, pp. 259–268, Cambridge University Press, Cambridge, U.K. (2006), doi:10.1017/S1743921306001980.

*Marsch, E.*: Solar wind responses to the solar activity cycle. Adv. Space Res. **38**, 921–930 (2006), doi:10.1016/j.asr.2005.07.029.

*Marsch, E., L. Zhao, and C.-Y. Tu*: Limits on the core temperature anisotropy of solar wind protons. Ann. Geophys. **24**, 2057–2063 (2006).

*Marsch, E., G.-Q. Zhou, J.-S. He, and C.-Y. Tu*: Magnetic structure of the solar transition region as observed in various ultraviolet lines emitted at different temperatures. Astron. & Astrophys. **457**, 699–706 (2006), doi:10.1051/0004-6361:20065665.

*Marsch, E., G.-Q. Zhou, J.-S. He, and C.-Y. Tu*: On the structure of the solar transition region. In: Proceedings of SOHO 17 - 10 Years of SOHO and Beyond, 7-12 May 2006, Giardini Naxos, Sicily, Italy, ed. H. Lacoste, ESA SP-617, ESA Publ. Div., Noordwijk (2006), on CD.

*Matteini, L., S. Landi, P. Hellinger, M. Velli, M. Maksimovic, F. Pantellini, and E. Marsch*: On the role of the parallel proton fire hose instability in the expanding solar wind: Simulations and observations. In: Proceedings of SOHO 17 - 10 Years of SOHO and Beyond, 7-12 May 2006, Giardini Naxos, Sicily, Italy, ed. H. Lacoste, ESA SP-617, ESA Publ. Div., Noordwijk (2006), on CD.

*Mecheri, R. and E. Marsch*: Coronal waves: propagation in the multi-fluid description. Philosophical Transactions of the Royal Society A **364**, 537–540 (2006), doi:10.1098/rsta.2005.1716.

*Mecheri, R. and E. Marsch*: Drift-instabilities in a coronal funnel within the multi-fluid description. In: Proceedings of SOHO 17 - 10 Years of SOHO and Beyond, 7-12 May 2006, Giardini Naxos, Sicily, Italy, ed. H. Lacoste, ESA SP-617, ESA Publ. Div., Noordwijk (2006), on CD.

*Mellado, E. M., K. Hornung, and J. Kissel*: Ion formation by high velocity impacts on porous metal targets. Int. J. Impact Eng. **33**, 419–430 (2006), doi:10.1016/j.ijimpeng.2006.09.019.

*Michelsen, R., A. Nathues, and C. I. Lagerkvist*: Spectroscopy of near-Earth asteroids. Astron. & Astrophys. **451**, 331–337 (2006), doi:10.1051/0004-6361:20040443.

*Modolo, R., G. Chanteur, E. Dubinin, and A. Matthews*: Simulated solar wind plasma interaction with the Martian exosphere: influence of the solar EUV flux on the bow shock and the magnetic pile-up boundary. Ann. Geophys. **24**, 3403–3410 (2006).

*Narita, Y., K. H. Glassmeier, K. H. Fornaçon, I. Richter, S. Schäfer, U. Motschmann, I. Dandouras, H. Rème, and E. Georgescu*: Low-frequency wave characteristics in the upstream and downstream regime of the terrestrial bow shock. J. Geophys. Res. **111**, A01203 (2006), doi:10.1029/2005JA011231.

*Nielsen, E., D. D. Morgan, D. L. Kirchner, J. J. Plaut, and G. Picardi*: Absorption and reflection of radio waves in the Martian ionosphere. Planet. Space Sci. **55**, 864–870 (2006), doi:10.1016/j.pss.2006.10.005.

*Nielsen, E., H. Zou, D. A. Gurnett, D. L. Kirchner, D. D. Morgan, R. Huff, R. Orosei, A. Safaeinili, J. J. Plaut, and G. Picardi*: Observations of vertical reflections from the topside Martian ionosphere. Space Sci. Rev. **126**, 373–388 (2006), doi:10.1007/s11214-006-9113-y.

*Nilsson, H., E. Carlsson, H. Gunell, Y. Futaana, S. Barabash, R. Lundin, A. Fedorov, Y. Soobiah, A. Coates, M. Fränz, and E. Roussos*: Investigation of the Influence of Magnetic Anomalies on Ion Distributions at Mars. Space Sci. Rev. **126**, 355–372 (2006), doi:10.1007/s11214-006-9030-0.

*Nilsson, H., M. Waara, S. Arvelius, O. Marghitu, M. Bouhram, Y. Hobara, M. Yamauchi, R. Lundin, H. Reme, J. A. Sauvaud, I. Dandouras, A. Balogh, L. M. Kistler, B. Klecker, C. W. Carlson, M. B. Bavassano-Cattaneo, and A. Korth*: Characteristics of high altitude oxygen ion energization and outflow as observed by Cluster: a statistical study. Ann. Geophys. **24**, 1099–1112 (2006).

*Obreschkow, D., P. Kobel, N. Dorsaz, A. de Bosset, C. Nicollier, and M. Farhat*: Cavitation bubble dynamics inside liquid drops in microgravity. Phys. Rev. Lett. **97**, 094502 (2006), doi:10.1103/PhysRevLett.97.094502.

*Olson, P. and U. R. Christensen*: Dipole moment scaling for convection-driven planetary dynamos. Earth and Planetary Science Letters **250**, 561–571 (2006), doi:10.1016/j.epsl.2006.08.008.

*Panov, A. D., J. H. Adams, H. S. Ahn, G. L. Bashindzhagyan, K. E. Batkov, J. Chang, M. Christl, A. R. Fazely, O. Ganel, R. M. Gunasingha, T. G. Guzik, J. Isbert, K. C. Kim, E. N. Kouznetsov, M. I. Panasyuk, W. K. H. Schmidt, E. S. Seo, N. V. Sokolskaya, J. P. Wefel, J. Wu, and V. I. Zatsepin*: The energy spectra of heavy nuclei measured by the ATIC experiment. Adv. Space Res. **37**, 1944–1949 (2006), doi:10.1016/j.asr.2005.07.040.

*Panov, E. V., J. Büchner, M. Fränz, A. Korth, Y. Khotyaintsev, B. Nikutowski, S. Savin, K.-H. Fornaçon, I. Dandouras, and H. Rème*: Cluster spacecraft observation of a thin current sheet at the Earth's magnetopause. Adv. Space Res. **37**, 1363–1372 (2006), doi:10.1016/j.asr.2005.08.024.

*Panov, E. V., J. Büchner, M. Fränz, A. Korth, S. P. Savin, K.-H. Fornaçon, I. Dandouras, and H. Rème*: Cluster observation of collisionless transport at the magnetopause. Geophys. Res. Lett. **33**, L15109 (2006), doi:10.1029/2006GL026556.

*Pick, M., T. G. Forbes, G. Mann, H. V. Cane, J. Chen, A. Ciaravella, H. Cremades, R. A. Howard, H. S. Hudson, A. Klassen, K. L. Klein, M. A. Lee, J. A. Linker, D. Maia, Z. Mikic, J. C. Raymond, M. J. Reiner, G. M. Simnett, N. Srivastava, D. Tripathi, R. Vainio, A. Vourlidas, J. Zhang, T. H. Zurbuchen, N. R. Sheeley, and C. Marque*: Multi-wavelength observations of CMEs and associated phenomena. Space Sci. Rev. **123**, 341–382 (2006), doi:10.1007/s11214-006-9021-1.

*Preusse, S., A. Kopp, J. Büchner, and U. Motschmann*: A magnetic communication scenario for hot Jupiters. Astron. & Astrophys. **460**, 317–322 (2006), doi:10.1051/0004-6361:20065353.

*Preusse, S., A. Kopp, J. Büchner, and U. Motschmann*: Magnetic communication scenarii for close-in extrasolar planets. In: Tenth Anniversary of 51 Peg-b: Status of and prospects for hot Jupiter studies, eds. L. Arnold, F. Bouchy, and C. Moutou, ISBN-2-914601-17.4, pp. 274–281, Observatoire de Haute Provence, Frontier Group, Paris (2006).

*Preusse, S., A. Kopp, J. Büchner, and U. Motschmann*: MHD simulation scenarios of the stellar wind interaction with Hot Jupiter magnetospheres. Planet. Space Sci. **55**, 589–597 (2006), doi:10.1016/j.pss.2006.04.037.

*Pu, Z. Y., J. Wang, M. W. Dunlop, X. G. Zhang, Y. Wei, X. Z. Zhou, S. Y. Fu, C. J. Xiao, Q. G. Zong, Z. X. Liu, C. Carr, C. Perry, H. Rème, I. Dandouras, A. Fazakerley, P. Daly, F. Pitout, J. Davies, C. Shen, H. Laakso, P. Escoubet, C. J. Owen, Y. Bogdanova, and M. G. G. T. Taylor*: Cluster and TC1 five point observations of an FTE on Jan. 4, 2005: A preliminary study. In: Proceedings Cluster and Double Star Symposium – 5th Anniversary of Cluster in Space, Noordwijk, The Netherlands, 19–23 September 2005, eds. P. Escoubet, H. Laakso, M. Taylor, and A. Masson, ESA SP-598, ESA Publ. Div., Noordwijk (2006), on CD.

*Qu, Z. Q., C. L. Xu, X. Y. Zhang, X. L. Yan, and C. L. Jin*: On the influence of magnetic fields on level populations. Mon. Not. Roy. Astron. Soc. **370**, 1790–1796 (2006), doi:10.1111/j.1365-2966.2006.10598.x.

*Radioti, A., N. Krupp, J. Woch, A. Lagg, K. H. Glassmeier, and L. S. Waldrop*: Correction to "ion abundance ratios in the Jovian magnetosphere". J. Geophys. Res. **111**, A10224 (2006), doi:10.1029/2006JA011990.

*Raouafi, N.-E., J. W. Harvey, and S. K. Solanki*: Plasma dynamics in the polar coronal plumes. In: Solar Activity and its Magnetic Origin, Proc. IAU Symp. 233, eds. V. Bothmer and A. A. Hady, pp. 193–194, Cambridge University Press, Cambridge (2006), doi:10.1017/S1743921306001864.

*Raouafi, N.-E., J. W. Harvey, and S. K. Solanki*: Properties of plasma dynamics in the polar coronal plumes. In: SOHO-17: 10 Years of SOHO and Beyond, ed. H. Lacoste, ESA SP-617, ESA Publ. Div., Noordwijk (2006), on CD.

*Raouafi, N.-E. and S. K. Solanki*: Large temperature anisotropies in the polar coronal holes: How reliable are they? In: SOHO-17: 10 Years of SOHO and Beyond, ed. H. Lacoste, ESA SP-617, ESA Publ. Div., Noordwijk (2006), on CD.

*Raouafi, N.-E. and S. K. Solanki*: Sensitivity of solar off-limb line profiles to electron density stratification and the velocity distribution anisotropy. Astron. & Astrophys. **445**, 735–745 (2006), doi:10.1051/0004-6361:20042568.

*Rietveld, M. T. and P. Stubbe*: Comment on "The magnetic response of the ionosphere to pulsed HF heating" by K. Papadopoulos, T. Wallace, G. M. Milikh, W. Peter, and M. McCarrick. Geophys. Res. Lett. **33**, L07102 (2006), doi:10.1029/2005GL024853.

*Roth, M., L. Gizon, and A. C. Birch*: Sensitivity kernels for helioseismic travel times in spherical geometry - preliminary results. In: Proceedings of SOHO 18 / GONG 2006 / HELAS I - Beyond the spherical Sun, 7-11 August 2006, Sheffield, UK, ed. K. Fletcher, ESA SP-624, ESA Publ. Div., Noordwijk, The Netherlands (2006), on CD.

*Roth, M., O. v. d. Lühe, P. Pallé, M. J. Thompson, J. Christensen-Dalsgaard, M. J. P. F. G. Monteiro, L. Gizon, M. P. Di Mauro, C. Aerts, J. Daszynska-Daszkiewicz, and T. Corbard*: European helio- and asteroseismology network – HELAS. In: Proceedings of SOHO 18 / GONG 2006 / HELAS I – Beyond the spherical Sun, 7-11 August 2006, Sheffield, UK, ed. K. Fletcher, ESA SP-624, ESA Publ. Div., Noordwijk, The Netherlands (2006), on CD.

*Roth, M., O. v. d. Lühe, P. Pallé, M. J. Thompson, J. Christensen-Dalsgaard, M. J. P. F. G. Monteiro, L. Gizon, M. P. Di Mauro, C. Aerts, J. Daszynska-Daszkiewicz, and T. Corbard*: HELAS – European Helio- and Asteroseismology Network. In: Proceedings of SOHO 17 – 10 Years of SOHO and Beyond, 7-12 May 2006, Giardini Naxos, Sicily, Italy, ed. H. Lacoste, ESA SP-617, ESA Publ. Div., Noordwijk (2006), on CD.

*Rotvig, J. and C. A. Jones*: Multiple jets and bursting in the rapidly rotating convecting two-dimensional annulus model with nearly plane-parallel boundaries. J. Fluid Mech. **567**, 117–140 (2006), doi:10.1017/S0022112006002254.

*Russell, C. T., F. Capaccioni, A. Coradini, U. Christensen, M. C. de Sanctis, W. C. Feldman, R. Jaumann, H. U. Keller, A. Konopliv, T. B. McCord, L. A. McFadden, H. Y. McSween, S. Mottola, G. Neukum, C. M. Pieters, T. H. Prettyman, C. A. Raymond, D. E. Smith, M. V. Sykes, B. Williams, and M. T. Zuber*: Dawn discovery mission to Vesta and Ceres: Present status. Adv. Space Res. **38**, 2043–2048 (2006), doi:10.1016/j.asr.2004.12.041.

*Sahal-Brechot, S. and N. E. Raouafi*: Doppler redistribution of anisotropic radiation and resonance polarization in moving scattering media - Predicted results for the coronal O VI 1032 angstrom line. Astron. & Astrophys. **445**, 681–692 (2006), doi:10.1051/0004-6361:20052822.

*Saidi, M. Y.*: Développement d'une interface logicielle pour le calcul scienitifique à distance: Application à l'héliosismologie. Diplomarbeit, Universités Paris-Sud XI (2006), rapport de Master, supervised by Dr. L. Gizon, Max Planck Institute for Solar System Research.

*Sasso, C., A. Lagg, and S. K. Solanki*: Milne-Eddington inversions of the He I 10 830 Å Stokes profiles: influence of the Paschen-Back effect. Astron. & Astrophys. **456**, 367–371 (2006), doi:10.1051/0004-6361:20065257.

*Sasso, C., A. Lagg, S. K. Solanki, and H. Socas-Navarro*: Influence of the Paschen-Back effect on the results of polarimetric inversions of the He I 10830 Å triplet. Memorie della Societa Astronomica Italiana Supplement **9**, 126 (2006).

*Saur, J., B. H. Mauk, D. G. Mitchell, N. Krupp, K. K. Khurana, S. Livi, S. M. Krimigis, P. T. Newell, D. J. Williams, P. C. Brandt, A. Lagg, E. Roussos, and M. K. Dougherty*: Anti-planetward auroral electron beams at Saturn. Nature **439**, 699–702 (2006), doi:10.1038/nature04401.

*Savin, S., E. Amata, M. André, M. Dunlop, Y. Khotyaintsev, P. M. E. Décréau, J. L. Rauch, J. G. Trotignon, J. Büchner, B. Nikutowski, J. Blecki, A. Skalsky, S. Romanov, L. Zelenyi, A. M. Buckley, T. D. Carozzi, M. P. Gough, P. Song, H. Rème, A. Volosevich, H. Alleyne, and E. Panov*: Experimental study of nonlinear interaction of plasma flow with charged thin current sheets: 2. Hall dynamics, mass and momentum transfer. Nonlin. Proc. Geophys. **13**, 377–392 (2006).

*Scherer, S., K. Altwegg, H. Balsiger, J. Fischer, A. Jäckel, A. Korth, M. Mildner, D. Piazza, H. Rème, and P. Wurz*: A novel principle for an ion mirror design in time-of-flight mass spectrometry. Intern. Journal of Mass Spectrometry **251**, 73–81 (2006), doi:10.1016/j.ijms.2006.01.025.

*Schlegel, K.*: Space Weather and Alexander von Humboldt's Kosmos. Space Weather **4**, S01001 (2006), doi:10.1029/2005SW000166.

*Schrijver, C. J., M. L. DeRosaand, T. R. Metcalf, Y. Liu, J. McTiernan, S. Regnier, G. Valori, M. S. Wheatland, and T. Wiegelmann*: Nonlinear force-free modeling of coronal magnetic fields Part I: A quantitative comparison of methods. Solar Phys. **235**, 161–190 (2006), doi:10.1007/s11207-006-0068-7.

*Schrinner, M., K.-H. Rädler, D. Schmitt, M. Rheinhardt, and U. Christensen*: Mean-field view on geodynamo models. Magnetohydrodynamics **42**, 111–122 (2006).

*Schüssler, M. and I. Baumann*: Modelling the Sun's open magnetic flux. Astron. & Astrophys. **459**, 945–953 (2006), doi:10.1051/0004-6361:20065871.

*Schüssler, M. and A. Vögler*: Magnetoconvection in a sunspot umbra. Astrophys. J. **641**, L73–L76 (2006), doi:10.1086/503772.

*Schwenn, R.*: Solar wind sources and their variations over the solar cycle. Space Sci. Rev. **124**, 51–76 (2006), doi:10.1007/s11214-006-9099-5.

*Schwenn, R., J. C. Raymond, D. Alexander, A. Ciaravella, N. Gopalswamy, R. Howard, H. Hudson,* *P. Kaufmann, A. Klassen, D. Maia, G. Munoz-Martinez, M. Pick, M. Reiner, N. Srivastava, D. Tripathi, A. Vourlidas, Y.-M. Wang, and J. Zhang*: Coronal Observations of CMEs. Space Sci. Rev. **123**, 127–176 (2006), doi:10.1007/s11214-006-9016-y.

*Seitz, R., J. C. Raymond, J. Kissel, and M. I. Petaev*: Xenomict energy in cold solids in space. Naturwissenschaften **93**, 88–91 (2006), doi:10.1007/s00114-005-0067-9.

*Selwa, M., S. K. Solanki, K. Murawski, T. J. Wang, and U. Shumlak*: Numerical simulations of impulsively generated vertical oscillations in a solar coronal arcade loop. Astron. & Astrophys. **454**, 653–661 (2006), doi:10.1051/0004-6361:20054286.

*Sergis, N., K. Dialynas, E. Roussos, and X. Moussas*: Magnetospheric Electron Flows In The Martian Ionosphere. Detection And Implications. In: Recent Advances in Astronomy and Astrophysics: 7th International Conference of the Hellenic Astronomical Society. AIP Conference Proceedings, vol. 848, pp. 263–272 (2006), doi:10.1063/1.2347990.

*Sergis, N., K. Dialynas, E. Roussos, and X. Moussas*: Mars: Determination of the most appropriate electron energy for the bow shock identification, using MGS data. In: Recent Advances in Astronomy and Astrophysics: 7th International Conference of the Hellenic Astronomical Society. AIP Conference Proceedings, vol. 848, pp. 163–167 (2006), doi:10.1063/1.2347973.

*Setiawan, J., M. Roth, P. Weise, and M. P. Doelinger*: Multi-periodic oscillations of HD 32887 and HD 81797. Mem. S.A.It. **77**, 510–514 (2006).

*Silin, I. and J. Büchner*: Three-dimensional Vlasov-code simulations of magnetopause-like current sheets. Adv. Space Res. **37**, 1354–1362 (2006), doi:10.1016/j.asr.2005.05.025.

*Siscoe, G. and R. Schwenn*: CME Disturbance Forecasting. Space Sci. Rev. **123**, 453–470 (2006), doi:10.1007/s11214-006-9024-y.

*Skorov, Y. V., G. N. Markelov, and H. U. Keller*: Direct statistical simulation of the near-surface layers of a cometary atmosphere. II: A nonspherical nucleus. Solar System Research **40**, 219–229 (2006).

*Solanki, S. K., B. Inhester, and M. Schüssler*: The solar magnetic field. Reports on Progress in Physics **69**, 563–668 (2006), doi:10.1088/0034-4885/69/3/R02.

*Solanki, S. K. and N. A. Krivova*: Solar variability of possible relevance for planetary climates. Space Sci. Rev. **125**, 25–37 (2006), doi:10.1007/s11214-006-9044-7.

*Solanki, S. K., A. Lagg, R. Aznar Cuadrado, D. Orozco, M. Collados, T. Wiegelmann, J. Woch, C. Sasso, and N. Krupp*: Measuring the magnetic vector with the He I 10830 Å line: A rich new world. In: Solar Polarization 4, eds. R. Casini and B. W. Lites, *ASP Conference Series*, vol. 358, pp. 431–436 (2006).

*Solanki, S. K. and E. Marsch*: Solar microscopy: unveiling the Sun's basic physical processes at their intrinsic scales. In: Proceedings of SOHO 17 - 10 Years of SOHO and Beyond, 7-12 May 2006, Giardini Naxos, Sicily, Italy, ed. H. Lacoste, ESA SP-617, ESA Publ. Div., Noordwijk (2006), on CD.

*Solanki, S. K., N.-E. Raouafi, A. Gandorfer, U. Schühle, and A. Lagg*: Solar coronal magnetic field mapper. In: SOHO-17: 10 Years of SOHO and Beyond, ed. H. Lacoste, ESA SP-617, ESA Publ. Div., Noordwijk (2006), on CD.

*Sonnemann, G. R., M. Grygalashvyly, P. Hartogh, and C. Jarchow*: Behaviour of mesospheric ozone under nearly polar night conditions. Adv. Space Res. **38**, 2402–2406 (2006), doi:10.1016/j.asr.2006.09.011.

*Soobiah, Y., A. J. Coates, D. R. Linder, D. O. Kataria, J. D. Winningham, R. A. Frahm, J. R. Sharber, J. R. Scherrer, S. Barabash, R. Lundin, M. Holmstrom, H. Andersson, M. Yamauchi, A. Grigoriev, E. Kallio, H. Koskinen, T. Sales, P. Riihela, W. Schmidt, J. Kozyra, J. Luhmann, E. Roelof, D. Williams, S. Livi, C. C. Curtis, K. C. Hsieh, B. R. Sandel, M. Grande, M. Carter, J. A. Sauvaud, A. Fedorov, J. J. Thocaven, S. McKenna-Lawler, S. Orsini, R. Cerulli-Irelli, M. Maggi, P. Wurz, P. Bochsler, N. Krupp, J. Woch, M. Fränz, K. Asamura, and C. Dierker*: Observations of magnetic anomaly signatures in Mars Express ASPERA-3 ELS data. Icarus **182**, 396–405 (2006), doi:10.1016/j.icarus.2005.10.034.

*Squyres, S. W., R. E. Arvidson, D. Bollen, J. F. Bell, J. Bruckner, N. A. Cabrol, W. M. Calvin, M. H. Carr, P. R. Christensen, B. C. Clark, L. Crumpler, D. J. D. Marais, C. d'Uston, T. Economou, J. Farmer, W. H. Farrand, W. Folkner, R. Gellert, T. D. Glotch, M. Golombek, S. Gorevan, J. A. Grant, R. Greeley, J. Grotzinger, K. E. Herkenhoff, S. Hviid, J. R. Johnson, G. Klingelhofer, A. H. Knoll, G. Landis, M. Lemmon, R. Li, M. B. Madsen, M. C. Malin, S. M. McLennan, H. Y. McSween, D. W. Ming, J. Moersch, R. V. Morris, T. Parker, J. W. Rice, L. Richter, R. Rieder, C. Schroder, M. Sims, M. Smith, P. Smith, L. A. Soderblom, R. Sullivan, N. J. Tosca, H. Wanke, T. Wdowiak, M. Wolff, and*

*A. Yen*: Overview of the Opportunity Mars Exploration Rover mission to Meridiani Planum: Eagle crater to Purgatory ripple. J. Geophys. Res. **111**, E12S12 (2006), doi:10.1029/2005JE002495.

*Srama, R., N. Altobelli, J. de Kam, S. Kempf, H. Krüger, S. Lera, G. Moragas-Klostermeyer, M. Rachev, A. Srovig, M. Landgraf, Q. Vo, and E. Grün*: DUNE-eXpress - dust astronomy with ConeXpress. Adv. Space Res. **38**, 2093–2101 (2006), doi:10.1016/j.asr.2005.09.009.

*Srama, R., S. Kempf, G. Moragas-Klostermeyer, S. Helfert, T. J. Ahrens, N. Altobelli, S. Auer, U. Beckmann, J. G. Bradley, M. Burton, V. V. Dikarev, T. Economou, H. Fechtig, S. F. Green, M. Grande, O. Havnes, J. K. Hillier, M. Horanyi, E. Igenbergs, E. K. Jessberger, T. V. Johnson, H. Krüger, G. Matt, N. McBride, A. Mocker, P. Lamy, D. Linkert, G. Linkert, F. Lura, J. A. M. McDonnell, D. Mohlmann, G. E. Morfill, F. Postberg, M. Roy, G. H. Schwehm, F. Spahn, J. Svestka, V. Tschernjawski, A. J. Tuzzolino, R. Wasch, and E. Grün*: In situ dust measurements in the inner Saturnian system. Planet. Space Sci. **54**, 967–987 (2006), doi:10.1016/j.pss.2006.05.021.

*Sunshine, J. M., M. F. A'Hearn, O. Groussin, J. Y. Li, M. J. S. Belton, W. A. Delamere, J. Kissel, K. P. Klaasen, L. A. McFadden, K. J. Meech, H. J. Melosh, P. H. Schultz, P. C. Thomas, J. Veverka, D. K. Yeomans, I. C. Busko, M. Desnoyer, T. L. Farnham, L. M. Feaga, D. L. Hampton, D. J. Lindler, C. M. Lisse, and D. D. Wellnitz*: Exposed water ice deposits on the surface of comet 9P/Tempel 1. Science **311**, 1453–1455 (2006), doi: 10.1126/science.1123632.

*Taylor, M. G. G. T., G. D. Reeves, R. H. W. Friedel, M. F. Thomsen, R. C. Elphic, J. A. Davies, M. W. Dunlop, H. Laakso, B. Lavraud, D. N. Baker, J. A. Slavin, C. H. Perry, C. P. Escoubet, A. Masson, H. J. Opgenoorth, C. Vallat, P. W. Daly, A. N. Fazakerley, and E. A. Lucek*: Cluster encounter with an energetic electron beam during a substorm. J. Geophys. Res. **111**, A11203 (2006), doi:10.1029/2006JA011666.

*Tereshchenko, E. D., B. Z. Khudukon, M. T. Rietveld, B. Isham, T. Hagfors, and A. Brekke*: The relationship between small-scale and large-scale ionospheric electron density irregularities generated by powerful HF electromagnetic waves at high latitudes. Ann. Geophys. **24**, 2901–2909 (2006), doi: www.ann-geophys.net/24/2901/2006/.

*Tereshchenko, E. D., R. Y. Yurik, B. Z. Khudukon, M. T. Rietveld, B. Isham, V. Belyey, A. Brekke, T. Hagfors, and M. Grill*: Directional features of the downshifted peak observed in HF-induced stimulated electromagnetic emission spectra obtained using an interferometer. Ann. Geophys. **24**, 1819–1827 (2006).

*Teriaca, L., A. Falchi, R. Falciani, G. Cauzzi, and L. Maltagliati*: Dynamics and evolution of an eruptive flare. Astron. & Astrophys. **455**, 1123–1133 (2006), doi:10.1051/0004-6361:20065065.

*Teriaca, L., A. Lagg, R. Aznar Cuadrado, C. Sasso, and S. K. Solanki*: The dynamics and structure of the solar atmosphere as obtained from combined SUMER/SOHO and TIP2/VTT observations. In: Proceedings of SOHO 17 - 10 Years of SOHO and Beyond, 7-12 May 2006, Giardini Naxos, Sicily, Italy, ed. H. Lacoste, ESA SP-617, ESA Publ. Div., Noordwijk, The Netherlands (2006), on CD.

*Teriaca, L., U. Schühle, S. K. Solanki, W. Curdt, and E. Marsch*: The dynamic nature of the solar transition region as revealed by spectroscopy of the hydrogen Lyman-alpha line. In: Proceedings of SOHO 17 - 10 Years of SOHO and Beyond, 7-12 May 2006, Giardini Naxos, Sicily, Italy, ed. H. Lacoste, ESA SP-617, ESA Publ. Div., Noordwijk (2006), on CD.

*Tishkovets, V. P. and K. Jockers*: Multiple scattering of light by densely packed random media of spherical particles: Dense media vector radiative transfer equation. J. Quant. Spectrosc. Radiat. Transf. **101**, 54–72 (2006), doi:10.1016/j.jqsrt.2005.10.001.

*Titov, D. V., H. Svedhem, D. Koschny, R. Hoofs, S. Barabash, J.-L. Bertaux, P. Drossart, V. Formisano, B. Häusler, O. Korablev, W. J. Markiewicz, D. Nevejans, M. Pätzold, G. Piccioni, T. L. Zhang, D. Merritt, O. Witasse, J. Zender, A. Accomazzo, M. Sweeney, D. Trillard, M. Janvier, and A. Clochet*: Venus Express science planning. Planet. Space Sci. **54**, 1279–1297 (2006), doi:10.1016/j.pss.2006.04.017.

*Titov, D. V., H. Svedhem, D. McCoy, J. P. Lebreton, S. Barabash, J. L. Bertaux, P. Drossart, V. Formisano, B. Häusler, O. I. Korablev, W. Markiewicz, D. Neveance, M. Pätzold, G. Piccioni, T. L. Zhang, F. W. Taylor, E. Lellouch, D. Koschny, O. Witasse, M. Warhaut, A. Accomazzo, J. Rodriguez-Cannabal, J. Fabrega, T. Schirmann, A. Clochet, and M. Coradini*: Venus Express: Scientific goals, instrumentation, and scenario of the mission. Cosmic Research **44**, 334–348 (2006), doi: 10.1134/S0010952506040071.

*Titov, D. V., H. Svedhem, and F. W. Taylor*: The atmosphere of Venus: current knowledge and future investigations. In: Solar System Update, eds. P. Blondel and J. W. Mason, pp. 87–110, Springer-Praxis (2006).

*Tripathi, D.*: EUV and coronagraphic observations of coronal mass ejections. J. Astrophys. Astron. **27**, 193–200 (2006).

*Tripathi, D., S. K. Solanki, R. Schwenn, V. Bothmer, M. Mierla, and G. Stenborg*: Observation of a bright coronal downflow by SOHO/EIT. Astron. & Astrophys. **449**, 369–378 (2006), doi:10.1051/0004-6361:20053840.

*Tsurutani, B. T., W. D. Gonzalez, A. L. C. Gonzalez, F. L. Guarnieri, N. Gopalswamy, M. Grande, Y. Kamide, Y. Kasahara, G. Lu, I. Mann, R. McPherron, F. Søraas, and V. M. Vasyliūnas*: Corotating solar wind streams and recurrent geomagnetic activity: A review. J. Geophys. Res. **111**, A07S01 (2006), doi:10.1029/2005JA011273.

*Tu, C.-Y., J.-S. He, and E. Marsch*: Plasma Outflows and Open Magnetic Fields in a Quiet-Sun Region. In: Proceedings of SOHO 17 - 10 Years of SOHO and Beyond, 7-12 May 2006, Giardini Naxos, Sicily, Italy, ed. H. Lacoste, ESA SP-617, ESA Publ. Div., Noordwijk (2006), on CD.

*Ulamec, S., S. Espinasse, B. Feuerbacher, M. Hilchenbach, D. Moura, H. Rosenbauer, H. Scheuerle, and R. Willnecker*: Rosetta lander – Philae: Implications of an alternative mission. Acta Astronautica **58**, 435–441 (2006), doi:10.1916/j.actaastro.2005.12.009.

*Usoskin, I. G., S. K. Solanki, and M. Korte*: Solar activity reconstructed over the last 7000 years: The influence of geomagnetic field changes. Geophys. Res. Lett. **33**, L08103 (2006), doi:10.1029/2006GL025921.

*Usoskin, I. G., S. K. Solanki, G. A. Kovaltsov, J. Beer, and B. Kromer*: Solar proton events in cosmogenic isotope data. Geophys. Res. Lett. **33**, L08107 (2006), doi:10.1029/2006GL026059.

*Usoskin, I. G., S. K. Solanki, C. Taricco, N. Bhandari, and G. A. Kovaltsov*: Long-term solar activity reconstructions: direct test by cosmogenic $^{44}$Ti in meteorites. Astron. & Astrophys. **457**, L25–L28 (2006), doi:10.1051/0004-6361:20065803.

*Vasyliūnas, V. M.*: Ionospheric and boundary contributions to the Dessler-Parker-Sckopke formula for Dst. Ann. Geophys. **24**, 1085–1097 (2006).

*Vasyliūnas, V. M.*: Reinterpreting the Burton-McPherron-Russell equation for predicting Dst. J. Geophys. Res. **111**, A07S04 (2006), doi:10.1029/2005JA011440.

*Villanueva, G. and P. Hartogh*: The high resolution chirp transform spectrometer for the SOFIA-GREAT instrument. Experimental Astronomy **18**, 77–91 (2006), doi:10.1007/s10686-005-9004-3.

*Villanueva, G. L., P. Hartogh, and L. Reindl*: A Digital Dispersive Matching Network for SAW Devices in Chirp Transform Spectrometers. IEEE Trans. Microw. Theory Tech. **54**, 1415–1424 (2006).

*Wade, G. A., A. W. Fullerton, J. F. Donati, J. D. Landstreet, P. Petit, and S. Strasser*: The magnetic field and confined wind of the O star theta(1) Orionis C. Astron. & Astrophys. **451**, 195–206 (2006), doi:10.1051/0004-6361:20054380.

*Wade, G. A., M. A. Smith, D. A. Bohlender, T. A. Ryabchikova, C. T. Bolton, T. Lueftinger, J. D. Landstreet, P. Petit, S. Strasser, M. Blake, and G. M. Hill*: The magnetic Bp star 36 Lyncis. I. Magnetic and photospheric properties. Astron. & Astrophys. **458**, 569–580 (2006), doi:10.1051/0004-6361:20054759.

*Wang, T. J., D. E. Innes, and S. K. Solanki*: Fe XIX observations of active region brightenings in the corona. Astron. & Astrophys. **455**, 1105–1113 (2006), doi:10.1051/0004-6361:20065126.

*Wenzler, T., S. K. Solanki, N. A. Krivova, and C. Fröhlich*: Reconstruction of solar irradiance variations in cycles 21-23 based on surface magnetic fields. Astron. & Astrophys. **460**, 583–595 (2006), doi:10.1051/0004-6361:20065752.

*White, S. M., M. Loukitcheva, and S. K. Solanki*: High-resolution millimeter-interferometer observations of the solar chromosphere. Astron. & Astrophys. **456**, 697–711 (2006), doi:10.1051/0004-6361:20052854.

*Wiegelmann, T. and B. Inhester*: Magnetic Stereoscopy. Solar Phys. **236**, 25–40 (2006), doi:10.1007/s11207-006-0153-y.

*Wiegelmann, T., B. Inhester, B. Kliem, G. Valori, and T. Neukirch*: Testing non-linear force-free coronal magnetic field extrapolations with the Titov-Démoulin equilibrium. Astron. & Astrophys. **453**, 737–741 (2006), doi:10.1051/0004-6361:20054751.

*Wiegelmann, T., B. Inhester, and T. Sakurai*: Preprocessing of vector magnetograph data for a nonlinear force-free magnetic field reconstruction. Solar Phys. **233**, 215–232 (2006), doi:10.1007/s11207-006-2092-z.

*Wiegelmann, T. and T. Neukirch*: An optimization principle for the computation of MHD equilibria in the solar corona. Astron. & Astrophys. **457**, 1053–1058 (2006), doi:10.1051/0004-6361:20065281.

*Wilhelm, K.*: Solar coronal-hole plasma densities and temperatures. Astron. & Astrophys. **455**, 697–708 (2006), doi:10.1051/0004-6361:20054693.

*Wilhelm, K.*: Solar VUV measurements obtained by SOHO instruments and their radiometric calibration. Adv. Space Res. **37**, 225–233 (2006), doi: 10.1016/j.asr.2004.12.057.

*Willingale, R., P. T. O'Brien, S. W. H. Cowley, G. H. Jones, D. J. McComas, K. O. Mason, J. P. Osborne, A. Wells, M. Chester, S. Hunsberger, D. N. Burrows, N. Gehrels, J. A. Nousek, L. Angelini, L. R. Cominsky, S. L. Snowden, and G. Chincarini*: Swift X-Ray Telescope Observations of the Deep Impact Collision. Astrophys. J. **649**, 541–552 (2006), doi: 10.1086/506315.

*Wimmer-Schweingruber, R. F., N. U. Crooker, A. Balogh, V. Bothmer, R. J. Forsyth, P. Gazis, J. T. Gosling, T. Horbury, A. Kilchenmann, I. G. Richardson, J. D. Richardson, P. Riley, L. Rodriguez, R. von Steiger, P. Wurz, and T. H. Zurbuchen*: Understanding interplanetary coronal mass ejection signatures. Space Sci. Rev. **123**, 177–216 (2006), doi:10.1007/s11214-006-9017-x.

*Winningham, J. D., R. A. Frahm, J. R. Sharber, A. J. Coates, D. R. Linder, Y. Soobiah, E. Kallio, J. R. Espley, R. Lundin, S. Barabash, M. Holmstrom, H. Andersson, M. Yamauchi, A. Grigoriev, J. R. Scherrer, S. J. Jeffers, D. O. Kataria, J. U. Kozyra, J. G. Luhmann, E. C. Roelof, D. J. Williams, S. Livi, C. C. Curtis, K. C. Hsieh, B. R. Sandel, H. Koskinen, T. Sales, P. Riihela, W. Schmidt, M. Grande, M. Carter, J. A. Sauvaud, A. Fedorov, J. J. Thocaven, S. McKenna-Lawler, S. Orsini, R. Cerulli-Irelli, M. Maggi, P. Wurz, P. Bochsler, N. Krupp, J. Woch, M. Fränz, K. Asamura, and C. Dierker*: Electron oscillations in the induced Martian magnetosphere. Icarus **182**, 360–370 (2006), doi:10.1016/j.icarus.2005.10.033.

*Wüllner, U., U. R. Christensen, and M. Jordan*: Joint geodynamical and seismic modelling of the Eifel plume. Geophys. J. Int. **165**, 357–372 (2006), doi: 10.1111/j.1365-246X.2006.02906.x.

*Xiao, C. J., X. G. Wang, Z. Y. Pu, H. Zhao, J. X. Wang, Z. W. Ma, S. Y. Fu, M. G. Kivelson, Z. X. Liu, Q.-G. Zong, K.-H. Glassmeier, A. Balogh, A. Korth, H. Rème, and C. P. Escoubet*: In situ evidence for the structure of the magnetic null in a 3D reconnection event in the Earth's magnetotail. Nature Physics **2**, 478–483 (2006), doi:10.1038/nphys342.

*Yamauchi, M., P. C. Brandt, Y. Ebihara, I. Dandouras, H. Nilsson, R. Lundin, H. Rème, C. Vallat, P. A. Lindqvist, A. Balogh, and P. W. Daly*: Source location of the wedge-like dispersed ring current in the morning sector during a substorm. J. Geophys. Res. **111**, A11S09 (2006), doi:10.1029/2006JA011621.

*Yamauchi, M., Y. Futana, A. Fedorov, E. Dubinin, R. Lundin, J.-A. Savaud, J. W. Winningham, R. Frahm, S. Barabash, M. Holmstrom, J. Woch, M. Fraenz, E. Budnik, H. Borg, R. Sharber, A. Coates, H. Soobiah, H. Koskinen, E. Kallio, K. Asamura, H. Hayakawa, C. Curtis, K. C. Hsieh, B. R. Sandel, M. Grande, A. Grigoriev, P. Wurz, S. Orsini, P. Brandt, S. McKenna-Lawler, J. Kozyra, and J. Luhmann*: IMF direction derived from cycloid-like ion distributions observed by Mars Express. Space Sci. Rev. **126**, 239–266 (2006), doi: 10.1007/s11214-006-9090-1.

*Zhang, H., Z. Y. Pu, X. Cao, S. Y. Fu, C. J. Xiao, Z. X. Liu, A. Korth, M. Frazen, Z. Qiugong, H. Rème, K. H. Glassmeier, R. Friedel, G. D. Reeves, and M. W. Dunlop*: Correlation between continuous lobe reconnection in the mid magnetotail and substorm expansion onset. Chin. Sci. Bull. **51**, 2795–2804 (2006), doi:10.1007/s11434-006-2198-6.

*Zong, Q.-G., H. Zhang, T. A. Fritz, S. Y. Fu, Z. Y. Pu, M. L. Goldstein, W. Keith, M. W. Dunlop, A. Korth, P. W. Daly, H. Rème, A. Balogh, and A. N. Fazakerley*: The magnetospheric cusp: Structure and dynamics. In: Proceedings Cluster and Double Star Symposium – 5th Anniversary of Cluster in Space, Noordwijk, The Netherlands, 19–23 September 2005, eds. P. Escoubet, H. Laakso, M. Taylor, and A. Masson, ESA SP-598, ESA Publ. Div., Noordwijk (2006), on CD.

*Zou, H., J. S. Wang, and E. Nielsen*: Reevaluating the relationship between the Martian ionospheric peak density and the solar radiation. J. Geophys. Res. **111**, A07305 (2006), doi:10.1029/2005JA011580.

## **Veröffentlichungen 2007 /** Publications 2007


*Agarwal, J., M. Mueller, H. Boehnhardt, and E. Gruen*: Imaging the Dust Trail and Neckline of 67P/Churyumov-Gerasimenko. In: Workshop on Dust in Planetary Systems, 26-30 September 2005, Kauai, Hawaii, ed. A. Wilson, ESA SP-643 (2007).

*Almeida, J. S., L. Teriaca, P. Suetterlin, D. Spadaro, U. Schühle, and R. J. Rutten*: Search for photospheric footpoints of quiet Sun transition region loops. Astron. & Astrophys. **475**, 1101–1109 (2007), doi:10.1051/0004-6361:20078124.

*Amit, H., P. Olson, and U. Christensen*: Tests of core flow imaging methods with numerical dynamos. Geophys. J. Int. **168**, 27–39 (2007), doi:10.1111/j.1365-246X.2006.03175.x.

*Apatenkov, S. V., V. A. Sergeev, M. V. Kubyshkina, R. Nakamura, W. Baumjohann, A. Runov, I. Alexeev, A. Fazakerley, H. Frey, S. Mühlbachler, P. W. Daly, J.-A. Sauvaud, N. Ganushkina, T. Pulkkinen, G. D. Reeves, and Y. Khotyaintsev*: Multi-spacecraft observation of plasma dipolarization/injection in the inner magnetosphere. Ann. Geophys. **25**, 801–814 (2007).

*Araneda, J. A., E. Marsch, and A. F. Vinas*: Collisionless damping of parametrically unstable Alfvén waves. J. Geophys. Res. **112**, A04104 (2007), doi:10.1029/2006JA011999.

*Aschwanden, M. J., J. K. Lee, G. A. Gary, M. Smith, and B. Inhester*: Comparison of Five Numerical Codes for Automated Tracing of Coronal Loops. Solar Phys. **248**, 359–377 (2007), doi:10.1007/s11207-007-9064-9.

*Aurnou, J., M. Heimpel, and J. Wicht*: The effects of vigorous mixing in a convective model of zonal flow on the ice giants. Icarus **190**, 110–126 (2007), doi:10.1016/j.icarus.2007.02.024.

*Auster, H. U., I. Apathy, G. Berghofer, A. Remizov, R. Roll, K. H. Fornaçon, K. H. Glassmeier, G. Haerendel, I. Hejja, E. Kührt, W. Magnes, D. Moehlmann, U. Motschmann, I. Richter, H. Rosenbauer, C. T. Russell, J. Rustenbach, K. Sauer, K. Schwingenschuh, I. Szemerey, and R. Waesch*: ROMAP: Rosetta magnetometer and plasma monitor. Space Sci. Rev. **128**, 221–240 (2007), doi:10.1007/s11214-006-9033-x.

*Aznar Cuadrado, R., S. K. Solanki, and A. Lagg*: Velocity distribution of chromospheric downflows. In: Modern Solar Facilities - Advanced Solar Science, eds. F. Kneer, K. G. Puschmann, and A. D. Wittmann, pp. 173–176, Universitätsverlag Göttingen (2007).

*Balmaceda, L., N. A. Krivova, and S. K. Solanki*: Reconstruction of solar irradiance using the Group sunspot number. Adv. Space Res. **40**, 986–989 (2007), doi:10.1016/j.asr.2007.02.077.

*Balsiger, H., K. Altwegg, P. Bochsler, P. Eberhardt, J. Fischer, S. Graf, A. Jäckel, E. Kopp, U. Langer, M. Mildner, J. Müller, T. Riesen, M. Rubin, S. Scherer, P. Wurz, S. Wüthrich, E. Arijs, S. Delanoye, J. De Keyser, E. Neefs, D. Nevejans, H. Rème, C. Aoustin, C. Mazelle, J.-L. Médale, J. A. Sauvaud, J.-J. Berthelier, J.-L. Bertaux, L. Duvet, S. A. Fuselier, A. G. Ghielmetti, T. T. Magoncelli, E. G. Shelley, A. Korth, K. Heerlein, H. Lauche, S. Livi, A. Loose, U. Mall, B. Wilken, F. Gliem, B. Fiethe, T. I. Gombosi, B. Block, G. R. Carignan, L. A. Fisk, J. H. Waite, D. T. Young, and H. Wollnik*: ROSINA - ROSETTA orbiter spectrometer for ion and neutral analysis. Space Sci. Rev. **128**, 745–801 (2007), doi:10.1007/s11214-006-8335-3.

*Bamert, K., R. Kallenbach, M. Hilchenbach, and C. W. Smith*: Determination of the eddy turn-over time in the solar wind. In: Turbulence and Nonlinear Processes in Astrophysical Plasmas; 6th Annual International Astrophysics Conference, eds. D. Shaikh and G. P. Zank, vol. 932, pp. 69–74 (2007).

*Barabash, S., A. Fedorov, J. A. Sauvaud, R. Lundin, C. T. Russell, Y. Futaana, T. L. Zhang, H. Andersson, K. Brinkfeldt, A. Grigoriev, M. Holmstrom, M. Yamauchi, K. Asamura, W. Baumjohann, H. Lammer, A. J. Coates, D. O. Kataria, D. R. Linder, C. C. Curtis, K. C. Hsieh, B. R. Sandel, M. Grande, H. Gunell, H. E. J. Koskinen, E. Kallio, P. Riihela, T. Sales, W. Schmidt, J. Kozyra, N. Krupp, M. Fränz, J. Woch, J. Luhmann, S. McKenna-Lawlor, C. Mazelle, J. J. Thocaven, S. Orsini, R. Cerulli-Irelli, M. Mura, M. Milillo, M. Maggi, E. Roelof, P. Brandt, K. Szego, J. D. Winningham, R. A. Frahm, J. Scherrer, J. R. Sharber, P. Wurz, and P. Bochsler*: The loss of ions from Venus through the plasma wake. Nature **450**, 650–653 (2007), doi:10.1038/nature06434.

*Barabash, S., J. A. Sauvaud, H. Gunell, H. Andersson, A. Grigoriev, K. Brinkfeldt, M. Holinstroem, R. Lundin, M. Yamauchi, K. Asamura, W. Baumjohann, T. L. Zhang, A. J. Coates, D. R. Linder, D. O. Kataria, C. C. Curtis, K. C. Hsieh, B. R. Sandel, A. Fedorov, C. Mazelle, J. J. Thocaven, M. Grande, H. E. J. Koskinen, E. Kallio, T. Sales, P. Riihela, J. Kozyra, N. Krupp, J. Woch, J. Luhmann, S. McKenna-Lawlor, S. Orsini, R. Cerulli-Irelli, M. Mura, M. Milillo, M. Maggi, E. Roelof,* *P. Brandt, C. T. Russell, K. Szego, J. D. Winningham, R. A. Frahm, J. Scherrer, J. R. Sharber, P. Wurz, and P. Bochsler*: The analyser of space plasmas and energetic atoms (ASPERA-4) for the Venus express mission. Planet. Space Sci. **55**, 1772–1792 (2007), doi:10.1016/j.pss.2007.01.014.

*Basilevsky, A. T. and H. U. Keller*: Craters, smooth terrains, flows, and layering on the comet nuclei. Solar System Research **41**, 109–117 (2007), doi:10.1134/S0038094607020037.

*Baumgaertel, K., K. Sauer, E. Mjolhus, and E. Dubinin*: Fluid versus simulation model of solitons in solar wind: Application to Ulysses observations. J. Geophys. Res. **112**, A12101 (2007), doi:10.1029/2007JA12557.

*Bedding, T., A. S. Brun, J. Christensen-Dalsgaard, A. Crouch, P. De Cat, R. A. Garcia, L. Gizon, F. Hill, H. Kjeldsen, J. Leibacher, J.-P. Maillard, S. Mathis, M. C. Rabello-Soares, J.-P. Rozelot, M. Rempel, I. W. Roxburgh, R. Samadi, S. Talon, and M. J. Thompson*: Highlights of recent progress in the seismology of the Sun and sun-like stars. In: Proc. IAU XXVI General Assembly, Highlights of Astronomy, ed. K. A. van der Hucht, vol. 14, pp. 491–516 (2007).

*Belton, M. J. S., P. Thomas, J. Veverka, P. Schultz, M. F. A'Hearn, L. Feaga, T. Farnham, O. Groussin, J. Y. Li, C. Lisse, L. McFadden, J. Sunshine, K. J. Meech, W. A. Delamere, and J. Kissel*: The internal structure of Jupiter family cometary nuclei from Deep Impact observations: The "talps" or "layered pile" model. Icarus **187**, 332–344 (2007), doi:10.1016/j.icarus.2006.09.005.

*Bertaux, J.-L., A.-C. Vandaele, O. Korablev, E. Villard, A. Fedorova, D. Fussen, E. Quémerais, D. Belyaev, A. Mahieux, F. Montmessin, C. Muller, E. Neefs, D. Nevejans, V. Wilquet, J. P. Dubois, A. Hauchecorne, A. Stepanov, I. Vinogradov, A. Rodin, M. Cabane, E. Chassefière, J. Y. Chaufray, E. Dimarellis, F. Leblanc, P. Rannou, E. Villard, D. Fussen, E. Van Ransbeeck, L. Zasova, F. Forget, S. Lebonnois, D. Titov, S. Rafkin, G. Durry, J. C. Gérard, and B. Sande.*: A warm layer in Venus cryosphere and high-altitude measurements of HF, HCl, $H_2O$ and HDO. Nature **450**, 646–649 (2007), doi:10.1038/nature05974.

*Bibring, J.-P., H. Rosenbauer, H. Boehnhardt, S. Ulamec, J. Biele, S. Espinasse, B. Feuerbacher, P. Gaudon, P. Hemmerich, P. Kletzkine, D. Moura, R. Mugnuolo, G. Nietner, B. Pätz, R. Roll, H. Scheuerle, K. Szegö, K. Wittmann, Philae Project Office, and the Entire Philae Team*: The Rosetta Lander ("Philae") Investigations. Space Sci. Rev. **128**, 205–220 (2007), doi:10.1007/s11214-006-9138-2.

*Birch, A. C. and L. Gizon*: Linear sensitivity of helioseismic travel times to local flows. Astron. Nachr. **328**, 228–233 (2007), doi:10.1002/asna.200610724.

*Birch, A. C., L. Gizon, B. W. Hindman, and D. A. Haber*: The linear sensitivity of helioseismic ring diagrams to local flows. Astrophys. J. **662**, 730–737 (2007), doi:10.1086/513683.

*Bloomfield, D. S., A. Lagg, and S. K. Solanki*: Observations of running waves in a sunspot chromosphere. In: The Physics of Chromospheric Plasmas, eds. P. Heinzel, I. Dorotovič, and R. J. Rutten, *Astron. Soc. Pacific Conf. Ser.*, vol. 368, pp. 239–244, ASP, San Francisco (2007).

*Bloomfield, D. S., A. Lagg, S. K. Solanki, and J. M. Borrero*: Modified $p$-modes in penumbral filaments. In: Modern Solar Facilities - Advanced Solar Science, eds. F. Kneer, K. G. Puschmann, and A. D. Wittmann, pp. 241–244, Universitätsverlag Göttingen (2007).

*Bloomfield, D. S., S. K. Solanki, A. Lagg, J. M. Borrero, and P. S. Cally*: Modified $p$-modes in penumbral filaments? Astron. & Astrophys. **469**, 1155–1161 (2007), doi:10.1051/0004-6361:20077330.

*Bloomfield, S., A. Lagg, and S. K. Solanki*: The nature of running penumbral waves revealed. Astrophys. J. **671**, 1005–1012 (2007), doi:10.1086/523266.

*Boehnhardt, H., E. Pompei, G. P. Tozzi, O. Hainaut, N. Ageorges, S. Bagnulo, L. Barrera, T. Bonev, H. U. Käufl, F. Kerber, G. LoCurto, O. Marco, E. Pantin, H. Rauer, I. Saviane, F. Selman, C. Sterken, and M. Weiler*: Broad- and narrowband visible imaging of comet 9P/Tempel 1 at ESO around the time of the Deep Impact event. Astron. & Astrophys. **470**, 1175–1183 (2007), doi:10.1051/0004-6361:20066577.

*Borrero, J. M.*: The structure of sunspot penumbrae - IV. MHS equilibrium for penumbral flux tubes and the origin of dark core penumbral filaments and penumbral grains. Astron. & Astrophys. **471**, 967–975 (2007), doi:10.1051/0004-6361:20066776.

*Bößwetter, A., S. Simon, T. Bagdonat, U. Motschmann, M. Fränz, E. Roussos, N. Krupp, J. Woch, J. Schüle, S. Barabash, and R. Lundin*: Comparison of plasma data from ASPERA-3/Mars-Express with a 3-D hybrid simulation. Ann. Geophys. **25**, 1851–1864 (2007).

*Breuer, D., S. A. Hauck, II, M. Buske, M. Pauer, and T. Spohn*: Interior evolution of Mercury. In: Mercury, eds. A. Balogh, L. Ksanfomality, and R. von Steiger, Space Sciences Series of ISSI, pp. 47–78, Springer, Dordrecht/Boston/London (2007), doi:10.1007/s11214-007-9228-9.

*Büchner, J.*: Astrophysical reconnection and collisionless dissipation. Plasma Phys. Control. Fusion **49**, B325–B339 (2007), doi:10.1088/0741-3335/49/12B/S30.

*Büchner, J.*: Investigation of Reconnection in the Solar Corona by Numerical Simulation Based on Solar-B Observations. In: New Solar Physics with Solar-B Mission, eds. K. Shibata, S. Nagata, and T. Sakurai, vol. 369, pp. 407–420, Astronomical Society of the Pacific (2007).

*Büchner, J.* (ed.): Magnetic coupling at sun and stars. Elsevier Ltd., Oxford, Orlando and Tokyo (2007).

*Büchner, J.*: Theory and simulation of reconnection. In: Solar Dynamics and its Effects on the Heliopshere and Earth, eds. D. N. Baker, B. Klecker, S. J. Schwartz, R. Schwenn, and R. von Steiger, pp. 345–360, Springer, Dordrecht (2007).

*Büchner, J.*: Vlasov-code simulation. In: Advanced methods for space simulations, eds. H. Usui and Y. Omura, pp. 23–46, TERRAPUB, Tokyo (2007).

*Büchner, J. and W. Daughton*: Role of current-aligned instabilities in reconnection. In: Reconnection of Magnetic Fields: Magnetohydrodynamics, Collisionless Theory and Observations, eds. J. Birn and E. Priest, pp. 144–153, Cambridge University Press, Cambridge, UK (2007).

*Büchner, J., K.-H. Glassmeier, and J. Saur*: Ein Plasmalabor im Weltraum. Physik Journal **6**, 51–56 (2007).

*Buffett, B. A. and U. R. Christensen*: Magnetic and viscous coupling at the core-mantle boundary: inferences from observations of the Earth's nutations. Geophys. J. Int. **171**, 145–152 (2007), doi:10.1111/j.1365-246X.2007.03543.x.

*Busà, I., R. Aznar Cuadrado, L. Terranegra, V. Andretta, and M. T. Gomez*: The CaII infrared triplet as a stellar activity diagnostic - II. Test and calibration with high resolution observations. Astron. & Astrophys. **466**, 1089–1098 (2007), doi:10.1051/0004-6361:20065588.

*Cai, H. T., S. Y. Ma, Y. Fan, Y. C. Liu, and K. Schlegel*: Climatological features of electron density in the polar ionosphere from long-term observations of EISCAT/ESR radar. Ann. Geophys. **25**, 2561–2569 (2007).

*Cameron, R., L. Gizon, and K. Daiffallah*: SLiM: a code for the simulation of wave propagation through an inhomogeneous, magnetised solar atmosphere. Astron. Nachr. **328**, 313–318 (2007), doi:10.1002/asna.200610736.

*Cameron, R. and M. Schüssler*: Solar Cycle Prediction Using Precursors and Flux Transport Models. Astrophys. J. **659**, 801–811 (2007), doi:10.1086/512049.

*Cameron, R., M. Schüssler, and A. Vögler*: Photospheric magnetoconvection. In: Convection in Astrophysics, eds. F. Kupka, I. Roxburgh, and K. Chan, no. 239 in IAU-Symposium, pp. 488–493, Cambridge University Press (2007), invited paper.

*Cameron, R., M. Schüssler, A. Vögler, and V. Zakharov*: Radiative MHD simulations of solar pores. Astron. & Astrophys. **474**, 261–272 (2007), doi:10.1051/0004-6361:20078140.

*Carbary, J. F., D. G. Mitchell, S. M. Krimigis, D. C. Hamilton, and N. Krupp*: Charged particle periodicities in Saturn's outer magnetosphere. J. Geophys. Res. **112**, A06246 (2007), doi:10.1029/2007JA012351.

*Carbary, J. F., D. G. Mitchell, S. M. Krimigis, D. C. Hamilton, and N. Krupp*: Spin-period effects in magnetospheres with no axial tilt. Geophys. Res. Lett. **34**, L18107 (2007), doi:10.1029/2007GL030483.

*Carbary, J. F., D. G. Mitchell, S. M. Krimigis, and N. Krupp*: Electron periodicities in Saturn's outer magnetosphere. J. Geophys. Res. **112**, A03206 (2007), doi:10.1029/2006JA012077.

*Carbary, J. F., D. G. Mitchell, S. M. Krimigis, and N. Krupp*: Evidence for spiral pattern in Saturn's magnetosphere using the new SKR longitudes. Geophys. Res. Lett. **34**, L13105 (2007), doi:10.1029/2007GL030167.

*Carr, C. M., T. S. Horbury, A. Balogh, S. D. Bale, W. Baumjohann, B. Bavassano, A. Breen, D. Burgess, P. J. Cargill, N. Crooker, G. Erdos, L. Fletcher, R. J. Forsyth, J. Giacalone, K.-H. Glassmeier, T. Hoeksema, M. L. Goldstein, M. Lockwood, W. Magnes, M. Maksimovic, E. Marsch, W. H. Matthaeus, N. Murphy, V. Nakariakov, J. R. Pacheco, J. L. Pinçon, P. Riley, C. T. Russell, S. J. Schwartz, A. Szabo, M. Thompson, R. Vainio, M. Velli, S. Vennerstrom, R. Walsh, R. Wimmer-Schweingruber, and G. Zank*: A Magnetometer For The Solar Orbiter Mission. In: The Second Solar Orbiter Workshop, 16-20 October 2006, Athens, Greece, eds. E. Marsch, K. Tsinganos,

R. Marsden, and L. Conroy, ESA SP-641, ESA Publ. Div., Noordwijk (2007), on CD.

*Cheung, M., M. Schüssler, and F. Moreno-Insertis*: The origin of the reversed granulation in the solar photosphere. Astron. & Astrophys. **461**, 1163–1171 (2007), doi:10.1051/0004-6361:20066390.

*Cheung, M. C. M., M. Schüssler, and F. Moreno-Insertis*: Magnetic flux emergence in granular convection: radiative MHD simulations and observational signatures. Astron. & Astrophys. **467**, 703–719 (2007), doi:10.1051/0004-6361:20077048.

*Christensen, U. R., J. Aubert, and P. Olson*: Convection-driven planetary dynamos. In: Convection in Astrophysics, Proceedings IAU Symposium No. 239, 2006, eds. F. Kupka, I. W. Roxburgh, and K. L. Chan, pp. 188–195, International Astronomical Union (2007), doi:10.1017/S1743921307000403.

*Christensen, U. R. and J. Wicht*: Numerical Dynamo Simulations. In: Core Dynamics, ed. P. Olson, *Treatise on Geophysics*, vol. 8, pp. 245–282, Elsevier, Amsterdam (2007).

*Collados, M., A. Lagg, J. J. Díaz García, E. Hernández Suárez, R. López López, E. Páez Mañá, and S. K. Solanki*: Tenerife Infrared Polarimeter II. In: The Physics of Chromospheric Plasmas, eds. P. Heinzel, I. Dorotovič, and R. J. Rutten, *Astron. Soc. Pacific Conf. Ser.*, vol. 368, pp. 611–616, ASP, San Francisco (2007).

*Constantinescu, O. D., K. H. Glassmeier, P. M. E. Décréau, M. Fränz, and K. H. Fornaçon*: Low frequency wave sources in the outer magnetosphere, magnetosheath, and near Earth solar wind. Ann. Geophys. **25**, 2217–2228 (2007).

*Corbard, T., L. Gizon, and M. Roth*: Editors' note. Astron. Nachr. **328**, 203 (2007), doi:10.1002/asna.200790000.

*Curdt, W. and E. Landi*: The transition region above sunspots. In: Solar and Stellar Physics Through Eclipses, eds. O. Demircan, S. O. Selam, and B. Albayrak, *ASP Conferences Series*, vol. 370, p. 40 (2007).

*Czechowski, A. and M. Hilchenbach*: Neutral solar wind and the inner source of the pick-up ions. In: The Second Solar Orbiter Workshop, 16-20 October 2006, Athens, Greece, eds. E. Marsch, K. Tsinganos, R. Marsden, and L. Conroy, ESA SP-641 (2007).

*Czechowski, A., R. Kallenbach, and M. Hilchenbach*: Diagnostics of the heliospheric interface: high energy ENAs. In: The Physics of the Heliospheric Boundaries, eds. V. Izmodenov and R. Kallenbach, no. SR-005 in ISSI Scientific Reports, pp. 311–334, ESA Publ. Div., Noordwijk, Netherlands (2007).

*D'Amicis, R., S. Orsini, E. Antonucci, A. M. Di Lellisand, M. Hilchenbach, D. Telloni, A. Mura, A. Milillo, S. Fineschi, and R. Bruno*: Numerical simulations of coronal hole-associated neutral solar wind as expected at the Solar Orbiter position. J. Geophys. Res. **112**, A06110 (2007), doi:10.1029/2006JA011969.

*Danilović, S., S. K. Solanki, W. Livingston, N. A. Krivova, and I. Vince*: Magnetic source of the solar cycle variation of the Mn I 539.4 nm line. In: Modern solar facilities – Advanced Solar Science, eds. F. Kneer, K. G. Puschmann, and A. D. Wittmann, pp. 189–192, Universitätsverlag Göttingen, Göttingen (2007).

*Defise, J.-M., J.-P. Halain, D. Berghmans, F. Denis, E. Mazy, T. Thibert, J.-H. Lecat, P. Rochus, B. Nicula, A. De Groof, J.-F. Hochedez, U. Schühle, M.-F. Ravet, and F. Delmotte*: SWAP: a novel EUV telescope for space weather. In: Solar Physics and Space Weather Instrumentation II, eds. S. Fineschi and R. A. Viereck, *Proceedings SPIE*, vol. 6689, pp. 0S1–0S12, SPIE (2007), doi:10.1117/12.731784.

*Dikarev, V., O. Preuss, S. K. Solanki, H. Krüger, and A. Krivov*: Understanding the WMAP results: low-order multipoles and dust in the vicinity of the solar system. Earth, Moon and Planets **102**, 555–561 (2007), doi:10.1007/s11038-007-9172-4.

*Drossart, P., G. Piccioni, A. Adriani, F. Angrilli, G. Arnold, K. H. Baines, G. Bellucci, J. Benkhoff, B. Bezard, J. P. Bibring, A. Blanco, M. I. Blecka, R. W. Carlson, A. Coradini, A. D. Lellis, T. Encrenaz, S. Erard, S. Fonti, V. Formisano, T. Fouchet, R. Garcia, R. Haus, J. Helbert, N. I. Ignatiev, P. G. J. Irwin, Y. Langevin, S. Lebonnois, M. A. Lopez-Valverde, D. Luz, L. Marinangeli, V. Orofino, A. V. Rodin, M. C. Roos-Serote, B. Saggin, A. Sanchez-Lavega, D. M. Stam, F. W. Taylor, D. Titov, G. Visconti, M. Zambelli, R. Hueso, C. C. C. Tsang, C. F. Wilson, and T. Z. Afanasenko*: Scientific goals for the observation of Venus by VIRTIS on ESA/Venus Express mission. Planet. Space Sci. **55**, 1653–1672 (2007), doi:10.1016/j.pss.2007.01.003.

*Drossart, P., G. Piccioni, J. C. Gerard, M. A. Lopez-Valverde, A. Sanchez-Lavega, L. Zasova, R. Hueso, F. W. Taylor, B. Bezard, A. Adriani, F. Angrilli, G. Arnold, K. H. Baines, G. Bellucci, J. Benkhoff, J. P. Bibring, A. Blanco, M. I. Blecka, R. W. Carlson, A. Coradini, A. D. Lellis, T. Encrenaz, S. Erard, S. Fonti, V. Formisano, T. Fouchet, R. Gar-*

*cia, R. Haus, J. Helbert, N. I. Ignatiev, P. Irwin, Y. Langevin, S. Lebonnois, D. Luz, L. Marinangeli, V. Orofino, A. V. Rodin, M. C. Roos-Serote, B. Saggin, D. M. Stam, D. Titov, G. Visconti, M. Zambelli, and C. Tsang*: A dynamic upper atmosphere of Venus as revealed by VIRTIS on Venus Express. Nature **450**, 641–645 (2007), doi:10.1038/nature06140.

*Dubinin, E., M. Maksimovic, N. Cornilleau-Werhlin, D. Fontane, P. Travnicek, A. Mangeney, O. Alexandrova, K. Sauer, M. Fraenz, I. Dandouras, E. Lucek, A. Fazakerley, A. Balogh, and M. Andre*: Coherent whistler emissions in the magnetosphere-Cluster observations. Ann. Geophys. **25**, 303–315 (2007).

*Ermolli, I., A. Tlatov, S. K. Solanki, N. A. Krivova, and J. Singh*: Solar Activity and Irradiance Studies with Ca II Spectroheliograms: Potential and Problems. In: The Physics of Chromospheric Plasmas, eds. P. Heinzel, I. Dorotovič, and R. J. Rutten, *ASP Conference Series*, vol. 368, p. 533, ASP, San Francisco (2007).

*Fear, R. C., S. E. Milan, A. N. Fazakerley, C. J. Owen, T. Asikainen, M. G. G. T. Taylor, E. A. Lucek, H. Rème, I. Dandouras, and P. W. Daly*: Motion of flux transfer events: a test of the Cooling model. Ann. Geophys. **25**, 1669–1690 (2007).

*Feng, L., B. Inhester, S. K. Solanki, T. Wiegelmann, B. Podlipnik, R. A. Howard, and J.-P. Wuelser*: First stereoscopic coronal loop reconstructions from STEREO/SECCHI images. Astrophys. J. **671**, L205–L208 (2007), doi:10.1086/525525.

*Feng, L., T. Wiegelmann, B. Inhester, S. K. Solanki, W. Q. Gan, and P. Ruan*: Magnetic Stereoscopy of Coronal Loops in NOAA 8891. Solar Phys. **241**, 235–249 (2007), doi:10.1007/s11207-007-0370-z.

*Flandes, A. and H. Krüger*: Solar wind modulation of Jupiter dust stream detection. In: Proceedings of "Dust in Planetary Systems", Kauai, Hawaii, USA, 26-30 September 2005, eds. H. Krüger and A. L. Graps, ESA SP-643, pp. 87–90, ESA Publ. Div., Noordwijk (2007), on CD.

*Fontenla, J. M., W. Curdt, E. H. Avrett, and J. Harder*: Log-normal intensity distribution of the quiet-Sun FUV continuum observed by SUMER. Astron. & Astrophys. **468**, 695–699 (2007), doi:10.1051/0004-6361:20066854.

*Fornasier, S., E. Dotto, O. Hainaut, F. Marzari, H. Boehnhardt, F. de Luise, and M. A. Barucci*: Visible spectroscopic and photometric survey of Jupiter Trojans: Final results on dynamical families. Icarus **190**, 622–642 (2007), doi:10.1016/j.icarus.2007.03.033.

*Fouchet, T., E. Lellouch, N. I. Ignatiev, F. Forget, D. V. Titov, M. Tschimmel, F. Montmessin, V. Formisano, A. Giuranna, A. Maturilli, and T. Encrenaz*: Martian water vapor: Mars Express PFS/LW observations. Icarus **190**, 32–49 (2007), doi:10.1016/j.icarus.2007.03.003.

*Gandorfer, A. M., S. K. Solanki, P. Barthol, V. Martínez Pillet, W. Schmidt, A. M. Title, M. Knölker, and the SUNRISE team*: SUNRISE: High resolution UV/VIS observations of the Sun from the stratosphere. In: Modern Solar Facilities - Advanced Solar Science, eds. F. Kneer, K. G. Puschmann, and A. D. Wittmann, pp. 69–76, Universitätsverlag Göttingen (2007).

*Garnier, P., I. Dandouras, D. Toublanc, P. C. Brandt, E. C. Roelof, D. G. Mitchell, S. M. Krimigis, N. Krupp, D. C. Hamilton, and H. Waite*: The exosphere of Titan and its interaction with the Kronian magnetosphere: MIMI observations and modeling. Planet. Space Sci. **55**, 165–173 (2007), doi:10.1016/j.pss.2006.07.006.

*Gaudio, S., J. Jackiewicz, and K. Bedell*: Many body exchange effects close to the s-wave Feshbach resonance in two-component Fermi systems: Is a triplet superfluid possible? Phil. Mag. Lett. **87**, 713–721 (2007).

*Gizon, L.*: Helioseismologie. In: Jahrbuch 2007, pp. 589–594, Max-Planck-Gesellschaft (2007), on CD.

*Gizon, L.*: Helioseismology with Solar Orbiter: Science Objectives, Observational Strategies and Requirements. In: The Second Solar Orbiter Workshop, 16-20 October 2006, Athens, Greece, eds. E. Marsch, K. Tsinganos, R. Marsden, and L. Conroy, ESA SP-641, ESA Publ. Div., Noordwijk (2007), on CD.

*Gizon, L., R. Cameron, J. Jackiewicz, M. Roth, H. Schunker, and T. Stahn*: Helioseismology at MPS. In: Modern Solar Facilities – Advanced Solar Science, eds. F. Kneer, K. G. Puschmann, and A. D. Wittmann, pp. 89–102, Universitätsverlag Göttingen, Göttingen, Germany (2007).

*Gizon, L. and M. J. Thompson*: Outstanding problems in local helioseismology. Astron. Nachr. **328**, 204–210 (2007), doi:10.1002/asna.200610720.

*Glassmeier, K.-H., H. Boehnhardt, D. Koschny, E. Kuehrt, and I. Richter*: The Rosetta Mission: Flying Towards the Origin of the Solar System. Space Sci. Rev. **128**, 1–21 (2007), doi:10.1007/s11214-006-9140-8.

*Goesmann, F., H. Rosenbauer, R. Roll, C. Szopa, F. Raulin, R. Sternberg, G. Israel, U. Meierhenrich, W. Thiemann, and G. Munoz-Caro*: COSAC, the cometary sampling and composition experiment on Philae. Space Sci. Rev. **128**, 257–280 (2007), doi:10.1007/s11214-006-9000-6.

*Graf, U. U., S. Heyminck, R. Güsten, P. Hartogh, H.-W. Hübers, J. Stutzki, J. Faist, M. Fischer, K. Jacobs, M. Phillip, D. Rabanus, A. Semenov, P. van der Waal, A. Wagner-Gentner, C. Walther, and M. Wiedner*: GREAT: the German first light heterodyne instrument for SOFIA. In: Proceeding of SPIE, ed. M. Strojnik-Scholl, *Infrared Spaceborne Remote Sensing and Instrumentation XV*, vol. 6678 (2007), doi:10.1117/12.768027.

*Graham, J. P., D. D. Holm, P. D. Mininni, and A. Pouquet*: Highly turbulent solutions of the Lagrangian-averaged Navier-Stokes alpha model and their large-eddy-simulation potential. Phys. Rev. E **76**, 056310 (2007), doi:10.1103/PhysRevE.76.056310.

*Grande, M., B. J. Kellett, C. Howe, C. H. Perry, B. Swinyard, S. Dunkin, J. Huovelin, L. Alha, L. C. D'Uston, S. Maurice, O. Gasnault, S. Couturier-Doux, S. Barabash, K. H. Joy, I. A. Crawford, D. Lawrence, V. Fernandes, I. Casanova, M. Wieczorek, N. Thomas, U. Mall, B. Foing, D. Hughes, H. Alleyne, S. Russell, M. Grady, R. Lundin, D. Baker, C. D. Murray, J. Guest, and A. Christou*: The D-CIXS X-ray spectrometer on the SMART-1 mission to the Moon: First results. Planet. Space Sci. **55**, 494–502 (2007), doi:10.1016/j.pss.2006.08.004.

*Griessmeier, J. M., S. Preusse, M. Khodachenko, U. Motschmann, G. Mann, and H. O. Rucker*: Exoplanetary radio emission under different stellar wind conditions. Planet. Space Sci. **55**, 618–630 (2007), doi:10.1016/j.pss.2006.01.008.

*Grün, E., R. Srama, S. Helfert, G. Moragas-Klostermeyer, H. Krüger, N. Altobelli, A. Sigfried, V. Dikarev, D. Harris, M. Horanyi, M. Rachev, A. Srowig, and Z. Sternovsky*: Prospects of Dust Astronomy missions. In: Proceedings of "Dust in Planetary Systems", Kauai, Hawaii, USA, 26-30 September 2005, eds. H. Krüger and A. L. Graps, ESA SP-643, pp. 245–249, ESA Publ. Div., Noordwijk (2007), on CD.

*Gruszecki, M., K. Murawski, S. K. Solanki, and L. Ofman*: Attenuation of Alfvén waves in straight and curved coronal slabs. Astron. & Astrophys. **469**, 1117–1121 (2007), doi:10.1051/0004-6361:20066924.

*Grygalashvyly, M., G. R. Sonnemann, and P. Hartogh*: Long-term trends of the concentration of the minor constituents in the mesosphere - a model study. Atmos. Chem. Phys. Discuss. **7**, 15 453–15 494 (2007).

*Gulkis, S., M. Allen, C. Backus, G. Beaudin, N. Biver, D. Bockelee-Morvan, J. Crovisier, D. Despois, P. Encrenaz, M. Frerking, M. Hofstadter, P. Hartogh, W. Ip, M. Janssen, L. Kamp, T. Koch, E. Lellouch, I. Mann, D. Muhlemann, H. Rauer, P. Schloerb, and T. Spilker*: Remote sensing of a comet at millimeter and submillimeter wavelengths from an orbiting spacecraft. Planet. Space Sci. **55**, 1050–1057 (2007), doi:10.1016/j.pss.2006.11.011.

*Hartogh, P., A. S. Medvedev, and C. Jarchow*: Middle atmosphere polar warmings on Mars: Simulations and study on the validation with submillimeter observations. Planet. Space Sci. **55**, 1103–1112 (2007), doi:10.1016/j.pss.2006.11.018.

*He, J.-S., C.-Y. Tu, and E. Marsch*: Can the solar wind originate from a quiet Sun region? Astron. & Astrophys. **468**, 307–312 (2007), doi:10.1051/0004-6361:20066423.

*Heber, B., H. Fichtner, K. Scherer, J. Büchner, and H. Peter*: Das Internationale Heliophysikalische Jahr. Sterne und Weltraum **4**, 18–21 (2007).

*Hedman, M. M., J. A. Burns, M. S. Tiscareno, C. C. Porco, G. H. Jones, E. Roussos, N. Krupp, C. Paranicas, and S. Kempf*: The Source of Saturn's G Ring. Science **317**, 653 – 656 (2007), doi:10.1126/science.1143964.

*Heuer, M. and E. Marsch*: Diffusion plateaus in the velocity distributions of fast solar wind protons. J. Geophys. Res. **112**, A03102 (2007), doi:10.1029/2006JA011979.

*Hilchenbach, M., S. Orsini, K. C. Hsieh, E. Antonucci, S. Barabash, K. Bamert, R. Bruno, M. R. Collier, A. Czechowski, R. D'Amicis, E. De Angelis, I. Dandouras, A. M. Di Lellis, R. Esser, J. Giacalone, M. Gruntman, S. R. Habbal, J. R. Jokipii, E. Kallio, J. Kota, H. Kucharek, R. Leoni, S. Livi, I. Mann, E. Marsch, E. Möbius, A. Mura, R. B. Sheldon, W. Schmidt, S. Selci, K. Szego, J. Woch, P. Wurz, and T. H. Zurbuchen*: Solar Orbiter Neutral Solar Wind Detector. In: The Second Solar Orbiter Workshop, 16-20 October 2006, Athens, Greece, eds. E. Marsch, K. Tsinganos, R. Marsden, and L. Conroy, ESA SP-641, ESA Publ. Div., Noordwijk (2007), on CD.

*Hirzberger, J., L. Gizon, S. K. Solanki, and T. L. Duvall, Jr.*: Structure and evolution of supergranulation from local helioseismology. In: Modern Solar Facilities - Advanced Solar Science, eds. F. Kneer,

K. G. Puschmann, and A. D. Wittmann, pp. 103–106, Universitätsverlag Göttingen, Göttingen, Germany (2007).

*Hochedez, J.-F., T. Appourchaux, J.-M. Defise, L. K. Harra, U. Schühle, F. Auchère, W. Curdt, B. Hancock, M. Kretzschmar, G. Lawrence, J.-C. Leclec'h, E. Marsch, R. Mercier, S. Parenti, E. Podladchikova, M.-F. Ravet, P. Rochus, L. Rodriguez, F. Rouesnel, S. Solanki, L. Teriaca, L. Van Driel, J. C. Vial, B. Winter, and A. Zhukov*: EUI, The Ultraviolet Imaging Telescopes Of Solar Orbiter. In: The Second Solar Orbiter Workshop, 16-20 October 2006, Athens, Greece, eds. E. Marsch, K. Tsinganos, R. Marsden, and L. Conroy, ESA SP-641, ESA Publ. Div., Noordwijk (2007), on CD.

*Holzwarth, V.*: Magnetic flux emergence in fast rotating stars. In: Coronae of stars and accretion disks, eds. M. Massi and T. Preibisch, vol. 78, pp. 271–278, Memorie della Società Astronomica Italiana (2007).

*Holzwarth, V. and M. Jardine*: Mass loss rates and wind ram pressures of cool stars. In: Modern Solar Facilities – Advanced Solar Science, eds. F. Kneer, K. G. Puschmann, and A. D. Wittmann, pp. 371–374, Universitätsverlag Göttingen (2007).

*Holzwarth, V. and M. Jardine*: Theoretical mass loss rates of cool main-sequence stars. Astron. & Astrophys. **463**, 11–21 (2007), doi:10.1051/0004-6361:20066486.

*Holzwarth, V., D. H. Mackay, and M. Jardine*: Formation of polar starspots through meridional circulation. Astronomische Nachrichten **328**, 1108–1110 (2007), doi:10.1002/asna.200710854.

*Holzwarth, V., M. Schüssler, and D. Schmitt*: Flow instabilities of magnetic flux tubes - II. Longitudinal flow. Astron. & Astrophys. **469**, 11–17 (2007), doi:10.1051/0004-6361:20077269.

*Işik, E., D. Schmitt, and M. Schüssler*: A coupled model of magnetic flux generation and transport in stars. Astron. Nachr. **328**, 1111–1113 (2007), doi:10.1002/asna.200710865.

*Işik, E., M. Schüssler, and S. K. Solanki*: Magnetic flux transport and the lifetimes of spots on active cool stars. In: Modern Solar Facilities - Advanced Solar Science, eds. F. Kneer, K. G. Puschmann, and A. D. Wittmann, pp. 367–369, Universitätsverlag Göttingen (2007).

*Işik, E., M. Schüssler, and S. K. Solanki*: Magnetic flux transport on active cool stars and starspot lifetimes. Astron. & Astrophys. **464**, 1049–1057 (2007), doi:10.1051/0004-6361:20066623.

*Imada, S., R. Nakamura, P. W. Daly, M. Hoshino, W. Baumjohann, S. Mühlbachler, A. Balogh, and H. Rème*: Energetic electron acceleration in the downstream reconnection outflow region. J. Geophys. Res. **112**, A03202 (2007), doi:10.1029/2006JA011847.

*Inhester, B., L. Feng, and T. Wiegelmann*: Segmentation of Loops from Coronal EUV Images. Solar Phys. **248**, 379–393 (2007), doi:10.1007/s11207-007-9027-1.

*Izmodenov, V. and R. Kallenbach* (eds.): The Physics of the Heliospheric Boundaries. No. SR-005 in ISSI Scientific Reports, ESA Publ. Div., Noordwijk, Netherlands (2007).

*Jackiewicz, J., L. Gizon, A. C. Birch, and T. L. Duvall, Jr.*: Time-distance helioseismology: Sensitivity of f-mode travel times to flows. Astrophys. J. **671**, 1051–1064 (2007), doi:10.1086/522914.

*Jackiewicz, J., L. Gizon, A. C. Birch, and M. J. Thompson*: A procedure for the inversion of f-mode travel times for solar flows. Astron. Nachrichten **328**, 234–239 (2007), doi:10.1002/asna.200610725.

*Jess, D. B., A. Andic, M. Mathioudakis, D. S. Bloomfield, and F. P. Keenan*: High-frequency oscillations in a solar active region observed with the RAPID DUAL IMAGER. Astron. & Astrophys. **473**, 943–950 (2007), doi:10.1051/0004-6361:20077142.

*Jorda, L., P. Lamy, G. Faury, H. U. Keller, S. Hviid, M. Küppers, D. Koschny, J. Lecacheux, P. Gutiérrez, and L. M. Lara*: Properties of the dust cloud caused by the Deep Impact experiment. Icarus **187**, 208–219 (2007), doi:10.1016/j.icarus.2006.10.004.

*Jordan, S., R. Aznar Cuadrado, R. Napiwotzki, H. M. Schmid, and S. K. Solanki*: The fraction of DA white dwarfs with kilo-Gauss magnetic fields. Astron. & Astrophys. **462**, 1097–1101 (2007), doi:10.1051/0004-6361:20066163.

*Jordan, S., R. Aznar Cuadrado, R. Napiwotzki, H. M. Schmid, and S. K. Solanki*: The fraction of DA White Dwarfs with kilo-Gauss magnetic fields. In: 15th European Workshop on White Dwarfs, *Astron. Soc. Pacific Conf. Ser.*, vol. 372, pp. 169–172, ASP, San Francisco (2007).

*Kallenbach, R., K. Bamert, and M. Hilchenbach*: Isotopic Composition of the Solar Wind Inferred from In-Situ Spacecraft Measurements. Space Sci. Rev. **130**, 173–182 (2007), doi:10.1007/s11214-007-9216-0.

*Kallenbach, R., A. Czechowski, M. Hilchenbach, and P. Wurz*: Turbulence and ion acceleration in the outer heliosphere. In: The Physics of the Heliospheric Boundaries, eds. V. Izmodenov and R. Kallenbach, no. SR-005 in ISSI Scientific Reports, pp. 203–243, ESA Publ. Div., Noordwijk, Netherlands (2007).

*Kallenbach, R. and V. Izmodenov*: Summary of the results of INTAS Project WP 01-270: Physics of the Heliosheath Plasma Flow and Structure of the Termination Shock. In: The Physics of the Heliospheric Boundaries, eds. V. Izmodenov and R. Kallenbach, no. SR-005 in ISSI Scientific Reports, pp. 391–413, ESA Publ. Div., Noordwijk, Netherlands (2007).

*Karkoschka, E., M. G. Tomasko, L. R. Doose, C. See, E. A. McFarlane, S. E. Schröder, and B. Rizk*: DISR imaging and the geometry of the descent of the Huygens probe within Titan's atmosphere. Planet. Space Sci. **55**, 1896–1935 (2007), doi:10.1016/j.pss.2007.04.019.

*Keller, H. U., C. Barbieri, P. Lamy, H. Rickman, R. Rodrigo, K.-P. Wenzel, H. Sierks, M. F. A'Hearn, F. Angrilli, M. Angulo, M. E. Bailey, P. Barthol, M. A. Barucci, J.-L. Bertaux, G. Bianchini, J.-L. Boit, V. Brown, J. A. Burns, I. Büttner, J. M. Castro, G. Cremonese, W. Curdt, V. Da Deppo, S. Debei, M. D. Cecco, K. Dohlen, S. Fornasier, M. Fulle, D. Germerott, F. Gliem, G. P. Guizzo, S. F. Hviid, W.-H. Ip, L. Jorda, D. Koschny, J. R. Kramm, E. Kührt, M. Küppers, L. M. Lara, A. Llebaria, A. López, A. López-Jimenez, J. López-Moreno, R. Meller, H. Michalik, M. D. Michelena, R. Müller, G. Naletto, A. Origné, G. Parzianello, M. Pertile, C. Quintana, R. Ragazzoni, P. Ramous, K.-U. Reiche, M. Reina, J. Rodríguez, G. Rousset, L. Sabau, A. Sanz, J.-P. Sivan, K. Stöckner, J. Tabero, U. Telljohann, N. Thomas, V. Timon, G. Tomasch, T. Wittrock, and M. Zaccariotto*: OSIRIS – The Scientific Camera System onboard Rosetta. Space Sci. Rev. **128**, 433–506 (2007), doi:10.1007/s11214-006-9128-4.

*Keller, H. U., M. Küppers, S. Fornasier, P. J. Gutiérrez, S. F. Hviid, L. Jorda, J. Knollenberg, S. C. Lowry, M. Rengel, I. Bertini, G. Cremonese, W.-H. Ip, D. Koschny, R. Kramm, E. Kührt, L.-M. Lara, H. Sierks, N. Thomas, C. Barbieri, P. Lamy, H. Rickman, R. Rodrigo, M. F. A'Hearn, F. Angrilli, M.-A. Barucci, J.-L. Bertaux, V. da Deppo, B. J. R. Davidsson, M. de Cecco, S. Debei, M. Fulle, F. Gliem, O. Groussin, J. J. Lopez Moreno, F. Marzari, G. Naletto, L. Sabau, A. Sanz Andrés, and K.-P. Wenzel*: Observations of Comet 9P/Tempel 1 around the Deep Impact event by the OSIRIS cameras onboard Rosetta. Icarus **187**, 87–103 (2007), doi:10.1016/j.icarus.2006.09.023.

*Kinch, K. M., J. Sohl-Dickstein, J. F. Bell, J. R. Johnson, W. Goetz, and G. A. Landis*: Dust deposition on the Mars Exploration Rover Panoramic Camera (Pancam) calibration targets. J. Geophys. Res. **112**, E06S03 (2007), doi:10.1029/2006JE002807.

*Kissel, J., K. Altwegg, B. C. Clark, L. Colangeli, H. Cottin, S. Czempiel, J. Eibl, C. Engrand, H. M. Fehringer, B. Feuerbacher, M. Fomenkovao, A. Glasmachers, J. M. Greenberg, E. Grün, G. Haerendel, H. Henkel, M. Hilchenbach, H. von Hoerner, H. Höfner, K. Hornung, E. K. Jessberger, A. Koch, H. Krüger, Y. Langevin, P. Parigger, F. Raulin, F. Rudenauer, J. Rynö, E. R. Schmid, R. Schulz, J. Silen, W. Steiger, T. Stephan, L. Thirkell, R. Thomas, K. Torkar, N. G. Utterback, K. Varmuza, K. P. Wanczek, W. Werther, and H. Zscheeg*: COSIMA - High resolution time-of-flight secondary ion mass spectrometer for the analysis of cometary dust particles onboard Rosetta. Space Sci. Rev. **128**, 823–867 (2007), doi:10.1007/s11214-006-9083-0.

*Koch, Ch. and J. Müller*: ICC on Planetary Geodesy. In: National Report of the Federal Republic of Germany on the Geodetic Activities in the years 2003 – 2007, eds. J. Müller and H. Hornik, no. 315 in Reihe B, pp. 159–161, Deutsche Geodätische Kommission bei der Bayrischen Akademie der Wissenschaften, München, Germany (2007).

*Kofman, W., A. Herique, J.-P. Goutail, T. Hagfors, I. P. Williams, E. Nielsen, J.-P. Barriot, Y. Barbin, C. Elachi, P. Edenhofer, A.-C. Levasseur-Regourd, D. Plettemeier, G. Picardi, R. Seu, and V. Svedhem*: The comet nucleus sounding experiment by radiowave transmisssion (CONSERT): A short description of the instrument and of the commissioning stages. Space Sci. Rev. **128**, 413–432 (2007), doi:10.1007/s11214-006-9034-9.

*Korokhin, V. V., Y. I. Velikodsky, Y. G. Shkuratov, and U. Mall*: The phase dependence of brightness and color of the lunar surface: a study based on integral photometric data. Solar System Research **41**, 19–27 (2007), doi:10.1134/S0038094607010029.

*Korth, A., E. Echer, F. L. Guarnieri, M. Fränz, R. Friedel, W. D. Gonzales, C. G. Mouikis, and H. Rème*: Cluster observations of plasma sheet activity during the September 14-28, 2003 corotating high speed stream event. In: Proceedings of the Eighth International Conference on Substorms

(ICS-8), eds. Syrjäsuo and Donovan, pp. 133–138, University of Calgary, Alberta, Canada (2007).

*Kramar, M. and B. Inhester*: Inversion of coronal Zeeman and Hanle Observations to reconstruct the coronal magnetic field. Memorie della Società Astronomica Italiana **78**, 120–125 (2007).

*Krieger, L., M. Roth, and O. von der Lühe*: Estimating the solar meridional circulation by normal mode decomposition. Astron. Nachr. **328**, 252–256 (2007), doi:10.1002/asna.200710745.

*Krimigis, S. M., N. Sergis, D. G. Mitchell, D. C. Hamilton, and N. Krupp*: A dynamic, rotating ring current around Saturn. Nature **450**, 1050–1053 (2007), doi:10.1038/nature06425.

*Krivova, N. A., L. Balmaceda, and S. K. Solanki*: Reconstruction of solar total irradiance since 1700 from the surface magnetic flux. Astron. & Astrophys. **467**, 335–346 (2007), doi:10.1051/0004-6361:20066725.

*Kronberg, E., K.-H. Glassmeier, J. Woch, N. Krupp, A. Lagg, and D. Michele*: A possible intrinsic mechanism for the quasi-periodic dynamics of the Jovian magnetosphere. J. Geophys. Res. **112**, A05203 (2007), doi:10.1029/2006JA011994.

*Krüger, H. and A. L. Graps* (eds.): Proceedings of "Dust in Planetary Systems", Kauai, Hawaii, USA, 26-30 September 2005, ESA SP-643, ESA Publ. Div., Noordwijk (2007), on CD.

*Krüger, H. and E. Grün*: Dust measurements during Ulysses' 2nd Jupiter encounter. In: Proceedings of "Dust in Planetary Systems", Kauai, Hawaii, USA, 26-30 September 2005, eds. H. Krüger and A. L. Graps, ESA SP-643, pp. 69–72, ESA Publ. Div., Noordwijk (2007), on CD.

*Krüger, H., M. Landgraf, N. Altobelli, and E. Grün*: Interstellar dust in the solar system. Space Sci. Rev. **130**, 401–408 (2007), doi:10.1007/s11214-007-9181-7.

*Krupp, N.*: New Surprises in the Largest Magnetosphere of Our Solar System. Science **318**, 216–217 (2007), doi:10.1126/science.1150448.

*Kunow, H., N. U. Crooker, J. A. Linker, R. Schwenn, and R. von Steiger* (eds.): Coronal Mass Ejections. Springer-Verlag, New York (2007).

*Küppers, M., H. U. Keller, E. Kührt, and the CNSR Team*: A comet nucleus sample return (CNSR) mission in ESAs Cosmic Vision program. Geochim. Cosmochim. Acta **71**, A531 (2007).

*Küppers, M., S. Mottola, S. C. Lowry, M. A. A'Hearn, C. Barbieri, M. A. Barucci, S. Fornasier, O. Groussin, P. Gutiérrez, S. F. Hviid, H. U. Keller, and P. Lamy*: Determination of the light curve of the Rosetta target asteroid (2867) Steins by the OSIRIS cameras onboard Rosetta. Astron. & Astrophys. **462**, L13–L16 (2007), doi:10.1051/0004-6361:20066694.

*Kuroda, T. and P. Hartogh*: Comparison of microwave observations of Martian temperature and wind with general circulation model simulations. In: Advances in Geosciences, Vol. 7: Planetary Science, eds. W.-H. Ip, A. Bhardwaj, C. Y. R. Wu, F. Leblanc, P. Hartogh, and Y. Kasaba, pp. 13–20, World Scientific Publishing Co, Singapore (2007).

*Kuroda, T., A. S. Medvedev, P. Hartogh, and M. Takahashi*: Seasonal changes of the baroclinic wave activity in the northern hemisphere of Mars simulated with a GCM. Geophys. Res. Lett. **34**, L09203 (2007), doi:10.1029/2006GL028816.

*Kutepov, A. A., A. G. Feofilov, A. S. Medvedev, A. W. A. Pauldrach, and P. Hartogh*: Small-scale temperature fluctuations associated with gravity waves cause additional radiative cooling of the mesopause region. Geophys. Res. Lett. **34**, L24807 (2007), doi:10.1029/2007GL032392.

*Kuznetsov, E. A., S. P. Savin, E. Amata, M. Dunlop, Y. Khotyaintsev, L. M. Zelenyi, J. Büchner, and J. Blecki*: Strong space plasma magnetic barriers and Alfvénic collapse. JETP letters **85**, 288–293 (2007).

*Lagg, A., J. Woch, S. K. Solanki, and N. Krupp*: Supersonic Downflows in the Vicinity of a Growing Pore: Evidence of unresolved magnetic fine structure at chromospheric heights. Astron. & Astrophys. **462**, 1147–1155 (2007), doi:10.1051/0004-6361:20054700.

*Lagg, A., L. Yelles, J. Hirzberger, J. Woch, and S. K. Solanki*: The performance of the SOLO-VIM instrument: Effects of instrumental noise and lossy data compression. In: The Second Solar Orbiter Workshop, eds. E. Marsch, K. Tsinganos, R. Marsden, and L. Conroy, ESA SP-641, ESA Publ. Div., Noordwijk (2007), on CD.

*Lara, L. M., H. Boehnhardt, R. Gredel, P. J. Gutierrez, R. Rodrigo, and M. J. Vidal-Nunez*: Behavior of Comet 9P/Tempel 1 around the Deep Impact event. Astron. & Astrophys. **465**, 1061–1067 (2007), doi:10.1051/0004-6361:20065534.

*Lasky, P. D., A. W. C. Lun, and R. B. Burston*: Initial value formalism for Lemaitre-Tolman-Bondi collapse. ANZIAM J. **49**, 53–73 (2007).

*Lazutin, L. L., T. V. Kozelova, N. P. Meredith, M. Danielides, B. V. Kozelov, J. Jussila, and A. Korth*: Studies of substorm on March 12, 1991: 2. Auroral electrons. Acceleration, injection, and dynamics. Cosmic Research **45**, 89–96 (2007), doi:10.1134/S0010952507020013.

*Lazutin, L. L., T. V. Kozelova, N. P. Meredith, M. Danielides, B. V. Kozelov, J. Jussila, and A. Korth*: Studies of the substorm on March 12, 1991: 1. Structure of substorm activity and auroral ions. Cosmic Research **45**, 27–38 (2007), doi:10.1134/S0010952507010042.

*Lee, K. W., J. Büchner, and N. Elkina*: Current driven low-frequency electrostatic waves in the solar corona: Linear theory and nonlinear saturation. Phys. Plasmas **14**, 112903 (2007), doi:10.1063/1.2805448.

*Leitner, M., C. J. Farrugia, C. Mostl, K. W. Ogilvie, A. B. Galvin, R. Schwenn, and H. K. Biernat*: Consequences of the force-free model of magnetic clouds for their heliospheric evolution. J. Geophys. Res. **112**, A06113 (2007), doi:10.1029/2006JA011940.

*Lindsey, C., H. Schunker, and P. S. Cally*: Magnetoseismic signatures and flow diagnostics beneath magnetic regions. Astron. Nachr. **328**, 298–304 (2007), doi:10.1002/asna.200610733.

*Lowry, S. C., A. Fitzsimmons, P. Pravec, D. Vokrouhlický, H. Boehnhardt, P. A. Taylor, J.-L. Margot, A. Galád, M. Irwin, J. Irwin, and P. Kusnirák*: Direct Detection of the Asteroidal YORP Effect. Science **316**, 272–274 (2007), doi:10.1126/science.1139040, originally published in Science Express.

*Madjarska, M. S., J. G. Doyle, D. E. Innes, and W. Curdt*: Jets or High-Velocity Flows Revealed in High-Cadence Spectrometer and Imager Co-observations? Astrophys. J. **670**, L57–L60 (2007), doi:10.1086/524013.

*Madjarska, M. S. and T. Wiegelmann*: Evolution of coronal hole boundaries seen in EIT 195 Å and TRACE 171 Å images. In: Modern Solar Facilities – Advanced Solar Science, eds. F. Kneer, K. G. Puschmann, and A. D. Wittmann, pp. 249–252, Universitätverlag Göttingen (2007).

*Markiewicz, W. J., D. V. Titov, N. Ignatiev, H. U. Keller, D. Crisp, S. S. Limaye, R. Jaumann, R. Moissl, N. Thomas, L. Esposito, S. Watanabe, B. Fiethe, T. Behnke, I. Szemerey, H. Michalik, H. Perplies, M. Wedemeier, I. Sebastian, W. Boogaerts, S. F. Hviid, C. Dierker, B. Osterloh, W. Böker, M. Koch, H. Michaelis, D. Belyaev, A. Dannenberg, M. Tschimmel, P. Russo, T. Roatsch, and K. D. Matz*: Venus monitoring camera for Venus express. Planet. Space Sci. **55**, 1701–1711 (2007), doi:10.1016/j.pss.2007.01.004.

*Markiewicz, W. J., D. V. Titov, S. S. Limaye, H. U. Keller, N. Ignatiev, R. Jaumann, N. Thomas, H. Michalik, R. Moissl, and P. Russo*: Morphology and dynamics of the upper cloud layer of Venus. Nature **450**, 633–636 (2007), doi:10.1038/nature06320.

*Marsch, E.*: Status Of Knowledge After Helios, Ulysses And SOHO Of The Microstate Of The Coronal And Solar-Wind Plasma. In: The Second Solar Orbiter Workshop, 16-20 October 2006, Athens, Greece, eds. E. Marsch, K. Tsinganos, R. Marsden, and L. Conroy, ESA SP-641, ESA Publ. Div., Noordwijk (2007), on CD.

*Marsch, E.*: The radial wavefunction of a relativistic binary of two fermions bound by the Coulomb force. Annalen der Physik **16**, 553–562 (2007), doi:10.1002/andp.200610248.

*Martínez González, M. J., M. Collados, B. Ruiz Cobo, and S. K. Solanki*: Low-lying magnetic loops in the solar internetwork. Astron. & Astrophys. **469**, L39–L42 (2007), doi:10.1051/0004-6361:20077505.

*Mason, K. O., M. Chester, A. Cucchiara, C. Gronwall, D. Grupe, S. Hunsberger, G. H. Jones, S. Koch, J. Nousek, P. T. O'Brien, J. Racusin, P. Roming, P. Smith, A. Wells, R. Willingale, G. Branduardi-Raymont, and N. Gehrels*: Swift ultraviolet photometry of the Deep Impact encounter with Comet 9P/Tempel 1. Icarus **187**, 123–131 (2007), doi:10.1016/j.icarus.2006.09.021.

*Mathew, S. K., V. Martínez Pillet, S. K. Solanki, and N. A. Krivova*: Properties of sunspots in cycle 23. I. Dependence of brightness on sunspot size and cycle phase. Astron. & Astrophys. **465**, 291–304 (2007), doi:10.1051/0004-6361:20066356.

*Matteini, L., S. Landi, P. Hellinger, F. Pantellini, M. Maksimovic, M. Velli, B. E. Goldstein, and E. Marsch*: Evolution of the solar wind proton temperature anisotropy from 0.3 to 2.5 AU. Geophys. Res. Lett. **34**, L20105 (2007), doi:10.1029/2007GL030920.

*McComas, D. J., M. I. Desai, F. Allegrini, M. Berthomier, R. Bruno, P. Louran, E. Marsch, C. J. Owen, N. A. Schwadron, and T. H. Zurbuchen*: The Solar Wind Proton And Alpha Sensor For The Solar Orbiter. In: The Second Solar Orbiter Workshop, 16-20 October 2006, Athens, Greece, eds. E. Marsch, K. Tsinganos, R. Marsden, and L. Conroy, ESA SP-641, ESA Publ. Div., Noordwijk (2007), on CD.

*McIntosh, S. W., A. R. Davey, D. M. Hassler, J. D. Armstrong, W. Curdt, K. Wilhelm, and G. Lin*: Observations supporting the role of magnetoconvection in energy supply to the quiescent solar atmosphere. Astrophys. J. **654**, 650–664 (2007), doi:10.1086/509071.

*McKenzie, J. F., E. Dubinin, and K. Sauer*: Comment on "Obliquely propagating large amplitude solitary waves in charge neutral plasmas" by Verheest, Nonlin. Processes Geophys., 14,49-57, 2007. Nonlin. Proc. Geophys. **14**, 543–544 (2007).

*Mecheri, R. and E. Marsch*: Coronal ion-cyclotron beam instabilities within the multi-fluid description. Astron. & Astrophys. **474**, 609–615 (2007), doi:10.1051/0004-6361:20077648.

*Mecheri, R. and E. Marsch*: Ray tracing of ion-cyclotron waves in a coronal funnel. In: Modern Solar Facilities – Advanced Solar Science, eds. F. Kneer, K. G. Puschmann, and A. D. Wittmann, pp. 355–358, Universitätsverlag Göttingen (2007).

*Medvedev, A. S.*: Definition of a generalized diabatic circulation based on a variational approach. Izv. Atmos. Ocean. Phys. **43**, 436–441 (2007), doi:10.1134/S0001433807040056.

*Medvedev, A. S. and P. Hartogh*: Winter polar warmings and the meridional transport on Mars simulated with a general circulation model. Icarus **186**, 97–110 (2007), doi:10.1016/j.icarus.2006.08.020.

*Melchiorri, R., T. Encrenaz, T. Fouchet, P. Drossart, E. Lellouch, B. Gondet, J. P. Bibring, Y. Langevin, B. Schmitt, D. Titov, and N. Ignatiev*: Water vapor mapping on Mars using OMEGA/Mars express. Planet. Space Sci. **55**, 333–342 (2007), doi:10.1016/j.pss.2006.05.040.

*Menietti, J. D., R. A. Frahm, A. Korth, F. S. Mozer, and Y. Khotyaintsev*: Polar and Cluster observations of a dayside inverted-V during conjunction. Ann. Geophys. **25**, 543–555 (2007).

*Middleton, K., V. Da Deppo, L. Poletto, U. Schühle, R. J. Thomas, and P. R. Young*: Optical Design of the Extreme Ultravioletspectrometer (EUS) on Board Solar Orbiter. In: The Second Solar Orbiter Workshop, eds. E. Marsch, K. Tsinganos, R. Marsden, and L. Conroy, ESA SP-641, ESA Publ. Div., Noordwijk (2007), on CD.

*Mierla, M., R. Schwenn, L. Teriaca, G. Stenborg, and B. Podlipnik*: The dynamics of the minimum solar corona during the period August – October 1996. Adv. Space Res. **40**, 1049–1053 (2007), doi:10.1016/j.asr.2007.01.083.

*Narita, Y., K. H. Glassmeier, M. Fränz, Y. Nariyuki, and T. Hada*: Observations of linear and nonlinear processes in the foreshock wave evolution. Nonlin. Proc. Geophys. **14**, 361–371 (2007).

*Nielsen, E., M. Fraenz, H. Zou, J.-S. Wang, D. A. Gurnett, D. L. Kirchner, D. D. Morgan, R. Huff, A. Safaeinili, J. J. Plaut, G. Picardi, J. D. Winningham, R. A. Frahm, and R. Lundin*: Local plasma processes and enhanced electron densities in the lower ionosphere in magnetic cusp regions on Mars. Planet. Space Sci. **55**, 2164–2172 (2007), doi:10.1016/j.pss.2007.07.003.

*Nielsen, E., X.-D. Wang, D. A. Gurnett, D. L. Kirchner, R. Orosie, A. Safaeinili, J. J. Plaut, and G. Picardi*: Vertical sheets of dense plasma in the top side Martian ionosphere. J. Geophys. Res. **112**, E02003 (2007), doi:10.1029/2006je002723.

*Nuño, B. S. A., R. Centeno, K. G. Puschmann, J. T. Bueno, J. B. Rodriguez, and F. Kneer*: Spicule emission profiles observed in He-I 10830 Å. Astron. & Astrophys. **472**, L51–L54 (2007), doi:10.1051/0004-6361:20077936.

*Otto, A., J. Büchner, and B. Nikutowski*: Force-free magnetic field extrapolation for MHD boundary conditions in simulations of the solar atmosphere. Astron. & Astrophys. **468**, 313–321 (2007), doi:10.1051/0004-6361:20054495.

*Paganini, L. and P. Hartogh*: Description of a New 400 MHz Bandwidth Chirp Transform Spectrometer. In: Advances in Geosciences, Vol. 7: Planetary Science, eds. A. Bhardwaj *et al.*, pp. 45–53, World Scientific Publishing Co., Singapore (2007).

*Paganini, L., P. Hartogh, and L. Reindl*: An improved method for nonlinearity detection applied to a new 400-MHz Bandwidth Chirp Transform Spectrometer. In: Proceedings of the Fourth IEEE International Multi-Conference on Systems, Signals & Devices, vol. 4, p. 381 (2007).

*Panov, E., S. Savin, J. Büchner, and A. Korth*: On the thickness of the outer boundary of the magnetosphere obtained by the four Cluster spacecraft. Space Res. **45**, 1–5 (2007), in Russian.

*Panov, E. V., S. P. Savin, J. Büchner, and A. Korth*: Current sheet thickness of the outer boundary of the magnetosphere as observed by four Cluster satellites. Cosmic Research **45**, 268–272 (2007), doi:10.1134/S0010952507030136.

*Paranicas, C., B. H. Mauk, K. Khurana, I. Jun, H. Garrett, N. Krupp, and E. Roussos*: Europa's near-surface radiation environment. Geophys. Res. Lett. **34**, L15103 (2007), doi:10.1029/2007GL030834.

*Paranicas, C., D. G. Mitchell, E. C. Roelof, B. H. Mauk, S. M. Krimigis, P. C. Brandt, M. Kusterer, F. S. Turner, J. Vandegriff, and N. Krupp*: Energetic electrons injected into Saturns neutral gas cloud. Geophys. Res. Lett. **34**, L02109 (2007), doi:10.1029/2006GL028676.

*Pätzold, M., B. Häusler, K. Aksnes, J. D. Anderson, S. W. Asmar, J.-P. Barriot, M. K. Bird, H. Boehnhardt, W. Eidel, E. Grün, W. H. Ip, E. Marouf, T. Morley, F. M. Neubauer, H. Rickman, N. Thomas, B. T. Tsurutani, M. K. Wallis, N. C. Wickramasinghe, E. Mysen, O. Olson, S. Remus, S. Tellmann, T. Andert, L. Carone, M. Fels, C. Stanzel, I. Audenrieth-Kersten, A. Gahr, A.-L. Müller, D. Stupar, and C. Walter*: Rosetta Radio Science Investigations (RSI). Space Sci. Rev. **128**, 599–627 (2007), doi:10.1007/s11214-006-9117-7.

*Pauluhn, A. and S. K. Solanki*: A nanoflare model of quiet Sun EUV emission. Astron. & Astrophys. **462**, 311–322 (2007), doi:10.1051/0004-6361:20065152.

*Peter, H., R. Schlichenmaier, and M. Roth*: Vom Kern zur Korona. Physik Journal **6**, 35–41 (2007).

*Petrova, E., V. P. Tishkovets, and K. Jockers*: Modelling of opposition effects with ensembles of clusters: Interplay of various scattering mechanisms. Icarus **188**, 233–245 (2007), doi:10.1016/j.icarus.2006.11.011.

*Piccioni, G., P. Drossart, A. Sanchez-Lavega, R. Hueso, F. W. Taylor, C. F. Wilson, D. Grassi, L. Zasova, M. Moriconi, A. Adriani, S. Lebonnois, A. Coradini, B. Bezard, F. Angrilli, G. Arnold, K. H. Baines, G. Bellucci, J. Benkhoff, J. P. Bibring, A. Blanco, M. I. Blecka, R. W. Carlson, A. D. Lellis, T. Encrenaz, S. Erard, S. Fonti, V. Formisano, T. Fouchet, R. Garcia, R. Haus, J. Helbert, N. I. Ignatiev, P. G. J. Irwin, Y. Langevin, M. A. Lopez-Valverde, D. Luz, L. Marinangeli, V. Orofino, A. V. Rodin, M. C. Roos-Serote, B. Saggin, D. M. Stam, D. Titov, G. Visconti, and M. Zambelli*: South-polar features on Venus similar to those near the North Pole. Nature **450**, 637–640 (2007), doi:10.1038/nature06209.

*Plaut, J. J., G. Picardi, A. Safaeinili, A. B. Ivanov, S. M. Milkovich, A. Cicchetti, W. Kofman, J. Mouginot, W. M. Farrell, R. J. Phillips, S. M. Clifford, A. Frigeri, R. Orosei, C. Federico, I. P. Williams, D. A. Gurnett, E. Nielsen, T. Hagfors, E. Heggy, E. R. Stofan, D. Plettemeier, T. R. Watters, C. J. Leuschen, and P. Edenhofer*: Subsurface radar sounding of the south polar layered deposits of Mars. Science **316**, 92–95 (2007), doi:10.1126/science.1139672.

*Preusse, S., A. Kopp, J. Büchner, and U. Motschman*: MHD simulation scenarios of the stellar wind interaction with Hot Jupiter magnetospheres. Planet. Space Sci. **55**, 589–597 (2007), doi:10.1016/j.pss.2006.04.037.

*Protopapa, S., T. Herbst, and H. Boehnhardt*: Surface Ice Spectroscopy of Pluto, Charon and Triton. The Messenger **129**, 58–60 (2007).

*Radioti, A., J. Woch, E. A. Kronberg, N. Krupp, A. Lagg, K.-H. Glassmeier, and M. K. Dougherty*: Energetic ion composition during reconfiguration events in the Jovian magnetotail. J. Geophys. Res. **112**, A06221 (2007), doi:10.1029/2006JA012047.

*Ramos, A. A., H. Socas-Navarro, A. L. Ariste, and M. J. M. González*: The intrinsic dimensionality of spectropolarimetric data. Astrophys. J. **660**, 1690–1699 (2007), doi:10.1086/513069.

*Raouafi, N.-E., J. W. Harvey, and S. K. Solanki*: Properties of solar polar coronal plumes constrained by UVCS data. Astrophys. J. **658**, 643–656 (2007), doi:10.1086/510286.

*Rengel, M., K. Hodapp, and J. Eisloeffel*: SK 1: A Possible Case of Triggered Star Formation in Perseus. In: Triggered Star Formation in a Turbulent Interstellar Medium (IAU S237), eds. B. Elmegreen and J. Palous, Cambridge University Press (2007).

*Rengel, M., M. Küppers, H. U. Keller, and P. Gutierrez*: Modeling of the Terminal Velocities of the Dust Ejected Material by the Impact. In: Deep Impact as a World Observatory Event – Synergies in Space, Time, eds. H. U. Kaeufl and C. Sterken, Springer Verlag (2007).

*Ribe, N., A. Davaille, and U. Christensen*: Fluid Dynamics of Mantle Plumes. In: Mantle Plumes – A Multidisciplinary Approach, eds. J. R. R. Ritter and U. R. Christensen, pp. 1–48, Springer-Verlag, Berlin, Heidelberg (2007).

*Ritter, J. R. R. and U. R. Christensen* (eds.): Mantle Plumes – A Multidisciplinary Approach. Springer-Verlag, Berlin, Heidelberg (2007).

*Rodriguez, J. B., O. V. Okunev, K. G. Puschmann, F. Kneer, and B. S. A. Nuño*: On the properties of faculae at the poles of the Sun. Astron.

& Astrophys. **474**, 251–259 (2007), doi:10.1051/0004-6361:20077739.

*Roth, M.*: Future missions for helioseismology. In: Modern Solar Facilities – Advanced Solar Science, eds. F. Kneer, K. G. Puschmann, and A. D. Wittmann, pp. 85–88, Universitätsverlag Göttingen, Göttingen, Germany (2007).

*Roth, M.*: The Network Activities in HELAS. Comm. in Asteroseismology **150**, 287–291 (2007).

*Roth, M., L. Gizon, and J. G. Beck*: Measuring helioseismic travel times. Astron. Nachr. **328**, 215–222 (2007), doi:10.1002/asna.200610722.

*Rother, M., K. Schlegel, and H. Lühr*: CHAMP observation of intense kilometre-scale field-aligned currents, evidence for an ionospheric Alfvén resonator. Ann. Geophys. **25**, 1603–1615 (2007).

*Roussos, E., G. H. Jones, N. Krupp, C. Paranicas, D. G. Mitchell, A. Lagg, J. Woch, U. Motschmann, S. M. Krimigis, and M. K. Dougherty*: Electron microdiffusion in the Saturnian radiation belts: Cassini MIMI/LEMMS observations of energetic electron absorption by the icy moons. J. Geophys. Res. **112**, A06214 (2007), doi:10.1029/2006JA012027.

*Russell, C. T., F. Capaccioni, A. Coradini, M. C. De Sanctis, W. C. Feldmann, R. Jaumann, H. U. Keller, T. B. McCord, L. A. McFadden, S. Mottola, C. M. Pieters, T. H. Prettyman, C. A. Raymond, M. V. Sykes, D. E. Smith, and M. T. Zuber*: Dawn Mission to Vesta and Ceres – Symbiosis between Terrestrial Observations and Robotic Exploration. Earth, Moon and Planets **101**, 65–91 (2007), doi:10.1007/s11038-007-9151-9.

*Safari, H., D. E. Innes, S. K. Solanki, and A. Pauluhn*: Nanoflare model of emission line radiance distributions in active region coronae. In: Modern Solar Facilities - Advanced Solar Science, eds. F. Kneer, K. G. Puschmann, and A. D. Wittmann, pp. 359–362, Universitätsverlag Göttingen (2007).

*Santos, J. C. and J. Büchner*: MHD simulation of electric currents in the solar atmosphere caused by photospheric plasma motion. ASTRA **3**, 29–33 (2007).

*Santos, J. C., J. Büchner, B. Nikutowski, and M. V. Alves*: Calculations of Photospheric Plasma Velocity Fields using Photospheric Magnetic Field Measurements. In: New Solar Physics with Solar-B Mission, eds. K. Shibata, S. Nagata, and T. Sakurai, vol. 369, pp. 183–192, Astronomical Society of the Pacific (2007).

*Sasso, C., A. Lagg, and S. K. Solanki*: Spectropolarimetry in the chromospheric He I 1083.0 nm multiplet. In: 1st Workshop of Astronomy and Astrophysics for Students, eds. N. R. Napolitano and M. Paolillo, pp. 43–46, INFN-Naples (2007).

*Sasso, C., A. Lagg, S. K. Solanki, R. Aznar Cuadrado, and M. Collados*: Full-Stokes observations and analysis of He I 10830 Å in a flaring region. In: The Physics of Chromospheric Plasmas, eds. P. Heinzel, I. Dorotovič, and R. J. Rutten, *Astron. Soc. Pacific Conf. Ser.*, vol. 368, pp. 467–471, ASP, San Francisco (2007).

*Sauer, K., E. Mjolhus, E. Dubinin, and K. Baumgaertel*: Banana-polarized solitons in anisotropic plasmas related to Ulysses observations. Geophys. Res. Lett. **34**, L11109 (2007), doi:10.1029/2007GL029583.

*Schlegel, K.*: Das Institut und die URSI. In: 60 Jahre Forschung in Lindau, 1946-2006, eds. P. Czechowsky and R. Rüster, pp. 87–90, Copernicus Publications (2007).

*Schlegel, K.*: In Memoriam: Tor Hagfors (1930-2007). Radio Science Bulletin **320**, 65–66 (2007).

*Schlegel, K.*: The URSI Board of Officers: URSI White Paper on Solar Power Satellite Systems (SPS). The Radio Science Bulletin **321**, 13–27 (2007).

*Schrinner, M., K.-H. Rädler, D. Schmitt, M. Rheinhardt, and U. R. Christensen*: Mean-field concept and direct numerical simulations of rotating magnetoconvection and the geodynamo. Geophys. Astrophys. Fluid Dynamics **101**, 81–116 (2007), doi:10.1080/03091920701345707.

*Schühle, U.*: Instrumental Approaches to Achieve the Measurements Required for Exploring the Energetics, Dynamics, and Fine-Scale Structure of the Sun's Magnetized Atmosphere. In: The Second Solar Orbiter Workshop, eds. E. Marsch, K. Tsinganos, R. Marsden, and L. Conroy, ESA SP-641, ESA Publ. Div., Noordwijk (2007), on CD.

*Schühle, U., S. K. Mathew, M. Wedemeier, H. Hartwig, E. Ballesteros, V. Martinez Pillet, and S. K. Solanki*: Space Qualification of a Thin Wafer Lithium Niobate Etalon for the Visible Light Imager and Magnetograph (VIM). In: The Second Solar Orbiter Workshop, eds. E. Marsch, K. Tsinganos, R. Marsden, and L. Conroy, ESA SP-641, ESA Publ. Div., Noordwijk (2007), on CD.

*Schühle, U., H. Uhlig, W. Curdt, T. Feigl, A. Theissen, and L. Teriaca*: Thin Silicon Carbide Coating of the Primary Mirror of VUV Imaging Instruments for Solar Orbiter. In: The Second Solar Orbiter Workshop, eds. E. Marsch, K. Tsinganos, R. Marsden, and L. Conroy, ESA SP-641, ESA Publ. Div., Noordwijk (2007), on CD.

*Schunker, H., D. C. Braun, and P. S. Cally*: Surface magnetic field effects in local helioseismology. Astron. Nachr. **328**, 292–297 (2007), doi:10.1002/asna.200610732.

*Schüssler, M.*: Are solar cycles predictable? Astron. Nachr./AN **328**, 1087–1091 (2007), doi:10.1002/asna.200710836.

*Schüssler, M. and A. Ferriz-Mas*: Flow instabilities of magnetic flux tubes I. Perpendicular flow. Astron. & Astrophys. **463**, 23–29 (2007), doi:10.1051/0004-6361:20066344.

*Schüssler, M. and A. Vögler*: A solar surface dynamo. Astron. & Astrophys. **465**, L43–L46 (2007), doi:10.1051/0004-6361:20077253.

*Selwa, M., K. Murawski, S. K. Solanki, and T. J. Wang*: Energy leakage as an attenuation mechanism for vertical kink oscillations in solar coronal wave guides. Astron. & Astrophys. **462**, 1127–1135 (2007), doi:10.1051/0004-6361:20065122.

*Sergeev, V., V. Semenov, M. Kubyshkina, V. Ivanova, W. Baumjohann, R. Nakamura, T. Penz, A. Runov, T. L. Zhang, K.-H. Glassmeier, V. Angelopoulos, H. Frey, J.-A. Sauvaud, P. Daly, J. B. Cao, H. Singer, and E. Lucek*: Observation of repeated intense near-Earth reconnection on closed field lines with Cluster, Double Star, and other spacecraft. Geophys. Res. Lett. **34**, L02103 (2007), doi:10.1029/2006GL028452.

*Sergis, N., S. M. Krimigis, D. G. Mitchell, D. C. Hamilton, N. Krupp, B. M. Mauk, E. C. Roelof, and M. Dougherty*: Ring current at Saturn: Energetic particle pressure in Saturn's equatorial magnetosphere measured with Cassini/MIMI. Geophys. Res. Lett. **34**, L09102 (2007), doi:10.1029/2006GL029223.

*Shelyag, S., M. Schüssler, S. K. Solanki, and A. Vögler*: Stokes diagnostics of simulated solar magneto-convection. Astron. & Astrophys. **469**, 731–747 (2007), doi:10.1051/0004-6361:20066819.

*Shkuratova, Y., N. Opanasenko, E. Zubko, Y. Grynko, V. Korokhin, C. Pieters, G. Videen, U. Mall, and A. Opanasenko*: Multispectral polarimetry as a tool to investigate texture and chemistry of lunar regolith particles. Icarus **187**, 406–416 (2007), doi:10.1016/j.icarus.2006.10.012.

*Sonnemann, G. R. and M. Grygalashvyly*: The relationship between the occurrence rate of major stratospheric warmings and solar Lyman-alpha flux. J. Geophys. Res. **112**, D20101 (2007), doi:10.1029/2007JD008718.

*Sonnemann, G. R., P. Hartogh, C. Jarchow, M. Grygalashvyly, and U. Berger*: On the winter anomaly of the night-to-day ratio of ozone in the middle to upper mesosphere in middle to high latitudes. Adv. Space Res. **40**, 846–854 (2007), doi:10.1016/j.asr.2007.01.039.

*Sonnemann, G. R., P. Hartogh, C. Jarchow, M. Grygalashvyly, and U. Berger*: The winter anomaly of the night-to-day ratio of ozone in the middle to upper mesosphere in middle latitudes - a comparison between measurements and model calculations. In: Advances in Geosciences, Vol.9: Solid Earth, Ocean Science & Atmospheric Science (2006), eds. W.-H. Ip and Y.-T. Chen, pp. 177–190, World Scientific Publishing Company, Singapore (2007).

*Soobiah, Y., A. J. Coates, D. R. Linder, D. O. Kataria, J. D. Winningham, R. A. Frahm, J. R. Sharber, J. R. Scherrer, S. Barabash, R. Lundin, M. Holmstrom, H. Andersson, M. Yamauchi, A. Grigoriev, E. Kallio, H. Koskinen, T. Sales, P. Riihela, W. Schmidt, J. Kozyra, J. Luhmann, E. Roelof, D. Williams, S. Livi, C. C. Curtis, K. C. Hsieh, B. R. Sandel, M. Grande, M. Carter, J. A. Sauvaud, A. Fedorov, J. J. Thocaven, S. McKenna-Lawler, S. Orsini, R. Cerulli-Irelli, M. Maggi, P. Wurz, P. Bochsler, N. Krupp, J. Woch, M. Fränz, K. Asamura, and C. Dierker*: Erratum to "Observations of magnetic anomaly signatures in Mars Express ASPERA-3 ELS data" [Icarus 182 (2006) 396–405]. Icarus **187**, 623–625 (2007), doi:10.1016/j.icarus.2005.11.025.

*Spanswick, E., E. Donovan, R. Friedel, and A. Korth*: Ground based identification of dispersionless electron injections. Geophys. Res. Lett. **34**, L03101 (2007), doi:10.1029/2006GL028329.

*Stenzel, O. J., B. Grieger, H. U. Keller, R. Greve, K. Fraedrich, E. Kirk, and F. Lunkeit*: Coupling Planet Simulator Mars, a general circulation model of the Martian atmosphere, to the ice sheet model SICOPOLIS. Planet. Space Sci. **55**, 2087–2096 (2007), doi:10.1016/j.pss.2007.09.001.

*Svedhem, H., D. V. Titov, D. Mccoy, J. P. Lebreton, S. Barabash, J. L. Bertaux, P. Drossart, V. Formisano, B. Hausler, O. Korablev, W. J. Markiewicz, D. Nevejans, M. Patzold, G. Piccioni, T. L. Zhang, F. W. Taylor, E. Lellouch, D. Koschny, O. Witasse, H. Eggel, M. Warhaut, A. Accomazzo, J. Rodriguez-Canabal, J. Fabrega, T. Schirmann, A. Clochet, and M. Coradini*: Venus express - The first European mission to Venus. Planet. Space Sci.

**55**, 1636–1652 (2007), doi:10.1016/j.pss.2007.01.013.

*Svedhem, H., D. V. Titov, F. W. Taylor, and O. Witasse*: Venus as a more Earth-like planet. Nature **450**, 629–632 (2007), doi:10.1038/nature06432.

*Tachihara, K., M. Rengel, Y. Nakajima, N. Yamaguchi, P. André, R. Neuhäuser, T. Onishi, Y. Fukui, and A. Mizuno*: Gas and Dust Condensations and a Peculiar Class 0 Object in the Lupus 3 Star-Forming Cloud. Astrophys. J. **659**, 1382–1393 (2007), doi:10.1086/512093.

*Tarcea, N., T. Frosch, P. Roesch, M. Hilchenbach, T. Stuffler, S. Hofer, H. Thiele, R. Hochleitner, and J. Popp*: Raman Spectroscopy: A Powerful Tool for in situ Planetary Science. Space Sci. Rev. (2007), doi:10.1007/s11214-007-9279-y, available only online pending paper publication.

*Taylor, F. W., H. Svedhem, and D. V. Titov*: Venus Express and terrestrial planet climatology. In: Exploring Venus as terrestrial Planet, eds. L. W. Esposito, E. R. Stofan, and T. E. Cravens, no. 176 in AGU Geophysical Monographs, pp. 157–170, American Geophysical Union, Washington, DC (2007).

*Teriaca, L., U. Schühle, S. K. Solanki, W. Curdt, and E. Marsch*: The Lower Transition Region As Seen In The H I Lyman-alpha Line. In: The Second Solar Orbiter Workshop, 16-20 October 2006, Athens, Greece, eds. E. Marsch, K. Tsinganos, R. Marsden, and L. Conroy, ESA SP-641, ESA Publ. Div., Noordwijk (2007), on CD.

*Theissen, A., A. BenMoussa, U. Schühle, J.-F. Hochedez, and W. Schmutz*: LYRA – a solar UV radiometer using diamond detectors. In: Modern Solar Facilities – Advanced Solar Science, Proceedings of a Workshop held at Göttingen September 27-29, 2006, eds. F. Kneer, K. G. Puschmann, and A. D. Wittmann, pp. 27–30, Universitätsverlag Göttingen (2007).

*Thomas, N., T. Spohn, J. P. Barriot, W. Benz, G. Beutler, U. Christensen, V. Dehant, C. Fallnich, D. Giardini, O. Groussin, K. Gunderson, E. Hauber, M. Hilchenbach, L. Iess, P. Lamy, L. M. Lara, P. Lognonne, J. J. Lopez-Moreno, H. Michaelis, J. Oberst, D. Resendes, J. L. Reynaud, R. Rodrigo, S. Sasakio, K. Selferlin, M. Wieczorek, and J. Whitby*: The BepiColombo laser altimeter (BELA): Concept and baseline design. Planet. Space Sci. **55**, 1398–1413 (2007), doi:10.1016/j.pss.2007.03.003.

*Tian, H., C.-Y. Tu, J.-S. He, and E. Marsch*: Emission heights of coronal bright points on Fe XII radiance map. Adv. Space Res. **39**, 1853–1859 (2007), doi:10.1016/j.asr.2007.03.065.

*Titov, D., M. Bullock, D. Crisp, N. Renno, F. W. Taylor, and L. V. Zasova*: Radiation in the atmosphere of Venus. In: Exploring Venus as terrestrial Planet, eds. L. W. Esposito, E. R. Stofan, and T. E. Cravens, no. 176 in AGU Geophysical Monographs, pp. 121–138, American Geophysical Union, Washington, DC (2007).

*Tothova, D., D. E. Innes, and S. K. Solanki*: Wavelet-based method for coronal loop oscillations analysis. In: Modern Solar Facilities - Advanced Solar Science, eds. F. Kneer, K. G. Puschmann, and A. D. Wittmann, pp. 265–267, Universitätsverlag Göttingen (2007).

*Tozzi, G. P., H. Boehnhardt, L. Kolokolova, T. Bonev, E. Pompei, S. Bagnulo, N. Ageorges, L. Barrera, O. Hainaut, H. U. Käufl, F. Kerber, G. LoCurto, O. Marco, E. Pantin, H. Rauer, I. Saviane, C. Sterken, and M. Weiler*: Dust observations of Comet 9P/Tempel 1 at the time of the Deep Impact. Astron. & Astrophys. **476**, 979–988 (2007), doi:10.1051/0004-6361:20077615.

*Tripathi, D., S. K. Solanki, H. E. Mason, and D. F. Webb*: A bright coronal downflow seen in multi-wavelength observations: Evidence of a bifurcating flux-rope? Astron. & Astrophys. **472**, 633–642 (2007), doi:10.1051/0004-6361:20077707.

*Tsiropoula, G., K. Tziotziou, J. Giannikakis, P. Young, U. Schühle, and P. Heinzel*: Multi-wavelength Analysis of a Solar Quiet Region. In: Coimbra Solar Physics Meeting on "The Physics of Chromospheric Plasmas", eds. P. Heinzel, I. Dorotovic, and R. J. Rutten, *ASP Conference Series*, vol. 368, pp. 171–176, Astronomical Society of the Pacific, San Francisco (2007).

*Tsiropoula, G., K. Tziotziou, T. Wiegelmann, Th. Zachariadis, C. Gontikakis, and H. Dara*: Evolution of a Coronal Loop System. Solar Phys. **240**, 37–48 (2007), doi:10.1007/s11207-006-0247-6.

*Tubiana, C., R. Duffard, L. Barrera, and H. Boehnhardt*: Photometric and spectroscopic observations of (132524) 2002 $JF_{56}$: fly-by target of the New Horizons mission. Astron. & Astrophys. **463**, 1197–1199 (2007), doi:10.1051/0004-6361:20066518.

*Usoskin, I. G., S. K. Solanki, and G. A. Kovaltsov*: Grand minima and maxima of solar activity: New observational constraints. Astron. & Astrophys. **471**, 301–309 (2007), doi:10.1051/0004-6361:20077704.

*Vallat, C., N. Ganushkina, I. Dandouras, C. P. Escoubet, M. G. G. T. Taylor, H. Laakso, A. Masson, J.-A. Sauvaud, H. Rème, and P. Daly*: Ion multi-nose structures observed by Cluster in the inner Magnetosphere. Ann. Geophys. **25**, 171–190 (2007).

*Vasyliūnas, V. M.*: The mechanical advantage of the magnetosphere: solar-wind-related forces in the magnetosphere-ionosphere-Earth system. Ann. Geophys. **25**, 255–269 (2007).

*Vasyliūnas, V. M. and D. H. Pontius, Jr.*: Rotationally driven interchange instability: Reply to André and Ferrière. J. Geophys. Res. **112**, A10204 (2007), doi:10.1029/2007JA012457.

*Vršnak, B., A. M. Veronig, J. K. Thalmann, and T. Zic*: Large amplitude oscillatory motion along a solar filament. Astron. & Astrophys. **471**, 295–299 (2007), doi:10.1051/0004-6361:20077668.

*Wang, T. J., D. E. Innes, and J. Qiu*: Determination of the coronal magnetic field from hot-loop oscillations observed by SUMER and SXT. Astrophys. J. **656**, 598–609 (2007), doi:10.1086/510424.

*Weinstock, J., G. P. Klaassen, and A. S. Medvedev*: Reply to “Comments on the gravity wave theory of J. Weinstock concerning dissipation induced by nonlinear effects”. J. Atmos. Sci. **64**, 1027–1041 (2007), doi:10.1175/JAS3865.1.

*Wicht, J., M. Mandea, F. Takahashi, U. R. Christensen, M. Matsushima, and B. Langlais*: The origin of Mercury’s internal magnetic field. In: Mercury, eds. A. Balogh, L. Ksanfomality, and R. von Steiger, Space Sciences Series of ISSI, pp. 79–108, Springer, Dordrecht/Boston/London (2007), doi:10.1007/s11214-007-9280-5.

*Wiegelmann, T.*: Computing Nonlinear Force-Free Coronal Magnetic Fields in Spherical Geometry. Solar Phys. **240**, 227–239 (2007), doi:10.1007/s11207-006-0266-3.

*Wiegelmann, T., T. Neukirch, P. Ruan, and B. Inhester*: Optimization approach for the computation of magnetohydrostatic coronal equilibria in spherical geometry. Astron. & Astrophys. **475**, 701–706 (2007), doi:10.1051/0004-6361:20078244.

*Wiegelmann, T., S. K. Solanki, A. Lagg, and L. Yelles*: Nonlinear force-free magnetic field modelling for VIM on SO. In: The Second Solar Orbiter Workshop, eds. E. Marsch, K. Tsinganos, R. Marsden, and L. Conroy, ESA SP-641, ESA Publ. Div., Noordwijk (2007), on CD.

*Wiehr, E., G. Stellmacher, and J. Hirzberger*: Two-dimensional mapping of the He D-3/H beta emission ratio in solar prominences. Solar Phys. **240**, 25–36 (2007), doi:10.1007/s11207-006-0226-y.

*Wilhelm, K., E. Marsch, B. N. Dwivedi, and U. Feldman*: Observations of the Sun at Vacuum-Ultraviolet Wavelengths from Space. Part II: Results and Interpretations. Space Sci. Rev. **133**, 103–179 (2007), doi:10.1007/s11214-007-9285-0.

*Woch, J. and L. Gizon*: The Solar Orbiter mission and its prospects for helioseismology. Astron. Nachr. **328**, 362–367 (2007), doi:10.1002/asna.200610743.

*Yamashita, Y., T. Kuroda, and M. Takahashi*: Maintainance of zonal wind variability associated with the annular mode on Mars. Geophys. Res. Lett. **34**, L16819 (2007), doi:10.1029/2007GL030069.

*Yankulova, I. M., V. K. Golev, and K. Jockers*: The luminous infrared composite Seyfert 2 galaxy NGC 7679 through the [O III] λ 5007 emission line. Astron. & Astrophys. **469**, 891–898 (2007), doi:10.1051/0004-6361:20077440.

*Zakharov, V., A. Gandorfer, S. K. Solanki, and A. Löfdahl*: Erratum in “A comparative study of the contrast of solar magnetic elements in CN and CH” (vol 437, pg L43, 2005). Astron. & Astrophys. **461**, 695–695 (2007), doi:10.1051/0004-6361:20066135.

*Zakharov, V. V., A. Gandorfer, and S. K. Solanki*: High-resolution CN spectroscopy of small-scale solar magnetic features. In: Modern Solar Facilities - Advanced Solar Science, eds. F. Kneer, K. G. Puschmann, and A. D. Wittmann, pp. 161–164, Universitätsverlag Göttingen (2007).

*Zhang, J., S. K. Solanki, and J. Woch*: Discovery of inward moving magnetic enhancements in sunspot penumbrae. Astron. & Astrophys. **475**, 695–700 (2007), doi:10.1051/0004-6361:20077829.

*Zhang, J., S. K. Solanki, J. Woch, and J. Wang*: The velocity structure of moving magnetic feature pairs around sunspots: Support for the U-loop model. Astron. & Astrophys. **471**, 1035–1041 (2007), doi:10.1051/0004-6361:20077900.

*Zhou, G.-Q., J.-S. He, C.-Y. Tu, and E. Marsch*: Correlation Height of the Source Region of Si II Emission Lines in Coronal Hole Regions. Chinese Astronomy and Astrophysics **31**, 137–145 (2007), doi:10.1016/j.chinastron.2007.04.001.

*Zong, Q.-G., S. Y. Fu, D. N. Baker, M. L. Goldstein, P. Song, J. A. Slavin, T. A. Fritz, J. B. Cao, O. Amm, H. Frey, A. Korth, P. W. Daly, H. Rème, and A. Pedersen*: Earthward flowing plasmoid: Structure and its related ionospheric signature. J. Geophys. Res. **112**, A07203 (2007), doi:10.1029/2006JA012112.

*Zong, Q.-G., X.-Z. Zhou, X. Li, P. Song, S. Y. Fu, D. N. Baker, Z. Y. Pu, T. A. Fritz, P. Daly, A. Balogh, and H. Rème*: Ultralow frequency modulation of energetic particles in the dayside magnetosphere. Geophys. Res. Lett. **34**, L12105 (2007), doi:10.1029/2007GL029915.

Max-Planck-Institut für
Sonnensystemforschung
Max-Planck-Straße 2
37191 Katlenburg-Lindau
Tel: 05556-979-0
Fax: 05556-979-240
E-Mail: presseinfo@mps.mpg.de